

Characterisation of organic osmolytes and biomarkers of  
smoltification in the Atlantic salmon (*Salmo salar*)

Claire Alexandra Dagen



University of  
St Andrews

This thesis is submitted in partial fulfilment for the degree of

Doctor of Philosophy (PhD)

at the University of St Andrews

September 2019



## **Candidate's declaration**

I, Claire Alexandra Dagen, do hereby certify that this thesis, submitted for the degree of PhD, which is approximately 59,000 words in length, has been written by me, and that it is the record of work carried out by me, or principally by myself in collaboration with others as acknowledged, and that it has not been submitted in any previous application for any degree.

I was admitted as a research student at the University of St Andrews in September 2013.

I received funding from an organisation or institution and have acknowledged the funder(s) in the full text of my thesis.

Date 05/11/20

Signature of candidate

## **Supervisor's declaration**

I hereby certify that the candidate has fulfilled the conditions of the Resolution and Regulations appropriate for the degree of PhD in the University of St Andrews and that the candidate is qualified to submit this thesis in application for that degree.

Date 05/11/20

Signature of supervisor

## **Permission for publication**

In submitting this thesis to the University of St Andrews we understand that we are giving permission for it to be made available for use in accordance with the regulations of the University Library for the time being in force, subject to any copyright vested in the work not being affected thereby. We also understand, unless exempt by an award of an embargo as requested below, that the title and the abstract will be published, and that a copy of the work may be made and supplied to any bona fide library or research worker, that this thesis will be electronically accessible for personal or research use and that the library has the right to migrate this thesis into new electronic forms as required to ensure continued access to the thesis.

I, Claire Alexandra Dagen, confirm that my thesis does not contain any third-party material that requires copyright clearance.

The following is an agreed request by candidate and supervisor regarding the publication of this thesis:

**Printed copy**

No embargo on print copy.

**Electronic copy**

No embargo on electronic copy.

Date 05/11/20

Signature of candidate

Date 05/11/20

Signature of supervisor

## **Underpinning Research Data or Digital Outputs**

### **Candidate's declaration**

I, Claire Alexandra Dagen, understand that by declaring that I have original research data or digital outputs, I should make every effort in meeting the University's and research funders' requirements on the deposit and sharing of research data or research digital outputs.

Date 05/11/20

Signature of candidate

### **Permission for publication of underpinning research data or digital outputs**

We understand that for any original research data or digital outputs which are deposited, we are giving permission for them to be made available for use in accordance with the requirements of the University and research funders, for the time being in force.

We also understand that the title and the description will be published, and that the underpinning research data or digital outputs will be electronically accessible for use in accordance with the license specified at the point of deposit, unless exempt by award of an embargo as requested below.

The following is an agreed request by candidate and supervisor regarding the publication of underpinning research data or digital outputs:

No embargo on underpinning research data or digital outputs.

Date 05/11/20

Signature of candidate

Date 05/11/20

Signature of supervisor



## Acknowledgements

I should like to thank Dr N. Hazon and Dr G. Cramb for the provision of research facilities and express my gratitude for their guidance and advice throughout this work. My thanks also go to past and present members of Dr Cramb's research group. I am indebted to Dr Paul Yancey of Whitman College, University of Washington for his collaboration in running HPLC analysis and Dr Steve McCormick of the Conte Anadromous Fish Research Centre for his kind donation of antibodies for this project. Sincere thanks are due to the technical staff of the Chemistry Departments of the University of St Andrews and the University of Edinburgh for their assistance in identifying the structure of the novel osmolyte hypoxanthine. I am also indebted to Ragna Hegbo, Simon Wadsworth, Louise Buttle and Mali Hartviksen and the staff of the EWOS Innovation facility in Dirdal, Norway for their assistance in designing the feeding trial study and their help in the collection of samples, and their hospitality while I was working at their facility. I should also like to thank Teresa Garzon and the staff of the Marine Harvest facilities at Loch Lochy, Invasion Bay and Fort William for providing fish for sampling and assisting in the collection of samples. Finally, I thank my family and friends for their help and support throughout this work.

This work was supported by EWOS Innovation (4327 Sandnes, Norway), Marine Harvest (Rosyth, Admiralty Park, Admiralty Road, Rosyth, Fife, KY11 2YW), and the University of St Andrews (School of Biology).

Research data underpinning this thesis are available at the University of St Andrews Library.



# Contents

Abstract.....	v
Abbreviations.....	vi
List of figures.....	ix
1. Introduction.....	3
1.1 Global seafood production.....	3
1.2 The expansion of the aquaculture industry .....	5
1.3 Sustainability.....	8
1.4 Increasing efficiency.....	10
1.5 Atlantic salmon .....	12
1.6 Importance of salmonids to Scottish economy .....	13
1.7 Salmon life cycle.....	14
1.8 Salmon Parr-Smolt Transformation.....	15
1.9 Osmoregulation.....	21
1.10 Osmoregulation in stenohaline fish .....	22
1.11 Osmoregulation in Euryhaline fish .....	25
1.12 Organic osmolytes .....	26
1.13 Functional feeds.....	29
1.14 This project .....	34
2. Materials and Methods.....	37
2.1 Tissue sampling .....	37
2.2 Gene expression.....	37
2.2.1 RNA extraction from tissues.....	37
2.2.2 RNA extraction from skin.....	38
2.2.3 cDNA synthesis .....	39
2.2.4 Polymerase Chain Reaction (PCR).....	40
2.2.5 Gel electrophoresis and extraction of DNA.....	40
2.2.6 SOPE resin purification of PCR products.....	41
2.2.7 Cloning of DNA fragments.....	42
2.2.8 Sequencing.....	45

2.2.9 Real Time Quantitative Polymerase Chain reaction (RT-qPCR) – relative gene expression .....	46
2.2.10 Primer design .....	50
2.3 Western Blotting .....	51
2.3.1 Protein extraction from tissues.....	51
2.3.2 Protein assays.....	51
2.3.3 Sodium Dodecylsulphate Polyacrylamide Gel Electrophoresis (SDS-PAGE).....	52
2.3.4 Immunostaining .....	52
2.4 Osmolyte extraction .....	53
2.4.1 Hypoxanthine characterisation.....	54
2.5 Industrial smoltification time course trial sampling .....	54
2.5.1 Initial samples .....	54
2.5.2 Second time course .....	54
2.5.3 Trial with SW challenge .....	55
2.6 Nucleotide supplement feeding trial design.....	55
2.6.1 Trial design .....	56
2.6.2 Time course.....	57
2.6.3 Tissue collection .....	58
2.8 Statistical analysis.....	58
3. Novel organic osmolyte in Atlantic salmon.....	61
3.1 Osmotic stress and organic osmolytes .....	61
3.2 Identification of a novel osmolyte in the skin of Atlantic salmon.....	63
3.2.1 Interpretation of spectra .....	64
3.2.2 Hypoxanthine levels in the skin - pilot .....	69
3.3 Hypoxanthine levels in acute seawater transfer trial .....	70
3.3.1 Methods.....	70
3.3.2 Results.....	71
3.4 Hypoxanthine levels in feeding trial with gradual seawater transfer.....	73
3.4.1. Methods.....	73
3.4.2 Results.....	74
3.5 Purine metabolism gene expression.....	75
3.5.1 Initial investigation .....	75
3.5.2 Method.....	77
3.5.3 Results of initial purine metabolism investigation.....	77

3.5.4 RT-qPCR investigation of purine metabolism genes.....	79
3.5.5 Xanthine dehydrogenase.....	98
3.6 Discussion.....	113
3.6.1 Hypoxanthine.....	113
3.6.2 Purine metabolism gene expression.....	115
4. Established organic osmolytes.....	131
4.1 The range of organic osmolytes.....	131
4.2 Organic osmolyte levels - direct transfer trial and SW challenge .....	135
4.2.1 Method.....	135
4.2.2 Results.....	136
4.3 Organic osmolyte levels – nucleotide supplement feeding trial .....	145
4.3.1 Method.....	145
4.3.2 Results.....	146
4.4 Discussion.....	158
4.4.1 Total osmolyte .....	158
4.4.2 Glucose .....	158
4.4.3 Myoinositol.....	163
4.4.4 Taurine .....	165
4.4.5 Glycerophosphocholine .....	167
4.4.6 Urea.....	169
4.4.7 Amino acids .....	175
4.4.8 Glycine betaine .....	179
4.4.9 Creatine.....	182
5. Biomarkers of smoltification .....	187
5.1 Smoltification in an aquaculture setting .....	187
5.1.1 Ion transport in the gill.....	188
5.1.2 Lipid transport and metabolism .....	190
5.1.3 Biomarker candidates involved in the immune system .....	192
5.1.4 Other biomarker candidates .....	194
5.1.5 Objectives .....	196
5.1.6 Procedures.....	196
5.2 Results.....	198
5.2.1 Ion transport.....	198

5.2.2 Lipid metabolism .....	210
5.2.3 Immunity.....	213
5.2.4 Other biomarker candidates .....	221
5.3 Discussion.....	227
5.3.1 Na <sup>+</sup> -K <sup>+</sup> -ATPase α-subunits.....	227
5.3.2 Na <sup>+</sup> -K <sup>+</sup> -ATPase β-subunit .....	230
5.3.3 Other osmoregulatory genes .....	230
5.3.4 Lipid metabolism genes .....	231
5.3.5 Immune genes .....	233
5.3.6 Other Biomarker Candidates.....	237
6. Discussion.....	245
6.1 Organic osmolytes .....	245
6.1.1 Novel osmolyte hypoxanthine .....	248
6.1.2 Short term SW adaptation.....	253
6.1.3 Long term SW adaptation .....	254
6.1.4 Nucleotide supplementation.....	255
6.1.5 Organic osmolyte position within the skin .....	260
6.2 The energy cost of osmoregulation.....	261
6.3 Biomarkers of smoltification .....	263
6.4 Conclusions.....	264
7. References.....	231
Appendix 1 – Feeding trial growth data .....	I
Appendix 2 – Hypoxanthine and purine metabolism .....	II
Appendix 3 – Salmon xanthine dehydrogenase full sequence.....	XVIII
Appendix 4 – Established osmolytes .....	XXVIII
Appendix 5 – Biomarkers of smoltification.....	XXXIV
Appendix 6 – SWATH methodology .....	LVI

## Abstract

Atlantic salmon are an economically important species, particularly in Scotland. The aquaculture of this species is complicated by its anadromous life cycle, requiring transfer to seawater. Smoltification is a complex process whereby fish prepare for entry to seawater, the “smolt window” is the time at which fish are best adapted for the transition to seawater. In the aquaculture setting fish are unable to self-select and may be transferred to the marine environment outwith their optimal smolt window, it is thus important that the mechanisms involved in seawater adaptation are well understood. The accumulation of organic osmolytes forms an important part of the adaptation to seawater, allowing fish to maintain osmotic and ionic balance within their tissues. A novel osmolyte identified in a pilot study was characterised and the metabolism of this compound investigated. The novel compound was identified as hypoxanthine, a purine involved in the nucleotide salvage pathway. This osmolyte and taurine were found to be accumulated in the skin of Atlantic salmon in the days and weeks following seawater transfer. A number of potential biomarkers of smoltification were also investigated with an aim to develop a more robust set of markers of the hypo-osmoregulatory ability of fish. Genes involved in the transport of ions were found to be the most reliable indicators of smoltification.

# Abbreviations

AdD	Adenosine deaminase
ADP	Adenosine diphosphate
AGAT	arginine-glycine transamidinase
AHR	Aryl hydrocarbon receptor
AMP	Adenosine monophosphate
AMPD	Adenosine monophosphate deaminase
AMPK	Adenosine monophosphate kinase
ANF	Anti-nutritional factor
Apo A	Apolipoprotein A
ApoB100	Apolipoprotein B100
ATP	Adenosine triphosphate
BCA	Bicinchoninic acid
BGT1	betaine/ GABA transporter 1
cDNA	complementary DNA
CFTR	Cystic fibrosis transmembrane conductance regulator
CK	creatine kinase
CKA	creatine kinase A
CLM8	CMRF35-like molecule 8
CMP	Cytosine monophosphate
CNT	Concentrative nucleotide transporter
CPT	Carnitine palmitoyltransferase
DDA	data dependent acquisition
DIA	data independent acquisition
DNA	Deoxyribonucleic acid
DOC	sodium deoxycholate
DTT	dithiothreitol
ECF	Extracellular fluid
EDTA	ethylenediaminetetraacetic acid
ENT	Equilibrative nucleotide transporter
FAO	Food and Agriculture Organisation
FIFO	Fish-in to fish-out
FM	Fishmeal
FO	Fish oil
FW	Freshwater
G6-P	glucose-6-phosphate
GAMT	guanidinoacetate methyltransferase
GH	Growth hormone
GPC	Glycerophosphocholine
HBA	hydrogen bond acceptors
HBD	hydrogen bond donors
HPLC	High performance liquid chromatography
Hprt	Hypoxanthine phosphoribosyltransferase

IAA	iodoacetamide
ICF	Intracellular fluid
IgD	Immunoglobulin D
IgK	Immunoglobulin $\kappa$
IMPD	Inosine monophosphate dehydrogenase
LC	liquid chromatography
LDL	Low density lipoprotein
LEI	Leukocyte elastase inhibitor
MFGM	milk fat globule membrane
MI	myocardial infarction
MIPS	Myo-inositol phosphate synthase
MRC	Mitochondria rich cell
MS	Mass spectroscopy
NAA	North Atlantic area
NAD <sup>+</sup>	nicotinamide adenine dinucleotide
NKA	Na <sup>+</sup> -K <sup>+</sup> -ATPase
NKCC	Na <sup>+</sup> -K <sup>+</sup> -Cl <sup>-</sup> -cotransporter
NMR	nuclear magnetic resonance spectroscopy
Ntc	Cytosolic purine 5-nucleotidase
NTE	neuropathy target esterase
Ostf1	Osmotic stress transcription factor 1
PCA	perchloric acid
PCR	Polymerase chain reaction
pIgR	Polymeric immunoglobulin receptor
pIgRL	Polymeric immunoglobulin receptor like transcript
PNP	Purine nucleoside phosphorylase
RAS	Recirculating aquaculture systems
RNA	Ribonucleic acid
RPLP0	Ribosomal Protein Lateral Stalk Subunit P0
RT-qPCR	Real time quantitative polymerase chain reaction
RVD	regulatory volume decrease
RVI	Regulatory volume increase
SBM	Soybean meal
SMIT	sodium-dependent myo-inositol transporters
SSPO	Scottish Salmon Producers' Organisation
SW	Seawater
SWATH	Sequential Windowed Acquisition of All Theoretical Fragments
T3	Triiodothyronine
T4	Thyroxine
TB	Terrific Broth
TCEP	tris 2-carboxyethyl phosphine hydrochloride
TFA	trifluoroacetic acid
TMAO	Trimethylamine-N-oxide
TonEBP	Tonicity-responsive enhancer binding protein
TSH	Thyroid stimulating hormone

TTP	Tristetraprolin
UP584	Unknown protein 584
VLDL	Very low density lipoprotein
XPB	X-box binding protein
XDH	Xanthine dehydrogenase
XOD	Xanthine oxidase
ZG16	Zymogen granule protein 16

# List of figures

Figure 1.1. The salmon life cycle. Illustration by Claire Dagen.	14
Figure 1.2. Parr-smolt transformation. Illustration by Claire Dagen.	16
Figure 1.3. Illustration of Atlantic salmon showing gill and kidney representing the osmoregulatory processes in fish living in freshwater. Diffusion perturbs osmotic balance. Gill and kidney act to maintain homeostasis. Illustration by Claire Dagen.	23
Figure 1.4. Illustration of Atlantic salmon showing gill and digestive tract representing the osmoregulatory processes in fish living in seawater. Diffusion perturbs osmotic balance. Gill and digestive tract act to maintain homeostasis. Illustration by Claire Dagen.	24
Figure 1.5. Structure of azadirachtin.	32
Figure 2.1. pCR <sup>®</sup> 4-TOPO <sup>®</sup> vector, taken from Invitrogen TOPO <sup>®</sup> TA Cloning manual (Life Technologies).	42
Figure 2.2. Randomised design of feeding trial. Diet 1 in red, 2 in orange, 3 in yellow, 4 in green, 5 in blue and 6 in purple.	56
Figure 2.3. Timeline of sampling in EWOS feeding trial showing dates of sampling and of SW transfer.	57
Figure 3.1. HPLC trace of extract from the skin of Atlantic salmon smolts following seawater transfer, supplied by P. H. Yancey.	63
Figure 3.2. Structure of hypoxanthine showing position of hydrogen atoms labels (A-D) correspond to Table 3.1.	64
Figure 3.3. Structure of lactic acid showing position of hydrogen atoms labels (A-D) correspond to Table 3.2.	64
Figure 3.4. <sup>1</sup> HNMR spectrum in D <sub>2</sub> O of unknown peak. The blue line is the same sample doped with hypoxanthine. Spectrum obtained from a Bruker Avance III 800 MHz spectrophotometer by Dr Jura Bella, Department of Chemistry, Edinburgh University.	65
Figure 3.5. <sup>1</sup> HNMR spectrum of unknown peak. The blue line is the same sample doped with lactic acid. Spectrum obtained from a Bruker Avance III 800 MHz spectrophotometer by Dr Jura Bella, Department of Chemistry, Edinburgh University.	66
Figure 3.6. <sup>1</sup> HNMR spectrum of unknown peak. Spectrum obtained from a Bruker Avance III 500 MHz spectrophotometer by Dr Tomas Lebl, Department of Chemistry, University of St Andrews.	67
Figure 3.7. Time of flight mass spectrum of sample believed to be hypoxanthine. Upper trace (A) shows background control. Lower trace (B) shows sample.	68
Figure 3.8. Hypoxanthine levels in the skin. Error bars denote standard deviation (n=3 in all groups but adult where n=2).	69
Figure 3.9. Hypoxanthine levels (mmol/kg wet tissue) extracted from the skin in the months before and days following acute SW transfer. Error bars denote standard error, n=5 or 6.	71
Figure 3.10: Hypoxanthine levels (mmol/kg wet tissue) extracted from the skin of fish sampled in the months leading to acute SW transfer before and after SW challenge. At the first two timepoints samples were collected 6 hours following SW transfer while at the third time point samples were collected 24 hours after SW transfer. Error bars denote standard error, n=5 or 6.	72
Figure 3.11. Hypoxanthine levels (mmol/kg wet tissue) extracted from the skin of Atlantic salmon over a time course leading up to and following smoltification fed on six diets with varying nucleotide supplements. Error bars represent standard error. The first time point represents fish sampled before feeding with experimental diets began and is universal for all diet groups.	74
Figure 3.12. Purine metabolism pathway associated with the production of hypoxanthine. AdD - Adenosine deaminase; AMPD - Adenosine monophosphate deaminase; Hprt - Hypoxanthine phosphoribosyltransferase; IMPD - Inosine monophosphate dehydrogenase; Ntc - Cytosolic purine nucleotidase; PNP - Purine nucleotide phosphorylase; XDH - Xanthine dehydrogenase.	75
Figure 3.13. Expression of purine metabolism genes in the gill (G), skin (S), liver (L) and kidney (K) of Atlantic salmon measured in pooled cDNA from parr and freshwater and seawater smolts. Ladders show up to 500bp.	78
Figure 3.14. Mean fold change in the expression of <i>AMPKα2a</i> relative to <i>RPLP0</i> in the skin of Atlantic salmon shortly before and following direct SW transfer. Error bars denote standard error, -24 hours and 6 hours n=6, 24 hours n=5.	79
Figure 3.15. Mean fold change in the expression of <i>Hprt1</i> relative to <i>RPLP0</i> in the skin of Atlantic salmon shortly before and following direct SW transfer. Error bars denote standard error, -24 hours and 6 hours n=6, 24 hours n=5.	80

Figure 3.16. Mean fold change in the expression of *PNP5a* relative to *RPLP0* in the skin of Atlantic salmon shortly before and following direct SW transfer. Error bars denote standard error, -24 hours and 6 hours n=6, 24 hours n=5. 81

Figure 3.17. Mean fold change in the expression of *PNP5b* relative to *RPLP0* in the skin of Atlantic salmon shortly before and following direct SW transfer. Error bars denote standard error, -24 hours and 6 hours n=6, 24 hours n=5. 82

Figure 3.18. Mean fold change in the expression of *PNP6b* relative to *RPLP0* in the skin of Atlantic salmon shortly before and following direct SW transfer. Error bars denote standard error, -24 hours and 6 hours n=6, 24 hours n=5. 83

Figure 3.19. Mean fold change in the expression of *PNP6c* relative to *RPLP0* in the skin of Atlantic salmon shortly before and following direct SW transfer. Error bars denote standard error, -24 hours and 6 hours n=6, 24 hours n=5. 84

Figure 3.20. Mean fold change in the expression of *AMPKa2a* relative to *RPLP0* in the skin of Atlantic salmon fed on diets containing varying proportions of nucleotide supplement. Time point 1 represents the baseline before feeding with supplemented diets began. Fish were transferred to SW between time points 3 and 4. Error bars denote standard error. 85

Figure 3.21. Mean fold change in the expression of *Hprt1* relative to *RPLP0* in the skin of Atlantic salmon fed on diets containing varying proportions of nucleotide supplement. Time point 1 represents the baseline before feeding with supplemented diets began. Fish were transferred to SW between time points 3 and 4. Error bars denote standard error. 86

Figure 3.22. Mean fold change in the expression of *PNP5a* relative to *RPLP0* in the skin of Atlantic salmon fed on diets containing varying proportions of nucleotide supplement. Time point 1 represents the baseline before feeding with supplemented diets began. Fish were transferred to SW between time points 3 and 4. Error bars denote standard error. 87

Figure 3.23. Mean fold change in the expression of *PNP5b* relative to *RPLP0* in the skin of Atlantic salmon fed on diets containing varying proportions of nucleotide supplement. Time point 1 represents the baseline before feeding with supplemented diets began. Fish were transferred to SW between time points 3 and 4. Error bars denote standard error. 88

Figure 3.24. Mean fold change in the expression of *PNP6b* relative to *RPLP0* in the skin of Atlantic salmon fed on diets containing varying proportions of nucleotide supplement. Time point 1 represents the baseline before feeding with supplemented diets began. Fish were transferred to SW between time points 3 and 4. Error bars denote standard error. 89

Figure 3.25. Mean fold change in the expression of *PNP6c* relative to *RPLP0* in the skin of Atlantic salmon fed on diets containing varying proportions of nucleotide supplement. Time point 1 represents the baseline before feeding with supplemented diets began. Fish were transferred to SW between time points 3 and 4. Error bars denote standard error. 90

Figure 3.26. Mean fold change in the expression of *CNT3* relative to *RPLP0* in the skin of Atlantic salmon shortly before and following direct SW transfer. Error bars denote standard error, -24 hours and 6 hours n=6, 24 hours n=5. 91

Figure 3.27. Mean fold change in the expression of *CNT3* relative to *RPLP0* in the skin of Atlantic salmon at two time points in FW. Error bars represent standard error, n=12 at -5 weeks and n=6 on each diet at -24 hours. 92

Figure 3.28. Mean fold change in the expression of *ENT1a* relative to *RPLP0* in the skin of Atlantic salmon at two time points in FW. Error bars represent standard error, n=12 at -5 weeks and n=6 on each diet at -24 hours. 93

Figure 3.29. Mean fold change in the expression of *ENT1b* relative to *RPLP0* in the skin of Atlantic salmon at two time points in FW. Error bars represent standard error, n=12 at -5 weeks and n=6 on each diet at -24 hours. 94

Figure 3.30. Mean fold change in the expression of *ENT2* relative to *RPLP0* in the skin of Atlantic salmon at two time points in FW. Error bars represent standard error, n=12 at -5 weeks and n=6 on each diet at -24 hours. 95

Figure 3.31. Mean fold change in the expression of *ENT3* relative to *RPLP0* in the skin of Atlantic salmon at two time points in FW. Error bars represent standard error, n=12 at -5 weeks and n=6 on each diet at -24 hours. 96

Figure 3.32. Mean fold change in the expression of *ENT4* relative to *RPLP0* in the skin of Atlantic salmon at two time points in FW. Error bars represent standard error, n=12 at -5 weeks and n=6 on each diet at -24 hours. 97

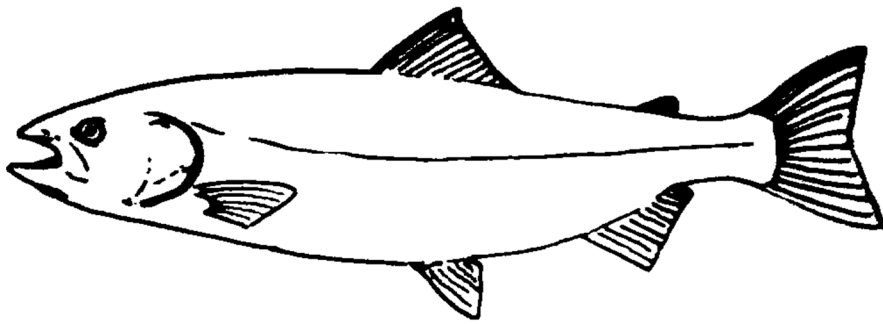
Figure 3.33. Mean fold change in the expression of *XDH* relative to *RPLP0* in the skin of Atlantic salmon fed on diets containing varying proportions of nucleotide supplement. Error bars denote standard error. 112

Figure 3.34. Structure of hypoxanthine.	113
Figure 3.35. The difference in the structure of hypoxanthine and guanine.	115
Figure 4.1. Mean sum of combined organic osmolytes extracted from the skin of Atlantic salmon in a time course leading to smoltification and SW transfer. Plot A shows levels of osmolyte extracted from the skin of fish under normal production conditions. Plot B shows levels extracted from fish exposed to SW challenge at three points on the time course. Error bars represent standard error.	136
Figure 4.2. Mean glucose level extracted from the skin of Atlantic salmon in a time course leading to smoltification and SW transfer. Plot A shows levels of glucose extracted from the skin of fish under normal production conditions. Plot B shows levels extracted from fish exposed to SW challenge at three points on the time course. Error bars represent standard error.	137
Figure 4.3. Mean myoinositol level extracted from the skin of Atlantic salmon in a time course leading to smoltification and SW transfer. Plot A shows levels of myoinositol extracted from the skin of fish under normal production conditions. Plot B shows levels extracted from fish exposed to SW challenge at three points on the time course. Error bars represent standard error.	138
Figure 4.4. Mean taurine level extracted from the skin of Atlantic salmon in a time course leading to smoltification and SW transfer. Plot A shows levels of taurine extracted from the skin of fish under normal production conditions. Plot B shows levels extracted from fish exposed to SW challenge at three points on the time course. Error bars represent standard error, n=6.	139
Figure 4.5. Mean GPC level extracted from the skin of Atlantic salmon in a time course leading to smoltification and SW transfer. Plot A shows levels of GPC extracted from the skin of fish under normal production conditions. Plot B shows levels extracted from fish exposed to SW challenge at three points on the time course. Error bars represent standard error, n=6.	140
Figure 4.6. Mean alanine level extracted from the skin of Atlantic salmon in a time course leading to smoltification and SW transfer. Plot A shows levels of alanine extracted from the skin of fish under normal production conditions. Plot B shows levels extracted from fish exposed to SW challenge at three points on the time course. Error bars represent standard error, n=6.	141
Figure 4.7. Mean betaine level extracted from the skin of Atlantic salmon in a time course leading to smoltification and SW transfer. Plot A shows levels of betaine extracted from the skin of fish under normal production conditions. Plot B shows levels extracted from fish exposed to SW challenge at three points on the time course. Error bars represent standard error, n=6.	142
Figure 4.8. Mean glycine level extracted from the skin of Atlantic salmon in a time course leading to smoltification and SW transfer. Plot A shows levels of glycine extracted from the skin of fish under normal production conditions. Plot B shows levels extracted from fish exposed to SW challenge at three points on the time course. Error bars represent standard error, n=6.	143
Figure 4.9. Mean creatine level extracted from the skin of Atlantic salmon in a time course leading to smoltification and SW transfer. Plot A shows levels of creatine extracted from the skin of fish under normal production conditions. Plot B shows levels extracted from fish exposed to SW challenge at three points on the time course. Error bars represent standard error, n=6.	144
Figure 4.10. Mean sum of combined organic osmolytes extracted from the skin of fish from nucleotide supplement feeding trial. The first time point, 5 weeks before SW transfer, represents baseline before feeding with experimental diets began. Error bars represent standard error.	146
Figure 4.11. Mean glucose level extracted from the skin of fish from nucleotide supplement feeding trial including arbitrary values for samples in which glucose was reported as undetected. The first time point, 5 weeks before SW transfer, represents baseline before feeding with experimental diets began. Error bars represent standard error. Bars without error bars represent groups in which two or fewer samples contained glucose.	148
Figure 4.12. Mean myoinositol level extracted from the skin of fish from nucleotide supplement feeding trial. The first time point, 5 weeks before SW transfer, represents baseline before feeding with experimental diets began. Error bars represent standard error.	149
Figure 4.13. Mean taurine level extracted from the skin of fish from nucleotide supplement feeding trial. The first time point, 5 weeks before SW transfer, represents baseline before feeding with experimental diets began. Error bars represent standard error.	150
Figure 4.14. Mean GPC level extracted from the skin of fish from nucleotide supplement feeding trial. The first time point, 5 weeks before SW transfer, represents baseline before feeding with experimental diets began. Error bars represent standard error.	151
Figure 4.15. Mean urea level extracted from the skin of fish from nucleotide supplement feeding trial including arbitrary values for samples in which urea was reported as undetected. The first time point, 5 weeks before SW transfer, represents baseline before feeding with experimental diets began. Error bars represent standard error.	153
Figure 4.16. Mean alanine level extracted from the skin of fish from nucleotide supplement feeding	154

trial. The first time point, 5 weeks before SW transfer, represents baseline before feeding with experimental diets began. Error bars represent standard error.	
Figure 4.17. Mean betaine level extracted from the skin of fish from nucleotide supplement feeding trial. The first time point, 5 weeks before SW transfer, represents baseline before feeding with experimental diets began. Error bars represent standard error.	155
Figure 4.18. Mean creatine level extracted from the skin of fish from nucleotide supplement feeding trial. The first time point, 5 weeks before SW transfer, represents baseline before feeding with experimental diets began. Error bars represent standard error.	156
Figure 4.19. Mean expression of CKA in the skin of Atlantic salmon at time points 24 hours before and 24 hours after SW transfer on all six diets on the nucleotide supplement feeding trial. Error bars represent standard error.	157
Figure 4.20. Structure of glucose molecule.	159
Figure 4.21. Structure of myo-inositol.	163
Figure 4.22. Structure of taurine showing equilibrium between charge neutral molecule and zwitterion.	165
Figure 4.23. Structure of glycerophosphocholine.	157
Figure 4.24. Structure of urea	169
Figure 4.25. The pathway of purine oxidation to urea.	170
Figure 4.26. The pathway of pyrimidine degradation.	171
Figure 4.27. Structure of alanine.	175
Figure 4.28. Structure of glycine	176
Figure 4.29. Factors influencing the intracellular amino acid pool.	177
Figure 4.30. Structure of glycine betaine.	179
Figure 4.31. Structure of creatine	182
Figure 5.1. Ion transport in the MRC of the teleost gill in seawater (SW). $\text{Na}^+\text{-K}^+\text{-ATPase}$ (NKA) actively transports $3\text{Na}^+$ into the ECF and $2\text{K}^+$ into the cell. $\text{Na}^+\text{-K}^+\text{-}2\text{Cl}^-$ -cotransporter (NKCC) imports $\text{Na}^+$ , $\text{K}^+$ and $2\text{Cl}^-$ into the cell from the ECF. $\text{Cl}^-$ leaves the cell through cystic fibrosis transmembrane conductance regulator (CFTR), and $\text{K}^+$ re-enters the ECF through $\text{K}^+$ channels. $\text{Na}^+$ leaves the body across leaky tight junctions between cells.	189
Figure 5.2. Mean expression of two $\text{Na}^+\text{-K}^+\text{-ATPase}$ $\alpha$ subunit paralogues relative to <i>RPLP0</i> in the gill of Atlantic salmon at various life stages ranging from parr to adult. Error bars represent standard error, n=6 in all groups except adult where n=3.	198
Figure 5.3. Mean expression of two $\text{Na}^+\text{-K}^+\text{-ATPase}$ $\alpha$ subunit paralogues relative to <i>RPLP0</i> in the gill of Atlantic salmon at various time points as fish progressed from parr to smolts and were transferred to SW. Error bars represent standard error, n=5 or 6.	200
Figure 5.4. Western blot showing $\text{Na}^+\text{-K}^+\text{-ATPase}$ $\alpha 1a$ levels in the gill of Atlantic salmon during development from parr to smolt. Time intervals (-68 d to +3 d) relate to the time of seawater transfer.	201
Figure 5.5. Quantification of western blot immunoreactive bands showing levels of three peptides detected using an antibody to salmon $\text{Na}^+\text{-K}^+\text{-ATPase}$ $\alpha 1a$ in the gill of Atlantic salmon during development from parr to smolt. Error bars indicate standard error, n=6.	202
Figure 5.6. Western blot showing $\text{Na}^+\text{-K}^+\text{-ATPase}$ $\alpha 1a$ levels in the gill of Atlantic salmon during development from parr to smolt. Time intervals (-68 d to +3 d) relate to the time of seawater transfer.	203
Figure 5.7. Quantification of western blot immunoreactive bands showing levels of three peptides detected using an antibody to salmon $\text{Na}^+\text{-K}^+\text{-ATPase}$ $\alpha 1a$ in the gill of Atlantic salmon during development from parr to smolt. Error bars indicate standard error, n=6.	204
Figure 5.8. Expression of $\text{Na}^+\text{-K}^+\text{-ATPase}$ $\beta 2a/b$ (A), $\text{Na}^+\text{-K}^+\text{-ATPase}$ $\beta 2c$ (B), $\text{Na}^+\text{-K}^+\text{-ATPase}$ $\beta 3b$ (C) and $\text{Na}^+\text{-K}^+\text{-ATPase}$ $\beta 4$ (d) mRNA relative to <i>RPLP0</i> in Atlantic salmon gill between 0 hours and 68 days post vaccination in FW. Error bars denote standard error (n=3).	205
Figure 5.9. Expression of $\text{Na}^+\text{-K}^+\text{-ATPase}$ $\beta 3c$ mRNA relative to <i>RPLP0</i> in Atlantic salmon gill between 0 hours and 68 days post vaccination in FW. Error bars denote standard error (n=3).	206
Figure 5.10. Expression of $\text{Na}^+\text{-K}^+\text{-}2\text{Cl}^-$ -cotransporter 1 ( <i>NKCC1</i> ) mRNA relative to <i>RPLP0</i> in Atlantic salmon gill on a FW time course (A) and in fish exposed to SW challenge (B). Error bars represent standard error (n=3 in A, n=5 or 6 in B).	207
Figure 5.11. Expression of <i>cystic fibrosis transmembrane conductance regulator</i> ( <i>CFTR</i> ) mRNA relative to <i>RPLP0</i> in Atlantic salmon gill on a FW time course (A) and in fish exposed to SW challenge (B). Error bars represent standard error (n=3 in A, n=5 or 6 in B).	208
Figure 5.12. Expression of $\text{Ca}^{2+}\text{-ATPase}$ mRNA relative to <i>RPLP0</i> in Atlantic salmon gill on a FW time course. Error bars represent standard error (n=3).	209
Figure 5.13. Expression of <i>LDL receptor</i> mRNA relative to <i>RPLP0</i> in Atlantic salmon gill on a FW time course. Error bars represent standard error (n=3).	210
Figure 5.14. Expression of <i>ApoA1</i> (A), <i>ApoA1b</i> (B), <i>ApoA4</i> (C) and <i>ApoB100</i> (D) mRNA relative to	211

<i>RPLP0</i> in Atlantic salmon gill between 0 hours and 68 days post vaccination in FW. Error bars denote standard error (n=3).	
Figure 5.15. Expression of <i>CPT2</i> mRNA relative to <i>RPLP0</i> in Atlantic salmon gill between 0 hours and 68 days post vaccination in FW. Error bars denote standard error (n=3).	212
Figure 5.16. Expression of <i>pIgR</i> mRNA relative to <i>RPLP0</i> in Atlantic salmon gill in fish exposed to SW challenge. Error bars represent standard error (n=5 or 6).	213
Figure 5.17. Expression of <i>pIgRL1</i> mRNA relative to <i>RPLP0</i> in Atlantic salmon gill on a FW time course (A) and in fish exposed to SW challenge (B). Error bars represent standard error (n=3 in A, n=5 or 6 in B).	214
Figure 5.18. Expression of <i>pIgRL2</i> mRNA relative to <i>RPLP0</i> in Atlantic salmon gill in fish exposed to SW challenge. Error bars represent standard error (n=5 or 6).	215
Figure 5.19. Expression of <i>CLM8</i> mRNA relative to <i>RPLP0</i> in Atlantic salmon gill in fish exposed to SW challenge. Error bars represent standard error (n=5 or 6).	216
Figure 5.20. Expression of <i>IgK</i> (A) and <i>IgD</i> (B) mRNA relative to <i>RPLP0</i> in Atlantic salmon gill on a FW time course. Error bars represent standard error (n=3).	217
Figure 5.21. Expression of <i>AHRT1</i> mRNA relative to <i>RPLP0</i> in Atlantic salmon gill in fish exposed to SW challenge. Error bars represent standard error (n=5 or 6).	218
Figure 5.22. Expression of <i>XBPI</i> mRNA relative to <i>RPLP0</i> in Atlantic salmon gill in fish exposed to SW challenge. Error bars represent standard error (n=5 or 6).	219
Figure 5.23. Expression of <i>LEI</i> mRNA relative to <i>RPLP0</i> in Atlantic salmon gill on a FW time course. Error bars represent standard error (n=3).	220
Figure 5.24. Expression of <i>Gelsolin</i> mRNA relative to <i>RPLP0</i> in Atlantic salmon gill on a FW time course. Error bars represent standard error (n=3).	221
Figure 5.25. Expression of <i>ZG16</i> mRNA relative to <i>RPLP0</i> in Atlantic salmon gill on a FW time course (A) and in fish exposed to SW challenge (B). Error bars represent standard error (n=3 in A, n=5 or 6 in B).	222
Figure 5.26. Expression of <i>TTP1</i> (A) and <i>TTP2</i> (B) mRNA relative to <i>RPLP0</i> in Atlantic salmon gill in fish exposed to SW challenge. Error bars represent standard error (n=5 or 6).	223
Figure 5.27. Expression of <i>AnnA1</i> (A), <i>AnnA2</i> (B), <i>AnnA3</i> (C) and <i>AnnA6b</i> (D) mRNA relative to <i>RPLP0</i> in Atlantic salmon gill on a FW time course. Error bars represent standard error (n=3).	224
Figure 5.28. Expression of <i>UP584</i> mRNA relative to <i>RPLP0</i> in Atlantic salmon gill on a FW time course. Error bars represent standard error (n=3).	226
Figure 6.1. Structure of hypoxanthine indicating atoms which act as hydrogen bond donors (HBD) and hydrogen bond acceptors (HBA).	249
Figure 6.2. The pathway of purine oxidation to urea.	258
Figure A1.1. Mean length (A) weight (B) condition factor (C) and Na <sup>+</sup> K <sup>+</sup> -ATPase enzyme activity (D) throughout the feeding trial time course. Error bars represent standard error (n=19 or 20).	I





# Introduction



# 1. Introduction

## *1.1 Global seafood production*

As the world population continues to grow, the demand for high quality protein for human consumption increases. This rising demand for food necessitates increasing output from all food producing sectors (Godfray *et al.*, 2010). Fish have historically been an important source of protein in the human diet, having been predominantly provided throughout history by capture fisheries (Ellis *et al.*, 2016). In 2014, on average fish made up 20% of the total animal protein consumed by the world's population, and up to 50% in some small coastal areas (Moffitt & Cajas-Cano, 2014; Smith *et al.*, 2010). Production from wild capture fisheries has plateaued since the 1970s, as the majority of fish stocks have in recent decades reached maximum sustainable yield, or crashed, due to intensification and increases mechanisation (FAO, 2016).

An example of stock decline is that of the North Sea cod (*Gadus morhua*) which has been declining continuously for the last four decades (Nicolas *et al.*, 2014). In previous decades fisheries management has been dictated by the results obtained from mathematical models, which assume a stable carrying capacity. However, as pressures on fish populations alter during this period of climate change, these models are no longer adequate to predict the influence of fishing on stocks (Arreguín-Sánchez *et al.*, 2015). It is now accepted that North Sea cod is an overfished stock, which has led to a dependence on recruitment to maintain sustainable breeding stock. Nicolas *et al.* (2014) found that the greatest driving factor in the most recent decline in cod recruitment was the spring sea surface temperature, which influences primary production and thus has knock-on effects on zooplankton populations, an important source of food for the larval stages of many fish species. As biotic and abiotic

pressures must now be taken into account in predicting the resilience of populations, successful modelling of the influence of exploitation pressure on fish stocks becomes more complex. Changes in ocean surface temperature influence levels of primary productivity in an ecosystem, and so the effects of climate change can negatively impact populations of exploited fish. Reductions in primary productivity can lead to reduced stock recruitment, making it essential to take into account the many different factors which affect the size and resilience of heavily exploited stocks. Furthermore, range shifts in the prey species of fish stocks can have a highly damaging effect on populations. As an example, the abundance of the copepod *Calanus finmarchicus* in the North Sea fell from 80% of the calanoid biomass in the 1960s to approximately 20% in the early 2000s as a result of increasing temperatures (Papworth *et al.*, 2016). In the North Sea *C. finmarchicus* exists at the upper limit of its thermal niche (Papworth *et al.*, 2016), thus, as sea temperatures have increased, the population of this species has shifted further north to access the deeper, cooler waters in the North Atlantic. This shift has major implications for a number of important fish stocks as this large copepod species plays an important role in the North Sea food web. North Sea cod are particularly heavily reliant on this lipid-rich species (Nicolas *et al.*, 2014). As changes in the world climate alter the seasonal temperature patterns in different regions of the planet it is essential to take into account the influence of asynchronies in ecosystems. Temperature changes influence the distribution and development of many species, which can lead to lags in the ecosystem. Changes in the timing of the peak production of a prey species can have deleterious effects on recruitment of populations: either through reduced larval survival, or through reduced female condition, leading to lower fecundity, reducing the number and quality of eggs and offspring produced. With so many confounding factors it is increasingly difficult to predict the effects of anthropogenic exploitation on stocks around the world.

It is currently not possible to increase production sustainably to provide fish for a growing population from wild caught fisheries (Godfray *et al.*, 2010; Smith *et al.*, 2010). Aquaculture production has been increasing since the mid-20<sup>th</sup> century, to increase the seafood available for the market, contributing 42% of all seafood produced in 2012 (FAO, 2014). As seafood currently provides on average 20% of the dietary animal protein consumed by almost half of the global human population, and almost 7% of the total dietary protein consumed worldwide, increased production to sustain a growing population is essential (FAO, 2016; Smith *et al.*, 2010). Further expansion of aquaculture will have a key role in ensuring food security in the future. Such expansion will require increases in efficiency as the sites and resources available for development are finite (Godfray *et al.*, 2010).

### *1.2 The expansion of the aquaculture industry*

While food from terrestrial sources has been cultivated for many thousands of years, and agriculture has outstripped hunting as the major method of food production on land, wild capture fisheries still provide approximately half of the food fish consumed by the world's population (FAO, 2016). Due to the high fishing pressures to which they are exposed, many wild fisheries have been greatly depleted in recent decades, and there has been a number of different attempts by governments to control fishing and reduce these pressures, as outlined by the FAO in the Code of Conduct for Responsible Fisheries (FAO, 2010; Tacon *et al.*, 2010). Therefore, the production from these systems is likely to decrease in coming years as stocks are allowed to recover. In contrast, production through aquaculture offers opportunities for further expansion.

In the past century there has been a rapid expansion of both domestic and industrial scale aquaculture production to provide fish for human consumption (FAO, 2016). In the early 1970s aquaculture provided only 7% of the fish produced globally for human consumption

(FAO, 2016). Production rose steadily throughout the following decades, and now a limited number of aquaculture species represent approximately 50% of the food-fish produced worldwide (FAO, 2016). For the first time, in 2014, the proportion of food-fish produced through aquaculture was higher than that produced from wild capture fisheries (FAO, 2016). These increases in production have overtaken the rate of world population growth, allowing the average annual *per capita* fish consumption to increase from approximately 10 kg in the 1960s to as much as 20 kg in 2015 (FAO, 2016). While the contribution to the diet in developing countries is lower, this has also increased over recent decades, providing a range of health benefits (FAO, 2016). Fish in the diet provides a variety of nutrients essential for growth and development, such as essential amino acids and long chain fatty acids vital for the development and maintenance of the nervous system, particularly in pregnancy and childhood (FAO, 2016; Li *et al.*, 2016). There is further potential, in developing countries where fish consumption is still low, for expansion of the industry, particularly in the production of non-fed species, which derive nutrition from their environment without a requirement for feed input from farmers (FAO, 2016; Moffitt & Cajas-Cano, 2014).

As well as providing an abundant and nutrient-rich food source, aquaculture production also benefits the economies of developing countries, as the aquaculture sector provides 33% of the jobs associated with food-fish production (FAO, 2016). A wide variety of different species are cultured around the world. Finfish production in ponds predominates in the developing world, with the bulk of production occurring in Asia (FAO, 2016). The vast majority of global finfish production is of freshwater species, with various species of carp, catfish and tilapia being commonly cultured in Asia and Africa. These species are typically herbivorous or omnivorous, thus occupy relatively low trophic levels, converting a higher proportion of their dietary intake to body mass than do carnivorous species (Tacon *et al.*, 2010). Conversely, in economically developed countries, aquaculture tends to focus on carnivorous

fish such as Atlantic salmon and rainbow trout, because of their high economic value (Tacon *et al.*, 2010). Such species, occupying a high trophic level, require a much more complex dietary input and convert their food less efficiently. The global trend now appears to be favouring the expansion of culture of species from higher trophic levels to improve financial returns, however, this practice is not sustainable while fed-fish aquaculture is reliant on external sources of feed (Ellis *et al.*, 2016; Tacon *et al.*, 2010). By culturing locally indigenous species, some problems associated with aquaculture, such as escapes of alien species, can be avoided (Tacon *et al.*, 2010). There can be other benefits. In China, the introduction of edible fish, such as the common carp (*Cyprinus carpio*) and grass carp (*Ctenopharyngodon idella*), to rice paddies has brought a range of benefits to local communities (Lane & Crosskey, 1993). These larvivorous fish species have been shown to reduce both the populations of malaria carrying *Anopheles* mosquitos and transmission of malaria in areas where they have been introduced (Wu *et al.*, 1991). Culturing these fish alongside rice also increased the level of protein in human diets, improving the health of the community. Furthermore, the carp consumed various plant pests as well as mosquito larvae, improving the yield of rice (Wu *et al.*, 1991). This is an example of a system in which aquaculture has brought both social and economic benefits to rural communities. The increased development of aquaponics systems, in which aquaculture and hydroponic systems are combined (Love *et al.*, 2015), allows food production in areas where space is limited, such as urban centres. In these systems the waste produced by fish is used to provide nutrients for crop plants, while the plants filter the recirculating water (Love *et al.*, 2015). In this way, aquaculture can benefit urban communities as well as those in rural areas.

### 1.3 Sustainability

While expansion of the aquaculture industry is desirable, it is essential to ensure that environmental concerns are taken into account, so that increased production does not come at an ecological cost. Godfray *et al.* (2010) advocate sustainable intensification, a process whereby yield is increased, while reducing the impacts of production on the environment. This is in line with the United Nations initiatives which aim to reduce the environmental impact of production systems, in order to conserve biodiversity and combat climate change (FAO, 2016). By measuring yields relative to costs in the form of resource inputs, such as feeds and space, and farming outputs such as emissions and effects on biodiversity, strategies can be found which allow yields to grow while environmental costs are reduced (Godfray *et al.*, 2010). In an aquaculture context, yields can be improved by an increase in feed conversion efficiency (the growth achieved per mass of feed) and in carnivorous species by reducing the ratio of fish-in to fish-out (FIFO), so that the input mass of wild caught fish required to produce an aquaculture species does not exceed the output (Ellis *et al.*, 2016). By improving these parameters, the overall production efficiency can be enhanced at current farm sites, reducing the need for more space to be turned over to farming. As feeds represent a very high economic cost to the industry, increased efficiency of feed conversion has economic benefits. Garnett *et al.* (2013) suggest that sustainable intensification should also take into account animal welfare, as well as the nutritional quality of the products and the impact of farming practices on rural economies. Expanding the use of aquaculture will allow the production of foods, which contain a variety of micronutrients, providing an essential part of a balanced human diet.

Treatment of diseases within stocks has welfare benefits for farmed fish as disease states are stressful, and tissue damage caused by diseases can cause osmoregulatory stress. However,

treatment protocols can also be problematic, often requiring fish to be confined within a small area, causing overcrowding stress. The drugs used to treat farmed stocks are costly and can pose health risks to the people working with them, and thus require safety procedures and protective clothing, which represent economic costs to the industry, and operatives in food production wearing chemical hazard suits can lead to problems in public relations. The use of drugs in the environment is also costly as inevitably some of these chemicals escape into the surrounding environment, with often unforeseen effects on wildlife. Preventative measures such as vaccination reduce the need for treatments; however, these still require handling of the fish, raising stress levels. Administering treatments through feed minimises handling and overcrowding stress, though this can lead to accumulation of drugs in the environment if too much is used. The use of non-drug health modulating feed ingredients is an alternative approach, which benefits fish welfare as well as reducing the impact of farm sites on their surrounding environment.

While attempting to ensure food security for the future, the different species farmed for seafood must be considered. Non-fed species are more sustainable as they gain nutrition from their environment (Ellis *et al.*, 2016). These non-fed species include seaweeds, filter feeders such as mussels and other bivalves, as well as some fish species such as the silver carp (FAO, 2016). In contrast fed species, including finfish such as the salmonids, rely on feeds produced either from products derived from wild fish populations, or terrestrial crops (FAO, 2014, 2016). The production of these feeds is costly as it requires significant resource input, either from highly exploited fish populations, or in the form of land, irrigation and fertilisers used in terrestrial farming. Nonetheless, in recent decades the increases in production of fed species has outstripped that of non-fed species (FAO, 2016). It is likely that the preferential increase in finfish production is driven by market pressures, as finfish are generally viewed as a luxury food, and are thus desirable in developed countries (Ellis *et al.*, 2016; FAO, 2014).

Some non-fed fish, such as tilapia species when included in the human diet, provide similar health benefits to those provided by salmonids and other finfish species. As these species do not require a large input of feeds, they represent a possible option for future sustainable aquaculture expansion (FAO, 2014).

#### *1.4 Increasing efficiency*

As the number of available new farm sites decreases, the growth of the aquaculture sector requires an increase in the efficiency of production at existing farm sites, allowing yields to increase without the requirement for new sites. The development of offshore aquaculture increases the opportunity for expansion, though this method of fish farming presents other challenges such as high initial investment, and reduced accessibility relative to inshore farms. Recirculating aquaculture systems (RAS) also provide an alternative to traditional inshore systems, however, like offshore aquaculture, RAS require a high level of initial investment. Both of these operating styles have their benefits. RAS has greatly reduced water use relative to flow through systems, while farming in the more dynamic environment of offshore waters, allows for the dispersal of organic waste, and avoids its accumulation on the benthos below sites. As these systems have not yet been widely established throughout the areas where the aquaculture industry is prevalent, improved efficiency in current systems is desirable.

As feeds represent the largest expense to the fed fish aquaculture industry, achieving increased efficiency by improving the digestibility of diets, and thereby improving the food conversion ratios achieved, would be greatly beneficial to the sector (Godfray *et al.*, 2010; Tacchi *et al.*, 2011). Efforts to improve the palatability and digestibility of diets are complicated by changes in feed formulation aimed at reducing pressure on natural populations of anchoveta species, which are heavily fished in the Pacific to supply fish for the production of fishmeal (FM) and fish oil (FO) routinely used in fish feeds. Currently, efforts

are being made to reduce and replace the FM and FO content of feeds that is derived from natural populations, to reduce both the environmental impact of the industry and the economic cost to farmers (Kiron, 2012; Tacon & Metian, 2008). As a result, dietary supplementation is of growing importance in the culture of many finfish species. Plant products, in the form of protein meals and concentrates, as well as vegetable oils, are being used to replace the traditional FM and FO ingredients in aquafeeds. However, the inclusion of these products in diets has presented challenges to the industry.

As plant products are increasingly used as the basis of aquafeeds, it is necessary to ensure that the nutritional quality of feeds is not reduced, and that optimal growth rates are maintained. Protein from plant sources, particularly in the form of cereal-based meals, can contain a number of different anti-nutritional factors (ANFs) which can have a negative effect on the health of the gastrointestinal tract (Król *et al.*, 2016; Tacchi *et al.*, 2012). These effects of ANFs are more pronounced in carnivorous fish as these species have not, in their evolutionary history, been exposed to plants and the associated ANFs in their diet (Król *et al.*, 2016). Krogdahl *et al.* (2003) found that the inclusion of soybean meal (SBM) in the diets of Atlantic salmon caused inflammation of the gastrointestinal tract, leading to enteritis, which reduced the absorptive ability of the intestine, ultimately reducing growth. Further they found that increasing inclusion levels of SBM in diets led to increased pathology within the intestine, giving a dose-dependent response, with diets containing higher levels on SBM causing greater pathology (Krogdahl *et al.*, 2003). The use of partially purified plant protein concentrates rather than meals can reduce the levels of pathology-causing ANFs in the diet, through further processing. However, the production of these concentrates requires increased resource inputs in terms of processing time and purification processes, and does not entirely remove ANFs from the protein source (Król *et al.*, 2016). A further problem associated with the use of plant proteins to replace fish meal relates to difference in amino acid composition,

with protein from plant sources lacking adequate levels of some amino acids, such as lysine and methionine, which are essential for fish growth (Gaylord *et al.*, 2007; Li *et al.*, 2009).

### *1.5 Atlantic salmon*

Atlantic salmon (*Salmo salar*) represent an economically important aquaculture species. Salmon production has increased dramatically since the establishment of the industry, from the 1 tonne produced in Norway in 1964, to world-wide production in eleven different countries in excess of 2 million tonnes in 2012 (Ellis *et al.*, 2016). Atlantic salmon production is the fastest growing food production system in the world. Salmon aquaculture has spread from Norway across the natural range of the species, the north Atlantic, and also to the north and south Pacific. Aquaculture production of salmon now greatly exceeds that of the wild fishery which has undergone a dramatic decline in recent decades, with catch falling from 4,106 tonnes in 1991 to 1,134 tonnes in 2014 (NASCO, 2014), thus aquaculture of this species is essential to meet the consumer demand (Ellis *et al.*, 2016). Since 2012 global annual production has continued to exceed 2 million tonnes. The North Atlantic area (NAA) produces approximately 1.45 million tonnes of this, with the majority in Norway and Scotland (ICES, 2016). It is estimated that production outside the NAA represented 23% of the total produced in 2015, predominantly from Chile (ICES, 2016). In recent years Chilean production has exceeded that of Scotland (Ellis *et al.*, 2016). The popularity of salmon, traditionally regarded as a luxury food, and more recently promoted as an excellent source of long chain  $\omega$ -3-unsaturated fatty acids, important for cardiovascular health, has led to increased demand. The resultant rapid expansion of the industry in the Northern hemisphere in recent years has led to further increases in production (Ellis *et al.*, 2016). However, as the availability of new sites suitable for farming has greatly declined, it is now necessary to

develop systems which will improve the efficiency of production without requiring an increase in the number or size of farms.

### *1.6 Importance of salmonids to Scottish economy*

Marine Scotland estimates that the aquaculture industry in Scotland contributes a value of £800 million to the Scottish economy, providing approximately 4800 jobs (Marine Scotland, 2014). The aquaculture industry forms an important part of Scottish Government plans for economic growth, with aims to reach production levels of 210,000 tonnes for finfish and 13,000 tonnes for shellfish by the year 2020 (Marine Scotland, 2015). Aquaculture in Scotland is dominated by the production of Atlantic salmon, with production reaching 179,022 tonnes in 2014, the highest level recorded, representing 80% of the total tonnage of finfish and shellfish produced by Scottish aquaculture (Marine Scotland, 2015; Munro & Wallace, 2015). Plans to increase the scale of the Scottish aquaculture industry largely relate to increases in the level of Atlantic salmon production as this species represents a valuable export (Marine Scotland, 2015; Scottish Government, 2011). In the year 2014 the salmonid aquaculture industry in Scotland employed 1,747 people in production, 1,634 of these working in the production of Atlantic salmon, and the remaining 113 in the production of rainbow and brown trout (Munro & Wallace, 2015). Further, it was estimated that in 2013 approximately 3,960 jobs were provided across Scotland, in both production and processing, by companies associated with the Scottish Salmon Producers' Organisation (SSPO); more than three quarters of these in the Highlands and Islands (SSPO, 2013). The Scottish salmon aquaculture industry is an important employer in the north west of Scotland, greatly contributing to the economies of the rural communities in the Highlands and Islands (SSPO, 2013). If the growth targets for the sector for 2020 are met it is estimated that the Scottish aquaculture industry will provide 8,000 jobs in the country, an increase of 3,200 on the

current estimate of 4,800 working in finfish and shellfish culture, contributing approximately £2 billion to the Scottish economy (Marine Scotland, 2014).

### *1.7 Salmon life cycle*

A complicating factor in the production of Atlantic salmon is the natural anadromous lifecycle of this species, beginning life in freshwater, before migrating downriver to seawater where they grow to full size (Figure 1.1). Returning salmon spawn in the autumn months, depositing eggs in redds (nests dug by females) in gravel river-beds. Eggs then remain on the river-bed until the following spring, when they hatch as alevins, which remain in the gravel, gaining nutrition from their yolk sac. Later the fish emerge from the gravel as fry and commence feeding. The fish are known as parr after their first year of life. Following a period of one to seven years, depending on latitude (NASCO, n.d.), the parr undergo the parr-smolt transformation which prepares them for entry to seawater, and migrate downriver to seawater in the spring. After one or more years at sea, during which the largest growth phase occurs, salmon migrate back to their natal rivers to spawn (Marine Scotland, n.d.). The majority of adults die after spawning.

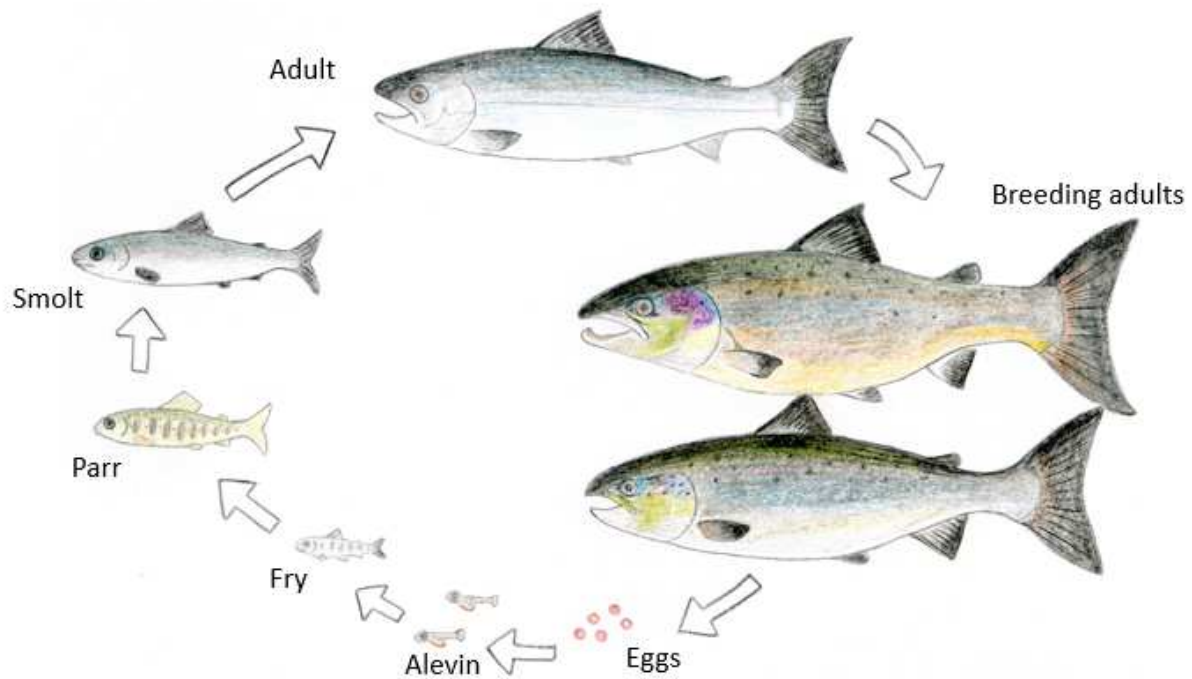


Figure 1.1. The salmon life cycle. Illustration by Claire Dagen.

This complex life history strategy requires the aquacultured fish to be transferred from freshwater to seawater at a stage of their development where natural physiological adaptations in key osmoregulatory tissues allow the fish to successfully acclimate to the higher salinities found in seawater. The physiological and morphological changes that take place during a period known as “smoltification” allow juvenile freshwater parr to develop into seawater migratory smolts.

### *1.8 Salmon Parr-Smolt Transformation*

The life cycle of *Salmo salar* is anadromous, beginning in freshwater, with the major growth phase of the fish occurring in seawater. This euryhaline life cycle requires individuals to adapt to the challenges of two vastly different environments. In order to cope with the transition, salmon undergo a number of physiological, morphological, and behavioural

changes, during a process known as the parr-smolt transformation. Smolting is a developmental phenomenon and fish must attain a certain size before they will respond to environmental cues to smolt (Metcalf, 1998). During this process juvenile fish lose their parr markings, undergoing the process of silvering as guanine and hypoxanthine crystals are deposited in the skin and scales (Figure 1.2), providing cryptic coloration suitable for life in the marine environment (Hoar, 1988; McCormick *et al.*, 1998). In preparation for active swimming at sea, the body shape of the salmon is altered, with an elongation of the body making the animal more streamlined for a pelagic lifestyle (McCormick *et al.*, 1998). Other physiological adaptations include changes in the pigments of the retina, shifting from porphyropsin to rhodopsin commonly found in marine fish (Alexander *et al.*, 1994). These changes are mediated by the action of thyroid hormones (Björnsson *et al.*, 2011).

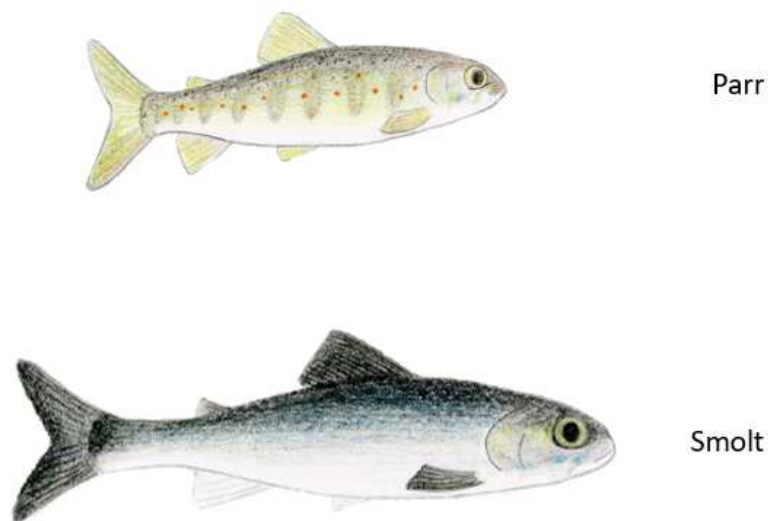


Figure 1.2. Parr-smolt transformation. Illustration by Claire Dagen.

Behavioural changes form an important part of the smoltification process. As parr, salmon exhibit territorial behaviour as they defend food sources in resource-poor rivers; they exhibit rheotaxis, orientating themselves to face upriver to maintain their position in rivers and

streams; low swim bladder volumes also aid in the maintenance of position in river systems (McCormick *et al.*, 1998; Stefansson *et al.*, 2008). In contrast, as smolts salmon show reduced territorial behaviour, forming schools, which are thought to reduce the risk of predation during the seaward migration (McCormick *et al.*, 1998). A combination of increased negative rheotaxis and more highly inflated swim bladders, increase buoyancy and aid fish in their journey towards the sea and the adopted pelagic lifestyle in the marine environment (McCormick *et al.*, 1998). Smolts also show an increased preference for more saline waters (McCormick *et al.*, 1998). It is thought that the urge for downstream migration is dependent on increases in blood levels of the thyroid hormones, thyroxine (T4) and triiodothyronine (T3) which occur during smoltification, although these increases are not dependent on an increase in circulating levels of thyroid stimulating hormone (TSH) (Björnsson *et al.*, 2011).

Perhaps the best-studied aspect of the smolting process is that of the osmoregulatory adaptations made as fish move from freshwater to seawater environments. When in freshwater, fish are exposed to an environmental osmolality of  $< 5$  mOsm/kg, however, in seawater they are faced with salinities of approximately 1000 mOsm/kg. The consequences of the change in environmental salinity are discussed in more detail below (see section 1.9) however, a number of physiological and morphological adaptations in key osmoregulatory tissues are essential if the fish are to survive and grow following migration to a hyperosmotic environment. Many of these adaptations take place in the gill, with a reversal of the role of the mitochondria-rich ionocytes from conserving ions in freshwater to excreting ions in seawater (Stefansson *et al.*, 2008). Another aspect of the hyperosmotic adaptations which occur during smoltification is the changes seen in the intestine, which becomes a major conduit for the absorption of water following the initiation of drinking (Björnsson *et al.*,

2011; Stefansson *et al.*, 2008). These physiological changes are initiated, at least in part, by elevated levels of growth hormone (GH) and cortisol (Björnsson *et al.*, 2011).

The combination of these physiological and behavioural changes create a physiological “smolt window” during which smolts are likely to move down rivers and survive the transition to seawater (McCormick *et al.*, 1998). The synchronisation of these changes, mediated by changes in photoperiod and temperature, ensures that this physiological smolt window coincides with the environmental conditions most suited for survival following seawater entry, or the “ecological smolt window” (Björnsson *et al.*, 2011; McCormick *et al.*, 1998). If smolts are held in freshwater, either trapped behind dams in the wild, or in an artificial setting, they undergo a process of “desmolting” whereby they lose a number of the traits developed during smoltification, such as their increased salinity tolerance and migratory urge (McCormick *et al.*, 1998; Stefansson *et al.*, 2008). This process occurs more rapidly at higher water temperatures (Duston *et al.*, 1991; McCormick *et al.*, 1999, 1998), and so in warmer years the “smolt window” is likely to be shorter, posing problems for both wild stocks and the aquaculture industry. Logistical problems associated with the transport of smolts from freshwater to seawater facilities can cause problems for the aquaculture industry as they can lead to transfer occurring outwith the physiological smolt window.

In the wild, salmon undergo the parr-smolt transformation in the spring, the change being triggered by increases in day length and temperature (McCormick *et al.*, 1998; Stefansson *et al.*, 2008). To increase production, the salmon aquaculture industry has developed methods to produce smolts year-round. By manipulating the photoperiod and water temperature during rearing, smolting can be triggered at different times of the year (Handeland & Stefansson, 2001; Johansson *et al.*, 2016). Fish are graded as parr by size and subjected to different rearing regimens to trigger smolting at different times, allowing the production of

“off-season” smolts (Handeland & Stefansson, 2001). Larger fish are usually selected for smolting at an early age, less than 12 months; the majority of farmed fish go to sea between 12-18 months, although fish are also put to sea at 19-24 months, and particularly slow growing fish can be put to sea after 24 months (Ellis *et al.*, 2016). By first exposing fish to extended day length, increased growth rates can be achieved in parr, however, exposure to photoperiod regimes simulating naturally increasing daylight is required for smolting to occur (Handeland & Stefansson, 2001).

Smolting and transfer to seawater represent a major bottleneck in the production of Atlantic salmon. At this life stage, the stress of altering osmoregulatory processes creates a period when salmon are vulnerable to infectious diseases (Johansson *et al.*, 2016). The condition factor, the relationship between length and weight, is used to assess the health of fish. During smoltification the condition factor decreases, largely due to the elongation of the body as fish become more streamlined (Stefansson *et al.*, 2008). This does not appear to increase susceptibility to disease in wild fish, however, morbidity and mortality are increased in farmed fish following seawater transfer (Stefansson *et al.*, 2008). This could be in part due to difficulties associated with transfer outwith the smolt window and selective breeding for rapid growth, which may lead to loss of traits which are protective in the wild population. Osmoregulatory stress can cause cellular damage, as well as being very energy expensive for an organism (Bourque, 2008). Unlike Atlantic salmon in the wild, farmed salmon cannot gradually acclimatise to increased salinity by pausing their migration in brackish estuarine waters, but must instead rapidly adapt to high salinities, either directly into 100% seawater or at least > 50% seawater, with transfers often mediated through stress-inducing pipe systems. This stress has been shown to cause a reduction in growth which can be observed up to 6 months after transfer (Alne *et al.*, 2011). In the wild, following more natural migration to the marine environment, smolts generally do not suffer significant ionic disturbance with the

consequent reduction in appetite or increased susceptibility to disease (McCormick *et al.*, 1998). However, farmed fish are unable to select their time of transfer to coincide with the time that they are most fit to migrate to seawater. The majority of deaths in farmed salmon smolts occur during the first 6 months following transfer (Ellis *et al.*, 2016). Increased mortality is likely to be due to immune suppression caused by increases in plasma stress hormones, including cortisol, mediated by the stress of transfer (Niklasson *et al.*, 2014).

Traditionally, the distinction between parr and smolt was determined purely based on the appearance of the fish, with the disappearance of parr markings and the development of silvering taken as a sign of smoltification (McCormick & Saunders, 1987). However, under intensive culture conditions, these morphological changes can become uncoupled from the other physiological changes which have an important role in ensuring smolt survival in seawater (McCormick & Saunders, 1987). Thus, it is essential to determine whether smolts have developed the ability to hypo-osmoregulate before they are transferred to seawater.

One of the major physiological changes undergone by salmon during smoltification is the change in branchial mitochondria rich cell function from ion conserving to ion excreting (Stefansson *et al.*, 2008). This change enables fish to osmoregulate in the marine environment. In the gill the activity of the enzyme  $\text{Na}^+\text{-K}^+\text{-ATPase}$  (NKA) increases, as do the functions associated with the  $\text{Na}^+\text{-K}^+\text{-Cl}^-$ -cotransporter (NKCC) and the chloride channel known as the cystic fibrosis transmembrane conductance regulator (CFTR) (Nilsen *et al.*, 2007). The increased activity of NKA in the gill has long been used as a biomarker of smoltification both in research and the aquaculture industry. A number of studies have shown that the increase in the activity of this ion transporter is tied to the photoperiod cues which trigger smoltification in Atlantic salmon (Björnsson *et al.*, 2011; Stefansson *et al.*, 2007).

The preparedness of smolts for seawater transfer is tested in the industrial setting by subjecting smolts to seawater challenge. Fish are transferred from freshwater directly to seawater. Following seawater challenge, the level of Cl<sup>-</sup> in the blood is measured, as this gives an indication of hypo-osmoregulatory ability. During the period of the parr-smolt transformation, gill samples are tested for NKA activity using methods such as that developed by McCormick (1993). However, Zydlewski & Zydlewski (2012) have shown that NKA activity in smolts did not predict the long term fitness of fish in seawater.

During smoltification there is also a switch in the type of  $\alpha$ -subunit paralogues of NKA expressed in the gill, with mRNA expression of  $\alpha$ 1a decreasing as fish smoltify, while  $\alpha$ 1b expression increases. The  $\alpha$ -subunit of NKA contains the active site of the enzyme (Nilsen *et al.*, 2007). It is possible that this change could be used as a sign of smoltification if a reliable test were developed. As smoltification is a complex process, involving many different aspects of the fish's physiology (Stefansson *et al.*, 2008), it is likely that there will be a suite of different changes in the molecular biology of the cell which could be used as a biomarker of smoltification. The development of more reliable biomarkers would be beneficial to the salmon aquaculture industry, as fish transferred to seawater during the "smolt window" are far more likely to grow successfully in seawater.

### *1.9 Osmoregulation*

All euryhaline species are faced with the challenge of maintaining body electrolyte homeostasis in the face of osmotic perturbations from their diet and more so, at certain times, from changes in the salinity of the environment. The osmolality of the intracellular fluid (ICF) is influenced by the osmolality of the extracellular fluid (ECF), and alterations to cellular osmolality can influence the function and activity of biologically important molecules such as proteins and nucleic acids (Bourque, 2008). The semi-permeable nature of

the cell membrane, allowing the movement of water and certain solutes into and out of the cell, allows changes in the osmolality of the ECF to directly influence cell volume and cell solute composition (Kultz, 2012). Osmotic perturbations, such as changes in osmolality and solute composition in the extracellular fluid and cytosol, may alter the structure and function of cellular proteins, in turn altering metabolism within the cell, causing osmotic stress (Kultz, 2012; Parsegian *et al.*, 1995; Seale *et al.*, 2012). Such effects on macromolecules can occur as a result of increases in the concentration of intracellular inorganic ions, often caused by the dehydration created by an excessively hypertonic extracellular environment (Kultz, 2012). Cell function can be further perturbed by osmotic stress through alteration of the concentrations of molecular messengers such as hormones, cytokines and reactive oxygen species, altering and sometimes impeding cell communication (Pasantés-Morales *et al.*, 2006; Sauer *et al.*, 2001). Due to the importance of osmotic balance, a large proportion of an organism's energy budget is invested in the maintenance of osmotic homeostasis (Edwards, 1982; Kidder *et al.*, 2006; Kostecki, 1982; Seale *et al.*, 2012).

### *1.10 Osmoregulation in stenohaline fish*

While some marine teleost species are osmo-conformers, maintaining cellular osmolality equivalent to that of their environment, for many animals living in aquatic habitats, their survival is dependent on the maintenance of their internal body fluids at a different osmolality from that of the surrounding environment (Al-Jandal & Wilson, 2011; Bourque, 2008). As all species living in aqueous environments are involved in direct exchange of fluids and gases with their environments (Fiol & Kultz, 2007), especially across the highly vascularised gills, fish and other aquatic animals are faced with a trade-off between the need for respiratory gas exchange and difficulties in maintaining ionic balance and osmotic homeostasis (Evans *et al.*, 1999; Evans, 2010). Due to the different challenges faced by animals living in different

aquatic environments, the majority of aquatic species including teleost fish, are stenohaline organisms, expressing specialised features which allow survival in only freshwater (FW) or seawater (SW). Teleosts living in freshwater must maintain their internal fluids at concentrations hypertonic to that of their surroundings, this involves the active uptake of ions across the gills to counter the effects of diffusive loss of ions, and high glomerular filtration rates in the kidney to allow for the excretion of water which passively enters the fish through the permeable gill tissue (Figure 1.3).

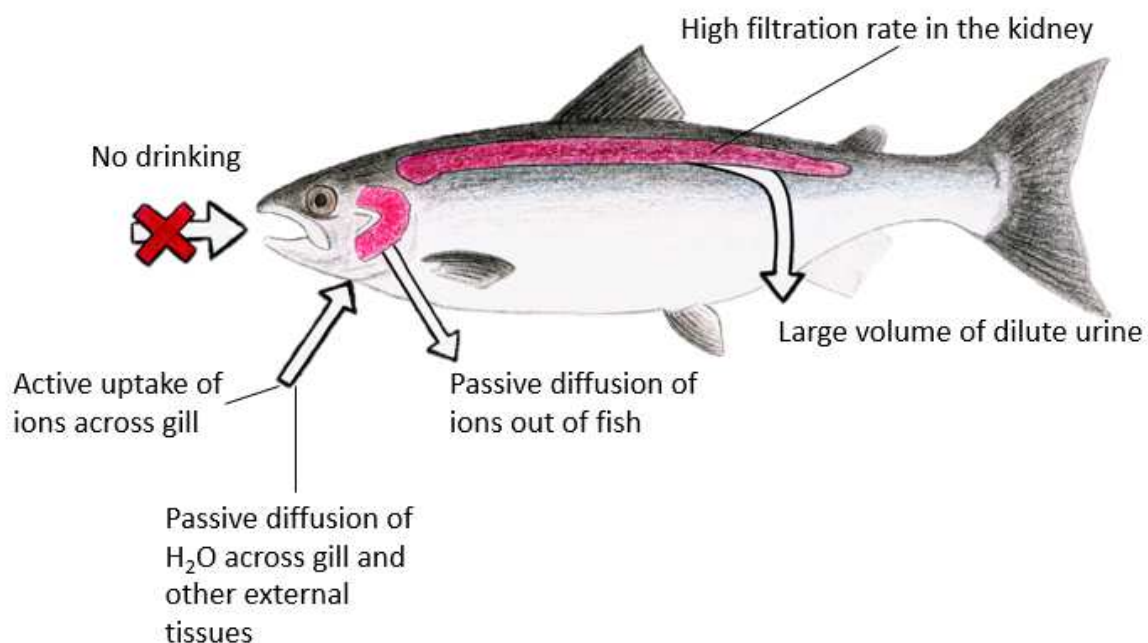


Figure 1.3. Illustration of Atlantic salmon showing gill and kidney representing the osmoregulatory processes in fish living in freshwater. Diffusion perturbs osmotic balance. Gill and kidney act to maintain homeostasis. Illustration by Claire Dagen.

Surviving the marine environment requires a different set of evolutionary adaptations in the osmoregulatory tissues. In marine teleosts, the body fluids are maintained hypotonic to that of the environment. As a consequence, the fish loses water to, and gains ions from, the environment by passive diffusion across permeable body surfaces (mainly the gill). To maintain body fluid volume the fish excretes only a small volume of isotonic urine and has to

drink the seawater to recover water lost by osmosis. As a result of drinking, the fish gastrointestinal tract is directly exposed to the high salinity of the external environment, and thus this tissue has an important osmoregulatory function, (Lavery & Skadhauge, 2012; Taylor & Grosell, 2006). After desalination of the imbibed seawater in the upper reaches of the gastro-intestinal tract, water can then be osmotically recovered from the intestinal lumen to maintain extracellular fluid volume and blood pressure (Marshall, 2013). The absorbed ions are actively excreted by the gills to prevent excessive increases in plasma osmolality. These processes are summarised in Figure 1.4.

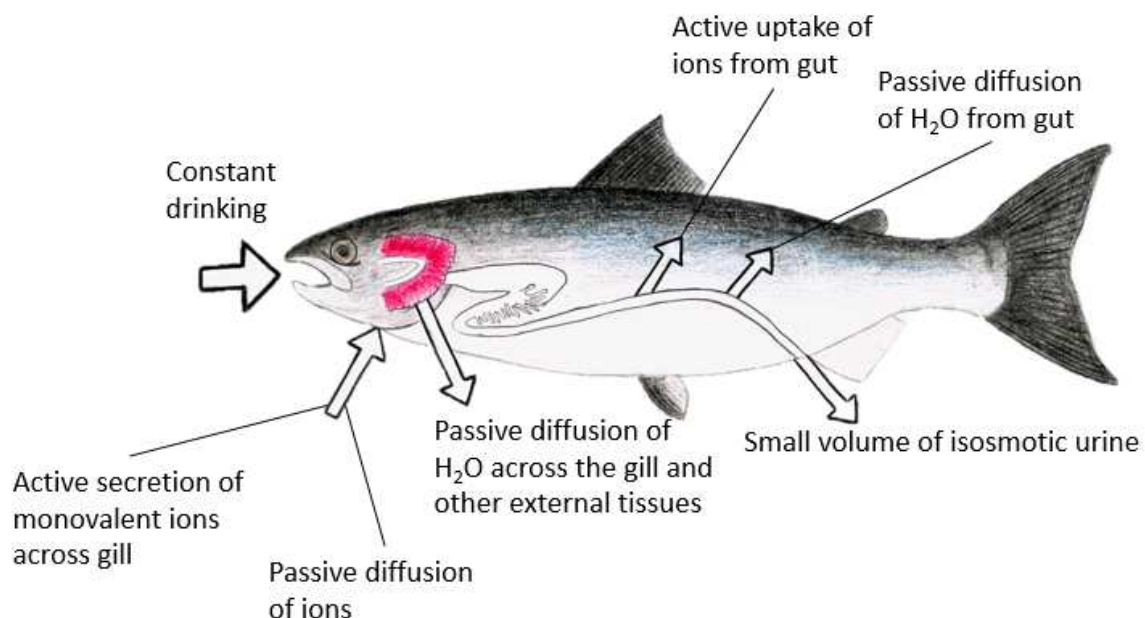


Figure 1.4. Illustration of Atlantic salmon showing gill and digestive tract representing the osmoregulatory processes in fish living in seawater. Diffusion perturbs osmotic balance. Gill and digestive tract act to maintain homeostasis. Illustration by Claire Dagen.

Unlike in mammals, where the kidneys are the main organ of osmoregulation, in fish a number of organs are equally involved in the maintenance of osmotic balance (Nishimura & Fan, 2003). The importance of the gills in osmoregulation in both FW- and SW-adapted fish has long been studied, with a great deal of focus on the NKA, as the action of this enzyme is

vitaly important to the maintenance of physiologically optimal ionic concentrations of both the intracellular and extracellular fluids (Evans *et al.*, 1999; Handeland & Stefansson, 2002; Le Bras *et al.*, 2011; Robertson & McCormick, 2012). Other ion transporters such as the  $\text{Na}^+/\text{Cl}^-$  and  $\text{Na}^+/\text{K}^+/\text{Cl}^-$  -cotransporters,  $\text{Na}^+/\text{H}^+$ -exchangers,  $\text{H}^+$ -ATPase and chloride ion channels also play vital roles in the maintenance of ionic balance in both FW and SW (Bystriansky & Schulte, 2011; Pan *et al.*, 2004; Pelis *et al.*, 2001). Cells which express high levels of these ion transport systems are often known as ionocytes, with those located in the branchial epithelium called mitochondria-rich cells (MRCs); previously known as chloride cells (Hiroi & McCormick, 2012). In the gill, these cells can be involved in either uptake or excretion of monovalent ions, as the ion requirements of an organism differ between freshwater and seawater environments (Scott & Brix, 2013). Although the kidneys do play a key role in the excretion of water in freshwater-adapted fish, their function is perhaps more limited in species inhabiting the marine environment where their main osmoregulatory role is in the excretion of small amounts of divalent ions in limited volumes of water (Hiroi & McCormick, 2012; McCormick, 2009).

### *1.11 Osmoregulation in Euryhaline fish*

Euryhaline fish can encounter and successfully adapt to wide range of environmental salinities (Kidder *et al.*, 2006). Some species, such as tilapia (*Oreochromis mossambicus*) and killifish (*Fundulus heteroclitus*) live in coastal environments with constantly varying salinities and can survive in hypersaline environments, such as salt lakes, marshes and lagoons where salinities of up to four times greater than that of sea water are experienced (Fiess *et al.*, 2007; Laverty & Skadhauge, 2012). These species can also adapt to repeated changes in salinity, such as in estuaries with the tidal cycle every 12 hours. True euryhaline species can tolerate direct transfer from FW to SW and from SW to FW at all life stages,

unlike diadromous species which usually only survive such transfers at specific life stages (Marshall, 2012). Euryhaline fish require epithelia with the ability to absorb and excrete ions. Organic osmolytes play a vital role in the osmoregulatory ability of euryhaline fish, enabling them to survive in their highly fluctuating environment.

Anadromous and catadromous fish species migrate between hypo-osmotic and hyper-osmotic environments only occasionally at specific periods of their life cycle that are often associated with reproduction. At these critical life stages fish undergo various physiological and anatomical transformations that are required for developmental maturation and salinity acclimation (Pan *et al.*, 2004). Such physiological changes allow species such as Atlantic salmon (*S. salar*) and the European eel (*Anguilla anguilla*) to utilise environments of different salinities. The catadromous European eel spawns in SW. Larvae are passively transported to coastal waters, fish then enter estuaries as “glass eels”, and mature as “yellow eels” in FW where they may grow for up to 20 years, before migrating to the Sargasso Sea to reproduce as “silver eels” (Zydlewski & Wilkie, 2012). This situation is reversed in anadromous fish, such as the Atlantic salmon. Salmon begin life in FW where they remain until reaching a particular size threshold, of approximately 10 cm, as parr, before undergoing the parr-smolt transformation which prepares them for a migration to SW where they feed for a variable number of years before famously returning to their natal streams to spawn (Zydlewski & Wilkie, 2012).

### *1.12 Organic osmolytes*

Organic osmolyte levels increase in almost all cell types experiencing hyperosmotic stress (Burg & Ferraris, 2008; Yancey *et al.*, 1982). As an initial response to hypertonic conditions and to avoid cell shrinkage, cells accumulate inorganic ions, which causes the retention of water, thus maintaining cell volume. However, the intracellular accumulation of elevated

concentrations of inorganic ions has deleterious effects as this can cause damage to protein structure and function (Burg & Ferraris, 2008). Therefore, following their initial influx the elevated inorganic ions are gradually replaced by various organic osmolytes, which are more compatible with the maintenance of protein function (Yancey *et al.*, 1982). As well as acting as compatible solutes, another protective mechanism provided by organic osmolytes is the stabilisation of protein structure (Burg & Ferraris, 2008; Yancey *et al.*, 1982).

An important example of the role of organic osmolyte systems is that seen in the mammalian renal medulla. The cells of this tissue are exposed to chronically high levels of NaCl and urea due to their function in the production of concentrated urine (Burg *et al.*, 2007). As a result, cells of the renal medulla must adapt to chronic hypertonicity. A number of different compatible organic osmolytes can be accumulated in this tissue to allow the maintenance of ion gradients that are essential to cell function under hypertonic conditions. Increased transcription of the enzyme aldol reductase, mediated by hypertonicity, results in increased cellular levels of sorbitol (Burg *et al.*, 2007). The expression of the enzymes responsible for the synthesis of glycerophosphocholine (GPC) and phosphocholine, its precursor, are also upregulated by hypertonic conditions (Burg *et al.*, 2007; Gallazzini *et al.*, 2006). The transcription of the enzyme involved in the breakdown of GPC is downregulated by hypertonicity, leading to further concentration of this osmolyte within the tissue (Burg *et al.*, 2007). The transcription of the transporters for the organic osmolytes betaine, inositol and taurine is upregulated by increased intracellular NaCl concentrations (Burg *et al.*, 2007). These osmolytes are accumulated by increased transport into the cell rather than by increased synthesis. The uptake of many of these organic osmolytes is mediated by sodium- and proton-dependent transporters driven by transmembrane ion gradients (Burg *et al.*, 2007). The mechanisms for the concentration of all of the above osmolytes are controlled by the same transcription factor, tonicity-responsive enhancer binding protein (TonEBP), which is

sensitive to osmotic changes (Burg *et al.*, 2007; Gallazzini *et al.*, 2006). Thus, it is possible for one compatible osmolyte to replace another while maintaining osmoprotection of cells (Burg *et al.*, 2007), an example of this is the increased degradation of GPC when intracellular concentrations of inositol and betaine are increased (Burg, 1996).

TonEBP is a transcription factor found in the renal tissues of mammals involved in the response to hypertonicity, and homologues have been found in the genomes of a number of fish species (Fiol & Kültz, 2007). There is relatively little known about TonEBP in fish (López-Bojórquez *et al.*, 2007), however, in mammalian renal tissue this transcription factor has been well studied. Genes targeted by TonEBP all contain one or more DNA consensus motifs known as a tonicity-responsive enhancer or an osmotic response element (Burg *et al.*, 2007). As well as influencing many genes involved in the accumulation of organic osmolytes as detailed above, TonEBP is known to increase the transcription of water channels and urea transporter genes, both important in concentrating urine in mammals, and expression of heat shock proteins which stabilise proteins in the presence of high inorganic ion concentrations (Burg *et al.*, 2007; Hasler *et al.*, 2006; Nakayama *et al.*, 2000; Woo *et al.*, 2002).

In recent years the osmotic stress transcription factor 1 (Ostf1) was identified in fish (Fiol & Kültz, 2005). Ostf1 is specifically induced by osmotic stress, and is not influenced by either heat shock or oxidative stress (Fiol & Kültz, 2005). Ostf1 is upregulated within a few hours of the onset of hyperosmotic stress (Fiol & Kültz, 2005). This fast responding transcription factor is sensitive to osmotic changes and the presence of cortisol, an important hormone in salinity acclimation (McGuire *et al.*, 2010). Ostf1 is believed to influence the expression of ion transporters and water channels in the gill (Tse, 2014). Ostf1 has also been implicated in remodelling of the cytoskeleton, and as an important gene during development in the model

species *Danio rerio* (Tse, 2014). Much further research is required to determine the full suite of roles played by this transcription factor.

Compatible organic osmolytes play an essential role in cells exposed to hypertonic conditions for chronic periods, such as in the kidney of mammalian species, and in the external tissues of animals living in the marine environment. The accumulation of these molecules under certain conditions or at key life stages plays a vital role in the survival of euryhaline fish species.

### *1.13 Functional feeds*

Now that the amino acids essential for growth in farmed fish (primarily lysine and methionine) have been identified and are routinely added to plant based feeds (He *et al.*, 2013; Nunes *et al.*, 2014; Sveier *et al.*, 2001), there has been increased interest in the development of “functional feeds” which may increase the overall quality of fish by improving health and welfare (Kiron, 2012; Tacchi *et al.*, 2011). The need for “functional” additives may be increased by the introduction of plant protein concentrates into aquafeeds, which, while reducing the difficulties caused by ANFs in plant meals, may contain lower levels of many of the other macromolecules present in less processed forms of biological matter. These include nucleic acids, which can be removed during the processing of protein sources due to their solubility in the aqueous alcohol used in the purification process (Berk, 1992). These feeds aim to replace substances, often present in fishmeal, beyond those required for basic nutrition, which may have beneficial effects on fish growth, health and welfare that have yet to be elucidated (Oliva-Teles, 2012; Tacchi *et al.*, 2011). The development of functional feeds also allows the production of specialised diets targeted for the needs of specific life stages of a species (Tacchi *et al.*, 2011). Diets can also be

formulated to aid in the immune response and reduce the risk of fish developing a variety of pathologies at vulnerable periods in the production cycle (Tacchi *et al.*, 2011).

In the past decade there has been an increase in scientific interest in the development of functional feeds, or immunonutrition, aiming to use dietary formulations to influence fish immune function and stress tolerance (Kiron, 2012). The United Nations' body, the Food and Agriculture Organisation (FAO) has produced a list of topics it considers to be important for further research to aid the sustainable expansion of the aquaculture industry (Subasinghe, 1997), these are:

1. "The role of good nutrition in improving aquatic animal health"
2. "Harnessing the host's specific and non-specific defence mechanisms in controlling aquatic disease"
3. "Use of immunostimulants and non-specific immune enhancers to reduce susceptibility to disease"
4. "Use of probiotics and bioaugmentation for the improvement of aquatic environmental quality"
5. "To reduce the use of chemicals and drugs in aquaculture"

Functional feeds have already been produced containing probiotics, live microorganisms, many of which have been shown to improve overall fish health by influencing the gut microbiota and thereby increasing the efficiency of feed conversion (Balcázar *et al.*, 2006; Merrifield *et al.*, 2010; Tacchi *et al.*, 2011). Merrifield *et al.* (2010) found that inclusion of two strains of *Bacillus* spp. (*B. subtilis* and *B. licheniformis*) alongside *Enterococcus faecium* in feeds for rainbow trout (*Oncorhynchus mykiss*) led to elevated levels of these species occurring in the intestinal mucosa of the posterior intestine, suggesting that these organisms successfully colonised the gut. Increased feed conversion ratios were observed with these

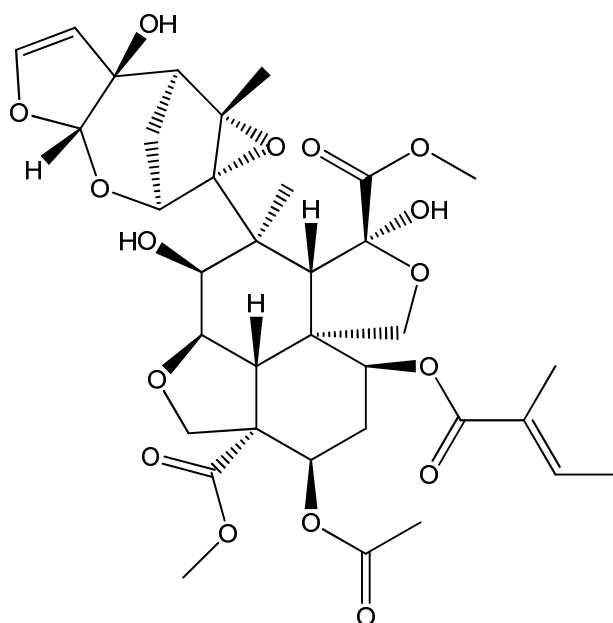
probiotics (Merrifield *et al.*, 2010). Probiotics have also been shown to have a beneficial impact on the fish immune system (Nayak, 2010). Sakai *et al.* (1995) found that *Clostridium butyricum* delivered orally to rainbow trout promoted the phagocytic activity of leukocytes, increasing resistance to vibriosis. One difficulty associated with the use of probiotics relates to the optimal growth conditions for probiotic organisms. The majority of aquaculture settings are subject to environmental change, such as seasonal temperature changes, and as a result the beneficial effects of probiotic supplements can be undermined by changes in the culture environment (Gonçalves & Gallardo-Escárate, 2017). A variety of other additives have been used in feeds including prebiotics, immunostimulants, vitamins, and nucleotides, all of which are reported to potentiate fish health and welfare (Burrells *et al.*, 2001a; Sakai, 1999). These can be used in combination to give optimal results (Tacchi *et al.*, 2011).

Prebiotics are defined as non-digestible ingredients in feeds which benefit the host by selectively benefiting populations of health-promoting bacteria (Gibson & Roberfroid, 1995; Merrifield *et al.*, 2010). These generally take the form of oligosaccharides (Merrifield *et al.*, 2010). Staykov *et al.* (2007) found that the addition of the plant mannose containing polysaccharide, mannan, to commercial diets fed to rainbow trout resulted in significantly higher body mass, relative to fish fed a control diet. They also found that a number of immune status indicators were increased by the addition of this prebiotic (Staykov *et al.*, 2007).

Immunostimulants are defined as naturally occurring compounds which increase host disease resistance by modulating the host's immune system (Bricknell & Dalmo, 2005; Ringø *et al.*, 2011). The polysaccharides found in the cell walls of fungal and bacterial cell walls, known as  $\beta$ -glucans, are commonly used as immunostimulants in aquaculture feeds (Wang *et al.*, 2017). These act on pattern recognition receptors, stimulating the immune system (Bricknell

& Dalmo, 2005; Wang *et al.*, 2017). Chansue *et al.* (2000) found that feeding tilapia (*Oreochromis niloticus*)  $\beta$ -1,3-glucan led to increased production of a number of different immune-related proteins, including cytokines, interleukins and tumour necrosis factor  $\alpha$ . Administration of  $\beta$ -glucan by injection to grass carp (*Ctenopharyngodon idella*) increased expression of immune-related genes and reduced mortality following a challenge with grass carp haemorrhage virus (Kim *et al.*, 2009).

Limnoid extract which is derived from the neem tree (*Azadirachta indica*), a plant native to the Indian subcontinent, has been added to feeds for Atlantic salmon to treat sea lice infestations (Walker & Gunari, 2015). This extract has been used for hundreds of years in India to protect crops, as its presence causes pest species to stop eating, and inhibits the production of eggs. Similar effects have been observed on sea lice, with reduced egg production, and detachment from the fish (Walker & Gunari, 2015). This treatment offers an alternative to established neurotoxic treatments such as SLICE<sup>®</sup> (emamectin benzoate) to which resistance has emerged (Igboeli *et al.*, 2012; Saksida *et al.*, 2013). The most potent compound in the neem tree extract is azadirachtin (I, Figure 1.5), which has a number of molecular targets, and is specific to arthropods (Walker & Gunari, 2015). As azadirachtin can be administered through the feed, fish need not be subjected to stressful bath treatments, as is the case with hydrogen peroxide treatments.



I

Figure 1.5. Structure of azadirachtin.

Burrells *et al.* (2001a) found that the addition of nucleotides to diets fed to salmonids improved survival following infections with the bacteria *Vibrio anguillarum*, also known as *Listonella anguillarum*, and infectious salmon anaemia virus. They also showed that numbers of infesting sea lice of the species *Lepeophtheirus salmonis* were significantly reduced in coho salmon (*Oncorhynchus kisutch*) fed nucleotide supplemented diets (Burrells *et al.*, 2001a). It was shown that reduced mortality due to *L. anguillarum* was more pronounced in fish fed nucleotide supplemented diets than in those fed diets supplemented with the immunostimulant  $\beta$ -glucan (Burrells *et al.*, 2001a). Further beneficial effects were found following the addition of nucleotides to the diets of Atlantic salmon (Burrells *et al.*, 2001b). These include increased vaccination efficiency and improved growth following stressors relative to control (Burrells *et al.*, 2001b). Reduced blood chloride levels following transfer to seawater suggests that the osmoregulatory capacity of fish was also increased by the inclusion of nucleotide supplements in diets (Burrells *et al.*, 2001b).

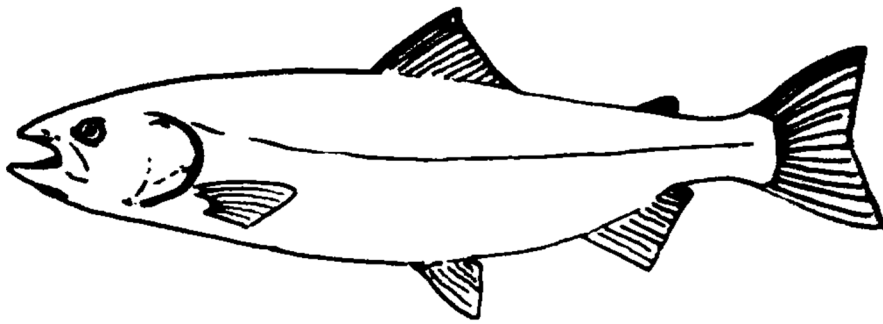
### *1.14 This project*

Smoltification, the process by which salmon prepare for entry to seawater, is a crucial phase of the life cycle of Atlantic salmon and represents an economically important phase in the production cycle in the aquaculture of this species. The purpose of this project was to investigate the molecules accumulated in the skin of Atlantic salmon during smoltification and following seawater transfer. A novel osmolyte was detected in the salmon skin in a pilot study, this project aimed to characterise this molecule, and identify when in the life cycle this compound was accumulated. The effects of dietary supplementation with precursors of this novel osmolyte were investigated, along with the expression of genes involved in the metabolism of this compound. A number of genes involved in ion transport, the immune response and cellular metabolism were investigated in the gill as potential biomarkers of smoltification to give a more robust indicator of the “smolt window” during which fish are well adapted to entry to seawater. This project aimed to:

1. Characterise the novel osmolyte in salmon skin identified in a pilot study.
2. Test the hypothesis that altering the levels of precursors for this osmolyte available in the diet would alter the level of this compound found in the skin.
3. Test the hypothesis that the levels of the novel osmolyte in the skin would be influenced by seawater transfer.
4. Test the hypothesis that the expression of genes involved in the metabolism of the novel osmolyte is influenced by seawater transfer.
5. Identify the effect of seawater transfer on a suite of established organic osmolytes in the skin of Atlantic salmon.
6. Determine whether levels of these established organic osmolytes are affected by diets designed to influence the level of the novel osmolyte.

7. Test the viability of genes observed to be differentially expressed in freshwater and seawater at the time of smoltification as possible biomarkers of this process.





# Materials and Methods



## 2. Materials and Methods

### 2.1 *Tissue sampling*

The tissues selected for sampling were those involved in whole body osmoregulation. Focus was placed on the gill, skin, fin, intestine and kidney. Fish were sacrificed by treatment with anaesthetic (MS222) before tissues were collected. All protocols were conducted in accordance with the Animals -Scientific Procedures- Act, 1986, under Home Office Project License No. 603805. Tissues were dissected using scalpels and scissors. All four gill arches were collected, the second gill arch was used for extraction experiments. Skin samples were taken from the left side of the fish, samples included epidermis, and dermis along with scales. Muscle tissue was removed from skin samples as far as possible. Pectoral fins were collected. Contents of intestine were mechanically removed as far as possible. Head kidney was not collected with kidney samples. After tissues were dissected they were frozen either on dry ice or in liquid nitrogen. Samples were transported on dry ice and stored at -80°C.

### 2.2 *Gene expression*

#### 2.2.1 *RNA extraction from tissues*

Tissue samples were stored at -80°C. Approximately 70 mg of tissue was homogenised at room temperature in a Precellys<sup>®</sup>24 homogeniser (3 x 5500 rpm for 20 s) using 2 ml tubes containing 6 ceramic beads (2.8 mm) and 1 ml of Ribozol (Amresco). Samples were vortexed for 15 seconds and centrifuged at 14000 rpm (20817 x g), Eppendorf 5417C microfuge, for 1 minute at room temperature. The supernatant was sampled (900 µl) into a 1.5 ml microfuge tube and 250 µl of bromo-3-chloro-propane added and vortexed vigorously for 15 seconds before incubation at room temperature for 3 minutes. Tubes were centrifuged

at 10000 rpm (11816 x g) in a Beckman J2M centrifuge (JA18.1 rotor) for 10 minutes at 4°C. The upper aqueous phase was sampled (approx. 500 µl) and placed in a fresh 1.5 ml microfuge tube and 500 µl of isopropanol added, vortexed for 10 seconds and incubated at room temperature for 5 minutes to precipitate RNA. Tubes were then centrifuged at 10000 rpm (11816 x g) for 10 minutes at 4°C as above to pellet the RNA. The isopropanol was carefully aspirated and the pellet washed with 500 µl of 70% ethanol and centrifuged at 10000 rpm (11816 x g) for 5 minutes at 4°C as before. The ethanol was aspirated and the washing step repeated. RNA pellets were dried in a vacuum oven at room temperature for approx. 5 minutes and dissolved in MilliQ water (generally 40 µl, although a lower volume of 20 µl was used for very small pellets).

### *2.2.2 RNA extraction from skin*

The extraction procedure was modified slightly for extraction of RNA from skin by including a second phenol extraction before precipitation with isopropanol. The aqueous phase (approx. 500 µl) from the first Ribozol/ bromo-3-chloro-propane extraction was collected and placed in a fresh 1.5 ml microfuge tube, 500 µl of Ribozol was added and the solution vortexed vigorously for 15 seconds. To this was added 125 µl of bromo-3-chloro-propane and the sample vortexed and incubated at room temperature for 3 minutes. Tubes were again centrifuged in a Beckman J2M centrifuge at 10000 rpm (11816 G, JA18.1 rotor) for 10 minutes at 4°C. The aqueous phase was collected (approx. 700 µl) and 700 µl of isopropanol added to precipitate RNA. Washing with 70% ethanol was then carried out as described above.

### 2.2.3 cDNA synthesis

The concentration of RNA in each sample was measured by absorbance at 260 nm using a Nanovue Plus spectrophotometer (GE Healthcare), and these data were used to calculate the dilution required to give 2 µg of RNA for synthesis of cDNA. RNA used in cDNA synthesis was diluted to 2 µg in 4µl with MilliQ water and added to a 0.2 ml tube. This diluted RNA was treated with DNase (Promega) as detailed below (Table 2.1). The program was run in a Biometra T-Gradient PCR thermocycler.

Table 2.1: DNase mixture and program run in Biometra T-Gradient PCR thermocycler.

DNase mix		Program	
Reagent	µl for 1 reaction	Temp.	Time
RNA	4		
DNase (1 u/µl)	0.5	37°C	30 min
10 x DNase buffer	0.8		
H <sub>2</sub> O	2.7		

After incubation with DNase, 2 µl of oligo dT (0.25 ug/µl) was added and incubated at 70°C for 5 minutes before rapid cooling on ice for 2 minutes. Samples were incubated in a Biometra T-Gradient PCR thermocycler.

The RNA was then reverse transcribed to make cDNA in a reaction using reagents from Promega as listed below (Table 2.2). Reverse transcription reaction program was run in a Biometra T-Gradient PCR thermocycler.

Table 2.2: Reverse transcription mixture and program run in Biometra T-Gradient PCR thermocycler.

Reverse transcription mix		Program	
Reagent	$\mu\text{l}$ for 1 reaction	Temp.	Time
DNase/oligo dT treated RNA	10		
5x first strand buffer	5	40 °C	10 min
10 mM dNTPs	1.5	42 °C	60 min
RNAsin (40 u/ $\mu\text{l}$ )	0.5	55 °C	10 min
Reverse transcriptase (200 u/ $\mu\text{l}$ )	1	70 °C	10 min
H <sub>2</sub> O	7	4 °C	hold

### 2.2.4 Polymerase Chain Reaction (PCR)

To test whether genes were expressed, standard PCR was employed, using Taq polymerase (Taq Gold; Biogene). For each reaction 0.5  $\mu\text{l}$  of the cDNA synthesis reaction mixture was added to a 0.2 ml tube and the following mix added (Table 2.3).

Table 2.3: PCR mixture and program run in Biometra T-Gradient PCR thermocycler.

PCR mix		Reaction (*35 cycles)	
Reagent	$\mu\text{l}$ for 1 reaction	Temp (°C)	Time
cDNA template	0.5	95	2 min
H <sub>2</sub> O	14.8	94*	10 sec
10x PCR buffer (Biogene)	2	60*	30 sec
10 mM dNTPs (Promega)	0.4	72*	1 min
Taq (500 u/ $\mu\text{l}$ ) (Biogene)	0.3	4	hold
Primers (5 pmol/ $\mu\text{l}$ )	1 of each		

This technique was used to test for expression and view the expected size of amplicons for every gene investigated. The results of these tests were used to inform later RT-qPCR experiments.

### 2.2.5 Gel electrophoresis and extraction of DNA

PCR products or isolated plasmid DNAs were separated on the basis of size by agarose gel electrophoresis. A stock 10 x gel loading buffer (composition in Table 2.4) was added to the

DNA containing solutions (1:10 v:v) and 10-20  $\mu$ l added to the sample wells of 1% agarose (Biogene) gels containing 1 x TAE (1 x TAE buffer stock composed of 20 ml 50 x TAE (composition in Table 2.5, made up with 980 ml distilled water) and 0.1  $\mu$ g/ml ethidium bromide. Gels were run at 80 volts (30 ml gels) or 160 volts (100 ml gel) for 15-30 minutes in 1 x TAE buffer before viewing the separated fragments on a transilluminator (Herolab UVT-20M).

Table 2.4: Composition of 10 x gel loading buffer.

<u>Reagent</u>	<u>Volume</u>
glycerol	3.9 ml
10% (w/v) SDS	500 $\mu$ l
0.5 M EDTA	200 $\mu$ l
bromophenol blue	0.025 g
xylene cyanol	0.025 g
H <sub>2</sub> O	10 ml

Table 2.5: Composition of 50 x TAE.

<u>Reagent</u>	<u>Volume</u>
Tris base	242 g
Glacial acetic acid	57.1 ml
0.5M EDTA (pH 8.0)	100 ml

Following gel electrophoresis, the amplified DNA fragments were visualised using a UV transilluminator under low intensity to prevent DNA damage and cut from gel using a clean scalpel blade. Excess gel was removed before processing to extract the DNA. Extraction was carried out using a QIAquick Gel Extraction Kit as per the manufacturer's instructions.

### *2.2.6 SOPE resin purification of PCR products*

Under conditions where only a single DNA fragment was amplified purification could be undertaken directly from the PCR cocktail without the need for gel electrophoresis. For each PCR reaction, 3  $\mu$ l SOPE resin (Edge Biosystems) was added to 15-20  $\mu$ l of amplified

product, mixed well and left at room temperature for 2-3 minutes. For each sample 200 µl of a 2:1 (v/v) slurry of swollen Sephacryl S400 in water was added to a spin tube insert in a 1.5 ml microfuge tube and centrifuged at 2800 rpm (833 x g) for 3 minutes in an Eppendorf 5417C microfuge. The eluate was discarded, and the insert transferred to a clean 1.5 ml tube and the sample (PCR product + SOPE resin) was added directly to the S400 column before centrifuging again at 2800 rpm (833 x g) for 3 minutes. DNA eluting from the beads was quantified by absorption at 260 nm or estimated by image analysis after visualisation by ethidium bromide-containing agarose gel electrophoresis using known quantified amounts of DNA ladder as standards (NEB 100 bp ladder).

#### *2.2.7 Cloning of DNA fragments*

PCR fragments purified either by gel extraction or SOPE resin cleaning were cloned using a pCR<sup>®</sup>4-TOPO<sup>®</sup> TA Cloning<sup>®</sup> Kit (Life Technologies) using One Shot<sup>®</sup> TOP10 chemically competent *E. coli* according to the supplier's instructions. The pCR<sup>®</sup>4-TOPO<sup>®</sup> vector is shown in Figure 2.1.

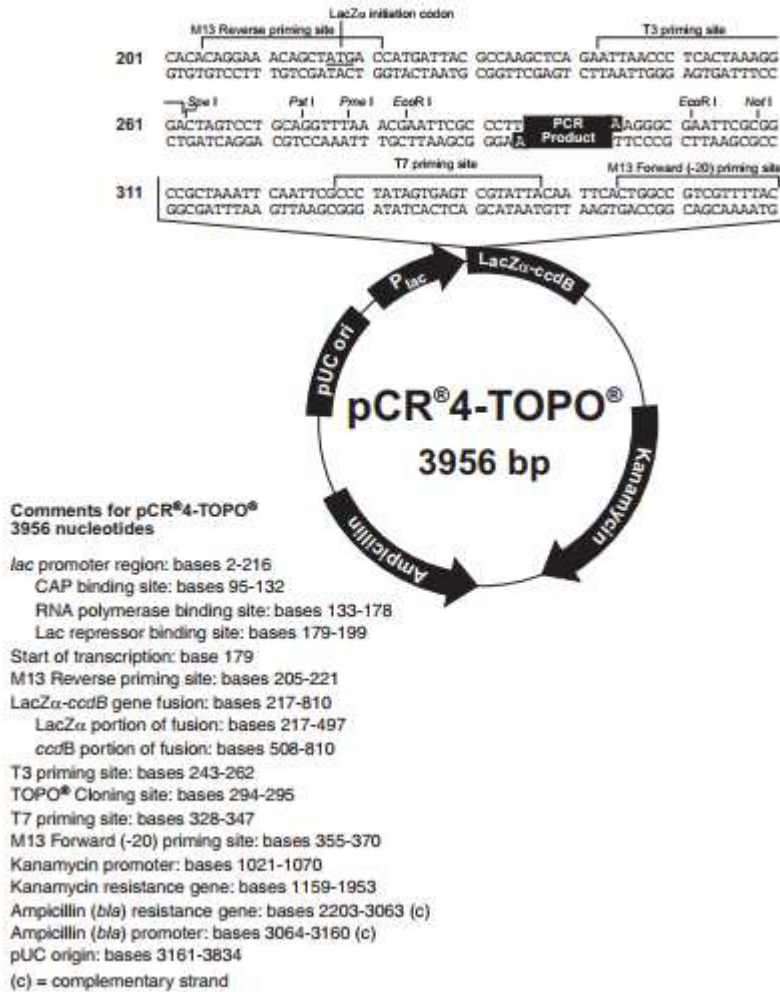


Figure 2.1. pCR®4-TOPO® vector, taken from Invitrogen TOPO® TA Cloning manual (Life Technologies).

PCR product for cloning was incubated for 5-20 minutes at room temperature with the vector in the mixture detailed in Table 2.6.

Table 2.6: Vector mixture for cloning.

Reagent	Volume
Fresh PCR product	2 $\mu$ l
Salt Solution	1 $\mu$ l
Sterile water	2.5 $\mu$ l
4-TOPO® vector	0.5 $\mu$ l

Following incubation of the vector with the PCR product, 2  $\mu$ l of this mixture was added to a vial of One Shot® TOP10 chemically competent *E. coli* and incubated on ice for 5-30

minutes. Cells were then heat shocked at 42°C for 30 seconds before being transferred back to ice. 250 µl of S.O.C. medium (Invitrogen) was added to the vial, and cells were incubated at 37°C for 1 hour, shaking at 200 rpm. Aliquots (20-100 µl) of this suspension were then spread on an agar plate (LB agar in H<sub>2</sub>O containing 50 µg/ml carbenicillin; composition in Table 2.7). Colonies derived from a single cell were selected from the plate with a sterile pipette tip, and transferred to a sterile 1.5 ml tube containing 1 ml of Terrific Broth (composition in Table 2.8) containing 50 µg/ml carbenicillin.

Table 2.7: Composition of agar used to pour plates, ~25 ml used per plate.

Reagent	Volume
LB agar (Fisher Scientific)	35 g
H <sub>2</sub> O	1 L
Autoclaved before addition of antibiotic	
Antibiotic (carbenicillin 1 µg/ml)	50 ml

Table 2.8: Composition of Terrific Broth (TB).

Reagent	Volume
TB powder (Fisher Scientific)	47.6 g
glycerol	10 g
H <sub>2</sub> O	1 L
Autoclaved before addition of antibiotic	
Antibiotic (carbenicillin 1 µg/ml)	50 ml

These were incubated at 37°C for 3-24 hours, shaking at 200 rpm. Samples (50 µl) of suspensions showing colony growth were transferred to fresh sterile 1.5 ml tubes and centrifuged for 1 minute at 14000 rpm (20817 x g), Eppendorf 5417C microfuge, at room temperature. The supernatants were removed, and the pellets resuspended in 100-500 µl of H<sub>2</sub>O. A sample (1 µl) of the suspended cells was transferred to a 0.2 ml PCR tube for PCR, using M13 forward and reverse primers (250 nM final concentration). Colonies containing the expected insert size were then used for sequencing or further processing. The reaction mixture used for colony PCR is detailed in Table 2.9.

Table 2.9: Colony PCR mixture and program run in Biometra T-Gradient PCR machine.

PCR mix		Reaction (*35 cycles)	
Reagent	µl for 1 reaction	Temp (°C)	Time
Template	1		
H <sub>2</sub> O	14.3	95	2 min
10x PCR buffer (Biogene)	2	94*	10 sec
10 mM dNTPs (Promega)	0.4	60*	30 sec
Taq (500 u/µl) (Biogene)	0.3	72*	1 min
Primers (5 pmol/µl)	1 of each	4	hold

The product of this PCR reaction was SOPE cleaned, as detailed above, and a sample (1-5 µl) visualised following agarose gel electrophoresis. This product was quantified by absorption at 260 nm or by image analysis of gels and then used for sequencing.

### 2.2.8 Sequencing

Each sample was diluted to give approximately 40 ng of purified DNA fragment in a final volume of 6 µl containing 1 µl of 5 µM T3 or T7 primer. To this mixture was added 4 µl of Big Dye reaction mixture (Applied Biosystems; detailed in Table 2.10) and the samples were placed in a PCR thermocycler for the cycle sequencing reaction (detailed below, Table 2.10). Following the cycle sequencing, 1.25 µl of 250 mM EDTA pH 8.0 was added to samples, before transferring to a 1.5 ml microfuge tube and then precipitating the amplified DNA by the addition of 28 µl of absolute ethanol. Tubes were incubated at room temperature for 5 minutes, then centrifuged at 14000 rpm (20817 x g) in Eppendorf 5417C microfuge for 30 minutes at room temp. The aqueous layer was carefully aspirated and the pellet washed with 400 µl of 80% ethanol before re-centrifuging at 14000 rpm (20817 x g) for 20 minutes as above. The ethanol was again carefully aspirated and the pelleted samples dried for 5 minutes in a vacuum oven at room temperature. The samples were sent to PNAACL at the University of Leicester for sequencing.

Table 2.10: Big dye mixture and program run in Biometra T-Gradient PCR thermocycler.

Big Dye Reaction mixture		Sequencing reaction (25 cycles)	
Reagent	Volume for 1 reaction	Temp. (°C)	Time
Big dye	0.5µl	96	10 sec
5x buffer	1.75µl	58	5 sec
H <sub>2</sub> O	1.75µl	60	4 min
Total volume	4µl	4	hold

### 2.2.9 Real Time Quantitative Polymerase Chain reaction (RT-qPCR) – relative gene expression

To quantitatively determine gene expression, RT-qPCR (7300 Real-Time PCR System, Applied Biosystems) was used and expression was calculated relative to the normalising gene, ribosomal protein large-P0 (RPLP0). This reference gene was selected because it is universally expressed in almost all tissues and its expression in previous studies has shown that it is not significantly altered during parr/smolt development nor by changes in environmental salinity (Cramb, personal communication). The primers used to amplify all transcripts are listed in Tables 2.12, 2.13, 2.14 and 2.15.

RT-qPCR samples were prepared as detailed in Table 2.11 in 96 well plates. After setup, plates were centrifuged at 2000 rpm (473 x g) for 2 minutes at 4°C (Beckman J6-MI centrifuge, JA18.1 rotor). SYBR<sup>®</sup> Green was the fluorescent dye used to detect the amplification of PCR products. At the end of each cycle the fluorescence was measured. ROX<sup>™</sup> dye was used as the internal passive reference dye. The fluorescence in each sample was measured at the end of each cycle of amplification, and this was plotted by the 7300 Real-Time PCR System software to give amplification curves. This data was then analysed using the 7300 Real-Time PCR System software to give Ct values (the number of cycles required for the fluorescence to cross the set threshold) used for further analysis. The Ct values of the reference gene were subtracted from that of the gene of interest to give the  $\Delta$ Ct.

The  $\Delta C_t$  was subjected to an exponential expression transformation ( $2^{-\Delta C_t}$ ), and this number was used for further analysis.

Table 2.11: RT-qPCR mixture and program run in 7300 Real-Time PCR System machine.

PCR mix		Reaction (*40 cycles)	
Reagent	$\mu$ l for 1 reaction	Temp ( $^{\circ}$ C)	Time
H <sub>2</sub> O	2	50	2 min
2x PerfeCTa SYBR Green FastMix ROX (Quanta Biosciences)	10	95	10 min
Primers (5 pmol/ $\mu$ l)	1 of each	95*	15 sec
cDNA dilution		60*	1 min
		Dissociation stage	
cDNA	0.25	95	15 sec
H <sub>2</sub> O	5.75	60	1 min
		95	15 sec
Total reaction volume	20 $\mu$ l	60	15 sec

Dissociation curves were created by running the dissociation stage given in Table 2.11, with the block temperature increasing from 60-95 $^{\circ}$ C to give the melting point of the product. These curves were used to ensure that only one product amplified during the sample run.

Following amplification qPCR products were also run out by agarose gel electrophoresis to confirm that a single amplicon of the expected size was present.

Table 2.12: Sequences of primers used to investigate expression of genes involved in purine metabolism.

Gene	Sense/ antisense	Sequence (5' - 3')	Expected amplicon size
Purine nucleoside phosphorylase 4b	S	GCTTCTGAGCCGGACGAGACATAGG	256 bp
	AS	CCGCACCGGGAATGTGACCTTACAGAGTGAA	
Purine nucleoside phosphorylase 5a1	S	GCTGAAGGGAAGGCCATGTGTGTGC	307 bp
	AS	AGCCAGCTGCTGCAGCTCTCTGTGC	
Purine nucleoside phosphorylase 5b	S	GAATGGCTCCTGTCCCCTACAGAGATA	274 bp
	AS	GCAGCTTGAAAATCCGCATGGGCATTGTT	
Purine nucleoside phosphorylase 6a	S	GCCGCTTCCACTTCTACGAAGGCTACAA	293 bp
	AS	GTCCTCAGCAGTCTCTTTGGCCATTA	
Purine nucleoside phosphorylase 6b	S	CTGCTGGGGGTGGAGACCTTGATCATT	228 bp
	AS	CTCCTCAGCAGTCTCTTTGGCCAGAC	
Purine nucleoside phosphorylase 6c	S	GACGTACCCGGTGCCTGTGTTACT	253 bp
	AS	CTCCTCTGCCACCTCTCGAGCCAAA	

Hypoxanthine phosphoribosyl-transferase 1	S AS	GCACCATATCGTGGCTCTCTGCGTG GTCTGGTATGTAGCCAACACTCCTTGGTG	355 bp
Hypoxanthine phosphoribosyl domain containing protein 1	S AS	CAGTTCTGTGCTGACTTGGTGGAGAGG GGGAGACATCCTGAACTGTTGGCACTC	311 bp
Xanthine dehydrogenase	S AS	GCCCTACTGCTGCCTCCGCTTC ATCTCCACCTCAGAGCAGGCCACTC	268 bp
Cytosolic purine 5-nucleotidase C3	S AS	GACTCCAGCAGCACAACGTGCC GTCTCCGAGCAGCACGATGTTGC	320bp
Cytosolic purine 5-nucleotidase A	S AS	CAGAGGAGATGCTGCCTGGCCTAAG CGAGGCAGAGTATGTGAGGCCGTACC	306bp
Cytosolic purine 5-nucleotidase C1	S AS	CAGCCCGCAGTGCAGCCAGCTC AGGCACGTGTGCAGCGATGGTCC	263 bp
Cytosolic purine 5-nucleotidase C2	S AS	GCCCAGACATCAGTGCCATTGAGACC GCAGGTGGAAGAGTACAGGTCAGCG	158 bp
Cytosolic purine 5-nucleotidase C3a	S AS	GGATGTGGTGAAGGAGTCCGATGCT GGACGTTGTGGCGTGACTTGAGCTCC	305 bp
Cytosolic purine 5-nucleotidase C3b	S AS	GTTGGTGAACAGAGGGCTACAGAAGG GGGCGCCGTCGTGCTTGTGTAAC	293 bp
Cytosolic purine 5-nucleotidase D1a	S AS	GAGGAGCCGTTGACAGTGTCTGGAC GGCATCGGAGTAGAGGGCCAGGG	240 bp
Cytosolic purine 5-nucleotidase D1b	S AS	GGGGAACAGACTCACGCTGTGTTG GGCATCGGAGTAGAGGGCCAGGG	202 bp
Cytosolic purine 5-nucleotidase D2	S AS	CATATGCAGTTCTACACCGTCTGGCAAGC GACCTGGCCCTTATCCAAGCTCTTGATC	251 bp
Cytosolic purine 5-nucleotidase E1	S AS	GCTTCAGTGAACCATGTTAGCTCCTG GAGAATCCGTCTCCTCCTCCACC	396 bp
Cytosolic purine 5-nucleotidase E2	S AS	CTGGGAATGTGGTGAAGGCCAATGGA GTCCTTATGCCTCCACTGTTGAGGATGCAT	298 bp
Equilibrative nucleotide transporter 1a	S AS	GACCCGCGCTCGAAGGCTTAGTGA CAGACAGGGAGCCGGCGATACGGT	196bp
Equilibrative nucleotide transporter 1b	S AS	GACCCGCGCGTTGAGGGCTCAGCTA CAGACAGGCAGCCAGCAATACGCC	196bp
Equilibrative nucleotide transporter 2	S AS	CGTGTGTGAC TGGATCGGCAGAACCGTC GGACATGGAGAGGCAGACGCAGTAGC	235bp
Equilibrative nucleotide transporter 3	S AS	CTGTGCTATCGCAAGTGGCTCGGAGATAA CAGCGATGGTAGACTTGACATCCACA	371bp
Equilibrative nucleotide transporter 4	S AS	CAGAGAGAAGGTCCGGATTGCTGTCAGTC CAGGTGTGGCAGTAGTAAGTAGCTGAGC	370bp
Concentrative nucleotide transporter 1	S AS	CTCTTGGCTGGCTGGGAGGCCTGG GACTGAGATCCATTGCCTCTCATCGCC	252bp
Concentrative nucleotide transporter 3	S AS	GGCGCTCTGTCATGGCTGGGCAACATG CAGAGTGGACAGACAGGTAAGTAAACG	262bp
Adenosine monophosphate kinase $\alpha$ 1	S AS	GTCAGGTCAGTGTCAAGACCTGTCC GTCGCACTAAGCACCATCACACCATC	245 bp
Adenosine monophosphate kinase $\alpha$ 2a	S AS	GATTGGAGAGCACCAGTTGACAGGTC GTGCACCACCATGTGTCTGTGGC	318 bp
Adenosine monophosphate kinase $\alpha$ 3	S AS	CTGGCACTGTCAATAATGTCATTCAGGTG GAGATGGTTGAGCATCACATGGTTGGGC	280 bp
Adenosine monophosphate kinase $\beta$ 1	S AS	GTGCAGACATGTCAGACCTCTCGAGTTCC CGGCTTGTACAGAAGTGTGGTCACATAC	289 bp
Adenosine monophosphate kinase $\gamma$ 1	S AS	CGTTGATGACAACGGACGAGTGGTGGACAT GTGAGAACCAGTGCCTGGAGGATGTCTGAG	284 bp
Adenosine monophosphate deaminase 1	S AS	CCCTAATGAGTGGACCAAGCTCTCAA GATGCTGAGCTCAGGGTTGGCGTG	205 bp
Adenosine monophosphate deaminase 3	S AS	CAGGTCGAAGAAGATAGTACAGAACTTCGC CGTTCCTTCCCTCAGGTTGTTGAGGAC	287 bp
Adenosine deaminase 1a	S AS	GTGCTGTACAAACAACCTCTGGAGCAG CTCAGGCAAGAAGCTGGAGTTAGCG	275 bp

Table 2.13: Primers used to investigate expression of annexins in Atlantic salmon tissues.

Gene	Sense/antisense	Sequence (5' - 3')	Expected amplicon size
Annexin 1	S	CTGTCTGACTGCCGTAGTGAAGTGTGC	246 bp
	AS	GAGAAGATCCTACTGGCCCTGTGTGG	
Annexin 2	S	GAGTCTGCTGTTGGCCCTGGTACAG	236 bp
	AS	CGACATGCAGGAGAGCATCAGGAAGG	
Annexin 3	S	CACACATGTGGATGCAGCCAAGGCCA	296 bp
	AS	CTGCATCAAGGCATGAAGGGCGGAG	
Annexin 6b	S	GAGGAGATCCACGCCATGAACGCTG	261 bp
	AS	CTCTGTACCAGGAGCTTCCCACATCTC	

Table 2.14: Primers used to investigate the expression of other biomarker candidates in Atlantic salmon tissues.

Gene	Sense/antisense	Sequence (5' - 3')	Expected amplicon size
Na <sup>+</sup> -K <sup>+</sup> -ATPase $\alpha$ 1a	S	CCCAAACCTCGTAGTCCCGATTTTAGC	212 bp
	AS	GGAATTGAAATTGATCACTTCATTGAAATC	
Na <sup>+</sup> -K <sup>+</sup> -ATPase $\alpha$ 1b	S	GATCGCTGAGATTCCCTTCAACTCCACCAACAAATAT	206 bp
	AS	GCTCTTCGTAGGCGTTCTGGAAGGC	
Na <sup>+</sup> -K <sup>+</sup> -ATPase $\beta$ 2c	S	CCTACTACGGCAAGAAGGCCCAGC	140 bp
	AS	CACTGAAGACTGGAGGAGAGAGAGAC	
Na <sup>+</sup> -K <sup>+</sup> -ATPase $\beta$ 3b	S	GGAGGGCGAGGTGGGCGAGC	357 bp
	AS	CAGAGCTGACCATCGAATGCCGGAT	
Na <sup>+</sup> -K <sup>+</sup> -ATPase $\beta$ 3c	S	GTTCAAGCGCAATCTGCTCCGGCAG	334 bp
	AS	GGAGTGTAAGATCGAGGGCTCCAAC	
Na <sup>+</sup> -K <sup>+</sup> -ATPase $\beta$ 4	S	GAGACACGTGAACTACACAGCGCCG	210 bp
	AS	CCTACTGTTGGTGTGATGTCCTCATGAC	
LDL receptor	S	GTCACCACTCAGGACATCCGCCATG	236 bp
	AS	CCGTCTGGACTGTGGCTCCTGC	
ApoB100	S	GCAGACAAGTACGGGATCTTCATGCAC	210 bp
	AS	GAGGAGCACAGGCAGGTGGTTATC	
ApoA1	S	CAAGCTCATGCCCATCGTGGAGACC	234 bp
	AS	GCCTGGCTGATGGTCTCGTAGAAAGC	
ApoA1b	S	GAC CCA GAG AAC TCA GGA TCT CCA GC	133 bp
	AS	CTGGATCTTCTTGGTGAAGGAGTCCC	
ApoA4	S	CTACACTGACGAGCTGAAGCAGAAGGTG	226 bp
	AS	GGTGTGGTGAAGGCCTGGTAGAGG	
Immunoglobulin kappa	S	GAG AAG GAC GGT CTG TAT AGC TGG AG	191 bp
	AS	GGAACCAGCGTCTCTCTCCACAG	
Immunoglobulin D	S	CAG GAC AGT GAT GAC ACA GAC TGA GGT A	227 bp
	AS	GGTTGAAGCAGCGATGTTTCACTCTG	
Na <sup>+</sup> -K <sup>+</sup> -Cl <sup>-</sup> cotransporter	S	GAGGCCCAACACTCTGGTATTGGC	190bp
	AS	GATGACCTGCTGTCTGTCGACAGGAG	
Cystic fibrosis transmembrane conductance regulator	S	CTGAGTAACGGACACAAGCAGCTCATGTG	189bp
	AS	GTCAGAACACAGAGTGAACCACTGCTG	
Zymogen granule protein 16	S	CAGAGTGTGGGAGACCAACAACAAC	180 bp
	AS	CCAGACACCTCGACGATGGACTC	
Tristetraprolin 1	S	CTATGGCGCCCGCTGTCACTTC	195 bp
	AS	GCCCTGGAGAACAGCATGGTCTC	
Tristetraprolin 2	S	GCCCCTATGGCGCGCGATG	199 bp
	AS	GCCCTAGAGAACAGCATGGGCTC	

Aryl hydrocarbon receptor-like 1	S AS	CAA CAT TAT CCA CAG GTC CCA TCC ACC T CGG CTG CAT CCT CAA CGA CAC CAA C	201 bp
Polymeric immunoglobulin receptor	S AS	GCTGTCTACATCCTGGTCACTCCTCC CCATGGCAGCAGCACCAGAACCATC	246 bp
Polymeric immunoglobulin receptor-like transcript 1	S AS	CCGCCACAGTAGACTCTGCTCTGAC GCTCAGTCATCTCTCCTTCCACAGGTC	309 bp
Polymeric immunoglobulin receptor-like transcript 2	S AS	CCGTCATCAGCAGGCTTCACCAACAG GGGCGTCGTCATCATCATCAACATCATC	295 bp
X-box binding protein 1	S AS	GGATCGGGTCTTCTGAGTCTGC CCTGGATCTCCTGCTCACCG	206 bp
CMRF35-like molecule 8	S AS	GAGCAACAGCCGAGGACAGTGGC GGAAGAGGAAGAGCATCCAGCGCAG	325 bp
Unknown protein 584	S AS	CTCCATCAGAACCGCATTATCCTGCC GGATTCTCAGCCACTCAGGAGTCAG	225bp

Table 2.15: Primers used to amplify the reference gene RPLP0 in Atlantic salmon tissues.

Gene	Sense/antisense	Sequence (5' - 3')	Expected amplicon size
RPLP0	S	GAGCGATGTGATGCTCATCAAGCCTG	163 bp
	AS	ATCCTCAGTAATGTGCGAGCACCTCAG	

### 2.2.10 Primer design

The sequences of transcripts listed in the SalmonDB database were aligned using Clustal Omega. Primers were then selected to produce amplicons from specific paralogues of the genes. For primers, sequences of 24-30 nucleotides with a GC content of 50-60% were selected. Oligocalc software (<http://biotools.nubic.northwestern.edu/OligoCalc.html>) was used to optimise primer melting temperature ( $T_m$ ) to 60-62 °C and to check for possible self-complementarity.

Primer efficiencies were measured using a standard dilution of cDNA to give a standard curve as per the Sigma Aldrich standard protocol for use with SYBR<sup>®</sup> Green ReadyMix<sup>™</sup>. To ensure quality control a random selection of samples for each experiment were re-run to determine whether results were reproducible. Amplification curves and dissociation curves were inspected and where abnormalities were observed qPCR experiments were repeated and

when necessary RNA extraction and cDNA synthesis were repeated. If samples continued to give abnormal readings after these measures were taken these samples were discarded and not included in analysis.

### *2.3 Western Blotting*

#### *2.3.1 Protein extraction from tissues*

Frozen tissue samples of between 50 and 100 mg in weight were homogenised in 1 ml of ice-cold homogenisation buffer (50 mM Tris, 0.25 M sucrose, 5 mM MgCl<sub>2</sub>, 1 mM EDTA pH 8.0) containing 1 x Roche protease inhibitors (Roche Applied Science). Tissues were disrupted in 2 ml screw-capped sample tubes in a Precellys<sup>®</sup>24 homogeniser (3 x 5500 rpm for 20 s) containing 7 ceramic beads (2.8 mm). Samples were kept on ice for 3 minutes between each period of tissue disruption with the beads. Samples were then centrifuged at 14000 rpm (20817 x g) for 10 seconds at room temperature (Eppendorf 5417C microfuge) and 0.8-0.9 ml of infranatant (between pellet and any floating lipid material) was collected and transferred to a new 1.5 ml microfuge tube. This was then centrifuged at 15500 rpm (28388 x g) in a Beckman J2M centrifuge (JA18.1 rotor) at 4°C for 90 minutes. The supernatants were removed into fresh 1.5 ml microfuge tubes and the pellets resuspended in 100-150 µl of original homogenisation buffer. Samples were then aliquoted and frozen at -20°C.

#### *2.3.2 Protein assays*

Bradford Assay: Samples were diluted 1:50 with water and 10 µl samples were added to 96 well plates along with a series of BSA standards (15 – 1000 µg/ml) and 100 µl of 1:1 diluted Bradfords reagent (Sigma Aldrich) was added. Samples were left for 10-15 minutes at room temperature before measuring the absorbance and 600 nm on a Dynex plate reader.

### *2.3.3 Sodium Dodecylsulphate Polyacrylamide Gel Electrophoresis (SDS-PAGE).*

Protein samples were diluted to 1 mg/ml in Laemmli sample preparation buffer (60 mM Tris-HCl, 2% SDS, 10% glycerol, 5% 2-mercaptoethanol, 0.01% bromophenol blue, pH 6.8.) and heated to 99°C for 10 minutes before vortexing and then cooling to room temperature. Samples were then centrifuged at 14000 rpm (20817 x g) for 1 min (Eppendorf 5417C microfuge) and then 10 µl (10 µg protein) added to the wells of Nu-Page Bis-Tris 4-12% PAGE gels (Thermo Fisher Scientific) and electrophoresed in 1 x Mes SDS running buffer (Thermo Fisher Scientific) at constant 160 volts for 1 h. Lanes containing standard pre-stained proteins (Page Ruler 15-140 kDa pre-stained protein ladder, Thermo Fisher Scientific) were also run to estimate protein molecular weights. Gels were removed and assembled into cassettes and proteins transferred onto an Immobilon<sup>®</sup>-FL Transfer Membrane (0.45 µm pore (Thermo Fisher Scientific)) by electroblotting (at 160 volts for 1 h) in ice cold 1 x Transfer buffer (Thermo Fisher Scientific) containing 10% methanol and 0.01% SDS.

### *2.3.4 Immunostaining*

Following transfer, the PVDF membrane was removed from the cassette and placed in a square petri dish with 20 ml blocking Solution 1 (PBS containing 10% non-fat milk and 0.2% Tween 20) and incubated on a reciprocal shaker for 1 hour at room temp. The blocking solution was removed and 10 ml of Solution 2 (PBS containing 2% non-fat milk and 0.5% Tween 20) containing the appropriately diluted primary antibody was added and the membrane incubated on a reciprocal shaker overnight at 4°C. The antibody solution was poured off and the membrane washed rapidly 5 times with approx. 20 ml of Solution 3 (PBS containing 0.2% Tween 20) and then washed twice in Solution 3 with reciprocal shaking for 15 min at room temperature. Following washes, Solution 3 was removed and 20 ml of Solution 4 (PBS containing 5% non-fat milk and 0.5% Tween 20) containing a 1/20000

dilution of secondary antibody (HRP-conjugated donkey anti-rabbit or anti chicken) was added to the membrane and incubated with gentle shaking for 1.5 hours at room temperature. Solution 4 was poured off and the membrane washed with Solution 3 as above. PVDF membranes were placed on a piece of white roll to remove excess Solution 3 and incubated for 3 min at room temperature with ECL reagent (Pierce Dura or Femto ECL; Thermo Fisher Scientific) according to the supplier's instructions. The membrane was blotted to remove excess ECL reagent and placed between two layers of plastic film and chemiluminescence detected and image captured using a Fuji Imager (LAS-3000). A white light image was also taken to show the position of the standards. The intensity of the chemiluminescent image was quantified using a Fuji LAS-3000 Imager and Aida Image Analysis software (Rayte).

The primary antibodies used in Western Blotting to measure NKA  $\alpha$ -subunit paralogous protein expression were raised to the epitopes as detailed by McCormick *et al.* (2009). The antibody to the  $\alpha$ 1a paralogue was raised in chicken and used in a final dilution of 1:3000, while the  $\alpha$ 1b paralogue was raised in rabbit and used in a final dilution of 1:50000. These antigen-affinity purified antibodies were a generous gift from Dr Stephen McCormick, Conte Anadromous Fish Research Center, Turner Falls, MA, USA.

#### *2.4 Osmolyte extraction*

Tissue samples were stored at -80°C until extraction. Approximately 150 mg of tissue was homogenised in 9 volumes (wt/vol) of 7% perchloric acid (PCA) (approximately 1350  $\mu$ l) using a Polytron PT-3100 homogeniser. The homogenate was transferred to a 1.5 ml microfuge tube and maintained at 4°C for  $\geq$  3 hours. The homogenate was then centrifuged at 14000 rpm (20817 G, Beckman J2 centrifuge; JA18.1 rotor) for 30 min at 4°C and 1 ml of supernatant was transferred into a fresh 1.5 ml microfuge tube. The extracts were neutralised (pH 6.8 to 7.8) by addition of 2 M KOH. The neutralised samples were then stored at 4°C

overnight before centrifuging at 14000 rpm (20817 G, Beckman J2 centrifuge; JA18.1 rotor) for 30 min at 4°C to remove the precipitate. A known volume of supernatant was then sampled into a fresh 1.5 ml microfuge tube and freeze-dried. The freeze-dried samples were then sent to Dr Paul Yancey, Whitman College, University of Washington, USA for HPLC analysis. HPLC analysis was carried out using a Sugar Pak I cation exchange column (Waters, Milford, MA), and the mobile phase HPLC grade water degassed with helium with 50 mg/L calcium disodium EDTA as described in Wolff *et al.* (1989). Using a series of known standards, osmolytes were quantified and expressed as mmol/kg wet weight of tissue.

#### *2.4.1 Hypoxanthine characterisation*

The unknown osmolyte peak was collected from the HPLC column and was characterised using mass spectrometry and NMR. This work was carried out at the Departments of Chemistry at the University of St Andrews and The University of Edinburgh.

### *2.5 Industrial smoltification time course trial sampling*

#### *2.5.1 Initial samples*

Atlantic salmon were sampled in November 2013 at the Marine Harvest FW facility at Loch Lochy. Tissues were sampled from parr, smolts in FW, and after a 24 hour SW challenge. SW challenge was conducted by transferring fish directly to aerated 100% SW at ambient temperature. The tissues collected were gill, fin, skin, liver, kidney, gut, brain, eye, spleen and skeletal muscle. Six fish were sampled in each group.

#### *2.5.2 Second time course*

Atlantic salmon were sampled at a number of life stages as detailed above and also from fish at Marine Harvest's SW facility at Invasion Bay, where fish were sampled after 12 weeks in

SW. Adult fish at harvest were sampled at the Marine Harvest processing plant in Fort William. The tissues collected were gill, fin, skin, gut, kidney and liver. Six fish were sampled in each group except adult fish, of which three were sampled.

### 2.5.3 Trial with SW challenge

Juvenile Atlantic salmon were sampled between August and October 2016 at the Marine Harvest FW facility at Loch Lochy, the time course covered fish from parr through to smoltification. Fish were sampled directly from FW pens, and following short 6-72 hour SW challenge/transfer. SW challenge was conducted by transferring fish directly from freshwater to aerated 100% seawater at ambient temperature. Time points at which fish were exposed to SW challenge and SW transfer are detailed in Table 2.16. All fish in the stock were transferred to SW 0 days to SW transfer time point. Tissues collected were skin and gill.

Table 2.16: Time course of sampling at Marine Harvest and SW challenge.

Time to SW transfer	SW challenge /transfer
68 days	N/A
67 days	N/A
61 days	N/A
57 days	6hr
54 days	6hr
44 days	6hr
30 days	6hr
16 days	6hr
0 days	6hr
-1 days	24hr
-2 days	48hr
-3 days	72hr

### 2.6 Nucleotide supplement feeding trial design

A feeding trial was conducted at EWOS Innovation’s study facility in Dirdal between 2<sup>nd</sup> of March and 1<sup>st</sup> of June 2015.

### 2.6.1 Trial design

24 experimental 490 L tanks, each containing 105 fish weighing approx. 70g of the Salmobreed strain. Tanks were maintained at ambient temperature (8-11 °C).

The experiment consisted of 6 experimental groups fed diets containing different purine and pyrimidine nucleotide contents as detailed in Table 2.17. Nucleotide supplements were prepared to a final concentration of 0.2% wt/wt of the total diet composition. Pyrimidine supplements took the form of cytosine monophosphate (CMP), and purine supplements adenosine monophosphate (AMP). An additional diet with a purine supplement of inosine was also prepared.

Table 2.17: proportions of purines and pyrimidines in nucleotide supplements in experimental diets.

Diet number	Nucleotide proportions
1	100% pyrimidine
2	75% pyrimidine / 25% purine
3	50% pyrimidine / 50% purine
4	25% pyrimidine / 75% purine
5	100% purine
6	100% purine (inosine)

The trial was conducted using a randomised design as depicted in Figure 2.2.

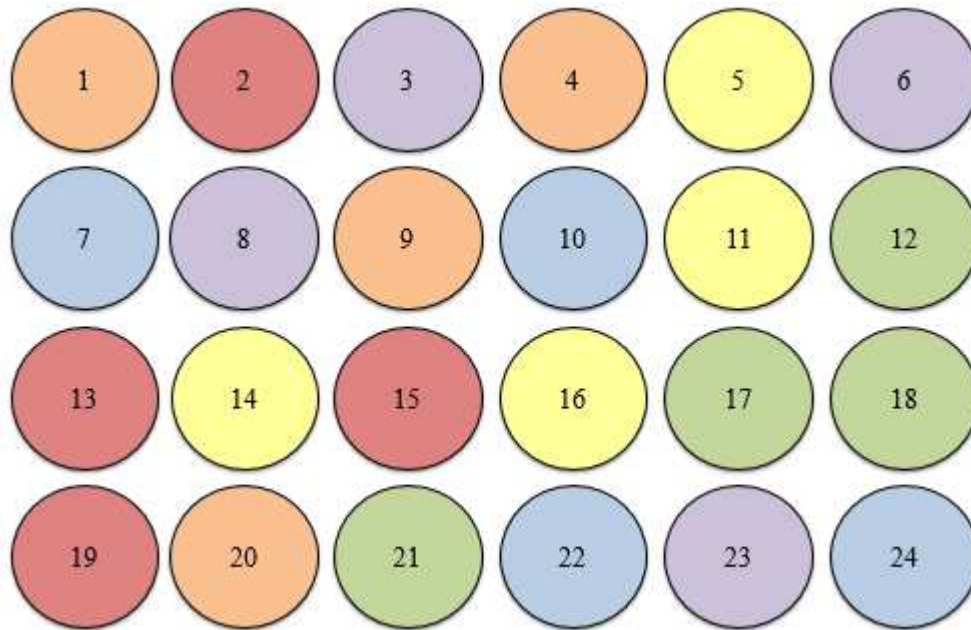


Figure 2.2. Randomised design of feeding trial. Diet 1 in red, 2 in orange, 3 in yellow, 4 in green, 5 in blue and 6 in purple.

### 2.6.2 Time course

On the 2<sup>nd</sup> of March 2015 fish were placed in FW in experimental tanks and fed on the facility's standard diet for a two-week acclimation period. Samples were taken immediately before introduction to experimental diets, these function as an experimental control. It would have been preferable to have maintained a group of fish in the standard non-supplemented diet throughout the time course to act as a control group, however, despite discussions and requests from ourselves, no fish were maintained on the standard diet after feeding with experimental diet began, as this was deemed unnecessary by EWOS statisticians.

Experimental feeding began on the 17<sup>th</sup> of March. Samples were collected after 3 weeks of feeding with experimental diets, and again after 5 weeks. Following the 5 week sampling point fish were then gradually transferred from FW to full SW. SW transfer was achieved by closing the FW supply and starting the SW supply, allowing the water in the tanks to gradually reach full SW concentration over a period of 6 hours. Tissue samples were

collected 24 hours after SW transfer was initiated. Further samples were collected after 3 weeks and 6 weeks in SW. Sampling timeline is given in Figure 2.3.

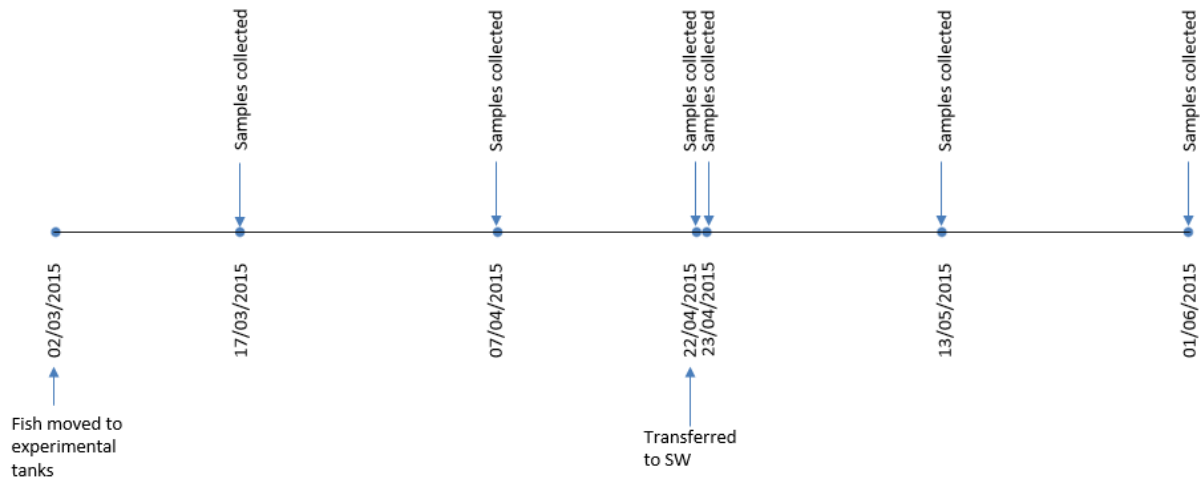


Figure 2.3. Timeline of sampling in EWOS feeding trial showing dates of sampling and of SW transfer.

### 2.6.3 Tissue collection

The tissues dissected from fish were the gill, skin, fin, liver and kidney. Twelve fish were sampled at the control time point, 6 fish per diet were sampled at the second time point, and 10 fish per tank were sampled for at the following time points. Following dissection tissue samples were wrapped in labelled foil and flash frozen in liquid nitrogen before being stored at  $-80^{\circ}\text{C}$ . Samples were shipped from Norway to the lab in St Andrews on dry ice. In St Andrews samples were again stored at  $-80^{\circ}\text{C}$ .

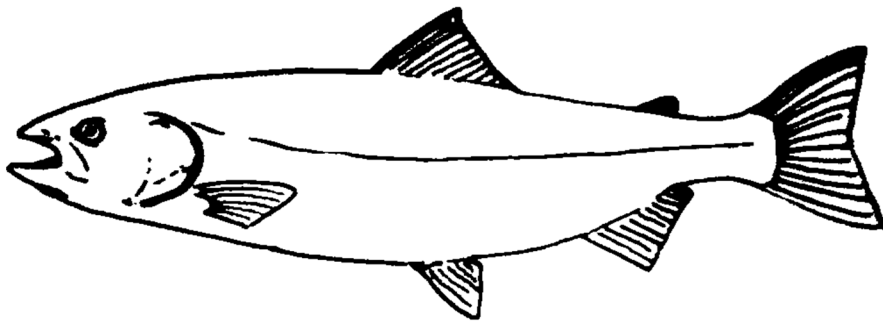
Growth data from the feeding trial is presented in Appendix 1.

## 2.8 Statistical analysis

Statistical analysis was conducted using R version 3.6.1. The package “ggpubr” was used to visualise data, “car” was used to conduct initial analysis. Where data were found to have equal variance and a normal distribution ANOVA was used for analysis, for non-normal data

with one exploratory variable Kruskal Wallis H test was used. Where data sets contained groups of different sizes type 2 ANOVA was used. For data sets with more than one exploratory variable found not to fit the assumptions of parametric tests the packages “fitsdistrplus” and “logspline” were used to find a distribution which approximately matched the data set for analysis. Generalised linear models were used to analyse these data. The packages “FAS”, “stats” and “emmeans” were used to conduct post hoc analysis.





# Novel osmolyte in Atlantic salmon



### 3. Novel organic osmolyte in Atlantic salmon

#### 3.1 Osmotic stress and organic osmolytes

Throughout evolutionary history cellular metabolism has developed to function optimally in a highly specific stable ionic milieu within the intracellular environment (Yancey, 2001). Changes in the osmolality of an organism's ECF lead to alterations in osmolality within cells, which in some cases alters the optimal concentrations of intracellular electrolytes and macromolecules such as proteins and nucleic acids (Bourque, 2008). These alterations in cell volume and osmotic concentration occur due to the semipermeable nature of the cell membrane, allowing the passive movement of water and some solutes into and out of the cell (Kultz, 2012). Such changes in the osmotic pressure within cells can lead to damage to cell structure, particularly the plasma membrane, which in turn may lead to irreversible tissue damage (Steenbergen *et al.*, 1985). Perturbations of the osmotic balance of the ECF and cytosol cause osmotic stress, which can also alter the structure and function of cellular proteins, this in turn alters cellular metabolism (Kultz, 2012; Parsegian *et al.*, 1995; Seale *et al.*, 2012). These disruptive effects on macromolecules often result from dehydration induced by hypertonicity of the extracellular environment which causes increased concentrations of intracellular inorganic ions (Kultz, 2012). Cell function can further be perturbed by osmotic stress through the alteration of the concentrations of molecular messengers, altering and sometimes impeding cell communication (Pasantes-Morales *et al.*, 2006).

Many species live in environments in which they are exposed to fluctuations in ionic concentrations, be that due to changes in salinity in aquatic environments, dehydration in desert environments, or water loss due to freezing in sub-zero temperatures. Hypertonicity of

fluids surrounding cells causes changes in cell volume as water leaves the cell by osmosis to equilibrate the osmolality of the cell and ECF, this leads to crowding of macro-molecules and increased concentrations of inorganic ions within the cell (Kultz, 2012). As high concentrations of inorganic ions can alter the tertiary structure of some proteins, often disrupting their function, organisms exposed to high or fluctuating levels of salts must adapt to counteract such perturbations.

Halobacteria have adapted to life in highly saline environments by extensively altering the amino acids sequences of their proteins to allow them to function in the presence of high concentrations of inorganic ions, sometimes up to 7 molar  $K^+$  (Yancey *et al.*, 1982). This extreme form of adaptation has led to a situation where many of the proteins produced by halobacteria require high concentrations of  $K^+$  to function optimally, limiting these species to a halophilic lifestyle in highly saline environments (Lanyi, 1974; Yancey *et al.*, 1982). As this adaptation places such constraints on the organisms, it may be seen as a sub-optimal adaptation to the challenge of surviving at high ionic concentrations, this strategy precludes adaptation to colonise new habitat types.

All other extant life on earth has favoured a different solution to the problem of coping with high levels of inorganic ions, namely employing organic osmolytes to maintain cell volume and metabolic function (Yancey *et al.*, 1982). Organic osmolytes are small molecules produced by cells to increase the osmolality of the intracellular fluid in response to hypertonic stressors, resisting cell shrinkage (Kultz, 2012). These compounds often perform functions other than those related to osmotic balance, and can belong to a number of different chemical groups, such as poly-alcohols, modified amino acids and short chain peptides (Kultz, 2012; Yancey *et al.*, 1982).

### 3.2 Identification of a novel osmolyte in the skin of Atlantic salmon

In a pilot study, osmolytes were extracted from the skin of Atlantic salmon smolts from the Marine Harvest facility at Lochailort, Scotland, shortly after transfer to seawater, using an acid extraction method with perchloric acid (Materials and Methods section 2.4). These were fractionated using an established HPLC method.

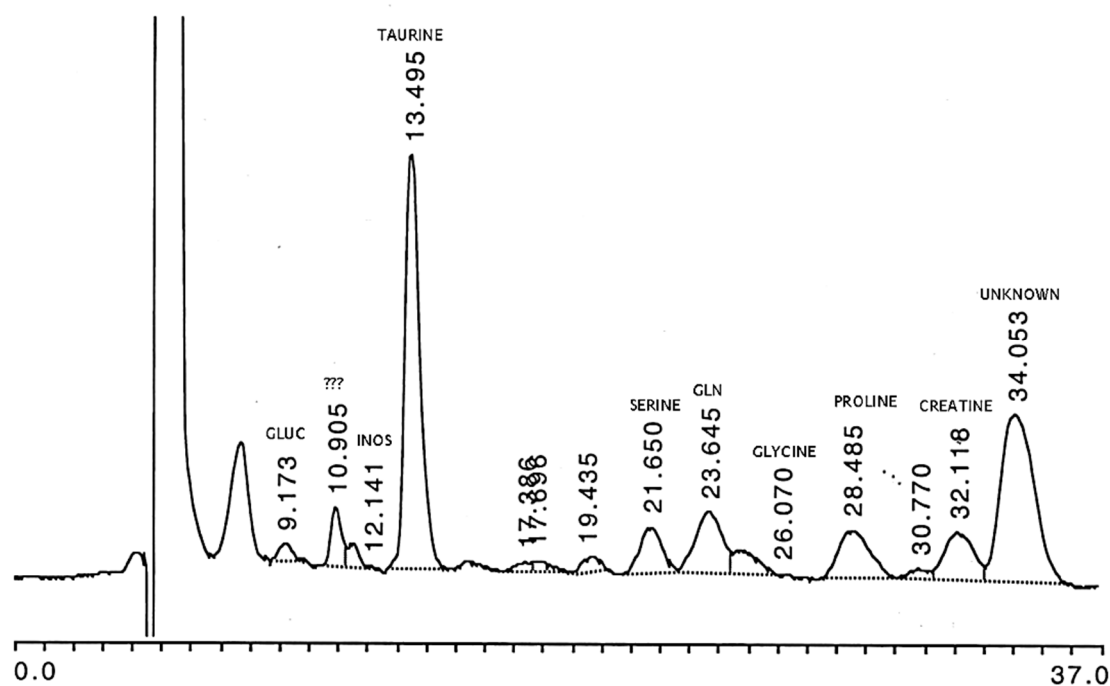


Figure 3.1. HPLC trace of extract from the skin of Atlantic salmon smolts following seawater transfer, supplied by P. H. Yancey.

The HPLC trace (Figure 3.1) showed a peak with a retention time of 34 minutes, labelled “unknown” on Figure 3.1, which was not observed in other euryhaline species, namely tilapia and European eel.

The first objective of this study was the characterisation of the novel osmolyte. The peak eluted at 34.053 minutes was collected and characterised using mass spectrometry and proton nuclear magnetic resonance spectroscopy ( $^1\text{H}$ NMR). The NMR results, detailed below,

indicated that the sample contained a mixture of hypoxanthine (II, Figure 3.2) and lactic acid (III, Figure 3.3).

### 3.2.1 Interpretation of spectra

Details of spectra obtained from the AIST database, shown below, were compared with the NMR spectra obtained from the unknown sample (Tables 3.1 and 3.2, Figure 3.2 and 3.3).

Table 3.1: <sup>1</sup>HNMR hypoxanthine in D6 DMSO from AIST database. Structure in Figure 3.2.

proton	chemical shift (δ)	multiplicity	integration
H <sub>A</sub> (NH)	12.4	doublet	1
H <sub>B</sub> (NH)	12.2	doublet	1
H <sub>C</sub>	8.14	doublet	1
H <sub>D</sub>	7.9	doublet	1

Spectral database for organic compounds AIST

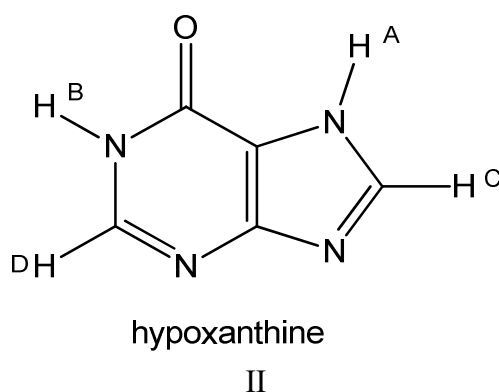
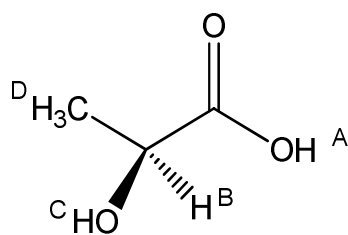


Figure 3.2. Structure of hypoxanthine showing position of hydrogen atoms labels (A-D) correspond to Table 3.1.

Table 3.2: <sup>1</sup>HNMR lactic acid in D6 DMSO from AIST database. Structure in Figure 3.3.

proton	chemical shift (δ)	multiplicity	integration
H <sub>A</sub> (COOH)	12.4	broad singlet	1
H <sub>B</sub> (C-H)	4.045	quartet	1
H <sub>C</sub> (OH)	3.4	broad variable δ	1
H <sub>D</sub> methyl	1.236	doublet	3

Spectral database for organic compounds AIST



lactic acid

III

Figure 3.3. Structure of lactic acid showing position of hydrogen atoms labels (A-D) correspond to Table 3.2.

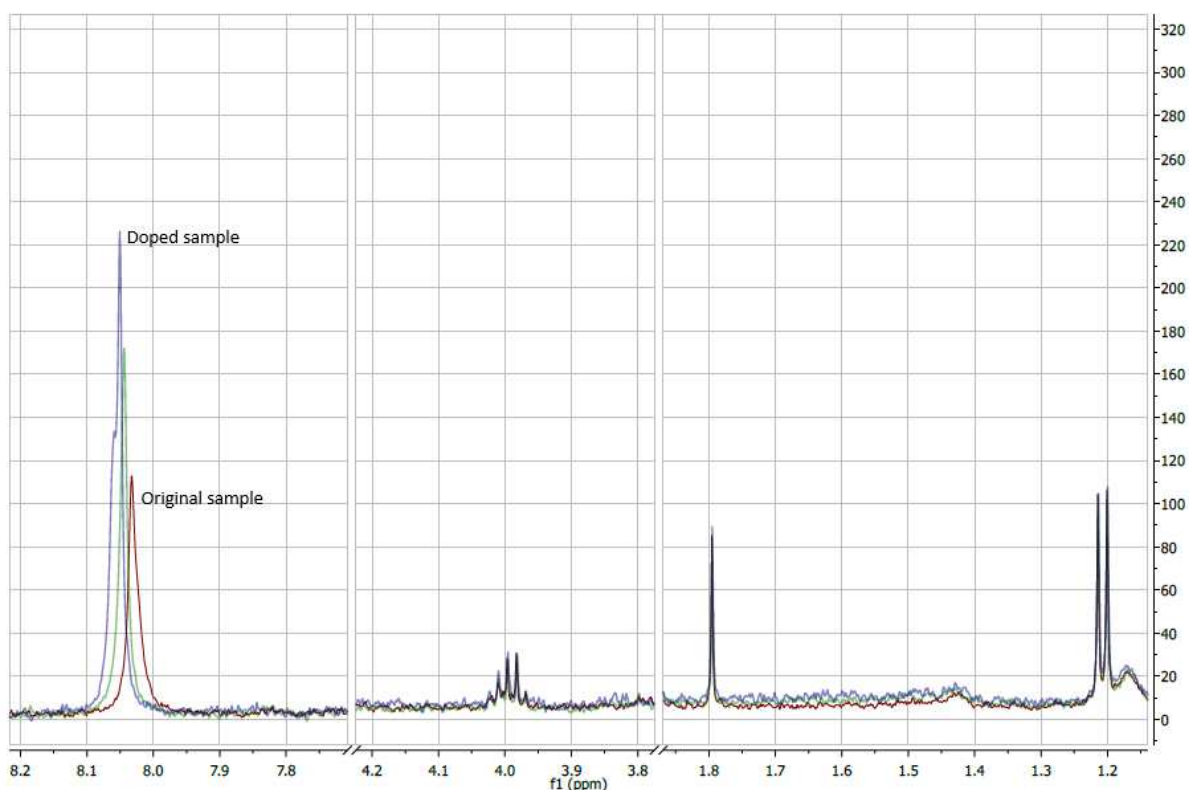


Figure 3.4.  $^1\text{H}$ NMR spectrum in  $\text{D}_2\text{O}$  of unknown peak. The blue line is the same sample doped with hypoxanthine. Spectrum obtained from a Bruker Avance III 800 MHz spectrophotometer by Dr Jura Bella, Department of Chemistry, Edinburgh University.

Table 3.3:  $^1\text{H}$ NMR unknown peak from spectra in Figure 3.2.

chemical shift ( $\delta$ )	multiplicity
8.05	broad
4	quartet
1.21	doublet

The spectrum has a doublet at  $\delta$  1.21 which is due to the methyl group of lactic acid (Figure 3.4, Table 3.3). The methyl group signal is split to a doublet by the adjacent proton labelled

H<sup>B</sup> shown above (Figure 3.4). The quartet at  $\delta$  4 is due to proton H<sup>B</sup> which is split to a quartet by the 3 adjacent hydrogens of the methyl group. No signal for the hydroxyl group is observed due to proton exchange, because the spectrum was run in D<sub>2</sub>O.

The broad peak at  $\delta$  8.05 is believed to be due to the CH protons of hypoxanthine (Figure 3.4). Doping the sample with hypoxanthine increased the area under this peak. It had no effect on the peaks due to lactic acid. It is believed that the small peak at  $\delta$  1.8 is due to an unknown trace impurity.

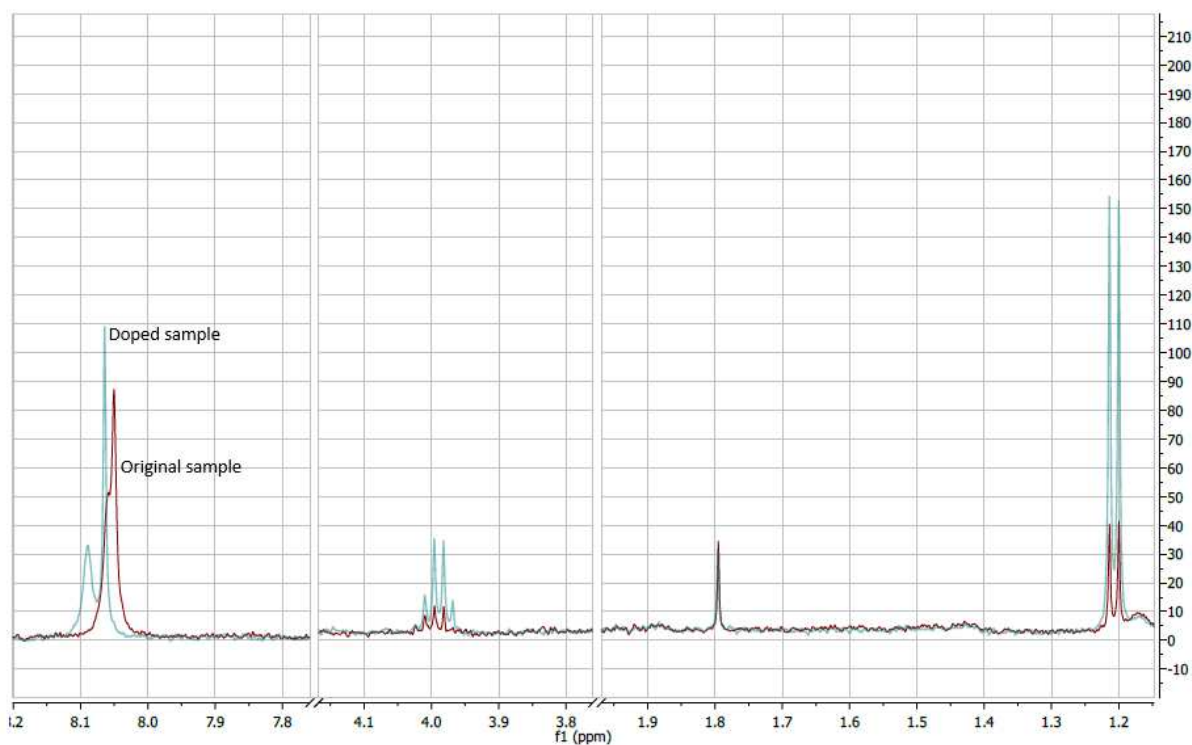


Figure 3.5. <sup>1</sup>H NMR spectrum of unknown peak. The blue line is the same sample doped with lactic acid. Spectrum obtained from a Bruker Avance III 800 MHz spectrophotometer by Dr Jura Bella, Department of Chemistry, Edinburgh University.

Doping with lactic acid increased the area under the peaks attributed to lactic acid (Figure 3.5).

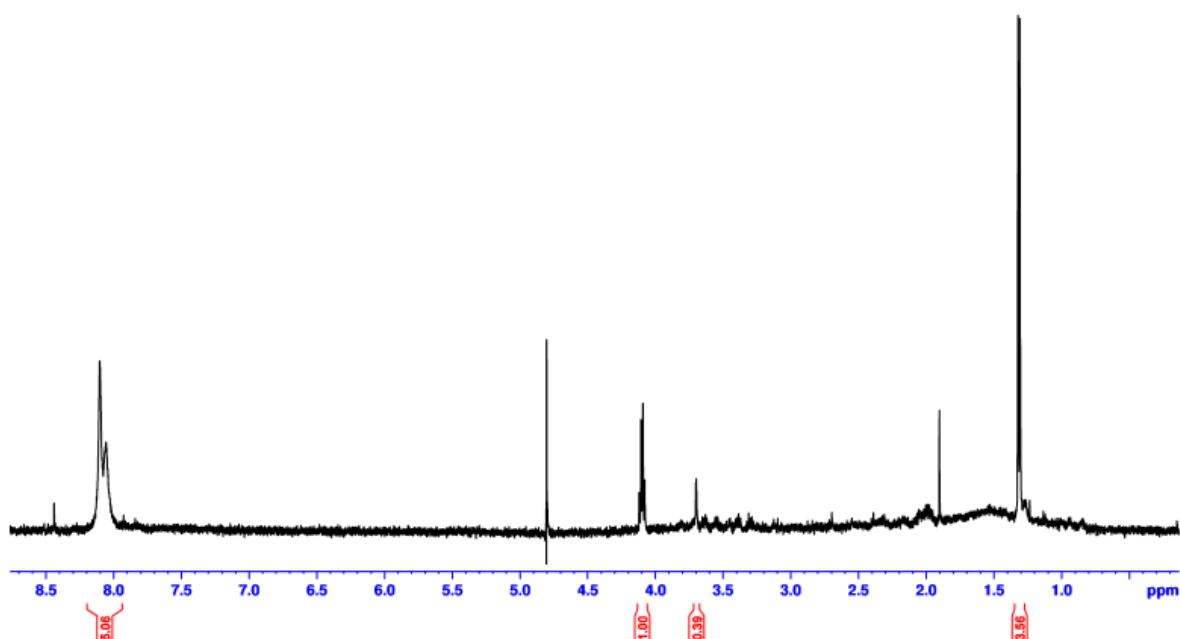


Figure 3.6.  $^1\text{H}$ NMR spectrum of unknown peak. Spectrum obtained from a Bruker Avance III 500 MHz spectrophotometer by Dr Tomas Lebl, Department of Chemistry, University of St Andrews.

Table 3.4:  $^1\text{H}$ NMR of unknown peak with integrations.

proton	chemical shift ( $\delta$ )	multiplicity	integration	
	8.0-8.2	Two peaks	5.06	Hypoxanthine
H (C-H)	4.1	quartet	1	
H (OH)	3.7	Broad	variable	Lactic acid
		$\delta$		
H methyl	1.3	doublet	3.56	

The peak integration is a measure of the number of equivalent protons giving rise to the peak. The multiplicity of the peak is  $n+1$  where  $n$  is the number of adjacent protons (Table 3.4). The doublet at  $\delta$  1.3 due to the methyl group of lactic acid integrates to 3.56 (Figure 3.6, Table 3.4). The quartet at 4.1 due to  $\text{H}^{\text{B}}$  of lactic acid integrates to 1. The small peak at 3.7 is consistent with the proton of the hydroxyl group of lactic acid. These signals are variable, often broad, and chemical shift can be solvent dependent. The signal would be very weak or absent in  $\text{D}_2\text{O}$  due to solvent exchange. The peak at  $\delta$  8.1 due to hypoxanthine integrates to 5.06, suggesting that it is due to approximately four protons. This peak is believed to be due to the CH proton of hypoxanthine. There are two of these per molecule. An integration of 4

as compared to the methyl integration strongly suggests that the sample contains hypoxanthine and lactic acid in the ratio of 2:1.

Hypoxanthine has the molecular formula  $C_5H_4N_4O$  with formula weight 136. The sample believed to be hypoxanthine was analysed by time of flight mass spectroscopy.

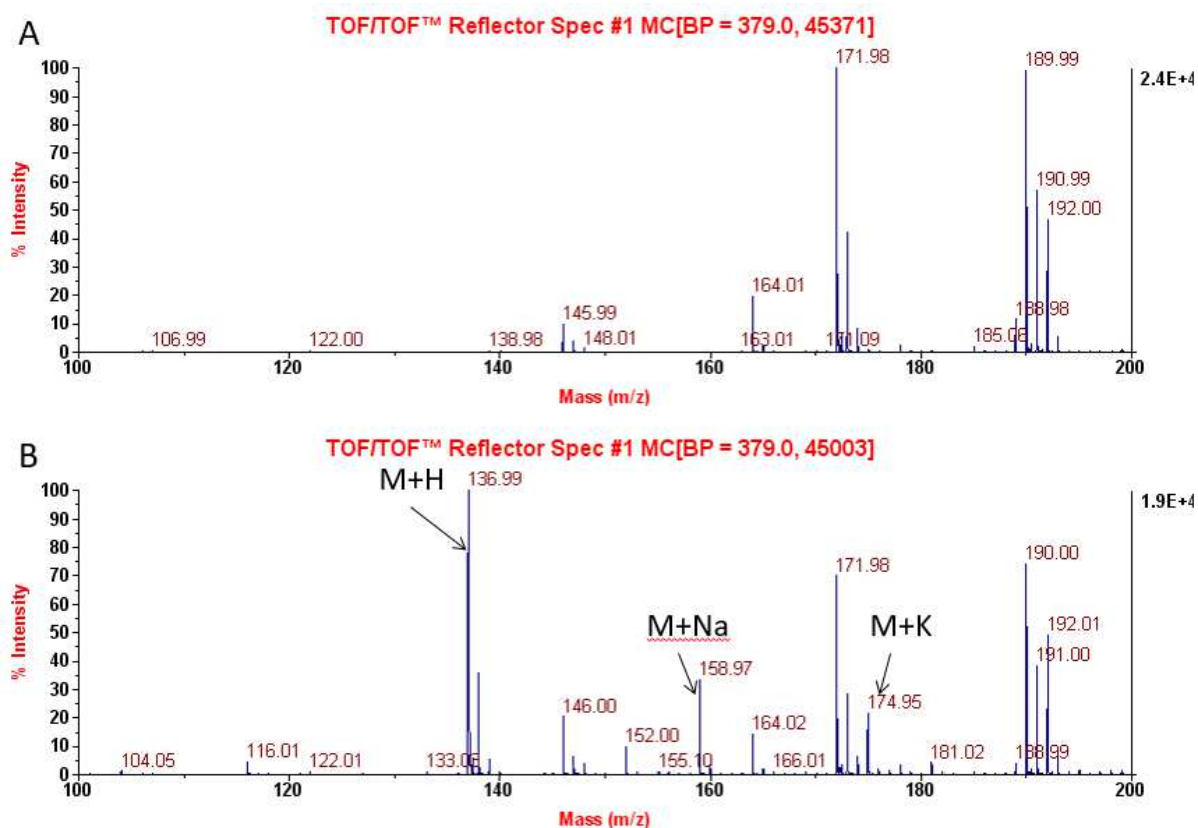


Figure 3.7. Time of flight mass spectrum of sample believed to be hypoxanthine. Upper trace (A) shows background control. Lower trace (B) shows sample.

The 100% peak at mass 136.99, represents M+1 due to the molecular ion ( $M+H^+$ ). Significant peaks at 158.97 and 174.95 are consistent with the adducts  $M+Na^+$  and  $M+K^+$ . Based on the NMR and mass spec data, the unknown compound has been identified as hypoxanthine.

### 3.2.2 Hypoxanthine levels in the skin - pilot

Levels of hypoxanthine were then measured in the skin of Atlantic salmon at a number of developmental stages. Levels were found to be higher in smolts 6 hours after seawater transfer, remained higher after 2 months in seawater, and were found to be higher in adults than in parr or freshwater smolts (Figure 3.8).

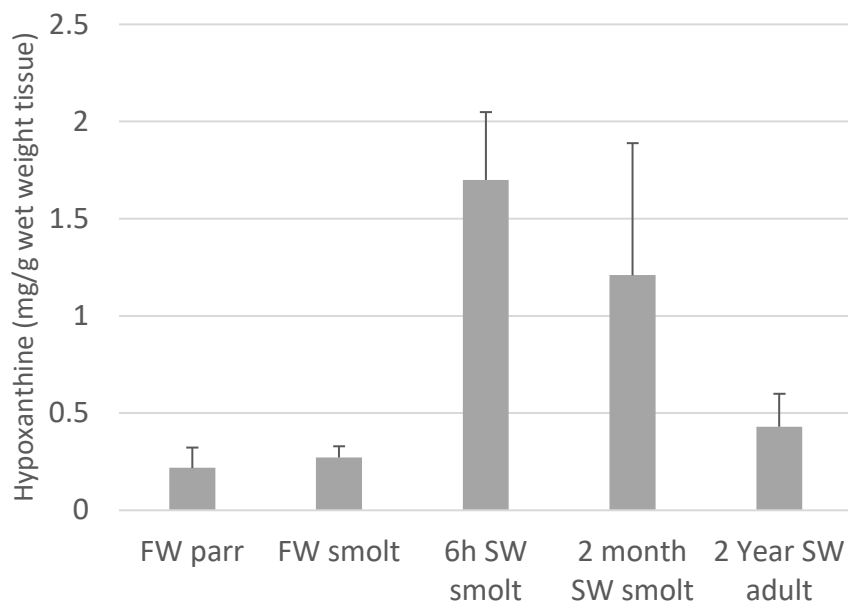


Figure 3.8. Hypoxanthine levels in the skin. Error bars denote standard deviation (n=3 in all groups but adult where n=2).

### *3.3 Hypoxanthine levels in acute seawater transfer trial*

Studies were carried out to determine the effect of SW transfer in an aquaculture setting on the level of the novel osmolyte hypoxanthine in skin.

The levels of the novel osmolyte hypoxanthine in the skin of Atlantic salmon were measured over a time course leading up to smoltification and following SW transfer at a freshwater loch site in the Scottish Highlands. At certain time points fish were given a SW challenge and samples were collected after 6 hours in SW. The effects of time and SW challenge on the level of hypoxanthine in total skin were investigated.

#### *3.3.1 Methods*

Osmolytes were extracted and quantified as detailed in General Methods Section 2.4 from total skin samples collected from salmon during the period of smoltification as detailed in General Methods Section 2.6.

These results were analysed in R using type II analysis of variance (ANOVA) as not all groups contain the same number of individuals. ANOVA results were then interrogated using the Tukey's Honest Significant Difference test. Code is given in Appendix 2.

### 3.3.2 Results

The level of hypoxanthine extracted from the skin (Figure 3.9) increased following SW transfer ( $F_{5,29} = 9.63$ ,  $p = 1.7 \times 10^{-5}$ ), with the levels significantly higher after 72 hours in SW (time point 6) than at any of the FW time points ( $p = 0.0009$ ,  $p = 0.00005$  and  $p = 0.03$  respectively). Levels at 24 hours after SW transfer were higher than seen in parr at the first two time points ( $p = 0.05$  and  $p = 0.004$  respectively) and remained elevated after 48 hours in SW ( $p = 0.017$  and  $p = 0.0009$  respectively).

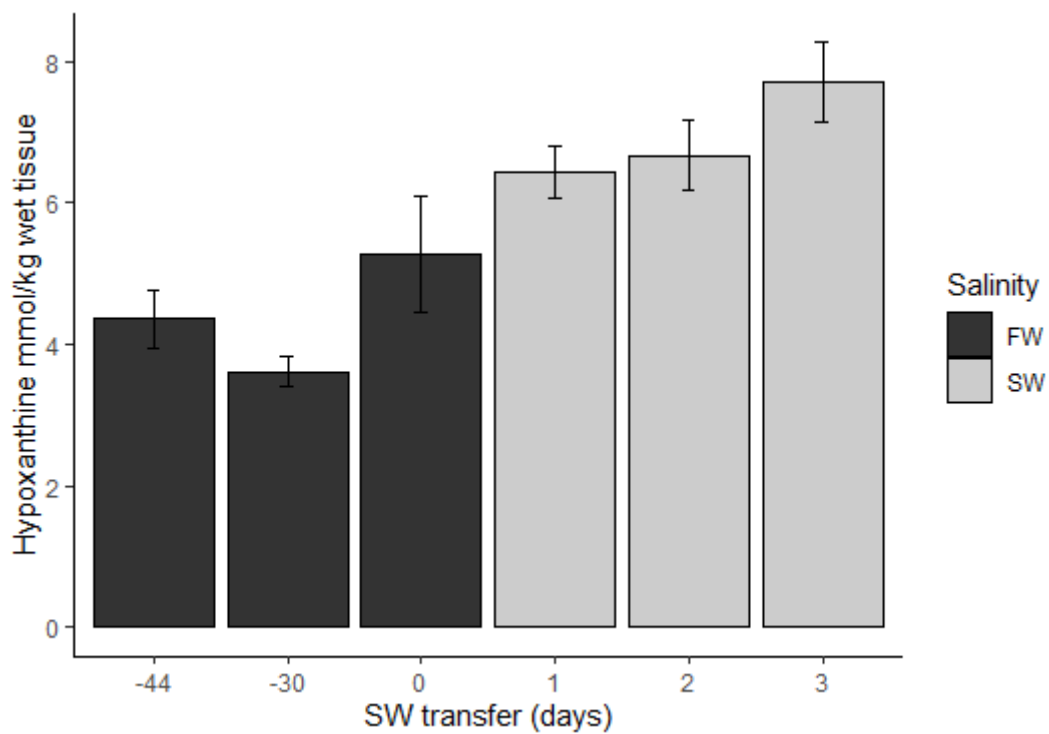


Figure 3.9. Hypoxanthine levels (mmol/kg wet tissue) extracted from the skin in the months before and days following acute SW transfer. Error bars denote standard error,  $n=5$  or  $6$ .

Fish were also exposed to seawater challenge at earlier time points before smoltification had occurred (Figure 3.10). No effect of SW challenge was observed ( $F_{1,28} = 1.84$ ,  $p = 0.19$ ). There was a significant effect of time point, with levels being significantly higher in smolts at the 3<sup>rd</sup> time point than in parr at the earlier two time points ( $p = 0.0004$  and  $p = 0.0002$  respectively).

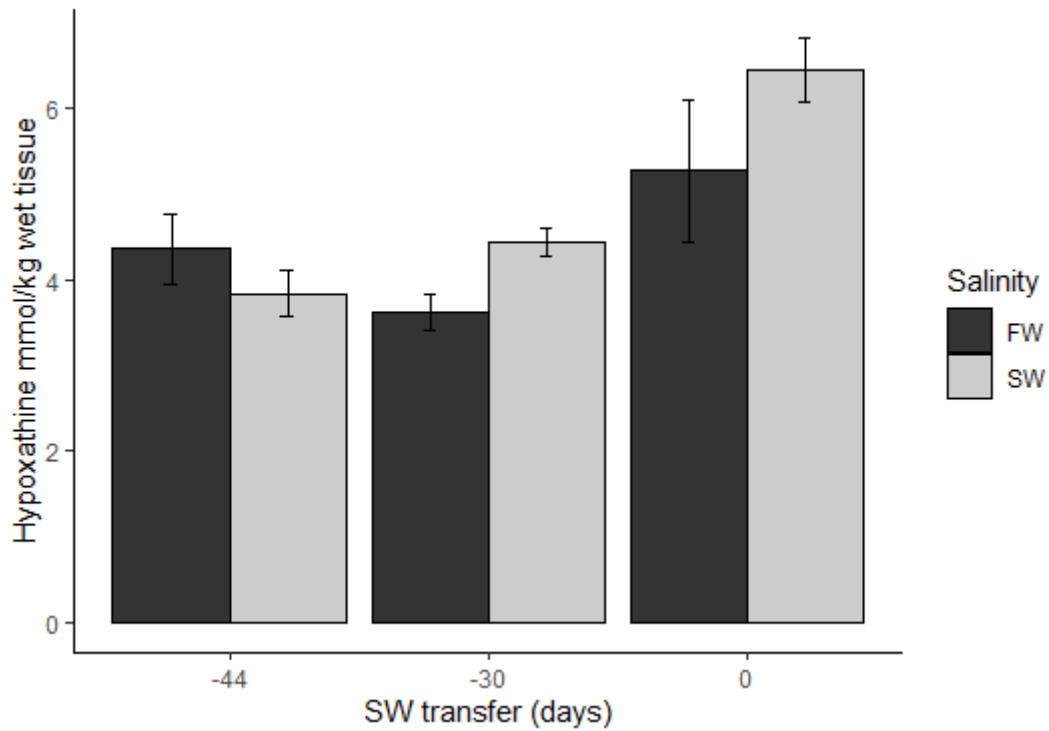


Figure 3.10: Hypoxanthine levels (mmol/kg wet tissue) extracted from the skin of fish sampled in the months leading to acute SW transfer before and after SW challenge. At the first two timepoints samples were collected 6 hours following SW transfer while at the third time point samples were collected 24 hours after SW transfer. Error bars denote standard error,  $n=5$  or  $6$ .

### *3.4 Hypoxanthine levels in feeding trial with gradual seawater transfer*

Work by Burrells *et al.* (2001a, 2001b) highlighted nucleotide supplements as a valuable addition to the diets of salmonid fish. However, little further investigation of these supplements has been conducted since. This feeding trial aimed to determine the effects of altering the proportions of nucleotide supplements in Atlantic salmon feed on the levels of the organic osmolyte hypoxanthine, which is a purine. This trial was conducted in conjunction with EWOS Innovation, as EWOS produce a commercial diet “Adapt” for smoltifying fish which contains nucleotide supplements.

#### *3.4.1. Methods*

Osmolytes were also extracted and quantified as above from total skin samples collected from salmon during the period of smoltification as detailed in General Methods section 2.7. SW transfer was gradual rather than acute in line with Norwegian welfare legislation for animals in research.

These results were analysed in R using a generalised linear model as data was found not to meet the assumptions of analysis of variance. Code is given in Appendix 2.

### 3.4.2 Results

The level of hypoxanthine in the skin (Figure 3.11) was found to be significantly influenced by time point on the feeding trial ( $F_{5,302} = 30.74$ ,  $p < 2 \times 10^{-16}$ ). No significant effect of diet was detected ( $F_{5,302} = 1.13$ ,  $p = 0.34$ ), nor was there a significant effect of the interaction between time point and diet ( $F_{25,302} = 1.05$ ,  $p = 0.4$ ). The level of hypoxanthine in the skin at the baseline timepoint 5 weeks prior to SW transfer was not significantly different from levels 2 weeks before SW transfer ( $p = 0.42$ ). At the third time point, one day before SW transfer levels of hypoxanthine were higher than baseline levels, and levels 2 weeks before SW transfer ( $p < 0.0001$ ). Hypoxanthine levels remained elevated following SW transfer up to 6 weeks post transfer and were significantly higher at all SW time points than baseline levels ( $p < 0.0001$ ) and at the second time point 2 weeks before SW transfer ( $p < 0.005$ ).

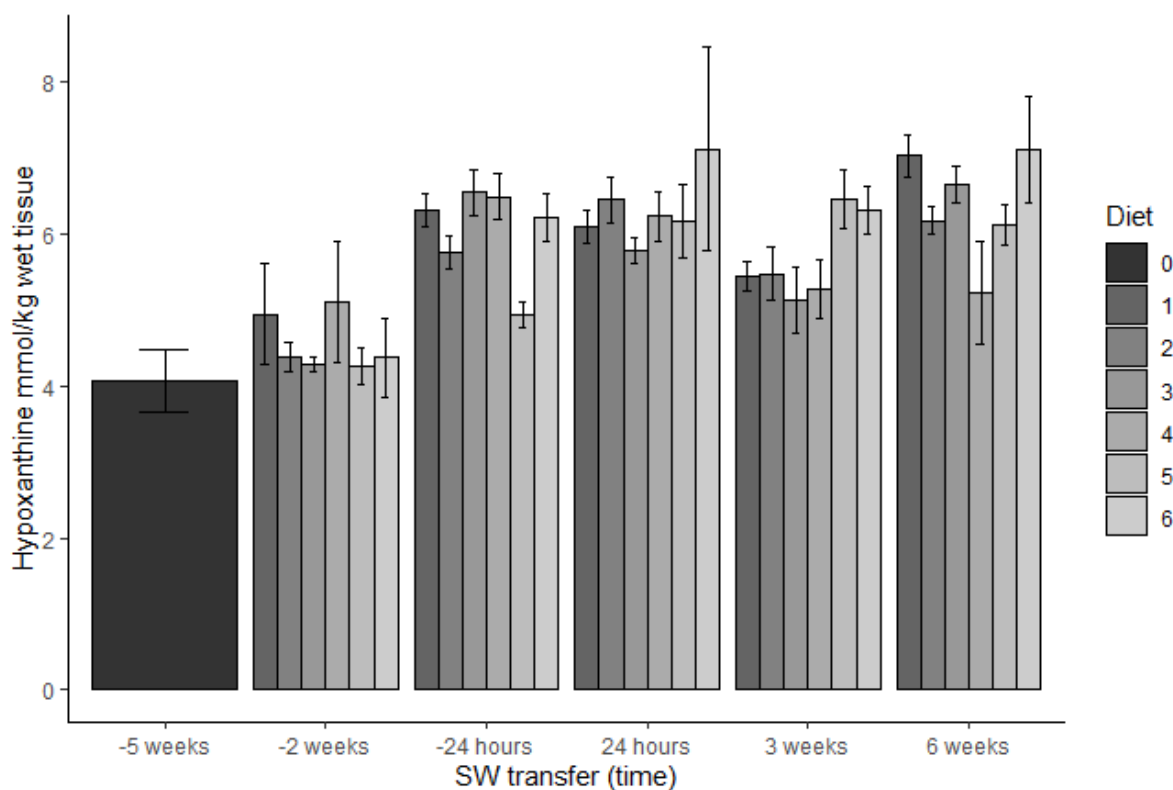


Figure 3.11. Hypoxanthine levels (mmol/kg wet tissue) extracted from the skin of Atlantic salmon over a time course leading up to and following smoltification fed on six diets with varying nucleotide supplements. Error bars represent standard error. The first time point represents fish sampled before feeding with experimental diets began and is universal for all diet groups.

### 3.5 Purine metabolism gene expression

Following the identification of hypoxanthine, a purine, as an organic osmolyte in the skin of Atlantic salmon, the expression of a number of genes involved in purine metabolism was investigated to determine how the expression of these genes was affected by changing demands for hypoxanthine and by different availability of purines in the diet. The section of the purine metabolism pathway relating to hypoxanthine is given in the Figure 3.12.

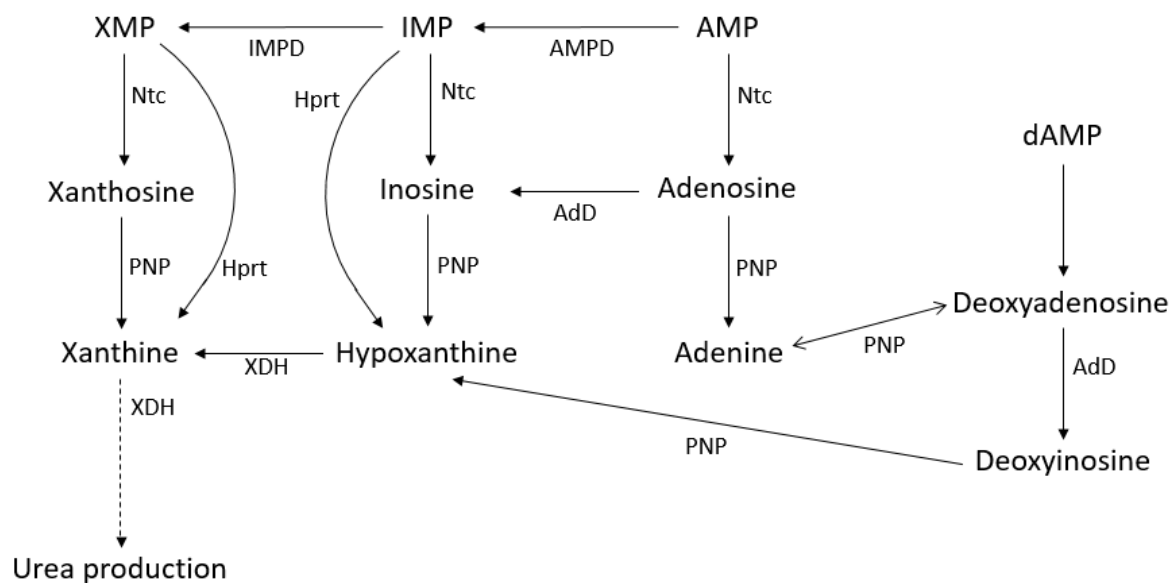


Figure 3.12. Purine metabolism pathway associated with the production of hypoxanthine. AdD - Adenosine deaminase; AMPD - Adenosine monophosphate deaminase; Hprt - Hypoxanthine phosphoribosyltransferase; IMPD - Inosine monophosphate dehydrogenase; Ntc - Cytosolic purine nucleotidase; PNP -Purine nucleotide phosphorylase; XDH - Xanthine dehydrogenase.

#### 3.5.1 Initial investigation

As salmonid species have undergone four whole genome duplications during their evolutionary history (Christensen & Davidson, 2017), several paralogues exist for many genes in these fish. The genes involved in purine metabolism identified in the SalmonDB are listed in Table 3.7. As changing the proportions of nucleotides in the diet may alter the levels of different metabolites within the purine metabolism pathway, the expression of the gene

encoding the enzyme adenosine mono-phosphate kinase (AMPK) was also studied. This enzyme group is involved in energy metabolism, responding to levels of adenosine monophosphate (AMP) relative to other phosphorylated adenine nucleotides. Therefore, this enzyme could be involved in changes in metabolic rate mediated by changes in nucleotide proportions in the diet.

Table 3.7. Full names of the paralogues of the enzymes involved in the purine metabolism pathway or involved in influencing levels of purines in tissues investigated.

Acronym	Full name
PNP5a	Purine nucleoside phosphorylase 5a
PNP5b	Purine nucleoside phosphorylase 5b
PNP6	Purine nucleoside phosphorylase 6
PNP6b	Purine nucleoside phosphorylase 6b
PNP6c	Purine nucleoside phosphorylase 6c
Hprt1	Hypoxanthine phosphoribosyltransferase 1
XDH	Xanthine dehydrogenase
Nt5c3	5'-nucleotidase, cytosolic IIIa
AMPK $\alpha$ 1	Adenosine monophosphate (AMP) kinase $\alpha$ 1
AMPK $\alpha$ 2a	AMP kinase $\alpha$ 2a
AMPK $\alpha$ 3	AMP kinase $\alpha$ 3
AMPK $\beta$ 1	AMP kinase $\beta$ 1
AMPK $\gamma$ 1	AMP kinase $\gamma$ 1
AMPD1	AMP deaminase 1
AMPD3	AMP deaminase 3
AdD1	Adenosine deaminase 1
CNT1	Concentrative nucleotide transporter 1
CNT3	Concentrative nucleotide transporter 3
ENT1a	Equilibrative nucleotide transporter 1a
ENT1b	Equilibrative nucleotide transporter 1b
ENT2	Equilibrative nucleotide transporter 2
ENT3	Equilibrative nucleotide transporter 3
ENT4	Equilibrative nucleotide transporter 4

### *3.5.2 Method*

The expression of purine metabolism genes identified in the SalmonDB (Table 3.7) was investigated in the gill, fin, skin and kidney. The cDNA of parr and freshwater and seawater smolts were pooled for each tissue. This was conducted using standard PCR with Taq polymerase as detailed in General Methods section 2.2.4. Samples were then visualised using gel electrophoresis as detailed in General Methods section 2.2.5, and the genes that were observed to be expressed at the highest levels were selected for further investigation using RT-qPCR as detailed in General Methods section 2.2.9. Code used for statistical analysis is given in Appendix 2.

### *3.5.3 Results of initial purine metabolism investigation*

The results of the initial investigation into the expression of genes involved in purine metabolism are shown in Figure 3.13. Following the investigation of these genes using PCR and gel electrophoresis, more paralogous forms of purine nucleotide phosphorylase were identified in the SalmonDB database. These are detailed below and were used in RT-qPCR studies.

The genes selected for further investigation are listed in Table 3.8.

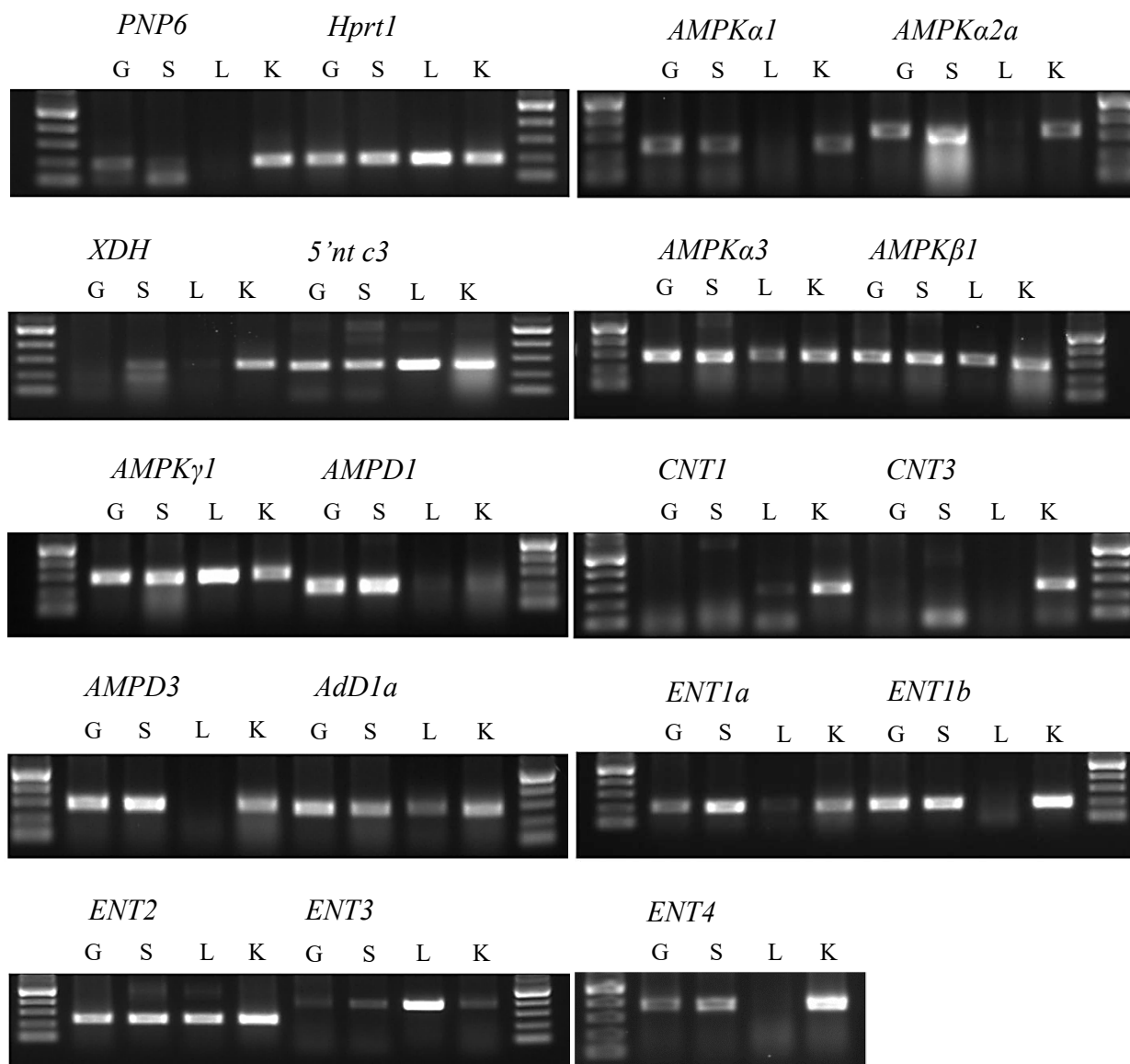


Figure 3.13. Expression of purine metabolism genes in the gill (G), skin (S), liver (L) and kidney (K) of Atlantic salmon measured in pooled cDNA from parr and freshwater and seawater smolts. Ladders show up to 500bp.

Table 3.8. Purine metabolism genes selected for further investigation with RT-qPCR.

Acronym	Full name
AMPK $\alpha$ 2a	Adenosine monophosphate kinase $\alpha$ 2a
Hprt1	Hypoxanthine phosphoribosyltransferase 1
PNP5a	Purine nucleotide phosphorylase 5a
PNP5b	Purine nucleotide phosphorylase 5b
PNP6b	Purine nucleotide phosphorylase 6b
PNP6c	Purine nucleotide phosphorylase 6c

### 3.5.4 RT-qPCR investigation of purine metabolism genes

#### 3.5.4.1 Purine metabolism gene expression on direct transfer trial

The expression of *AMPK $\alpha$ 2a* (Figure 3.14) was not found to be significantly influenced by direct SW transfer ( $F_{2,14} = 2.03$ ,  $p = 0.17$ ).

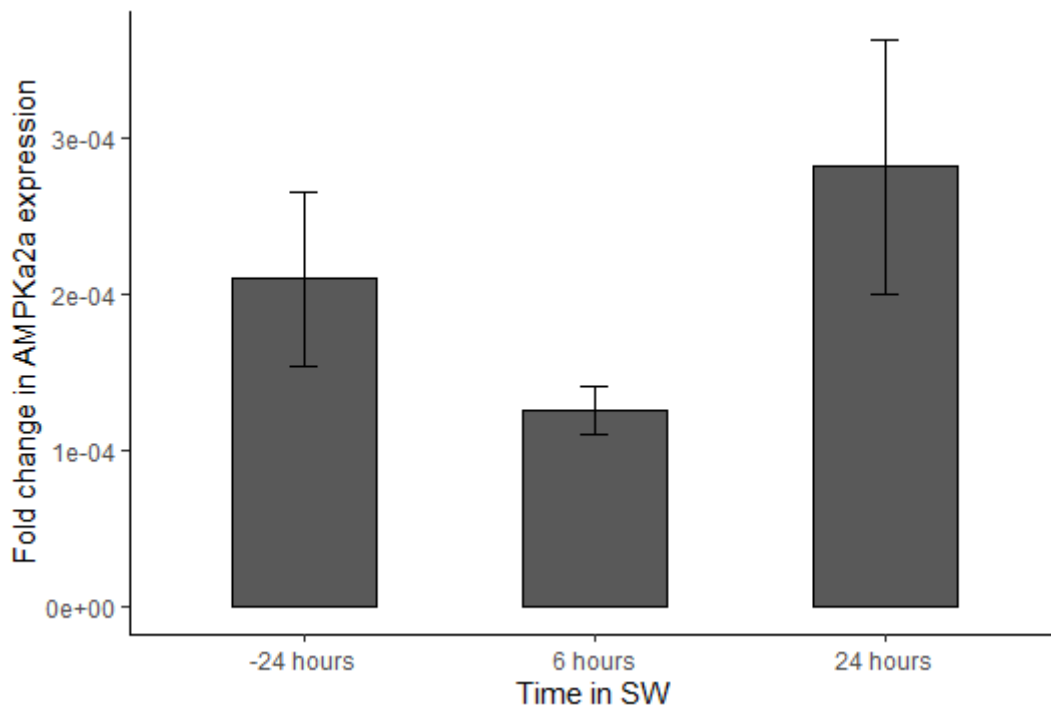


Figure 3.14. Mean fold change in the expression of *AMPK $\alpha$ 2a* relative to *RPLP0* in the skin of Atlantic salmon shortly before and following direct SW transfer. Error bars denote standard error, -24 hours and 6 hours  $n=6$ , 24 hours  $n=5$ .

*Hprt1* expression, shown in Figure 3.15, was not found to be significantly influenced by direct SW transfer in the 24 hours following transfer ( $F_{2,14} = 0.26$ ,  $p = 0.78$ ).

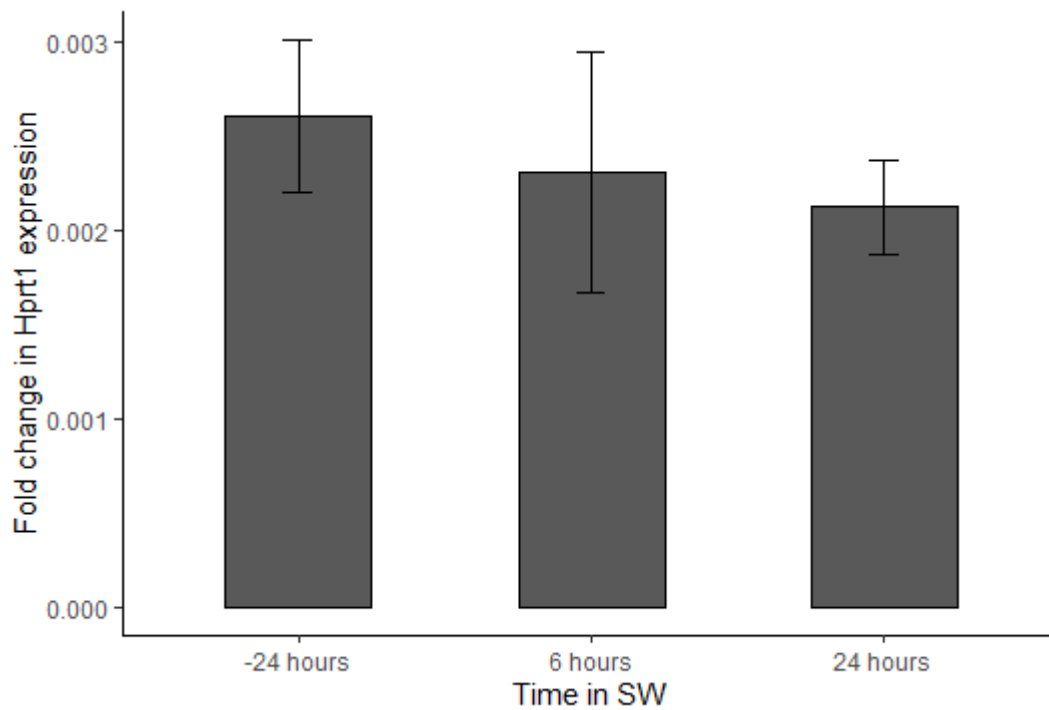


Figure 3.15. Mean fold change in the expression of *Hprt1* relative to *RPLP0* in the skin of Atlantic salmon shortly before and following direct SW transfer. Error bars denote standard error, -24 hours and 6 hours  $n=6$ , 24 hours  $n=5$ .

*PNP5a* expression (Figure 3.16) was found by linear model to be significantly influenced by direct transfer ( $F_{2,14} = 5.44$ ,  $p = 0.018$ ), however, the data were found by Leven's test to have unequal variance ( $F_{2,14} = 7.49$ ,  $p = 0.006$ ). Analysis with Kruskal Wallis rank sum test also found that Direct SW transfer had a significant effect on *PNP5a* expression ( $H_2 = 8.57$ ,  $p = 0.013$ ). Expression of *PNP5a* was significantly lower at 24 hours post SW transfer than at 24 hours prior to SW transfer ( $p = 0.01$ ).

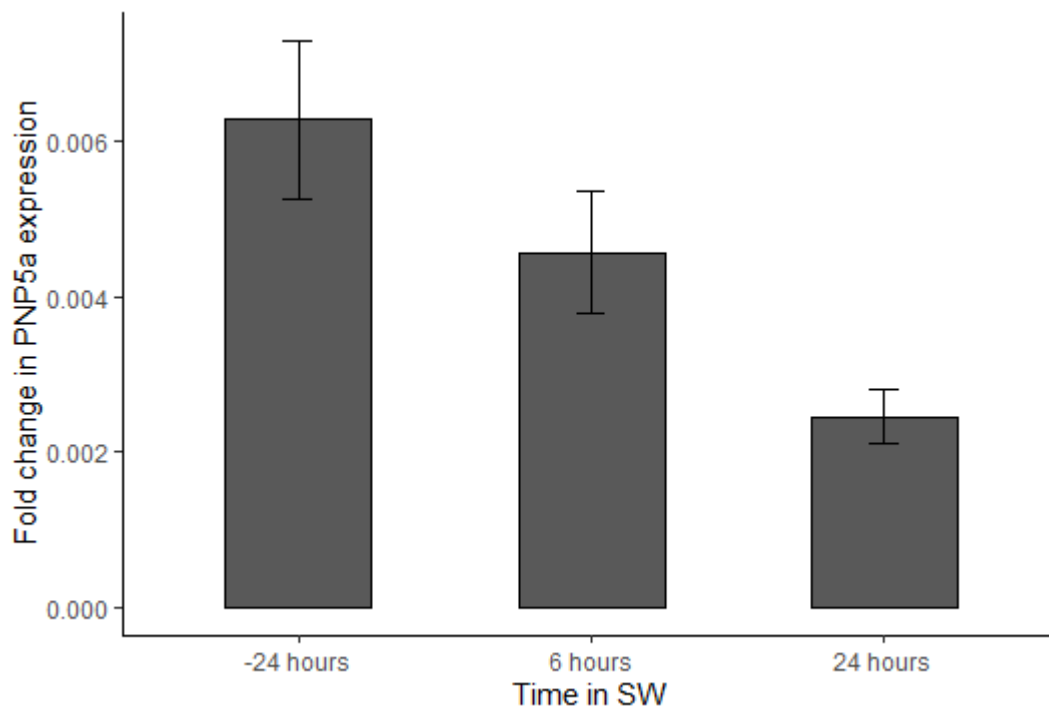


Figure 3.16. Mean fold change in the expression of *PNP5a* relative to *RPLP0* in the skin of Atlantic salmon shortly before and following direct SW transfer. Error bars denote standard error, -24 hours and 6 hours  $n=6$ , 24 hours  $n=5$ .

No significant effect of direct SW transfer on the expression of *PNP5b* ( $F_{2,14} = 0.67$ ,  $p = 0.53$ ), Figure 3.17.

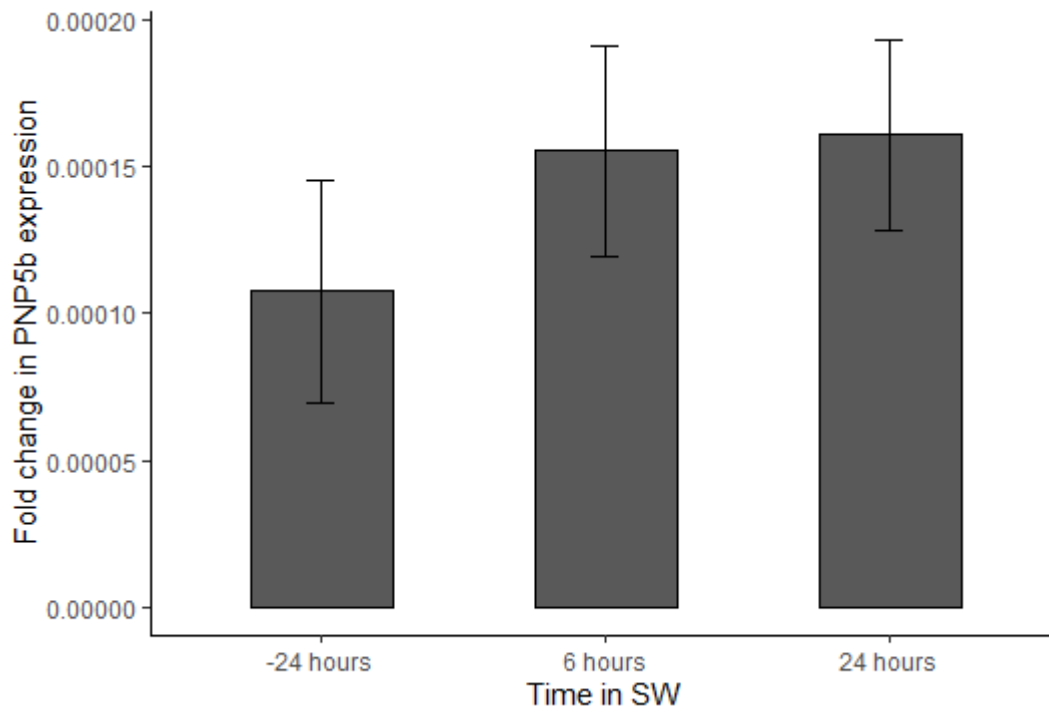


Figure 3.17. Mean fold change in the expression of *PNP5b* relative to *RPLP0* in the skin of Atlantic salmon shortly before and following direct SW transfer. Error bars denote standard error, -24 hours and 6 hours  $n=6$ , 24 hours  $n=5$ .

*PNP6b* expression (Figure 3.18) was not found to be significantly influenced by direct SW transfer up to 24 hours post transfer ( $F_{2,14} = 0.37$ ,  $p = 0.7$ ).

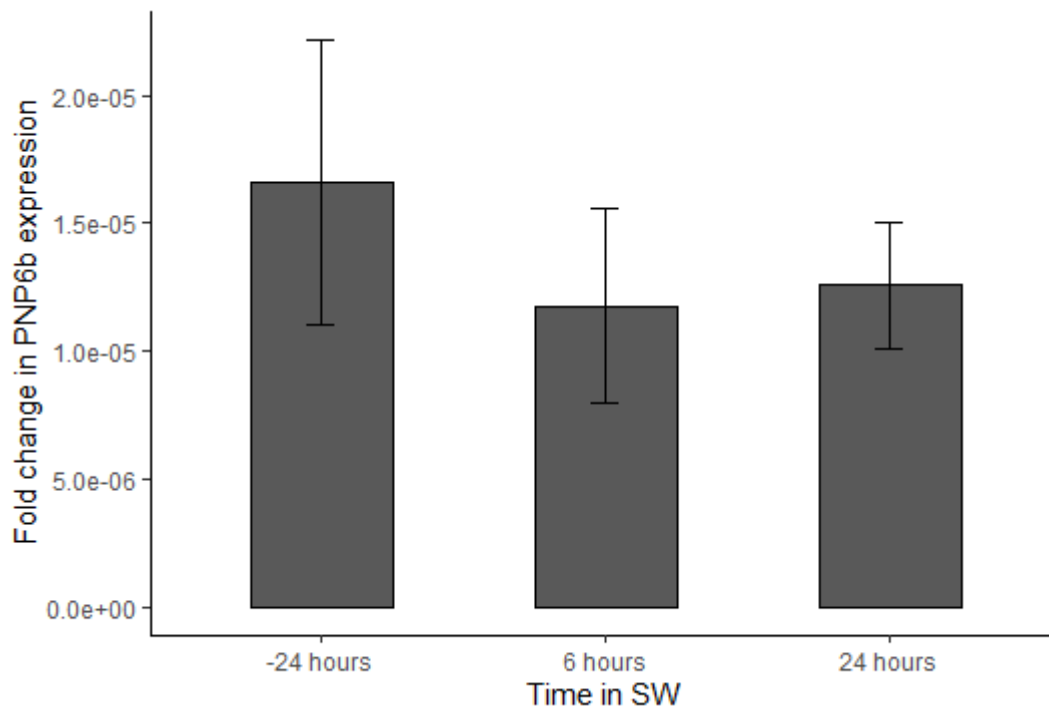


Figure 3.18. Mean fold change in the expression of *PNP6b* relative to *RPLP0* in the skin of Atlantic salmon shortly before and following direct SW transfer. Error bars denote standard error, -24 hours and 6 hours  $n=6$ , 24 hours  $n=5$ .

There was a significant effect of SW transfer on the expression of *PNP6c* ( $F_{2,14} = 7.66$ ,  $p = 0.006$ ). At 6 hours and 24 hours post SW transfer the level of *PNP6c* expression was significantly lower than at 24 hours before SW transfer ( $p = 0.007$  and  $p = 0.02$  respectively).

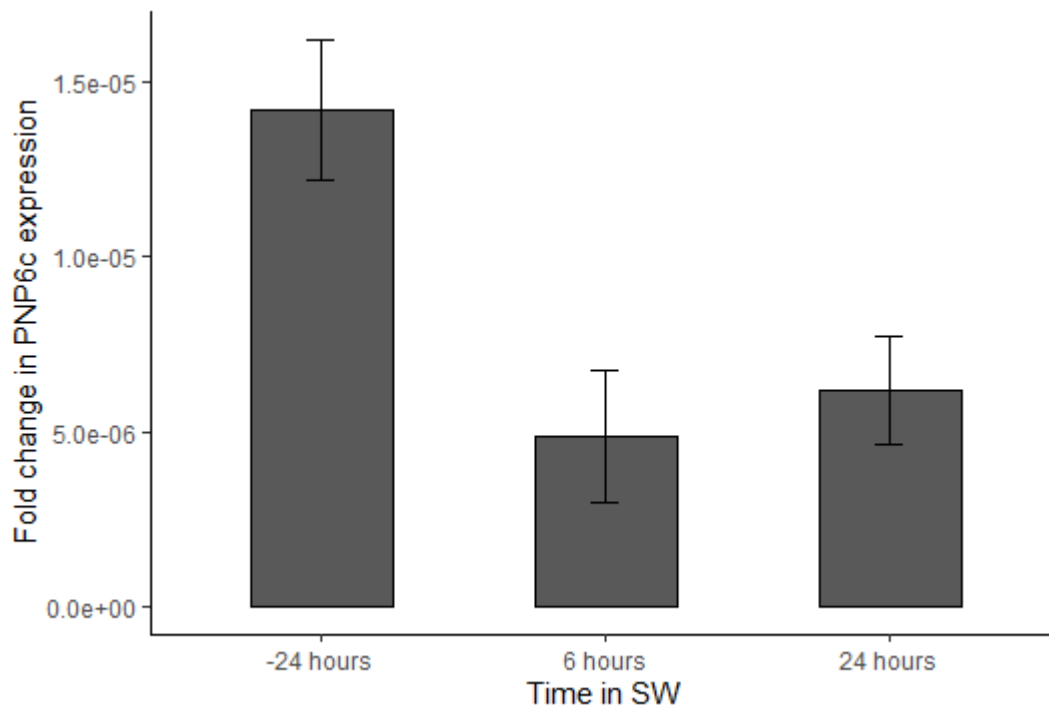


Figure 3.19. Mean fold change in the expression of *PNP6c* relative to *RPLP0* in the skin of Atlantic salmon shortly before and following direct SW transfer. Error bars denote standard error, -24 hours and 6 hours  $n=6$ , 24 hours  $n=5$ .

### 3.5.3.2 Purine metabolism gene expression in fish on the nucleotide supplement feeding trial

*AMPK $\alpha$ 2a* expression was highly variable on some treatments, particularly diet 4 at the time points 2 weeks prior to SW transfer and 3 weeks post SW transfer, and diet 5 24 hours before SW transfer. The level of *AMPK $\alpha$ 2a* expression (Figure 3.20) was found to be significantly influenced by both time point ( $F_{5,309} = 37.65$ ,  $p < 2.2 \times 10^{-16}$ ) and diet ( $F_{5,309} = 5.39$ ,  $p = 9.1 \times 10^{-5}$ ) and the interaction between these variables ( $F_{25,309} = 4.6$ ,  $p = 3.86 \times 10^{-11}$ ). However, when these differences were investigated with pairwise comparisons with correction for multiple comparisons the only significant differences detected were due to time point. Overall expression was higher at baseline, 5 weeks before SW transfer, than at all other time points ( $p < 0.05$ ), at 3 weeks post SW transfer expression of *AMPK $\alpha$ 2a* was lower than at 24 hours post transfer ( $p = 0.007$ ), and 6 weeks post transfer expression was lower than at all previous time points ( $p < 0.0005$ ).

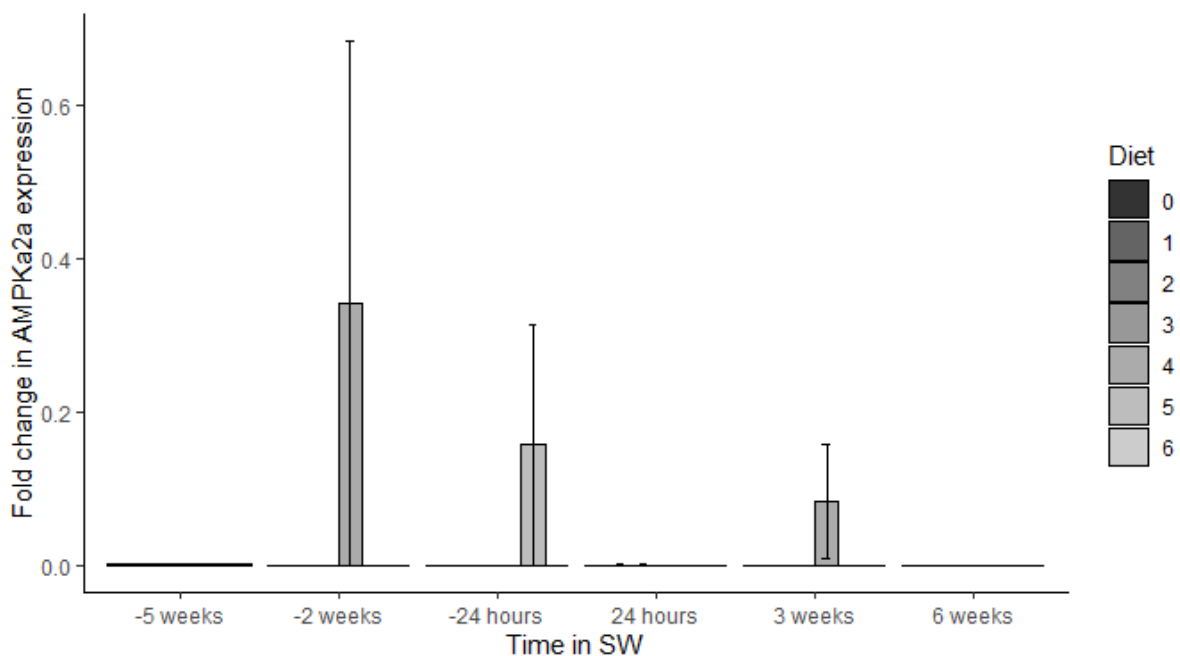


Figure 3.20. Mean fold change in the expression of *AMPK $\alpha$ 2a* relative to *RPLP0* in the skin of Atlantic salmon fed on diets containing varying proportions of nucleotide supplement. Time point 1 represents the baseline before feeding with supplemented diets began. Fish were transferred to SW between time points 3 and 4. Error bars denote standard error.

A significant effect of time point on the expression of *Hprt1* (Figure 3.21) was observed ( $F_{5,307} = 16.13$ ,  $p = 4.02 \times 10^{-14}$ ), along with a significant effect of the interaction between time point and diet ( $F_{25,307} = 2.41$ ,  $p = 0.0003$ ). However, when these differences were investigated with pairwise comparisons with correction for multiple comparisons the only significant differences detected were due to time point. *Hprt1* expression was higher overall at the baseline time point than at 2 weeks and 24 hours before SW transfer ( $p < 0.02$ ), and higher than at 24 hours and 6 weeks post SW transfer ( $p < 0.002$ ). Expression 3 weeks after SW transfer was significantly higher than at all other time points after experimental feeding began ( $p < 0.05$ ).

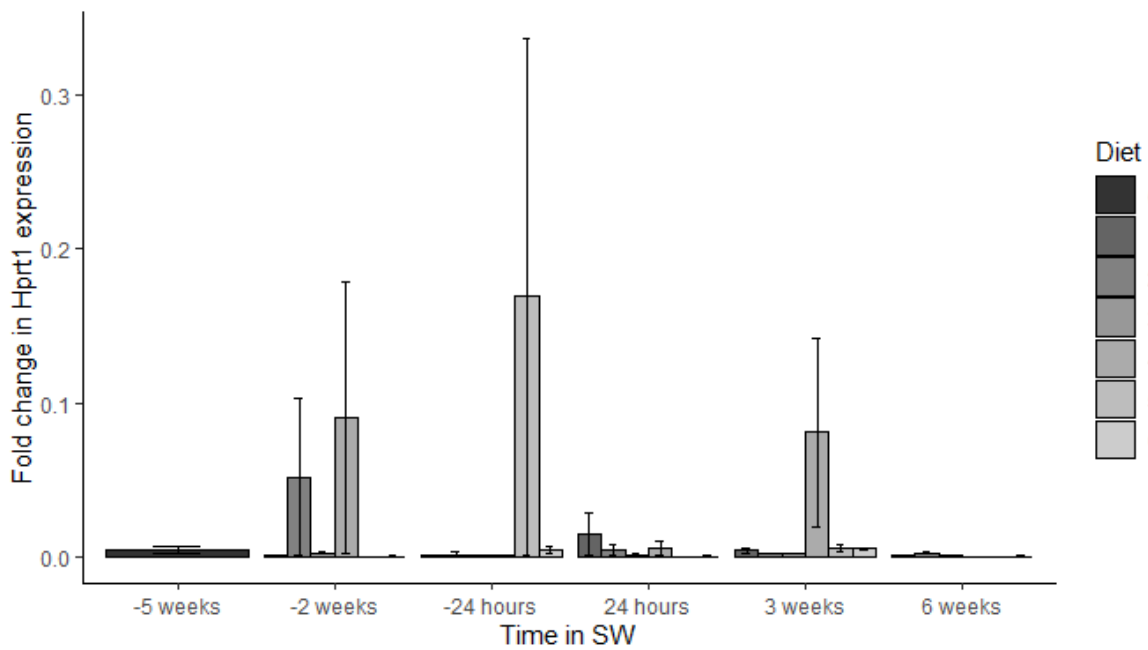


Figure 3.21. Mean fold change in the expression of *Hprt1* relative to *RPLP0* in the skin of Atlantic salmon fed on diets containing varying proportions of nucleotide supplement. Time point 1 represents the baseline before feeding with supplemented diets began. Fish were transferred to SW between time points 3 and 4. Error bars denote standard error.

The expression of *PNP5a* (Figure 3.22) was found to be significantly influenced by time point ( $F_{5,307} = 36.07$ ,  $p < 2.2 \times 10^{-16}$ ), diet ( $F_{5,307} = 2.81$ ,  $p = 0.02$ ) and the interaction between these two variables ( $F_{25,307} = 2.69$ ,  $p = 3.95 \times 10^{-5}$ ). However, when these differences were investigated with pairwise comparisons with correction for multiple comparisons the only significant differences detected were due to time point. *PNP5a* expression was overall significantly higher at the baseline time point 5 weeks before SW transfer than at all other timepoints ( $p < 0.05$ ). Expression 2 weeks before transfer was higher than at 24 hours before transfer ( $p = 0.005$ ) and 6 weeks post transfer ( $p < 0.0001$ ). At 3 weeks post SW transfer *PNP5a* expression were higher than at 24 hours before SW transfer ( $p = 0.0005$ ), 24 hours post SW transfer ( $p = 0.004$ ) and 6 weeks post transfer ( $p < 0.0001$ ).

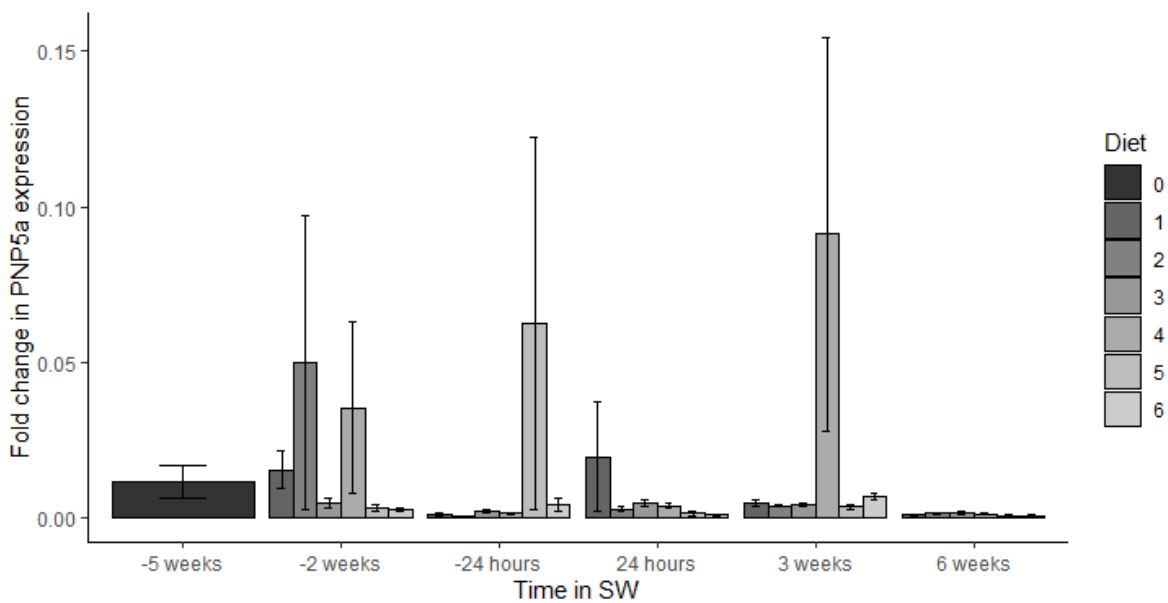


Figure 3.22. Mean fold change in the expression of *PNP5a* relative to *RPLP0* in the skin of Atlantic salmon fed on diets containing varying proportions of nucleotide supplement. Time point 1 represents the baseline before feeding with supplemented diets began. Fish were transferred to SW between time points 3 and 4. Error bars denote standard error.

The expression of *PNP5b* (Figure 3.23) was found to be significantly affected by time point ( $F_{3,201} = 13.02$ ,  $p = 8.28 \times 10^{-8}$ ) and the interaction between time point and diet ( $F_{15,201} = 5.51$ ,  $p = 2.53 \times 10^{-9}$ ). However, when these differences were investigated with pairwise comparisons with correction for multiple comparisons the only significant differences detected were due to time point. At baseline, 5 weeks before SW transfer, *PNP5b* expression was significantly higher than at the other time points investigated, and significantly higher than at 2 weeks before SW transfer ( $p = 0.046$ ) and 24 hours post SW transfer ( $p = 0.009$ ).

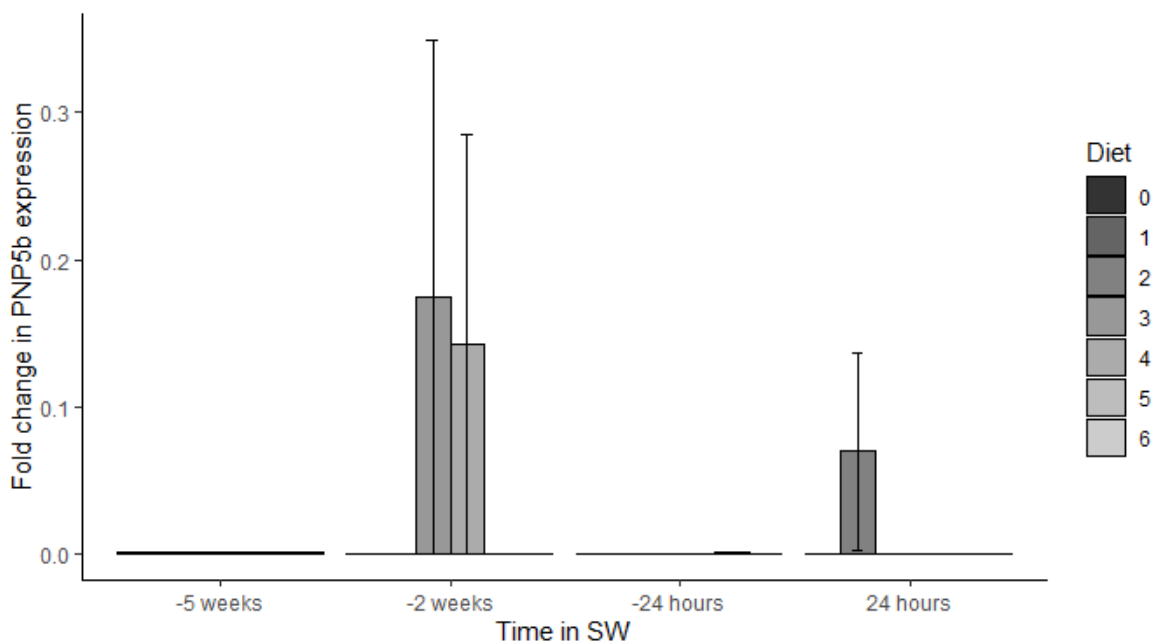


Figure 3.23. Mean fold change in the expression of *PNP5b* relative to *RPLP0* in the skin of Atlantic salmon fed on diets containing varying proportions of nucleotide supplement. Time point 1 represents the baseline before feeding with supplemented diets began. Fish were transferred to SW between time points 3 and 4. Error bars denote standard error.

*PNP6b* expression (Figure 3.24) was found to be significantly affected by time point ( $F_{3,201} = 60.95$ ,  $p < 2.2 \times 10^{-16}$ ) and by the interaction between time point and diet ( $F_{15,201} = 6.42$ ,  $p = 4.29 \times 10^{-11}$ ). However, when these differences were investigated with pairwise comparisons with correction for multiple comparisons the only significant differences detected were due to time point. *PNP6b* expression at baseline, 5 weeks before SW transfer, was significantly higher than at 24 hours before SW transfer ( $p = 0.036$ ).

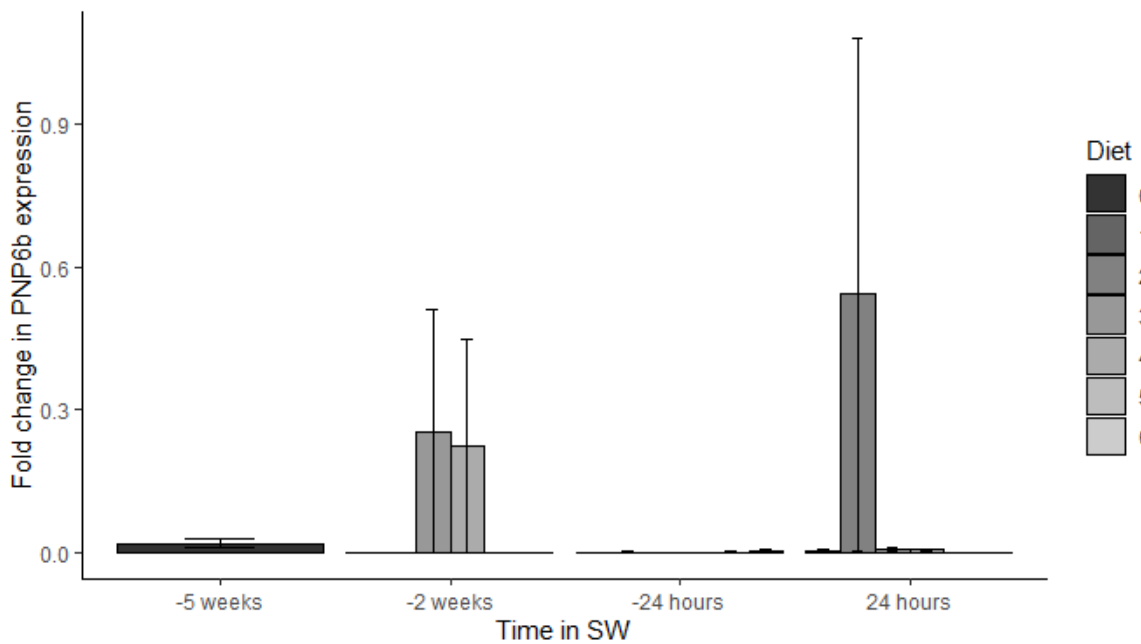


Figure 3.24. Mean fold change in the expression of *PNP6b* relative to *RPLP0* in the skin of Atlantic salmon fed on diets containing varying proportions of nucleotide supplement. Time point 1 represents the baseline before feeding with supplemented diets began. Fish were transferred to SW between time points 3 and 4. Error bars denote standard error.

The expression of *PNP6c* (Figure 3.25) was found to be significantly influenced by time point ( $F_{3,200} = 73.6, p < 2.2 \times 10^{-16}$ ) and the interaction between time point and diet ( $F_{15,200} = 6.59, p = 2.08 \times 10^{-11}$ ). However, when these differences were investigated with pairwise comparisons with correction for multiple comparisons the only significant differences detected were due to time point. Expression was significantly higher at baseline, 5 weeks before SW transfer, than at the following time points ( $p < 0.05$ ). After 24 hours in SW, *PNP6c* expression was significantly higher than at 2 weeks before SW transfer ( $p = 0.039$ ).

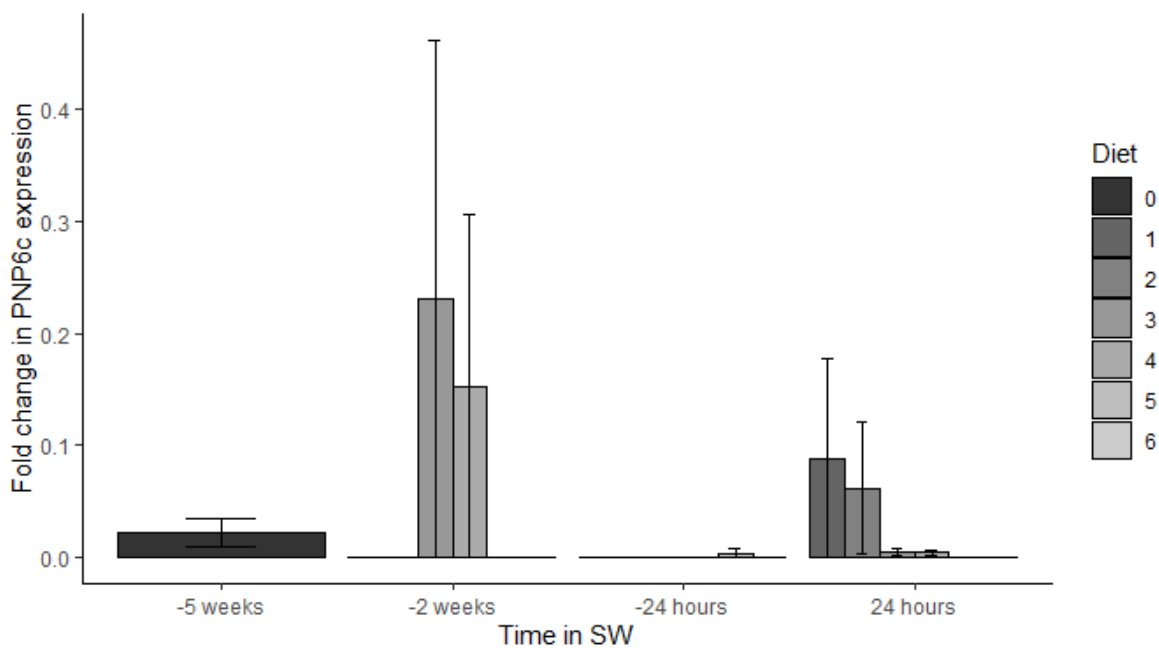


Figure 3.25. Mean fold change in the expression of *PNP6c* relative to *RPLP0* in the skin of Atlantic salmon fed on diets containing varying proportions of nucleotide supplement. Time point 1 represents the baseline before feeding with supplemented diets began. Fish were transferred to SW between time points 3 and 4. Error bars denote standard error.

### 3.5.4.2 Expression of nucleoside transporter genes

Alongside genes involved in purine metabolism, a number of nucleoside transporters were investigated in the skin with the aim of determining whether purine transport was affected by SW transfer or nucleotide supplementation. *Concentrative nucleoside transporter 3 (CNT3)* expression was examined on the direct SW transfer trial. On the nucleotide supplement feeding trial *CNT3* and a number of equilibrative nucleoside transporters were investigated.

No significant effect of direct SW transfer was observed on the expression of *CNT3* expression ( $H_2 = 0.54$ ,  $p = 0.76$ ), Figure 3.26.

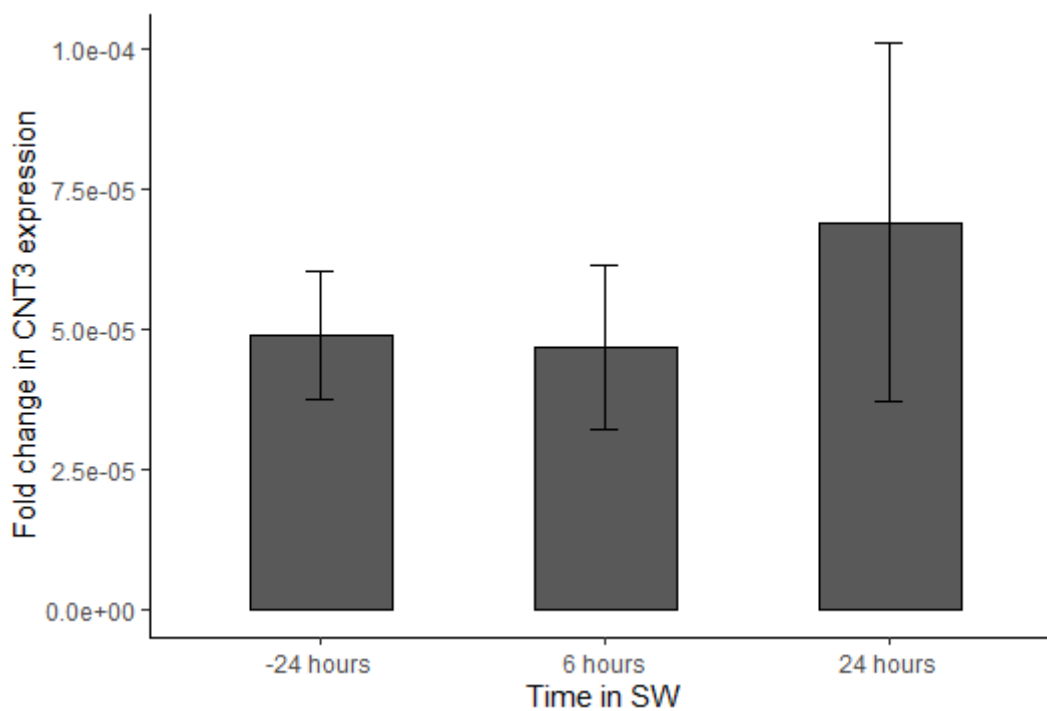


Figure 3.26. Mean fold change in the expression of *CNT3* relative to *RPLP0* in the skin of Atlantic salmon shortly before and following direct SW transfer. Error bars denote standard error, -24 hours and 6 hours n=6, 24 hours n=5.

On the nucleotide supplement feeding trial the level of nucleoside transporters was measured in the skin of fish sampled at the baseline time point before feeding with experimental diets began and at the 24 hours to SW transfer time point on all six diets. This time point was selected because an increase in hypoxanthine levels in the skin had been detected by this stage (Figure 3.11).

*CNT3* expression data (Figure 3.27) were found not to have equal variance ( $F_{1,46} = 20.06$ ,  $p = 4.94 \times 10^{-5}$ ) and were not normally distributed ( $W = 0.5$ ,  $p = 1.49 \times 10^{-11}$ ), results were analysed using a generalised linear model. *CNT3* expression was found to be significantly influenced by time point ( $F_{1,96} = 169.98$ ,  $p < 2.2 \times 10^{-16}$ ) and the interaction between time point and diet ( $F_{5,96} = 4.20$ ,  $p = 0.002$ ). However, when these results were investigated by pairwise comparison with correction for multiple tests, the only significant effect identified was due to time point. *CNT3* expression was significantly lower 24 hours before SW transfer than at the baseline time point 5 weeks before SW transfer ( $p = 0.0001$ ).

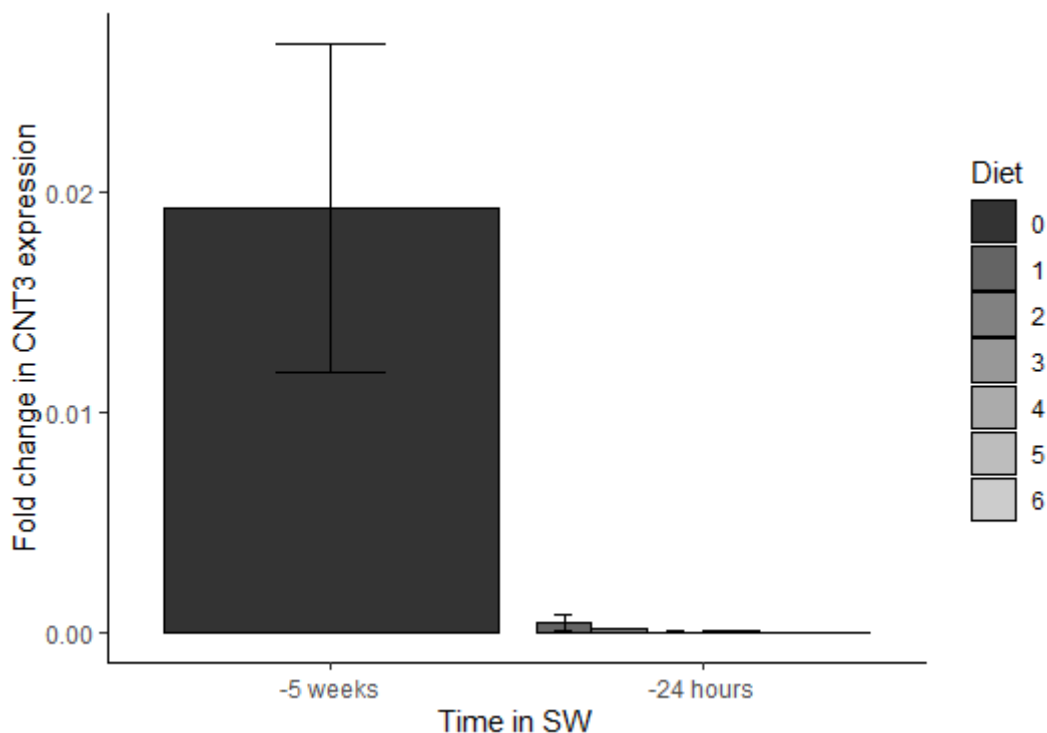


Figure 3.27. Mean fold change in the expression of *CNT3* relative to *RPLP0* in the skin of Atlantic salmon at two time points in FW. Error bars represent standard error,  $n=12$  at -5 weeks and  $n=6$  on each diet at -24 hours.

No significant effect of diet or time point was observed on the expression of *ENT1a* in the skin (Figure 3.28).

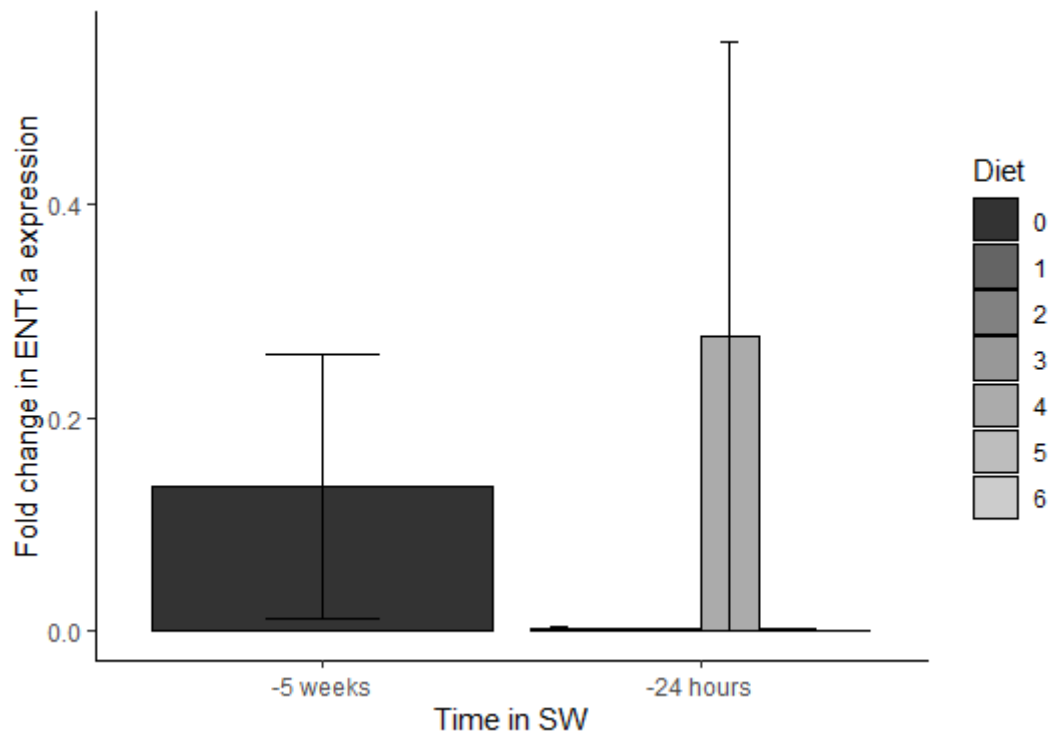


Figure 3.28. Mean fold change in the expression of *ENT1a* relative to *RPLP0* in the skin of Atlantic salmon at two time points in FW. Error bars represent standard error, n=12 at -5 weeks and n=6 on each diet at -24 hours.

The expression of *ENT1b* (Figure 3.29) was significantly influenced by time point ( $F_{1,96} = 52.37$ ,  $p = 1.13 \times 10^{-10}$ ). Expression of *ENT1b* was significantly lower at the 24 hours to SW transfer time point than at baseline ( $p < 0.0001$ ).

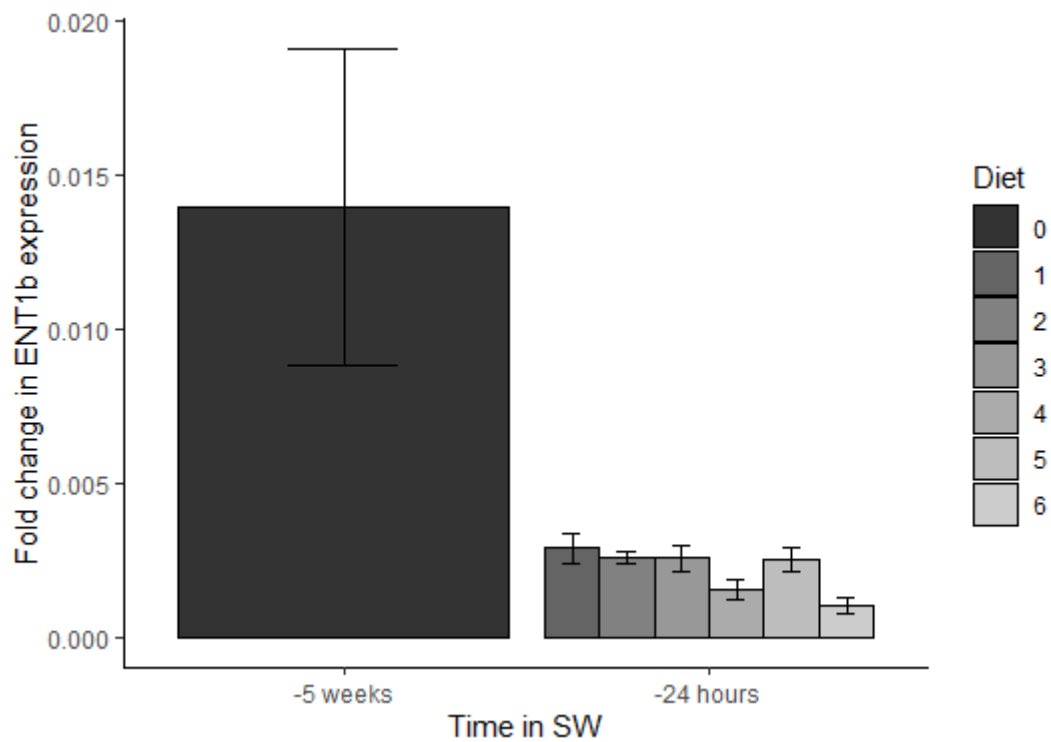


Figure 3.29. Mean fold change in the expression of *ENT1b* relative to *RPLP0* in the skin of Atlantic salmon at two time points in FW. Error bars represent standard error,  $n=12$  at -5 weeks and  $n=6$  on each diet at -24 hours.

*ENT2* expression (Figure 3.30) was significantly affected by time point ( $F_{1,96} = 166.31$ ,  $p < 2 \times 10^{-16}$ ). Expression was significantly lower at the 24 hours to SW transfer time point than at baseline ( $p < 0.0001$ ).

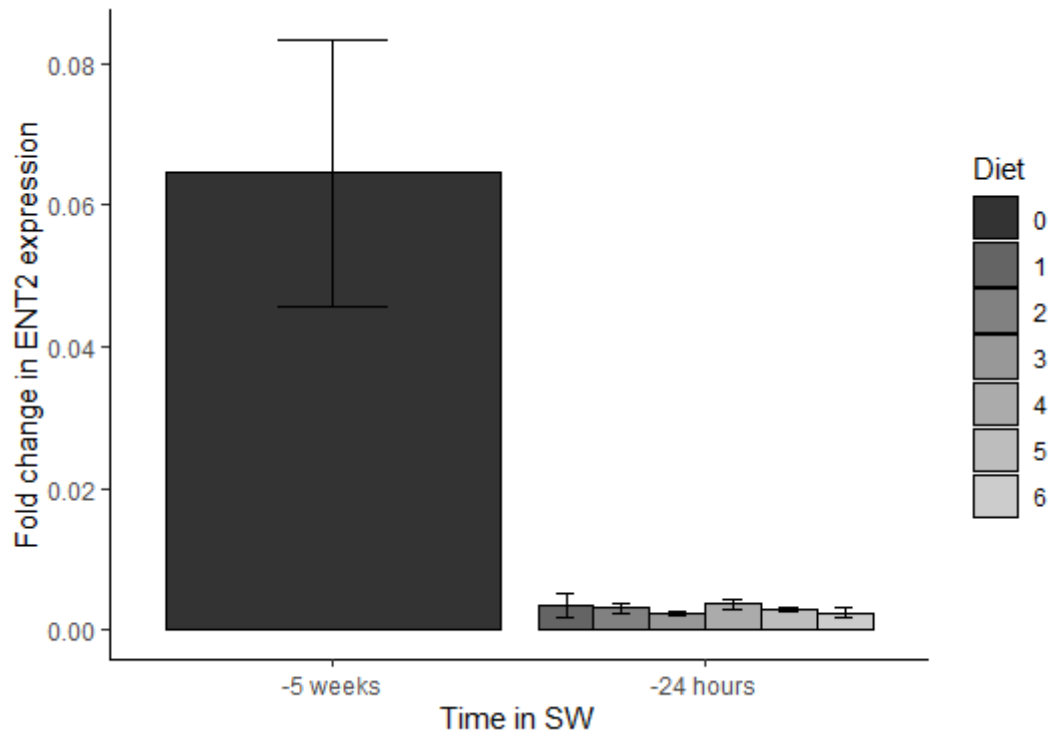


Figure 3.30. Mean fold change in the expression of *ENT2* relative to *RPLP0* in the skin of Atlantic salmon at two time points in FW. Error bars represent standard error,  $n=12$  at -5 weeks and  $n=6$  on each diet at -24 hours.

The expression of *ENT3* (Figure 3.31) was significantly influenced by time point ( $F_{1,96} = 19.79$ ,  $p = 2.32 \times 10^{-5}$ ). However, investigation by pairwise comparison with adjustment for multiple comparisons did not give a statistically significant difference between expression at the two time points ( $p = 0.13$ ).

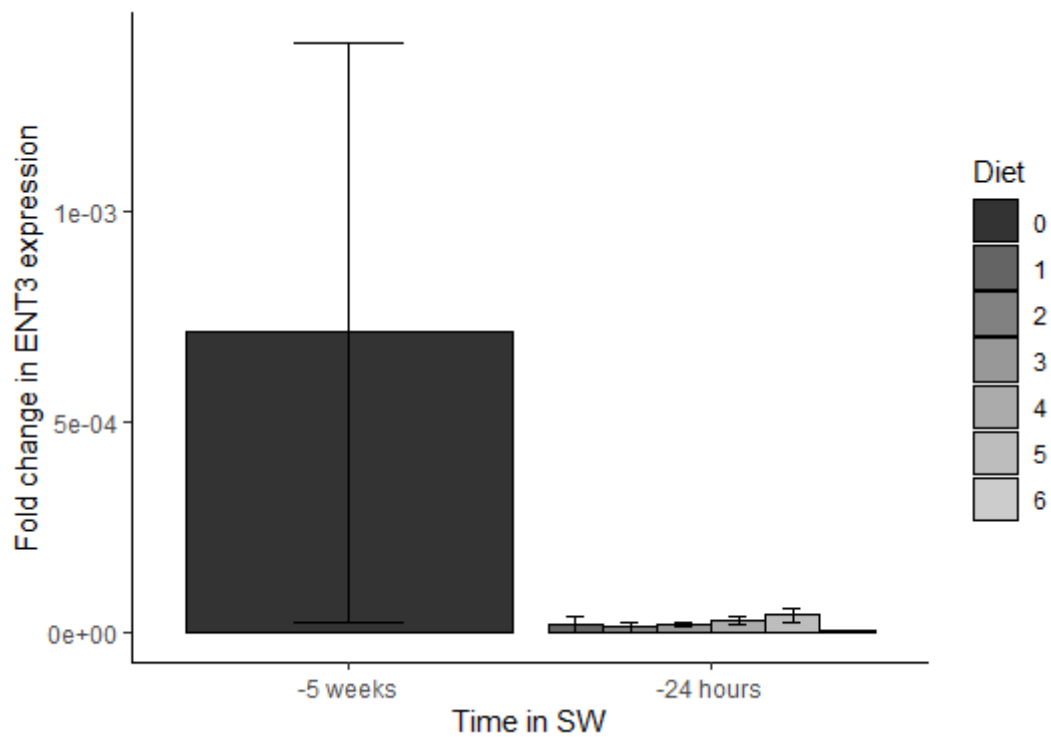


Figure 3.31. Mean fold change in the expression of *ENT3* relative to *RPLP0* in the skin of Atlantic salmon at two time points in FW. Error bars represent standard error,  $n=12$  at -5 weeks and  $n=6$  on each diet at -24 hours.

*ENT4* expression was significantly influenced by time point ( $F_{1,96} = 112.85$ ,  $p < 2 \times 10^{-16}$ ), Figure 3.32. Expression was significantly lower at the 24 hours to transfer time point than at baseline ( $p < 0.001$ ).

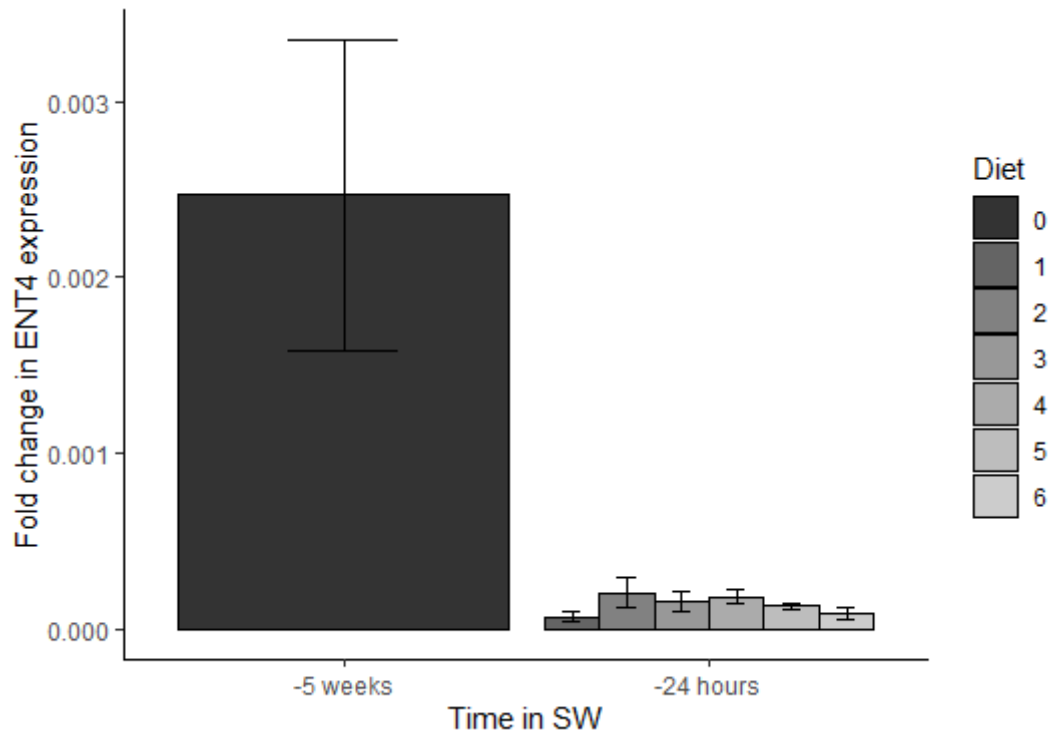


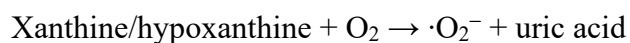
Figure 3.32. Mean fold change in the expression of *ENT4* relative to *RPLP0* in the skin of Atlantic salmon at two time points in FW. Error bars represent standard error,  $n=12$  at -5 weeks and  $n=6$  on each diet at -24 hours.

### 3.5.5 Xanthine dehydrogenase

Xanthine dehydrogenase (XDH) is related to aldehyde oxidases (AOX), however, XDH preferentially acts on the purines hypoxanthine and xanthine, while the substrate specificity of AOX is broad (Terao *et al.*, 2016). A single functional XDH gene has been identified in all vertebrate genomes investigated (Terao *et al.*, 2016). XDH is important in the breakdown of purines as it converts hypoxanthine to xanthine, and xanthine to uric acid (Terao *et al.*, 2016). In humans XDH can exist in two enzymatic forms, xanthine dehydrogenase (XDH) and xanthine oxidase (XOD). These enzymes catalyse the rate limiting step in the breakdown of purines (Chung *et al.*, 1997). Both forms of the enzyme convert xanthine and/or hypoxanthine to uric acid, using different co-factors. XDH catalyses the reaction:



producing NADH and uric acid. While XOD catalyses the reaction:



producing a super oxide ion and uric acid.

In mammals the XDH form of the protein can be reversibly converted to the XOD form by the oxidation of amino acid residues containing sulphhydryl groups, or irreversibly converted to the XOD form by proteolytic processes (Terao *et al.*, 2016). XOD is viewed as a source of free radicals which cause oxidative damage. While the fish XDH does not contain the equivalent motifs which allow the mammalian form to be converted to XOD, it appears that fish XDH does show XOD activity, producing H<sub>2</sub>O<sub>2</sub> which can perform a role in the innate immune response, targeting microbes and ectoparasites (Sinha *et al.*, 2015; Xu *et al.*, 2012; Zhao *et al.*, 2014).

### 3.5.5.1 Objectives and methods

Over the course of this project the SalmonDB database was the primary source of salmonid sequence information (<http://salmondb.cmm.uchile.cl/>). The sequence of *xanthine dehydrogenase* (*XDH*) in the SalmonDB was incomplete (sequence alignments in Appendix 3). When *XDH* sequence fragments from the SalmonDB (SS2U045801, SS2U039842, SS2U007333, SS2U007334, SS2U038182, SS2U018457, SS2U036705, SS2U006602, SS2U045801) and NCBI (BT072730.1) databases were aligned two gaps in the sequence were identified. Sequencing was carried out with the aim of completing the sequence.

Primers were designed to amplify sections of the sequence which overlapped with the missing fragments and the surrounding known sequence. The primers used to amplify *XDH* sequences are listed in Table 1. The amplified fragments were cloned and sequenced as detailed in the Material and Methods sections 2.6 – 2.9.

Table 1: primers used to amplify the *XDH* sequence.

Primer sequence 5'-3'	Sense/Antisense	Amplicon size	Primer use
GAGCAACTCCGCTGGTTTGCTGGAC	S	408 bp	Primers used to amplify missing sections of <i>XDH</i> sequence
GGCCATGACGGTAGTAGCAGCCATC	AS		
GTCAACCGTCGTCAAGCACCTGGCC	S	863 bp	
CACACAGGCTGACCACATTCTGGAGG	AS		
GCCCTACTGCTGCCTCCGCTTC	S	268 bp	Primers used for RT-qPCR
ATCTCCACCTCAGAGCAGGCCACTC	AS		

### 3.5.5.2 Sequencing results

The Clustal O (1.2.3) multiple sequence alignments for the fragments sequenced in this project and those in the SalmonDB and NCBI databases are given below.

CLUSTAL O (1.2.3) multiple sequence alignment for the consensus sequence for the 408bp fragment sequenced in this project and the SS2U007333 and SS2U007334 sequence fragments from SalmonDB.

```
SS2U007333      GAGGACGTGTTGTGGTGGCAAGGGGAAGGAAAACGGCTGCTGCATGACCGACGGTGACAA
XDH408bpfragment -----
SS2U007334      -----

SS2U007333      GACTAAAGGGTACTGACGATCATGTCACCAGGACCTCAGTGTTCCTGCTCCTCTCTA
XDH408bpfragment -----
SS2U007334      -----

SS2U007333      CAACCCAGCTGACTTCCTCCCTCTGGACCCCACTCAGGAGATCATCTCCACCGGAGCT
XDH408bpfragment -----
SS2U007334      -----

SS2U007333      GATGTCCCTGTGTAAAGGCCAGTCCTCTCAACAGCTGAGGTTTACAGAGAGAGAGGGTCT
XDH408bpfragment -----
SS2U007334      -----

SS2U007333      GTGGCTCCAGCCAGCTTCTCTGGATCAACTTCTAGAGCTTAAGACTCAGTACCCCAACGC
XDH408bpfragment -----
SS2U007334      -----

SS2U007333      CAAGATGGTGGTTGGTAACACGGAAGTCGGTATTGAGATGAAGTTAAGAACCTGTTGTA
XDH408bpfragment -----
SS2U007334      -----

SS2U007333      TCCTGTTATTCTGGCCCCGGCGTACATCCCCGAGCTCAACGCCATACAGCACACTGACGA
XDH408bpfragment -----
SS2U007334      -----

SS2U007333      GGGTATAGTATTTGGAGCATCCTGTTCCCTGACCCTGCTGGGTGATGTGCTGAAGGAAGC
XDH408bpfragment -----
SS2U007334      -----

SS2U007333      GGTGGGTAAACTGCCCTCTACCAGACTGAAGTCTTCACCTCTATACTGGAGCAACTCCG
XDH408bpfragment -----GAGCAACTCCG
SS2U007334      -----

SS2U007333      CTGGTTTGCTGGACTACAGATACGCAACGTGGCAGCCGTTGGAGGTAACATCATGACTGC
XDH408bpfragment CTGGTTTGCTGGACTACAGATACGCAACGTGGCAGCCGTTGGAGGTAACATCATGACTGC
SS2U007334      -----

SS2U007333      CAGCCCCATCTCCGACCTCAACCCTGTCTTTATGGCTGCTGGCTGCAAGCTCACACTCAT
XDH408bpfragment CAGCCCCATCTCCGACCTCAACCCTGTCTTTATGGCTGCTGGCTGCAAGCTCACACTCAT
SS2U007334      -----
```

```

SS2U007333          GTCCAAAGGTGGTGGTGAGCGTGTGGTTGTGATGAATGAGAAGTTCTTCCCAGGTTACAG
XDH408bpfragment    GTCCAAAGGTGGTGGTGAGCGTGTGGTTGTGATGGATGAGAAGTTCTTCCCAGGTTACAG
SS2U007334          -----

```

```

SS2U007333          AAGAACCATTCTGACACCTGAGGAGGTTCTTCTATGTGTCCTGAT-----
XDH408bpfragment    AAGAACCATC-CTGACACCTGAGGAGGTTCTTCTATGTGTCCTGATCCCGTACACCAAGA
SS2U007334          -----TC-CTGACACCTGAGGAGGTTCTTTTATGTGTCCTGATCCCGTACACCAAGA

```

```

SS2U007333          -----
XDH408bpfragment    AGGGTCAGTATTTTGTGCCTATAAGCAGTCTCCTCGTCGTGAGGATGACATCAGCATTG
SS2U007334          AGGGTCAGTATTTTGTGCCTATAAGCAGTCTCCTCGTCGTGAGGATGACATCAGCATTG

```

The SS2U045801 sequence reported here is cropped beyond the point of overlap with the sequences produced in this project. The full sequence can be found in Appendix 3.

CLUSTAL O (1.2.3) multiple sequence alignment for the 863bp fragment sequenced in this project from three clones and the SS2U007334 and SS2U045801 sequence fragments from SalmonDB.

```

SS2U007334          TCCTGACACCTGAGGAGGTTCTTTTATGTGTCCTGATCCCGTACACCAAGAAGGGTCAGT
SS2U045801          -----
XDH863c13T3revcomp -----
XDH863c13T7          -----
XDH863c11T3revcomp -----
XDH863c11T7          -----
XDH863c12T3          -----
XDH863c12T7revcomp -----

```

```

SS2U007334          ATTTTGTGCCTATAAGCAGTCTCCTCGTCGTGAGGATGACATCAGCATTGTGACGTCAG
SS2U045801          -----
XDH863c13T3revcomp -----
XDH863c13T7          -----
XDH863c11T3revcomp -----
XDH863c11T7          -----
XDH863c12T3          -----
XDH863c12T7revcomp -----

```

```

SS2U007334          GGATGAGTGTGACATTGCCGAGGGGTCAACCGTCGTCAAGCACCTGGCCCTTAGTTACG
SS2U045801          -----
XDH863c13T3revcomp -----GTC AACCGTCGTCAAGCACCTGGCCCTTAGTTACG
XDH863c13T7          -----GTC AACCGTCGTCAAGCACCTGGCCCTTAGTTACG
XDH863c11T3revcomp -----GTC AACCGTCGTCAAGCACCTGGCCCTTAGTCACG
XDH863c11T7          -----GTC AACCGTCGTCAAGCACCTGGCCCTTAGTCACG
XDH863c12T3          -----GTC AACCGTCGTCAAGCACCTGGCCTTTAGTTACG
XDH863c12T7revcomp -----GTC AACCGTCGTCAAGCACCTGGCCTTTAGTTACG

```

```

SS2U007334          GAGGGATGGCTGCTACTACCGTCATGGCCAAGAACACAGCCAGCAGACTTTTGGGAC---
SS2U045801          -----
XDH863c13T3revcomp GAGGGATGGCTGCTACTACCGTCATGGCCAAGAACACAGCCAGCAGACTTTTGGGACAAC
XDH863c13T7          GAGGGATGGCTGCTACTACCGTCATGGCCAAGAACACAGCCAGCAGACTTTTGGGACAAC
XDH863c11T3revcomp GAGGGATGGCTGCTACTACCGTCATGGCCAAGAACACAGCCAGCAGACTTTTGGGACAAC
XDH863c11T7          GAGGGATGGCTGCTACTACCGTCATGGCCAAGAACACAGCCAGCAGACTTTTGGGACAAC
XDH863c12T3          GAGGGGTGGCTGCTACTACCGTCATGGCCAAGAACACAGCCAGCAGACTTTTGGGACAAC
XDH863c12T7revcomp GAGGGGTGGCTGCTACTACCGTCATGGCCAAGAACACAGCCAGCAGACTTTTGGGACAAC

```

SS2U007334  
SS2U045801  
XDH863c13T3revcomp AATGGGGGGAAGAGCTTCTGCAGGATGCTTGTTCCTCATTGGCTGAGGAGATGACCCTTC  
XDH863c13T7 AATGGGGGGAAGAGCTTCTGCAGGATGCTTGTTCCTCATTGGCTGAGGAGATGACCCTTC  
XDH863c11T3revcomp AATGGGGGGAAGAGCTTCTGCAGGATGCTTGTTCCTCATTGGCTGAGGAGATGACCCTTC  
XDH863c11T7 AATGGGGGGAAGAGCTTCTGCAGGATGCTTGTTCCTCATTGGCTGAGGAGATGACCCTTC  
XDH863c12T3 AATGGGGGGAAGAGCTTCTGCAGGATGCTTGTTCCTCATTGGCTGAGGAGATGACCCTTC  
XDH863c12T7revcomp AATGGGGGGAAGAGCTTCTGCAGGATGCTTGTTCCTCATTGGCTGAGGAGATGACCCTTC

SS2U007334  
SS2U045801  
XDH863c13T3revcomp ACCCCTCTGTGCCGGGTGGCATGGTGACCTACAGACGAACTCTGACCCTCAGCCTGTTTT  
XDH863c13T7 ACCCCTCTGTGCCGGGTGGCATGGTGACCTACAGACGAACTCTGACCCTCAGCCTGTTTT  
XDH863c11T3revcomp ACCCCTCTGTGCCGGGTGGCATGGTGACCTACAGACGAACTCTGACCCTCAGCCTGTTTT  
XDH863c11T7 ACCCCTCTGTGCCGGGTGGCATGGTGACCTACAGACGAACTCTGACCCTCAGCCTGTTTT  
XDH863c12T3 ACCCCTCTGTGCCGGGTGGCATGGTGACCTACAGACGAACTCTGACCCTCAGCCTGTTTT  
XDH863c12T7revcomp ACCCCTCTGTGCCGGGTGGCATGGTGACCTACAGACGAACTCTGACCCTCAGCCTGTTTT

SS2U007334  
SS2U045801  
XDH863c13T3revcomp ACAAGTTTTACCTGACTGTACAACAGAACTGGCCAGTGAGGGTGCAGATATGGAGGGTG  
XDH863c13T7 ACAAGTTTTACCTGACTGTACAACAGAACTGGCCAGTGAGGGTGCAGATATGGAGGGTG  
XDH863c11T3revcomp ACAAGTTTTACCTGACTGTACAACAGAACTGGCCAGTGAGGGTGCAGATATGGAGGGTG  
XDH863c11T7 ACAAGTTTTACCTGACTGTACAACAGAACTGGCCAGTGAGGGTGCAGATATGGAGGGTG  
XDH863c12T3 ACAAGTTTTACCTGACTGCACAACAGAACTGGCCAGTGAGGGTGCAGATATGGAGGGTG  
XDH863c12T7revcomp ACAAGTTTTACCTGACTGCACAACAGAACTGGCCAGTGAGGGTGCAGATATGGAGGGTG

SS2U007334  
SS2U045801  
XDH863c13T3revcomp TCAGGGCTGACTACATCAGTGCTACAGAGATCTACCACCAGACGTCCCCCTCCAGTGTCC  
XDH863c13T7 TCAGGGCTGACTACATCAGTGCTACAGAGATCTACCACCAGACGTCCCCCTCCAGTGTCC  
XDH863c11T3revcomp TCAGGGCTGACTACATCAGTGCTACAGAGATCTACCACCAGACGTCCCCCTCCAGTGTCC  
XDH863c11T7 TCAGGGCTGACTACATCAGTGCTACAGAGATCTACCACCAGACGTCCCCCTCCAGTGTCC  
XDH863c12T3 TCAGGGCTGACTACATCAGTGCTACAGAGATCTACCACCAGACGTCCCCCTCCAGTGTCC  
XDH863c12T7revcomp TCAGGGCTGACTACATCAGTGCTACAGAGATCTACCACCAGACGTCCCCCTCCAGTGTCC

SS2U007334  
SS2U045801  
XDH863c13T3revcomp -----GTTGGACGGTCAGAAGGAGGAGGACGTGGTGGGCCGTCCCATGA  
XDH863c13T7 AGATTCTCCAGGCGGTTCCAGACGGTCAGAAGGAGGAGGACGTGGTGGGCCGTCCCATGA  
XDH863c11T3revcomp AGATTCTCCAGGCGGTTCCAGACGGTCAGAAGGAGGAGGACGTGGTGGGCCGTCCCATGA  
XDH863c11T7 AGATTCTCCAGGCGGTTCCAGACGGTCAGAAGGAGGAGGACGTGGTGGGCCGTCCCATGA  
XDH863c12T3 AGATTCTCCAGGCGGTTCCAGACGGTCAGAAGGAGGAGGACGTGGTGGGCCGTCCCATGA  
XDH863c12T7revcomp AGATTCTCCAGGCGGTTCCAGACGGTCAGAAGGAGGAGGACGTGGTGGGCCGTCCCATGA

SS2U007334  
SS2U045801  
XDH863c13T3revcomp TGCACCTCTCAGCCATGAAGCAGGCGACGGGCGAGGCGGTTTACTGTGATGACATCCCTC  
XDH863c13T7 TGCACCTCTCAGCCATGAAGCAGGCGACGGGCGAGGCGGTTTACTGTGATGACATCCCTC  
XDH863c11T3revcomp TGCACCTCTCAGCCATGAAGCAGGCGACGGGCGAGGCGGTTTACTGTGATGACATCCCTC  
XDH863c11T7 TGCACCTCTCAGCCATGAAGCAGGCGACGGGCGAGGCGGTTTACTGTGATGACATCCCTC  
XDH863c12T3 TGCACCTCTCAGCCATGAAGCAGGCGACGGGCGAGGCGGTTTACTGTGATGACATCCCTC  
XDH863c12T7revcomp TGCACCTCTCAGCCATGAAGCAGGCGACGGGCGAGGCGGTTTACTGTGATGACATCCCTC

SS2U007334  
SS2U045801  
XDH863c13T3revcomp TCTACGAGAATGAACCTACCTCTGTCTTATAACCAGCACCAAGGCCACGCACGCATAC  
XDH863c13T7 TCTACGAGAATGAACCTACCTCTGTCTTATAACCAGCACCAAGGCCACGCACGCATAT  
XDH863c11T3revcomp TCTACGAGAATGAACCTACCTCTGTCTTATAACCAGCACCAAGGCCACGCACGCATAC  
XDH863c11T7 TCTACGAGAATGAACCTACCTCTGTCTTATAACCAGCACCAAGGCCACGCACGCATAC  
XDH863c12T3 TCTACGAGAATGAACCTACCTCTGTCTTATAACCAGCACCAAGGCCACGCACGCATAC  
XDH863c12T7revcomp TCTACGAGAATGAACCTACCTCTGTCTTATAACCAGCACCAAGGCCACGCACGCATAC

SS2U007334  
SS2U045801  
XDH863c13T3revcomp  
XDH863c13T7  
XDH863c11T3revcomp  
XDH863c11T7  
XDH863c12T3  
XDH863c12T7revcomp

-----  
AGTCTATAGCTACATCGGAGGCAGAGAGTATGCCAGGTGTGGTGACGTGTGTGTTTGCCA  
AGTCTATAGATAACATCGGAGGCAGAGAGTATGCCAGGTGTGGTGACGTGTGTGTTTGCCA  
AGTCTATAGATAACATCGGAGGCAGAGAGTATGCCAGGTGTGGTGACGTGTGTGTTTGCCA  
AGTCTATAGATAACATCGGAGGCAGAGAGTATGCCAGGTGTGGTGACGTGTGTGTTTGCCA  
AGTCTATAGATAACATCGGAGGCAGAGAGTATGCCAGGTGTGGTGACGTGTGTGTTTGCCA  
AGTCTATAGATAACATCGGAGGCAGAGAGTATGCCAGGTGTGGTGACGTGTGTGTTTGCCA  
AGTCTATAGATAACATCGGAGGCAGAGAGTATGCCAGGTGTGGTGACGTGTGTGTTTGCCA

SS2U007334  
SS2U045801  
XDH863c13T3revcomp  
XDH863c13T7  
XDH863c11T3revcomp  
XDH863c11T7  
XDH863c12T3  
XDH863c12T7revcomp

-----  
AGGACATCCCTGGCAGCAACATGACAGGACCTATCATCTACGATGAGACTGTCTCTCGCTG  
AGGACATCCCTGGCAGCAACATGACAGGACCTATCATCTACGGTGAGACTGTCTCTCGCTG  
AGGACATCCCTGGCAGCAACATGACAGGACCTATCATCTACGGTGAGACTGTCTCTCGCTG  
AGGACATCCCTGGCAGCAACATGACAGGACCTATCATCTACGATGAGACTGTCTCTCGCTG  
AGGACATCCCTGGCAGCAACATGACAGGACCTATCATCTACGATGAGACTGTCTCTCGCTG  
AGGACATCCCTGGCAGCAACATGACAGGACCTATCATCTACGATGAGACTGTCTCTCGCTG  
AGGACATCCCTGGCAGCAACATGACAGGACCTATCATCTACGATGAGACTGTCTCTCGCTG  
AGGACATCCCTGGCAGCAACATGACAGGACCTATCATCTACGATGAGACTGTCTCTCGCTG

SS2U007334  
SS2U045801  
XDH863c13T3revcomp  
XDH863c13T7  
XDH863c11T3revcomp  
XDH863c11T7  
XDH863c12T3  
XDH863c12T7revcomp

-----  
TTGACACGGTGACCTGTGTGGGCCACATCATAGGAGCGGTAGTAGCAGACACTCAGGCTC  
TTGACACGGTGACCTGTGTGGGCCACATCATAGGAGCGGTAGTAGCAGACACTCAGGCTC  
TTGACACGGTGACCTGTGTGGGCCACATCATAGGAGCGGTAGTAGCAGACACTCAGGCTC  
TTGACACGGTGACCTGTGTGGGCCACATCATAGGAGCGGTAGTAGCAGACACTCAGGCTC  
TTGACACGGTGACCTGTGTGGGCCACATCATAGGAGCGGTAGTAGCAGACACTCAGGCTC  
TTGACACGGTGACCTGTGTGGGCCACATCATAGGAGCGGTAGTAGCAGACACTCAGGCTC  
TTGACACGGTGACCTGTGTGGGCCACATCATAGGAGCGGTAGTAGCAGACACTCAGGCTC  
TTGACACGGTGACCTGTGTGGGCCACATCATAGGAGCGGTAGTAGCAGACACTCAGGCTC

SS2U007334  
SS2U045801  
XDH863c13T3revcomp  
XDH863c13T7  
XDH863c11T3revcomp  
XDH863c11T7  
XDH863c12T3  
XDH863c12T7revcomp

-----  
ACGCTCAGAGAGCAGCCAAGGCTGTGAGGATCACCTACCAAGAACTACAGCCTGTAATCA  
ACGCTCAGAGAGCAGCCAAGGCTGTGAGGATCACCTACCAAGAACTACAGCCTGTAATCA  
ACGCTCAGAGAGCAGCCAAGGCTGTGAGGATCACCTACCAAGAACTACAGCCTGTAATCA  
ACGCTCAGAGAGCAGCCAAGGCTGTGAGGATCACCTACCAAGAACTACAGCCTGTAATCA  
ACGCTCAGAGAGCAGCCAAGGCTGTGAGGATCACCTACCAAGAACTACAGCCTGTAATCA  
ACGCTCAGAGAGCAGCCAAGGCTGTGAGGATCACCTACCAAGAACTACAGCCTGTAATCA  
ACGCTCAGAGAGCAGCCAAGGCTGTGAGGATCACCTACCAAGAACTACAGCCTGTAATCA  
ACGCTCAGAGAGCAGCCAAGGCTGTGAGGATCACCTACCAAGAACTACAGCCTGTAATCA

SS2U007334  
SS2U045801  
XDH863c13T3revcomp  
XDH863c13T7  
XDH863c11T3revcomp  
XDH863c11T7  
XDH863c12T3  
XDH863c12T7revcomp

-----  
TCACCATAAGGATGCCATTACACACCAGTCCTTCTTCCAGCCTGTTAGAACCATCCAGA  
TCACCATAAGGATGCCATTACACACCAGTCCTTCTTCCAGCCTGTTAGAACCATCCAGA  
TCACCATAAGGATGCCATTACACACCAGTCCTTCTTCCAGCCTGTTAGAACCATCCAGA  
TCACCATAAGGATGCCATTACACACCAGTCCTTCTTCCAGCCTGTTAGAACCATCCAGA  
TCACCATAAGGATGCCATTACACACCAGTCCTTCTTCCAGCCTGTTAGAACCATCCAGA  
TCACCATAAGGATGCCATTACACACCAGTCCTTCTTCCAGCCTGTTAGAACCATCCAGA  
TCACCATAAGGATGCCATTACACACCAGTCCTTCTTCCAGCCTGTTAGAACCATCCAGA  
TCACCATAAGGATGCCATTACACACCAGTCCTTCTTCCAGCCTGTTAGAACCATCCAGA

SS2U007334  
SS2U045801  
XDH863c13T3revcomp  
XDH863c13T7  
XDH863c11T3revcomp  
XDH863c11T7  
XDH863c12T3  
XDH863c12T7revcomp

-----  
GAGGAGACCTGGACCAAGGGTTTACACAGGCTGACCACATTCTGGAGGTGAGATGCATA  
GAGGAGACCTGGACCAAGGGTTTACACAGGCTGACCACATTCTGGAGG-----  
GAGGAGACCTGGACCAAGGGTTTACACAGGCTGACCACATTCTGGAGG-----  
GAGGAGACCTGGACCAAGGGTTTACACAGGCTGACCACATTCTGGAGG-----  
GAGGAGACCTGGACCAAGGGTTTACACAGGCTGACCACATTCTGGAGG-----  
GAGGAGACCTGGACCAAGGGTTTACACAGGCTGACCACATTCTGGAGG-----  
GAGGAGACCTGGACCAAGGGTTTACACAGGCTGACCACATTCTGGAGG-----  
GAGGAGACCTGGACCAAGGGTTTACACAGGCTGACCACATTCTGGAGG-----

Subsequently the SalmoBase database was published (<http://salmobase.org/>), containing a sequence for *XDH* (XM\_014200934.1, Gene ID: 100380763). However, there are differences between the published sequence in SalmoBase and the one resolved by the sequencing carried out in this project. It is suggested that these may represent different paralogues of the gene or alternatively different N-terminal splice variants, possibly associated with different physiological functions. An alignment of the compiled sequence (SalmonXDHcompiled) from this study and that in SalmoBase (XM\_014200934.1) is given below, differences between the consensus sequence and the sequence from SalmoBase are highlighted in grey.

CLUSTAL O multiple sequence alignment for the compiled XDH sequence from this project and the published SalmoBase XM\_014200934.1 sequence.

```

SalmonXDHcompiled -----
XM_014200934.1      tcctcatattcagtcxaaaggttgagactttatccttttatgacgcttatatcctcctgt

SalmonXDHcompiled -----
XM_014200934.1      ctagctacatgaagacagagatatagaggaacagggacagggcggacgtaggaggttaa

SalmonXDHcompiled -----
XM_014200934.1      ctttaaagggtctagagagaaagacagaaggagagagagcgggagagagaggggtgata

SalmonXDHcompiled -----
XM_014200934.1      cagggtgactgaatgagcatattcattgtcacacgataacatagcagtcctcactgacaa

SalmonXDHcompiled -----AGCGCGCAAACCCCTAGCCTAAACATGTCGGCCCTGACCTACGGAGAGCAGACT
XM_014200934.1      cagttagagcgcgcaaaccactagcctaaacatgtcggaccctgacctacggagagcagact

SalmonXDHcompiled AACAGGAATAATCTGACGGATCACAACATGAGCGGAGATGAACTTGTTCCTTTGTAAAT
XM_014200934.1      aacaggaataatctgacggatcacaacatgagcggagatgaacttgtttccttgtaaat

SalmonXDHcompiled GGAAAAAAGATAACAGAGAAGCATGCTGATCCAGAGATGACCCTGCTGACATACCTCAGG
XM_014200934.1      ggaaaaaagataacagagaagcatgctgatccagagatgacactgctgacatacctcagg

SalmonXDHcompiled AGAAAGTTGGGTTTGACAGGTAAGCTAGGCTGTGCAGAGGGAGGATGTGGAGCCTGT
XM_014200934.1      agaaagttgggtttgacaggtactaagctaggctgtgcagagggaggatgtggagcctgt

SalmonXDHcompiled ACTGTGATGCTCTCCAAATATCAGCCCCCCTCAGAAGAGTGCTTCCCTCGGTGAAT
XM_014200934.1      actgtgatgctctccaaatatcagccccactcagaagagtgcttccactcgggtgaat

SalmonXDHcompiled GGGTGTCTGGCCCCCTCTGTGTTCTCTCCATCCCTGTGCTGTCCGACGGTGAAGGGATC

```

XM_014200934.1	gggtgtctggccctctgtgttctctccatcactgtgctgtcacgacggtggaagggatc
SalmonXDHcompiled XM_014200934.1	GGCAGCGTGGCAGGGAACTACCCCCTGTGCAGGAGGGTATCGCTAAGTCTCATGGTTCT ggcagcgtggcagggaaactacaccctgtgcaggagcgtatcgctaagtctcatggttct
SalmonXDHcompiled XM_014200934.1	CAGTGTGGGTTCGTACCCCAGGTATCGTCATGTTTATGTATTTTTGCTCAGGAACAAC cagtgtgggttctgtaccccaggtatcgcatgtctatgtattctctgctcaggaacaac
SalmonXDHcompiled XM_014200934.1	CCTACCCCGCATGGCCGACATAGAGGAGGCCTTCCAAGGGAACCTGTGTCGCTGTACT cctacaccacgcatggccgacatagaggaggccttccaagggaaacctgtgctgctgtact
SalmonXDHcompiled XM_014200934.1	GGTTACAGACCAATTTGGAGGGGTACAAGACATTCCTCAAAGAGAGGACGTGTTTGGT ggttacagaccaattctggaggggtacaagacattcaccaaagagaggacgtggtgtggt
SalmonXDHcompiled XM_014200934.1	GGCAAGGGGAAGGAAAACGGCTGCTGCATGCCGACGGTGACAAGAAGAAAGGGTACACT ggcaaggggaaggaaaaacggctgctgcatgaccgacggtgacaagactaaagggtaact
SalmonXDHcompiled XM_014200934.1	GACGATCATGTCACCAGGACCTCAGTGTTCCTGCTCCTCTCTACAACCCAGCTGACTTC gacgatcatgtcaccaggacctcagtgttctctgctcctctctacaaccagctgacttc
SalmonXDHcompiled XM_014200934.1	CTCCCTCTGGACCCCACTCAGGAGATCATCTTCCCACCGGAGCTGATGTCCCTGTGTAAA ctccctctggaccccaactcaggagatcatcttcccaccggagctgatgtccctgtgtaaa
SalmonXDHcompiled XM_014200934.1	GGCCAGTCCTCTCAACAGCTGAGGTTCAAGGAGAGAGGGTTCTGTGGTCCAGCCAGCT ggccagtctctcaacagctgaggttcagaggagagagggttctgtggctccagccagct
SalmonXDHcompiled XM_014200934.1	TCTCTGGATCAACTTCTAGAGCTTAAGACTCAGTACCCCAACGCCAAGATGGTGGTTGGT tctctggatcaacttctagagcttaagactcagtaccccaacgcccaagatggtggttgg
SalmonXDHcompiled XM_014200934.1	AACACGGAAGTCGGTATTGAGATGAAGTTTAAAGAACCTGTTGTATCCTGTTATTCTGGCC aacacggaagtggattgagatgaagtttaagaacctggtgtatcctggtattctggcc
SalmonXDHcompiled XM_014200934.1	CCGGCGTACATCCCCGAGCTCAACGCCATACAGCACACTGACGAGGGTATAGTATTTGGA ccggcgtacatccccgagctcaacgccatacagcacactgacgagggatagatatttgga
SalmonXDHcompiled XM_014200934.1	GCATCCTGTTCCCTGACCCTGCTGGGTGATGTGCTGAAGGAAGCGGTGGGTAAACTGCC gcatcctgttccctgaccctgctgggtgatgtgctgaaggaagcgggtgggtaactgcc
SalmonXDHcompiled XM_014200934.1	TCCTACCAGACTGAAGTCTTACCTCTATACTGGAGCAACTCCGCTGGTTTGCTGGACTA tcctaccagactgaagtcttcacctctatactggagcaactccgctggtttgctggacta
SalmonXDHcompiled XM_014200934.1	CAGATACGCAACGTGGCAGCCGTTGGAGGTAACATCATGACTGCCAGCCCATCTCCGAC cagatacgcaacgtggcagccgttggaggtaacatcatgactgccagcccatctccgac
SalmonXDHcompiled XM_014200934.1	CTCAACCCTGTCTTTATGGCTGCTGGCTGCAAGCTCACACTCATGTCCAAGGTGGTGGT ctcaaccctgtctttatggctgctggctgcaagctcacactcatgtccaaaggtggtggt
SalmonXDHcompiled XM_014200934.1	GAGCGTGTGGTTGTGATGAATGAGAAGTTCTTCCCAGGTTACAGAAGAACCATCCTGACA gagcgtgtggttgtgatgaatgagaagttcttcccaggttacagaagaaccatcctgaca

SalmonXDHcompiled XM_014200934.1	CCTGAGGAGGTTCTTTATGTGTCTGATCCCGTACACCAAGAAGGGTCAGTATTTTGCT cctgaggaggttctctatgtgtcctgatcccgtacaccaagaagggtcagtatTTTgct
SalmonXDHcompiled XM_014200934.1	GCCTATAAGCAGTCTCTCGTCGTGAGGATGACATCAGCATTGTGACGTCAGGGATGAGT gcctataagcagctctcctcgtcgtgaggatgacatcagcattgtgacgtcagggatgagt
SalmonXDHcompiled XM_014200934.1	GTGACATTGCGCGAGGGGTCAACCGTCGTCAAGCACCTGGCCCTTAGTTACGGAGGGATG gtgacattcgccgaggggtcaaccgtcgtcaagcacctggcccttagttacggagggatg
SalmonXDHcompiled XM_014200934.1	GCTGCTACTACCGTCATGGCCAAGAACACAGCCAGCAGACTTTTGGGACAACAATGGGGG gctgctactaccgtcatggccaagaacacagccagcagactTTTgggacaacaatggggg
SalmonXDHcompiled XM_014200934.1	GAAGAGCTTCTGCAGGATGCTTGTTCCTCATTGGCTGAGGAGATGACCCTTACCCCTCT gaagagcttctgcaggatgcttgttcctcattggctgaggagatgacccttaccctctct
SalmonXDHcompiled XM_014200934.1	GYGCCGGGTGGCATGGTGACCTACAGACGAACCTTGACCCTCAGCCTGTTTTACAAGTTT gycgggggtggcatggtgacctacagacgaactctgaccctcagcctgttttacaagttt
SalmonXDHcompiled XM_014200934.1	TACCTGACTGYACAACAGAACTGGCCAGTGAGGGTGCAGATATGGAGGGTGTGAGGGCT tacctgactgtacaacagaaactggccagtgaggggtgcagatatggaggggtgcagggct
SalmonXDHcompiled XM_014200934.1	GACTACATCAGTGCTACAGAGATCTACCACCAGACGTCCCCCTCCAGTGTCCAGATTTC gactacatcagtgctacagagatctaccaccagacgtccccctccagtgtccagatttctc
SalmonXDHcompiled XM_014200934.1	CAGGCGGTTCCAGACGGTCAGAAGGAGGAGGACGTGGTGGGCCGTCCCATGATGCACCTC caggcggttccagacggtcagaaggaggaggacgtggtgggcccgtcccatgatgcacctc
SalmonXDHcompiled XM_014200934.1	TCAGCCATGAAGCAGGCGACGGGCGAGGCGGTTTACTGTGATGACATCCCTCTCTACGAG tcagccatgaagcaggcgacgggcgaggcggtttactgtgatgacatccctctctacgag
SalmonXDHcompiled XM_014200934.1	AATGAACTCTACCTCTGTCTTATAACCAGCACCAAGGCCACGCACGCATAYAGTCTATA aatgaactctacctctgtcttataaccagcaccaaggcccacgcacgcatacagctctata
SalmonXDHcompiled XM_014200934.1	GATACATCGGAGGCAGAGAGTATGCCAGGTGTGGTGACGTGTGTGTTGCCAAGGACATC gatacatcggaggcagagagtatgccaggtgtggtgacgtgtgtgtttgccaaggacatc
SalmonXDHcompiled XM_014200934.1	CCTGGCAGCAACATGACAGGACCTATCATCTACGARGAGACTGTCCTCGCTGTTGACACG cctggcagcaacatgacaggacctatcatctacgatgagactgtcctcgtctgttgacagc
SalmonXDHcompiled XM_014200934.1	GTGACCTGTGTGGGCCACATCATAGGAGCGGTAGTAGCAGACACTCAGGCTYACGCTCAG gtgacctgtgtgggccaatcataggagcggtagtagcagacactcaggctcagcctcag
SalmonXDHcompiled XM_014200934.1	AGAGCAGCCAAGGCTGTGAGGATCACCTACCAAGAATAACAGCCTGTAATCATCACCATA agagcagccaaggctgtgaggatcacctaccaagaactacagcctgtaaatcatcaccata
SalmonXDHcompiled XM_014200934.1	CAGGATGCCATTACACACCAGTCCTTCTTCCAGCCTGTTAGAACCATCCAGAGAGGAGAC caggatgccattacacaccagtccttcttccagcctgttagaacatccagagaggagac
SalmonXDHcompiled XM_014200934.1	CTGGACCAAGGGTTCACACAGGCTGACCACATTCTGGAGGGTGAGATGCATATGGGAGGC ctggaccaagggttcacacaggctgaccacattctggagggtgagatgcataatgggaggc

SalmonXDHcompiled XM_014200934.1	CAGGAACACTTCTACCTGGAGACCAATGTTACTGTAGCTGTACCTAGAGGAGAGGATGGA caggaacacttctacctggagaccaatgttactgtagctgtacctagaggagaggatgga
SalmonXDHcompiled XM_014200934.1	GAGATGGAGCTGTTTGTCTCTACTCAGTCTGCTACCAAAACCCAGTCTCTGGTAGCTAAG gagatggagctgtttgtctctactcagtctgctacaaaaccagctctctggtagctaag
SalmonXDHcompiled XM_014200934.1	GCGTTGAGTGTCCCGGCCAGTAGAGTGGTGATCAGAGTGAAGAGGATGGGAGGAGGATTC gcgttgagtgtcccggccagtagagtggatgatcagagtgaagaggatgggaggaggatctc
SalmonXDHcompiled XM_014200934.1	GGAGGGAAGGAGAGCAGGTCCACCACCCTGTCCACCGTGGTCGCTGTGGCCGCTCAGAAG ggaggaaggagagcaggtccaccaccctgtccacgtggtcgctgtggccgctcagaag
SalmonXDHcompiled XM_014200934.1	TTGAAGAGGCCAGTGAGATGTATGTTGGATAGAGATGAAGACATGCTGGTGACGGGGGGG ttgaagaggccagtgagatgtatgttggatagagatgaagacatgctggtgacggggggg
SalmonXDHcompiled XM_014200934.1	CGACACCCCTTCTATGGACGTTACAAGTGGGCTTTATGAAGTCAGTAAAGTGGTGGCT cgacaccccttctatggacgttacaagtgggctttatgaagttagttaaagtggtagct
SalmonXDHcompiled XM_014200934.1	CTAGAAGTGACCTACTACAACAACGCAGGAACTCCATAGACCTCTCTCTCAATCATG ctagaagttagcctactacaacaacgcaggaaactccatagacctctctctcaatcatg
SalmonXDHcompiled XM_014200934.1	GAGCGTGCGTTGTTCCACATGGAGAACTCTTACAGCATCGCTAACATTAGAGGGCGTGGC gagcgtgcggttgttccacatggagaactcttacagcatcgctaacattagagggcgtagc
SalmonXDHcompiled XM_014200934.1	TACGTGTGTAAGACACACCTCCCGTCCAACACGGCCTCCGAGGCTTTGGCGGGCCGCAA tacgtgtgtaagacacacctcccgtccaacacggcctccgaggctttggcggggccgcaa
SalmonXDHcompiled XM_014200934.1	GGAATGCTGATTGCTGAGAGTTGGATGAGTGACGTAGCTCTGAGCCTCGGGCTGCCTGCT ggaatgctgattgctgagagttggatgagtgacgttagctctgagcctcgggctgcctgct
SalmonXDHcompiled XM_014200934.1	GAACAGGTGCGTCGCTGAACATGTACATCCAGGGAGAGACGACTCCCTACAGCCAGATC gaacaggtgcgctcgtctgaacatgtacatccagggagagacgactccctacagccagatc
SalmonXDHcompiled XM_014200934.1	CTGGATCACATCACCTGGACCGCTGCTGGACCAATGTCTGGAGATATCATCCTTCAAC ctggatcacatcacctggaccgctgctgggaccaatgtctggagatatcatccttcaac
SalmonXDHcompiled XM_014200934.1	CAACGCAGAGCTGGAGTAGAGACATAACAAGGGACCACCGTTGGACTAAGCGAGGGCTG caacgcagagctggagttagagacataacaagggaccaccgcttgactaagcgagggctg
SalmonXDHcompiled XM_014200934.1	TCTGTCGTCCCCACCAAGTTCGGCATCAGCTTCACCGCTCTCTTCTTAACCAGGCCGGT tctgtcgtccccaccaagttcggcatcagcttcaccgctctcttcttaaccaggccggt
SalmonXDHcompiled XM_014200934.1	GCGTTGGCTCATATTTACACAGACGGCTCCGTGCTGTTGACTCACGGAGGGACTGAGATG gcgttggctcatatttacacagacggctccgtgctgttgactcacggagggactgagatg
SalmonXDHcompiled XM_014200934.1	GGACAGGGTCTACACACCAAGATGGTACAGGTGGCCAGTAGGACCCTGGGTATCCCCAGC ggacagggctacacaccaagatggtacaggtggccagtaggaccctgggtatccccagc
SalmonXDHcompiled XM_014200934.1	AGTAAGATCCACATCACAGAGACCAGCACCAACACTGTTCCCAACACCAGCCCTACTGCT agtaagatccacatcacagagaccagcaccaacactgttcccaacaccagccctactgct

SalmonXDHcompiled XM\_014200934.1 GCCTCCGCTTCCTCTGACCTCAATGGAGCCGCTGTGCATAATGCGTGTGAGATCCTACTC gcctccgcttcctctgacctcaatggagccgctgtgcataatgctgtgagatcctactc

SalmonXDHcompiled XM\_014200934.1 CACCGTCTAGAACCCTACAAGACCAAGAATCCCAAAGGATGCTGGGAGGACTGGGTGAAC caccgtctagaaccctacaagaccaagaatcccaaaggatgctgggaggactgggtgaac

SalmonXDHcompiled XM\_014200934.1 ACTGCCTACTTTGACCGGGTCAGTCTGTCTGCCAATGGATTCTACAAGACTCCAGACCTT actgcctactttgaccgggtcagtctgtctgccaatggattctacaagactccagacctt

SalmonXDHcompiled XM\_014200934.1 GGTTATGACTTTGAGACCAACACAGGTCGTCTTTCAACTACTTCAGTTATGGAGTGGCC ggttatgactttgagaccaacacaggtcgtcctttcaactacttcagttatggagtggcc

SalmonXDHcompiled XM\_014200934.1 TGCTCTGAGGTGGAGATAGACTGTCTGACCGGCAGCCACAAGAACATTCATACGTCCATC tgctctgaggtggagatagactgtctgaccggcagccacaagaacattcatacctccatc

SalmonXDHcompiled XM\_014200934.1 GTCATTGATGTGGGGAATAGTCTGAACCCAGCTCTGGACATAGGACAGGTAGAGGGGGGC gtcattgatgtggggaatagctctgaaccagctctggacataggacaggtagaggggggc

SalmonXDHcompiled XM\_014200934.1 TTTATGCAGGGTGTGGGTCTGTACACCTGGAGGAGCTGAAGTATTCTCTGAGGGATAC tttatgcaggggtgtgggtctgtacacctggaggagctgaagtattctcctgagggatac

SalmonXDHcompiled XM\_014200934.1 CTGTTACGCGAGGACCAGGCATGTACAAGATCCCCGCCTTTGGAGACATCCCCACTGAC ctgttcacgcgaggaccaggcattgtacaagatccccgcctttggagacatccccactgac

SalmonXDHcompiled XM\_014200934.1 CTCACAGTGTCTCTGCTCCGAGATGCACCCAACGACAAGGCCATCTTCTCTCCAAGGCG ctcacagtgtctctgctccgagatgcacccaacgacaaggccatcttctcctccaaggcg

SalmonXDHcompiled XM\_014200934.1 GTAGGTGAGCCTCCTCTCTTCTTGGCGCCTCAGTGTTTTTTGGCCATCAAAGATGCCATC ataggtgagcctcctctcttcttgcggcctcagtgTTTTTTGGCCATCAAAGATGCCATC

SalmonXDHcompiled XM\_014200934.1 ACCGCTGCCAGGAAGGAGTCAGGCCTTAGTGGGCCCTTCAGATTGGACAGCCCGGCCACA accgctgccaggaaggagtcaggccttagtgggcccctcagattggacagcccggccaca

SalmonXDHcompiled XM\_014200934.1 CCCGAGAGGATACGCAACACCTGCGAGGACCGCTTCACCAAACCTGTGCCCCCTGCAGAG cccgagaggatagcaaacacctgagaggaccgcttcaccaaactgtgccccctgagag

SalmonXDHcompiled XM\_014200934.1 CCAGGCACCTTCACTCCATGGGCTGTCTAGTGTAAAGACTAACAGAAGTAGAGAGAGAAT ccaggcaccttcaactccatgggctgtcgtagtgtAAAGACTAACAGAAGTAGAGAGAGAAT

SalmonXDHcompiled XM\_014200934.1 ACATGCAGAGGAGAGAGAGAGAGAGAGAGAGAGAAGAGGGGAGAGACGGAGGGGGAAAA acatgcagaggagaggagagagagagagagagagagaagaggggagagacggagggggaaaa

SalmonXDHcompiled XM\_014200934.1 GAATAGGATAGCAAGCAGAGAGAGAGAAGGATAATCTGCTCCGAATTTATGCCATTAAAT gaataggatagcaagcagagagagagaaggataatctgctccGAATTTATGCCATTAAAT

SalmonXDHcompiled XM\_014200934.1 TCCTTTGTCTCAGTCTGAGGAAACGGCTGTTCTAATCAGTTTGAATGGAATCAGAACCC tcctttgtctcagctgaggaaacggctgTTCTAATCAGTTTGAATGGAATCAGAACCC

SalmonXDHcompiled XM\_014200934.1 TAATCAGTTTGAACCTTACCCCAACGCACACATGGGTGGATCTCAGTGTAAAGGGGCT taatcagtttgaactcttaccccaacgcacacatgggtggatctcagtgtaaggggct

SalmonXDHcompiled XM_014200934.1	TCATCTCCTTGCTCTCCTGTCTCTCATCCTTACTGAGCTGAGAACTCAGAACAATATAGTG tcatctccttgctctcctgtctctcatccttactgagctgagaactcagaacaatatagtg
SalmonXDHcompiled XM_014200934.1	GATGTTGAGGGTCTGCTTTCACCTGTCCACTAGTTTTAGATCAGTGAAGAGGAAGAGACT gatgttgagggctgctttcacctgtccactagtttttagatcagtgaagaggaagagact
SalmonXDHcompiled XM_014200934.1	ATTAAGATGAAGCCCTGATCTGAAGCCTACCTGGCTATCAGCACTTTGACCTAGGAAGCA attaagatgaagccctgatctgaagcctacctggctatcagcactttgacctaggaagca
SalmonXDHcompiled XM_014200934.1	ATCCTAGTTCGGTCCGTCCCCCCCCCCCCCCCCCATAGCCACCATGGTGCATTGTGAA atcctagttcggtcgcccccccccc-----ccccccccccaccatggtgcattgtgaa
SalmonXDHcompiled XM_014200934.1	ATAGGTCAGGAGCCACAGATTCTGATTGGAGGAAAGTGTGCTGAGGCCGCGGGAAGTG ataggtcaggagccacagattctgattggaggaaagtgtcgctgagggcgcgggaactg
SalmonXDHcompiled XM_014200934.1	ACCAGACCAATCACACACCACATACAGTAACTGTTGAGGATCTTTTTCAAGGGATGTCAA accagaccaatcacacaccacatacagtaactgttgaggatcttttcaagggatgtcaa
SalmonXDHcompiled XM_014200934.1	TCATTTTCAGACCTCACTGCATATCATATACAAATGACCTATGATCAATTCAATATCTGT tcattttcagacctcactgcatatcatatacaaatgacctatgatcaattcaatatctgt
SalmonXDHcompiled XM_014200934.1	AATGATGCCTGTTATATACCTTTATCAAATAAGTCAACATCTTGTATTTGTGTGTA AAAAG aatgatgcctgttatatacctttatcaaataagtcaacatcttgtatttgtgtgtaaaaag
SalmonXDHcompiled XM_014200934.1	AGACAATATTTGTGTGTAAATTTAATAAATTTCCCTAAATGTATATTTTATACATATTA agacaatatttgtgtgttaaatttaataaatttcctaaatgtatattttatacatatta
SalmonXDHcompiled XM_014200934.1	ATTTAATTTGACTTTTACTAGCAGAAATGTGATTTTATTTAGTGTTATGTTGAGTGTAT atttaatttgacttttactagcagaaattgtgattttatttagtggttatgttgagtgat
SalmonXDHcompiled XM_014200934.1	AGAGATTTATTGAAATAATTTGTTTAAATTTATTTTATGTGTAATCTCAGGTTTTAGTAAA agagttttattgaaataaatttgtttaattttatgtgtaaatctcaggttttagtaaa
SalmonXDHcompiled XM_014200934.1	ACAGCACCATCTAGTGGCCGGTAGTGTGTCTGCAGTGCTACTGTTTTCAATTC AACTAGT acagcaccatctagtgccggtagtgtgtctgcagtgctactgTTTTCAATTC AACTAGT
SalmonXDHcompiled XM_014200934.1	TTAATACTACTTGACTGACACAGAATAACTCAATTACTTCAACTACTTGATTAGACTGAG ttaatactacttgactgacacagaataactcaattacttcaactacttgattagactgag
SalmonXDHcompiled XM_014200934.1	ACAAATGAAAAGAGACTATCAAGCAATGGTGTAATTGAAGAATTTGCTTTATTTTACATT acaaatgaaaagagactatcaagcaatggtgtaattgaagaatttgctttatTTTACATT
SalmonXDHcompiled XM_014200934.1	TCAATAATGTACAGAGTTAGTCTGTTGAATAAACATACATTTCCAATCAAAAAAAAAAAAA tcaataatgtacagagttagtctgTTGAATAAACATACATTTCCAATCAAAAAAAAAAAAA
SalmonXDHcompiled XM_014200934.1	AAAAAAAAAGA -----

These differences in the nucleic acid sequence of the *XDH* gene lead to changes in the amino acid sequence of the protein. The CLUSTAL O sequence alignment for the amino acid sequences is given below, differences between the sequences are highlighted in grey.

CLUSTAL O (1.2.4) multiple sequence alignment for the translated amino acid sequences of xanthine dehydrogenase from the SalmonBase XM\_014200934.1 sequence and the sequence identified in this project.

```

XM_014200934.1      MSDLTYGEQTNRNNLTDHNMSGDELVFFVNGKKITEKHADPEMTLLTYLRRKLGLTGTKL
salXDH_this_project MSALTYGEQTNRNNLTDHNMSGDELVFFVNGKKITEKHADPEMTLLTYLRRKLGLTGTKL

XM_014200934.1      GCAEGGCGACTVMLSKYQPHLRRVLHHSVNGCLAPLCSLHCAVTTVEGIGSVAGKLHPV
salXDH_this_project GCAEGGCGACTVMLSKYQPPLRRVLPPSVNGCLAPLCSLHCAVTTVEGIGSVAGKLPPV

XM_014200934.1      QERIAKSHGSQCGFCTPGIVSMYSLLRNNPTPRMADIEEAFQGNLCRCTGYRPILEGYK
salXDH_this_project QEGIAKSHGSQCGFCTPGIVMMYFLLRNNPTPRMADIEEAFQGNLCRCTGYRPILEGYK

XM_014200934.1      TFTKERTCCGGKGKENGCCMTDGDKTKGYTDDHVTRTSVFPAPLYNPADFLPLDPTQEII
salXDH_this_project TFPKERTCFGGKGKENGCCMPDGDKKKGYTDDHVTRTSVFPAPLYNPADFLPLDPTQEII

XM_014200934.1      FPPELMSLCKGQSSQLRFRGERVLWLQPASLDQLLELKTQYPNAKMVVGNTEVGIEMKF
salXDH_this_project FPPELMSLCKGQSSQLRFRGERVLWLQPASLDQLLELKTQYPNAKMVVGNTEVGIEMKF

XM_014200934.1      KNLLYPVILAPAYIPELNAIQHTDEGIVFGASCSLTLLGDVLKEAVGKLPSYQTEVFTSI
salXDH_this_project KNLLYPVILAPAYIPELNAIQHTDEGIVFGASCSLTLLGDVLKEAVGKLPSYQTEVFTSI

XM_014200934.1      LEQLRWFAGLQIRNVAAVGGNIMTASPISDLNPVFMAAGCKLTLMSKGGGERVVVMDEKF
salXDH_this_project LEQLRWFAGLQIRNVAAVGGNIMTASPISDLNPVFMAAGCKLTLMSKGGGERVVVMNEKF

XM_014200934.1      FPGYRRTILTPEEVLLCVLIPYTKKGQYFAAYKQSPREDDISIVTSGMSVTFAEGSTVV
salXDH_this_project FPGYRRTILTPEEVLLCVLIPYTKKGQYFAAYKQSPREDDISIVTSGMSVTFAEGSTVV

XM_014200934.1      KHLALSYGGMAATTVMAKNTASRLLGQQWGEELLQDACSSLAEEMTLHPSAPGGMVTYRR
salXDH_this_project KHLALSYGGMAATTVMAKNTASRLLGQQWGEELLQDACSSLAEEMTLHPSXPGGMVTYRR

XM_014200934.1      TLTLSLFYKFYLTVQQKLASEGADMEGVRADYISATEIYHQTSPSSVQIFQAVPDGQKEE
salXDH_this_project TLTLSLFYKFYLTXQQKLASEGADMEGVRADYISATEIYHQTSPSSVQIXQAVPDGQKEE

XM_014200934.1      DVVGRPMMHLSAMKQATGEAVYCDDIPLYENELYLCLITSTKAHARISIDTSEAESMPG
salXDH_this_project DVVGRPMMHLSAMKQATGEAVYCDDIPLYENELYLCLITSTKAHARIXSIDTSEAESMPG

XM_014200934.1      VVTCVFAKDIPGSNMTGPIIYDETVLAVDTVTCVGHIIGAVVADTQAHAQRAAKAVRITY
salXDH_this_project VVTCVFAKDIPGSNMTGPIIYXETVLAVDTVTCVGHIIGAVVADTQAXAQRAAKAVRITY

XM_014200934.1      QELQPVIITIQDAIHQSFFQPVRTIQRGDLDQGFTQADHILEGEMHMGGQEHFYLETNV
salXDH_this_project QELQPVIITIQDAIHQSFFQPVRTIQRGDLDQGFTQADHILEGEMHMGGQEHFYLETNV

XM_014200934.1      TVAVPRGEDGEMELFVSTQSATKTQSLVAKALSVPASRVVIRVKRMGGGFGGKESRSTLL
salXDH_this_project TVAVPRGEDGEMELFVSTQSATKTQSLVAKALSVPASRVVIRVKRMGGGFGGKESRSTLL

```

XM_014200934.1 salXDH_this_project	STVVAVAAQKLRPVRCLDRDEDMLVTGGRHPFYGRYKVGFMKSGKVVVALEVTYYNNAG STVVAVAAQKLRPVRCLDRDEDMLVTGGRHPFYGRYKVGFMKSGKVVVALEVTYYNNAG
XM_014200934.1 salXDH_this_project	NSIDL SLSIMERALFHMENSYSIANIRGRGYVCKTHLP SNTAFRFGGGPQGMLIAESWMS NSIDL SLSIMERALFHMENSYSIANIRGRGYVCKTHLP SNTAFRFGGGPQGMLIAESWMS
XM_014200934.1 salXDH_this_project	DVALSLGLPAEQVRRRLNMYIQGETTPYSQILDHITLDRCDWQCLEISSFNQRRAGVETYN DVALSLGLPAEQVRRRLNMYIQGETTPYSQILDHITLDRCDWQCLEISSFNQRRAGVETYN
XM_014200934.1 salXDH_this_project	RDHRWTKRGLSVVPTKFGISFTALFLNQAGALAHITYDGSVLLTHGGTEMGQGLHTKMVQ RDHRWTKRGLSVVPTKFGISFTALFLNQAGALAHITYDGSVLLTHGGTEMGQGLHTKMVQ
XM_014200934.1 salXDH_this_project	VASRTLGI PSSKI HITETSTNTVPNTSPTAASASSDLNGAAVHNACEILLHRLEPYKTKN VASRTLGI PSSKI HITETSTNTVPNTSPTAASASSDLNGAAVHNACEILLHRLEPYKTKN
XM_014200934.1 salXDH_this_project	PKGCWEDWVNTAYFDRVSL SANGFYKTPDLGYDFETNTGRPFNYFSYGVACSEVEIDCLT PKGCWEDWVNTAYFDRVSL SANGFYKTPDLGYDFETNTGRPFNYFSYGVACSEVEIDCLT
XM_014200934.1 salXDH_this_project	GSHKNIHTSIVIDVGNLSLNPALDIGQVEGGFMQGVGLYTL EELKYSPEGYLFTRGPGMYK GSHKNIHTSIVIDVGNLSLNPALDIGQVEGGFMQGVGLYTL EELKYSPEGYLFTRGPGMYK
XM_014200934.1 salXDH_this_project	IPAFGDIP TDLTVSLLRDAPNDKAI FSSKAI GEPPLFLAASVFFAIKDAITAARKESGLS IPAFGDIP TDLTVSLLRDAPNDKAI FSSKAVGEPPLFLAASVFFAIKDAITAARKESGLS
XM_014200934.1 salXDH_this_project	GPFRLDSPATPERIRNTCEDRFTKLCPPAEPGTFTPWAVVV GPFRLDSPATPERIRNTCEDRFTKLCPPAEPGTFTPWAVVV

### 3.5.5.3 Xanthine dehydrogenase gene expression results

As the level of hypoxanthine in the skin was observed to be higher in the later time points of the feeding trial study, the level of *XDH* expression was investigated in the skin of fish from the final two time points. It was hypothesised that elevated levels of hypoxanthine may be used as a precursor for the production of hydrogen peroxide, which is generated when hypoxanthine is broken down by *XDH*. This could have a function in aiding smolt adaptation to SW as  $H_2O_2$  plays an important role in the innate immune system which can be compromised by the stress of changing osmoregulatory challenges.

The expression of *XDH* (Figure 3.33) was found to be significantly influenced by timepoint ( $F_{1,60} = 59.42$ ,  $p = 1.54 \times 10^{-10}$ ) and the interaction between time point and diet ( $F_{5,60} = 8.53$ ,  $p = 3.81 \times 10^{-6}$ ). On all but diet 4, expression of *XDH* was significantly higher 6 weeks after SW transfer than at 3 weeks post SW transfer ( $p < 0.03$ ).

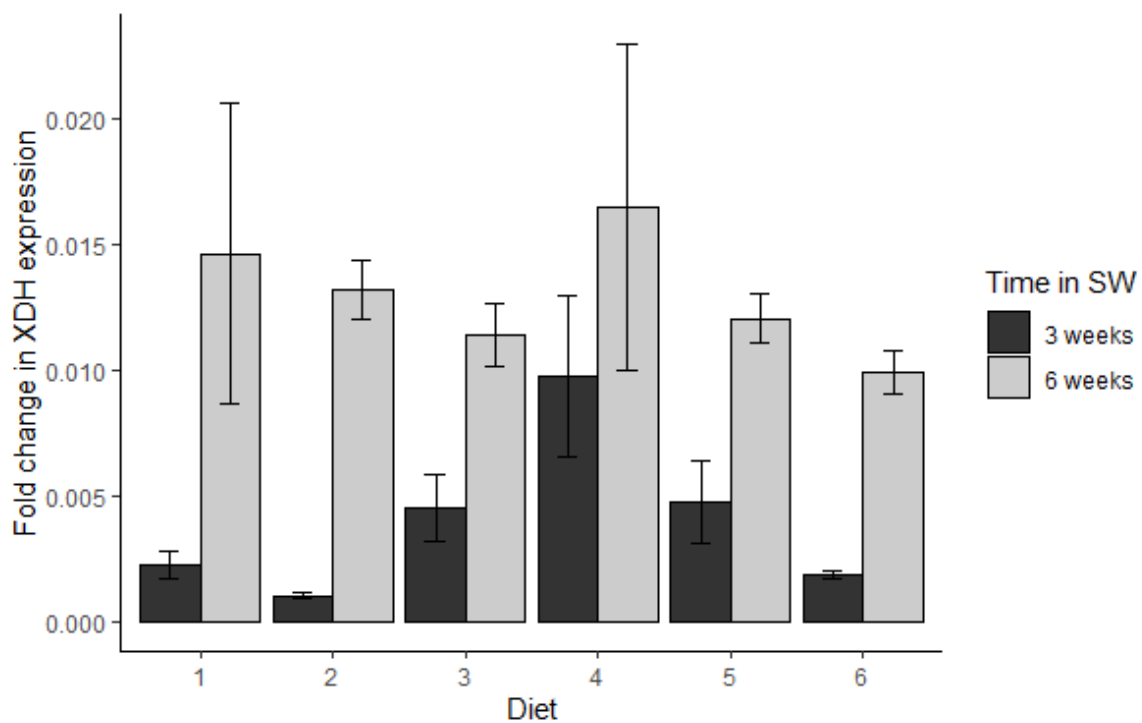


Figure 3.33. Mean fold change in the expression of *XDH* relative to *RPLP0* in the skin of Atlantic salmon fed on diets containing varying proportions of nucleotide supplement. Error bars denote standard error.

### 3.6 Discussion

#### 3.6.1 Hypoxanthine

Hypoxanthine (II, Figure 3.34) was identified as an organic osmolyte present in the skin of Atlantic salmon through an established HPLC method. This purine has not previously been identified in playing a major osmotic role in other euryhaline teleost species studied, and thus represents an important new discovery in the study of organic osmolytes in ichthyology.

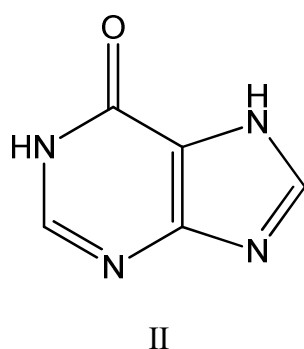


Figure 3.34. Structure of hypoxanthine.

The level of hypoxanthine in the skin was observed to rise over time during the smoltification process in fish sampled from an industrial aquaculture setting (Figure 3.9), and levels after 72 hours in SW were shown to be significantly higher than those in FW ( $p < 0.05$ ). Levels at 24 and 48 hours in SW were higher than in parr ( $p < 0.02$ ), though not higher than in FW smolts shortly before SW transfer. These results suggest that hypoxanthine may be accumulated in the skin prior to entry to SW in preparation for the osmotic challenges faced when moving from a hypotonic to a hypertonic environment.

In SW challenge trials, the level of hypoxanthine in the skin did not change within 6 to 24 hours of transfer to SW in either parr or smolts, unlike the results seen in the pilot study. Overall, the level of hypoxanthine in the skin of smolts was higher than in parr ( $p < 0.0005$ ), though short term SW challenge had no significant effect at either life stage. These results

support the above observation that hypoxanthine is accumulated during the smoltification process.

In a feeding trial testing the effect of altering the composition of nucleotide supplements the level of hypoxanthine in the skin was found to be higher in smolts approaching and following SW transfer than it was at the initial time point before the initiation of feeding with supplemented diets. However, no effect of diet on the level of hypoxanthine in the skin was observed.

The purine hypoxanthine is an intermediate in the nucleic acid salvage pathway. It is structurally very similar to guanine and can be produced by the spontaneous deamination of adenine. This can lead to an error in DNA transcription/replication as hypoxanthine binds to cytosine. Purines have potent anti-inflammatory and cytoprotective effects which are mediated by adenosine receptors (da Rocha Lapa *et al.*, 2012). Hypoxanthine protects against oxidant-induced cell injury by inhibiting activation of nuclear poly(ADP-ribose) polymerase (Virág & Csaba, 2001). Guanine and hypoxanthine have been observed to increase in the skin of salmonids during smoltification. In cells known as iridophores, anhydrous guanine crystals organised in layers with cytoplasm produce reflective structures (Leclercq *et al.*, 2010b; Levy-Lior *et al.*, 2010). The crystallisation of guanine accumulated in the skin of smolts is recognised as being responsible for the characteristic silvering seen during smoltification where fish lose their parr markings and freshwater colouration. Silver colouration is beneficial in a marine pelagic life style (Stefansson *et al.*, 2008). Hypoxanthine occurs at much lower levels in the skin than guanine in smolts (Leclercq *et al.*, 2010a). Hypoxanthine is more water soluble than guanine. Guanine can be produced by the amination of hypoxanthine and it is possible that hypoxanthine is accumulated as a precursor

for the production of guanine. The structures of hypoxanthine and guanine are given in Figure 3.35.

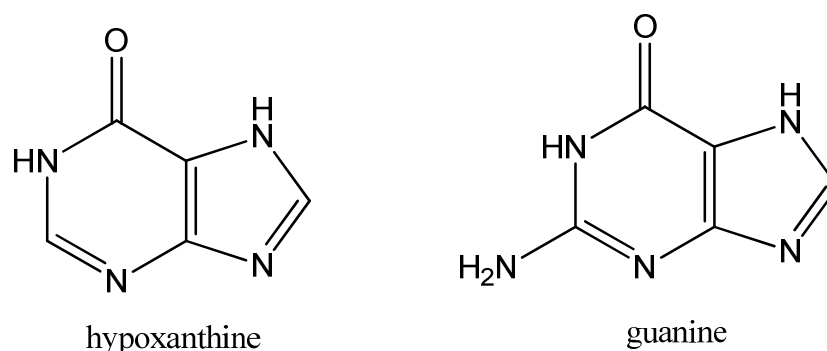


Figure 3.35. The difference in the structure of hypoxanthine and guanine.

It is plausible that hypoxanthine accumulated in the skin can play a role as an organic osmolyte, though this function has not been identified in other species. Hypoxanthine is a small molecule which can form hydrogen bonds and is readily available in cells as a product of purine catabolism. Therefore, it would be a useful metabolite as an organic osmolyte. The molecule contains a number of lone pairs of electrons which could act as hydrogen bond acceptors, and a number of electropositive hydrogens which act as hydrogen bond donors.

### 3.6.2 Purine metabolism gene expression

As hypoxanthine in Atlantic salmon represents such an important new finding in the study of organic osmolytes, the expression of a number of genes involved in the metabolism of purines was investigated in the skin of Atlantic salmon from both the direct SW transfer trial and the nucleotide supplement feeding trial. The sequence of the xanthine dehydrogenase enzyme in Atlantic salmon was also investigated, and the expression of this gene measured in fish from the feeding trial following SW transfer.

### 3.6.2.1 Adenosine mono-phosphate kinase

*Adenosine mono-phosphate kinase* expression was investigated, the  $\alpha 2a$  paralogue from the SalmonDB was selected for investigation as in pilot trials this gene was found to be expressed at relatively high levels. On the direct SW transfer trial there was no significant effect of SW transfer observed on the level of *AMPK $\alpha 2a$*  expression in the skin. In fish on the feeding trial, the expression of this gene at the baseline time point, before the commencement of feeding with supplemented diets, was significantly higher than at all later time points. Following SW transfer, there was a fall observed in *AMPK $\alpha 2a$*  expression between 24 hours and 3 weeks post transfer ( $p = 0.007$ ). At 6 weeks post transfer the level of *AMPK $\alpha 2a$*  expression was the lowest observed on the trial ( $p < 0.0005$ ).

AMPK is a regulator of cellular metabolism which is conserved in a wide range of eukaryotic species (Hardie *et al.*, 2011; Mihaylova & Shaw, 2011). Under conditions of depleted ATP, AMPK phosphorylates other enzymes which are involved in both catabolic processes which produce ATP, and in the inhibition of processes which consume ATP (Hardie *et al.*, 2011). AMPK is composed of three subunits,  $\alpha$ ,  $\beta$  and  $\gamma$ . The  $\alpha$  subunit contains the active site of the enzyme, the  $\beta$  and  $\gamma$  subunits have regulatory functions (Mihaylova & Shaw, 2011). When levels of intracellular adenosine mono-phosphate (AMP) and/or adenosine di-phosphate (ADP) are high these bind directly with the  $\gamma$  subunit, producing a conformational change which protects the phosphorylation that activates AMPK (Mihaylova & Shaw, 2011). It was thought that changes in dietary purine content may lead to changes in the expression of this enzyme as AMP, ADP and ATP are all involved in the purine metabolism pathway. The  $\alpha$  subunit paralogue *AMPK $\alpha 2a$*  was identified as being expressed in the skin (Figure 3.13) and was selected for investigation using RT-qPCR. However, the expression of *AMPK $\alpha 2a$*  was

not found to be significantly influenced by changes in the purine content of nucleotide supplements in feed.

### 3.6.2.2 Hypoxanthine-guanine phosphoribosyltransferase

Hypoxanthine-guanine phosphoribosyltransferase (Hprt) forms an important part of the purine salvage pathway, catalysing the conversion of hypoxanthine and guanine to inosine monophosphate and guanosine monophosphate respectively (Moriwaki *et al.*, 1999). Hprt expression occurs at high levels in some regions of the human brain (Moriwaki *et al.*, 1999).

In humans Lesch-Nyhan syndrome is a rare X-linked recessive condition in which the activity of the enzyme Hprt is absent or extremely low. Deficiency in this enzyme increases synthesis and reduces utilisation of purines, leading to an accumulation of uric acid in all body fluids. The resultant hyperuricaemia and hyperuricosuria lead to gout and kidney stone formation. This condition also causes severe neurological symptoms the aetiology of which is unknown, though low Hprt1 is associated with low brain dopamine. Certain *Hprt1* gene mutations give rise to Kelley-Seegmiller syndrome. In this condition Hprt1 levels are low and associated with gouty arthritis and the formation of uric acid kidney stones. This condition rarely causes neurological problems. Inhibition of xanthine oxidase activity, blocking the synthesis of uric acid from purines, prevents the development of nephropathy and gout (Torres *et al.*, 2007). Xanthine oxidase inhibition has no impact on the neurological symptoms which include characteristic self-injuring behaviours (Puig *et al.*, 2001).

On the direct transfer trial, *Hprt1* expression was found to be significantly influenced by SW transfer up to 24 hours after entry to SW. On the nucleotide supplement feeding trial, the level of *Hprt1* expression at the baseline time point was significantly higher than at the subsequent time points except for 3 weeks after SW transfer ( $p < 0.02$ ). At the time point 3

weeks after transfer, there was a rise in *Hprt1* expression to a level significantly higher than all other time points after the commencement of feeding with supplemented diets ( $p < 0.05$ ). No significant effect of diet was observed on the expression of *Hprt1* on the feeding trial.

As neurological changes play an important role in the smoltification process (Stefansson *et al.*, 2008), it is possible that hypoxanthine accumulation and *Hprt1* expression are linked to the changes in synaptic pathways observed as fish progress towards smoltification. A peak in dopamine levels is observed in the brains of smolts prior to SW entry, with levels then declining before downriver migration (Stefansson *et al.*, 2008). This may be influenced by the expression of *Hprt1*.

#### 3.6.2.3 Purine nucleotide phosphorylase

Purine nucleotide phosphorylase (PNP) plays an important role in the purine salvage pathway. This enzyme converts ribo- and deoxyribonucleosides to purine nucleotides (Bzowska *et al.*, 2000). Four paralogues of PNP were investigated in this study, *PNP5a*, *PNP5b*, *PNP6b* and *PNP6c*.

PNP is primarily located in the cytoplasm, though a mitochondrial form has also been identified (Yegutkin, 2008). This enzyme converts hypoxanthine to inosine (Yegutkin, 2008). In mammals PNP has been linked to the development of the immune system, particularly T-cell mediated immunity and PNP deficiency is linked to highly perturbed T-cell function (Moriwaki *et al.*, 1999). In mammalian species PNP is expressed in a wide range of tissues (Yegutkin, 2008).

*PNP5a* expression was found to fall after direct SW transfer, with expression significantly lower after 24 hours in SW than in fish sampled the day before SW transfer ( $p = 0.01$ ). On the feeding trial, *PNP5a* was found to be higher at the baseline time point than at all

subsequent time points ( $p < 0.05$ ). There was a fall in *PNP6* expression over the time course, with the lowest level of *PNP5a* expression occurring at the final time point, 6 weeks after SW transfer. No significant effect of diet was detected on the expression of this gene.

The expression of *PNP5b* was not found to be influenced by SW transfer on the direct transfer trial. On the feeding trial, baseline levels were higher than at 2 weeks before transfer and 24 hours post transfer ( $p < 0.05$ ). No effect of diet was detected.

*PNP6b* expression was not significantly affected by direct SW transfer. On the feeding trial there was no effect of diet detected, and little effect of time point.

*PNP6c* expression was significantly affected by SW transfer, with expression falling following SW transfer. *PNP6c* expression was higher at baseline on the nucleotide supplement feeding trial than at the subsequent time points ( $p < 0.03$ ).

#### 3.6.2.4 Nucleoside transporters

Two classes of nucleoside transporter have been identified,  $\text{Na}^+$ -independent equilibrative nucleoside transporters (ENTs) and  $\text{Na}^+$ -dependent concentrative nucleoside transporters (CNTs) (Gupta *et al.*, 2019). Nucleosides play a number of important roles in cellular and system biology. Adenosine has a number of important roles including the regulation of blood flow, myocardial action potentials and immune cell function as well as modulating inflammatory processes (Choi & Berdis, 2012). Nucleosides and deoxy-nucleosides are the monomers which make up RNA and DNA, necessary for cellular survival and reproduction. Therefore, the regulation of the concentration of these essential molecules in the intra- and extracellular fluid is essential.

On the direct transport trial, the level of *CNT3* was found not to be significantly affected by SW transfer up to 24 hours. On the purine supplement feeding trial nucleoside transporter expression was investigated at the baseline time point before the introduction of supplemented diets and 24 hours before SW transfer on all six experimental diets. On this trial the level of *CNT3* was significantly lower on all diets the day before SW transfer than at the time point 5 weeks before SW transfer. *ENT1a* and *ENT3* expression was not found to change significantly between the two time points. Both of these genes showed a high level of variability in expression at the 5 weeks to transfer time point, and *ENT1a* expression was also highly variable on diet 4 one day before SW transfer. The other ENT genes investigated (*ENT1b*, *ENT2*, and *ENT4*) all showed significantly lower expression 24 hours before SW transfer than at 5 weeks to SW transfer. It is possible that the introduction of nucleotide supplements into the diet reduced the need for nucleotide transporter expression as increased availability of these molecules in the ECF could make it disadvantageous to express equilibrative transporters as excessive levels of nucleoside could enter the cell down a concentration gradient. Likewise, increased levels of nucleosides in the ECF would reduce the need for the concentrative transporters.

#### 3.6.2.5 Xanthine dehydrogenase

Xanthine dehydrogenase (XDH) is an enzyme found in most vertebrate species (Terao *et al.*, 2016). This enzyme is similar in structure to the aldehyde oxidases (AOX) found in most eukaryotic branches of the tree of life (Terao *et al.*, 2016). It is hypothesised that the AOX genes evolved from an ancestral XDH gene through a gene duplication event in an early eukaryotic ancestor (Terao *et al.*, 2016). These enzymes belong to the group known as molybdoenzymes, requiring molybdenum as a cofactor for their catalytic activity (Mendel, 2013; Terao *et al.*, 2016). Unlike AOXs which have a wide range of substrates, XDH is very

specific to two purine substrates, catabolising hypoxanthine and xanthine to produce xanthine and uric acid respectively. Thus XDH is important in the catabolism of purines, with the oxidation of hypoxanthine and xanthine representing the rate limiting step in this breakdown pathway (Terao *et al.*, 2016).

In mammals XDH exists in two forms, the XDH form which uses nicotinamide adenine dinucleotide (NAD<sup>+</sup>) as an electron acceptor, and XOD which uses O<sub>2</sub> as an electron acceptor (Souza *et al.*, 2017). Saito & Nishino (1989) reported that in bovine milk the XDH form of the enzyme, while predominantly showing NAD<sup>+</sup> dependent activity, showed some O<sub>2</sub> dependent activity, though this activity was approximately a quarter of that observed in the XOD form of the enzyme. The XOD form has been identified as playing a role in the inflammatory response, producing H<sub>2</sub>O<sub>2</sub> at higher levels under the conditions associated with inflammation (Kelley *et al.*, 2010). XDH has also been found to show oxidase activity in conditions of low NAD<sup>+</sup>, such as the hypoxic microenvironment created in areas of inflammation (Harris & Massey, 1997). It has also been reported that XDH catalyses the conversion of inorganic nitrite to nitric oxide (NO) under hypoxic conditions (Finkel, 1999; Godber *et al.*, 2000). NO is a chemoattractant signal which draws neutrophils towards sites of injury and infection and also has antibacterial properties (Martin *et al.*, 2004).

The expression of XDH is predominantly observed in epithelia, suggesting that this enzyme is likely to have a role in the innate immune system (Brown *et al.*, 1995; Martin *et al.*, 2004). XDH has also been identified in bile secretions, known to be involved in antimicrobial activity in the gastrointestinal tract (Martin *et al.*, 2004). The oxidase activity of XOD and XDH produces H<sub>2</sub>O<sub>2</sub>, which acts as an attractant for neutrophils to sites of infection and injury (Kelley *et al.*, 2010; Martin *et al.*, 2004). High levels of XDH are found in mammalian milk, associated with the milk fat globule membrane (MFGM) (Patton & Keenan, 1975).

The MFGM surrounds fat globules in mammalian milk. This membrane is derived from the apical membrane of secretory cells in the mammary tissue, and thus bears antigens characteristic to epithelial membranes (Martin *et al.*, 2004). As pathogenic bacteria target epithelial cells, it is possible that they bind to the antigens present on the MFGM rather than the intestinal epithelia of infants (Keenan & Patton, 1995). XDH has an affinity for acidic polysaccharides which form part of many bacterial capsules, and binding of pathogenic bacteria to the MFGM brings these pathogens into contact with the XDH enzyme (Martin *et al.*, 2004). Oxidase activity of XDH is highest in mammalian milk in the first few weeks after birth, when it is of most benefit to the infant (Brown *et al.*, 1995).

The majority of organisms express only one form of the *XDH* gene, the product of which can be post translationally modified to give XOD, while a number of AOX paralogues are expressed in some mammalian species (Kurosaki *et al.*, 2013). However, this work suggests the possibility of two paralogues of XDH in Atlantic salmon. The nucleotide sequence differences identified between the sequence derived from the clones amplified and sequenced in this project, the sequences available on SalmonDB and the sequence published in SalmoBase suggest that more than one expressed form of XDH exists in the Atlantic salmon. Most of the nucleotide differences are found within the first half of the transcripts and especially towards the 5' end. On many occasions these differences in nucleotide sequence result in changes to the amino acid sequence, particularly at the N-terminal of the protein. Although not yet confirmed by RT-qPCR, it is possible that two paralogues of XDH exist in salmon. The different forms may be expressed in separate tissues, possibly performing distinct physiological roles. Further investigation is required to determine whether this is the case; as only a relatively small sample size was used in cloning experiments in this project the possibility of sequencing errors cannot be discounted.

The structure of salmonid XDH does not contain the amino acid motifs seen in mammalian XDH which allow this enzyme to be converted to the xanthine oxidase (XOD) form (see Clustal O alignment below), which produces reactive oxygen species which can form H<sub>2</sub>O<sub>2</sub>. However, there is evidence of XOD activity in fish tissue lysates (Sinha *et al.*, 2015; Xu *et al.*, 2012; Zhao *et al.*, 2014). The amino acid sequence of salmon XDH suggests that, while it lacks the cysteines present in the mammalian enzymes which allow the oxidation to reversibly form XOD, and the amino acids removed by proteolysis to create XOD, sites required for XOD activity are present (see Clustal O alignment below). It is possible that an as yet unidentified mechanism allows the conversion of salmon XDH to XOD or that a single form of the enzyme can catalyse both reactions, as has been seen in the results presented by Harris & Massey (1997).

In the Clustal O alignment below, the cysteine residues highlighted in **pale grey** are believed to form disulphide bonds in the structure of the enzyme. Highlighted in **dark grey** are the amino acid residues identified as playing a role in the active site of the enzyme (Nishino *et al.*, 2005). Four of these active site residues are cysteines in the mammalian sequences, however, in salmon three of these cysteine residues are absent, these differences are highlighted in **black**.

Four cysteine residues in the active site of the mammalian form of the enzyme have been identified as forming disulphide bonds when the enzyme is converted from the XDH to the XOD form (Nishino *et al.*, 2005). Nishino *et al.* (2005) reported that in mutant enzymes in which Cys<sup>535</sup> and Cys<sup>992</sup> were substituted for other amino residues the conversion of XDH to XOD was slowed, but still occurred. However, in mutants in which Cys<sup>1316</sup> or Cys<sup>1324</sup> were also substituted, conversion of XDH to XOD did not occur (Nishino *et al.*, 2005). As can be seen in the Clustal alignment below, the Atlantic salmon sequence lacks three of the four

cysteine residues identified by Nishino *et al.* (2005) as being responsible for the conversion of XDH to XOD.

CLUSTAL O (1.2.4) multiple sequence alignment of XDH amino acid sequences in salmon (*Salmo salar*), cow (*Bos taurus*), human (*homo sapiens*), mouse (*Mus musculus*) and rat (*Rattus rattus*).

```
salmonXDH  MSDLTYGEQTNRRNLT D H N M S G D E L V F F V N G K K I T E K H A D P E M T L L T Y L R R K L G L T G T K L
bovineXDH  -----M T A D E L V F F V N G K K V V E K N A D P E T T L L A Y L R R K L G L R G T K L
humanXDH   -----M T A D K L V F F V N G R K V V E K N A D P E T T L L A Y L R R K L G L S G T K L
mouseXDH   -----M T R T T V D E L V F F V N G K K V V E K N A D P E T T L L V Y L R R K L G L C G T K L
ratXDH     -----M T A D E L V F F V N G K K V V E K N A D P E T T L L V Y L R R K L G L C G T K L
```

```
salmonXDH  G C A E G G C G A C T V M L S K Y Q P H L R R V L H H S V N G C L A P L C S L H H C A V T T V E G I G S V A G K L H P V
bovineXDH  G C G E G G C G A C T V M L S K Y D R L Q D K I I H F S A N A C L A P I C T L H H V A V T T V E G I G S T K T R L H P V
humanXDH   G C G E G G C G A C T V M L S K Y D R L Q N K I V H F S A N A C L A P I C S L H H V A V T T V E G I G S T K T R L H P V
mouseXDH   G C G E G G C G A C T V M I S K Y D R L Q N K I V H F S V N A C L T P I C S L H H V A V T T V E G I G N T K - K L H P V
ratXDH     G C G E G G C G A C T V M I S K Y D R L Q N K I V H F S V N A C L A P I C S L H H V A V T T V E G I G N T Q - K L H P V
```

```
salmonXDH  Q E R I A K S H G S Q C G F C T P G I V M S M Y L L R N N P T P R M A D I E E A F Q G N L C R C T G Y R P I L E G Y K
bovineXDH  Q E R I A K S H G S Q C G F C T P G I V M S M Y T L L R N Q P E P T V E E I E D A F Q G N L C R C T G Y R P I L Q G F R
humanXDH   Q E R I A K S H G S Q C G F C T P G I V M S M Y T L L R N Q P E P T M E E I E N A F Q G N L C R C T G Y R P I L Q G F R
mouseXDH   Q E R I A K S H G S Q C G F C T P G I V M S M Y T L L R N K P E P T V E E I E N A F Q G N L C R C T G Y R P I L Q G F R
ratXDH     Q E R I A R S H G S Q C G F C T P G I V M S M Y T L L R N Q P E P T V E E I E N A F Q G N L C R C T G Y R P I L Q G F R
```

```
salmonXDH  T F T K E R T C C G G K G K E N G C C M T D G D K T K G Y T D D H V T R T S V F P A P L Y N P A D F L P L D P T Q E I I
bovineXDH  T F A K N G G C C G G N N P N C C M N Q K K D -----H T V T L S P S L F N P E E F M P L D P T Q E P I
humanXDH   T F A R D G G C C G D G N N P N C C M N Q K K D -----H S V S L S P S L F K P E E F T P L D P T Q E P I
mouseXDH   T F A K D G G C C G G S G N N P N C C M S Q T K D -----Q T I A P S S S L F N P E D F K P L D P T Q E P I
ratXDH     T F A K D G G C C G G S G N N P N C C M N Q T K D -----Q T V S L S P S L F N P E D F K P L D P T Q E P I
```

```
salmonXDH  F P P E L M S L C K G Q S S Q Q L R F R G E R V L W L Q P A S L D Q L L E L K T Q Y P N A K M V V G N T E V G I E M K F
bovineXDH  F P P E L L R L K - D V P P K Q L R F E G E R V T W I Q A S T L K E L L D L K A Q H P E A K L V V G N T E I G I E M K F
humanXDH   F P P E L L R L K - D T P R K Q L R F E G E R V T W I Q A S T L K E L L D L K A Q H P D A K L V V G N T E I G I E M K F
mouseXDH   F P P E L L R L K - D T P R K T L R F E G E R V T W I Q V S T M E E L L D L K A Q H P D A K L V V G N T E I G I E M K F
ratXDH     F P P E L L R L K - D T P Q K K L R F E G E R V T W I Q A S T M E E L L D L K A Q H P D A K L V V G N T E I G I E M K F
```

```
salmonXDH  K N L L Y P V I L A P A Y I P E L N A I Q H T D E G I V F G A S C S L T L L G D V L K E A V G K L P S Y Q T E V F T S I
bovineXDH  K N Q L F P M I I C P A W I P E L N A V E H G P E G I S F G A A C A L S S V E K T L L E A V A K L P T Q K T E V F R G V
humanXDH   K N M L F P M I V C P A W I P E L N S V E H G P D G I S F G A A C P L S I V E K T L V D A V A K L P A Q K T E V F R G V
mouseXDH   K N M L F P L I I C P A W I L E L T S V A H G P E G I S F G A A C P L S L V E S V L A D A I A T L P E Q R T E V F R G V
ratXDH     K N M L F P L I V C P A W I P E L N S V V H G P E G I S F G A S C P L S L V E S V L A E E I A K L P E Q K T E V F R G V
```

```
salmonXDH  L E Q L R W F A G L Q I R N V A A V G G N I M T A S P I S D L N P V F M A A G C K L T L M S K G G G E R V V M D E K F
bovineXDH  L E Q L R W F A G K Q V K S V A S L G G N I I T A S P I S D L N P V F M A S G T K L T I V S R G - T R R T V P M D H T F
humanXDH   L E Q L R W F A G K Q V K S V A S V G G N I I T A S P I S D L N P V F M A S G A K L T L V S R G - T R R T V Q M D H T F
mouseXDH   M E Q L R W F A G K Q V K S V A S I G G N I I T A S P I S D L N P V L M A S R A K L T L A S R G - T K R T V W M D H T F
ratXDH     M E Q L R W F A G K Q V K S V A S I G G N I I T A S P I S D L N P V F M A S G A K L T L V S R G - T R R T V R M D H T F
```

salmonXDH FPGYRRTILTPEEVLLCVLIPYTKKGQYFAAYKQSPRREDDISIVTSGMSVTF AEGSTVV  
bovineXDH FPSYRKTLGPEEILLSIEIPYSREDEFFSAFKQASRREDDIAKVTCGMRVLFQPGSMQV  
humanXDH FPGYRKTLLSPEEILLSIEIPYSREGEYFSAFKQASRREDDIAKVTCGMRVLFKPGTTEV  
mouseXDH FPGYRRTLLSPEEILVSIVIPYSRKGEFFSAFKQASRREDDIAKVTCGMRVLFKPGTTEV  
ratXDH FPGYRKTLLRPEEILLSIEIPYSKEGEFFSAFKQASRREDDIAKVTCGMRVLFKPGTIEV

salmonXDH KHLALS YGGMAATTVMKNTASRLLGQQWGEELLQDACSSLA EEMTLHPSAPGGMV TYRR  
bovineXDH KELALCYGGMADRTISALKTTQKQLSKFWNEKLLQDVCAGLAEELS LSPDAPGGMIEFRR  
humanXDH QELALCYGGMANRTISALKTTQRQLSKLWKEELLQDVCAGLAEELHLPDAPGGMVDFRC  
mouseXDH QELSLCFGGMADRTVSALKTTPKQLSKSWNEELLQDVCAGLAEELHLPDAPGGMVEFRR  
ratXDH QELSLCFGGMADRTISALKTTPKQLSKSWNEELLQSV CAGLAEELQLAPDAPGGMVEFRR

salmonXDH TLTLSLFYKFYLT VQQKLASEGAD--MEGVRADYISATEIYHQ TSPSSVQIFQAVPDGQK  
bovineXDH TLTLSFFFKFYLT V LKKGKD-SKDKCGKLDPTYTSATLLFQKHPPANIQLFQEV PNGQS  
humanXDH TLTLSFFFKFYLT V LQKLGQENLEDKCGKLDPTFASATLLFQKDP PADVQLFQEV PKQS  
mouseXDH TLTLSFFFKFYLT V LQKLG RADLEGMCGKLDPTFASATLLFQKDP PANVQLFQEV PKQS  
ratXDH TLTLSFFFKFYLT V LQKLG RADLED MCGKLDPTFASATLLFQKDP PANVQLFQEV PKDQS

salmonXDH EEDVVG R P M M H L S A M K Q A T G E A V Y C D D I P L Y E N E L Y L C L I T S T K A H A R I Q S I D T S E A E S M  
bovineXDH K E D T V G R P L P H L A A A M Q A S G E A V Y C D D I P R Y E N E L F L R L V T S T R A H A K I K S I D V S E A Q K V  
humanXDH E E D M V G R P L P H L A A D M Q A S G E A V Y C D D I P R Y E N E L S L R L V T S T R A H A K I K S I D T S E A K K V  
mouseXDH E E D M V G R P M P H L A A D M Q A S G E A V Y C D D I P R Y E N E L S L R L V T S T R A H A K I M S I D T S E A K K V  
ratXDH E E D M V G R P L P H L A A N M Q A S G E A V Y C D D I P R Y E N E L S L R L V T S T R A H A K I T S I D T S E A K K V

salmonXDH P G V V T C V F A K D I P G S N M T G P I I Y D E T V L A V D T V T C V G H I I G A V V A D T Q A H A Q R A A K A V R I  
bovineXDH P G F V C F L S A D D I P G S N E T G - L F N D E T V F A K D T V T C V G H I I G A V V A D T P E H A E R A A H V V K V  
humanXDH P G F V C F I S A D D V P G S N I T G - I C N D E T V F A K D K V T C V G H I I G A V V A D T P E H T Q R A A Q G V K I  
mouseXDH P G F V C F L T S E D V P G S N I T G - I F N D E T V F A K D E V T C V G H I I G A V V A D T P E H A H R A A R G V K I  
ratXDH P G F V C F L T A E D V P N S N A T G - L F N D E T V F A K D E V T C V G H I I G A V V A D T P E H A Q R A A R G V K I

salmonXDH T Y Q E L Q P V I I T I Q D A I T H Q S F F Q P V R T I Q R G D L D Q G F T Q A D H I L E G E M H M G G Q E H F Y L E T  
bovineXDH T Y E D L - P A I I T I E D A I K N N S F Y G S E L K I E K G D L K K G F S E A D N V V S G E L Y I G G Q D H F Y L E T  
humanXDH T Y E E L - P A I I T I E D A I K N N S F Y G P E L K I E K G D L K K G F S E A D N V V S G E I Y I G G Q E H F Y L E T  
mouseXDH T Y E D L - P A I I T I Q D A I K N N S F Y G P E V K I E K G D L K K G F S E A D N V V S G E L Y I G G Q E H F Y L E T  
ratXDH T Y E D L - P A I I T I Q D A I N N N S F Y G S E I K I E K G D L K K G F S E A D N V V S G E L Y I G G Q E H F Y L E T

salmonXDH N V T V A V P R G E D G E M E L F V S T Q S A T K T Q S L V A K A L S V P A S R V V I R V K R M G G G F G G K E S R S T  
bovineXDH H C T I A I P K G E E G E M E L F V S T Q N A M K T Q S F V A K M L G V P V N R I L V R V K R M G G G F G G K E T R S T  
humanXDH H C T I A V P K G E A G E M E L F V S T Q N T M K T Q S F V A K M L G V P A N R I V V R V K R M G G G F G G K E T R S T  
mouseXDH H C T I A V P K G E A G E M E L F V S T Q N T M K T Q S F I A K M L G V P D N R I V V R V K R M G G G F G G K E T R S T  
ratXDH N C T I A V P K G E A G E M E L F V S T Q N T M K T Q S F V A K M L G V P D N R I V V R V K R M G G G F G G K E T R S T

salmonXDH T L S T V V A V A A Q K L K R P V R C M L D R D E D M L V T G G R H P F Y G R Y K V G F M K S G K V V A L E V T Y Y N N  
bovineXDH L V S V A V A L A A Y K T G H P V R C M L D R N E D M L I T G G R H P F L A R Y K V G F M K T G T I V A L E V D H Y S N  
humanXDH V V S T A V A L A A Y K T G R P V R C M L D R D E D M L I T G G R H P F L A R Y K V G F M K T G T V V A L E V D H F S N  
mouseXDH L I S T A V A L A A Y K T G R P V R C M L D R D E D M L I T G G R H P F L A K Y K V G F M K T G T I V A L E V A H F S N  
ratXDH V V S T A L A L A A H K T G R P V R C M L D R D E D M L I T G G R H P F L A K Y K V G F M K T G T V V A L E V A H F S N

salmonXDH A G N S I D L S L S I M E R A L F H M E N S Y S I A N I R G R G Y V C K T H L P S N T A F R G F G G P Q G M L I A E S W

bovineXDH AGNSRDLSHSIMERALFHMDNCYKIPNIRGTGRLCKTNLSSNTAFRGGPQALFIAENW  
humanXDH VGNTQDLSQSIMERALFHMDNCYKIPNIRGTGRLCKTNLPSNTAFRGGPQGMLIAECW  
mouseXDH GGNSEDLSRSIMERA V F H M D N A Y K I P N I R G T G R I C K T N L P S N T A F R G G P Q G M L I A E Y W  
ratXDH GGNTEDLSRSIMERALFHMDNAYKIPNIRGTGRICKTNLPSNTAFRGGPQGMLIAEYW

salmonXDH MSDVALSLGLPAEQVRRNLNMYIQGETTPYSQILDHITLDRCDWQCLEISSFNQRRAGVET  
bovineXDH MSEVAVTCGLPAEEVRRKNMYKEGDLTHFNQRLEGFSVPRCWDECLKSSQYARKSEVDK  
humanXDH MSEVAVTCGMPAEEVRRKNLYKEGDLTHFNQKLEGFTLPRCWEECLASSQYHARKSEVDK  
mouseXDH MSEVAVTCGLPAEEVRRKNMYKEGDLTHFNQKLEGFTLPRCWDECIASSQYQARKMEVEK  
ratXDH MSEVAITCGLPAEEVRRKNMYKEGDLTHFNQKLEGFTLPRCWDECIASSQYLARKREVEK

salmonXDH YNRDHRWTKRGLSVVPTKFGISFTALFLNQAGALAHYTDGSVLLTHGGTEMGQGLHTKM  
bovineXDH FNKENCWKKRGLCIIPTKFGISFTVPFLNQAGALIHVYTDGSVLVSHGGTEMGQGLHTKM  
humanXDH FNKENCWKKRGLCIIPTKFGISFTVPFLNQAGALLHVYTDGSVLLTHGGTEMGQGLHTKM  
mouseXDH FNRENCWKKRGLCIIPTKFGISFTLSFLNQGGALVHVYTDGSVLLTHGGTEMGQGLHTKM  
ratXDH FNRENCWKKRGLCIIPTKFGISFTLPFLNQGGALVHVYTDGSVLLTHGGTEMGQGLHTKM

salmonXDH VQVASRTLGIPISSKIHIHITETSTNTVPNTSPTAASASSDLNGAAVHNACEILLHRLEPYKT  
bovineXDH VQVASKALKIPIISKIYISETSTNTVPNSSPTAASVSTDIYQAVYEACQIILKRLEPFKK  
humanXDH VQVASRALKIPIISKIYISETSTNTVPNTSPTAASVSADLNGQAVYAACQIILKRLEPYKK  
mouseXDH VQVASRALKIPIISKIHIHITETSTNTVPNTSPTAASASADLNGQAIYEACQIILKRLEPFKK  
ratXDH VQVASRALKIPIISKIHISETSTNTVPNTSPTAASASADLNGQGVYEACQIILKRLEPFKK

salmonXDH KNPKGCWEDWVNTAYFDRVSLSANGFYKTPDLGYDFETNTGRPFNYFSYGVACSEVEIDC  
bovineXDH KNPDGSWEDWVMAAYQDRVSLSTTFYRTPNLGYSFETNSGNPFHYFTYGVACSEVEIDC  
humanXDH KNP SG SWEDWVTAAYMDTVSLSATGFYRTPNLGYSFETNSGNPFHYFSYGVACSEVEIDC  
mouseXDH KNP SG SWESWVMDAYTSAVLSATGFYKTPNLGYSFETNSGNPFHYFSYGVACSEVEIDC  
ratXDH KKPTGPWEAWVMDAYTSAVLSATGFYKTPNLGYSFETNSGNPFHYFSYGVACSEVEIDC

salmonXDH LTGSHKNIHTSIVIDVGNSLNPALDIGQVEGGFMQGVGLYTLLEELKYSPEGYLFTTRGPGM  
bovineXDH LTGDHKNLRTDIVMDVGSLSLNPALDIGQVEGAFVQGLGLFTLEELHYSPEGLHTRGPST  
humanXDH LTGDHKNLRTDIVMDVGSLSLNPALDIGQVEGAFVQGLGLFTLEELHYSPEGLHTRGPST  
mouseXDH LTGDHKNLRTDIVMDVGSLSLNPALDIGQVEGAFVQGLGLFTMEELHYSPEGLHTRGPST  
ratXDH LTGDHKNLRTDIVMDVGSLSLNPALDIGQVEGAFVQGLGLFTMEELHYSPEGLHTRGPST

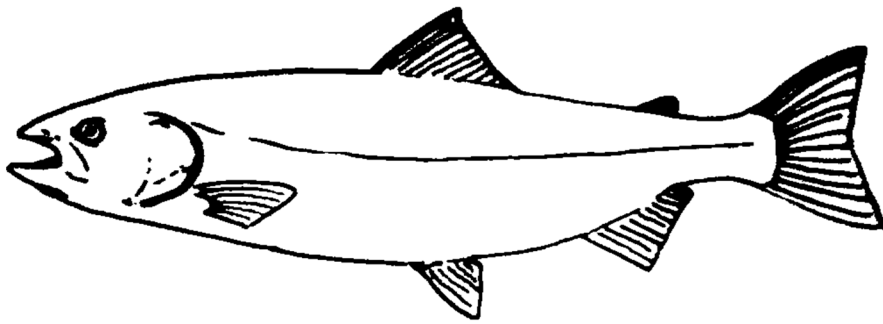
salmonXDH YKIPAFGDIPDLDLTVSLLRDAPNDKAIFFSSKAIGEPPLFLAASVFFAIKDAITAARKESG  
bovineXDH YKIPAFGSIPTEFRVSLLRDPCPNKAIYASKAVGEPPLFLGASVFFAIKDAIRAARAQHT  
humanXDH YKIPAFGSIPIEFRVSLLRDPCPNKAIYASKAVGEPPLFLAASIFFAIKDAIRAARAQHT  
mouseXDH YKIPAFGSIPIEFRVSLLRDPCPNKRAIYASKAVGEPPLFLASSIFFAIKDAIRAARAQHG  
ratXDH YKIPAFGSIPIEFRVSLLRDPCPNKRAIYASKAVGEPPLFLASSIFFAIKDAIRAARAQHG

salmonXDH ---LSGPFRLDSPATPERIRNTCEDRFTKLCPPAEPGTFTPWAVVV  
bovineXDH NNNTKELFRLDSPATPEKIRNACVDKFTTLCVTGAPGNCKPWSLRV  
humanXDH GNNVKELFRLDSPATPEKIRNACVDKFTTLCVTGVPENCKPWSVRV  
mouseXDH DSNAKQLFQLDSPATPEKIRNACVDQFTTLCATGTPENCKSWSVRI  
ratXDH D-NAKQLFQLDSPATPEKIRNACVDQFTTLCVTGVPENCKSWSVRI

While the amino acid sequence of XDH in salmon lacks three of the four cysteine residues involved in the conversion of XDH to the XOD form of the enzyme in mammals, there is evidence of XOD activity in fish tissue. Sinha *et al.* (2015) reported XOD activity in the liver of European Sea Bass (*Dicentrarchus labrax*) which was increased when fish were exposed to environmental pollutants. There was also an increase in the XOD activity in two species of carp (*Cyprinus carpio* and *Carassius auratus gibelio*) when exposed to pollutants (Xu *et al.*, 2012; Zhao *et al.*, 2014). Therefore, it is possible that teleost XDH may be converted to XOD through a different system to that in mammals.

It is possible that XDH, together with the increased levels of hypoxanthine in the skin of smolts identified in this work may play a role in the innate immune system, providing the substrate for the production of H<sub>2</sub>O<sub>2</sub> as a defence against potential pathogens and parasites. On all but one of the diets in the nucleotide supplement feeding trial the level of *XDH* expression increased between 3 and 6 weeks post transfer to SW ( $p < 0.03$ ). As the stress of seawater transfer produces problems with fish health, with increased infection risk during the first few months following transfer, it is possible that hypoxanthine is accumulated in smolts as a preparation for the increased risk from pathogens associated with transfer to seawater. Work to determine whether the expression of *XDH* in the skin increases during both smoltification and infection would be useful to determine whether this is a likely role for the increased hypoxanthine levels detected in the skin of smolts.





Established Osmolytes



## 4. Established organic osmolytes

### 4.1 *The range of organic osmolytes*

The previous chapter focussed on the novel osmolyte hypoxanthine and the metabolism of purines in the skin. While this represents an important discovery in this species, it is important to consider the whole picture. A variety of different osmolytes were extracted from the skin alongside hypoxanthine, as seen in the HPLC trace in Figure 3.1.

The range of organic osmolytes found in terrestrial and aquatic life can be categorised into two major groups, compatible and counteracting osmolytes (Kultz, 2012). Compatible osmolytes are small molecules with no net charge which have no effect on macromolecular structure, while counteracting osmolytes are molecules which occur in biological systems in pairs with counteracting effects on macromolecular structure which are cancelled out when they occur in particular ratios (Kultz, 2012; Yancey, 2005; Yancey *et al.*, 1982). A prominent example of counteracting osmolytes is that of urea and methylamines in cartilaginous fish. Urea is produced in many species as a product of nitrogen metabolism, usually as a waste product which is excreted, as even at low concentrations it can have damaging effects on macromolecular structure (Yancey *et al.*, 1982). However, cartilaginous fish accumulate urea in tissues at approximately 400 mM, despite the fact that the majority of proteins produced by these fish are similarly vulnerable to the effects of urea as those of animals which do not accumulate this osmolyte (Yancey *et al.*, 1982; Yancey & Somero, 1979). The presence of methylamines counteracts the denaturing effects of urea by providing a stabilising influence on proteins, with the counteracting effects of these two osmolytes found to be most effective when urea and methylamines occur in the ratio of 2:1, as found in elasmobranchs (Yancey *et al.*, 1982; Yancey & Somero, 1979).

Levels of compatible osmolytes in the intracellular fluid can be increased in response to osmotic stress, allowing maintenance of cell volume without disruption of metabolic function and without the requirement for the accumulation of a counteracting compound (Kultz, 2012; Yancey *et al.*, 1982). These molecules are not necessary for optimal activity of intracellular enzymes in the absence of osmotic perturbations, however, they can occur at high levels within cells without impeding metabolic functions in contrast to elevated intracellular inorganic ion concentrations which would have deleterious effects on various enzyme actions (Kultz, 2012; Yancey *et al.*, 1982). The molecules employed as osmolytes by phylogenetically distant eukaryote species all belong to a limited number of classes of small metabolic products: free amino acids and modified amino acids, such as taurine and  $\beta$ -alanine; polyhydric alcohols such as glycerol and inositol; and methylamines such as trimethylamine-N-oxide (TMAO), betaine and sarcosine, in combination with urea in some species (Yancey *et al.*, 1982). That only a relatively small number of compounds are utilised as osmolytes suggests that only specific molecules have the necessary properties to make them compatible solutes. For example, the amino acids taurine, proline, glycine, alanine, and  $\beta$ -alanine were all found to be compatible with enzyme function, while the basic, positively charged amino acids arginine and lysine cause disruption to the function of enzymes as these would interfere with the structure of the negatively charged macromolecules (Yancey *et al.*, 1982). The physicochemical interactions between water, solutes, and macromolecules dictates which solutes are compatible and which are unsuitable as osmolytes.

As the majority of extant species use a relatively limited range of organic osmolytes it appears that there is a strong selective pressure favouring these systems. Accumulating compatible osmolytes, or assemblages of counteracting osmolytes requires relatively little genetic adaptation as the only alterations required would be those associated with osmolyte production and transport (Yancey *et al.*, 1982). This system is more “genetically simple”

than the alteration of the amino acid sequences of proteins to allow them to function in the presence of the high concentrations of inorganic ions seen in halobacteria (Yancey *et al.*, 1982) and also allows species to be more flexible in their habitat use.

Organic osmolytes play a vital role in the lifecycle of euryhaline fish species as these transition between habitats with different environmental salinities. When animals are exposed to the effects of increased salinity either through movement into more saline environments, or due to changes in tidal systems, cells directly exposed to the environment undergo a process known as regulatory volume increase (RVI). In the initial response inorganic ions are rapidly accumulated within cells, quickly followed by an ingress of water, to regain osmotic balance and maintain cell volume (Kultz, 2012). When cells are faced with prolonged exposure to hypertonic environments these intracellular inorganic ions are replaced by the synthesis or accumulation of more biologically compatible organic osmolytes. Studies on teleosts and other vertebrates have focussed on the role of just a few organic osmolytes, including the polyhydric alcohol inositol and the modified amino acids taurine and betaine, as well as a few other related macromolecules (Kalujnaia & Cramb, 2009; Michell, 2008; Ripps & Shen, 2012; Yancey, 2005). As the blood osmolality of most euryhaline fish increases by as much as 100 mOsm kg<sup>-1</sup> following entry to seawater, to levels up to 450-500 mOsm kg<sup>-1</sup> as seen in Atlantic salmon, osmolytes form part of the intracellular adaptation of fish to their new environment (Bendiksen *et al.*, 2003; Marshall, 2012; Pan *et al.*, 2004).

In tilapia, myo-inositol has been identified as the major functional osmolyte (Kalujnaia *et al.*, 2013). Similarly, inositol has been shown to be a major organic osmolyte in the European eel (Kalujnaia *et al.*, 2013, 2010, 2009). This compatible osmolyte is synthesised from glucose-6-phosphate by two enzymes which are found to be up-regulated in several tissues when eels and tilapia are exposed to hyperosmotic stress (Kalujnaia *et al.*, 2013; Sacchi *et al.*, 2013). In

seawater acclimated eels and tilapia, inositol production is up-regulated predominantly in the tissues exposed to the external environment, such as the skin, fin and gills (Kalujnaia *et al.*, 2013). Dietary supplements of myo-inositol have been shown to increase the growth rate of juvenile tilapia, and hence this cyclic alcohol is considered an essential component in some dietary feeds used in aquaculture (Peres *et al.*, 2004; Shiau & Su, 2005). In Atlantic salmon, myo-inositol does not occur in tissues at levels sufficient to perform a significant osmotic role (this study), therefore other molecules must perform this essential function. The organic molecules responsible for the majority of osmotic function within Atlantic salmon are currently unknown. The identification of the organic osmolytes present in seawater-acclimated salmon awaits future experimentation.

As smolt transfer from the freshwater to seawater environments is such an integral part of Atlantic salmon aquaculture and poses a major bottleneck for the industry as a vulnerable life stage for fish, knowledge of the organic osmolytes employed by the species in seawater acclimation will aid in its culture.

## *4.2 Organic osmolyte levels - direct transfer trial and SW challenge*

Alongside hypoxanthine a number of other organic osmolytes was extracted from the skin and quantified by HPLC (Materials and Methods section 2.4). These osmolytes were investigated in the direct transfer trial with two aims:

1. to determine how osmolyte levels were affected by acute exposure to sea water
2. to determine the effect of SW challenge on osmolyte levels at different stages as fish progressed towards the time of smoltification and SW transfer.

### *4.2.1 Method*

Tissue samples were collected from parr and smolts from the Marine Harvest freshwater facility at Loch Lochy in the autumn of 2016 (Materials and Methods section 2.6.3). SW challenge was conducted by transferring fish directly to aerated SW. This differs from SW transfer as it was conducted at selected time points during the development of fish from parr to smolts before the time of whole stock transfer to SW. As stated above, organic osmolytes were extracted from the skin and quantified by an established HPLC method (Materials and Methods section 2.4). Code used for statistical analysis is given in Appendix 4.

## 4.2.2 Results

### 4.2.2.1 Total osmolyte

Total osmolyte levels, including hypoxanthine, were found to be significantly influenced by time point in a time course leading to smoltification and SW transfer, as seen in Figure 4.1 A ( $F_{5,29} = 6.21$ ,  $p = 0.0005$ ). Twenty-four hours before SW transfer the level of total osmolyte was significantly lower than at 30 days before transfer ( $p = 0.02$ ). On the two days following SW transfer the level of total osmolyte increased and was significantly higher than at the 0 days to transfer time point ( $p < 0.001$ ).

The level of total osmolyte was also affected by SW challenge ( $F_{2,28} = 7.14$ ,  $p = 0.003$ ). As seen in Figure 4.1 B the mean level of total osmolyte was higher in SW at the three time points investigated, this difference was statistically significant at 44 days to SW transfer ( $p = 0.0002$ ) and at the 0 days to transfer time point ( $p = 0.002$ ), but not at the 30 days to SW transfer time point ( $p = 0.42$ ).

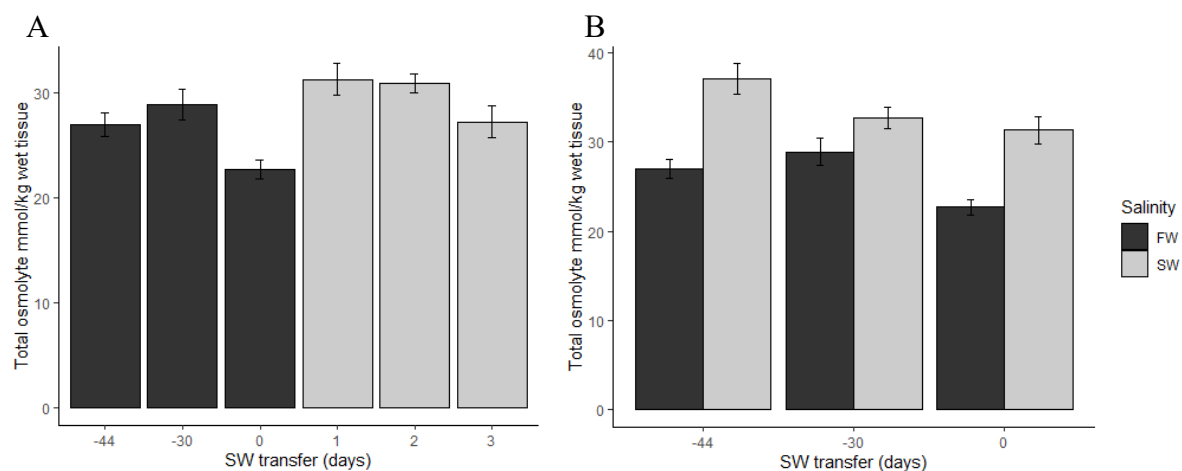


Figure 4.1. Mean sum of combined organic osmolytes extracted from the skin of Atlantic salmon in a time course leading to smoltification and SW transfer. Plot A shows levels of osmolyte extracted from the skin of fish under normal production conditions. Plot B shows levels extracted from fish exposed to SW challenge at three points on the time course. Error bars represent standard error.

#### 4.2.2.2 Glucose

Glucose levels were found not to be significantly affected by time point as fish progressed towards smoltification and SW transfer ( $F_{5,28} = 2.49$ ,  $p = 0.054$ ) as shown in Figure 4.2 A. When fish underwent SW challenge, a significant effect of time point ( $F_{2,27} = 9.02$ ,  $p = 0.001$ ) and salinity ( $F_{1,27} = 20.04$ ,  $p = 0.0001$ ) was detected. Following SW challenge the level of glucose detected in the skin was higher than in FW at each time point, though this trend only achieved statistical significance at the time point 30 days before SW transfer ( $p = 0.0001$ ), Figure 4.2 B.

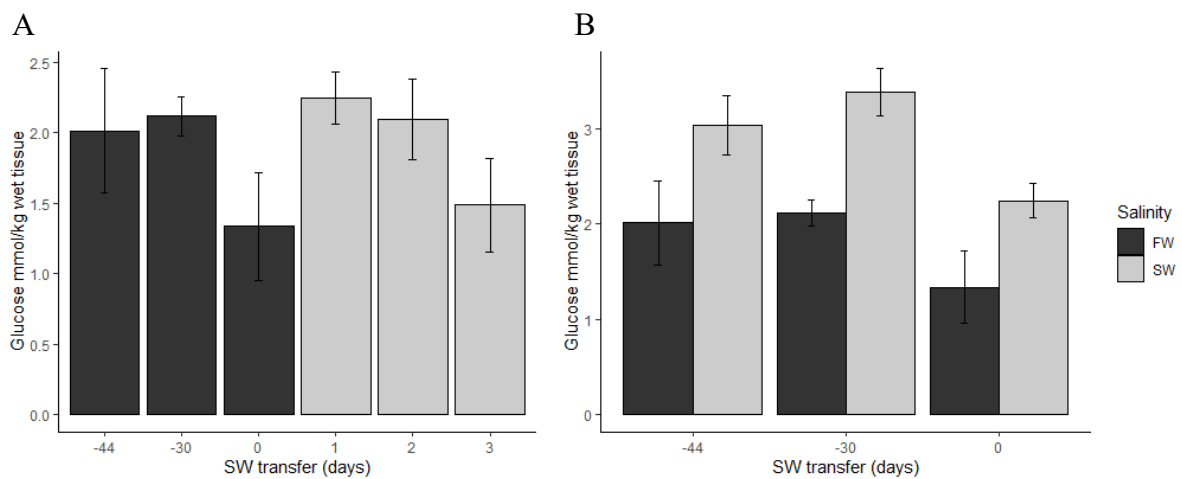


Figure 4.2. Mean glucose level extracted from the skin of Atlantic salmon in a time course leading to smoltification and SW transfer. Plot A shows levels of glucose extracted from the skin of fish under normal production conditions. Plot B shows levels extracted from fish exposed to SW challenge at three points on the time course. Error bars represent standard error.

#### 4.2.2.3 Myoinositol

Over the time course leading to smoltification the level of myoinositol in the skin was shown to be significantly affected by time point by one way ANOVA ( $F_{5,29} = 53.52$ ,  $p = 9.28 \times 10^{-14}$ ), however, the data were found not to be normally distributed ( $W = 0.84$ ,  $p = 0.0001$ ). The non-parametric Kruskal Wallis test was used to analyse the data and a significant effect was found ( $\chi^2_5 = 28.47$ ,  $p = 2.94 \times 10^{-5}$ ), Figure 4.3 A. The level of myoinositol was significantly higher at 44 days and 30 days to SW transfer than at 0 days to SW transfer ( $p < 0.005$ ). At 1 day post transfer the level remained lower than at the 30 days to transfer time point ( $p = 0.002$ ). The level of myoinositol was not found to be significantly influenced by SW challenge ( $F_{1,28} = 1.7748$ ,  $p = 0.19$ ), Figure 4.3 B.

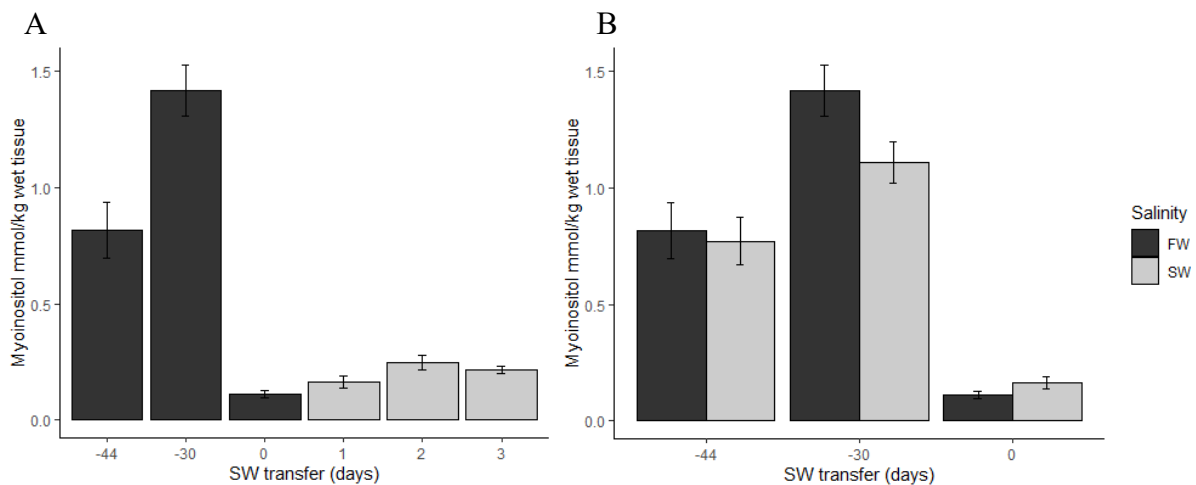


Figure 4.3. Mean myoinositol level extracted from the skin of Atlantic salmon in a time course leading to smoltification and SW transfer. Plot A shows levels of myoinositol extracted from the skin of fish under normal production conditions. Plot B shows levels extracted from fish exposed to SW challenge at three points on the time course. Error bars represent standard error.

#### 4.2.2.4 Taurine

Taurine levels in the skin were not found to be influenced by time point as fish progressed towards smoltification and SW transfer ( $F_{5,29} = 1.75$ ,  $p = 0.16$ , Figure 4.4 A), nor did the level of taurine change following SW challenge ( $F_{1,28} = 0.19$ ,  $p = 0.67$ , Figure 4.4 B). However, data were not normally distributed in the SW challenge analysis ( $W = 0.91$ ,  $p = 0.01$ ). Data were analysed using a generalised linear model which showed SW challenge did not have a significant effect on taurine level ( $F_{1,28} = 0.48$ ,  $p = 0.62$ ).

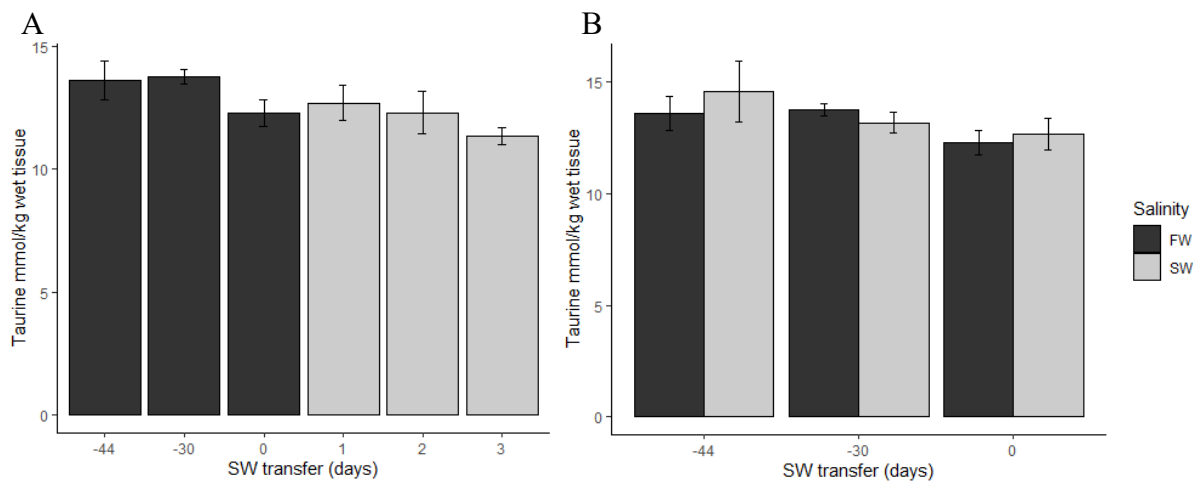


Figure 4.4. Mean taurine level extracted from the skin of Atlantic salmon in a time course leading to smoltification and SW transfer. Plot A shows levels of taurine extracted from the skin of fish under normal production conditions. Plot B shows levels extracted from fish exposed to SW challenge at three points on the time course. Error bars represent standard error,  $n=6$ .

#### 4.2.2.5 GPC

Levels of GPC were significantly influenced by time point as fish progressed towards SW transfer ( $F_{5,29} = 11.99$ ,  $p = 2.39 \times 10^{-6}$ ). 30 days before SW transfer the level of GPC was higher than at all other time points except on the first day after SW transfer (Figure 4.5 A). Immediately prior to SW transfer, the level of GPC detected was significantly lower than at the two preceding ( $p < 0.05$ ) and the two following time points ( $p < 0.01$ ), however, after 3 days in SW the level of GPC was not significantly different from that seen at the 0 days to SW transfer time point ( $p = 0.63$ ).

SW challenge had a significant effect on the level of GPC detected in the skin ( $F_{1,28} = 80.2$ ,  $p = 1.04 \times 10^{-9}$ ), with the level significantly higher following challenge at all three time points ( $p < 0.002$ ), Figure 4.5 B.

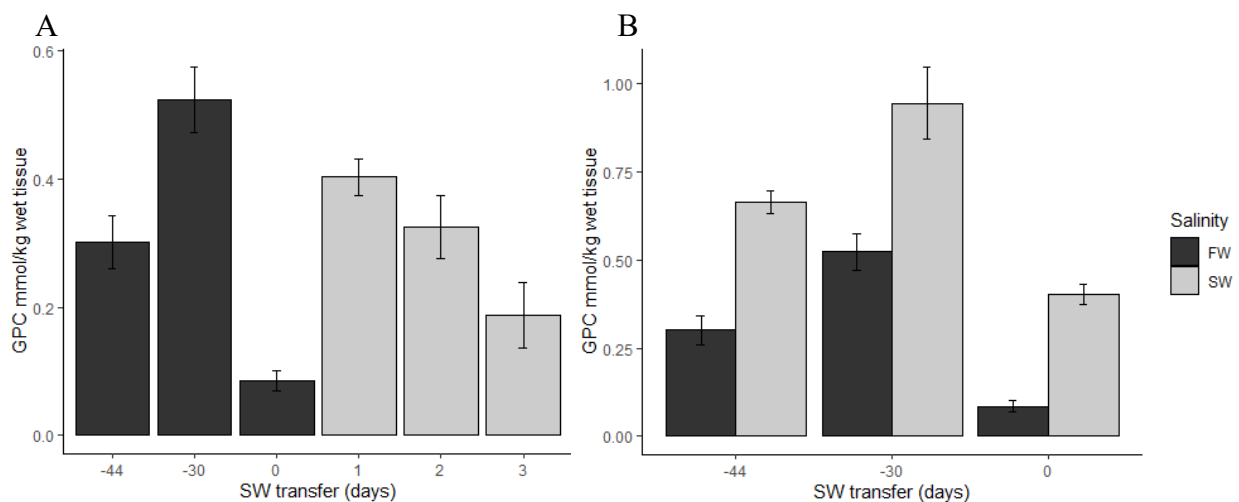


Figure 4.5. Mean GPC level extracted from the skin of Atlantic salmon in a time course leading to smoltification and SW transfer. Plot A shows levels of GPC extracted from the skin of fish under normal production conditions. Plot B shows levels extracted from fish exposed to SW challenge at three points on the time course. Error bars represent standard error,  $n=6$ .

#### 4.2.2.6 Alanine

Alanine levels were significantly affected by time point over the smoltification time course ( $F_{5,29} = 13.77$ ,  $p = 7.98 \times 10^{-7}$ ). As seen in Figure 4.6 A, there was a rise in alanine levels following SW transfer, with the level at 1 day and 2 days post transfer significantly higher than the preceding time points in FW ( $p < 0.05$ ). By the 3<sup>rd</sup> day in SW the level of alanine had returned to the lower levels seen in FW and was significantly lower than at the 1<sup>st</sup> day in SW ( $p = 0.00006$ ).

As Figure 4.6 B shows, SW challenge also influenced the level of alanine detected in the skin ( $F_{1,27} = 76.65$ ,  $p = 2.27 \times 10^{-9}$ ). At all three time points investigated, SW challenge led to an increase in alanine levels in the skin ( $p < 0.01$ ).

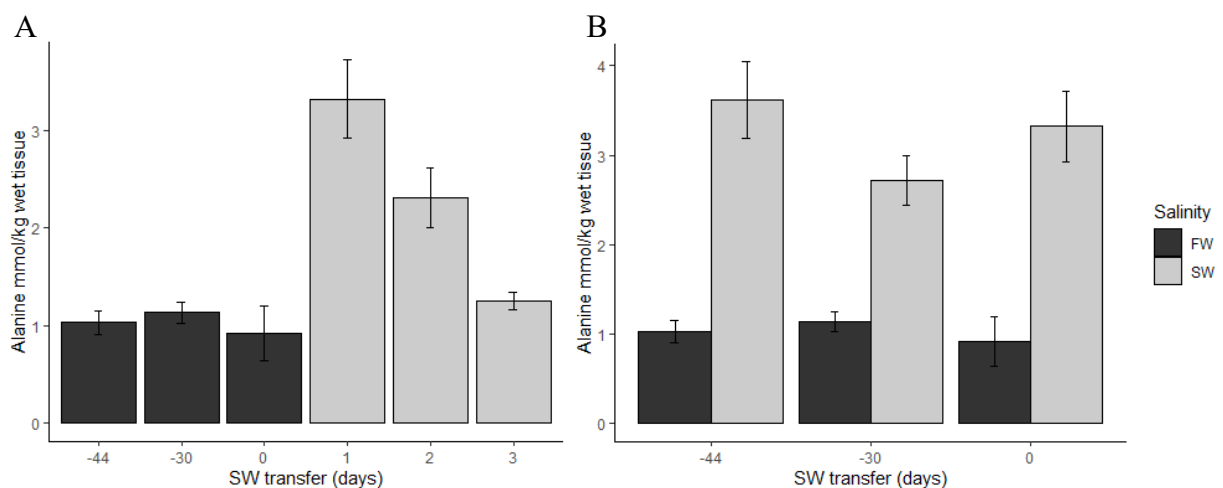


Figure 4.6. Mean alanine level extracted from the skin of Atlantic salmon in a time course leading to smoltification and SW transfer. Plot A shows levels of alanine extracted from the skin of fish under normal production conditions. Plot B shows levels extracted from fish exposed to SW challenge at three points on the time course. Error bars represent standard error, n=6.

#### 4.2.2.7 Glycine betaine

Betaine levels were significantly influenced by time point on the smoltification time course ( $F_{5,29} = 5.03$ ,  $p = 0.002$ ), Figure 4.7 A. The level of betaine was significantly higher at all time points following SW transfer than at the 44 and 0 days to transfer time points ( $p < 0.05$ ). At the 30 days to transfer time point the level of betaine measured was more variable, and levels did not differ significantly from any other time points investigated.

SW challenge also influenced the level of betaine measured in the skin ( $F_{1,28} = 12.94$ ,  $p = 0.001$ ), however, the data was not normally distributed ( $W = 0.88$ ,  $p = 0.002$ ). This non-normal result was due to one outlier in the FW group. When this point was excluded the same results was obtained ( $F_{1,27} = 30.43$ ,  $p = 7.63 \times 10^{-6}$ ), and as the variance of the original data was found to be equal by Leven's test ( $F_{5,28} = 0.92$ ,  $p = 0.48$ ), the result from the original data was accepted. A significant difference was detected when fish were exposed to SW challenge at the 0 hour to SW transfer time point ( $p < 0.03$ ), Figure 4.7 B.

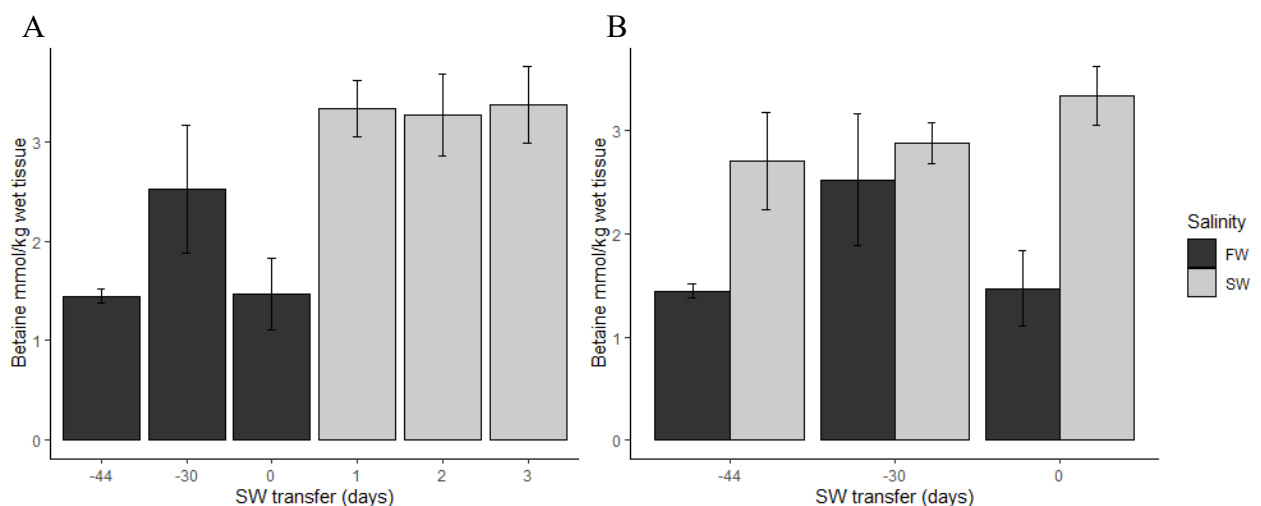


Figure 4.7. Mean betaine level extracted from the skin of Atlantic salmon in a time course leading to smoltification and SW transfer. Plot A shows levels of betaine extracted from the skin of fish under normal production conditions. Plot B shows levels extracted from fish exposed to SW challenge at three points on the time course. Error bars represent standard error,  $n=6$ .

#### 4.2.2.8 Glycine

Glycine levels in the skin were not found to be significantly influenced by time point over the smoltification time course ( $F_{5,25} = 2.18$ ,  $p = 0.09$ ), however, the data were not normally distributed ( $W = 0.89$ ,  $p = 0.005$ ). When an outlier was removed from the 2 days post SW transfer time point the data were found to be normally distributed ( $W = 0.98$ ,  $p = 0.86$ ), as with the original data, no significant effect of time point was observed on the level of glycine measured in the skin ( $F_{5,24} = 2.41$ ,  $p = 0.07$ ), Figure 4.8 A.

SW challenge had a significant effect on glycine levels in the skin ( $F_{1,19} = 22.90$ ,  $p = 0.0001$ ). However, there was no significant difference between levels in FW and SW at each time point ( $p > 0.05$ ), Figure 4.8 B.

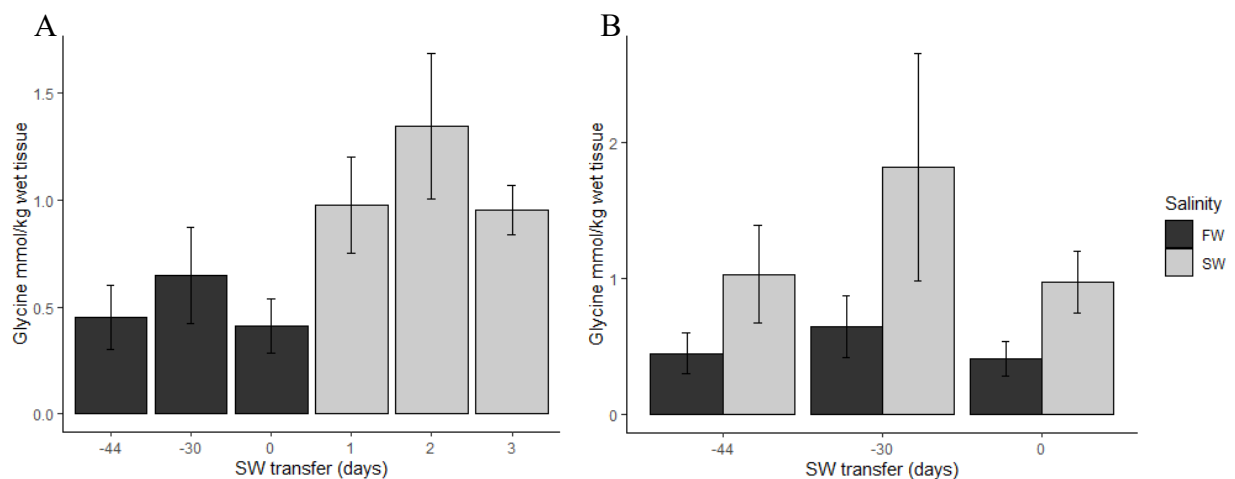


Figure 4.8. Mean glycine level extracted from the skin of Atlantic salmon in a time course leading to smoltification and SW transfer. Plot A shows levels of glycine extracted from the skin of fish under normal production conditions. Plot B shows levels extracted from fish exposed to SW challenge at three points on the time course. Error bars represent standard error,  $n=6$ .

#### 4.2.2.9 Creatine

Time point was found by ANOVA to have a significant effect on creatine levels in the skin as fish progressed towards smoltification and SW transfer ( $F_{5,29} = 2.85$ ,  $p = 0.03$ ), however data were not normally distributed ( $W = 0.88$ ,  $p = 0.001$ ). Analysis by Kruskal Wallis test also identified a significant effect of time point on creatine levels ( $\chi^2_5 = 16.55$ ,  $p = 0.005$ ). The level of creatine was significantly higher 30 days before SW transfer than at 0 days to transfer ( $p = 0.037$ ). Following SW transfer levels of creatine increased up to two days post transfer, before returning to a level significantly lower than at 30 days to SW transfer ( $p = 0.047$ ), results in Figure 4.9 A.

No significant effect if SW challenge on creatine levels in the skin was identified ( $F_{1,28} = 3.68$ ,  $p = 0.07$ ), Figure 4.9 B.

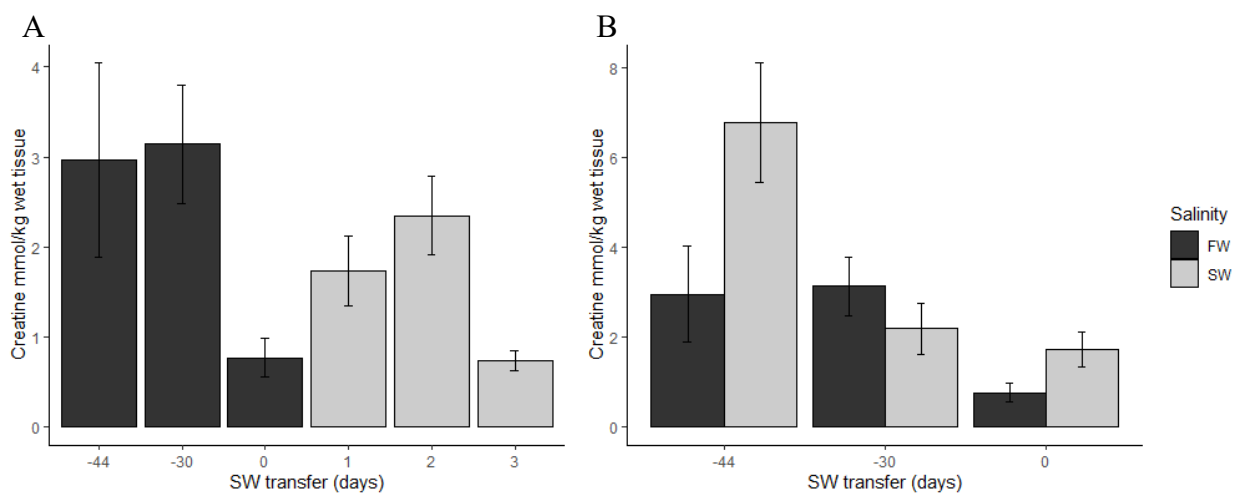


Figure 4.9. Mean creatine level extracted from the skin of Atlantic salmon in a time course leading to smoltification and SW transfer. Plot A shows levels of creatine extracted from the skin of fish under normal production conditions. Plot B shows levels extracted from fish exposed to SW challenge at three points on the time course. Error bars represent standard error, n=6.

### *4.3 Organic osmolyte levels – nucleotide supplement feeding trial*

As above in the direct transfer trial, a number of other osmolytes were extracted from the skin of fish on the nucleotide supplement feeding trial alongside hypoxanthine and quantified by HPLC (Materials and Methods section 2.4). These were analysed with two aims:

1. to determine the effect of the different nucleotide supplements on the levels of organic osmolytes in the skin
2. to examine the level of different organic osmolytes over a longer time course, up to 6 weeks after SW transfer.

#### *4.3.1 Method*

Tissue samples were collected from fish at the EWOS Innovation research facility at Dirdal, Norway. Fish were sampled before the commencement of feeding with experimental diets and this was taken as a baseline time point. Subsequently fish were sampled at two time points before SW transfer and three time points post SW transfer (Materials and Methods section 2.7). Osmolytes were then extracted and quantified by an established HPLC method (Materials and Methods section 2.4). Code used for statistical analysis in R is given in Appendix 4.

### 4.3.2 Results

#### 4.3.2.1 Total osmolyte

The sum of the combined organic osmolytes measured in the skin of Atlantic salmon in the feeding trail study is presented in Figure 4.10. The level of the total osmolyte was significantly affected by time point ( $F_{5,306} = 3.38$ ,  $p = 0.005$ ) but not by diet. Total osmolyte level was significantly higher 24 hours before SW transfer, than at baseline ( $p = 0.03$ ), 24 hours post SW transfer ( $p = 0.04$ ), and after 3 weeks in SW ( $p = 0.04$ ).

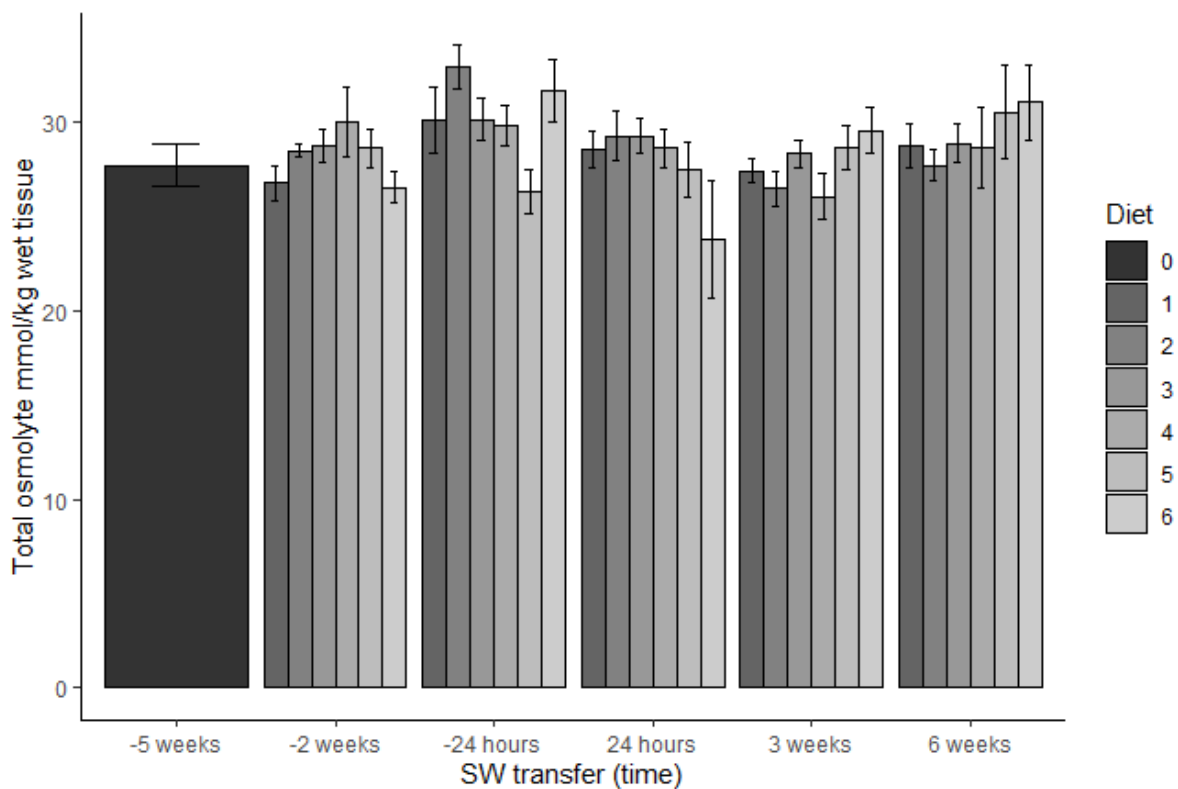


Figure 4.10. Mean sum of combined organic osmolytes extracted from the skin of fish from nucleotide supplement feeding trial. The first time point, 5 weeks before SW transfer, represents baseline before feeding with experimental diets began. Error bars represent standard error.

#### 4.3.2.2 Glucose

No effect of diet was detected on the level of glucose in the skin ( $F_{5,164}=0.41$ ,  $p = 0.46$ ). Relative to baseline measurements taken 5 weeks before SW transfer, glucose levels fell significantly by 2 weeks before SW transfer ( $p < 0.0001$ ). At all of the following time points glucose levels were below the limit of detection of the assay in some individuals on all diets. As it is unlikely that these “undetected” values were in fact 0 values, and to avoid using skewed means favouring higher values which were within the detection parameters of the assay, missing values were ascribed an arbitrary value to allow for interrogation and analysis. The lowest value reported was 1.079 mmol/kg and this was taken as close to the limit of detection. There are a number of ways used to compare data when a data set contains undetected values. One is to arbitrarily set undetectable values at half the limit of detection, another is to set the values to a number close to but below the limit of detection. The latter was chosen in this case and points below the level of detection were arbitrarily ascribed the value of 1. This value was chosen because overall a falling trend in glucose levels was observed and setting the value to just below the level of detection reduces the risk of inflating this effect but can give an indication of the trend.

When arbitrary values were included in the analysis both time point ( $F_{5,306} = 77.18$ ,  $p < 2.2 \times 10^{-16}$ ) and the interaction between time point and diet ( $F_{25,306} = 0.84$ ,  $p = 0.0004$ ) had a significant effect on glucose levels. Overall, on all diets glucose levels were significantly lower at 2 weeks to SW transfer than at baseline ( $p = 0.003$ ). At 24 hours to SW transfer the level of glucose was significantly lower than at 2 weeks to transfer ( $p = 0.004$ ). At the three time points following SW transfer glucose levels were significantly lower than at 24 hours before SW transfer ( $p < 0.0001$ ). On diets 5 and 6 at the last time point the level of glucose returned to within the assay range in all samples.

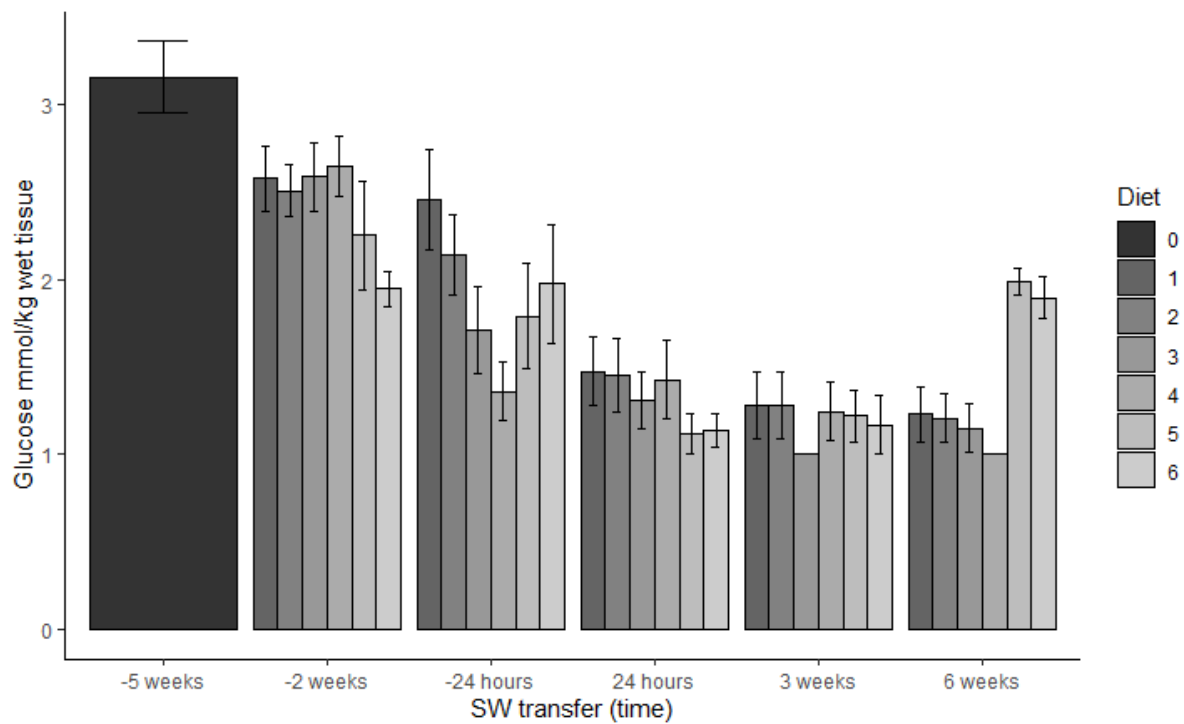


Figure 4.11. Mean glucose level extracted from the skin of fish from nucleotide supplement feeding trial including arbitrary values for samples in which glucose was reported as undetected. The first time point, 5 weeks before SW transfer, represents baseline before feeding with experimental diets began. Error bars represent standard error. Bars without error bars represent groups in which two or fewer samples contained glucose.

#### 4.3.2.3 Myoinositol

Myoinositol levels were significantly influenced by time point ( $F_{5,300} = 28.55$ ,  $p < 2 \times 10^{-16}$ ), and the interaction between time point and diet ( $F_{25,300} = 1.82$ ,  $p = 0.01$ ). As shown in Figure 4.12, there was a downward trend in levels of myoinositol in the skin over the course of the feeding trial. After 3 weeks in SW skin myoinositol was lower than baseline levels, achieving statistical significance on diets 2, 3 and 6 ( $p < 0.01$ ). At 6 weeks post SW transfer myoinositol levels had fallen further in the skin of fish on diet 4 ( $p = 0.004$ ).

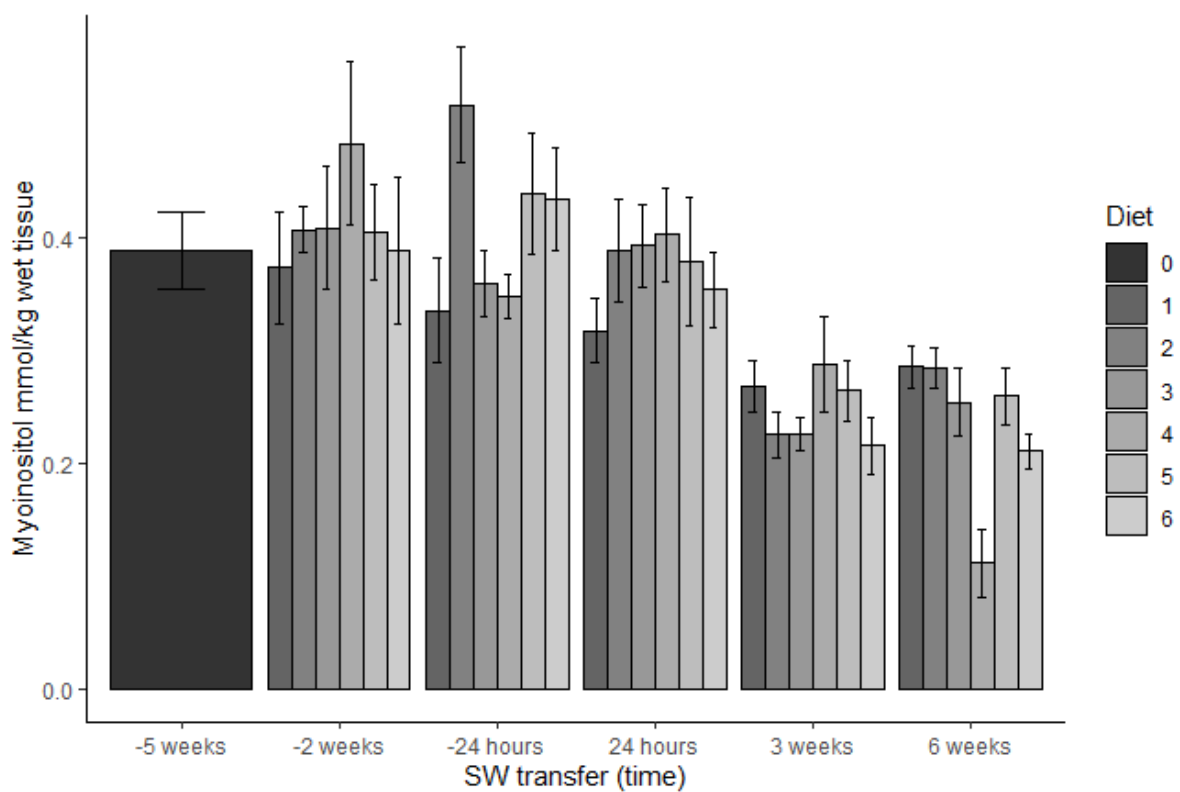


Figure 4.12. Mean myoinositol level extracted from the skin of fish from nucleotide supplement feeding trial. The first time point, 5 weeks before SW transfer, represents baseline before feeding with experimental diets began. Error bars represent standard error.

#### 4.3.2.4 Taurine

The level of taurine in the skin (Figure 4.13) was found to be affected by time point ( $F_{5,305} = 33.17, p < 2 \times 10^{-16}$ ). The level of taurine was significantly higher at 3 weeks and 6 weeks post SW transfer than at any previous time points ( $p < 0.0001$ ).

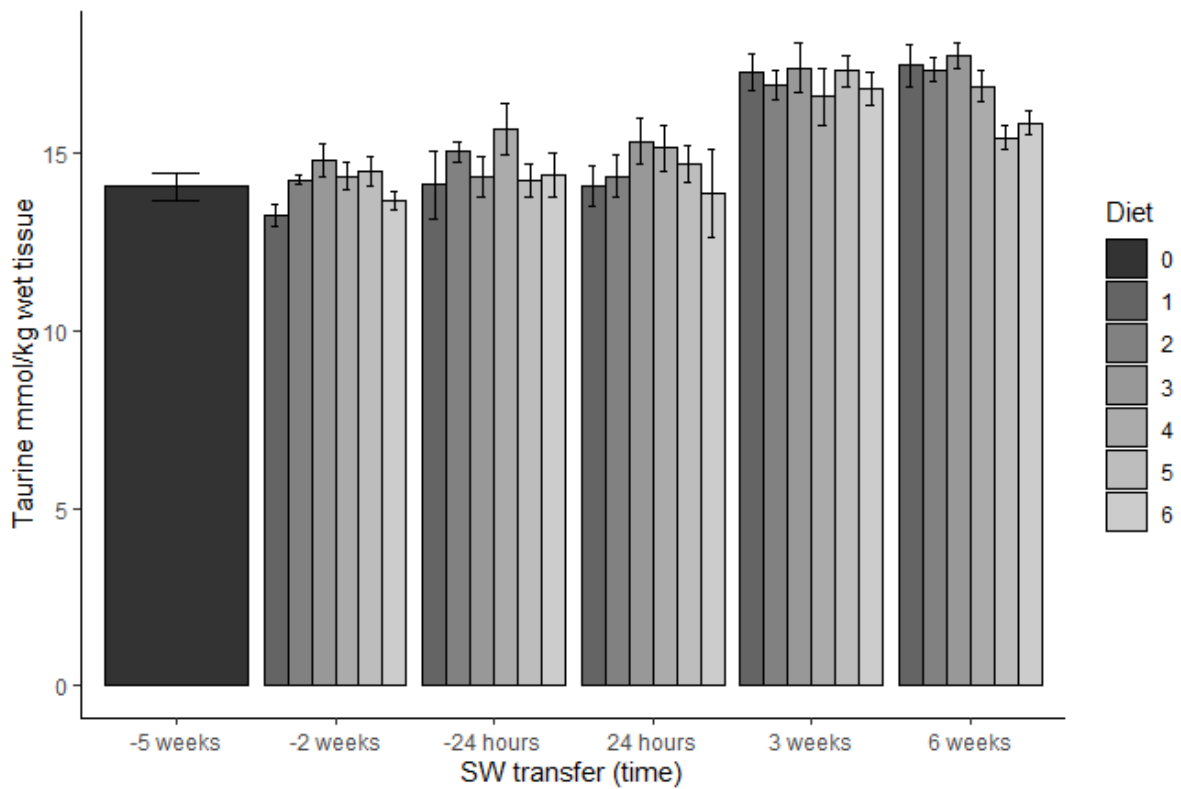


Figure 4.13. Mean taurine level extracted from the skin of fish from nucleotide supplement feeding trial. The first time point, 5 weeks before SW transfer, represents baseline before feeding with experimental diets began. Error bars represent standard error.

#### 4.3.2.5 GPC

GPC levels in the skin (Figure 4.14) were significantly influenced by time point ( $F_{5,304} = 23.26$ ,  $p < 2.2 \times 10^{-16}$ ) and by the interaction between time point and diet ( $F_{25,304} = 2.19$ ,  $p = 0.001$ ). On diets 2, 3 and 6 GPC levels were significantly higher the day before SW transfer than earlier time points ( $p < 0.05$ ) falling back to previous levels after 24 hours in SW ( $p < 0.05$ ). The downward trend continued, at 3 weeks post SW transfer GPC levels were lower than at 24 hours pre-SW transfer on all but diet 6 ( $p < 0.05$ ).

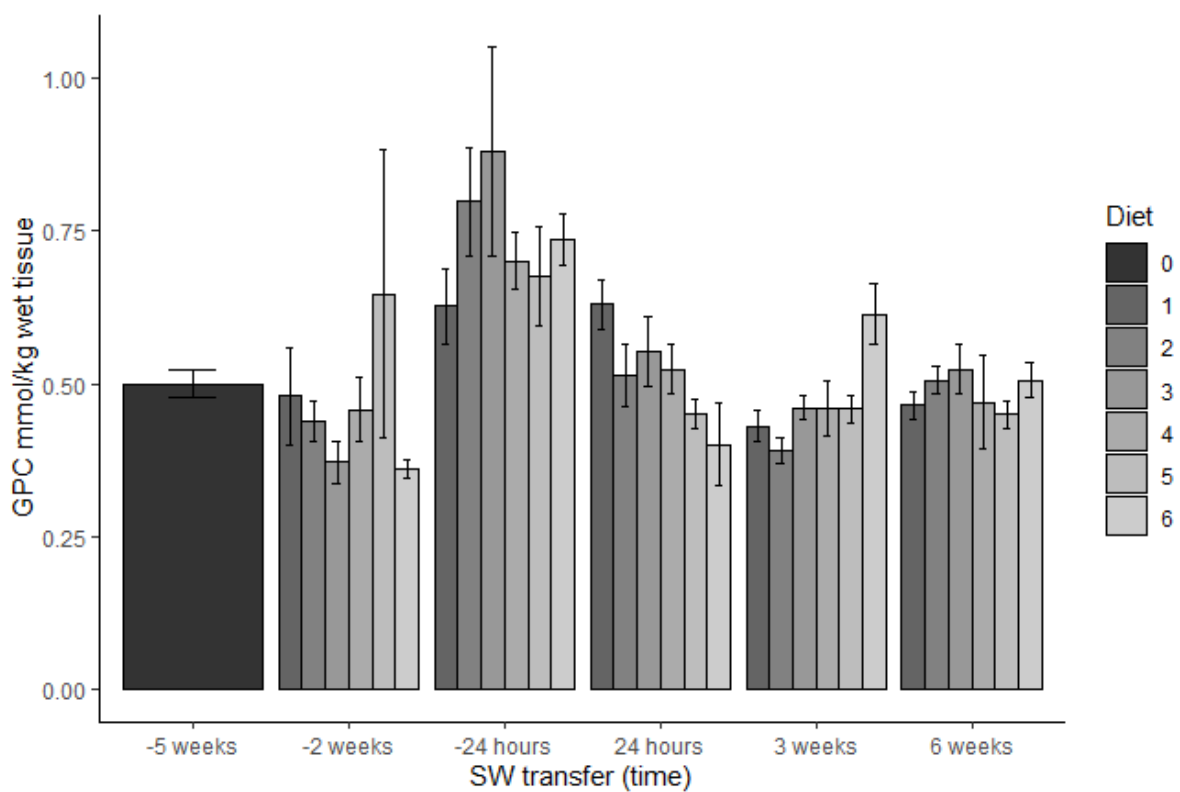


Figure 4.14. Mean GPC level extracted from the skin of fish from nucleotide supplement feeding trial. The first time point, 5 weeks before SW transfer, represents baseline before feeding with experimental diets began. Error bars represent standard error.

#### 4.3.2.6 Urea

The level of urea in the skin was significantly influenced by time point ( $F_{5,306} = 19.2669$ ,  $p < 2 \times 10^{-16}$ ). At the baseline time point urea levels were a little below 2 mmol/kg and at 2 weeks to SW transfer levels had not changed from baseline. At the later time points the level of urea was below the limit of detection of the assay on many of the samples. As it is unlikely that these “undetected” values were in fact 0 values, and to avoid using skewed means favouring higher values which were within the detection parameters of the assay, missing values were ascribed an arbitrary value to allow for interrogation and analysis. As with the glucose analysis above, the level of undetected samples was set slightly below the limit of detection of the assay. The lowest levels of urea reported was 0.17 mmol/kg which was taken to be close to the limit of detection. Undetected samples were set to 0.1 mmol/kg.

By 24 hours to SW transfer the level of urea dropped below baseline ( $p = 0.017$ ) and they remained below baseline at 24 hours post SW transfer ( $p = 0.0016$ ). By 3 weeks post transfer levels fell further ( $p = 0.0013$ ). At 6 weeks post transfer levels were significantly higher than at 3 weeks ( $p = 0.002$ ) and not significantly different from other time points. On a small number of samples on diets 4, 5 and 6 the level of urea was very high, approximately 8 mmol/kg on diet 4, between 10-20 mmol/kg on diet 5, and between 6-18 mmol/kg on diet 6.

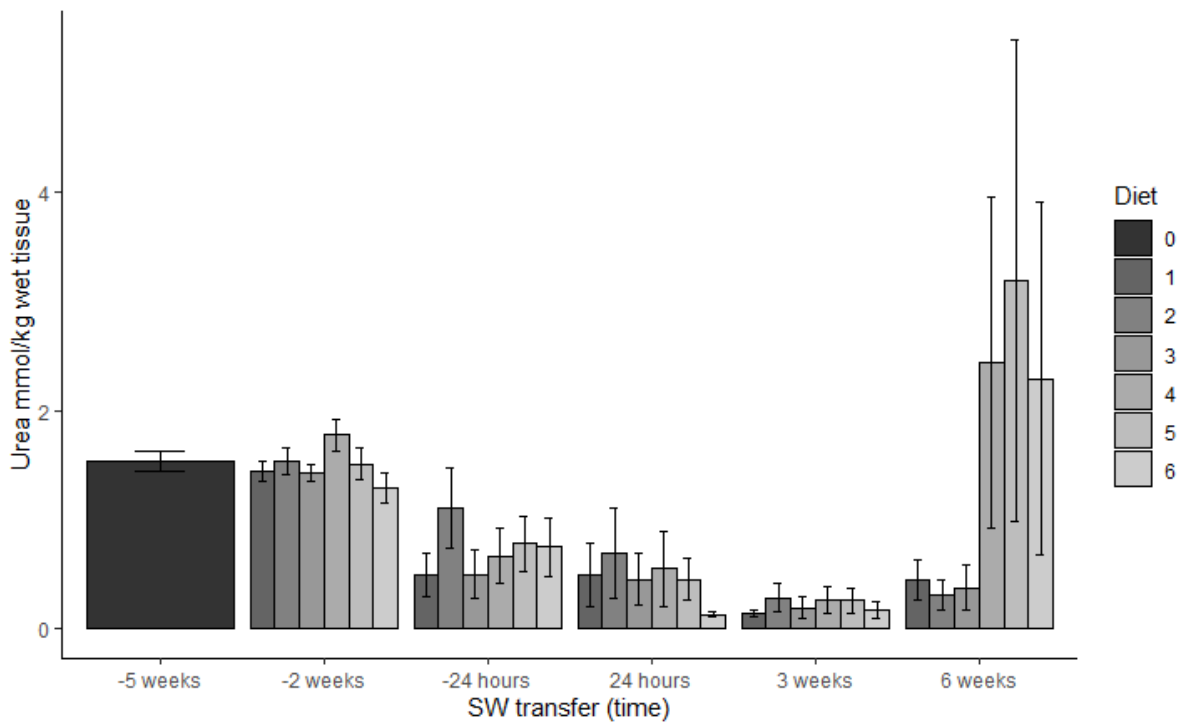


Figure 4.15. Mean urea level extracted from the skin of fish from nucleotide supplement feeding trial including arbitrary values for samples in which urea was reported as undetected. The first time point, 5 weeks before SW transfer, represents baseline before feeding with experimental diets began. Error bars represent standard error.

#### 4.3.2.7 Alanine

Alanine levels in the skin (Figure 4.16) were significantly influenced by both time point ( $F_{5,291} = 42.47$ ,  $p < 2.2 \times 10^{-16}$ ) and diet ( $F_{5,291} = 4.73$ ,  $p = 0.0004$ ), as well as the interaction between these two variables ( $F_{25,164} = 4.51$ ,  $p < 9.27 \times 10^{-11}$ ). There was a rise in alanine levels to above baseline levels prior to SW transfer which was significant at 2 weeks before SW transfer on diets 4 and 5 ( $p < 0.01$ ). This rise was maintained at the following time point, 24 hours prior to SW transfer, with all remaining diets achieving a statistically significant increase ( $p < 0.05$ ). Following SW transfer, levels of alanine fell, returning to baseline levels on diets 3-6, though levels remained elevated on diets 1 and 2 ( $p < 0.005$ ). After 3 weeks in SW the level of alanine in the skin fell to levels equivalent to baseline, and at the final time point, 6 weeks after SW transfer, the level of alanine in the skin remained at around baseline levels on diets 1-4, while on diets 5 and 6 levels were significantly higher than at baseline ( $p < 0.05$ ).

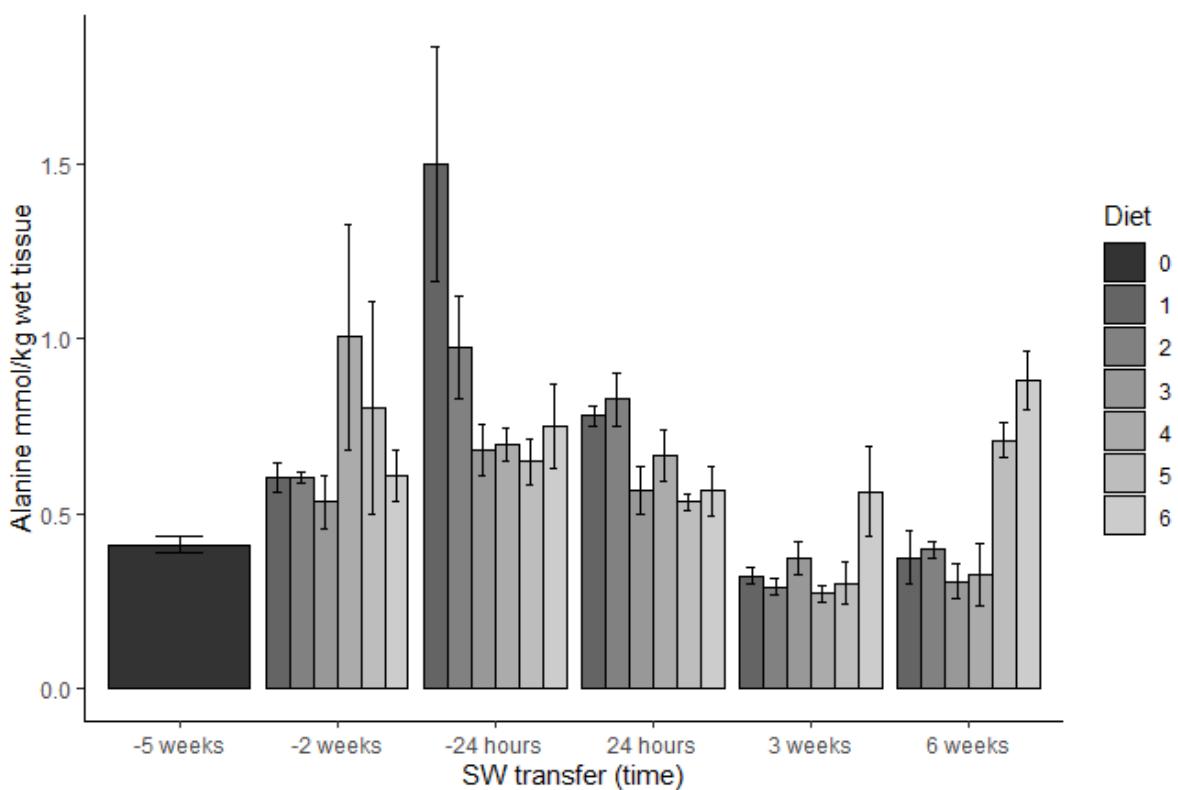


Figure 4.16. Mean alanine level extracted from the skin of fish from nucleotide supplement feeding trial. The first time point, 5 weeks before SW transfer, represents baseline before feeding with experimental diets began. Error bars represent standard error.

#### 4.3.2.8 Glycine betaine

The level of glycine betaine in the skin (Figure 4.17) was found to be significantly affected by time point ( $F_{5,305} = 58.27$ ,  $p < 2.2 \times 10^{-16}$ ) and the interaction between time point and diet ( $F_{25,305} = 27.55$ ,  $p < 6.2 \times 10^{-12}$ ). A slight increase in betaine levels was observed at 2 weeks before SW transfer compared to baseline, however, this was not statistically significant. 24 hours before SW transfer, betaine levels remained similar to the baseline on diets 1-5, though on diets 4 and 5 levels were significantly lower than those measured 2 weeks transfer ( $p < 0.005$ ). Meanwhile, on diet 6 betaine levels were the highest recorded in this study at around 50% higher than baseline levels ( $p = 0.0004$ ). After 24 hours in SW, fish on diet 6 showed lower levels of betaine in the skin compared with the previous time point ( $p < 0.0001$ ). Conversely, on diets 1-5 betaine levels increased, achieving statistical significance on diets 1, 2, 4 and 5 ( $p < 0.01$ ). After 3 weeks in SW the level of betaine in the skin had fallen on all diets and was significantly lower than baseline levels on diets 1-5 ( $p < 0.05$ ). Levels remained low at 6 weeks post transfer, with levels on diets 1 and 2 remaining below baseline ( $p < 0.05$ ).

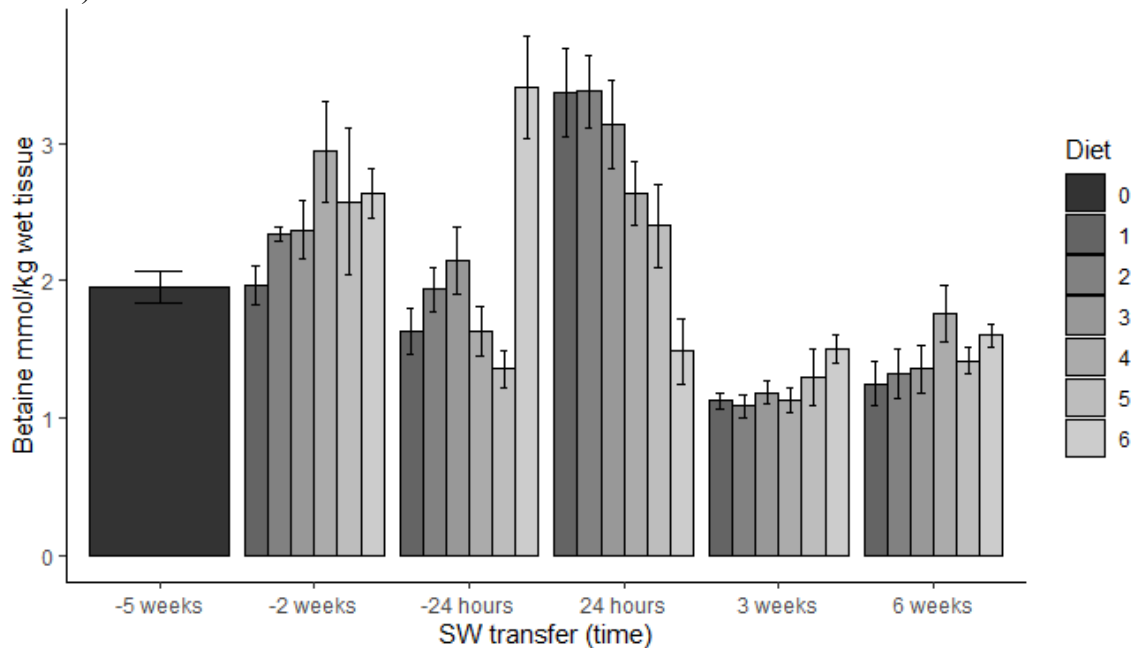


Figure 4.17. Mean betaine level extracted from the skin of fish from nucleotide supplement feeding trial. The first time point, 5 weeks before SW transfer, represents baseline before feeding with experimental diets began. Error bars represent standard error.

#### 4.3.2.9 Creatine

The level of creatine in the skin (Figure 4.18) was influenced by time point ( $F_{5,305} = 19.75$ ,  $p < 2 \times 10^{-16}$ ). Creatine levels were above baseline values 1 day prior to SW transfer ( $p < 0.0001$ ). The trended down towards baseline 1 day post SW transfer ( $p = 0.002$ ) and this downward trend continued, with levels below baseline at 6 weeks post SW transfer ( $p = 0.01$ ).

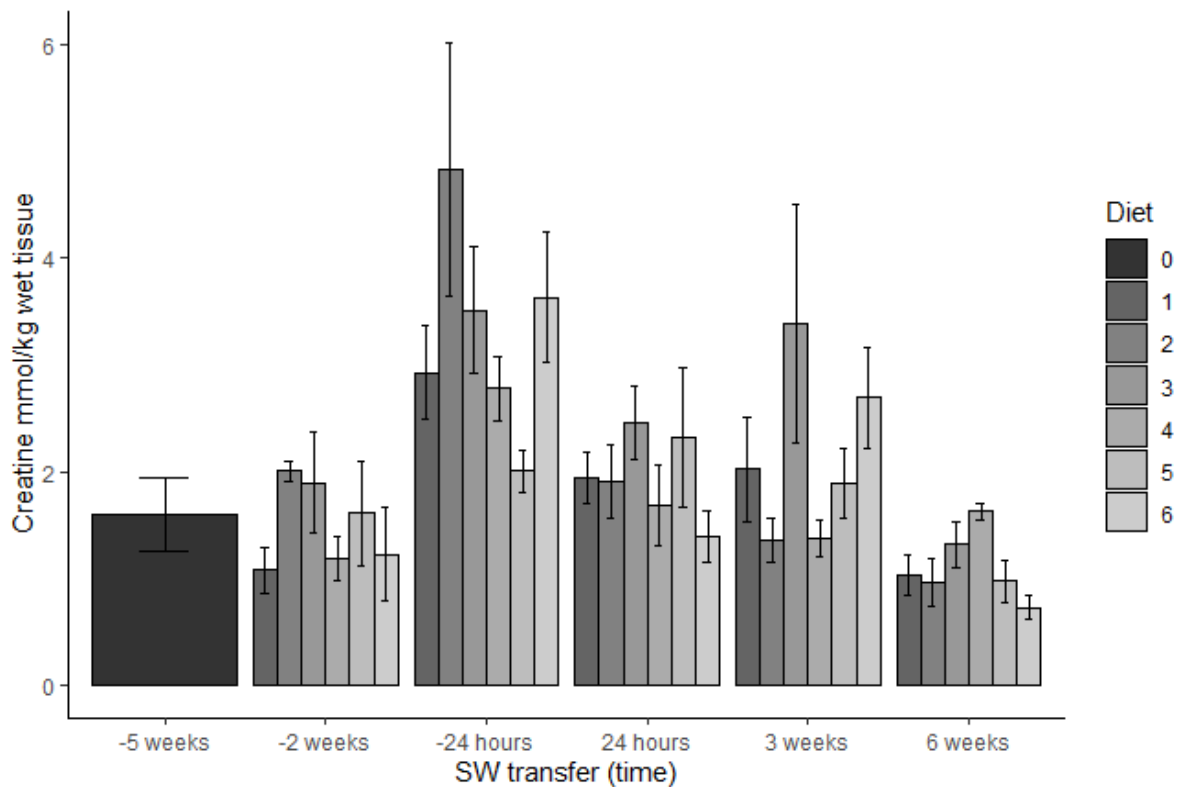


Figure 4.18. Mean creatine level extracted from the skin of fish from nucleotide supplement feeding trial. The first time point, 5 weeks before SW transfer, represents baseline before feeding with experimental diets began. Error bars represent standard error.

The level of creatine kinase A (CKA) expression as measured in the skin at the two time points, 24 hours before SW transfer and 24 hours after SW transfer (Figure 4.19). No significant effect of diet ( $F_{5,108} = 1.44$ ,  $p = 0.21$ ) or salinity ( $F_{1,108} = 0.14$ ,  $p = 0.71$ ) was detected, however there was a significant effect of the interaction of these two variables ( $F_{5,108} = 3.38$ ,  $p = 0.007$ ). On diet 6 CKA expression was significantly lower following SW transfer ( $p = 0.37$ ). No significant difference was detected on the other diets.

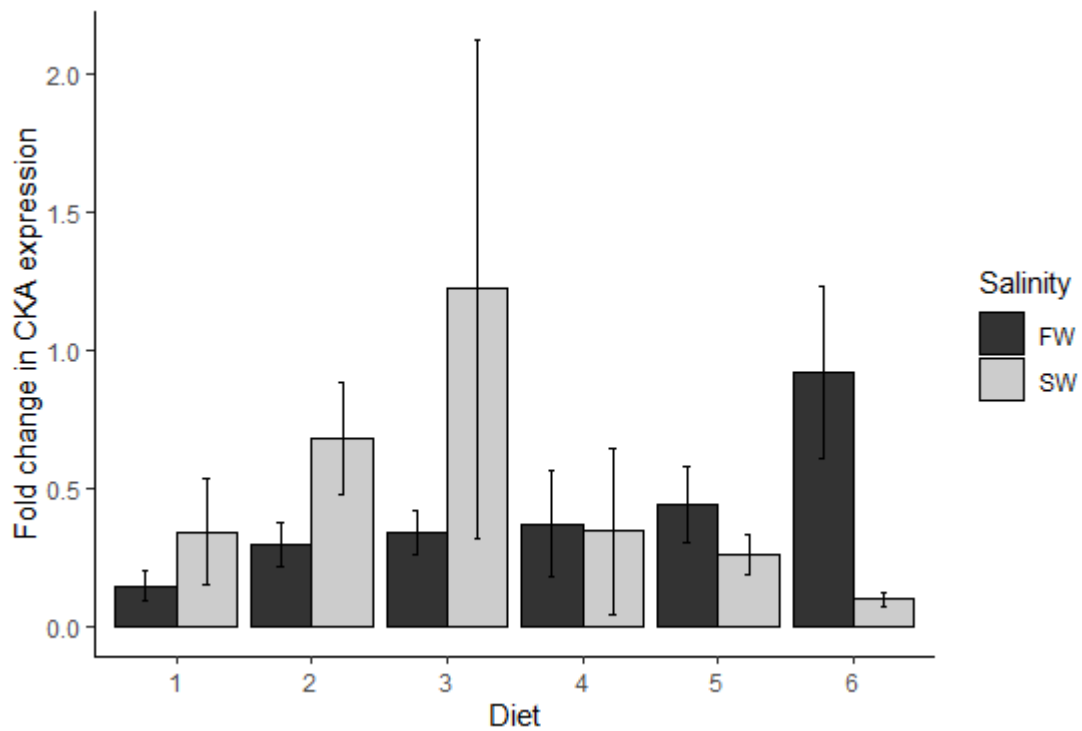


Figure 4.19. Mean expression of CKA in the skin of Atlantic salmon at time points 24 hours before and 24 hours after SW transfer on all six diets on the nucleotide supplement feeding trial. Error bars represent standard error.

#### *4.4 Discussion*

##### *4.4.1 Total osmolyte*

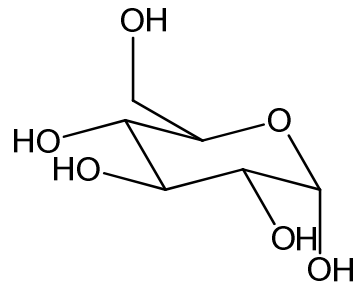
The level of total organic osmolyte extracted from the skin was observed to increase following SW challenge in parr, and a similar increase was observed in smolts when transferred directly to full concentration SW, with levels returning to those seen in FW 72 hours after SW transfer. This increase was not replicated in the fish from the feeding trial which were exposed to a more gradual SW transfer. It seems likely that the fish which underwent direct SW transfer had less time to acclimatise to the increasing salinity and thus overcompensated in response to the osmotic stress. When transfer to SW took place gradually over a period of 6 hours on the feeding trial, fish did not experience the same acute stress and did not produce the same elevated levels of organic osmolytes in the skin. The level of total organic osmolyte in the skin was observed to increase prior to SW transfer in fish which underwent gradual transfer, and this may have been a preparatory adaptation as fish smoltified and anticipated SW entry.

##### *4.4.2 Glucose*

No statistically significant change in skin glucose (IV, Figure 4.20) was observed in smolts transferred directly to SW. SW challenge of parr at the 30 days to transfer time point resulted in a significant increase in skin glucose. Other authors have reported increased tissue glucose levels in euryhaline species subjected to acute SW transfer, as discussed below.

On the feeding trial a drop in glucose levels was observed in the skin following the commencement of feeding with experimental supplemented diets which was maintained as fish progressed to smoltification and SW transfer. Following SW transfer glucose was not detected in the majority of skin samples, it is unclear whether this is due to the absence of

glucose at these time point or glucose levels below the limit of detection of the assay. It would be of interest to investigate glucose levels in the skin on a SW transfer time course with a glucose specific assay.



IV

Figure 4.20. Structure of glucose molecule.

Baltzegar *et al.* (2014) found that plasma glucose levels were elevated following acute seawater challenge in tilapia (*Oreochromis mossambicus*). The rise in plasma glucose occurred alongside an increase in the expression of leptin A in the liver, and it was suggested that this hyperglycaemic effect was due to an increase in glycogenolysis mediated by leptin A. Cortisol is believed to act synergistically with leptin A, increasing gluconeogenesis from amino acids following seawater transfer, in order to meet the increased energy demands for osmoregulation in hyperosmotic conditions (Baltzegar *et al.*, 2014). Sangiao-Alvarellos *et al.* (2005, 2003) detected increased activities of liver glycogen phosphorylase and gill hexokinase in gilthead sea bream (*Sparus auratus*) following seawater exposure, which were consistent with increased mobilisation of liver glycogen stores, resulting in increased availability of glucose for use in the gills.

In mammalian species glucose utilisation by most tissues is insulin dependent. Glucose intolerance, due to lack of insulin, or lack of responsive receptors, leads to hyperglycaemia, and in extreme cases the resultant plasma hyperosmolality leads to cellular dehydration, osmotic diuresis and ultimately death, if untreated (Gaw *et al.*, 2013). Tilapia have been

described as glucose intolerant, a clinical term that describes the phenomenon in mammals in which a glucose load leads to persistent hyperglycaemia. It has been observed that carnivorous fish are less efficient at clearing glucose from the bloodstream than omnivorous species, with herbivorous species being the most efficient (Furuichi & Yone, 1981). The lower body temperatures and metabolic rates observed in fish, compared to mammals, result in typical rates of resting glucose turnover in fish species 20-100 times lower than those found in mammals of equivalent body weight (Moon, 2001).

Glucose transport across membranes is facilitated by specific carrier proteins. In mammals there are five recognised forms of the GLUT glucose transporters (Moon, 2001). Tilapia do not appear to have the GLUT-4 insulin sensitive glucose transporter that facilitates glucose entry into most tissues in mammals (Wright *et al.*, 2000). Homologues of the mammalian GLUT transporters have been observed in a number of fish species (Navarro *et al.*, 1999). The insulin independent transporter GLUT-1 has been identified in the skeletal muscle of tilapia (Wright *et al.*, 2000). The high insulin levels found in teleost fish compared with mammals indicates that insulin deficiency is not the cause of the persistent hyperglycaemia observed in these species. It is likely that hyperglycaemia has an important role in the availability of glucose for use in peripheral tissue in teleosts (Moon, 2001). Given that glucose does not play an important role in the natural diet it is unsurprising that tilapia do not have a mechanism for rapidly clearing glucose from plasma into fat and muscle. Nonetheless, in tilapia, insulin has the effect of increasing liver glucose uptake which will increase glycogen stores. When required, liver glycogen can be rapidly mobilised to glucose which has an osmotic effect as well as being an energy source (Wright *et al.*, 2000).

Rapid breakdown of liver glycogen, leading to increased plasma glucose levels, is an important component of the mammalian stress response, mediated by cortisol and adrenaline.

The resultant hyperglycaemia provides a ready source of glucose for muscle and other organs. The increased plasma glucose and glycogen mobilisation seen in the fish stress response has a role in meeting energy requirements in specific tissues: for instance, through uptake of glucose by the zGLUT13a transporter found specifically in gill ionocytes (Tseng & Hwang, 2008). Phosphorylation of intracellular glucose to glucose-6-phosphate by hexokinase maintains favourable glucose gradients for transport. A high affinity hexokinase has been shown to be expressed in fish tissues (Moon, 2001).

Salinity challenges lead to an energy requirement for ion transport. Hwang & Lee (2007) reported that glycogen is accumulated as an energy reserve in glycogen rich cells in the gill of a tilapia. Tseng *et al.* (2007) found that salt water challenge of Mozambique tilapia led to increased activity of glycogen phosphorylase, indicating increased glycogenolysis in gill glycogen rich cells, and it is postulated that this provides energy to neighbouring mitochondria rich cells which are involved in ion transport (Tseng *et al.*, 2007; Tseng & Hwang, 2008).

It is likely that in fish the osmotic effect of glucose is important. Diouf *et al.* (2000) found that both plasma glucose and osmolality increased in response to stress, with increased plasma adrenaline leading to electrolyte changes due to increased gill permeability to both water and sodium.

It is clear that glucose levels increase acutely on seawater challenge, and there is good evidence that it is required to provide energy for physiological compensatory processes. However, the osmotic effect of raised glucose may also be important in the acute phase of the response, with other organic osmolytes becoming more important as the glucose is consumed by energy requirements. Glucose, as glucose-6-phosphate, is also the precursor of myo-

inositol, an important compatible osmolyte in the acute response to osmotic stress in a number of euryhaline species.

#### 4.4.3 Myoinositol

The level of myoinositol (V, Figure 4.21) in the skin fell significantly in the skin prior to SW transfer and remained lower in SW on the direct transfer trial, while on the feeding trial with gradual SW transfer myoinositol levels were not observed to fall significantly until the 3 weeks post transfer time point, and remained low at 6 weeks post transfer. It is possible that this difference is due to different rearing conditions or genetic strain. These results suggest that myo-inositol does not play an important role in the skin in the acclimation of salmon smolts to seawater.

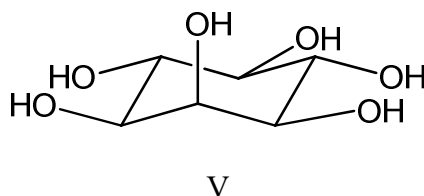


Figure 4.21. Structure of myo-inositol.

Myo-inositol may be obtained directly from the diet. It is synthesised *de novo* from glucose-6-phosphate (G6-P). The enzyme myo-inositol phosphate synthase (MIPS) converts G6-P to 1L-myo-inositol 1-phosphate which is hydrolysed to inositol by inositol monophosphatase (Kalujnaia *et al.*, 2013). Inositol is an essential polyalcohol, the precursor of numerous signalling molecules in the cells of all eukaryotic species. It has a role in calcium release and the phospholipid derivative phosphatidylinositol is a membrane component. Myo-inositol has an important role protecting cells from osmotic damage in a number of euryhaline fish species, where it is a compatible organic osmolyte. It is also a precursor of phosphoinositide compounds involved in osmotic stress signalling (Munnik & Vermeer, 2010). The expression and activities of the enzymes myo-inositol phosphate synthase and inositol monophosphatase 1 are upregulated in tilapia and the European eel (*A. anguilla*) following seawater exposure (Fiol *et al.*, 2006; Kalujnaia *et al.*, 2010, 2009).

Myo-inositol is a very stable molecule with a long half-life *in vivo*, important for accumulation of this organic osmolyte (Yancey *et al.*, 1982). This stability may be influenced by salinity. Dowd *et al.* (2010) demonstrated that inositol breakdown is increased in euryhaline elasmobranchs on exposure to reduced salinity. In contrast to this response to hypo-osmotic stress, tilapia exposed to increased salinity were found to accumulate myo-inositol (Fiess *et al.*, 2007).

Inositol is an important organic osmolyte in mammalian kidney and brain. Renal cells synthesise inositol but its increase in response to osmotic stress is due to increased uptake of the polyol from the ECF. Hypertonicity increases the number of sodium-dependent myo-inositol transporters (SMITs) by increasing transcription of the SMIT gene (Burg *et al.*, 2007).

#### 4.4.4 Taurine

Taurine (VI, Figure 4.22) is an important organic osmolyte. On both trials, taurine was present in much higher concentrations than the other osmolytes quantified in this study, representing on average 45.5% of the total osmolyte quantified on the direct transfer trial and 54.3% on the nucleotide supplement feeding trial. On the direct transfer trial, the level of taurine in the skin was not observed to change over the time course as fish progressed from parr to smolts and entered SW. This is supported by the results of the feeding trial as the level of taurine in the skin was not observed to increase until 3 weeks after SW transfer. It seems likely that taurine is used for long term adaptation to increased salinity and is not involved in the response to short term osmotic stress.

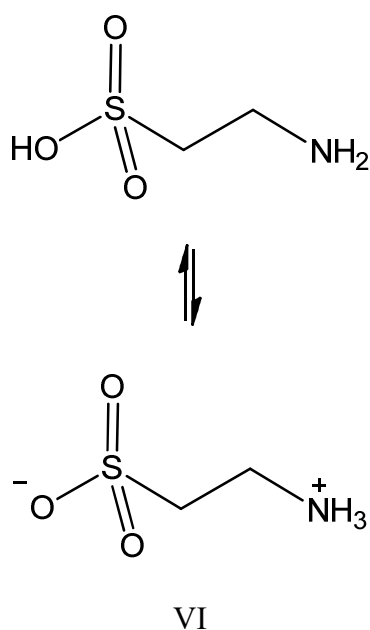


Figure 4.22. Structure of taurine showing equilibrium between uncharged molecule and zwitterion.

Taurine, sometimes described as an amino acid, is in fact an amino sulphonic acid, derived from cysteine *via* oxidation and decarboxylation. It is abundant in all vertebrates: in mammals it is synthesised in the pancreas, in fish it is synthesised predominantly in the liver (Liu *et al.*, 2017). Taurine is readily water soluble, is not incorporated into protein and is an

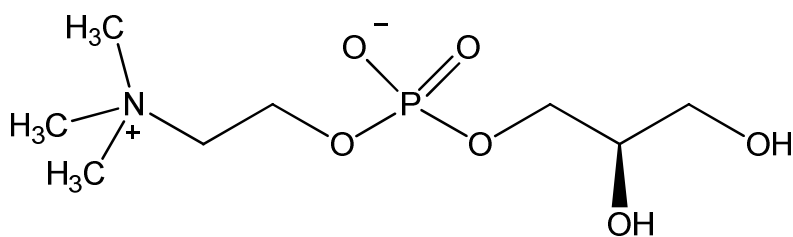
important osmolyte; a zwitterion at physiological pH (Figure 4.22), with millimolar intracellular concentrations achieved by active transport from the extracellular fluid where concentrations are micromolar (Chesney *et al.*, 1976). It has many roles in important physiological processes, including bile salt and xenobiotic conjugation, calcium homeostasis, central nervous system development, retinal development and function, cardiovascular function, muscle development and function and osmoregulation (Huxtable, 1992; Ripps & Shen, 2012). Despite being highly polar it crosses the blood brain barrier (Urquhart *et al.*, 1974), where it plays a number of cellular functions, including as a neurotransmitter, osmolyte and neuroprotectant and has a role in the prevention of epileptic seizures (Wu & Prentice, 2010). It is an antioxidant (Zhang *et al.*, 2004b) and its ability to reduce the secretion of apolipoprotein B100 by liver cells has led to studies into supplementation to reduce cardiovascular disease (Yanagita *et al.*, 2008). Dietary taurine reduces weight and lowers plasma cholesterol in obese young adults (Zhang *et al.*, 2004a) and is an inotrope, beneficial in congestive cardiac failure.

Taurine is an important osmolyte in renal medullary cells (Burg, 1996). The role of the mammalian renal medulla in concentrating urine results in very high concentrations of inorganic salts and urea, leading to the highest intracellular concentrations of organic osmolytes found in terrestrial mammals (Burg & Ferraris, 2008). Cells in other tissues also accumulate organic osmolytes when exposed to hyperosmolality. Taurine has an osmotic role in both the brain and liver (Häussinger, 1998; Law, 1994).

#### 4.4.5 Glycerophosphocholine

Glycerophosphocholine (VII, Figure 4.23) levels in the skin were found to fall in smolts immediately prior to SW transfer on the direct transfer trial before increasing back to levels seen in parr upon transfer to SW. After three days levels returned to those seen in FW smolts the day before transfer. This follows the pattern observed in total osmolyte levels, however, the change in GPC level does not account for the whole effect. The total level of osmolyte in the skin changed by approximately 10 mmol/kg while GPC levels never exceeded 1 mmol/kg.

Conversely, the level of GPC in the skin was observed to increase before SW transfer on the feeding trial, with levels returning to those seen at earlier time points by 24 hours post transfer. Levels remained low at 3 weeks and 6 weeks post SW transfer. On this trial the level of GPC also mirrored the trend in total osmolyte levels, though accounting for a relatively small proportion of the total.



VII

Figure 4.23. Structure of glycerophosphocholine.

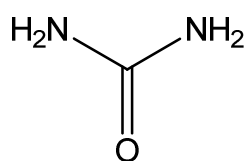
GPC is a product of the breakdown of phosphatidylcholines, phospholipids that are an important component of biological membranes found in all plant and animal cells. GPC is a methyl amine counteracting osmolyte, which can protect cells from high urea concentrations. It is important in the mammalian kidney, where its concentration varies directly with

extracellular osmolarity. Cells in the renal medulla accumulate GPC when exposed to high urea and NaCl concentrations (Zablocki *et al.*, 1991). Studies in mammalian renal epithelial cells have demonstrated that the accumulation of GPC in response to osmotic stress is due to inhibition of the degradative enzyme GPC:choline phosphodiesterase, resulting in a reduction of GPC breakdown, and an increase in GPC synthesis catalysed by the phospholipase, neuropathy target esterase (NTE) (Burg & Ferraris, 2008). High NaCl increases levels of this enzyme by upregulation of NTE gene transcription (Burg & Ferraris, 2008). Synthesis is regulated by osmolality, as well as the abundance of other osmolytes (Burg *et al.*, 2007). Urea levels have not been shown to have an impact on synthesis. The regulation of GPC by controlling both synthesis and degradation could enable a more rapid response to increases in osmolality than is possible with other osmolytes.

The response to osmotic stress involves contributions from several organic osmolytes, with sorbitol, GPC, betaine, and inositol contributing to the osmoprotection of the mammalian kidney, with the sum of the concentrations of these osmolytes correlating to the extracellular salt concentrations (Gallazzini & Burg, 2009). It would be expected that both GPC and betaine, as methyl amines would be suitable as counteracting osmolytes in the presence of urea, however, only GPC concentration correlates directly with that of urea in this tissue, betaine concentration does not. In the euryhaline species tilapia and the European eel, GPC levels were found to rise on seawater acclimation in the gill and fin which are important osmoregulatory tissues (Kalujnaia *et al.*, 2013).

#### 4.4.6 Urea

Urea (VIII, Figure 4.24) was only detected in the skin of fish on the feeding trial. Little change was observed in levels up until SW transfer. Following transfer urea was undetectable in the majority of samples, however, on a small number of samples on the high purine content diets urea was measured at very high levels (between approximately 6 mmol/kg and 20 mmol/kg). These samples led to a significant increase in urea levels being detected on diets 4, 5 and 6 which contained a 75% purine (AMP) supplement, 100% purine (AMP) supplement and 100% purine (inosine) supplement respectively. Extraction of osmolyte from these samples was repeated and replicates contained similarly high levels of urea. It is possible that samples were contaminated, however, this seems unlikely as it would require the original tissue sample to be contaminated with urea. It may be the case that these results represent inter-individual variation, with elevated purine levels in the diet leading to increases in urea accumulation in some individuals and not others. More work is required to determine whether high levels of purine supplementation in the diet produce elevated levels of urea in the skin and other tissues.



VIII

Figure 4.24. Structure of urea

Purines can be converted to urea as shown in Figure 4.25.

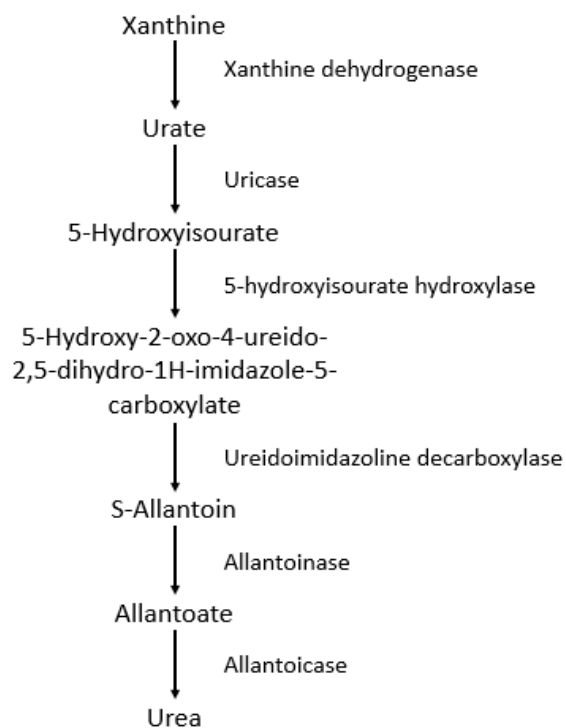


Figure 4.25. The pathway of purine oxidation to urea.

Pyrimidines are degraded to urea *via* an oxidative pathway in some microorganisms (Soong *et al.*, 2001), other species, including most microorganisms, use a reductive pathway leading to L-amino acids, ammonia and CO<sub>2</sub> as in Figure 4.26.

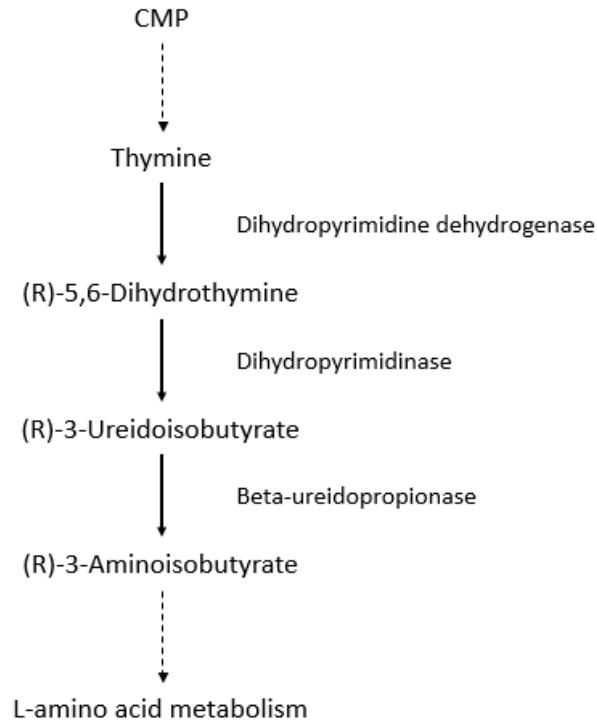


Figure 4.26. The pathway of pyrimidine degradation.

It is possible that the very high levels of urea in skin at 6 weeks post transfer are due to the high levels of purine in the diet since this was the only difference between the groups. Degradation of purines increases production of urea, which can function as a counteracting osmolyte and play a role in the long term adaptation of these fish to seawater when accumulated with methyl amines (Wright & Land, 1998). Alternatively, it is possible that by 6 weeks in seawater excess purines in the diet are being efficiently broken down to urea as a waste product, although that does not explain why the urea produced is not excreted. It is possible that the waste product is employed as an osmolyte opportunistically, avoiding the requirement for synthesis or import of other osmolytes.

High urea concentrations are damaging to cells. The globular structure of proteins is dependent on hydrophobic interactions. Urea is a chaotropic agent that disrupts these interactions (Auton & Bolen, 2005; Nozaki & Tanford, 1963; Yancey & Somero, 1979). It

can bind to proteins, having the potential for hydrogen bonding, hydrophobic, dipole-dipole and induced dipole interactions. These non-covalent interactions disrupt hydrogen bonds and alter the degree of solvation of the protein: both are important for the maintenance of protein structure and function (Patrick, 2017). High urea can also cause post-translational modification by carbonylation or carbamoylation at physiological pH (Kraus & Kraus, 2001; Nyström, 2005). Urea is described as a destabilising osmolyte due to its effect on protein structure.

Stabilising, or counteracting osmolytes, such as methyl amines do not bind to proteins. They are excluded from close approach to the protein backbone, acting as structure-making solutes, effectively increasing protein hydration, and do not disrupt structurally important non-covalent interactions (Street *et al.*, 2006). The opposing structure-breaking and structure-making effects of urea and counteracting osmolytes vary directly with concentration. Typically the effects counteract each other at a ratio of urea:stabilising osmolyte of 2:1 (Mello & Barrick, 2003).

Glycine also acts as a stabilising osmolyte in a variety of cell types (Foord & Leatherbarrow, 1998), however, it does not play that role in cells with high urea content. Khan *et al.* (2013) found that while methylated derivatives of glycine counteract the effect of urea on several proteins, glycine does not. This is unsurprising when the physicochemical properties of glycine are considered. Glycine is the simplest amino acid; it has no hydrophobic side chain. It is a small polar molecule and as such does not disrupt the hydrophobic interactions involved in protein folding. Methylated derivatives of glycine have a reduced polar surface area by comparison. This improves their ability to form hydrophobic interactions with urea. It is likely that dipole-dipole interactions and hydrogen bonding interactions between urea and counteracting osmolytes also play a role in their ability to prevent the disruption of

protein structure by high urea concentrations. Glycine cannot prevent the interaction of urea with proteins due to the lack of the important hydrophobic interaction with nonpolar methyl groups (Patrick, 2017).

In this study it was found that alanine levels in skin were increased at the same time point as very high urea levels were observed, with the greatest increases being on diets 5 and 6 which had the greatest increases in urea (discussed in Section 4.3.7 below). Although alanine concentrations increased from approximately 0.5 to 1 mmol/kg wet tissue, while urea concentrations increased from approximately 2 to 12 mmol/kg. It is possible that in this case alanine, which differs from glycine by one hydrophobic methyl group, makes some contribution to the sum of osmolyte counteracting urea. However, none of the osmolytes measured showed an increase of the magnitude of that observed in urea, so it is likely that urea is counteracted by a compound or combination of compounds that were not measured.

Elasmobranch and coelacanth fishes are unusual in that they accumulate high concentrations of urea to counteract the osmotic effect of seawater. Urea is the major nitrogenous waste product in elasmobranchs, whereas most fish species primarily excrete ammonia. High levels of ammonia are toxic but accumulation is avoided in fish by diffusion across the gills and dilution in the environment (Smith, 1929). Ammonia excretion is more energy efficient than converting it to urea *via* the urea cycle. Teleosts do excrete a small proportion of nitrogenous waste as urea but this is believed to be produced by argininolysis and uricolysis (Cvancara, 1969a, 1969b; Goldstein & Forster 1965; Wright, 1993). Many species express arginase and uricase in their livers (Cvancara, 1969a, 1969b; Goldstein & Forster, 1965; Hayashi *et al.*, 1989; Jenkinson *et al.*, 1996; Wilkie *et al.*, 1993).

Although most teleosts do not produce urea *via* the ornithine urea cycle it is believed that they have retained the genes for the urea cycle enzymes. A few species such as the tilapia

species *Oreochromis alcalicus grahami* that express all of the enzymes are both ureogenic and ureotelic. *O. a. grahami* are found in very alkaline lakes, where conditions do not favour passive diffusion of ammonia across gills into the surrounding environment. Ammonia is converted to urea *via* the urea cycle which is excreted mainly across the gills (Pärt *et al.*, 1998; Wood *et al.*, 1994). Other species found in alkaline lakes also excrete significant amounts of urea (Danulat & Kempe, 1992).

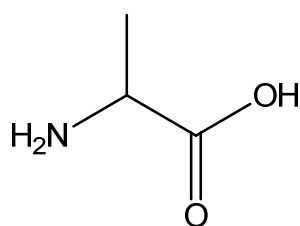
Most teleosts have very low or undetectable levels of the urea cycle enzymes (Anderson, 1980; Cao *et al.*, 1991; Huggins *et al.*, 1969; McGeer *et al.*, 1994; Mommsen & Walsh, 1989). However, it is believed that they have retained the genes and that the urea cycle is important in protecting embryos from high levels of ammonia that can accumulate during development. Urea cycle enzymes have been detected in early embryos of rainbow trout. It is likely that urea synthesis and excretion in the early developmental stages of trout prevents accumulation of damaging concentrations of ammonia (Wright & Land, 1998).

#### 4.4.7 Amino acids

##### 4.4.7.1 Alanine

Alanine (IX, Figure 4.27) levels in the skin increased following SW transfer before returning to approximately FW levels by 3 days post transfer on the direct transfer trial. SW challenge also increased alanine levels at the 44 days and 30 days to transfer time points. These results suggest that alanine is involved in short term response to osmotic stress due to increased salinity. The increase in alanine levels following SW transfer account for approximately 20% of the increase in total organic osmolyte at this time point.

On the feeding trial alanine levels increased before transfer to SW, falling back to baseline levels on four of the six diets by 24 hours post transfer. By 3 weeks post transfer levels had returned to baseline on all diets. At the final timepoint 6 weeks after SW transfer there was a rise in alanine levels on diets 5 and 6. At this time point the level of urea in the skin was elevated in some individuals. Alanine is a methyl amine



IX

Figure 4.27. Structure of alanine.

##### 4.4.7.2 Glycine

Glycine (X, Figure 4.28) was only detected in extracts from the direct transfer trial. Glycine levels did increase following SW transfer and SW challenge however, this change was not statistically significant.

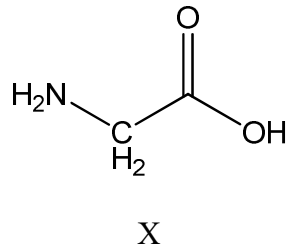


Figure 4.28. Structure of glycine

While methyl amines act as counteracting osmolytes to protect against the damaging effects of high urea concentrations, and polyols effectively protect against the osmotic effects of dehydration or desiccation, amino acids appear to be particularly effective in protecting against high extracellular salt concentrations (Bolen, 2001; Yancey *et al.*, 1982).

The role of amino acids as osmolytes has been widely investigated in mammalian brain cells. High concentrations of amino acids are also found in the kidney, though other osmolytes have been shown to be important in this tissue. There is comparatively little known about osmoregulation by amino acids in other tissues. Efflux of glycine and taurine has been shown to be involved in regulatory volume decrease (RVD) in ascites tumour cells (Hoffmann *et al.*, 1988; Hoffmann & Hendil, 1976). Hyperosmolarity has been shown to activate a Na<sup>+</sup>-dependent neutral amino acid transporter in cultured human fibroblasts, which has been shown to achieve complete RVI after dehydration induced by high concentrations of sucrose. This response requires the presence of amino acids in the medium (Franchi-Gazzola *et al.*, 2006; Gazzola *et al.*, 1991). Figure 4.29 illustrates the factors which influence the intracellular pool of amino acids.

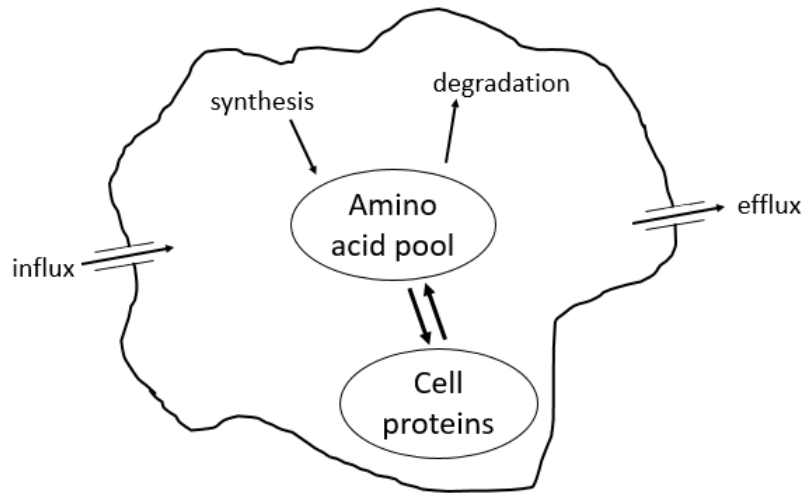


Figure 4.29. Factors influencing the intracellular amino acid pool.

This is dependent on synthesis and breakdown of proteins and amino acids, as well as transport across membranes, consumption in biosynthetic processes such as gluconeogenesis, and catabolism.

A number of amino acid transporters that facilitate cellular uptake of amino acids have been identified (Barker & Ellory, 1990; Christensen, 1990; Yudilevich & Boyd, 1987). NaCl-dependent and NaCl-independent efflux transporters have been identified in several cell types (Lambert & Hoffmann, 1993).

Although all amino acids in the cytosol contribute to ICF osmolality, not all amino acids are compatible osmolytes. Alanine, proline and glycine are compatible osmolytes and do not disrupt enzyme structure and function, whereas, basic amino acids such as arginine and lysine, with their positively charged side chains can destabilise macromolecules: neither has a role in response to osmotic stress in animal cells (Bowlus & Somero, 1979). Amino acids provide the main defence of the brain against osmotic stress, such as in dehydration, renal failure and hyperglycaemia (Heilig *et al.*, 1989). The straight chain aliphatic amino acids make a very important contribution to adaptive osmoprotection in the mammalian brain.

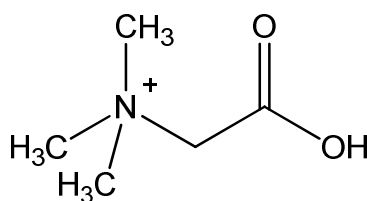
While there are variations, these same acids are osmoprotective in species other than mammals (Law, 1991).

Alanine has been shown to protect the stability of RNase-A against the harmful effects of urea, while glycine does not (Chowhan *et al.*, 2016). In this study, alanine levels in the skin were found to increase at the 6 weeks post seawater transfer time point in the high purine supplemented diets (5 and 6), this coincided with a large increase in urea in this tissue. It is possible that alanine was accumulated in the skin to protect against the damaging effects of urea on cellular proteins.

#### 4.4.8 Glycine betaine

On the direct transfer trial, the level of glycine betaine (XI, Figure 4.30) increased following SW transfer and remained elevated up to 72 hours post transfer. SW challenge only caused a statistically significant increase in betaine levels at the time of SW transfer. These results suggest that this osmolyte is important in the initial acclimation to increased salinity when smolts move to SW.

On the feeding trial the level of glycine betaine rose on diet 6 at the time point 24 hours before SW transfer. This increase was not seen on the other five diets at this time point, however, 24 hours after SW transfer betaine levels did increase on diets 1-5, while levels dropped on diet 6. At the next time point, 3 weeks after SW transfer the level of betaine in the skin of fish on diets 1-5 had fallen and was below baseline levels, and levels remained at or below baseline levels on all diets after 6 weeks in SW. The results seen on diets 1-5 suggest that glycine betaine is important in the initial adaptation of smolts to the increased salinity experienced when they move to SW. However, the increase on diet 6 occurred before SW transfer. It is possible that the peak in betaine levels on diet 6 before SW transfer was a pre-emptive version of the effect seen on the other five diets following SW transfer.



XI

Figure 4.30. Structure of glycine betaine.

The methyl amine glycine betaine is an effective osmolyte that accumulates in the cytoplasm of a wide range of prokaryotic and eukaryotic cells under conditions of osmotic stress. It is

synthesised from choline in a variety of species, this process involves the initial conversion of choline to betaine aldehyde, catalysed by either choline dehydrogenase or choline oxidase, followed by the conversion to glycine betaine by NAD<sup>+</sup>-dependent betaine aldehyde dehydrogenase (Kimura *et al.*, 2010). In *Myxococcus xanthus* glycine betaine is important for osmoprotection in cell growth and spore germination under hyperosmotic conditions. Kimura *et al.* (2010) found that this Gram-negative bacterium can synthesise glycine betaine from glycine, the first report of this pathway in a non-halophilic bacterial species.

Betaine accumulates in many cell types. Uptake from the ECF is increased in hypertonicity. Synthesis is not increased (Burg & Ferraris, 2008). Uptake is regulated by the transporter betaine/ GABA transporter 1 (BGT1). A small amount of BGT1 is present in the cytoplasm at normal osmolality. As tonicity increases these proteins localise in the plasma membranes and transcription of the BGT1 gene is up-regulated resulting in increased transport of betaine into the cell (Burg & Ferraris, 2008). While betaine is an important organic osmolyte in the mammalian renal medulla, high urea decreases betaine in renal medullary cells, while levels of GPC increase (Burg *et al.*, 2007).

Sorbitol is also an important organic osmolyte in the renal medulla in mammals. The synthesis of sorbitol from glucose is catalysed by aldose reductase, and inhibition of this enzyme in renal medullary cell cultures reduces cell survival. Addition of betaine to the growth medium prevents the harmful effects of inhibiting the enzyme. This is consistent with the observation that inhibition of aldose reductase, and the resultant reduction in sorbitol accumulation *in vivo* does not lead to kidney damage, suggesting that betaine can substitute for sorbitol in protecting renal cells from osmotic stress (Moriyama *et al.*, 1991). Petronini *et al.* (1993) found, in studies of cultured chick embryo cells exposed to hyperosmotic conditions, that synthesis of a heat shock protein was induced. Inclusion of betaine in the

growth medium led to reduced induction of this heat shock protein expression. As heat shock proteins have been implicated in the maintenance of protein conformation in kidney cells (Cohen *et al.*, 1991), it appears that betaine may have a similar role and can eliminate the need for production of these proteins in hyperosmotic stress.

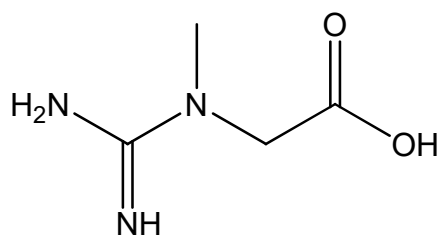
#### 4.4.9 Creatine

Creatine (XII, Figure 4.31) levels fell immediately prior to SW transfer on the direct transfer trial. Up to two days post transfer there was an increase in creatine levels which then fell by 72 hours post transfer to SW to levels equivalent to those seen 24 hours before SW entry. SW challenge had no significant effect on the accumulation of creatine in the skin at the time points investigated.

Conversely, on the feeding trial creatine levels increased at the time point 24 hours before SW transfer. Following transfer creatine levels trended downwards, dropping below baseline by 6 weeks post SW transfer.

These results suggest that creatine may play a role in the acute response to seawater transfer, but not in the long-term acclimation of fish to the marine environment.

The expression of creatine kinase A (CKA), an enzyme involved in the breakdown of creatine, was investigated both pre- and post-seawater transfer. On diet 6 there was a significant fall in the expression which coincided with a reduction in creatine levels. It is possible that a negative feedback loop reduced the expression of this gene as the substrate for the CKA enzyme reduced. Expression on the other five diets was highly variable, and no statistically significant difference was observed between fish in freshwater and seawater.



XII

Figure 4.31. Structure of creatine

Creatine is found in all vertebrates. Its synthesis from arginine, glycine and S-adenosylmethionine is dependent on the enzymes arginine-glycine transaminase (AGAT) (Bloch & Schoenheimer, 1941; Borsook & Dubnoff, 1941) and guanidinoacetate methyltransferase (GAMT) (Borsook *et al.*, 1940; Cantoni & Vignos, 1954). Creatine is transported in the blood, mainly to muscle, from its major sites of synthesis, the liver and kidney. It is also transported to the brain and other tissues (Brosnan & Brosnan, 2016). Entry into cells is dependent on the specific creatine transporter SLC6A8 (Braissant *et al.*, 2011). Creatine plays a critical role in the CNS, both in development and energy requirements as well as being a major CNS osmolyte (Bothwell *et al.*, 2002).

Mutations in the genes coding for the synthetic enzymes AGAT and GAMT, and the transporter SLC6A8 cause creatine deficiency syndromes that result in severe neurological defects (Braissant *et al.*, 2011). Neurological function can be improved by creatine supplementation in subjects with deficiencies of the synthetic enzymes (Schulze & Battini, 2007), but supplementation is not effective in patients with the transporter defect (Póo-Argüelles *et al.*, 2006).

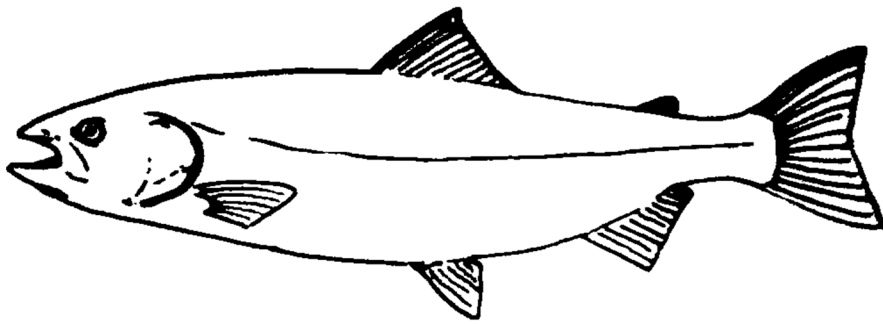
Creatine is phosphorylated by creatine kinase (CK) to phosphocreatine. ATP is rapidly re-synthesised from ADP by the CK/phosphocreatine system during periods of high energy demand (Wallimann *et al.*, 1992). CK is an important enzyme in cellular energy homeostasis. In mammals it exists in different tissue-specific molecular forms as the product of six different genes. Cytosolic CK exists as a dimer with three distinct isoenzymes of two genetic forms, MM, MB and BB (M = muscle type, B = brain type). In man plasma levels of CK are used as a marker of muscle injury and levels of isoenzymes are used in diagnosis of myocardial infarction (MI). CK-MM predominates in skeletal muscle, CK-BB in brain, and CK-MB in cardiac muscle. Muscle damage increases plasma CK-MM levels, while CK-MB

increases dramatically in MI (although change in total CK is small) however, CK-BB does not increase in response to brain injury (Gaw *et al.*, 2013). In addition, two mitochondrial CK enzymes are expressed as dimers or multimers of three different genes CKmt 1A, 1B and 2.

In tissues with high energy demand, phosphocreatine is accumulated as a phosphagen (energy storage compound), as increased concentrations of this metabolite within the cell do not disrupt macromolecular function as would high concentrations of adenosine phosphates (Cohen, 1968; Meyer, 1988). In vertebrates phosphocreatine is the only known phosphagen (Wallimann *et al.*, 1992). Another role of the CK/phosphocreatine system is generation of inorganic phosphate (Pi). Phosphocreatine hydrolysis releases Pi, which activates glycogenolysis and glycolysis in tissues subject to high energy demands, such as muscle, thus CK action indirectly regulates these pathways in tissues that depend on glycogenolysis (Davuluri *et al.*, 1981).

Most creatine is excreted by vertebrates as creatinine, which is the anhydride of creatine formed by the irreversible dehydration of phosphocreatine. Creatinine is filtered in the kidney and lost in the urine in mammals (Gaw *et al.*, 2013).

Fish excrete very little nitrogenous waste in urine, with urinary nitrogen excretion being typically lower in freshwater than in seawater species. Smith identified creatine as a major nitrogen source in fish urine, though creatinine was also detected (Smith, 1929).



# Biomarkers of Smoltification



## 5. Biomarkers of smoltification

### 5.1 Smoltification in an aquaculture setting

Smoltification is a complex process, involving many physiological and morphological changes in preparation for entry to seawater. As this process requires the development of systems, such as those for ion transport, that are maladaptive for life in freshwater, there is a limited time window, known as the “smoltification window” during which fish are best adapted to the transition to seawater (Stefansson *et al.*, 2008). Fish which enter the marine environment outside of this smoltification window are more likely to show lower feeding rates, reduced growth and increased disease susceptibility (Johansson *et al.*, 2016). In the wild, salmon are able to time their migration to sea so that it coincides with their smoltification window, however, fish reared in an aquaculture setting cannot control their time of seawater entry. Therefore, it is important for the condition of farmed fish to be monitored during the period of smoltification to determine the optimal time to transfer fish to seawater. A number of indices have been developed to determine the seawater readiness of farmed salmon. An increase in gill  $\text{Na}^+\text{K}^+$ -ATPase activity during smoltification prior to seawater entry has long been used as an indicator of seawater preparedness (Stefansson *et al.*, 2008). The ability of smolts to regulate plasma  $\text{Cl}^-$  when transferred to seawater is also an indicator of hypo-osmoregulatory ability. Parologue switching of the  $\text{Na}^+\text{K}^+$ -ATPase  $\alpha$ -subunit has been reported in the salmonid gill, and has been shown to be associated with smoltification and subsequent seawater entry (Nilsen *et al.*, 2007). A number of other osmoregulatory genes are also differently expressed in the branchial epithelia of smolts and parr, including the  $\text{Na}^+\text{-K}^+\text{-2Cl}^-$  cotransporter (NKCC) and the cystic fibrosis transmembrane conductance regulator (CFTR) chloride channel (Nilsen *et al.*, 2007).

A number of different biomarker candidates were considered due to their roles in the acclimation of fish to SW or the changes in metabolic processes which occur as fish smoltify. The results of a pilot study conducted by other members of our research group and Dr Silva Synowsky of the Mass spectrometry and proteomic facility in the Biomedical Sciences Research Complex Core Facility at the University of St Andrews using SWATH proteomics were used to inform the selection of genes for investigation. The genes encoding proteins which showed differences in expression in the gill of parr, smolts prior to SW transfer and smolts following SW transfer were investigated. The SWATH methodology employed is given in Appendix 6.

#### *5.1.1 Ion transport in the gill*

In gill mitochondria rich cells (MRCs) the  $\text{Na}^+\text{-K}^+\text{-ATPase}$  plays an essential role in the secretion (in SW fish) and absorption (in FW fish) of ions across the gill.  $\text{Na}^+\text{-K}^+\text{-ATPase}$ , located on the basolateral membrane of the MRC actively pumps 3  $\text{Na}^+$  out of the cell into the extracellular fluid (ECF), and 2  $\text{K}^+$  into the cell. Together with basolateral K-channels this creates an electrochemical gradient across the membrane which can be used to drive the secondary transport of other ions. In seawater fish the  $\text{Na}^+$  and  $\text{Cl}^-$  gradients created by  $\text{Na}^+\text{-K}^+\text{-ATPase}$  allow the basolateral NKCC to transport  $\text{Na}^+$ ,  $\text{K}^+$ , and  $2\text{Cl}^-$  from the ECF into the cell.  $\text{Cl}^-$  then leaves the cell *via* the apically situated CFTR chloride channel. The movement of  $\text{Cl}^-$  induces a trans-epithelial electrical potential which causes  $\text{Na}^+$  to leave the ECF through leaky tight junctions between the MRC and surrounding cells (Evans *et al.*, 2005; Zydlewski & Wilkie, 2012). These processes are summarised in Figure 5.1.

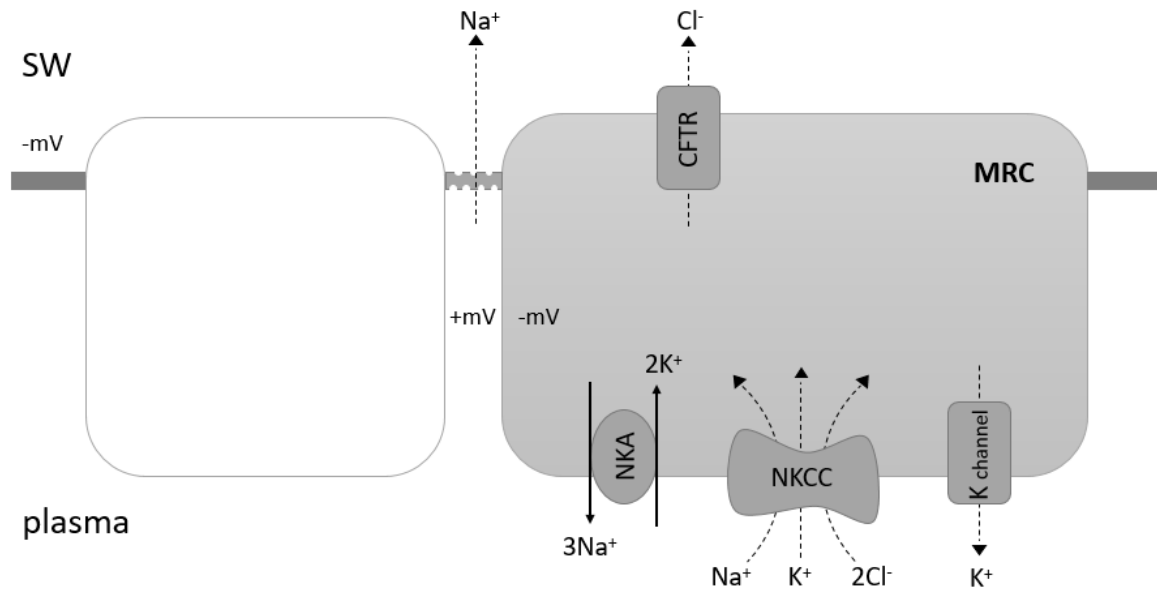


Figure 5.1. Ion transport in the MRC of the teleost gill in seawater (SW). Na<sup>+</sup>-K<sup>+</sup>-ATPase (NKA) actively transports 3Na<sup>+</sup> into the ECF and 2K<sup>+</sup> into the cell. Na<sup>+</sup>-K<sup>+</sup>-2Cl<sup>-</sup> cotransporter (NKCC) imports Na<sup>+</sup>, K<sup>+</sup> and 2Cl<sup>-</sup> into the cell from the ECF. Cl<sup>-</sup> leaves the cell through cystic fibrosis transmembrane conductance regulator (CFTR), and K<sup>+</sup> re-enters the ECF through K<sup>+</sup> channels. Na<sup>+</sup> leaves the body across leaky tight junctions between cells.

While Na<sup>+</sup>K<sup>+</sup>-ATPase activity has been favoured as a biomarker of smoltification, a number of other ion channels and transporters are also important in the acclimation of teleosts to increased salinity and could be considered as potential biomarkers of smoltification.

NKCC is recognised as playing an important role in the transport of ions across the gills (Evans *et al.*, 2005). Like Na<sup>+</sup>-K<sup>+</sup>-ATPase, NKCC is present on the basolateral membrane of gill MRC in several fish species, including Atlantic salmon (Evans *et al.*, 2005; Pelis *et al.*, 2001b). NKCC uses the electrochemical gradient of Na<sup>+</sup> produced by Na<sup>+</sup>-K<sup>+</sup>-ATPase to transport Na<sup>+</sup>, K<sup>+</sup>, and two Cl<sup>-</sup> into the cell from the extracellular fluid (Evans *et al.*, 2005). This has an important role in the maintenance of osmotic balance in the marine environment. As hypo-osmoregulatory ability is essential to the adaptation of Atlantic salmon to seawater, the expression of the *NKCC1* paralogue was investigated as a possible biomarker of smoltification.

CFTR is a chloride channel involved in the secretion of ions across the gill. This ion channel is situated on the apical membrane of gill MRC, responsible for the efflux of ions to the external environment. The accumulation of intracellular  $\text{Cl}^-$  by NKCC allows these ions to leave the cells through CFTR down an electrochemical gradient (Evans *et al.*, 2005). Mackie *et al.* (2007) have previously shown that the mRNA levels of *CFTR* in the gill is a useful indicator of hypo-osmoregulatory ability in salmon smolts, thus *CFTR* was selected as a potential biomarker for investigation.

As fish in the marine environment drink seawater to replace that lost by osmosis, and the concentration of divalent ions in SW is higher than that within the tissues of fish, a mechanism to secrete these ions is required (Evans *et al.*, 2005). The mRNA expression of *Ca<sup>2+</sup>-ATPase* in the gill was also investigated as a potential marker of divalent ion secretion.

### *5.1.2 Lipid transport and metabolism*

During smoltification there is a change in lipid metabolism as protein deposition is prioritised at the expense of stores of lipid and carbohydrate (Stefansson *et al.*, 2008). During smoltification an increase in circulating growth hormone leads to the mobilisation of lipids, allowing fish to grow in preparation for their migration to seawater. Also associated with smoltification is an increase in plasma cortisol (McCormick *et al.*, 2007), a hormone which mobilises lipid stores.

In Atlantic salmon there is a marked reduction in condition factor associated with smoltification, caused by the reduction of lipid content in the muscle (McCormick, 2012). Seawater adapted smolts have lower muscle lipid content than fish that have remained in freshwater and desmoltified (Stefansson *et al.*, 2008). It was hypothesised that increased lipid mobilisation could lead to changes in lipoproteins. Indeed, investigation of the proteins

expressed in the gill using SWATH proteomics suggested that lipoproteins may be differentially expressed in parr and smolts (Dr G. Cramb, personal communication).

In vertebrates exogenous and endogenous lipids are transported by plasma lipoproteins, complexes composed of proteins, phospholipids, triglycerides, cholesterol and cholesterol esters in varying proportions. Lipoproteins are classified according to their density. Specific apolipoproteins are associated with the different lipoprotein classes. In both mammals and fish, low density lipoprotein (LDL) and very low density lipoprotein (VLDL) predominantly contain apolipoprotein B100 (ApoB100), while apolipoprotein A (ApoA) is the major protein in high density lipoprotein (HDL) (Babin & Vernier, 1989). Blood lipid levels, both cholesterol and triglycerides, in teleosts are higher than in mammals. In fish HDL is the major lipoprotein (Babin & Vernier, 1989). Most of the blood cholesterol in mammals is found in LDL. ApoB100 binds to the LDL receptor and the complex is internalised providing cholesterol and other lipids for cellular requirements (Goldstein *et al.*, 1979; Goldstein & Brown, 2009). In mammals apolipoprotein A4 (ApoA4) is primarily expressed and secreted in the intestine, and is important in formation of chylomicrons, the method by which dietary lipids enter the bloodstream (Karathanasis *et al.*, 1986). The genes coding for these proteins were assessed as potential biomarkers of smoltification.

Carnitine palmitoyltransferase 2 (CPT2) is a protein found in the mitochondrial membrane involved in the oxidation of fatty acids in the mitochondria. In humans, deficiency of this protein leads to symptoms ranging from myopathy to neonatal death (Bonfont *et al.*, 2004; Sharma *et al.*, 2003). As lipid stores are metabolised during smoltification, *CPT2* expression was investigated in the gill of Atlantic salmon as they developed from parr to smolts in freshwater.

### 5.1.3 Biomarker candidates involved in the immune system

Smolts are particularly susceptible to infection after seawater transfer in an aquaculture setting (Johansson *et al.*, 2016). A number of genes associated with the immune system were investigated as potential biomarkers of smoltification. A number of genes involved in the immune system were also identified as potential biomarkers of smoltification from the SWATH proteomics data (Dr G. Cramb, personal communication).

Polymeric immunoglobulin receptor (pIgR) transports secretory immunoglobulins to mucosal epithelia, playing an important role in mucosal immune function. The mucosal layer on the skin of fish forms an important barrier between the fish and its external environment.

CMRF 35-like molecule 8 (CLM8) is an inhibitory receptor involved in the innate immune system, with some similarities in structure to polymeric immunoglobulin receptor (Tadiso *et al.*, 2011). This antigen is expressed on the surface of leukocytes and may be involved in intracellular signalling (Green *et al.*, 1998). Differences in the structure of CMRF 35-like molecules suggest different roles for these proteins. Green *et al.* (1998) suggest that differences in the cytosolic portion of the protein, with the same extracellular sequence may produce different intracellular signals in response to the same ligand.

Immunoglobulins form a vital part of the adaptive immune response. Unlike the innate immune response which produces a rapid, non-specific response to infectious agents, the adaptive immune system produces a pathogen specific response which is long lasting. T cells are responsible for the majority of cell-mediated immunity in the adaptive immune response, while B cells produce immunoglobulins, important in the humoral immune response (Alberts *et al.*, 2002). Functional immunoglobulins are composed of two heavy chains and two light chains (Criscitiello & Flajnik, 2007; Mashoof & Criscitiello, 2016). Immunoglobulin D

(IgD) is a form of heavy chain immunoglobulin, forming part of functional antibodies, which has been identified in a variety of teleost species (Mashoof & Criscitiello, 2016). Immunoglobulin Kappa (IgK) is a form of immunoglobulin light chain. IgK is found in all vertebrates except birds (Criscitiello & Flajnik, 2007). The genes for both of these immunoglobulins were identified as potential biomarkers from SWATH proteomics results (Dr G. Cramb, personal communication).

The aryl hydrocarbon receptor 1 (AHR1) is a transcription factor involved in the activation of a suite of genes involved in the innate immune system (Hansson *et al.*, 2004; Hansson & Hahn, 2008). X-box binding protein 1 (XBP1) is a transcription factor which regulates the expression of genes involved in cellular stress and the immune system (Hollien, 2013; Kaser *et al.*, 2008). These transcription factors were investigated as candidate biomarkers since the transfer to seawater subjects the fish to osmotic stress, and farmed fish at this point in the production cycle are particularly susceptible to infectious disease.

The expression of a predicted leukocyte elastase inhibitor (LEI), was investigated in the gill of Atlantic salmon smolts prior to seawater transfer. LEI protects the cell from proteases released into the cytoplasm during stress (Torriglia *et al.*, 2017). During infection neutrophils are attracted to sites of inflammation by cytokines released by the stressed tissue (Havixbeck & Barreda, 2015). Neutrophils represent a major part of the initial antimicrobial response in all vertebrates, using a number of strategies to fight infectious agents (Havixbeck & Barreda, 2015). LEI has been shown to be essential for the successful clearance of bacterial infection as this protease inhibitor protects neutrophils from high concentration of their own proteases which are produced as part of the host immune response (Torriglia *et al.*, 2017). This protective effect allows the recruitment of large numbers of neutrophils to the site of infection by increasing their survival in inflamed tissue (Torriglia *et al.*, 2017).

#### 5.1.4 Other biomarker candidates

Gelsolin is an important, calcium dependent, regulator of the assembly and disassembly of actin filaments (Sun *et al.*, 1999). Actin filaments play an essential role in uniting membrane and intracellular functions, and the maintenance of cell volume (Pedersen *et al.*, 2001; Sun *et al.*, 1999). Gelsolin is specifically involved in the severing and capping of actin filaments, producing short filaments which cannot re-join or elongate (Sun *et al.*, 1999). Gelsolin can also facilitate actin polymerisation, severing by gelsolin produces many filaments which, when uncapped, can elongate and allow remodelling of the cytoskeleton (Yin & Stull, 1999). As the cytoskeleton is important in the regulation of cell volume (Devos *et al.*, 1998), the expression of gelsolin was investigated in the gill of Atlantic salmon smolts prior to transfer to seawater to determine whether this gene may be useful as a biomarker of smoltification.

Zymogen granule protein 16 (ZP16), has been shown to be expressed in the digestive tract of mammals, and has been identified as a secretory protein (Cronshagen *et al.*, 1994; Kleene *et al.*, 1999). As a result of some earlier work in our laboratory this gene was highlighted as a possible biomarker of smoltification (Dr S. Kalujnaia & Dr G. Cramb, personal communication).

Tristetraprolin is a zinc containing protein involved in the regulation of the expression of genes such as tumour necrosis factor  $\alpha$  by binding to the AU-rich region of 3' untranslated mRNAs and inducing their degradation. Tristetraprolin was investigated as a possible biomarker of smoltification because of the high level of tissue remodelling which takes place in the gill during the smoltification process, and the associated change in gene expression. Two forms of tristetraprolin were identified in the SalmonDB database, *TTP1* and *TTP2*.

Smoltification is an important part of the life cycle of many salmonid species, including Atlantic salmon which undergo the majority of their growth in seawater. In the wild smoltification is triggered by a combination of changes in photoperiod in the winter and spring and concurrent changes in water temperature (Stefansson *et al.*, 2008). Seawater transfer represents a major bottleneck in the production cycle for Atlantic salmon, with many fish showing reduced growth and increased disease susceptibility in the months following seawater transfer (Johansson *et al.*, 2016). Smoltification has been linked with systemic downregulation of the immune system, and changes in condition factor as lipid metabolism changes (Johansson *et al.*, 2016; Stefansson *et al.*, 2008). The situation in aquaculture is further complicated by the fact that many fish are manipulated to smoltify off season, through artificial lighting and feed additives (Johansson *et al.*, 2016; Stefansson *et al.*, 2008). To date, the majority of studies investigating the process of smoltification have been conducted on fish collected from wild populations and maintained in aquaria, under strictly controlled light and temperature conditions and free from environmental stressors such as those caused by predation or infection (Nilsen *et al.*, 2007).

### *5.1.5 Objectives*

The purpose of this study was to determine whether the changes in gene expression seen in wild populations represent robust biomarkers in fish reared under industrial aquaculture conditions. Fish reared in aquaculture net pens are exposed to infectious agents in the environment and subjected to disease treatments and artificial photoperiods. As well as the ion channels and transporters mentioned above, the expression of a number of other genes associated with lipid metabolism, the immune system and cellular metabolism were investigated in the gill of Atlantic salmon.

The aim of this study was to determine whether the expression of the biomarker candidates mentioned above changed as Atlantic salmon progressed towards smoltification and SW transfer in an industrial salmon farming environment.

### *5.1.6 Procedures*

Genes were investigated in the gill of fish from the Marine Harvest facility at Loch Lochy sampled over two different time courses (Materials and methods section 2.6). Fish used were “Q4” smolts, manipulated to smolt in the autumn/winter rather than in the spring as they do in the natural system. Smoltification was triggered by changing the light regime from natural photoperiod to 24 hour illumination. Fish were maintained in freshwater net pens in Loch Lochy or in seawater tanks during seawater exposures. Na<sup>+</sup>-K<sup>+</sup>-ATPase  $\alpha$ -subunit paralogues were investigated in fish sampled between 9<sup>th</sup> and 11<sup>th</sup> of February 2015, ranging from parr to adults. The Na<sup>+</sup>-K<sup>+</sup>-ATPase  $\alpha$ -subunit paralogues and the other genes mentioned above were also investigated in fish sampled between 9<sup>th</sup> of August and the 29<sup>th</sup> of October 2016. All fish were exposed to 24 h artificial lights from 22<sup>nd</sup> October and transferred to sea cages during the first week of November. SW exposures were carried out in experimental SW

tanks at the Marine Harvest site at Loch Lochy. Tanks were automatically gassed with O<sub>2</sub> to 10 mg/l, and maintained at the loch temperature of 12°C, and fish were kept on 24 h artificial lights as in the loch pens. Tissue samples were collected (Materials and methods section 2.1) from fish ranging from parr to smolts between 68 days before the population was transferred to SW, and 3 days after SW transfer. Genes were studied using RT-qPCR experiments (Materials and method section 2.2.9). Code used in statistical analysis is given in Appendix 5.

## 5.2 Results

### 5.2.1 Ion transport

The expression of *NKA a1a* (Figure 5.2) was found to be significantly affected by life stage ( $H_6 = 31.01$ ,  $p = 2.52 \times 10^{-5}$ ). *NKA a1a* was expressed at a lower level in the gill of salmon after 12 weeks in SW and in adult individuals at harvest size than it was in parr ( $p = 0.001$ ,  $p = 0.01$  respectively) and FW smolts ( $p = 0.007$ ,  $p = 0.04$  respectively), and was lower at 12 weeks in SW than in smolts which had been in SW for 6 hours ( $p = 0.01$ ).

*NKA a1b* expression (Figure 5.2) was also found to be significantly affected by life stage ( $H_6 = 26.40$ ,  $p = 0.0002$ ). Smolts which had been in SW for 6 hours had significantly higher *NKA a1b* than parr ( $p = 0.004$ ), FW smolts ( $p = 0.007$ ) and adults ( $p = 0.002$ ).

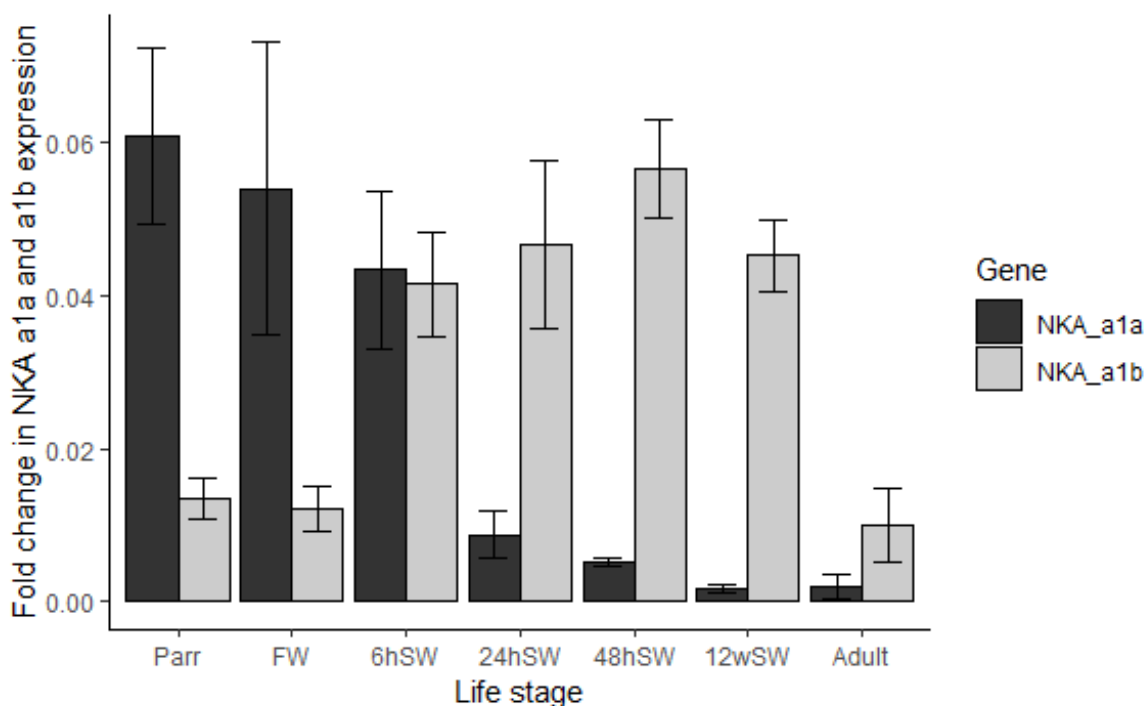


Figure 5.2. Mean expression of two  $Na^+K^+$ -ATPase  $\alpha$  subunit paralogues relative to *RPLP0* in the gill of Atlantic salmon at various life stages ranging from parr to adult. Error bars represent standard error,  $n=6$  in all groups except adult where  $n=3$ .

On the more comprehensive time course investigating smoltification (Figure 5.3), sampled between 9<sup>th</sup> of August and the 29<sup>th</sup> of October 2016, the expression of *NKA  $\alpha$ 1a* was found to be significantly influenced by time point ( $H_{11} = 43.26$ ,  $p = 9.8 \times 10^{-6}$ ). The mean level of *NKA  $\alpha$ 1a* expression was variable in FW at the beginning of time course, however, these changes were not statistically significant. There was a fall in *NKA  $\alpha$ 1a* expression following SW transfer. After 2 and 3 days in SW the level of *NKA  $\alpha$ 1a* expression was significantly lower than at 67 days, 61 days and 44 days before SW transfer ( $p < 0.04$ ). Levels at 3 days post SW transfer were also significantly lower than at 68 days before transfer.

On the same time course *NKA  $\alpha$ 1b* was also significantly influenced by time point ( $H_{11} = 54.72$ ,  $p = 8.73 \times 10^{-8}$ ). Expression of *NKA  $\alpha$ 1b* showed a declining trend in FW at the beginning of the time course, with levels at 57 days to SW transfer significantly lower than at 68 days to SW transfer ( $p = 0.01$ ). At 44 days to transfer levels increased again to levels that did not differ from the earlier time points. By 30 days to transfer expression was once again lower than at the first time point ( $p = 0.005$ ). At the time point 16 days before SW transfer the level of *NKA  $\alpha$ 1b* expression increased and was significantly higher than at 66 days, 57 days, and 30 days to SW transfer ( $p < 0.02$ ). Following SW transfer the level of *NKA  $\alpha$ 1b* expression was significantly higher at 1 day and 2 days post transfer than at 57 days and 30 days to SW transfer ( $p < 0.02$ ).

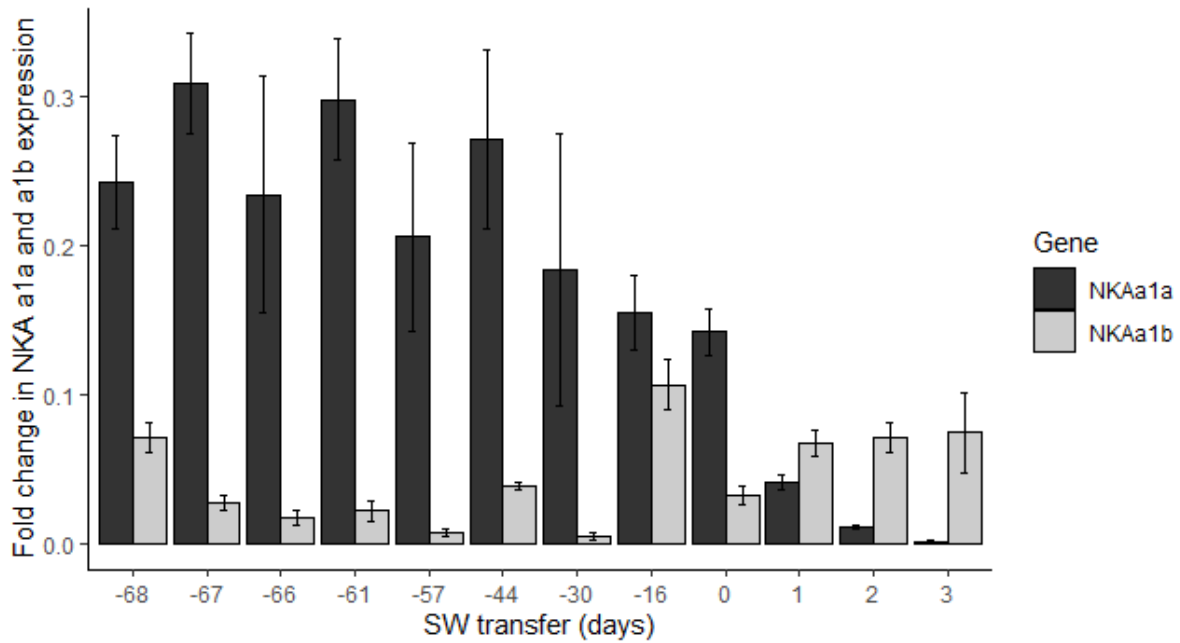


Figure 5.3. Mean expression of two  $Na^+K^+$ -ATPase  $\alpha$  subunit paralogues relative to *RPLP0* in the gill of Atlantic salmon at various time points as fish progressed from parr to smolts and were transferred to SW. Error bars represent standard error, n=5 or 6.

#### 5.2.1.1 $Na^+K^+$ -ATPase $\alpha$ -subunit protein levels

The protein levels of the  $Na^+K^+$ -ATPase  $\alpha$ -subunits,  $\alpha$ 1a and  $\alpha$ 1b were investigated in the gill of Atlantic salmon from the study investigating smoltification in an industrial setting, using Western blotting as detailed in the Materials and Methods.

The results obtained from Western blots using the NKA  $\alpha$ 1a antibody showed three immunoreactive protein bands, one at 180 kDa, one at 110 kDa, and one at 95 kDa (Figure 5.4). The expression of these was analysed individually and summed. The expression of all three bands was significantly affected by time point, 180 kDa ( $H_7 = 35.37$ ,  $p = 9.54 \times 10^{-6}$ ), 110 kDa ( $F_{7,40} = 4.0$ ,  $p = 0.002$ ), 95 kDa ( $H_7 = 30.64$ ,  $p = 7.24 \times 10^{-5}$ ). Results are summarised in Figure 5.5.

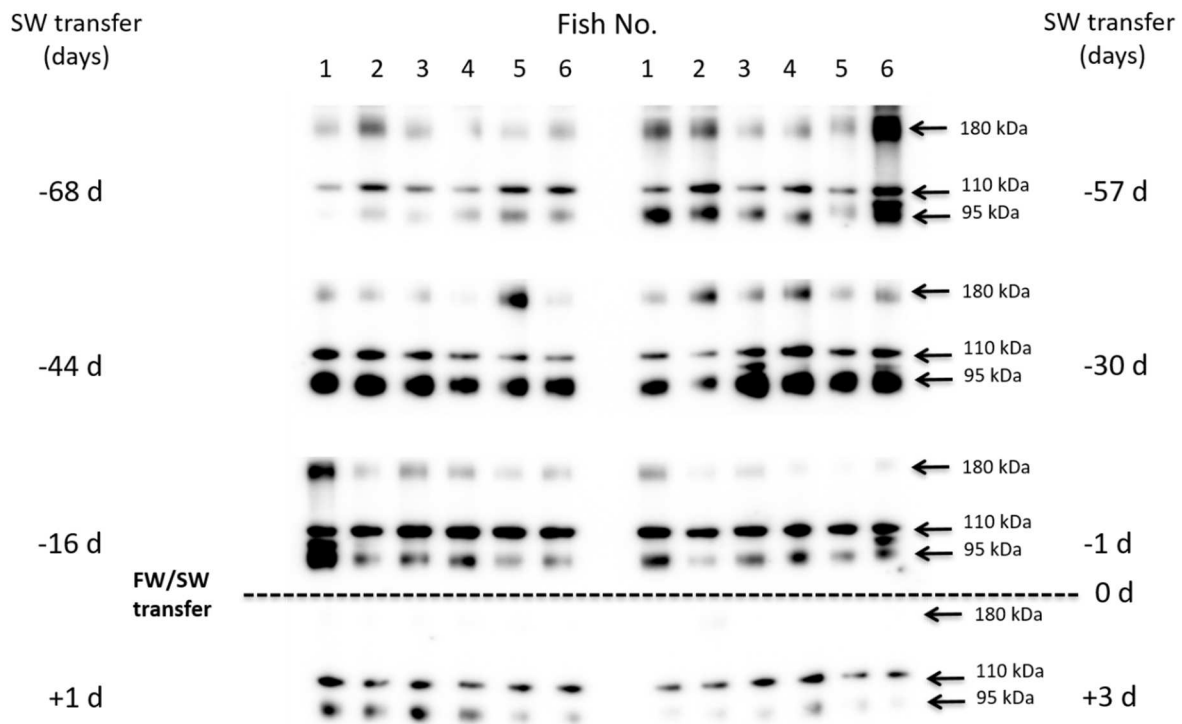


Figure 5.4. Western blot showing Na<sup>+</sup>-K<sup>+</sup>-ATPase  $\alpha$ 1a levels in the gill of Atlantic salmon during development from parr to smolt. Time intervals (-68 d to +3 d) relate to the time of seawater transfer.

The expression of the 180 kDa band was lower after 24 hours in SW than 68 ( $p = 0.006$ ) and 57 ( $p = 0.0004$ ) days before SW transfer. Similarly, the expression of this band after 3 days in SW was also lower than expression at the first two time points ( $p = 0.003$  and  $p = 0.0002$  respectively).

Expression of the 110 kDa band was significantly higher at 16 and 0 days before SW transfer than 68 days ( $p = 0.047$  and  $p = 0.009$  respectively). At 0 days to transfer the level of expression was also higher than that after 3 days in SW ( $p = 0.02$ ).

Expression of the 95 kDa was higher at 44 days to transfer than at 68 days ( $p = 0.02$ ). After three days in SW the expression of the 95 kDa band was significantly lower than 57 ( $p = 0.03$ ), 44 ( $p = 0.0006$ ), and 30 ( $p = 0.003$ ) days to SW transfer.

The sum of the expression of the three bands was also found to be significantly affected by time point ( $F_{7,40} = 5.17$ ,  $p = 0.0003$ ). Summed expression of NKA  $\alpha 1a$  was higher at the 57 days to transfer time point than 68 ( $p = 0.048$ ). Following SW transfer the level of summed NKA  $\alpha 1a$  protein expression was lower, with expression at 24 hours in SW significantly lower than at 57 days ( $p = 0.01$ ). After 3 days in SW was significantly lower than at 57 ( $p = 0.001$ ), 44 ( $p = 0.01$ ) and 30 ( $p = 0.01$ ) days to SW transfer.

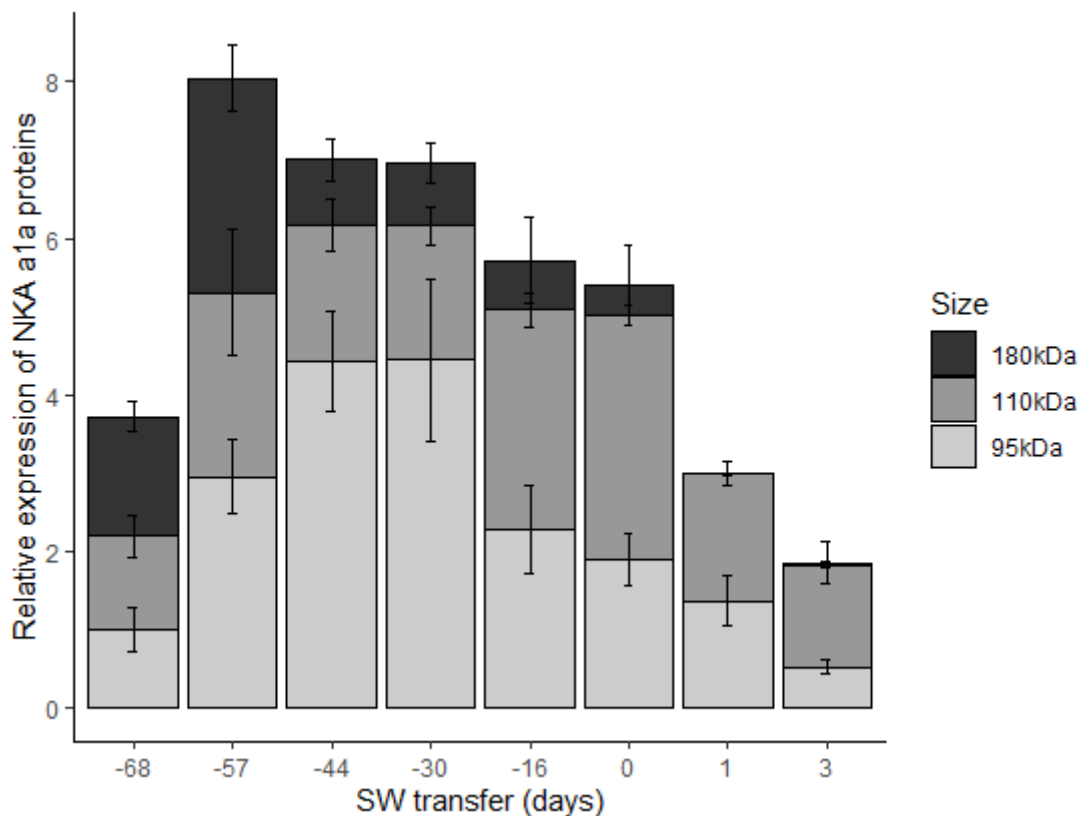


Figure 5.5. Quantification of western blot immunoreactive bands showing levels of three peptides detected using an antibody to salmon  $\text{Na}^+\text{-K}^+\text{-ATPase } \alpha 1a$  in the gill of Atlantic salmon during development from parr to smolt. Error bars indicate standard error,  $n=6$ .

NKA  $\alpha 1b$  protein expression (Figure 5.6) in the gill of salmon was found to be significantly affected by time point in the smoltification time course studied ( $H_7 = 35.233$ ,  $p = 1.011 \times 10^{-5}$ ). NKA  $\alpha 1b$  protein expression was in general significantly higher in the following SW transfer than in FW, with expression at 24 hours in SW significantly higher than 68 ( $p = 0.03$ ), 57 ( $p = 0.02$ ) and 30 ( $p = 0.008$ ) days before SW transfer. After three days in SW NKA  $\alpha 1b$  expression was higher than 68 ( $p = 0.01$ ), 57 ( $p = 0.03$ ), 44 ( $p = 0.02$ ), 30 ( $p = 0.002$ ) and 16 ( $p = 0.04$ ) days before SW transfer. Results summarised in Figure 5.7.

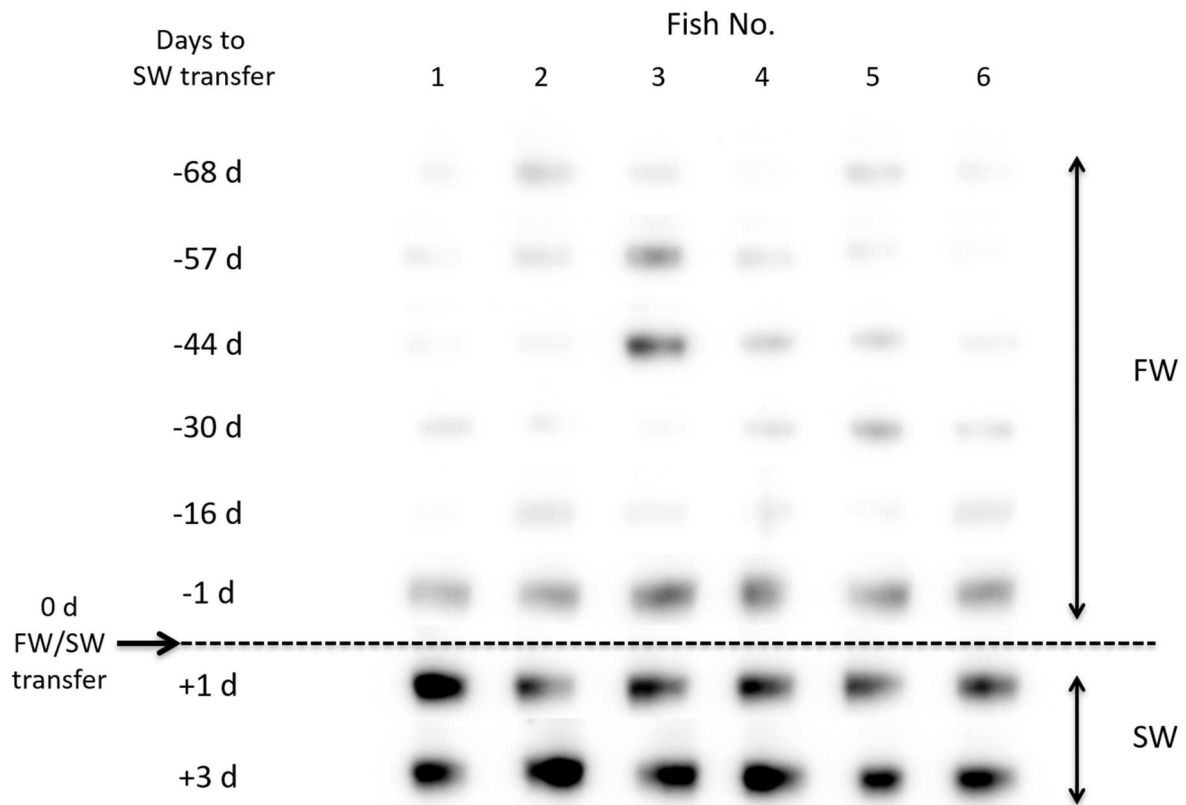


Figure 5.6. Western blot showing  $\text{Na}^+\text{-K}^+\text{-ATPase } \alpha 1b$  levels in the gill of Atlantic salmon during development from parr to smolt. Time intervals (-68 d to +3 d) relate to the time of seawater transfer.

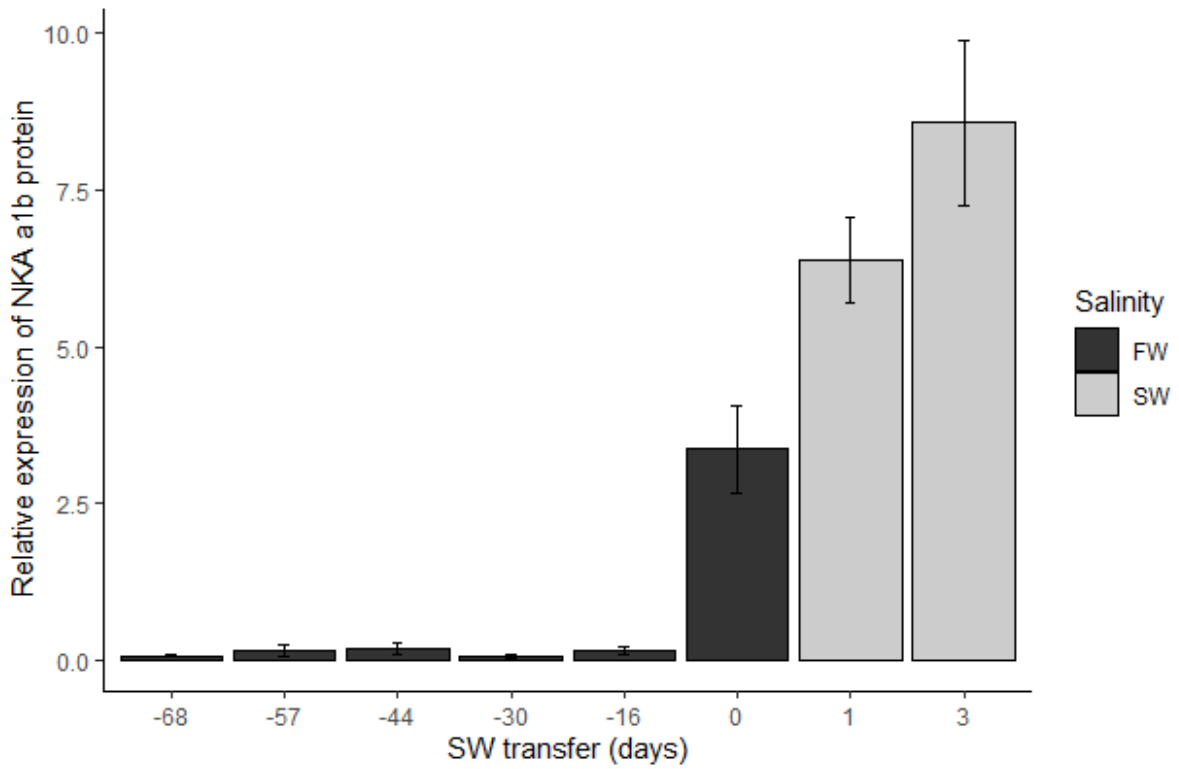


Figure 5.7. Quantification of western blot immunoreactive bands showing levels of three peptides detected using an antibody to salmon Na<sup>+</sup>-K<sup>+</sup>-ATPase α1b in the gill of Atlantic salmon during development from parr to smolt. Error bars indicate standard error, n=6.

No significant change in expression was observed in the expression of the genes *NKA β2ab* ( $F_{4,10} = 3.4$ ,  $p = 0.05$ , Figure 5.8), *β2c* ( $F_{4,10} = 1.5$ ,  $p = 0.28$ , Figure 5.8B), *β3b* ( $F_{4,10} = 1.2$ ,  $p=0.37$ , Figure 5.8C) and *β4* ( $F_{4,10} = 1.03$ ,  $p=0.44$ . Figure 5.8D).

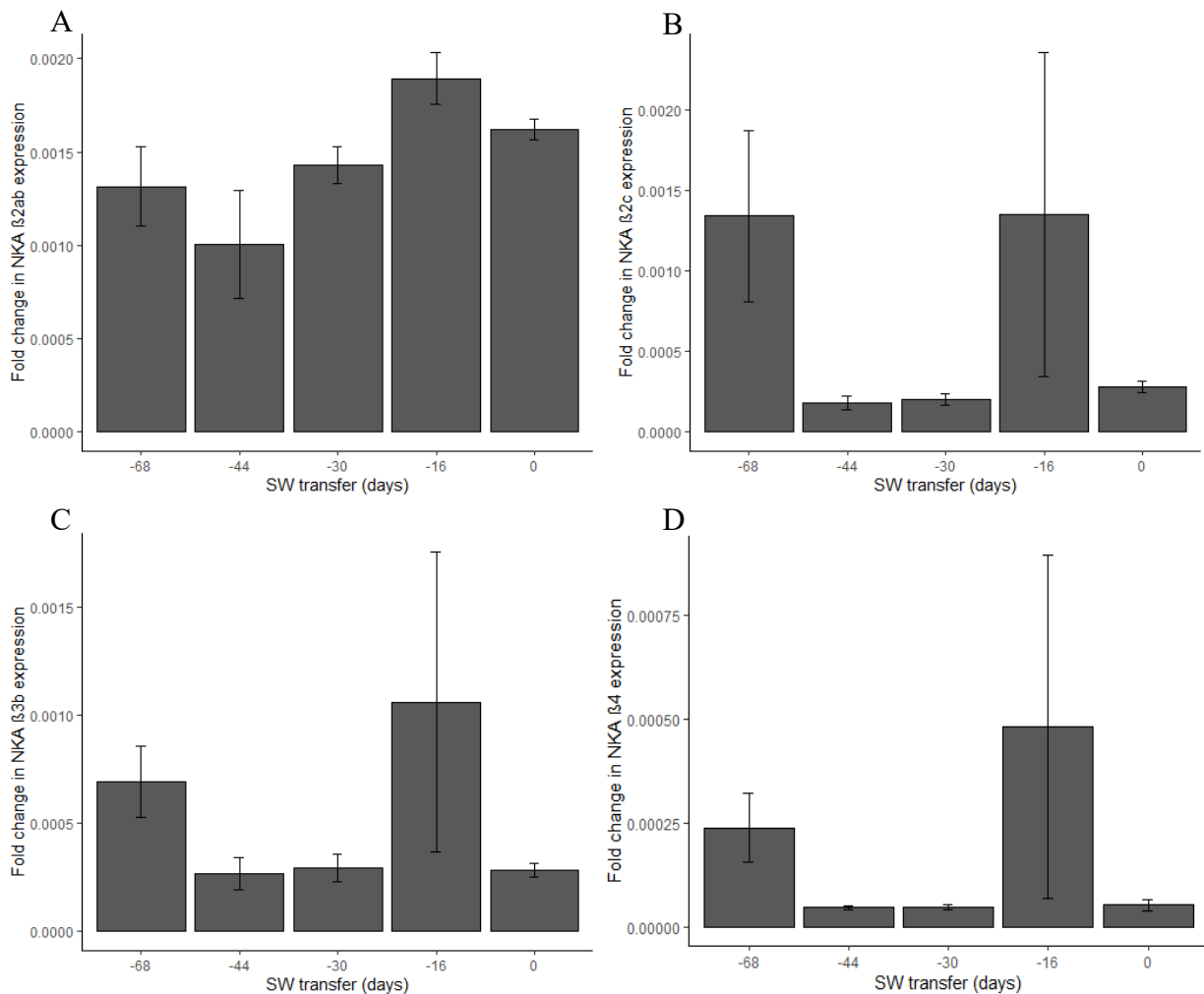


Figure 5.8. Expression of *Na<sup>+</sup>K<sup>+</sup>-ATPase β2a/b* (A), *Na<sup>+</sup>K<sup>+</sup>-ATPase β2c* (B), *Na<sup>+</sup>K<sup>+</sup>-ATPase β3b* (C) and *Na<sup>+</sup>K<sup>+</sup>-ATPase β4* (d) mRNA relative to *RPLP0* in Atlantic salmon gill between 0 hours and 68 days post vaccination in FW. Error bars denote standard error (n=3).

The expression of *NKA β3c* (Figure 5.9) was found to be significantly affected by the numbers of days to transfer ( $F_{4,10} = 6.93$ ,  $p = 0.006$ ) with expression at 68 days before SW transfer significantly higher than at 30, 16 and 0 days ( $p = 0.01$ ,  $p = 0.03$ ,  $p = 0.005$  respectively).

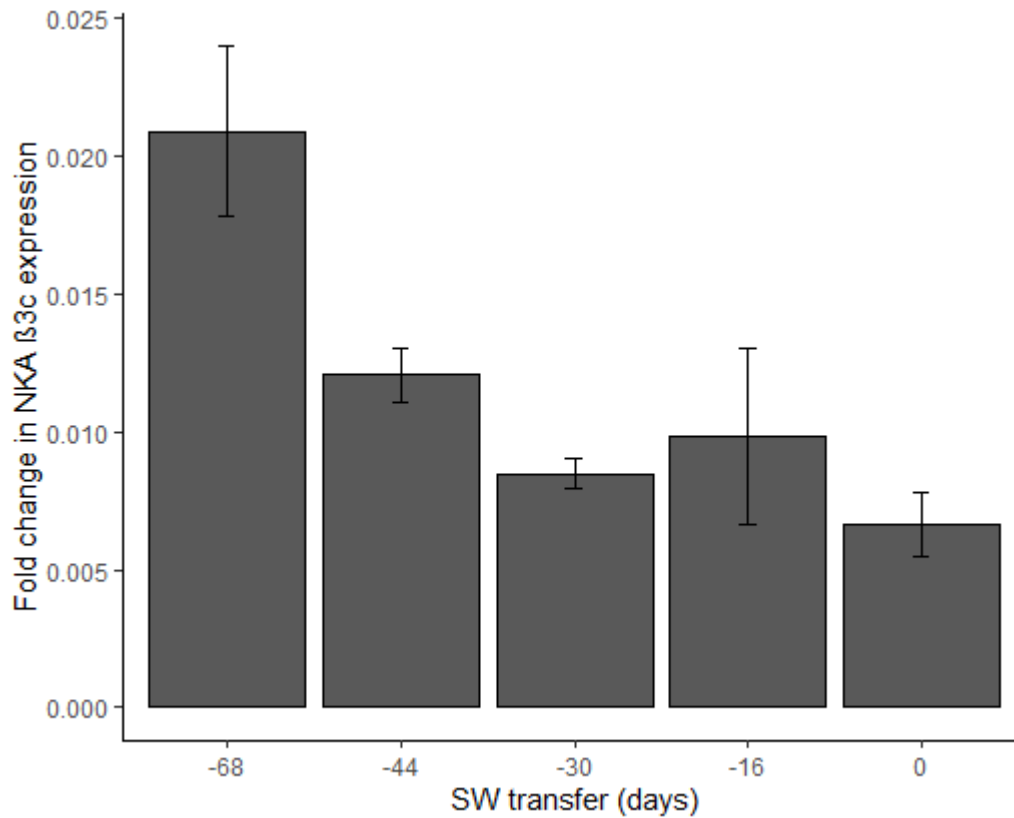


Figure 5.9. Expression of  $Na^+K^+ATPase \beta3c$  mRNA relative to *RPLP0* in Atlantic salmon gill between 0 hours and 68 days post vaccination in FW. Error bars denote standard error (n=3).

The expression of *NKCC1* was not observed to vary significantly in FW as fish progressed towards smoltification ( $F_{4,10} = 3.11$ ,  $p = 0.066$ ), Figure 5.10A. However, *NKCC1* was significantly affected by treatment in the SW challenge trial ( $F_{3,19} = 6.60$ ,  $p = 0.003$ ). Expression was significantly higher after 24 hours in SW than at the two time points in FW, 68 days ( $p = 0.003$ ) and 16 days ( $p = 0.03$ ) prior to the date of SW transfer, Figure 5.10B.

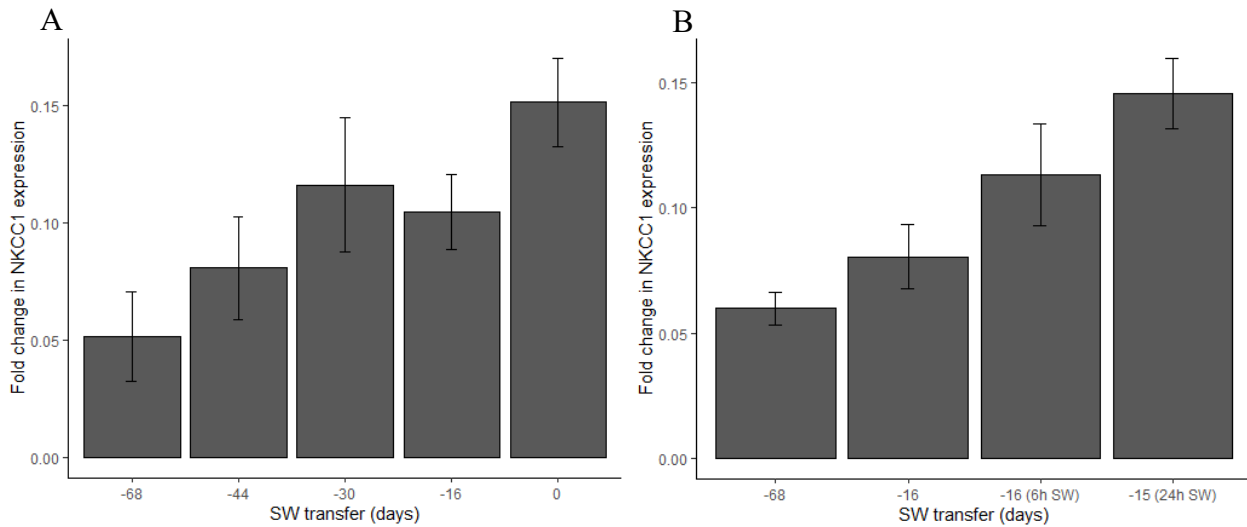


Figure 5.10. Expression of  $Na^+-K^+-2Cl^-$ -cotransporter 1 (*NKCC1*) mRNA relative to *RPLP0* in Atlantic salmon gill on a FW time course (A) and in fish exposed to SW challenge (B). Error bars represent standard error (n=3 in A, n=5 or 6 in B).

Expression of *CFTR* was found to vary significantly in FW as fish progressed towards smoltification in FW ( $F_{4,10}=7.78$ ,  $p=0.004$ ) Figure 5.11A. The level of *CFTR* expression was significantly higher on the day of SW transfer than at any of the previous time points, 68 days ( $p = 0.003$ ), 44 days ( $p = 0.018$ ), 30 days ( $p = 0.049$ ) and 16 days ( $p = 0.01$ ). However, no significant effect of time point or SW challenge was observed on the SW challenge trial ( $F_{3,19} = 1.65$ ,  $p = 0.21$ ), Figure 5.11B.

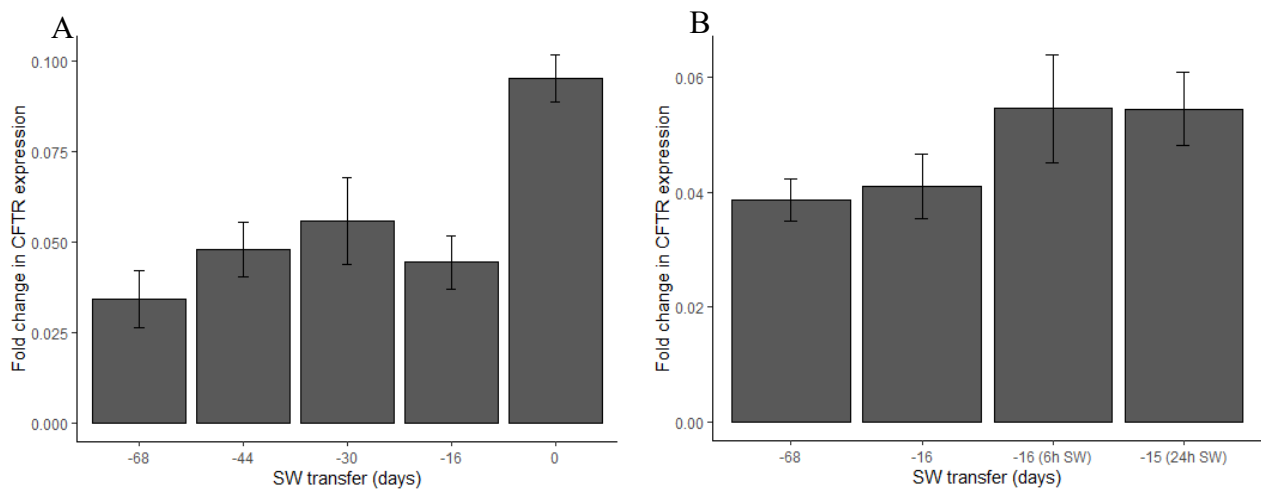


Figure 5.11. Expression of *cystic fibrosis transmembrane conductance regulator (CFTR)* mRNA relative to *RPLP0* in Atlantic salmon gill on a FW time course (A) and in fish exposed to SW challenge (B). Error bars represent standard error (n=3 in A, n=5 or 6 in B).

$Ca^{2+}$ -ATPase expression (Figure 5.12) did not show significant changes in the gill of fish during the time leading to smoltification ( $F_{4,10} = 1.84$ ,  $p = 0.2$ ).

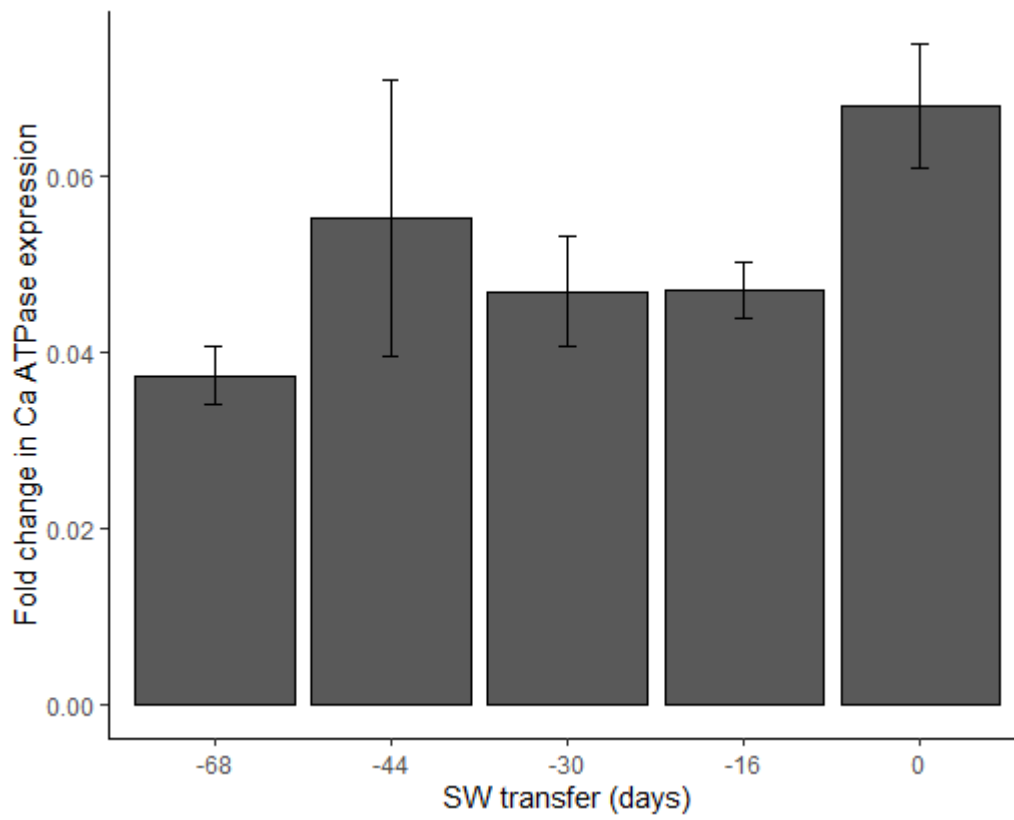


Figure 5.12. Expression of  $Ca^{2+}$ -ATPase mRNA relative to *RPLP0* in Atlantic salmon gill on a FW time course. Error bars represent standard error (n=3).

### 5.2.2 Lipid metabolism

Expression of *LDLR* is shown in Figure 5.13. *LDLR* expression was not observed to differ significantly as fish progressed towards smoltification over the time course investigated leading up to smoltification ( $F_{4,10} = 3.27$ ,  $p = 0.059$ ).

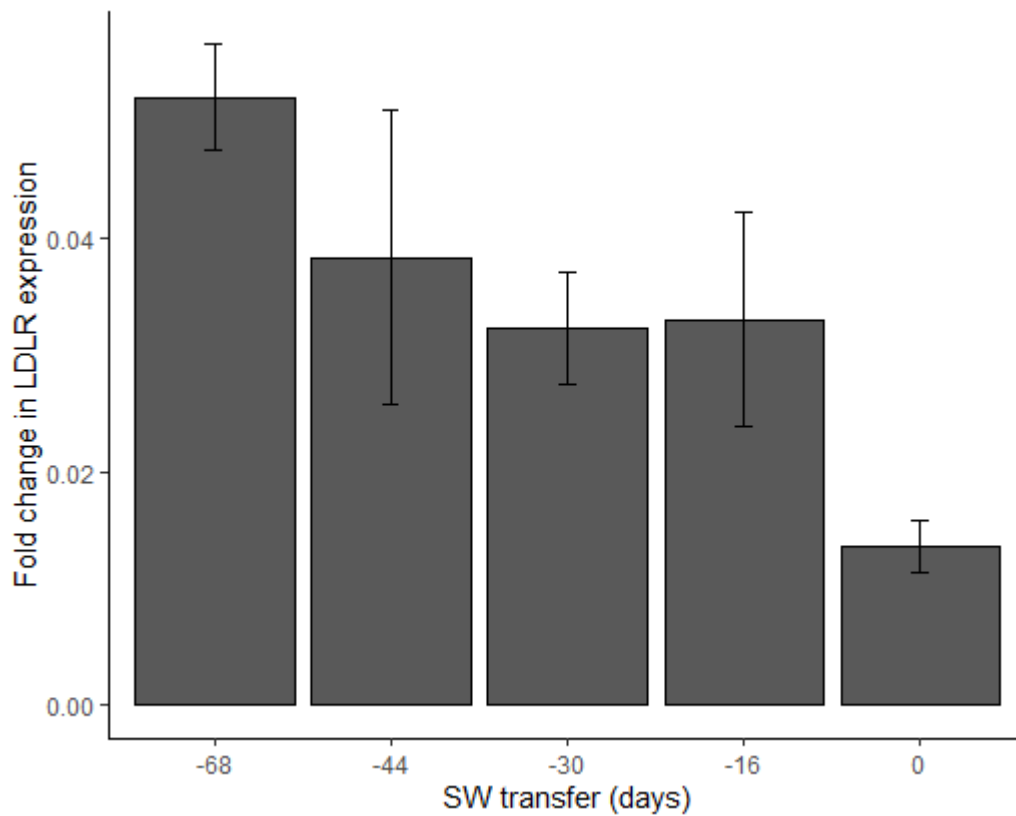


Figure 5.13. Expression of *LDL receptor* mRNA relative to *RPLP0* in Atlantic salmon gill on a FW time course. Error bars represent standard error (n=3).

As seen in Figure 5.14 the expression of *ApoA1* (A), *ApoA1b* (B) and *ApoA4* (C) was not found to differ significantly as salmon developed towards smoltification and SW transfer ( $F_{4,10} = 2.028$ ,  $p = 0.166$ ;  $F_{4,10} = 1.726$ ,  $p = 0.22$ ;  $F_{4,10} = 3.607$ ,  $p = 0.05$  respectively). An increase in variability was observed on all three of these genes at the 30 days to SW transfer time point (Figure 5.14A-C). *ApoB100* (Figure 5.14D) expression also did not vary significantly over the time course leading up to smoltification and SW transfer ( $F_{4,10} = 1.15$ ,  $p = 0.39$ ).

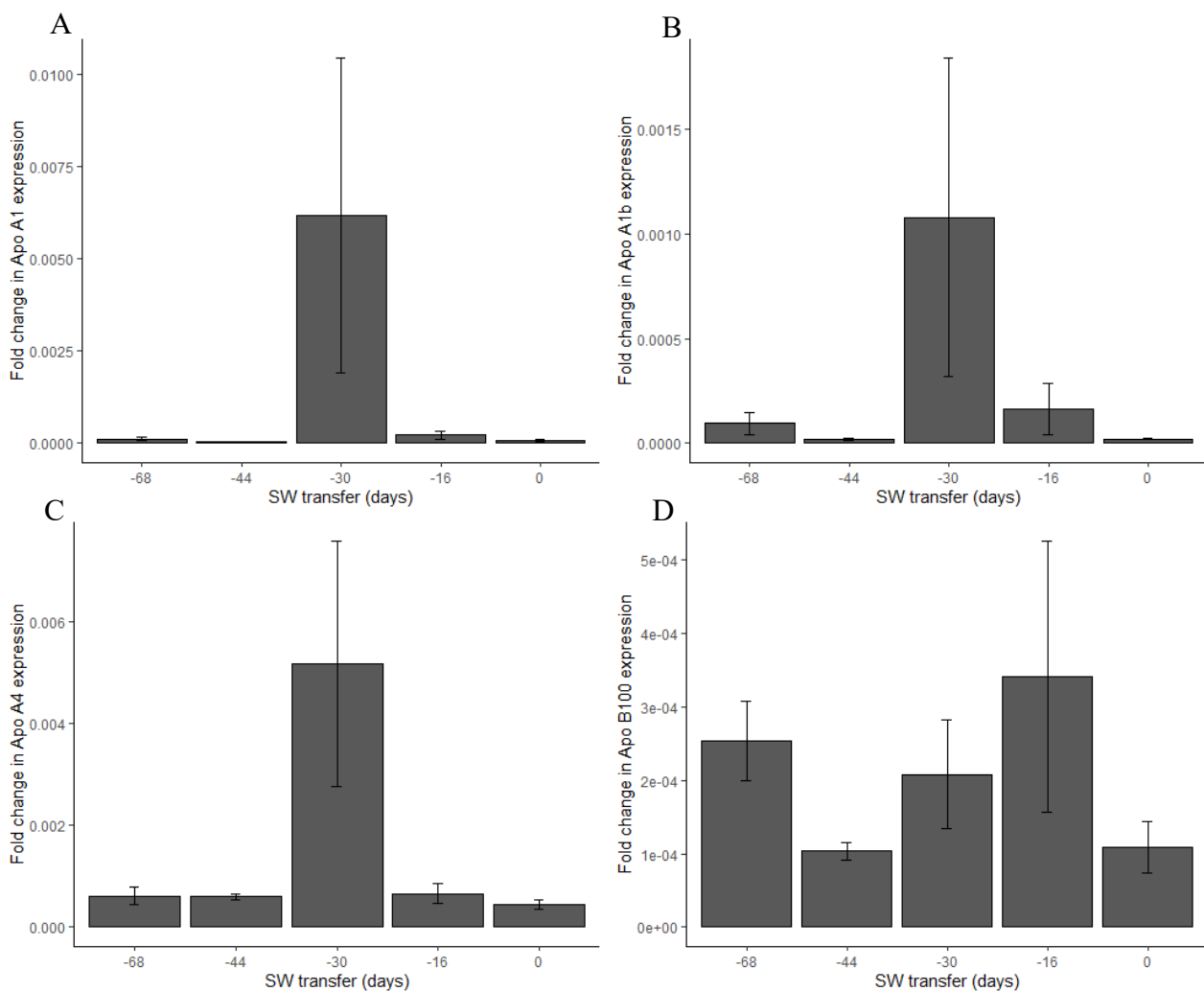


Figure 5.14. Expression of *ApoA1* (A), *ApoA1b* (B), *ApoA4* (C) and *ApoB100* (D) mRNA relative to *RPLP0* in Atlantic salmon gill between 0 hours and 68 days post vaccination in FW. Error bars denote standard error (n=3).

*CPT2* expression (Figure 5.15) was not observed to differ significantly as salmon progressed towards smoltification ( $F_{4,10}=3.16$ ,  $p=0.06$ ).

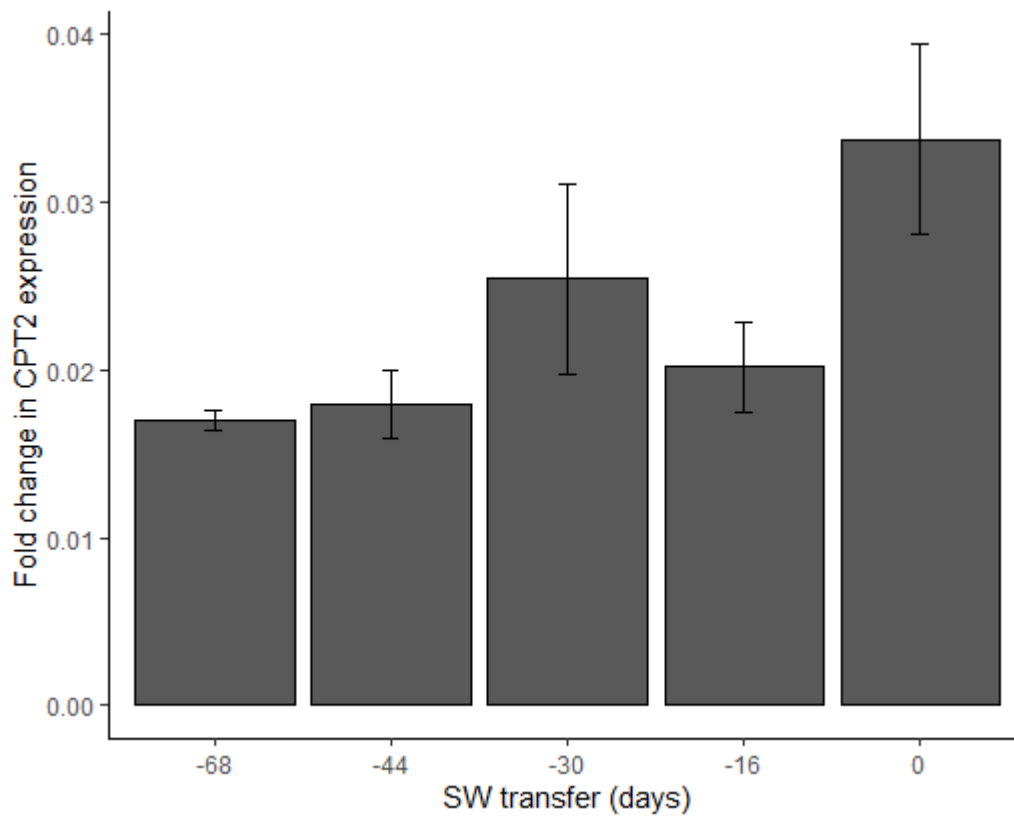


Figure 5.15. Expression of *CPT2* mRNA relative to *RPLP0* in Atlantic salmon gill between 0 hours and 68 days post vaccination in FW. Error bars denote standard error (n=3).

### 5.2.3 Immunity

Expression of *pIgR* (Figure 5.16) was not observed to change over time as fish progressed towards smoltification of following SW challenge ( $F_{3,19} = 0.47$ ,  $p = 0.71$ ).

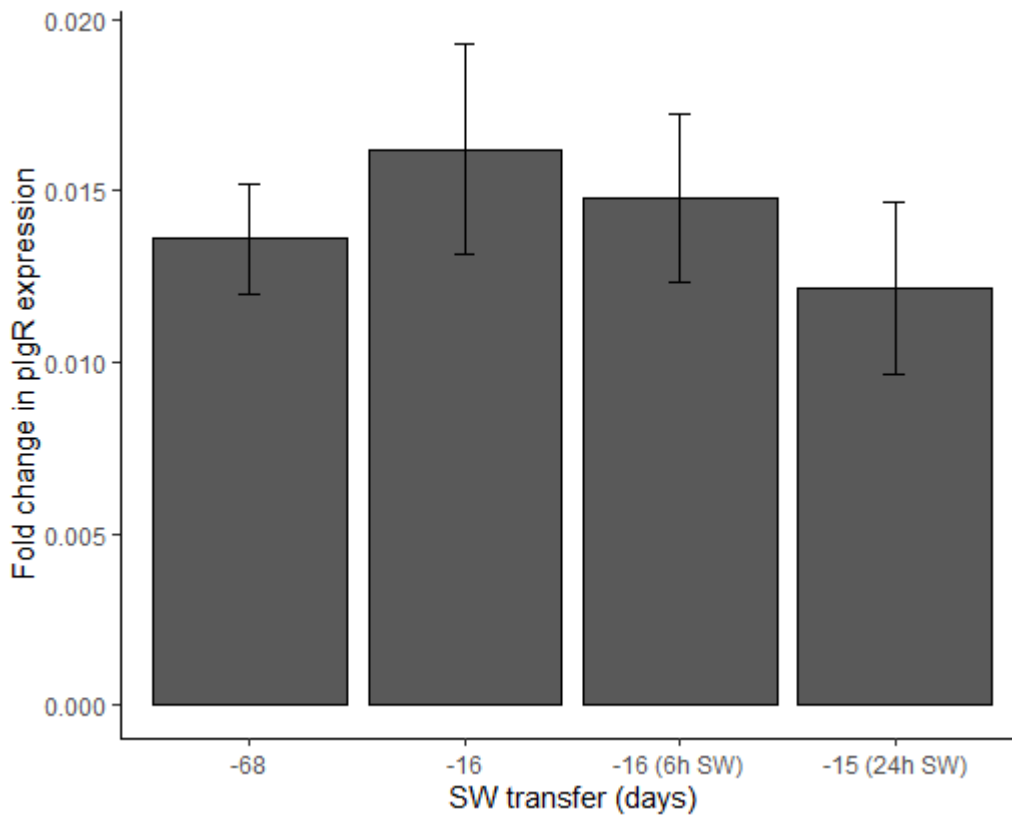


Figure 5.16. Expression of *pIgR* mRNA relative to *RPLP0* in Atlantic salmon gill in fish exposed to SW challenge. Error bars represent standard error (n=5 or 6).

The expression of *pIgRL1* was not found to change over the time course leading to smoltification in FW, Figure 5.17A ( $F_{4,10}=2.45$ ,  $p=0.11$ ). However, the level of *pIgRL1* was found to differ significantly between time points in the SW challenge trial, Figure 5.17B ( $F_{3,19} = 31.91$ ,  $p = 1.27 \times 10^{-7}$ ). Expression was higher after 6 hours in SW than at the first FW time point 68 days before the date of SW transfer ( $p = 0.037$ ). After 24 hours in SW the level of expression was higher than at the earlier time points in the SW challenge trial ( $p < 0.0001$ ).

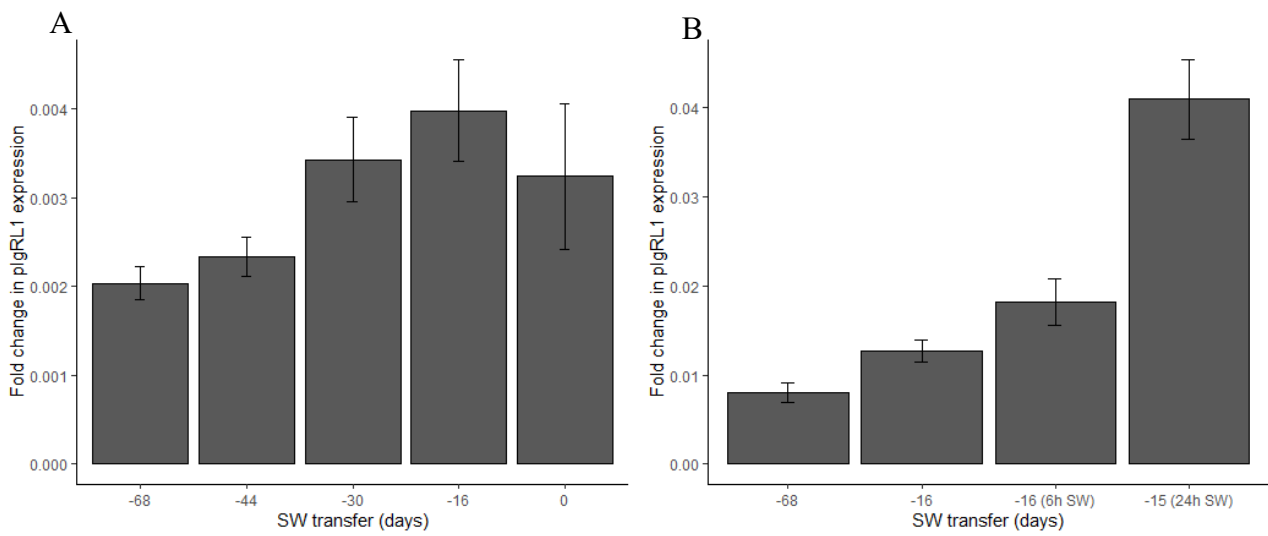


Figure 5.17. Expression of *pIgRL1* mRNA relative to *RPLP0* in Atlantic salmon gill on a FW time course (A) and in fish exposed to SW challenge (B). Error bars represent standard error ( $n=3$  in A,  $n=5$  or  $6$  in B).

The expression of *pIgRL2* (Figure 5.18) was found to be influenced by treatment in a SW challenge trial ( $F_{3,19} = 4.868$ ,  $p = 0.0112$ ). Expression was lower in the gill following 24 hours in SW than in seen at the FW time points (68 days before date of transfer  $p = 0.02$ , and 16 days before the date of SW transfer  $p = 0.01$ ).

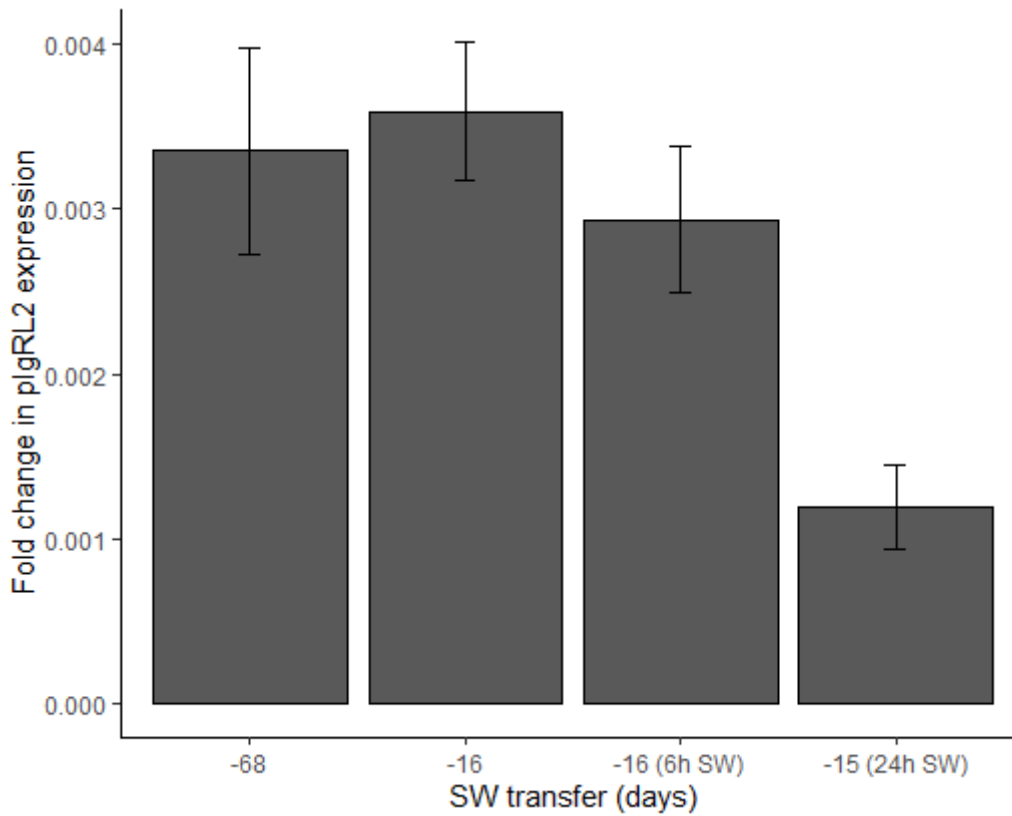


Figure 5.18. Expression of *pIgRL2* mRNA relative to *RPLP0* in Atlantic salmon gill in fish exposed to SW challenge. Error bars represent standard error (n=5 or 6).

The expression of *CLM8* (Figure 5.19) was found not to differ significantly throughout the SW challenge trial ( $F_{3,19} = 2.168$ ,  $p = 0.125$ ).

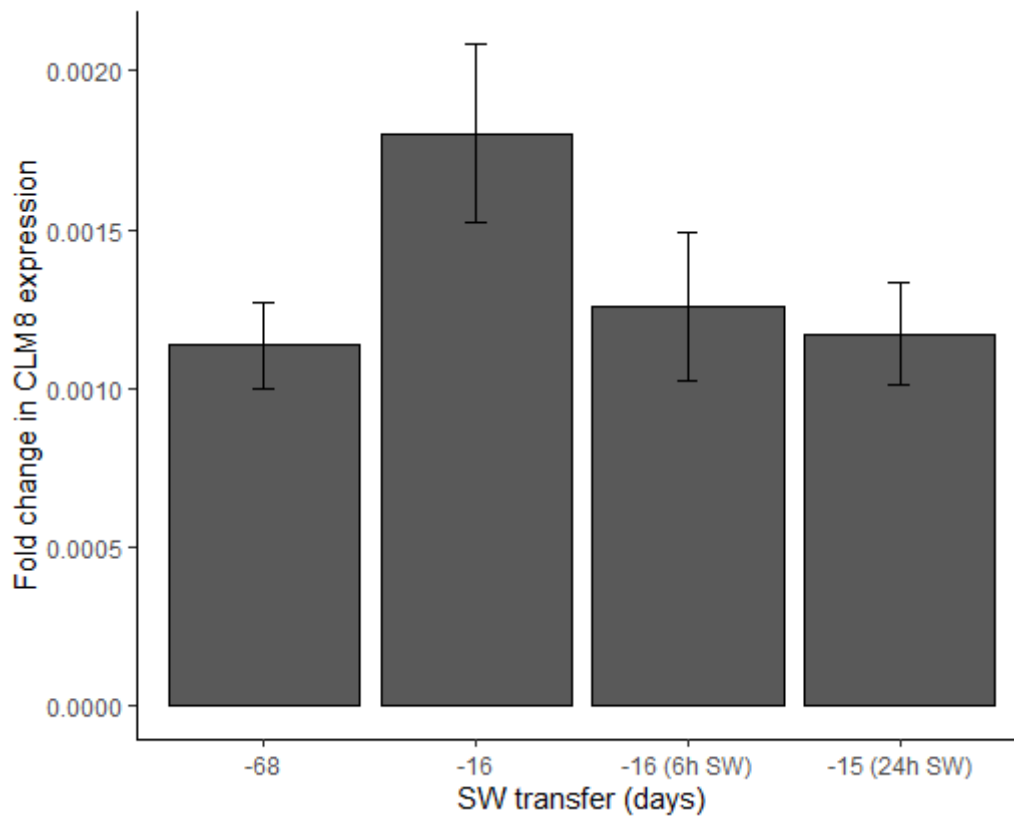


Figure 5.19. Expression of *CLM8* mRNA relative to *RPLP0* in Atlantic salmon gill in fish exposed to SW challenge. Error bars represent standard error ( $n=5$  or  $6$ ).

The expression of the immunoglobulin *IgK* (Figure 5.20A) was found to change significantly throughout the FW time course leading to smoltification ( $F_{4,10} = 6.885$ ,  $p = 0.00626$ ). Expression of *IgK* was higher in FW the day of SW transfer than at 68 days and 30 days prior previously ( $p = 0.009$  and  $p = 0.008$  respectively). The level of *IgD* (Figure 5.20B) expression was not observed to significantly differ over the FW time course ( $F_{4,10}=3.271$ ,  $p=0.0585$ ).

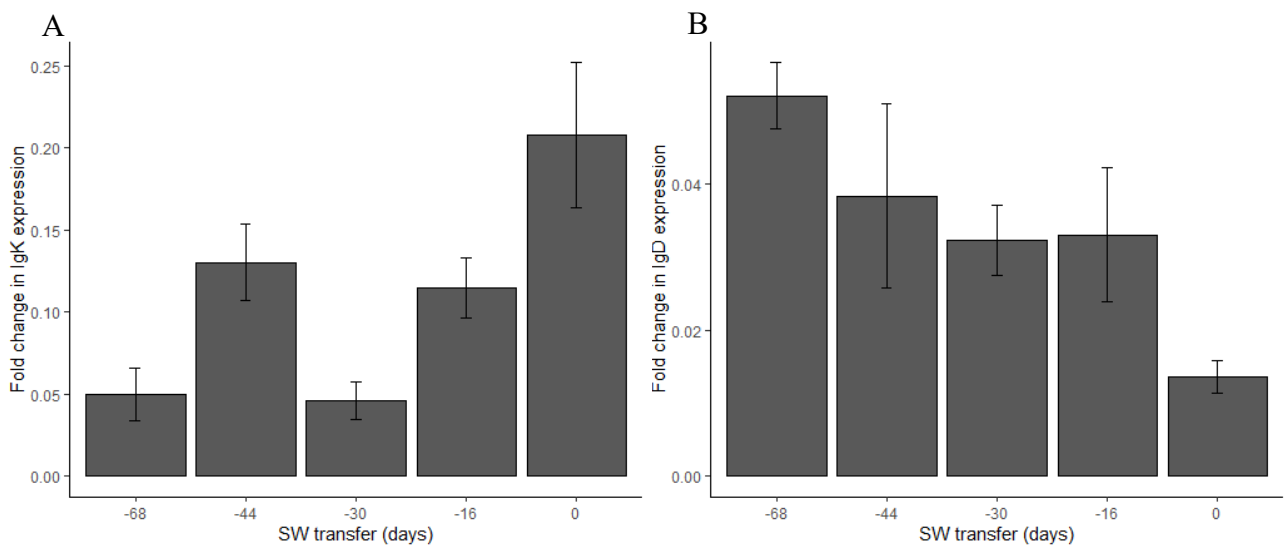


Figure 5.20. Expression of *IgK* (A) and *IgD* (B) mRNA relative to *RPLP0* in Atlantic salmon gill on a FW time course. Error bars represent standard error (n=3).

Expression of *AHRT1* (Figure 5.21) was not found to change in the SW challenge trial ( $F_{3,19} = 2.34, p = 0.11$ )

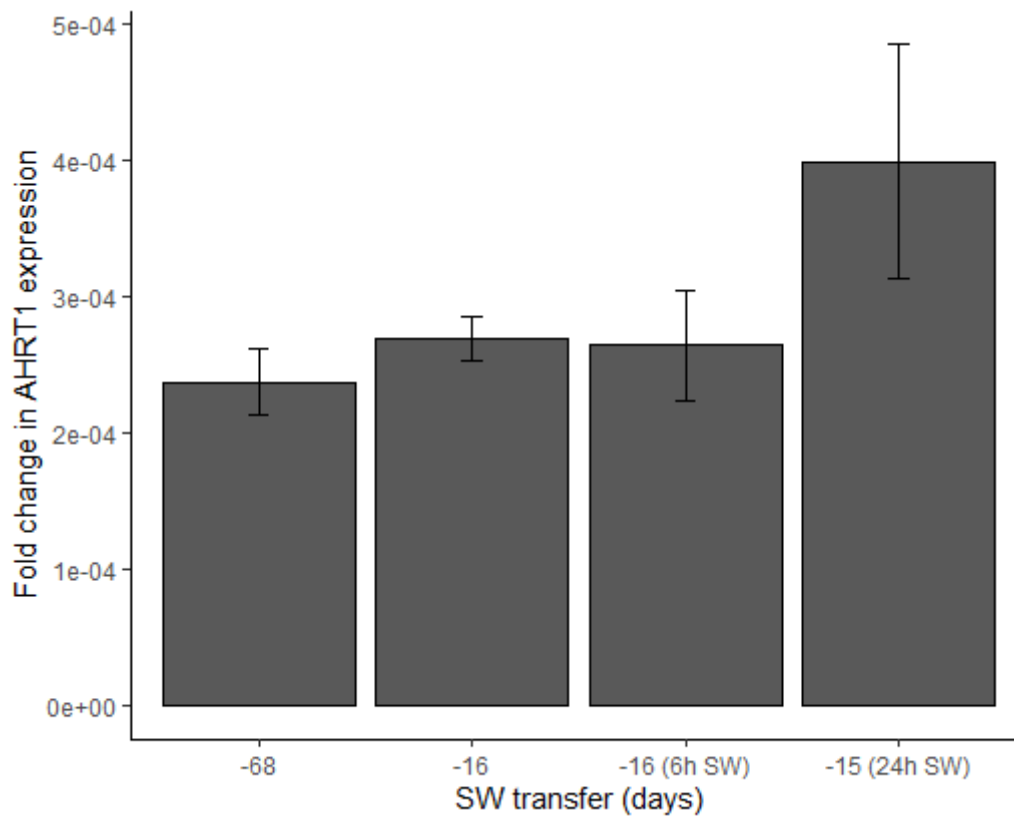


Figure 5.21. Expression of *AHRT1* mRNA relative to *RPLP0* in Atlantic salmon gill in fish exposed to SW challenge. Error bars represent standard error (n=5 or 6).

*XBPI* expression (Figure 5.22) was not found to be significantly affected by treatment in the SW challenge trial ( $F_{3,19} = 2.053$ ,  $p = 0.141$ ).

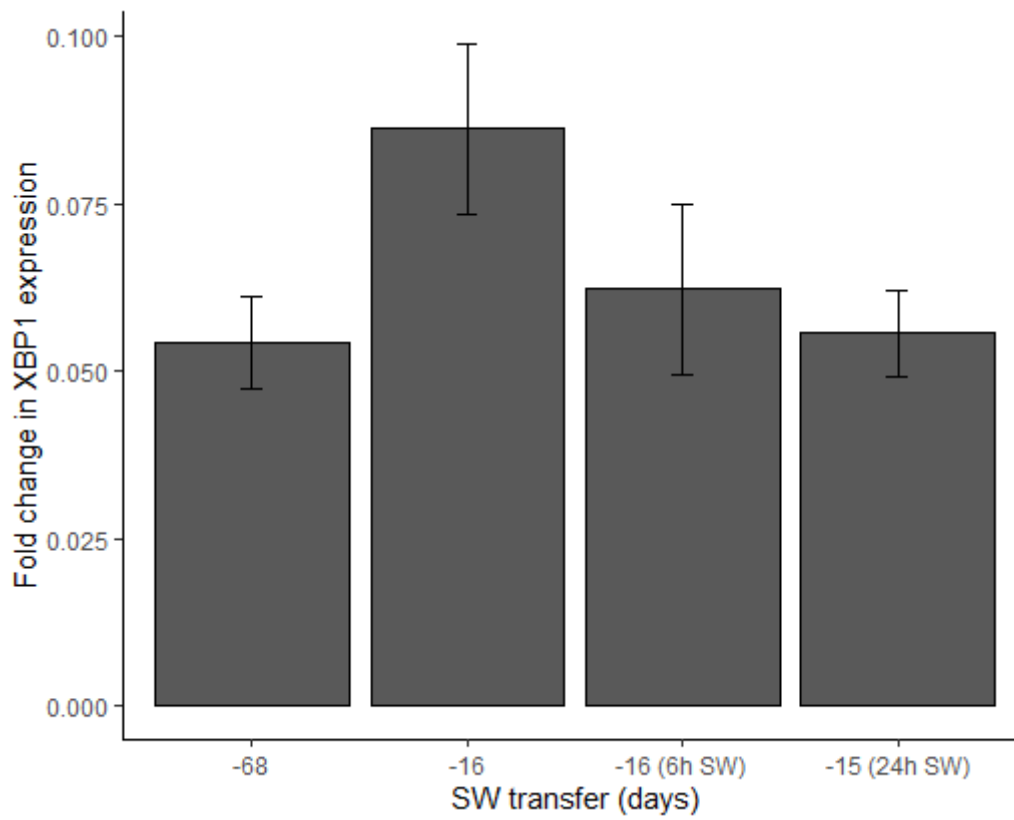


Figure 5.22. Expression of *XBPI* mRNA relative to *RPLP0* in Atlantic salmon gill in fish exposed to SW challenge. Error bars represent standard error ( $n=5$  or  $6$ ).

The expression of *LEI* (Figure 5.23) was found to be significantly affected by time point (days to SW) as salmon progressed towards smoltification ( $F_{4,10} = 4.21$ ,  $p = 0.0297$ ). Expression was significantly higher at 30 to SW transfer than at 68 days to transfer ( $p = 0.027$ ).

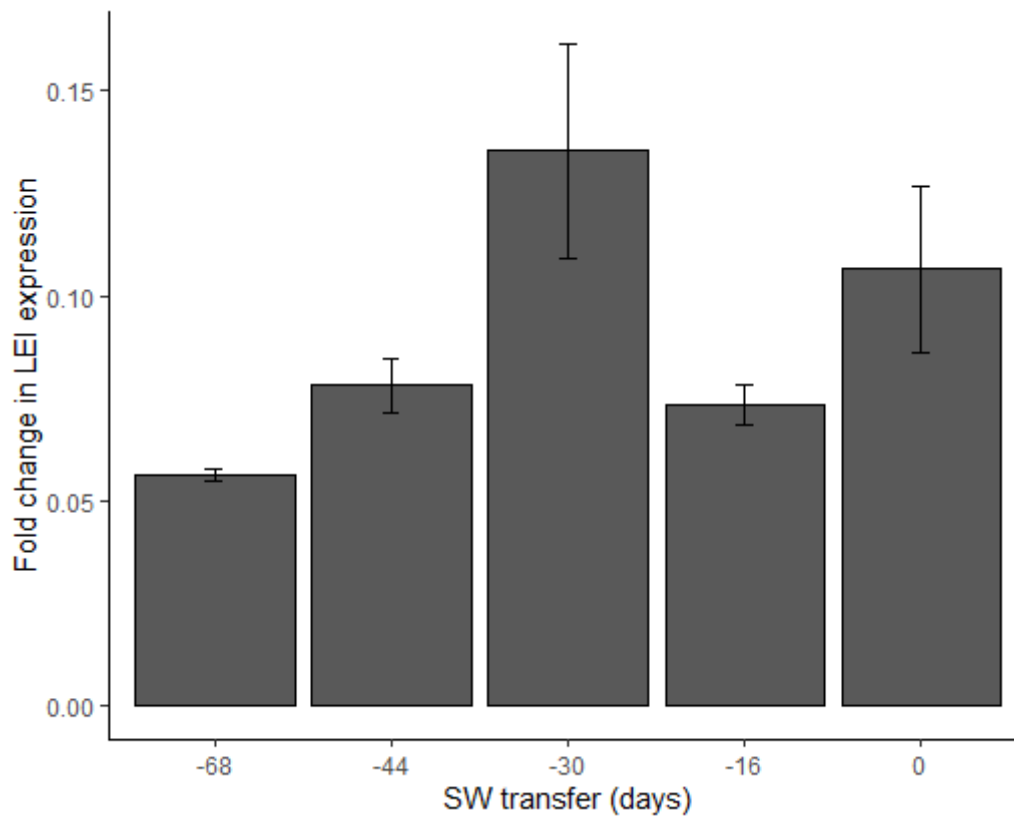


Figure 5.23. Expression of *LEI* mRNA relative to *RPLP0* in Atlantic salmon gill on a FW time course. Error bars represent standard error (n=3).

#### 5.2.4 Other biomarker candidates

*Gelsolin* expression (Figure 5.24) was not found to be significantly affected by the time point as salmon progressed towards smoltification ( $F_{4,10} = 1.56$ ,  $p = 0.26$ ).

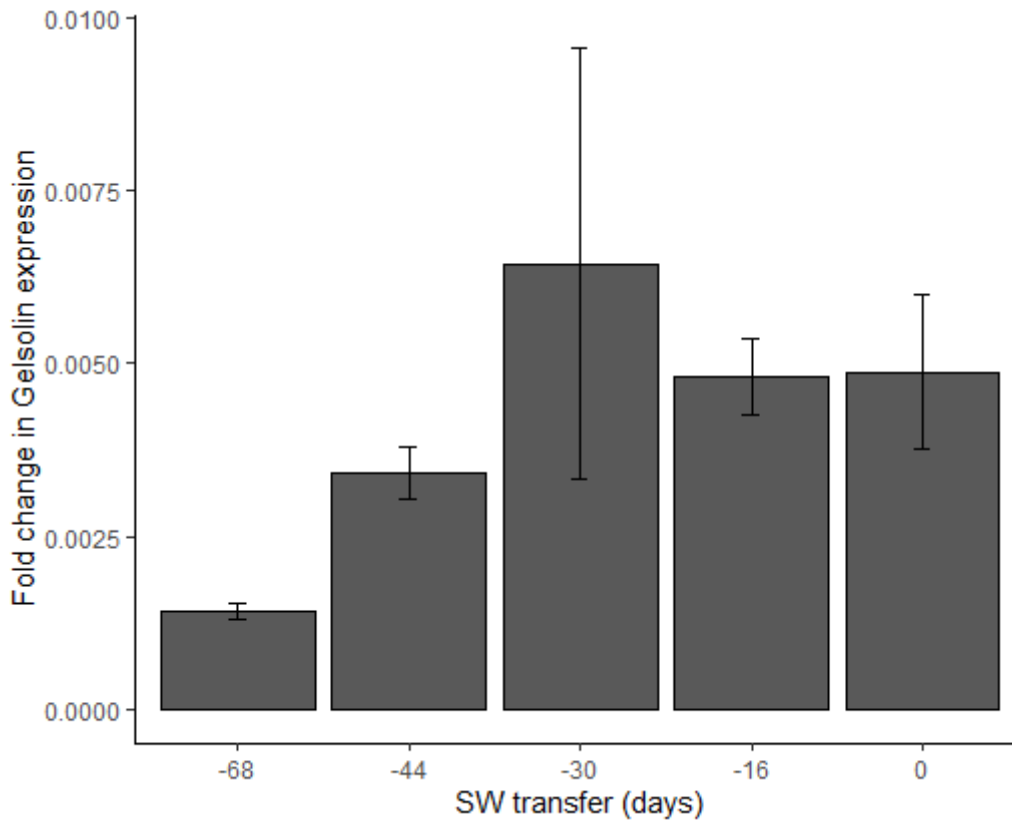


Figure 5.24. Expression of *Gelsolin* mRNA relative to *RPLP0* in Atlantic salmon gill on a FW time course. Error bars represent standard error (n=3).

The expression of *ZG16* was found to be significantly affected by time point leading up to smoltification in FW ( $F_{4,10} = 8.10$ ,  $p = 0.004$ ), Figure 5.25A. The level of the *ZG16* expression was significantly higher 0 days before the date of SW transfer than at 68 ( $p = 0.03$ ), 44 ( $p = 0.01$ ) and 16 ( $p = 0.002$ ) days before SW transfer. *ZG16* was not found to be significantly affected by time point in the SW challenge trial ( $F_{3,19} = 1.31$ ,  $p = 0.3$ ), Figure 5.25B.

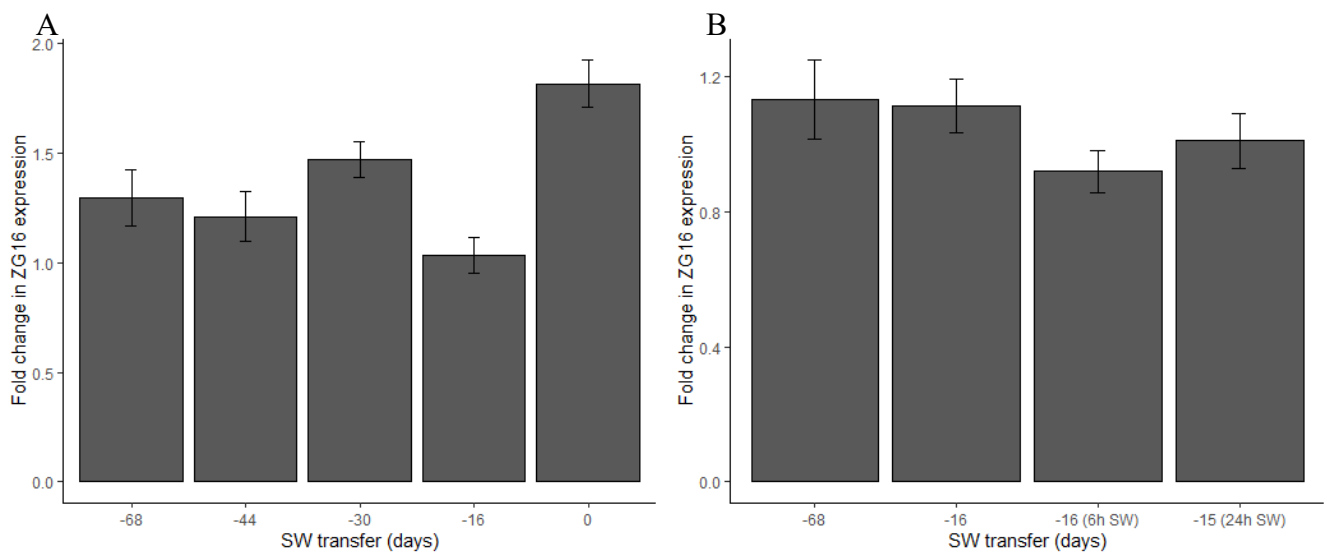


Figure 5.25. Expression of *ZG16* mRNA relative to *RPLP0* in Atlantic salmon gill on a FW time course (A) and in fish exposed to SW challenge (B). Error bars represent standard error ( $n=3$  in A,  $n=5$  or  $6$  in B).

The expression of *tristetrapolin 1* (*TTP1*:  $F_{3,19} = 1.49$ ,  $p = 0.25$ , Figure 5.26A) and 2 (*TTP2*:  $F_{3,19} = 2.46$ ,  $p = 0.094$ , Figure 5.26B) were not found to be significantly affected by time point in the SW challenge trial.

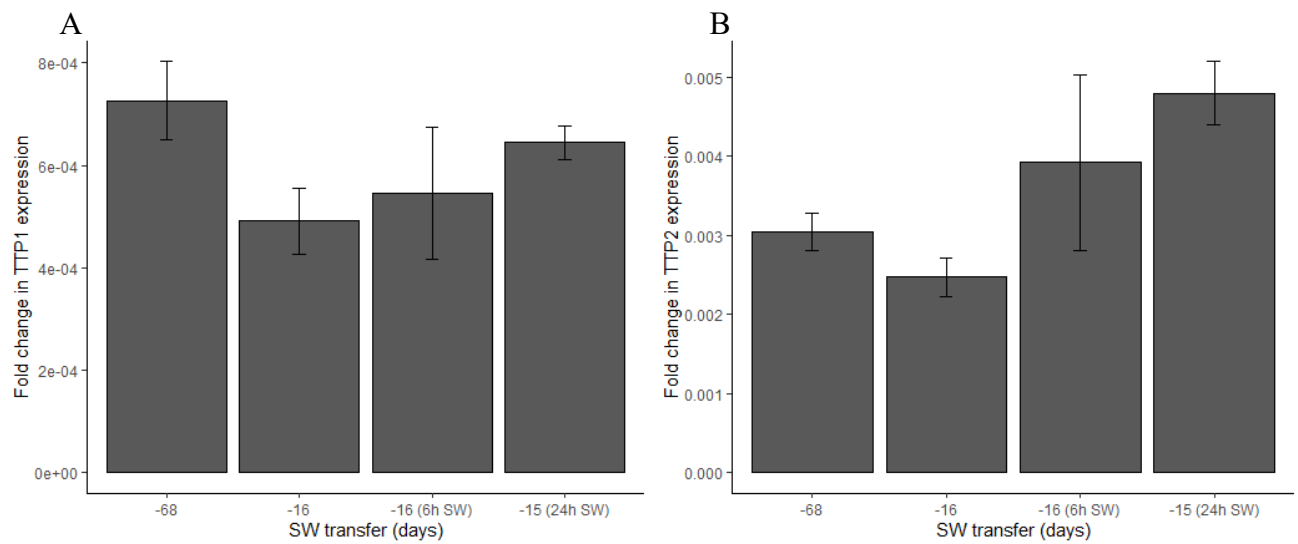


Figure 5.26. Expression of *TTP1* (A) and *TTP2* (B) mRNA relative to *RPLP0* in Atlantic salmon gill in fish exposed to SW challenge. Error bars represent standard error (n=5 or 6).

The expression of the annexins investigated was not found to be significantly affected by time point as salmon progressed towards smoltification in FW (Figure 5.27). *AnnA1*, Figure 5.27A,  $F_{4,10}=0.79$ ,  $p=0.56$ ; *AnnA2*, Figure 5.27B,  $F_{4,10}=3.30$ ,  $p=0.057$ ; *AnnA3*, Figure 5.27C,  $F_{4,10}=0.76$ ,  $p=0.58$ ; *AnnA6b*, Figure 5.27D,  $F_{4,10}=1.91$ ,  $p=0.19$ .

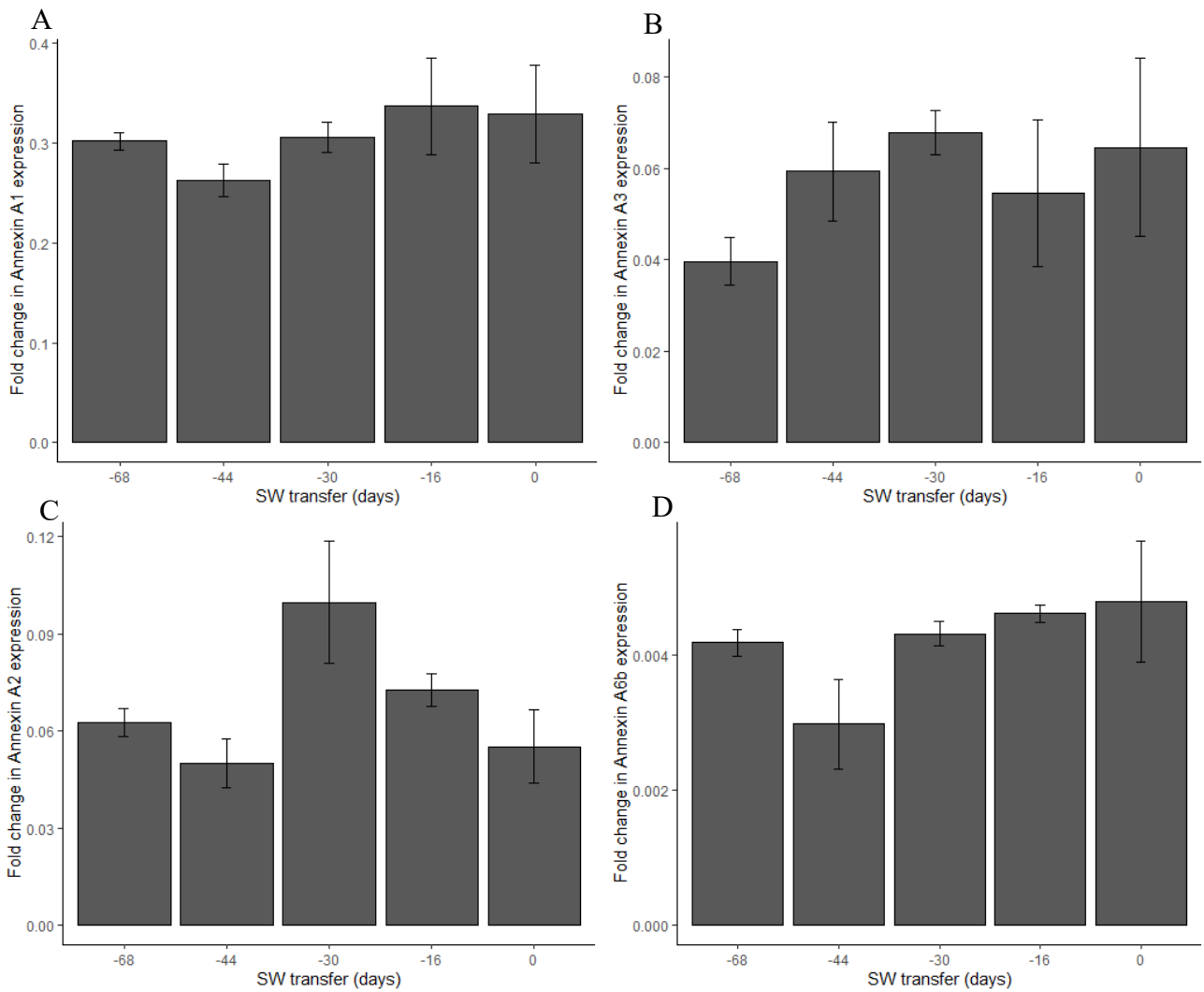


Figure 5.27. Expression of *AnnA1* (A), *AnnA2* (B), *AnnA3* (C) and *AnnA6b* (D) mRNA relative to *RPLP0* in Atlantic salmon gill on a FW time course. Error bars represent standard error (n=3).

### 5.2.4.1 Uncharacterised protein 584

An uncharacterised protein (Accession number XP\_014058600.1) designated UP584 was identified by SWATH as being up-regulated during the parr/smolt transformation in Atlantic salmon. BLAST searches failed to identify additional paralogues in the Atlantic salmon although homologues were identified in a number of other teleosts (Clustal O multiple sequence alignment below). The nucleotide sequence of this gene also exhibits high similarity with the 3' untranslated region of a gamma amino butyric acid receptor found in various salmonids. There is no significant similarity with any mammalian genes. The amino acid alignment of the sequence of the unknown protein in a number of teleost species is given below in Clustal O multiple sequence alignment.

CLUSTAL O multiple sequence alignment for the amino acid sequence of unknown protein 584 in the teleost species channel catfish (*Ictalurus punctatus*, XM\_017464418.1), Atlantic salmon (*Salmo salar*, XM\_014201850.1), Atlantic herring (*Clupea harengus*, XM\_012827895.1), common carp (*Cyprinus carpio*, XM\_019111548.1) and zebrafish (*Danio rerio*, XM\_005158186.3).

Channel catfish	-MITTNALGV-FVFITALIVTEGSWGSKGKNSYNYDLSRMSDLRKLKLYNSKVYRAERMTRP
Atlantic salmon	MFSIRTAFILPALLALLVVHVESFSGGGGGSYNYDISKMSDLRKLKLYNSKVYEAADRMRRP
Atlantic herring	MFSFKAATL-AVLAMLVVAHCGFGEG-TNSYNYDLSKMSDLRKLKLYNSKVYLCDRMTRP
Common carp	MMSFKTALGL-LLLAMVVMVAESEWGSKDGNSYSYDLSKMSDLRKLKLYNSKVYFAERMTRP
Zebrafish	MMSFKTALAL-LLLAMF SMVAESSWGNKGKNSYNYDLSKMSDLRKLKLYNSKVYFAERMTRP
Channel catfish	LEGLKVQAGILSHSGVRVTLADGTTWLVHKGDGFGISSQTVVVDARHMSRHVKVREVKNF
Atlantic salmon	LEGMTFQVVGILSHSGVRVTLADGSQWLVLHKGDGFGISTQTVVVAARHMSQDWKKVETKNE
Atlantic herring	LSGMSIQIGKLSHSGVRVTLADGTTWLVHKGDGFGISSQTVVVHARHMSNTWKIIVETKDF
Common carp	LKGVTFQVVGKLSHSGVRVTLADGTTWLVHKGDGFGISSQTVVVAARHMSNTWTIVETKDF
Zebrafish	LEGMSFQVGVLSHSGVRVTLADGTTWLVHKGDGFGISSQTVVVAARHMSNTWKIIVETKNE
Channel catfish	AGAKTVSDFVKAGGTDYSLLFNCHTAAGRMMDD
Atlantic salmon	RGSKTVSDFVKAGGTDYSLIFDNCHDAAGRME-
Atlantic herring	GGSKTVSDFVKAGGTDYSLIFDNCHDASGRMMGG
Common carp	RGSKTVSDFVKAGGTDYRLLFDNCHDAADRMMEG
Zebrafish	GGSKTVSDFVKAGGTDYKLLFDNCHDAANRMMGG

The expression of mRNA for this gene was investigated in the gill of parr and smolts from the Marine Harvest facility at Loch Lochy sampled Aug-Oct 2016.

Over the time course in FW as fish progressed towards SW transfer no significant effect of time was observed on the expression of *UP584* ( $F_{4,10} = 2.73$ ,  $p = 0.09$ ).

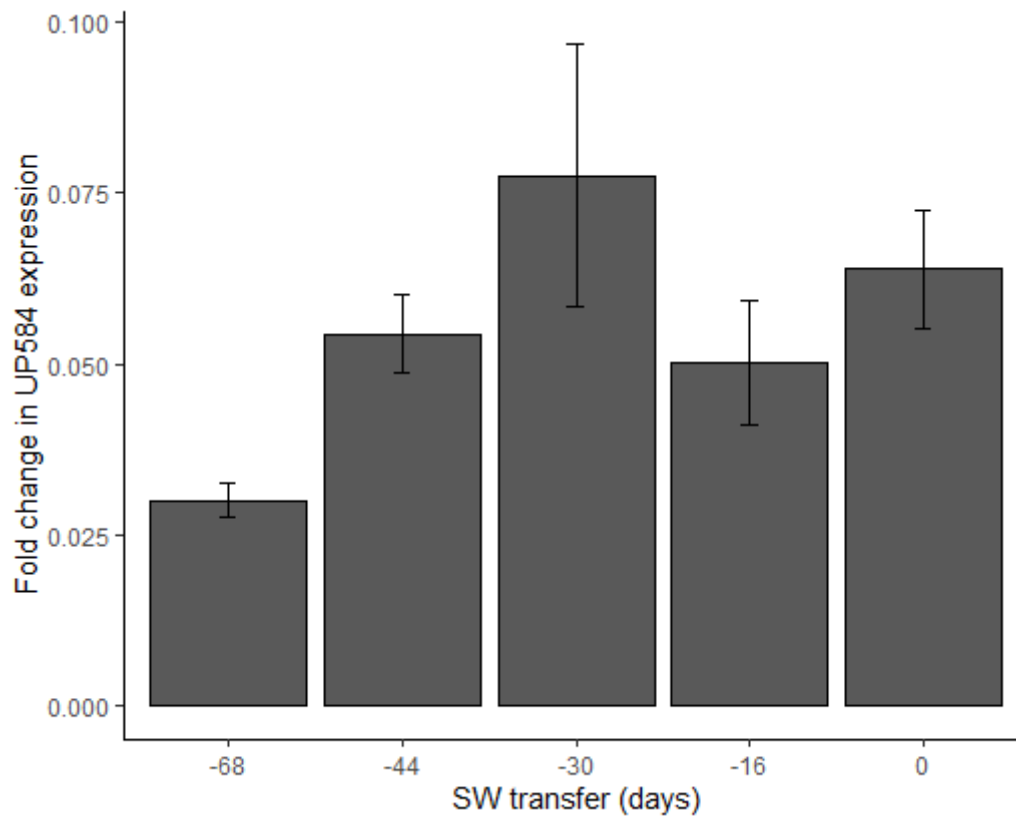


Figure 5.28. Expression of *UP584* mRNA relative to *RPLP0* in Atlantic salmon gill on a FW time course. Error bars represent standard error (n=3).

### 5.3 Discussion

Fish must maintain the osmolality within their cells at approximately 300-330 mOsm/kg to avoid damage to cell structure, and detrimental effects on biologically important macromolecules. The gill is a major site of ion transport, taking up ions in freshwater, and excreting them in seawater.  $\text{Na}^+\text{-K}^+\text{-ATPase}$  plays an important role in the transport of ions across the gill in both the freshwater and seawater environment. Increased  $\text{Na}^+\text{-K}^+\text{-ATPase}$  enzyme activity in the spring has been observed to be associated with increased ability to regulate plasma  $\text{Cl}^-$  (Robertson & McCormick, 2012). Therefore,  $\text{Na}^+\text{-K}^+\text{-ATPase}$  enzyme activity as an indicator of smolt hypo-osmoregulatory ability, has long been used as a biomarker of smoltification (Robertson & McCormick, 2012; Seidelin *et al.*, 2001). The important role played by this enzyme is demonstrated by the finding of Silva *et al.* (1977) that the hypo-osmoregulatory ability of seawater eels is reduced by ouabain inhibition of  $\text{Na}^+\text{-K}^+\text{-ATPase}$ .

#### 5.3.1 $\text{Na}^+\text{-K}^+\text{-ATPase}$ $\alpha$ -subunits

It has been widely reported that during smoltification there is an increase in activity of the  $\text{Na}^+\text{-K}^+\text{-ATPase}$ , prior to SW entry (Nilsen *et al.*, 2007; Stefansson *et al.*, 2008). Nilsen *et al.* (2007) found that mRNA levels of  $\text{Na}^+\text{-K}^+\text{-ATPase}$   $\alpha 1a$  were reduced in the gill of smolts in the months leading up to SW transfer, while over the same time the mRNA levels of the  $\alpha 1b$  paralogue increased. McCormick *et al.* (2013) showed that, in the natural environment, the protein level of the  $\alpha$ -subunit paralogue  $\alpha 1a$  was lower in smolts than in parr during the spring. Also during this period of smoltification McCormick *et al.* (2013) observed that levels of  $\alpha 1b$  protein were higher in smolts than in parr, and increased as fish prepared for the downstream migration to seawater.

In contrast to reports that mRNA expression of  $Na^+K^+ATPase \alpha1a$  subunit decreased and that the  $\alpha1b$  subunit increased in the gill of Atlantic salmon prior to movement to seawater, an initial investigation of  $Na^+K^+ATPase \alpha$ -subunit paralogue switching in this study found no change in  $\alpha1a$  mRNA expression before transfer to seawater. A fall was observed after 24 hours in seawater (Figure 5.2), however, the difference from FW levels was not found to be statistically significant until fish had spent 12 weeks in SW. It is possible that this is in part due lower statistical power of non-parametric test as the data were not normally distributed. Likewise, the expression of mRNA for  $\alpha1b$  subunit was only found to change following seawater transfer in this time course, however, in this case the change was found to be statistically significant after only 6 hours in SW (Figure 5.2). Levels were then observed to fall in adults back to levels similar to those seen in FW.

A further study of the  $Na^+K^+ATPase \alpha$ -subunit paralogue switching was carried out over a more comprehensive time course as detailed in the Material and Methods Section 2.5.3.

In this separate study (Figure 5.3) a fall in mRNA expression of the  $\alpha1a$  paralogue was observed in the gill of salmon prior to SW transfer, however, this was not statistically significant as levels in FW showed a high level of variability over the time course. There was a further drop following SW transfer which was statistically significant after 48 hours in SW.

Expression of the  $\alpha1b$  paralogue in this time course was also variable in FW. Following SW transfer expression was significantly higher than the lowest level seen in FW, but not significantly different from levels at other time points in FW.

In the gill of salmon sampled over the same time course, a fall in the protein level of  $Na^+K^+ATPase \alpha1a$  was observed following SW transfer. The Western blot results for  $Na^+K^+ATPase \alpha1a$  showed multiple immunoreactive bands rather than the single band reported by

McCormick *et al.* (2009). The expected size of the Na<sup>+</sup>-K<sup>+</sup>-ATPase  $\alpha$ 1a protein was 110 kDa, and McCormick *et al.* (2009) reported a band between 90-95kDa. The band at 95 kDa was assumed to represent the Na<sup>+</sup>-K<sup>+</sup>-ATPase  $\alpha$ 1a band observed by Dr McCormick.

This result is in agreement with the findings of McCormick *et al.* (2013), who showed that the protein abundance of the  $\alpha$ 1a paralogue fell upon entry to seawater. In the same samples, an increase in Na<sup>+</sup>-K<sup>+</sup>-ATPase  $\alpha$ 1b protein levels was observed prior to transfer to seawater, with a further increase following entry to seawater (Figure 5.7). Again these results are supported by those of McCormick *et al.* (2013). These results support the assertion that paralogue switching of the Na<sup>+</sup>-K<sup>+</sup>-ATPase  $\alpha$ -subunit occurs at least at the level of the protein, during the smoltification process. Therefore, it is likely that the *alpha*1a paralogue is involved in the uptake of ions across the gill in freshwater, while the *alpha*1b paralogue drives the branchial secretion of ions in seawater. Indeed, structural differences in these paralogues related to these different functions have been identified (Colina *et al.*, 2007). Differences in the Na<sup>+</sup>-K<sup>+</sup>-ATPase amino acid sequence of squid from that of terrestrial mammals results in differences in the electrostatics of the portion of the pump which interacts with Na<sup>+</sup> ions, allowing the efficient transport of ions under conditions of high extracellular Na<sup>+</sup> concentrations (Colina *et al.*, 2007).

The difference in the expression of the Na<sup>+</sup>-K<sup>+</sup>-ATPase  $\alpha$ -subunit paralogues on the two time courses in this project suggest that the change in  $\alpha$ -subunit paralogue expression may not represent a robust biomarker of smoltification. Both sampling time courses were conducted in the winter, with smoltification artificially triggered through photoperiod manipulation. As the expression of these paralogous genes did not change before seawater transfer on the first time course, monitoring the expression of these genes using RT-qPCR would not be useful as a biomarker of smoltification. The results of the second trial showed a trend similar to that

reported by other authors (McCormick *et al.*, 2013; Nilsen *et al.*, 2007), however, changes were not statistically significant in this study. It seems likely that changes in  $Na^+-K^+-ATPase$   $\alpha$ -subunit paralogue expression is not a robust biomarker of smoltification in all circumstances. Protein levels were observed to change following SW transfer as reported by McCormick *et al.* (2013), however, as these changes occurred following SW transfer this does not represent a useful biomarker of smoltification in FW.

### 5.3.2 $Na^+-K^+-ATPase$ $\beta$ -subunit

The  $\beta$ -subunit of  $Na^+K^+-ATPase$  is important in the stabilisation, location and transport of newly synthesised alpha subunits to the plasma membrane (Blanco & Mercer, 1998; Sundh *et al.*, 2014). Several paralogues of the  $\beta$ -subunit of  $Na^+-K^+-ATPase$  were investigated as possible biomarkers in the gill of Atlantic salmon. No difference in the expression of *NKA*  $\beta2ab$ ,  $\beta2c$ ,  $\beta3b$ , or  $\beta4$  was observed over the time course investigated. Expression of  $\beta3c$  was found to be significantly higher at the first time point than at later time points closer to that date of SW transfer (Figure 5.9). However, as the level of *NKA*  $\beta3c$  was not found to change between time points close to the date of smolt transfer to SW, it is likely that this would not represent a useful biomarker, as the change in expression happens too early to be a useful predictor of SW readiness.

### 5.3.3 Other osmoregulatory genes

A number of ion channels and transporters are involved in the secretion of ions across the gill in seawater. As outlined in Figure 5.1, the  $Na^+$  electrochemical gradient produced by  $Na^+-K^+-ATPase$  allows the uptake of  $Na^+$ ,  $K^+$ , and  $Cl^-$  ions through the NKCC ion transporter.  $Cl^-$  ions then leave the cell *via* CFTR  $Cl^-$  channels, and  $Na^+$  ions escape through leaky tight junctions. The expression of *NKCC1* was found to increase in pre-smolts following SW

challenge, however, the increase seen in Figure 5.10A in FW was not found to be statistically significant. These results are not in line with findings of Nilsen *et al.* (2007), who reported that in wild anadromous Atlantic salmon there was an increase in *NKCC* expression in the gill, accompanied by an increase in protein levels, between February and May, the period of natural smoltification. This increase in gill *NKCC* plays a role in the increased hypo-osmoregulatory ability of smolts. Therefore, it is possible that while monitoring *NKCC* expression could be useful in gaining a more holistic view of ion transport in the gill, this gene alone would not represent a reliable biomarker of smoltification.

*CFTR* expression was not found to be significantly affected by SW challenge in pre-smolts, although the level of *CFTR* expression in the gill was found to be significantly higher in FW the day of SW transfer than in all the preceding time points (Figure 5.11A). Nilsen *et al.* (2007) similarly reported that *CFTR1* expression in the gill increased during the period of smoltification in spring. While this gene plays an important role in osmoregulation, and the findings of this study indicate that it may be beneficial as a biomarker of smoltification, further work is required in the period immediately prior to transfer to determine whether there is sufficient increase, sufficiently early to be useful.

*Ca<sup>2+</sup>-ATPase* expression was not found to change in the gill over the FW smoltification time course studied.

#### 5.3.4 Lipid metabolism genes

As there is a change in the metabolism of body lipids during smoltification, leading to a reduction in condition factor (Stefansson *et al.*, 2008), a number of genes related to lipid metabolism were investigated. The level of *LDLR* expression was lower in smolts before SW transfer than in parr, however, this difference was not statistically significant. The expression

if the genes *ApoA1*, *ApoA1b* and *ApoA4* were all found not to differ significantly over the time course studies leading up to smoltification. However, it may be of note that the expression of all of these genes showed much greater variability at the time point 30 days prior to SW transfer. Four days prior to this the study population were switched from a natural photo period to 24-hour light. This is used to stimulate smoltification outside the natural seasonal period of smoltification, however, it is possible that this photoperiod manipulation may have unknown effects on metabolism of farmed populations. The expression of *ApoB100* was also found not to be significantly affected by time as salmon progressed towards smoltification, however, this gene did not show the high level of variability in expression seen in the *ApoA* genes at the 30 days to transfer time point. In this study these genes were investigated in the gill, as this tissue is already used routinely in the industry to determine Na<sup>+</sup>K<sup>+</sup>-ATPase enzyme activity levels, however, genes associated with lipid metabolism, particularly apolipoproteins, are primarily expressed in the liver. It would be of interest to investigate the changes in the expression of these genes in the liver as salmon undergo the complex metabolic changes associated with smoltification.

Carnitine palmitoyltransferase 2 (CPT2), a mitochondrial membrane protein, is involved in fatty acid oxidation in the mitochondria. Deficiency in CPT2 in humans exists in a number of forms ranging in severity. The “adult” form of the disease results in recurrent episodes of muscle damage, usually triggered by prolonged exercise, some medications or stressors such as infection, (Bonfont *et al.*, 2004). Affected individuals are clinically normal between attacks. More severe forms of the deficiency cause prenatal cardiac, renal and neural abnormalities, leading to early neonatal death (Bonfont *et al.*, 2004). In a mammalian model, supplementation with  $\omega$ -3 fatty acids leads to a lowering of plasma very low density lipoprotein (VLDL) levels (Willumsen *et al.*, 1997). Increased  $\beta$ -oxidation of fatty acids results in a reduction in triglyceride production resulting in reduced hepatic VLDL

production (Willumsen *et al.*, 1993). This effect is strongly correlated with increased activity of CPT2 (Surette *et al.*, 1992). Teleosts are hyperlipidaemic compared with mammals (Babin & Vernier, 1989). Lipids are an important energy source, with carnivorous fish relying on almost no dietary carbohydrate. *CPT2* expression was higher in smolts immediately before SW transfer than in parr, however, this difference was not statistically significant. This is unlikely to be a useful biomarker of smoltification.

### 5.3.5 Immune genes

Smoltification in the aquaculture setting poses problems associated with the immune system. During the 6 months following seawater transfer, fish are particularly susceptible to infectious disease (Johansson *et al.*, 2016; Stefansson *et al.*, 2008). It is possible that the impairment of the immune system seen in smolts and post-smolts may be due to increased levels of circulating cortisol (Eggset *et al.*, 1997), however, as this increased disease susceptibility is not observed in wild populations, this effect may be due to artificial rearing conditions (Stefansson *et al.*, 2008). The majority of pathogenic bacteria are opportunistic, and only produce pathological effects in individuals which are immunocompromised (Hansen & Olafsen, 1999). The gill, as well as being the organ of gas exchange and ionic regulation (Evans *et al.*, 2005), has been identified as an important site in primary entry of infectious agents (dos Santos *et al.*, 2001).

Very high numbers of antibody secreting cells have been found in the gill of sea bass (*Dicentrarchus labrax*) (dos Santos *et al.*, 2001). Immunisation by immersion, has been shown to be more effective in promoting gill antibody production than intraperitoneal injection, producing more effective protective responses to immersion challenge with infectious agents (Lumsden *et al.*, 1995, 1993). The gill has also been shown to produce many agents such as lysozymes and immunoglobulins involved in the innate immune

response (Rebl *et al.*, 2014). Therefore, the gill can be said to be an important organ in the defence of animals against infection. The expression of a number of genes associated with both the innate and adaptive immune systems were investigated in the gill as fish developed from parr to smolts.

The polymeric immunoglobulin receptor (pIgR), responsible for the transport of secretory immunoglobulins to mucosal epithelia, is important in these tissues. As the mucosal layer on the skin, gut, and gill is important as a barrier between body tissue and the external environment, these tissues represent the first line of defence against the initial entry of pathogens (Tadiso *et al.*, 2011). Expression of *pIgR* was not observed to change as parr developed into pre-smolts, nor was any change observed when pre-smolts were subjected to seawater challenge (Figure 5.16). This gene would not be useful as a biomarker of smoltification. Tadiso *et al.* (2011) reported one *polymeric immunoglobulin receptor like* transcript (*pIgRL*) along with salmon *pIgR*, identified as having a more highly conserved sequence relative to that of other teleosts. Expression of *pIgR* and *pIgRL* has been identified in a number of mucosal epithelia, including the skin and gill, with *pIgRL* expressed in the gill at higher levels than *pIgR* (Tadiso *et al.*, 2011). Two *polymeric immunoglobulin receptor-like* transcripts were identified in the NCBI GenBank database. No statistically significant change in *pIgRL1* expression was observed in FW as salmon progressed towards smoltification, however, the level of *pIgRL1* expression was found to increase significantly in pre-smolts after 24 hours of SW challenge (Figure 5.17B). The expression of *polymeric immunoglobulin receptor-like transcript 2* (*pIgRL2*) was significantly lower in pre-smolts following 24 hours of SW challenge than in FW. This gene was not investigated over the full time course in FW, it would be useful to determine whether the level of *pIgRL2* expression fell prior to the date of SW transfer. These genes would not make useful biomarkers of

smoltification. It is possible that their expression may change after exposure to SW due to the effects of stress hormones such as cortisol on the immune system.

The inhibitory receptor CMRF 35-like molecule 8 (CLM8) is a member of the immunoglobulin super family involved in the innate immune system and is structurally similar to pIgR (Tadiso *et al.*, 2011). CLM8 has a role in regulating the responses of monocytes and dendritic cells, preventing chronic inflammation (Clark *et al.*, 2009). The expression of *CLM8* did not vary between parr and pre-smolts, and the expression of *CLM8* in pre-smolts was not altered by seawater challenge up to 24 hours (Figure 5.19). It is unlikely that this gene would be useful as a biomarker of smoltification. *CLM8* expression has previously been identified in the gill, though at lower levels than *pIgR* and *pIgRL* (Tadiso *et al.*, 2011).

An immunoglobulin light chain (IgK) and heavy chain (IgD) were also investigated in the gill. Immunoglobulin Kappa (IgK) has been identified as one of the major light chain immunoglobulins in teleost fish (Mashoof & Criscitiello, 2016). The expression of *IgK* was significantly higher shortly before SW transfer than at the start of the time course. However, throughout the time course the level of *IgK* was fairly variable (Figure 5.20A). It is possible that the drop in *IgK* expression at the 30 days pre SW transfer time point was related to the change in photoperiod, in which case there may be a gradual increase in *IgK* expression. Immunoglobulin D (IgD) was originally believed to be present only in higher vertebrates, as it was found to be absent in avian species (Ramirez-Gomez *et al.*, 2017). Following the discovery of IgD in the channel catfish (*Ictalurus punctatus*) (Wilson *et al.*, 1997), further investigation of this immunoglobulin has led to its identification in a number of other teleost species, and IgD is now considered to be an ancestral immunoglobulin, present in the vertebrate ancestors of both teleosts and mammals (Ramirez-Gomez *et al.*, 2017; Wilson *et*

*al.*, 1997). *IgD* expression was lower in smolts than in parr (Figure 5.20B), however, this difference was not statistically significant. These genes do not represent reliable biomarkers of smoltification. Although *IgK* was expressed at a higher level in smolts, the variability of this gene over the time course suggests that this would be unreliable.

Two transcription factors, the aryl hydrocarbon receptor 1 (AHR1) and the X-box binding protein 1 (XBP1), associated with the activation of a suite of stress induced genes, were investigated in the gill. The aryl hydrocarbon receptor is a transcription factor responsible for the toxic responses produced following exposure to environmental pollutants (Hansson *et al.*, 2004; Poland & Knutson, 1982). The primers used to amplify *AHR1* were common to both *AHR1 $\alpha$*  and  *$\beta$* , two of six aryl hydrocarbon receptors found in the salmonid genome (Hansson & Hahn, 2008). It has been reported that the two *AHR1* paralogues are expressed at a lower level than the four *AHR2* forms (Hansson *et al.*, 2004). *AHR1* expression did not change as parr developed from parr to pre-smolts. Following seawater challenge there was no change in the expression of *AHR1* mRNA. This gene would not be useful as a biomarker of smoltification.

X-box binding protein 1 (XBP1) is important in the unfolded protein response, which is caused by endoplasmic reticulum (ER) stress (Hollien, 2013). ER stress is caused by an increase in the level of unfolded proteins in the ER. The signalling pathways for the unfolded protein response found in mammals have been shown to be conserved in the medaka (*Oryzias latipes*), a euryhaline teleost. No difference between parr and pre-smolts was detected, and no effect of SW challenge was observed. This gene does not represent a useful biomarker of smoltification.

As part of the innate immune response, cytokines are released that attract neutrophils to infection sites which attack infectious agents by releasing a number of antimicrobial agents

(Havixbeck & Barreda, 2015). Leukocyte elastase inhibitor (LEI) protects neutrophils from protease inhibitors which are released as part of the stress response at sites of infection. *LEI* expression was higher in pre-smolts and smolts than in parr (Figure 5.23). However, as levels in smolts did not differ from those in pre-smolts, this gene would not be a reliable biomarker of smoltification. Furthermore, as seen in other genes, there may have been an effect of the change of lighting regime on the expression of *LEI*, as expression appears to have increased at the 30 days pre SW transfer time point, although it was not statistically significantly higher than at other time points studied.

While some differences were detected in the mRNA expression of immune genes as fish developed from parr into smolts, using these genes as biomarkers may be unreliable. Fish growing in an aquaculture system which is open to the surrounding environment are at risk of infectious bacterial, viral and fungal diseases derived from the environment. It is possible that developmental changes in immune gene expression related to smoltification could be masked by upregulation of the immune response during infection events. It is possible that upregulation of genes related to the infection could be mistaken for an indicator of smoltification. Therefore, it is possible that using immune genes as biomarkers would not prove a robust method for determining whether fish are ready for transfer to seawater, however, these genes may prove useful in a whole system style of smolt determination, using a large suite of genes as indicators of smoltification.

#### *5.3.6 Other Biomarker Candidates*

Gelsolin is a calcium dependent regulator of actin filaments, mediating the remodelling of this part of the cytoskeleton (Sun *et al.*, 1999). Actin filaments are important in cell volume maintenance, with a number of different volume regulated transport proteins interacting with the cytoskeleton (Pedersen *et al.*, 2001). A number of ion channels, including epithelial Na<sup>+</sup>

channels and CFTR have been shown to be associated with actin filaments, and regulation of these transporters by actin has been linked to the formation of short actin filaments (Cantiello & Prat, 1996; Pedersen *et al.*, 2001). Gelsolin severing of actin filaments produces an increased number of short actin filaments which can then elongate following uncapping of gelsolin, allowing cytoskeleton remodelling (Sun *et al.*, 1999; Yin & Stull, 1999). Although there was a slight increase in *gelsolin* expression in smolts relative to parr, this difference was not statistically significant. There was also an increase in variability in the level of *gelsolin* expression at the 30 days to transfer time point, shortly after the change in photoperiod. *Gelsolin* expression would not represent a useful biomarker of smoltification.

Zymogen granule protein 16 (ZG16) is a secretory lectin the production of which, in mammals, has been identified in mucosal cells of the intestine. This protein has been shown to recognise and bind to fungal polyvalent mannose, forming an important part of the defence against pathogen invasion (Tateno *et al.*, 2012). Tateno *et al.* (2012) found that rat ZG16 bound to pathogenic fungi found in the digestive tract. As the gill is a mucosal tissue containing goblet cells similar to those in the intestine (Fletcher *et al.*, 1976), the expression of *ZG16* was investigated during the period of smoltification as a possible biomarker. *ZG16* expression was not significantly affected by SW challenge in pre-smolts (Figure 5.25B), however, levels were higher in FW smolts shortly before SW transfer than in earlier time points (Figure 5.25A). The expression of this gene was slightly higher at the 30 days to SW transfer time point. This is another gene which should be considered as possibly affected by the change in photoperiod. It is possible that this gene could be used in concert with other genes as part of a whole system approach to smolt assessment, however, alone this would not be a useful biomarker for smoltification.

Tristetraprolin (TTP) is involved in the destabilisation of cytokine mRNA, particularly that of TNF $\alpha$  produced as part of the inflammatory response (Carballo *et al.*, 1998). This effect is produced by the TTP binding to the AU-rich element of the RNA. TTP deficient mice develop serious problems associated with increased inflammation, including inflammatory arthritis and autoimmune pathologies (Carballo *et al.*, 1998). These symptoms are caused by elevated levels of TNF $\alpha$ . As there are immune compromising effects associated with smoltification, the expression of two TTP paralogues was investigated in the gill. Neither the expression of *TTP1* nor *TTP2* was found to differ between parr and pre-smolts (Figure 5.26). No effect of SW challenge was observed on the expression of these genes. It is unlikely that these tristetraprolins would prove useful as biomarkers of smoltification.

The annexins, also known as lipocortins, comprise a group of proteins which exhibit calcium dependent binding to phospholipids, and have a role in the innate immune response (Einarsson *et al.*, 2016; Rescher & Gerke, 2004). These proteins are characterised by the presence of a conserved sequence of 70 amino acids repeated four or eight times in different members of the group (Gerke & Moss, 1997). This “annexin domain” is considered to form a membrane binding module within the protein (Gerke & Moss, 2002). Although this “annexin repeat” is conserved, each member of the group possess a different N-terminus, thought to be responsible for the specific activity of the different members of the group (Gerke and Moss, 1997; Walther *et al.*, 2000). As multiple forms of this protein are co-expressed within the same cell types, it is suggested that these different members of the annexin group have different biological roles (Walther *et al.*, 2000). These roles and the mode of action are yet to be fully elucidated (Gerke & Moss, 2002, 1997; Walther *et al.*, 2000).

A number of different roles have been proposed for annexins, most of which are related to membrane function, including regulation of membrane organisation, traffic, cytoskeleton

interactions, and transmembrane ion conductance (Gerke and Moss, 2002, 1997). In humans, it has been found that the anti-inflammatory effects of glucocorticoids are mediated by annexin 1 (Walther *et al.*, 2000). There is a non-specific effect on inflammation, involving inhibition of phospholipase A<sub>2</sub>, the first enzyme in eicosanoid metabolism, resulting in a reduction in arachidonic acid production (Walther *et al.*, 2000). Annexin A1 has also been found to specifically inhibit trans-endothelial migration of neutrophils through interactions with formyl peptide receptors (Rescher & Gerke, 2004; Walther *et al.*, 2000). As these receptors are not restricted to leukocytes, it is possible that Annexin A1 may influence the migratory behaviour of other cells which express formyl peptide receptors in a range of tissues, including hepatocytes, dendritic cells, and alveolar type II cells (McCoy *et al.*, 1995; Rescher *et al.*, 2002; Sozzani *et al.*, 1998).

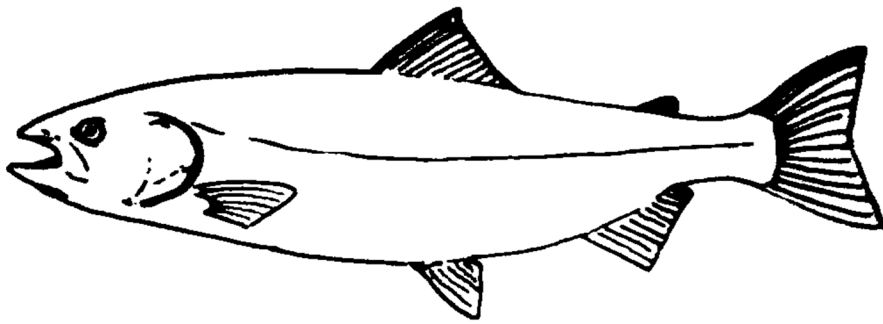
Annexins have been implicated in membrane-cytoskeleton interactions, particularly in Ca<sup>2+</sup> regulated exocytosis, though other functions have been proposed for some annexins (Gerke & Moss, 2002). Annexin A2, an actin filament binding protein, is associated with sites of actin membrane attachment (Rescher & Gerke, 2004). This may be important in osmosensing as cytoskeleton strain is thought to be a major contributor to intracellular osmosensing (Kultz, 2012).

The expression of the *annexins* investigated did not appear to be affected by the process of smoltification, with annexins *A1-3* and *6b* all showing similar expression in freshwater smolts as was seen in parr. It is thus unlikely that these genes would prove useful as biomarkers of smoltification. The increased expression of annexins *A2* and *A3* at the 30 days to SW transfer time point may be linked to the change in photoperiod the fish were exposed to at four days earlier when a 24-hour lighting regime began, to trigger smoltification.

The expression of the uncharacterised gene *UP584* was not found to change over the time course in FW as salmon developed from parr to smolts. An increase in variability was observed at the time point 30 days before SW transfer, suggesting that this gene may also be influenced by the change in photoperiod.

In conclusion, of the biomarkers investigated in this study, the mRNA expression of the ion channels *NKCC1* and *CFTR* represent the most reliable biomarkers of smoltification. There was a large increase in the expression of these genes prior to seawater transfer. These ion transporters are important in the acclimation of smolts to seawater due to their role in ion secretion, particularly across the gill. The mRNA expression of a number of immune genes did differ in the gill between parr and smolts. However, as fish reared in farms exposed to the external environment are at risk of exposure to pathogens present in the environment, the expression of immune genes may be unreliable as a biomarker since the expression of these genes is likely to change in response to infections. It appears that ion channels still represent the most useful biomarkers of smoltification in Atlantic salmon.





# Discussion



## 6. Discussion

The anadromous life cycle of Atlantic salmon creates complex challenges in the farming of this species. Smoltification is a complex process requiring the synchronisation of a number of physiological processes which in nature is triggered by environmental stimuli including photoperiod and temperature. In an aquaculture setting the environmental cues fish are exposed to can be artificially altered, which has allowed the production of “off season” fish. Smolts can be produced year round, primarily through photoperiod manipulation. While this brings financial benefits to the industry it also poses potential problems. The natural timing of smoltification has been selected as the optimal time for young fish to migrate to the marine environment, likely due to the availability of prey species and beneficial environmental conditions. While food availability is not a problem faced by fish growing in an aquaculture environment, they may be more likely to be faced with undesirable environmental conditions as fish in static aquaculture fixtures cannot move to more favourable areas when subjected to such conditions. An example of this is the algal blooms seen in the North Atlantic during the summer of 2019 which have killed large numbers of farmed salmon in parts of Norway (Norwegian Directorate of Fisheries, Fiskeridirektoratet, 2019).

### *6.1 Organic osmolytes*

Adaptation to the marine environment requires organisms to maintain the osmoregulatory balance within their tissues, resisting osmotic shrinkage as water diffuses out into the hypoosmotic medium around them. In euryhaline species this process is more complex as organisms are required to switch from adaptations enabling them to osmoregulate in FW to those which allow them to survive in SW. Organic osmolytes are involved in the long term acclimation of cells to high salinity. The permeability of the plasma membrane to water leads

to a challenge when cells are exposed to changes in extracellular osmolarity. The volume regulatory increase, which occurs following cellular dehydration caused by increased extracellular salinity, is mediated by the accumulation of inorganic ions inside the cell and allows a rapid response to decreases in cell volume (Wehner *et al.*, 2003). However, sustaining high levels of intracellular inorganic ions for long periods is damaging to the structure of important cellular macromolecules such as DNA and proteins. To avoid the need for high intracellular ion concentrations cells accumulate organic osmolytes, small molecules which influence the osmolality of the cell without changing the structure of cellular macromolecules (Burg & Ferraris, 2008).

Organic osmolytes can play a role either as compatible or counteracting osmolytes (Burg & Ferraris, 2008; Wehner *et al.*, 2003; Yancey *et al.*, 1982). Compatible osmolytes can be accumulated within cells without perturbing the structure and function of cellular macromolecules. An example of a compatible osmolyte is sorbitol, which, with no net charge, does not interact with the structure of macromolecules in cells. Compatible osmolytes generally either have no charge or are zwitterions at physiological pH. Counteracting osmolytes are accumulated in pairs, for instance, methyl amines counteract the destabilising effects of urea on proteins (Yancey, 2001), however, high levels of methyl amines in the absence of urea can have the effect of “over-stabilising” proteins, preventing them from functioning (Yancey *et al.*, 1982). Methyl amines are generally accumulated with urea at a ratio of 2:1 urea:methyl amine (Yancey, 2001).

A well-studied role for organic osmolytes is in the mammalian kidney. As this organ concentrates urine, the cells of the renal medulla are exposed to very high extracellular solute concentrations, and thus accumulate the highest intracellular osmolyte levels in any mammalian cells (Burg & Ferraris, 2008; Yancey *et al.*, 1982). Organic osmolytes are

accumulated by two different methods under hypertonic conditions, either by increased synthesis within the cell, or by increased transport across the cell membrane. In the mammalian kidney, the organic osmolyte sorbitol is produced from glucose through the action of the enzyme aldose reductase. The production of aldose reductase is increased under conditions of increased extracellular osmolality (Burg & Ferraris, 2008). In contrast, the production of glycine betaine, another organic osmolyte, does not increase when cells are exposed to increased extracellular concentrations, however, the transport of this molecule into the cell does increase (Burg & Ferraris, 2008).

Marine fish are exposed to high salinities throughout their lives, however, the majority of their proteins are not adapted to function at high salt concentrations, unlike those of halobacteria (Yancey *et al.*, 1982). Cartilaginous fish maintain high levels of urea in their tissues in order to maintain plasma osmolality similar to that of the external environment (Yancey *et al.*, 1982). High intracellular urea levels in elasmobranchs are generally associated with elevated levels of trimethylamine oxide (TMAO), accumulated in a ratio of 2:1 (Yancey, 2001). However, Bedford *et al.*, (1998) reported that the elephant fish (*Callorhincus millii*), a primitive species of the Chondrichthian class, accumulates the methyl amine glycine betaine. Teleosts do not rely on high intracellular urea levels to maintain osmotic balance. The majority of organic osmolytes used by teleost fish are amino acids with no net charge such as glycine, methyl amines such as TMAO, and the amino sulphonic acid taurine (Yancey *et al.*, 1982).

Euryhaline fish have a particular need to accumulate organic osmolytes as they experience changes in environmental salinity, either because they live in environments of fluctuating salinity, or in the case of catadromous and anadromous species, because they migrate between freshwater and seawater environments at different life stages. In the European eel

(*A. anguilla*), inositol has been identified as an important organic osmolyte in the osmoregulatory tissues when eels move to seawater (Kalujnaia *et al.*, 2007; Kalujnaia & Cramb, 2009). Similarly in tilapia (*O. mossambicus*), inositol has been shown to play a role as an organic osmolyte under conditions of increased osmolality (Kalujnaia *et al.*, 2013). The Atlantic salmon has an anadromous life cycle, migrating to seawater where the major growth phase of this species occurs. This transition to seawater requires changes in osmoregulatory strategy, and fish undergo the parr-smolt transformation in preparation for the journey to seawater.

#### *6.1.1 Novel osmolyte hypoxanthine*

In the skin of Atlantic salmon hypoxanthine was identified as a novel osmolyte which has not been observed in other euryhaline species such as tilapia and the European eel (Section 3.1). The structure of hypoxanthine suggests that it would be suitable as an organic osmolyte. As shown in Figure 6.1, the carbonyl oxygen and the nitrogen atoms can act as hydrogen bond acceptors (HBA) as these atoms possess lone pairs of electrons (Patrick, 2017). The hydrogen atoms covalently bonded to nitrogen in hypoxanthine can act as hydrogen bond donors (HBD), these atoms are  $\delta$ -positive as the electrons in the N-H bond are more strongly attracted to the electronegative nitrogen atom (Patrick, 2017). Therefore, there are many potential hydrogen bonding interactions which could occur between hypoxanthine and water. While hypoxanthine has many polar groups which potentially could be involved in non-covalent interactions, the molecule carries no overall charge, and thus will not interact in a damaging way with cellular macromolecules.

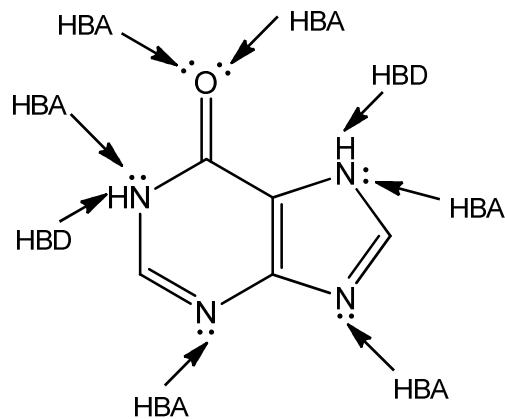


Figure 6.1. Structure of hypoxanthine indicating atoms which act as hydrogen bond donors (HBD) and hydrogen bond acceptors (HBA).

On the feeding trial hypoxanthine levels in the skin increased prior to SW transfer and were significantly higher than baseline levels at the time point 24 hours before SW transfer. Following SW transfer hypoxanthine levels remained at this elevated level up to the 6 weeks post transfer time point. Similarly, the level of hypoxanthine on the direct transfer trial showed an increasing trend in FW, which became statistically significant following SW transfer.

One of the aims of the nucleotide feeding trial was to determine whether increased availability of the precursors required for the production of hypoxanthine would lead to either an increased levels of this osmolyte before SW transfer, or an increase in the speed at which the osmolyte could be produced or accumulated following SW entry. It must be considered whether this would be beneficial to the fish, as increasing intracellular osmotic concentrations before movement to SW could have damaging effects, impairing the osmoregulatory ability of smolts in FW. As the different diets did not have a significant effect on the level of hypoxanthine detected in the skin, it is unlikely that the increased availability of purines did lead to an increased accumulation of hypoxanthine or its precursors before SW transfer occurred.

Possible alternative functional reasons for the accumulation of hypoxanthine in the skin of Atlantic salmon smolts include:

1. The nucleotide is a substrate for the production of guanine crystal production and silvering during smoltification.
2. Hypoxanthine is a substrate for XDH activity and the production of hydrogen peroxide as part of the innate immune response to skin infections.

#### *6.1.1.1 Hypoxanthine in silvering during smoltification*

During smoltification fish undergo morphological changes which include silvering, providing camouflage for their marine pelagic existence in the natural environment (Stefansson *et al.*, 2008). This silvering is achieved by the accumulation of guanine and hypoxanthine in the skin, leading to the formation of guanine crystals in the skin and scales which give the fish their silvery appearance (Johnston & Eales, 1967). Purine crystals are accumulated in reflective platelets in iridophores, which give blue and green metallic colouration, and leucophores which give white or cream colouration (Leclercq *et al.*, 2010b). These differences are due to the different organisation of platelets within cells. In iridophores reflective platelets are arranged in parallel stacks which produce an iridescent effect, while in leucophores purine crystals are poorly organised and reflect a broader range of wavelengths (Leclercq *et al.*, 2010b). While elevated levels of hypoxanthine have been detected in the reflective deposits within the skin of salmonids as fish smoltify (Johnston & Eales, 1967), the predominant purine in these deposits is guanine. Johnston & Eales (1967) reported that hypoxanthine levels associated with the purine deposits involved in silvering were elevated prior to smoltification and seawater transfer. The results of both trials show a trend of increasing hypoxanthine levels in the skin prior to SW transfer, with further increases following SW transfer. These results suggest that while increased skin hypoxanthine levels

may in part be due to the accumulation of purines associated with silvering, this does not account for all of the increase.

#### *6.1.1.2 Hypoxanthine accumulation for urea production*

During smoltification and movement to the seawater environment fish have been found to have increased susceptibility to infectious disease, with immune suppression observed in fish reared in an aquaculture setting (Johansson *et al.*, 2016). Sea lice infestation is also a risk encountered by fish upon entering the marine environment and represents a major cost to the salmon farming industry (Leclercq *et al.*, 2014). Therefore, it would be advantageous for fish to produce and or accumulate substrates which can reduce their susceptibility to infectious challenges.

Inflammation is part of the innate immune defence and usually the first response seen in tissues exposed to infective agents or experiencing physical injury, isolating the damaged tissue. This response involves the release of many different factors by injured cells, which lead to vasodilation around the site of injury and mediate the chemoattraction of various classes of immune cells to the site of the damage. Cellular generation of hydrogen peroxide ( $H_2O_2$ ) is important in the inflammatory response, attracting leukocytes to sites of infection (Wittmann *et al.*, 2012). Cell damage has been shown to lead to the production of a gradient of  $H_2O_2$  around the site of injury (Wittmann *et al.*, 2012). This gradient attracts leucocytes to the site of injury to deal with any initial infectious agents. As  $H_2O_2$  is a form of reactive oxygen species as well as a signalling molecule, this compound can also act as an antimicrobial agent, damaging proteins and DNA by oxidising these macromolecules. This non-specific defence forms the immediate response of the body to infection and injury.

Hypoxanthine forms part of the purine degradation pathway, it can be converted by xanthine dehydrogenase to xanthine, which can be further broken down to urea by the pathway shown in Figure 6.2. The enzyme xanthine dehydrogenase (XDH) is responsible for the conversion of the purines hypoxanthine and xanthine to xanthine and uric acid respectively.  $\text{H}_2\text{O}_2$  is a major byproduct of this reaction, and Kelley *et al.* (2010) state that in the inflammatory response xanthine oxidase is a critical source of reactive oxygen species, both superoxide ( $\cdot\text{O}_2^-$ ) and  $\text{H}_2\text{O}_2$ . As elevated levels of hypoxanthine were detected in the skin at the 3 weeks and 6 weeks post transfer time points on the feeding trial, the level of XDH expression was investigated at these two time points to determine whether the differences in hypoxanthine levels were related to differences in XDH expression. There was a trend for the activity of this enzyme to be increased in the skin between three and six weeks post seawater transfer. It is possible that increased hypoxanthine levels in the skin may represent the accumulation of a substrate for  $\text{H}_2\text{O}_2$  production. The increased mRNA expression of XDH at the final time point could be due to a feedback mechanism triggered by increased hypoxanthine levels.

Sea lice represent a major cost to the salmon aquaculture industry. Costello (2009) reported that in 2006 treatment for sea lice infection cost the industry €305 million. In terms of surveillance and treatment, sea lice represent the most economically costly parasite encountered by salmon farming (Aaen *et al.*, 2014). Further to the economic costs, sea lice also represent a cost to the aquaculture industry in terms of the public perception of fish farming, with concerns related to the ecological risks associated with sea lice transferring from farmed to wild populations. Hydrogen peroxide is a recognised treatment for sea lice infestation, predominantly used to remove pre-adult and adult life stages attached to the fish (Aaen *et al.*, 2014). Aaen *et al.* (2014) found that exposure of sea lice egg strings to  $\text{H}_2\text{O}_2$  at high concentrations (1000-2000  $\text{mgL}^{-1}$ ) prevented the successful hatching of larvae, and at a

lower concentration (470 mgL<sup>-1</sup>) prevented the hatched larvae from developing into the copepodid stage, the life stage at which these parasites attach to their host.

Staley & Ewing (1992) reported levels of hypoxanthine in the skin of coho salmon (*Oncorhynchus kisutch*) between 59-110 mmol/kg wet tissue, much higher than the levels of 4-8 mmol/kg detected in the skin of Atlantic salmon in this study. It has been demonstrated that coho salmon are more resistant to sea lice infection than other salmonid species, particularly Atlantic salmon (Tadiso *et al.*, 2011). The louse *L. salmonis*, which feeds initially on the host's skin mucus, and later skin, secretes prostaglandin E2 when attached to an Atlantic salmon host. This has been shown to down-regulate the inflammatory response in this host species (Fast *et al.*, 2005, 2004). It has been found that the mucus on the skin of coho salmon does not stimulate the release of prostaglandin secretions from *L. salmonis* to the same degree as that of species such as Atlantic salmon which are more susceptible to sea lice infection (Fast *et al.*, 2003). Burrells (2001) previously reported that the addition of nucleotide supplements to feed is beneficial in the control of sea lice infestation. In another publication Burrells *et al.* (2001) demonstrated that dietary nucleotide supplementation increased the resistance of salmonids to a number of different infectious agents, including bacteria, viruses and ectoparasitic sea lice. Increased dietary nucleotides provide substrates for the production of antimicrobial agents such as H<sub>2</sub>O<sub>2</sub> by the innate immune system.

#### *6.1.2 Short term SW adaptation*

Glycerophosphocholine (GPC) was found to increase in the skin of parr following SW challenge, and in smolts following direct SW transfer, falling back to FW levels by 3 days post transfer. Alanine levels in the skin were similarly found to increase following SW challenge of parr and SW transfer of smolts, returning to levels equivalent to those seen in FW by three days post transfer. Glycine betaine in the skin was observed to increase

following SW challenge in parr early in the time course and in smolts following transfer to SW. Levels in SW remained elevated up to 3 days post transfer. No significant change was observed following SW challenge at the 30 day before transfer time point, however, this may have been due to increased variation in the level detected in fish in FW at this time point. It must be considered that the change in photoperiod 4 days before this sampling point may have influenced the level of this osmolyte in the skin. It can be considered likely that these osmolytes are important in the initial adaptation of salmon to increased external salinity.

Hypoxanthine levels showed a gradual increasing trend in FW, with levels shortly after SW transfer significantly higher than in parr, and levels at three days post transfer significantly higher than in FW smolts the day before transfer. SW challenge had no discernible effect on the level of hypoxanthine in the skin in parr, suggesting that this is a smolt specific adaptation.

### *6.1.3 Long term SW adaptation*

Of the organic osmolytes detected in the skin of Atlantic salmon taurine occurred in the highest concentrations, between 10 and 20 mmol/kg wet tissue. This accounted for approximately 50% of the total osmolyte extracted from the skin. The level of taurine in the skin did not change significantly over the short time course when salmon were transferred directly to SW. On the feeding trial taurine levels were observed to increase on all diets by the 3 weeks post transfer time point and remained elevated at 6 weeks post SW transfer.

Taurine is an amino sulphonic acid, which is abundant in all vertebrates, and is predominantly synthesised in the liver in teleosts from the sulphur containing amino acids methionine and cysteine (Liu *et al.*, 2017). It is a zwitterion at physiological pH, thus very polar and unable to cross membranes, and is accumulated within cells by active transport

from the ECF by the taurine transporter (TauT) (Liu *et al.*, 2017), creating millimolar concentrations within cells (Chesney *et al.*, 1976).

In a number of mammalian species taurine plays a role as an intracellular organic osmolyte. Häussinger (1998) found that it played an osmotic role in the liver, while Law (1994) identified a similar role in the brain. Taurine is also an important osmolyte in the mammalian renal medulla, a tissue which requires regular adaptation to high solute conditions (Burg, 1996). Renal medullary cells are exposed to high concentrations of urea and salts as urine is concentrated, requiring cells in this tissue to accumulate the highest concentrations of organic osmolytes found in terrestrial mammalian tissue (Burg & Ferraris, 2008). As taurine is successful in providing protection from chronic conditions of high extracellular salt concentrations, it seems likely that it would play a similar role in fish, providing osmotic protection to tissues in contact with the marine environment. Indeed, taurine has been shown to play an osmotic role in the tissues of the yellowtail (*Seriola quinqueradiata*) (Takagi *et al.*, 2006).

#### *6.1.4 Nucleotide supplementation*

In the aquaculture industry, a variety of feed supplements have been developed to improve the growth and health of farmed species. Functional feeds have been developed to cater to the specific nutritional needs of fish at different life stages and in different environments. The parr-smolt transformation is an important phase of the salmon life cycle and represents a major bottleneck in the production of this species. The major growth phase of Atlantic salmon occurs following their entry to seawater, however, it has been reported that following seawater transfer smolts in an aquaculture setting are more susceptible to disease and ectoparasitic infections (Johansson *et al.*, 2016), and often show retarded growth in the months after seawater transfer. Burrells *et al.* (2001a) reported that the supplementation of

salmonid feeds with nucleotides reduced the incidence of mortality due to bacterial and viral infections. They found that mortalities due to infection stopped 4-5 days earlier in fish fed nucleotide supplemented diets than in fish on control diets (Burrells *et al.*, 2001a). Thus, it was posited that nucleotide supplementation improved survival of infection through more rapid immune activation (Burrells *et al.*, 2001a). Shiao *et al.* (2015) reported that in tilapia, supplementation with nucleotides in fish meal poor diets led to increased disease resistance relative to control, with increased lymphocyte production and a more rapid innate immune response. In another study, Burrells *et al.* (2001b) reported that dietary nucleotide supplementation improved the ability of salmonid species to adapt to stressors, such as handling, vaccination and seawater transfer. These authors also reported that the plasma chloride levels of fish three weeks after seawater transfer were significantly lower in fish fed nucleotide supplemented diets than in fish on a control diet (Burrells *et al.*, 2001b). Fish fed nucleotide supplements were also larger than those fed the control diet five weeks after seawater transfer, possibly due to the increased intestinal surface area seen in fish fed nucleotide supplements (Burrells *et al.*, 2001b).

While a majority of cells can produce nucleotides *de novo* endogenously, some cell types lack this ability (Quan, 1992). The nucleotide salvage pathways are more energy efficient than *de novo* synthesis, and are favoured when an exogenous source of nucleotides is available (Uauy, 1994). It has been reported in mammals that during periods of growth and physiological stress the requirement for exogenous nucleotides is increased (Carver, 1994; Jyonouchi, 1994). Nucleotides are essential for cell proliferation and the production of mRNA, required for protein production, important processes for growth. The requirement for nucleotide supplementation has been reported in a number of fish species. The strains of fish bred for aquaculture production are selected for rapid growth, and thus may have increased need for dietary nucleotides during times of stress to maintain their high growth rates.

In this project organic osmolytes were extracted from the skin of fish fed diets containing nucleotide supplements of differing proportions, varying from a 100% pyrimidine supplement (CMP) to two different 100% purine supplements (AMP and inosine).

No significant effect of diet was detected on the level of the novel osmolyte hypoxanthine in the skin. Of the other osmolytes investigated, diet had a statistically significant effect on the levels of urea and alanine, and there was a significant effect of the interaction between diet and time point on the levels of myo-inositol, GPC and glycine betaine.

Urea levels were very high in the skin of a small number of individuals on the diets containing 100% purine supplements at the final time point, 6 weeks after SW transfer. While it was considered that samples may have been contaminated, re-extraction and analysis gave similar results, suggesting that any contamination was at the level of the original tissue samples. It was determined that these high levels may be down to inter-individual variation, as concurrent increases in the methyl-amine alanine were also observed. As samples post SW transfer were taken at 3 week intervals, it is possible that if changes in urea levels in the skin were not synchronised between individuals this effect could have been missed in other fish.

It is proposed that the high levels of urea at the final time point in the nucleotide supplement feeding trial are due to the degradation of purines. Purines can be converted to urea by the pathway shown in Figure 6.2. The initial stage in this pathway is catalysed by xanthine dehydrogenase, which was found to be up regulated at the 6 weeks post transfer time point on diets 5 and 6. No significant change was observed on diet 4, however, measurements from fish on this diet did show increased variability.

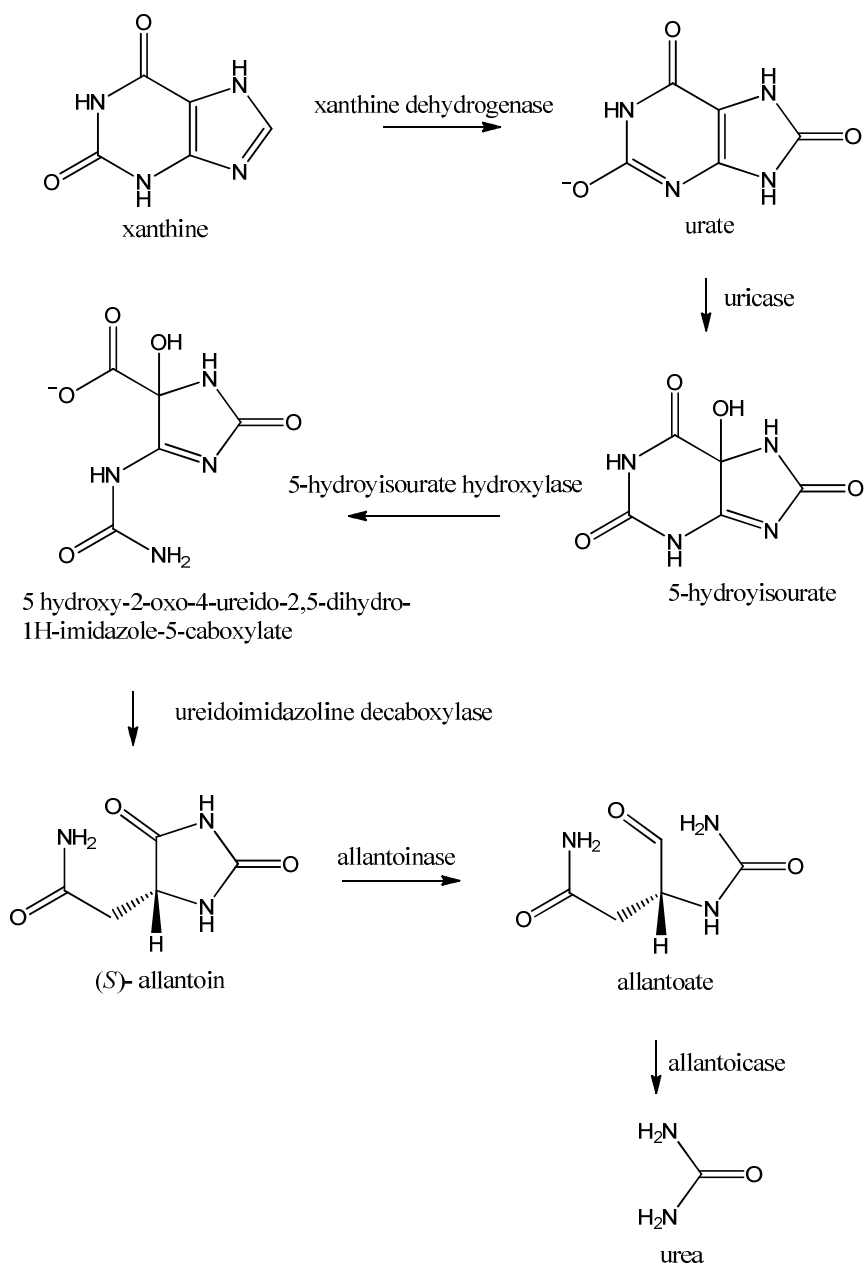


Figure 6.2. The pathway of purine oxidation to urea.

Pyrimidines are only converted to urea in some microorganisms, while the majority of species degrade pyrimidines to L-amino acids, ammonia and CO<sub>2</sub> through a reductive pathway (Soong *et al.*, 2001).

Urea can function as a counteracting osmolyte when accumulated with methyl amines, and play a role in the long term adaptation of fish to the marine environment (Wright & Land,

1998). Increased urea in the skin may be explained by the facultative use of this purine breakdown product as an organic osmolyte. As high urea concentrations inhibit the breakdown of GPC (Burg & Ferraris, 2008), a methyl amine, the opportunistic accumulation of these counteracting organic osmolytes together may be more energy efficient than accumulating other osmolytes that would have to be synthesised *de novo* or transported from other tissues. On the feeding trial GPC was not accumulated at a higher level in the high purine diets at the time point at which urea levels increased. However, alanine, another counteracting osmolyte, did show increased levels at this time point.

On the diets containing 100% purine supplements alanine levels were elevated at the final time point on the feeding trial. This increase was to levels above those seen around the point of SW transfer. It seems plausible that following an initial increase and subsequent drop off during the first stages of SW adaptation, alanine levels increased at this time point to combat the destabilising effects of high urea concentrations.

Hypoxanthine in muscle has been shown to increase in fish post mortem when stored in ice, and is associated with flesh spoiling, contributing a bitter taste (Özoğul *et al.*, 2011). This effect is seen in a variety of fish and shellfish species, and is due to the breakdown of adenosine phosphates (Massa *et al.*, 2002; Özoğul *et al.*, 2011). The ratio of hypoxanthine and inosine to total nucleotide content of muscle is used to determine the freshness of fish flesh stored in ice (Özoğul *et al.*, 2011; Tejada *et al.*, 2007). As there are increased levels of dietary purines available to the fish on diets 5 and 6 in the form of AMP and inosine, it is possible that the increased levels of hypoxanthine are simply due to increased breakdown of these nucleotides. This may be further broken down to form urea, which may have been used opportunistically as an osmolyte in fish on the high purine diets.

While it is entirely possible that the high levels of urea seen in a small number of samples are an artefact of contamination, this finding is of interest, and further work to determine whether high purine content in the diet leads to increased urea levels in the tissue would be valuable for a number of reasons. High levels of urea in the muscle of elasmobranchs gives the meat from these species an unpleasant taste if fillets are not soaked before cooking, if high levels of urea were accumulated in the muscle of Atlantic salmon this could reduce the desirability of the fillets to consumers. A study in which samples are collected more frequently may shed light on whether this result is an artefact or due to interindividual variation.

#### *6.1.5 Organic osmolyte position within the skin*

The organic osmolytes investigated in this study were measured in the aqueous fraction derived from extraction from total skin, i.e. the combination of epidermis, dermis, and scales, and likely contained a small amount of muscle tissue and skin mucus. The skin is a complex stratified tissue composed of different layers which play specific roles. The outer layer of the skin, the epidermis, is composed of a basal layer of cells which renew the tissue as old cells are sloughed off. These are covered by a layer of superficial cells which can migrate quickly in response to mechanical damage to promote healing (Jensen, 2015). The epidermis also contains goblet cells, responsible for the production of the mucosal body covering. Below the epidermis is the dermis in which scales are formed. This tissue is composed of an upper portion containing nerves, pigment cells and fibroblasts, and a lower portion known as the hypodermis which is highly vascularised and contains a high proportion of adipocytes (Jensen, 2015). Below the hypodermis lies the skeletal musculature. It would be useful to determine the distribution of organic osmolytes within the different layers of this tissue. Further work could focus on specific assays targeting osmolytes of interest to determine the localisation of these molecules within the different layers of the skin.

## 6.2 *The energy cost of osmoregulation*

Glucose levels increase in the skin of parr when exposed to SW challenge. Meanwhile a decreasing trend in glucose levels was observed on the feeding trial, with levels falling below the limit of detection of the assay in many samples at the later time points. It is possible that glucose was being consumed to produce energy for the maintenance of osmotic homeostasis following SW transfer.

Maintenance of osmotic homeostasis in the face of changing salinity is an energy expensive process, requiring ATP to drive the active transport of ions against electrochemical gradients (Evans *et al.*, 2005). Glucose is required to produce this energy. There is evidence of increased hepatic glycogenolysis in both tilapia (*O. mossambicus*) and gilthead sea bream (*S. auratus*) following seawater exposure (Baltzegar *et al.*, 2014; Sangiao-Alvarellos *et al.*, 2005, 2003). Baltzegar *et al.* (2014) suggested that increased leptin A activity produced the hyperglycaemic effect observed in tilapia, as increased expression of leptin A was associated with increased glucose levels. As circulating amino acid levels also increased on seawater challenge, it was proposed that cortisol triggered gluconeogenesis from amino acids to supply energy for osmoregulation once glycogen stores were depleted (Baltzegar *et al.*, 2014).

Differences from the classic mammalian paradigms in the action of hormones associated with energy metabolism have been identified in fish. A high glucose load does not lead to hyperinsulinaemia in fish as it does in mammals (Kelley, 1993), and the hormone glucagon-like peptide 1 which plays a hypoglycaemic role in mammalian species, leads to hyperglycaemia in fishes (Mommsen, 2000). The steroid hormone cortisol acts as a promoter of hyperglycaemia in both fish and mammals (Khani & Tayek, 2001; Vijayan *et al.*, 1996), however, this hormone, which is both a glucocorticoid and mineralocorticoid in mammals, is also important in the excretion of Na<sup>+</sup> across the gill epithelia during adaptation to increased

salinity (Evans *et al.*, 2005). Cortisol also promotes lipolysis in vertebrates (Mommensen *et al.*, 1999), however, no changes in the levels of circulating free fatty acids have been observed in salmonids exposed to salinity challenge (Bystriansky *et al.*, 2007).

Glycogen accumulation has been identified in the gill (Hwang & Lee, 2007), providing this tissue with a local energy source for rapid adaptation to changes in osmoregulatory demand. Tseng *et al.* (2007) reported increased glycogen phosphorylase activity following seawater challenge, suggestive of increased glycogenolysis within the gill tissue. The gill has an important role in the active secretion of ions when fish enter water of a higher salinity, and the presence of local energy stores facilitates the initial response to seawater entry, providing energy faster than is possible by mobilisation of liver stores. Tissues such as the skin may rely on the release of hepatic stores of glucose to provide energy for the maintenance of osmotic homeostasis.

It is possible that rather than being accumulated as an organic osmolyte, increased glucose levels in the skin following seawater challenge could represent an initial accumulation of glucose as an energy source for osmoregulatory processes, with levels returning to normal as fish acclimate to a higher salinity. It has been reported that the processes involved in the maintenance of osmotic balance account for between 20 and 60% of the energy metabolism of fish during their acclimation to increased salinity (Bœuf & Payan, 2001; Morgan *et al.*, 1997). However, it seems likely that the osmotic effect of increased glucose levels is also important in the initial response to hypertonic conditions. Glucose can be produced rapidly from glycogen stores in the liver, as well as in other tissues such as the gill (Tseng & Hwang, 2008). This rapid response may allow glucose to act as a “first responder” to changes in environmental osmolality, particularly in tissues directly exposed to the external environment, such as the skin and gill. The accumulation of other osmolytes such as taurine,

glycine betaine and hypoxanthine requires de novo synthesis or increased transport into the cell, processes which are more time-consuming than glucose mobilisation. Glucose can be mobilised quickly and can play a role as an organic osmolyte in the short term while other osmolytes are synthesised or transported around the body. These other organic osmolytes become more important as the glucose is consumed as an energy source.

It is worthy of note that on the nucleotide supplement feeding trial the level of glucose in the skin was within the measurable range of the assay in all samples collected at the final time point on the two diets containing 100% purine supplements. This could be due to the higher availability of purines leading to a reduced energetic demand in response to osmotic stress. It may be that there was a lower requirement for the transport or synthesis of other organic osmolytes due to the increased availability of the substrate required for the production of hypoxanthine. This is worthy of further investigation.

### *6.3 Biomarkers of smoltification*

In order to improve the performance of smolts transferred to SW tests are carried out on each stock to assess whether they are prepared for this change. The level of activity of the enzyme Na<sup>+</sup>K<sup>+</sup>-ATPase in the gill, alongside plasma chloride levels following SW challenge have been used for many years as indicators of hyperosmoregulatory ability. The results of this project indicated that genes encoding ion channels represent the most reliable of the genes investigated for predicting the ability of fish to adapt to SW transfer (Section 5.2). In future it may be useful to develop a more complex assay which takes into account a variety of different metabolic processes involved in smoltification to give a more robust measurement of the developmental stage of the fish.

The expression of a number of genes investigated as biomarkers, including those involved in lipid metabolism, the immune system and cytoskeleton remodelling, along with the gene for an uncharacterised protein (UP584) showed increased variability around the time that fish were exposed to a change in photoperiod from natural day length to 24 hour light. As photoperiod triggers are an important tool used in the manipulation of the development of salmon, used to initiate smoltification as well as to suppress or trigger sexual maturation, a better understanding of the metabolic effects of artificial photoperiod manipulation would be valuable. Further work to determine the changes in expression profiles of genes involved in different metabolic processes would give a useful insight into the effects of what is a standard practice in the industry. Of particular interest would be the effect of photoperiod manipulation on the expression of genes involved in the immune system as smoltification is associated with a suppression of the immune system in salmonids.

#### *6.4 Conclusions*

A novel osmolyte has been identified in the skin of Atlantic salmon. The purine hypoxanthine is highly suitable as an organic osmolyte as its structure contains many hydrogen bond donors and hydrogen bond acceptors.

Nucleotide supplementations, while a valuable addition to salmon feeds for the various benefits described by Burrells *et al.* (2001a, 2001b), did not have the effect of improving the ability of fish to accumulate the purine hypoxanthine.

The osmolytes detected in this study were measured using an assay optimised for a range of different molecules. It would be of interest to measure the levels of these osmolytes with specific assays to give a more definite picture of the accumulation of these molecules during

the smoltification process. This would be of particular value in further investigating the novel osmolyte hypoxanthine in salmonids.

It would be of value to study the effects of changes in photoperiod on the expression of a variety of genes involved in different metabolic processes to determine the effects of this treatment. It would also be interesting to determine the effects of photoperiod manipulation on the level of organic osmolytes in osmoregulatory tissues. A time course study to determine the duration of these effects could give useful insight into the most appropriate timing for such treatments, perhaps indicating whether there is an optimal length of time to allow fish to recover from this change before exposing them to additional stressors such as SW transfer or other handling events. Furthermore, when selecting biomarkers of changes in developmental stage, an understanding of the effects of treatments used to initiate such developmental changes would be invaluable and would reduce the risk of false readings caused by the treatments.



## 7. References

- Aaen, S.M., Aunsmo, A., Horsberg, T.E., 2014. Impact of hydrogen peroxide on hatching ability of egg strings from salmon lice (*Lepeophtheirus salmonis*) in a field treatment and in a laboratory study with ascending concentrations. *Aquaculture* 422–423, 167–171.
- Al-Jandal, N.J., Wilson, R.W., 2011. A comparison of osmoregulatory responses in plasma and tissues of rainbow trout (*Oncorhynchus mykiss*) following acute salinity challenges. *Comp. Biochem. Physiol. A. Mol. Integr. Physiol.* 159, 175–181.
- Alberts, B., Johnson, A., Lewis, J., Raff, M., Roberts, K., Walter, P., 2002. *Molecular biology of the cell*, 4th ed. Garland Science, New York.
- Alexander, G., Sweeting, R., Mckeown, B., 1994. The shift in visual pigment dominance in the retinae of juvenile coho salmon (*Oncorhynchus Kisutch*): an indicator of smolt status. *J. exp. Biol* 195, 185–197.
- Alne, H., Oehme, M., Thomassen, M., Terjesen, B., Rørvik, K.-A., 2011. Reduced growth, condition factor and body energy levels in Atlantic salmon *Salmo salar* L. during their first spring in the sea. *Aquac. Res.* 42, 248–259.
- Anderson, P.M., 1980. Glutamine- and N-acetylglutamate-dependent carbamoyl phosphate synthetase in elasmobranchs. *Science* 208, 291–293.
- Arreguín-Sánchez, F., del Monte-Luna, P., Zetina-Rejón, M.J., 2015. Climate change effects on aquatic ecosystems and the challenge for fishery management: pink shrimp of the Southern Gulf of Mexico. *Fisheries* 40, 15–19.
- Auton, M., Bolen, D.W., 2005. Predicting the energetics of osmolyte-induced protein folding/unfolding. *Proc. Natl. Acad. Sci. U. S. A.* 102, 15065–15068.
- Babin, P.J., Vernier, J.-M., 1989. Plasma lipoproteins in fish. *J. Lipid Res.* 30, 467–89.
- Balcázar, J.L., Blas, I. de, Ruiz-Zarzuela, I., Cunningham, D., Vendrell, D., Múzquiz, J.L., 2006. The role of probiotics in aquaculture 114, 173–186.
- Baltzegar, D.A., Reading, B.J., Douros, J.D., Borski, R.J., 2014. Role for leptin in promoting glucose mobilization during acute hyperosmotic stress in teleost fishes. *J. Endocrinol.* 220, 61–72.
- Barker, G., Ellory, J., 1990. The identification of neutral amino acid transport systems. *Exp. Physiol.* 75, 3–26.
- Bedford, J.J., Harper, J.L., Leader, J.P., Yancey, P.H., Smith, R.A.J., 1998. Betaine is the principal counteracting osmolyte in tissues of the elephant fish, *Callorhincus millii* (Elasmobranchii, Holocephali). *Comp. Biochem. Physiol. Part B* 119, 521–526.
- Bendiksen, E.Å., Arnesen, A.M., Jobling, M., 2003. Effects of dietary fatty acid profile and fat content on smolting and seawater performance in Atlantic salmon (*Salmo salar* L.). *Aquaculture* 225, 149–163.
- Berk, Z., 1992. *Technology of production of edible flours and protein products from soybeans*. Food and Agriculture Organization of the United Nations.

- Björnsson, B.T., Stefansson, S.O., McCormick, S.D., 2011. Environmental endocrinology of salmon smoltification. *Gen. Comp. Endocrinol.* 170, 290–298.
- Blanco, G., Mercer, R.W., 1998. Isozymes of the Na-K-ATPase: heterogeneity in structure, diversity in function. *Am. J. Physiol.* 275, 633–650.
- Bloch, K., Schoenheimer, R., 1941. The biological precursors of creatine. *J. Biol. Chem.* 138, 167–194.
- Bœuf, G., Payan, P., 2001. How should salinity influence fish growth? *Comp. Biochem. Physiol. Part C* 130, 411–423.
- Bolen, D.W., 2001. Protein stabilization by naturally occurring osmolytes. In: *Protein Structure, Stability, and Folding*. Humana Press, New Jersey, pp. 017–036.
- Bonnefont, J.-P., Djouadi, F., Prip-Buus, C., Gobin, S., Munnich, A., Bastin, J., 2004. Carnitine palmitoyltransferases 1 and 2: biochemical, molecular and medical aspects. *Mol. Aspects Med.* 25, 495–520.
- Borsook, H., Dubnoff, J.W., 1941. The formation of glycocholine in animal tissues. *J. Biol. Chem.* 138, 389–403.
- Borsook, H., Dubnoff, J.W., Kerckhoff, W.G., 1940. The formation of creatine from glycocholine in the liver. *J. Biol. Chem.* 132, 559–574.
- Bothwell, J.H., Styles, P., Bhakoo, K.K., 2002. Swelling-activated taurine and creatine effluxes from rat cortical astrocytes are pharmacologically distinct. *J. Membr. Biol.* 185, 157–164.
- Bourque, C.W., 2008. Central mechanisms of osmosensation and systemic osmoregulation. *Nat. Rev. Neurosci.* 9, 519–31.
- Bowlus, R.D., Somero, G.N., 1979. Solute compatibility with enzyme function and structure: Rationales for the selection of osmotic agents and end-products of anaerobic metabolism in marine invertebrates. *J. Exp. Zool.* 208, 137–151.
- Braissant, O., Henry, H., Béard, E., Uldry, J., 2011. Creatine deficiency syndromes and the importance of creatine synthesis in the brain. *Amino Acids* 40, 1315–1324.
- Bricknell, I., Dalmo, R., 2005. The use of immunostimulants in fish larval aquaculture. *Fish Shellfish Immunol.* 19, 457–472.
- Brosnan, M.E., Brosnan, J.T., 2016. The role of dietary creatine. *Amino Acids* 48, 1785–1791.
- Brown, A.-M., Benboubetra, M., Ellison, M., Powell, D., Reckless, J.D., Harrison, R., 1995. Molecular activation-deactivation of xanthine oxidase in human milk. *Biochim. Biophys. Acta* 1245, 248–254.
- Burg, M.B., 1996. Coordinate regulation of organic osmolytes in renal cells. *Kidney Int.* 49, 1684–1685.
- Burg, M.B., Ferraris, J.D., 2008. Intracellular organic osmolytes: function and regulation. *J. Biol. Chem.* 283, 7309–13.
- Burg, M.B., Ferraris, J.D., Dmitrieva, N.I., 2007. Cellular response to hyperosmotic stresses. *Physiol. Rev.* 87, 1441–1474.

- Burrells, C., Williams, P.D., Forno, P.F., 2001a. Dietary nucleotides: a novel supplement in fish feeds 1. Effects on resistance to disease in salmonids. *Aquaculture* 199, 159–169.
- Burrells, C., Williams, P.D., Southgate, P.J., Wadsworth, S.L., 2001b. Dietary nucleotides: a novel supplement in fish feeds 2. Effects on vaccination, salt water transfer, growth rates and physiology of Atlantic salmon (*Salmo salar* L.). *Aquaculture* 199, 171–184.
- Bystriansky, J.S., Frick, N.T., Ballantyne, J.S., 2007. Intermediary metabolism of Arctic char *Salvelinus alpinus* during short-term salinity exposure. *J. Exp. Biol.* 210, 1971–1985.
- Bystriansky, J.S., Schulte, P.M., 2011. Changes in gill H<sup>+</sup>-ATPase and Na<sup>+</sup>/K<sup>+</sup>-ATPase expression and activity during freshwater acclimation of Atlantic salmon (*Salmo salar*). *J. Exp. Biol.* 214, 2435–42.
- Bzowska, A., Kulikowska, E., Shugar, D., 2000. Purine nucleoside phosphorylases: properties, functions, and clinical aspects. *Pharmacol. Ther.* 88, 349–425.
- Cantiello, H.F., Prat, A.G., 1996. Chapter 17 Role of actin filament organization in ion channel activity and cell volume regulation. *Curr. Top. Membr.* 43, 373–396.
- Cantoni, G.L., Vignos, P.J., 1954. Enzymatic mechanism of creatine synthesis. *J. Biol. Chem.* 209, 647–659.
- Cao, X., Kemp, J.R., Anderson, P.M., 1991. Subcellular localization of two glutamine-dependent carbamoyl-phosphate synthetases and related enzymes in liver of *Micropterus salmoides* (largemouth bass) and properties of isolated liver mitochondria: comparative relationship with elasmobranchs. *J. Exp. Zool.* 258, 24–33.
- Carballo, E., Lai, W.S., Blackshear, P.J., 1998. Feedback inhibition of macrophage tumor necrosis factor- $\alpha$  production by tristetraprolin. *Science* (80- ). 281, 1001–1005.
- Carver, J.D., 1994. Dietary nucleotides: cellular immune, intestinal and hepatic system effects. *J. Nutr.* 124, 144–148.
- Chansue, N., Endo, M., Kono, T., Sakai, M., 2000. The stimulation of cytokine-like proteins in tilapia (*Oreochromis niloticus*) orally treated with  $\beta$ -1, 3-glucan. *Asian Fish. Sci.* 13, 271–278.
- Chesney, R.W., Scriver, C.R., Mohyuddin, F., 1976. Localization of the membrane defect in transepithelial transport of taurine by parallel studies in vivo and in vitro in hypertaurinuric mice. *J. Clin. Invest.* 57, 183–93.
- Choi, J.-S., Berdis, A.J., 2012. Nucleoside transporters: biological insights and therapeutic applications. *Future Med. Chem.* 4, 1461–1478.
- Chowhan, R.K., Ali, F., Bhat, M.Y., Rahman, S., Singh, L.R., Ahmad, F., Dar, T.A., 2016. Alanine counteracts the destabilizing effect that urea has on RNase-A. *Protein Pept. Lett.* 23, 795–9.
- Christensen, H.N., 1990. Role of amino acid transport and countertransport in nutrition and metabolism. *Physiol. Rev.* 70, 43–77.
- Christensen, K.A., Davidson, W.S., 2017. Autopolyploidy genome duplication preserves other ancient genome duplications in Atlantic salmon (*Salmo salar*). *PLoS One* 12, e0173053.
- Chung, H.Y., Baek, B.S., Song, S.H., Kim, M.S., Huh, J.I., Shim, K.H., Kim, K.W., Lee,

- K.H., 1997. Xanthine dehydrogenase/xanthine oxidase and oxidative stress. *Age (Omaha)*. 20, 127–140.
- Clark, G.J., Ju, X., Azlan, M., Tate, C., Ding, Y., Hart, D.N.J., 2009. The CD300 molecules regulate monocyte and dendritic cell functions. *Immunobiology* 214, 730–736.
- Cohen, D.M., Wasserman, J.C., Gullans, S.R., 1991. Immediate early gene and HSP70 expression in hyperosmotic stress in MDCK cells. *Am. J. Physiol. - Cell Physiol.* 261, 594–601.
- Cohen, G., 1968. *The Regulation of Cell Metabolism*. Holt, Rinehart and Winston.
- Colina, C., Rosenthal, J.J.C., Degiorgis, J.A., Srikumar, D., Iruku, N., Holmgren, M., 2007. Structural basis of Na<sup>+</sup>/K<sup>+</sup>-ATPase adaptation to marine environments. *Nat. Struct. Mol. Biol.* 14, 427–431.
- Costello, M.J., 2009. The global economic cost of sea lice to the salmonid farming industry. *J. Fish Dis.* 32, 115–118.
- Criscitello, M.F., Flajnik, M.F., 2007. Four primordial immunoglobulin light chain isotypes, including  $\lambda$  and  $\kappa$ , identified in the most primitive living jawed vertebrates. *Eur. J. Immunol.* 37, 2683–2694.
- Cronshagen, U., Voland, P., Kern, H.F., 1994. cDNA cloning and characterization of a novel 16 kDa protein located in zymogen granules of rat pancreas and goblet cells of the gut. *Eur. J. Cell Biol.* 65, 366–77.
- Cvancara, V.A., 1969a. Studies on tissue arginase and ureogenesis in fresh-water teleosts. *Comp. Biochem. Physiol.* 30, 489–496.
- Cvancara, V.A., 1969b. Comparative study of liver uricase activity in fresh-water teleosts. *Comp. Biochem. Physiol.* 28, 725–732.
- da Rocha Lapa, F., da Silva, M.D., de Almeida Cabrini, D., Santos, A.R.S., 2012. Anti-inflammatory effects of purine nucleosides, adenosine and inosine, in a mouse model of pleurisy: evidence for the role of adenosine A<sub>2</sub> receptors. *Purinergic Signal.* 8, 693–704.
- Danulat, E., Kempe, S., 1992. Nitrogenous waste excretion and accumulation of urea and ammonia in *Chalcalburnus tarichi* (Cyprinidae), endemic to the extremely alkaline Lake Van (Eastern Turkey). *Fish Physiol. Biochem.* 9, 377–386.
- Davuluri, S.P., Hird, F.J.R., McLean, R.M., 1981. A re-appraisal of the function and synthesis of phosphoarginine and phosphocreatine in muscle. *Comp. Biochem. Physiol. Part B Comp. Biochem.* 69, 329–336.
- Devos, E., Devos, P., Cornet, M., 1998. Effect of cadmium on the cytoskeleton and morphology of gill chloride cells in parr and smolt Atlantic salmon (*Salmo salar*). *Fish Physiol. Biochem.* 18, 15–27.
- Diouf, B., Rioux, P., Blier, P.U., Rajotte, D., 2000. Use of brook char (*Salvelinus fontinalis*) physiological responses to stress as a teaching exercise. *Adv. Physiol. Educ.* 23, 18–23.
- dos Santos, N.M.S., Taverne-Thiele, J.J., Barnes, A.C., van Muiswinkel, W.B., Ellis, A.E., Rombout, J.H.W.M., 2001. The gill is a major organ for antibody secreting cell production following direct immersion of sea bass (*Dicentrarchus labrax*, L.) in a

- Photobacterium damsela* ssp. *piscicida* bacterin: an ontogenetic study. *Fish Shellfish Immunol.* 11, 65–74.
- Dowd, W.W., Harris, B.N., Cech, J.J., Kultz, D., 2010. Proteomic and physiological responses of leopard sharks (*Triakis semifasciata*) to salinity change. *J. Exp. Biol.* 213, 210–224.
- Duston, J., Saunders, R.L., Knox, D.E., 1991. Effects of increases in freshwater temperature on loss of smolt characteristics in Atlantic salmon (*Salmo salar*). *Can. J. Fish. Aquat. Sci.* 48, 164–169.
- Edwards, B.Y.H.A., 1982. *Aedes Aegypti*: Energetics of osmoregulation. *J. Exp. Biol.* 101, 135–141.
- Eggset, G., Mortensen, A., Johansen, L.-H., Sommer, A.-I., 1997. Susceptibility to furunculosis, cold water vibriosis, and infectious pancreatic necrosis (IPN) in post-smolt Atlantic salmon (*Salmo salar* L.) as a function of smolt status by seawater transfer. *Aquaculture* 158, 179–191.
- Einarsson, E., Ástvaldsson, Á., Hultenby, K., Andersson, J.O., Svärd, S.G., Jerlström-Hultqvist, J., 2016. Comparative cell biology and evolution of annexins in diplomonads. *mSphere* 1.
- Ellis, T., Turnbull, J.F., Knowles, T.G., Lines, J.A., Auchterlonie, N.A., 2016. Trends during development of Scottish salmon farming: An example of sustainable intensification? *Aquaculture* 458, 82–99.
- Evans, D.H., Piermarini, P.M., Choe, K.P., 2005. The multifunctional fish gill: dominant site of gas exchange, osmoregulation, acid-base regulation, and excretion of nitrogenous waste. *Physiol. Rev.* 85, 97–177.
- Evans, D.H., Piermarini, P.M., Potts, W.T.W., 1999. Ionic transport in the fish gill epithelium 652, 641–652.
- Evans, T.G., 2010. Co-ordination of osmotic stress responses through osmosensing and signal transduction events in fishes. *J. Fish Biol.* 76, 1903–1925.
- FAO, 2010. *Aquaculture Development 4. Ecosystem approach to aquaculture.*
- FAO, 2014. *The state of world fisheries and aquaculture, Food and Agriculture Organization of the United Nations.*
- FAO, 2016. *The State of World Fisheries and Aquaculture.*
- Fiess, J.C., Kunkel-Patterson, A., Mathias, L., Riley, L.G., Yancey, P.H., Hirano, T., Grau, E.G., 2007. Effects of environmental salinity and temperature on osmoregulatory ability, organic osmolytes, and plasma hormone profiles in the Mozambique tilapia (*Oreochromis mossambicus*). *Comp. Biochem. Physiol. A. Mol. Integr. Physiol.* 146, 252–264.
- Finkel, T., 1999. Signal transduction by reactive oxygen species in non-phagocytic cells. *J. Leukoc. Biol.* 65, 337–340.
- Fiol, D.F., Chan, S.Y., Kültz, D., 2006. Identification and pathway analysis of immediate hyperosmotic stress responsive molecular mechanisms in tilapia (*Oreochromis mossambicus*) gill. *Comp. Biochem. Physiol. Part D* 1, 344–356.

- Fiol, D.F., Kültz, D., 2005. Rapid hyperosmotic coinduction of two tilapia (*Oreochromis mossambicus*) transcription factors in gill cells. *Proc. Natl. Acad. Sci. U. S. A.* 102, 927–932.
- Fiol, D.F., Kültz, D., 2007. Osmotic stress sensing and signaling in fishes. *FEBS J.* 274, 5790–5798.
- Fiskeridirektoratet, 2019. 11 600 tonn død laks i nord [WWW Document]. URL <https://www.fiskeridir.no/Akvakultur/Nyheter/2019/0519/11-600-tonn-doed-laks-i-nord> (accessed 8.21.20).
- Fletcher, T.C., Jones, R., Reid, L., 1976. Identification of glycoproteins in goblet cells of epidermis and gill of plaice (*Pleuronectes platessa* L.), flounder (*Platichthys flesus* (L.)) and rainbow trout (*Salmo gairdneri* Richardson). *Histochem. J.* 8, 597–608.
- Foord, R.L., Leatherbarrow, R.J., 1998. Effect of osmolytes on the exchange rates of backbone amide protons in proteins. *Biochemistry* 37, 2969–2978.
- Franchi-Gazzola, R., Dall’Asta, V., Sala, R., Visigalli, R., Bevilacqua, E., Gaccioli, F., Gazzola, G.C., Bussolati, O., 2006. The role of the neutral amino acid transporter SNAT2 in cell volume regulation. *Acta Physiol.* 187, 273–283.
- Furuichi, M., Yone, Y., 1981. Change of blood sugar and plasma insulin levels of fishes in glucose tolerance test. *Bull. Japanese Soc. Sci. Fish.* 47, 761–764.
- Gallazzini, M., Burg, M.B., 2009. What’s new about osmotic regulation of Glycerophosphocholine. *Physiology* 24, 245–249.
- Gallazzini, M., Ferraris, J.D., Kunin, M., Morris, R.G., Burg, M.B., 2006. Neuropathy target esterase catalyzes osmoprotective renal synthesis of glycerophosphocholine in response to high NaCl. *Proc. Natl. Acad. Sci. U. S. A.* 103, 15260–5.
- Garnett, T., Appleby, M.C., Balmford, A., Bateman, I.J., Benton, T.G., Bloomer, P., Burlingame, B., Dawkins, M., Dolan, L., Fraser, D., Herrero, M., Hoffmann, I., Smith, P., Thornton, P.K., Toulmin, C., Vermeulen, S.J., Godfray, H.C.J., 2013. Sustainable intensification in agriculture: premises and policies. *Science* (80-. ). 341, 33–4.
- Gaw, A., Murphy, M.J., Srivastava, R., Cowan, R., O’Reilly, D.S.J., 2013. *Clinical biochemistry : an illustrated colour text*, 5th ed. Churchill Livingstone/Elsevier.
- Gaylord, T.G., Barrows, F.T., Teague, A.M., Johansen, K. a., Overturf, K.E., Shepherd, B., 2007. Supplementation of taurine and methionine to all-plant protein diets for rainbow trout (*Oncorhynchus mykiss*). *Aquaculture* 269, 514–524.
- Gazzola, G.C., Dall’Asta, V., Nucci, F.A., Rossi, P.A., Bussolati, O., Hoffmann, E.K., Guidotti, G.G., 1991. Role of amino acid transport system A in the control of cell volume in cultured human fibroblasts. *Cell. Physiol. Biochem.* 1, 131–142.
- Gerke, V., Moss, S.E., 1997. Annexins and membrane dynamics. *Biochim. Biophys. Acta* 1357, 129–154.
- Gerke, V., Moss, S.E., 2002. Annexins: from structure to function. *Physiol. Rev.* 82, 331–371.
- Gibson, Y., Roberfroid, M.B., 1995. Dietary modulation of the human colonie microbiota: Introducing the concept of prebiotics. *J. Nutr.* 125, 1401–1412.

- Gillet, L.C., Navarro, P., Tate, S., Rö, H., Selevsek, N., Reiter, L., Bonner, R., Aebersold, R., 2012. Targeted Data Extraction of the MS/MS Spectra Generated by Data-independent Acquisition: A New Concept for Consistent and Accurate Proteome Analysis\* □ S.
- Godber, B.L.J., Doel, J.J., Sapkota, G.P., Blake, D.R., Stevens, C.R., Eisenthal, R., Harrison, R., 2000. Reduction of nitrite to nitric oxide catalyzed by xanthine oxidoreductase. *J. Biol. Chem.* 275, 7757–7763.
- Godfray, Beddington, Crute, Haddad, Lawrence, Muir, Pretty, Robinson, Thomas, Toulmin, 2010. Food Security: the challenge of feeding 9 billion people. *Science* (80-. ). 327, 812–818.
- Goldstein, J.L., Anderson, R.G.W., Brown, M.S., 1979. Coated pits, coated vesicles and receptor-mediated endocytosis. *Nature* 279, 679–685.
- Goldstein, J.L., Brown, M.S., 2009. History of Discovery: The LDL Receptor. *Arterioscler. Thromb. Vasc. Biol.* 29, 431–438.
- Goldstein, L., Forster, R.P., 1965. The role of uricolysis in the production of urea by fishes and other aquatic vertebrates. *Comp. Biochem. Physiol.* 14, 567–576.
- Gonçalves, A.T., Gallardo-Escárate, C., 2017. Microbiome dynamic modulation through functional diets based on pre- and probiotics (mannan-oligosaccharides and *Saccharomyces cerevisiae*) in juvenile rainbow trout (*Oncorhynchus mykiss*). *J. Appl. Microbiol.* 122, 1333–1347.
- Green, B.J., Clark, G.J., Hart, D.N.J., 1998. The CMRF-35 mAb recognizes a second leukocyte membrane molecule with a domain similar to the poly Ig receptor. *Int. Immunol.* 10, 891–899.
- Gupta, S., Dhanda, S., Sandhir, R., 2019. Anatomy and physiology of blood-brain barrier. In: Huile Gao, X.G. (Ed.), *Brain Targeted Drug Delivery System*. Elsevier, pp. 7–31.
- Handeland, S.O., Stefansson, S.O., 2001. Photoperiod control and influence of body size on off-season parr-smolt transformation and post-smolt growth. *Aquaculture* 192, 291–307.
- Handeland, S.O., Stefansson, S.O., 2002. Effects of salinity acclimation on pre-smolt growth, smolting and post-smolt performance in off-season Atlantic salmon smolts (*Salmo salar* L.). *Aquaculture* 209, 125–137.
- Hansen, G.H., Olafsen, J.A., 1999. Bacterial interactions in early life stages of marine cold water fish. *Microb Ecol* 38, 1–26.
- Hansson, M.C., Hahn, M.E., 2008. Functional properties of the four Atlantic salmon (*Salmo salar*) aryl hydrocarbon receptor type 2 (AHR2) isoforms. *Aquat. Toxicol.* 86, 121–130.
- Hansson, M.C., Wittzell, H., Persson, K., von Schantz, T., 2004. Unprecedented genomic diversity of AhR1 and AhR2 genes in Atlantic salmon (*Salmo salar* L.). *Aquat. Toxicol.* 68, 219–232.
- Hardie, D.G., Carling, D., Gamblin, S.J., 2011. AMP-activated protein kinase: also regulated by ADP? *Trends Biochem. Sci.* 36, 470–477.
- Harris, C.M., Massey, V., 1997. The oxidative half-reaction of xanthine dehydrogenase with NAD; reaction kinetics and steady-state mechanism. *J. Biol. Chem.* 272, 28335–28341.
- Hasler, U., Jeon, U.S., Kim, J.A., Mordasini, D., Kwon, H.M., Féraillé, E., Martin, P.-Y.,

2006. Tonicity-responsive enhancer binding protein is an essential regulator of aquaporin-2 expression in renal collecting duct principal cells. *J. Am. Soc. Nephrol.* 17, 1521–31.
- Häussinger, D., 1998. Osmoregulation of liver cell function: signalling, osmolytes and cell heterogeneity. *Contrib. Nephrol.* 123, 185–204.
- Havixbeck, J., Barreda, D., 2015. Neutrophil development, migration, and function in teleost fish. *Biology (Basel)*. 4, 715–734.
- Hayashi, S., Fujiwara, S., Noguchi, T., 1989. Degradation of uric acid in fish liver peroxisomes. Intraperoxisomal localization of hepatic allantoinase and purification of its peroxisomal membrane-bound form. *J. Biol. Chem.* 264, 3211–5.
- He, J.-Y., Tian, L.-X., Lemme, A., Gao, W., Yang, H.-J., Niu, J., Liang, G.-Y., Chen, P.-F., Liu, Y.-J., 2013. Methionine and lysine requirements for maintenance and efficiency of utilization for growth of two sizes of tilapia (*Oreochromis niloticus*). *Aquac. Nutr.* 19, 629–640.
- Heilig, C.W., Stromski, M.E., Blumenfeld, J.D., Lee, J.P., Gullans, S.R., 1989. Characterization of the major brain osmolytes that accumulate in salt-loaded rats. *Am. J. Physiol.* 257, 1108–1116.
- Hiroi, J., McCormick, S.D., 2012. New insights into gill ionocyte and ion transporter function in euryhaline and diadromous fish. *Respir. Physiol. Neurobiol.* 184, 257–68.
- Hoar, W.S., 1988. 4 The Physiology of smolting salmonids. In: Hoar, W.S., Randall, D.J. (Ed.), *Fish Physiology*. Academic Press, New York, pp. 275–343.
- Hoffmann, E.K., Hendil, K.B., 1976. The role of amino acids and taurine in isosmotic intracellular regulation in Ehrlich ascites mouse tumour cells. *J. Comp. Physiol. ? B* 108, 279–286.
- Hoffmann, E.K., Lambert, I.H., Simonsen, L.O., 1988. Mechanisms in volume regulation in Ehrlich ascites tumor cells. *Kidney Blood Press. Res.* 11, 221–247.
- Hollien, J., 2013. Evolution of the unfolded protein response. *Biochim. Biophys. Acta* 1833, 2458–2463.
- Huggins, A.K., Skutsch, G., Baldwin, E., 1969. Ornithine-urea cycle enzymes in teleostean fish. *Comp. Biochem. Physiol.* 28, 587–602.
- Huxtable, R.J., 1992. Physiological actions of taurine. *Physiol. Rev.* 72, 101–63.
- Hwang, P.-P., Lee, T.-H., 2007. New insights into fish ion regulation and mitochondrion-rich cells. *Comp. Biochem. Physiol. Part A Mol. Integr. Physiol.* 148, 479–497.
- ICES, 2016. ICES WGNAS REPORT 2016 International Council for the Exploration of the Sea Conseil International pour l'Exploration de la Mer 30.
- Igboeli, O.O., Fast, M.D., Heumann, J., Burka, J.F., 2012. Role of P-glycoprotein in emamectin benzoate (SLICE®) resistance in sea lice, *Lepeophtheirus salmonis*. *Aquaculture* 344–349, 40–47.
- Jenkinson, C.P., Grody, W.W., Cederbaum, S.D., 1996. Comparative properties of arginases. *Comp. Biochem. Physiol. B. Biochem. Mol. Biol.* 114, 107–132.

- Jensen, L.B., 2015. Nutritional and environmental impacts on the skin and mucus condition in Atlantic salmon (*Salmo salar* L.). University of Bergen.
- Johansson, L.-H., Timmerhaus, G., Afanasyev, S., Jørgensen, S.M., Krasnov, A., 2016. Smoltification and seawater transfer of Atlantic salmon (*Salmo salar* L.) is associated with systemic repression of the immune transcriptome. *Fish Shellfish Immunol.* 58, 33–41.
- Johnston, C.E., Eales, J.G., 1967. Purines in the integument of the Atlantic Salmon (*Salmo salar*) during parr-smolt transformation. *J. Fish. Res. Board Canada* 24, 955–964.
- Jyonouchi, H., 1994. Nucleotide actions on humoral immune responses. *J. Nutr.* 124, 138–143.
- Kalujnaia, S., Cramb, G., 2009. Regulation of expression of the myo-inositol monophosphatase 1 gene in osmoregulatory tissues of the European eel *Anguilla anguilla* after seawater acclimation. *Ann. N. Y. Acad. Sci.* 1163, 433–436.
- Kalujnaia, S., Gellatly, S. a, Hazon, N., Villasenor, A., Yancey, P.H., Cramb, G., 2013. Seawater acclimation and inositol monophosphatase isoform expression in the European eel (*Anguilla anguilla*) and Nile tilapia (*Oreochromis niloticus*). *Am. J. Physiol. Regul. Integr. Comp. Physiol.* 305, R369-84.
- Kalujnaia, S., McVee, J., Kasciukovic, T., Stewart, A.J., Cramb, G., 2010. A role for inositol monophosphatase 1 (IMPA1) in salinity adaptation in the euryhaline eel (*Anguilla anguilla*). *FASEB J.* 24, 3981–3991.
- Kalujnaia, S., McWilliam, I.S., Zaguinaiko, V.A., Feilen, A.L., Nicholson, J., Hazon, N., Cutler, C.P., Balment, R.J., Cossins, A.R., Hughes, M., Cramb, G., 2007. Salinity adaptation and gene profiling analysis in the European eel (*Anguilla anguilla*) using microarray technology. *Gen. Comp. Endocrinol.* 152, 274–80.
- Kalujnaia, S., Osborne, C.J., Cramb, G., 2009. Osmolytes and osmoregulation in the euryhaline European eel, *Anguilla anguilla*. *Comp. Biochem. Physiol. Part A Mol. Integr. Physiol.*
- Karathanasis, S.K., Oettgen, P., Haddad, I.A., Antonarakis, S.E., 1986. Structure, evolution, and polymorphisms of the human apolipoprotein A4 gene (APOA4). *Proc. Natl. Acad. Sci. U. S. A.* 83, 8457–8461.
- Kaser, A., Lee, A.-H., Franke, A., Glickman, J.N., Zeissig, S., Tilg, H., Nieuwenhuis, E.E.S., Higgins, D.E., Schreiber, S., Glimcher, L.H., Blumberg, R.S., 2008. XBP1 links ER stress to intestinal inflammation and confers genetic risk for human inflammatory bowel disease. *Cell* 134, 743–756.
- Keenan, T.Y., Patton, S., 1995. The structure of milk: Implications for sampling and storage A. The milk lipid globule membrane. In: R.G. Jensen (Ed.), *Handbook of Milk Composition*. Academic Press, New York, New York, pp. 5–50.
- Kelley, Eric E, Khoo, N.K.H., Hundley, N.J., Malik, U.Z., Freeman, B.A., Tarpey, M.M., 2010. Hydrogen peroxide is the major oxidant product of xanthine oxidase. *Free Radic. Biol. Med.* 48, 493–8.
- Kelley, Eric E., Khoo, N.K.H., Hundley, N.J., Malik, U.Z., Freeman, B.A., Tarpey, M.M., 2010. Hydrogen peroxide is the major oxidant product of xanthine oxidase. *Free Radic. Biol. Med.* 48, 493–498.

- Kelley, K.M., 1993. Experimental diabetes mellitus in a teleost fish. I. Effect of complete isletectomy and subsequent hormonal treatment on metabolism in the goby, *Gillichthys mirabilis*. *Endocrinology* 132, 2689–2695.
- Khan, S., Bano, Z., Singh, L.R., Hassan, M.I., Islam, A., Ahmad, F., 2013. Why is glycine not a part of the osmoticum in the urea-rich cells? *Protein Pept. Lett.* 20, 61–70.
- Khani, S., Tayek, J.A., 2001. Cortisol increases gluconeogenesis in humans: its role in the metabolic syndrome. *Clin. Sci.* 101, 739–47.
- Kidder, G.W., Petersen, C.W., Preston, R.L., 2006. Energetics of osmoregulation: II. Water flux and osmoregulatory work in the euryhaline fish, *Fundulus heteroclitus*. *J. Exp. Zool. A. Comp. Exp. Biol.* 305, 318–327.
- Kim, Y., Ke, F., Zhang, Q.-Y., 2009. Effect of  $\beta$ -glucan on activity of antioxidant enzymes and Mx gene expression in virus infected grass carp. *Fish Shellfish Immunol.* 27, 336–340.
- Kimura, Y., Kawasaki, S., Yoshimoto, H., Takegawa, K., 2010. Glycine betaine biosynthesized from glycine provides an osmolyte for cell growth and spore germination during osmotic stress in *Myxococcus xanthus*. *J. Bacteriol.* 192, 1467–1470.
- Kiron, V., 2012. Fish immune system and its nutritional modulation for preventive health care. *Anim. Feed Sci. Technol.* 173, 111–133.
- Kleene, R., Dartsch, H., Kern, H.-F., 1999. The secretory lectin ZG16p mediates sorting of enzyme proteins to the zymogen granule membrane in pancreatic acinar cells. *Eur. J. Cell Biol.* 78, 79–90.
- Kostecki, P.T., 1982. The effect of osmotic and ion-osmotic stresses on the mortality of rainbow trout (*Salmo gairdneri*) 15–17.
- Kraus, L.M., Kraus, A.P., 2001. Carbamoylation of amino acids and proteins in uremia. *Kidney Int.* 59, 102–107.
- Krogdahl, Å., Bakke-McKellep, A.M., Baeverfjord, G., 2003. Effects of graded levels of standard soybean meal on intestinal structure, mucosal enzyme activities, and pancreatic response in Atlantic salmon (*Salmo salar* L.). *Aquac. Nutr.* 9, 361–371.
- Król, E., Douglas, A., Tocher, D.R., Crampton, V.O., Speakman, J.R., Secombes, C.J., Martin, S.A.M., 2016. Differential responses of the gut transcriptome to plant protein diets in farmed Atlantic salmon. *BMC Genomics* 17.
- Kultz, D., 2012. The combinatorial nature of osmosensing in fishes. *Physiology* 27, 259–275.
- Kurosaki, M., Bolis, M., Fratelli, M., Barzago, M.M., Pattini, L., Perretta, G., Terao, M., Garattini, E., 2013. Structure and evolution of vertebrate aldehyde oxidases: from gene duplication to gene suppression. *Cell. Mol. Life Sci.* 70, 1807–1830.
- Lambert, I.H., Hoffmann, E.K., 1993. Regulation of taurine transport in Ehrlich ascites tumor cells. *J. Membr. Biol.* 131, 67–79.
- Lane, R.P., Crosskey, R.W., 1993. Medical insects and arachnids, Medical and Veterinary Entomology. Blackwell Publishing Ltd.
- Lanyi, J.K., 1974. Salt-dependent properties of proteins from extremely halophilic bacteria. *Bacteriol. Rev.* 38, 272–290.

- Lavery, G., Skadhauge, E., 2012. Adaptation of teleosts to very high salinity. *Comp. Biochem. Physiol. Part A Mol. Integr. Physiol.* 163, 1–6.
- Law, R.O., 1991. Amino acids as volume-regulatory osmolytes in mammalian cells. *Comp. Biochem. Physiol. Part A Physiol.* 99, 263–277.
- Law, R.O., 1994. Regulation of mammalian brain cell volume. *J. Exp. Zool.* 268, 90–96.
- Le Bras, Y., Dechamp, N., Krieg, F., Filangi, O., Guyomard, R., Boussaha, M., Bovenhuis, H., Pottinger, T.G., Prunet, P., Le Roy, P., Quillet, E., 2011. Detection of QTL with effects on osmoregulation capacities in the rainbow trout (*Oncorhynchus mykiss*). *BMC Genet.* 12, 46.
- Leclercq, E., Davie, A., Migaud, H., 2014. Delousing efficiency of farmed ballan wrasse (*Labrus bergylta*) against *Lepeophtheirus salmonis* infecting Atlantic salmon (*Salmo salar*) post-smolts. *Pest Manag. Sci.* 70, 1274–1282.
- Leclercq, E., Dick, J.R., Taylor, J.F., Bell, J.G., Hunter, D., Migaud, H., 2010a. Seasonal variations in skin pigmentation and flesh quality of atlantic salmon (*Salmo salar* L.): Implications for quality management. *J. Agric. Food Chem.* 58, 7036–7045.
- Leclercq, E., Taylor, J.F., Migaud, H., 2010b. Morphological skin colour changes in teleosts. *Fish Fish.* 11, 159–193.
- Levy-Lior, A., Shimoni, E., Schwartz, O., Gavish-Regev, E., Oron, D., Oxford, G., Weiner, S., Addadi, L., 2010. Guanine-Based biogenic photonic-crystal arrays in fish and spiders. *Adv. Funct. Mater.* 20, 320–329.
- Li, J., Yin, H., Bibus, D.M., Byelashov, O.A., 2016. The role of Omega-3 docosapentaenoic acid in pregnancy and early development. *Eur. J. Lipid Sci. Technol.* 118, 1692–1701.
- Li, P., Mai, K., Trushenski, J., Wu, G., 2009. New developments in fish amino acid nutrition: towards functional and environmentally oriented aquafeeds. *Amino Acids* 37, 43–53.
- Liu, C.-L., Watson, A.M., Place, A.R., Jagus, R., 2017. Taurine biosynthesis in a fish liver cell line (ZFL) adapted to a serum-free medium. *Mar. Drugs* 15.
- López-Bojórquez, L., Villalobos, P., García-G., C., Orozco, A., Valverde-R., C., 2007. Functional identification of an osmotic response element (ORE) in the promoter region of the killifish deiodinase 2 gene (FhDio2). *J. Exp. Biol.* 210, 3126–3132.
- Love, D.C., Fry, J.P., Li, X., Hill, E.S., Genello, L., Semmens, K., Thompson, R.E., 2015. Commercial aquaponics production and profitability: Findings from an international survey. *Aquaculture* 435, 67–74.
- Lumsden, J.S., Ostland, V.E., Byrne, P.J., Ferguson, H.W., 1993. Detection of a distinct gill-surface antibody response following horizontal infection and bath challenge of brook trout *Salvelinus fontinalis* with *Flavobacterium branchiophilum*, the causative agent of bacterial gill disease., *Diseases of Aquatic Organisms*. Inter-Research Science Center.
- Lumsden, J.S., Ostland, V.E., MacPhee, D.D., Ferguson, H.W., 1995. Production of gill-associated and serum antibody by rainbow trout (*Oncorhynchus mykiss*) following immersion immunization with acetone-killed *Flavobacterium branchiophilum* and the relationship to protection from experimental challenge. *Fish Shellfish Immunol.* 5, 151–165.

- Mackie, P.M., Gharbi, K., Ballantyne, J.S., McCormick, S.D., Wright, P. a., 2007.  $\text{Na}^+/\text{K}^+/\text{2Cl}^-$  cotransporter and CFTR gill expression after seawater transfer in smolts (0+) of different Atlantic salmon (*Salmo salar*) families. *Aquaculture* 272, 625–635.
- Marine Scotland, 2014. An assessment of the benefits to Scotland of aquaculture.
- Marine Scotland, 2015. Scotland's national marine plan - a single framework for managing our seas.
- Marine Scotland, n.d. Salmon [WWW Document]. URL <http://www.gov.scot/Topics/marine/marine-environment/species/fish/freshwater/salmon> (accessed 8.2.17).
- Marshall, W.S., 2012. Osmoregulation in estuarine and intertidal fishes, Euryhaline Fishes, *Fish Physiology*. Elsevier.
- Marshall, W.S., 2013. 8. Osmoregulation in estuarine and intertidal fishes. In: McCormick, S.D., Farrell, A.P., Brauner, C.J. (Eds.), *Fish Physiology*. Academic Press, pp. 395–434.
- Martin, H.M., Hancock, J.T., Salisbury, V., Harrison, R., 2004. Role of xanthine oxidoreductase as an antimicrobial agent. *Infect. Immun.* 72, 4933–4939.
- Mashoof, S., Criscitiello, M.F., 2016. Fish immunoglobulins. *Biology (Basel)*. 5, 45.
- Massa, A.E., Paredi, M.E., Crupkin, M., 2002. Nucleotide catabolism in cold stored adductor muscle of scallop (*Zygochlamys patagonica*). *J. Food Biochem.* 26, 295–305.
- McCormick, S.D., 1993. Methods for nonlethal gill biopsy and measurement of  $\text{Na}^+$ ,  $\text{K}^+$ -ATPase activity. *Can. J. Fish. Aquat. Sci.* 50, 656–658.
- McCormick, S.D., 2009. Evolution of the hormonal control of animal performance: Insights from the seaward migration of salmon. *Integr. Comp. Biol.* 49, 408–422.
- McCormick, S.D., 2012. Smolt physiology and endocrinology, Euryhaline Fishes, *Fish Physiology*. Elsevier.
- McCormick, S.D., Cunjak, R.A., Dempson, B., O'Dea, M.F., Carey, J.B., 1999. Temperature-related loss of smolt characteristics in Atlantic salmon (*Salmo salar*) in the wild. *Can. J. Fish. Aquat. Sci.* 56, 1649–1667.
- McCormick, S.D., Hansen, L.P., Quinn, T.P., Saunders, R.L., 1998. Movement, migration, and smolting of Atlantic salmon (*Salmo salar*). *Can. J. Fish. Aquat. Sci.* 55, 77–92.
- McCormick, S.D., Regish, A.M., Christensen, A.K., 2009. Distinct freshwater and seawater isoforms of  $\text{Na}^+/\text{K}^+$ -ATPase in gill chloride cells of Atlantic salmon. *J. Exp. Biol.* 212, 3994–4001.
- McCormick, S.D., Regish, A.M., Christensen, A.K., Björnsson, B.T., 2013. Differential regulation of sodium-potassium pump isoforms during smolt development and seawater exposure of Atlantic salmon. *J. Exp. Biol.* 216, 1142–1151.
- McCormick, S.D., Saunders, R.L., 1987. Preparatory physiological adaptations for marine life of salmonids: Osmoregulation, growth, and metabolism. *Am. Fish. Soc. Symp.* 1, 211–229.
- McCormick, S.D., Shrimpton, J.M., Moriyama, S., Björnsson, B.T., 2007. Differential hormonal responses of Atlantic salmon parr and smolt to increased daylength: A

- possible developmental basis for smolting. *Aquaculture* 273, 337–344.
- McCoy, R., Haviland, D.L., Molmenti, E.P., Ziambaras, T., Wetsel, R.A., Perlmutter, D.H., 1995. N-formylpeptide and complement C5a receptors are expressed in liver cells and mediate hepatic acute phase gene regulation. *J. Exp. Med.* 182, 207–217.
- McGeer, J.C., Wright, P.A., Wood, C.M., Wilkie, M.P., Mazur, C.F., Iwama, G.K., 1994. Notes: Nitrogen excretion in four species of fish from an alkaline lake. *Trans. Am. Fish. Soc.* 123, 824–829.
- McGuire, A., Aluru, N., Takemura, A., Weil, R., Wilson, J.M., Vijayan, M.M., 2010. Hyperosmotic shock adaptation by cortisol involves upregulation of branchial osmotic stress transcription factor 1 gene expression in Mozambique Tilapia. *Gen. Comp. Endocrinol.* 165, 321–329.
- Mello, C.C., Barrick, D., 2003. Measuring the stability of partly folded proteins using TMAO. *Protein Sci.* 12, 1522–1529.
- Mendel, R.R., 2013. The molybdenum cofactor. *J. Biol. Chem.* 288, 13165–13172.
- Merrifield, D.L., Dimitroglou, A., Bradley, G., Baker, R.T.M., Davies, S.J., 2010. Probiotic applications for rainbow trout (*Oncorhynchus mykiss* Walbaum) I. Effects on growth performance, feed utilization, intestinal microbiota and related health criteria. *Aquac. Nutr.* 16, 504–510.
- Merrifield, Daniel L., Dimitroglou, A., Foey, A., Davies, S.J., Baker, R.T.M., Bøggwald, J., Castex, M., Ringø, E., 2010. The current status and future focus of probiotic and prebiotic applications for salmonids. *Aquaculture* 302, 1–18.
- Metcalf, N.B., 1998. The interaction between behavior and physiology in determining life history patterns in Atlantic salmon (*Salmo salar*). *Can. J. Fish. Aquat. Sci.* 55, 93–103.
- Meyer, R.A., 1988. A linear model of muscle respiration explains monoexponential phosphocreatine changes. *Am. J. Physiol.* 254, 548–553.
- Michell, R.H., 2008. Inositol derivatives: evolution and functions. *Nat. Rev. Mol. Cell Biol.* 9, 151–61.
- Mihaylova, M.M., Shaw, R.J., 2011. The AMP-activated protein kinase (AMPK) signaling pathway coordinates cell growth, autophagy, & metabolism. *Nat. Cell Biol.* 13, 1016–1023.
- Moffitt, C.M., Cajas-Cano, L., 2014. Blue Growth: The 2014 FAO state of world fisheries and aquaculture 2415, 10–12.
- Mommsen, T.P., 2000. Glucagon-like peptide-1 in fishes: the liver and beyond. *Am. Zool.* 40, 259–268.
- Mommsen, T.P., Vijayan, M.M., Moon, T.W., 1999. Cortisol in teleosts: dynamics, mechanisms of action, and metabolic regulation. *Rev. Fish Biol. Fish.* 9, 211–268.
- Mommsen, T.P., Walsh, P.J., 1989. Evolution of urea synthesis in vertebrates: the piscine connection. *Science* (80-. ). 243, 72–75.
- Moon, T.W., 2001. Glucose intolerance in teleost fish: fact or fiction? *Comp. Biochem. Physiol. Part B Biochem. Mol. Biol.* 129, 243–249.

- Morgan, J.D., Sakamoto, T., Grau, E.G., Iwama, G.K., 1997. Physiological and respiratory responses of the Mozambique tilapia (*Oreochromis mossambicus*) to salinity acclimation. *Comp. Biochem. Physiol. Part A Physiol.* 117A, 391–398.
- Moriwaki, Y., Yamamoto, T., Higashino, K., 1999. Enzymes involved in purine metabolism—a review of histochemical localization and functional implications. *Histol. Histopathol.* 14, 1321–1340.
- Moriyama, T., Garcia-Perez, A., Olson, A.D., Burg, M.B., 1991. Intracellular betaine substitutes for sorbitol in protecting renal medullary cells from hypertonicity. *Am. J. Physiol.* 260, 494–497.
- Munnik, T., Vermeer, J.E.M., 2010. Osmotic stress-induced phosphoinositide and inositol phosphate signalling in plants. *Plant. Cell Environ.* 33, 655–69.
- Munro, L.A., Wallace, I.S., 2015. Scottish fish farm production survey 2014.
- Nakayama, Y., Peng, T., Sands, J.M., Bagnasco, S.M., 2000. The TonE/TonEBP pathway mediates tonicity-responsive regulation of UT-A urea transporter expression. *J. Biol. Chem.* 275, 38275–80.
- NASCO, 2014. 2014 Report of the thirty-first annual meeting of the council. Saint-Malo, France.
- NASCO, n.d. NASCO ~ The North Atlantic Salmon Conservation Organization [WWW Document]. URL <http://www.nasco.int/atlanticsalmon.html> (accessed 8.2.17).
- Navarro, I., Leibush, B., Moon, T.W., Plisetskaya, E.M., Baños, N., Méndez, E., Planas, J. V., Gutiérrez, J., 1999. Insulin, insulin-like growth factor-I (IGF-I) and glucagon: the evolution of their receptors. *Comp. Biochem. Physiol. B. Biochem. Mol. Biol.* 122, 137–53.
- Nayak, S.K., 2010. Probiotics and immunity: a fish perspective. *Fish Shellfish Immunol.* 29, 2–14.
- Nicolas, D., Rochette, S., Llope, M., Licandro, P., 2014. Spatio-temporal variability of the North Sea cod recruitment in relation to temperature and zooplankton. *PLoS One* 9, e88447.
- Niklasson, L., Sundh, H., Olsen, R.-E., Jutfelt, F., Skjødt, K., Nilsen, T.O., Sundell, K.S., 2014. Effects of cortisol on the intestinal mucosal immune response during cohabitant challenge with IPNV in Atlantic Salmon (*Salmo salar*). *PLoS One* 9, e94288.
- Nilsen, T.O., Ebbesson, L.O.E., Madsen, S.S., McCormick, S.D., Andersson, E., Björnsson, B.T., Prunet, P., Stefansson, S.O., 2007. Differential expression of gill Na<sup>+</sup>,K<sup>+</sup>-ATPase alpha- and beta-subunits, Na<sup>+</sup>,K<sup>+</sup>,2Cl<sup>-</sup> cotransporter and CFTR anion channel in juvenile anadromous and landlocked Atlantic salmon *Salmo salar*. *J. Exp. Biol.* 210, 2885–2896.
- Nishimura, H., Fan, Z., 2003. Regulation of water movement across vertebrate renal tubules. *Comp. Biochem. Physiol. A. Mol. Integr. Physiol.* 136, 479–498.
- Nishino, Tomoko, Okamoto, K., Kawaguchi, Y., Hori, H., Matsumura, T., Eger, B.T., Pai, E.F., Nishino, Takeshi, 2005. Mechanism of the conversion of xanthine dehydrogenase to xanthine oxidase. *J. Biol. Chem.* 280, 24888–24894.
- Nozaki, Y., Tanford, C., 1963. The solubility of amino acids and related compounds in

- aqueous urea solutions. *J. Biol. Chem.* 238, 4074–4081.
- Nunes, A.J.P., Sá, M.V.C., Browdy, C.L., Vazquez-Anon, M., 2014. Practical supplementation of shrimp and fish feeds with crystalline amino acids. *Aquaculture* 431, 20–27.
- Nyström, T., 2005. Role of oxidative carbonylation in protein quality control and senescence. *EMBO J.* 24, 1311–1317.
- Oliva-Teles, a, 2012. Nutrition and health of aquaculture fish. *J. Fish Dis.* 35, 83–108.
- Özoğul, Y., Boğa, E.K., Tokur, B., Özoğul, F., 2011. Changes in biochemical, sensory and microbiological quality indices of common sole (*Solea solea*) from the Mediterranean Sea, during ice storage. *Turkish J. Fish. Aquat. Sci.* 11, 243–251.
- Pan, F., Zarate, J., Choudhury, A., Rupprecht, R., Bradley, T.M., 2004. Osmotic stress of salmon stimulates upregulation of a cold inducible RNA binding protein (CIRP) similar to that of mammals and amphibians. *Biochimie* 86, 451–461.
- Papworth, D.J., Marini, S., Conversi, A., 2016. A novel, unbiased analysis approach for investigating population dynamics: a case study on *Calanus finmarchicus* and its decline in the North Sea. *PLoS One* 11, e0158230.
- Parsegian, V.A., Bezrukov, S.M., Vodyanoy, I., 1995. Watching small molecules move: interrogating ionic channels using neutral solutes. *Biosci. Rep.* 15, 503–14.
- Pärt, P., Wright, P.A., Wood, C.M., 1998. Urea and water permeability in dogfish (*Squalus acanthias*) gills. *Biochem. Physiol* 119, 117–123.
- Pasantes-Morales, H., Lezama, R., Ramos-Mandujano, G., Tuz, K., 2006. Mechanisms of cell volume regulation in hypo-osmolality. *Am. J. Med.* 119, S4-11.
- Patrick, G.L., 2017. An introduction to medicinal chemistry, 6th ed. Oxford University Press, Oxford.
- Patton, S., Keenan, T.W., 1975. The milk fat globule membrane. *Biochim. Biophys. Acta* 415, 273–309.
- Pedersen, S.F., Hoffmann, E.K., Mills, J.W., 2001. The cytoskeleton and cell volume regulation. *Comp. Biochem. Physiol. Part A* 130, 385–399.
- Pelis, R.M., Zydlewski, J., Cormick, S.D.M.C., Ryan, M., Stephen, D., 2001a. Gill Na<sup>+</sup>-K<sup>+</sup>-2Cl<sup>-</sup> cotransporter abundance and location in Atlantic salmon: effects of seawater and smolting. *Am. J. Physiol. Regul. Integr. Comp. Physiol.* 4156, 1844–1852.
- Pelis, R.M., Zydlewski, J., McCormick, S.D., 2001b. Gill Na<sup>+</sup>-K<sup>+</sup>-2Cl<sup>-</sup>-cotransporter abundance and location in Atlantic salmon: effects of seawater and smolting. *Am. J. Physiol. - Regul. Integr. Comp. Physiol.* 280, 1844–1852.
- Peres, H., Lim, C., Klesius, P.H., 2004. Growth, chemical composition and resistance to *Streptococcus iniae* challenge of juvenile Nile tilapia (*Oreochromis niloticus*) fed graded levels of dietary inositol. *Aquaculture* 235, 423–432.
- Petronini, P.G., De Angelis, E.M., Borghetti, A.F., Wheelert, K.P., 1993. Effect of betaine on HSP70 expression and cell survival during adaptation to osmotic stress. *Biochem. J* 293, 553–558.

- Poland, A., Knutson, J.C., 1982. 2,3,7,8-Tetrachlorodibenzo- p -dioxin and related halogenated aromatic hydrocarbons: examination of the mechanism of toxicity. *Annu. Rev. Pharmacol. Toxicol.* 22, 517–554.
- Póo-Argüelles, P., Arias, A., Vilaseca, M.A., Ribes, A., Artuch, R., Sans-Fito, A., Moreno, A., Jakobs, C., Salomons, G., 2006. X-Linked creatine transporter deficiency in two patients with severe mental retardation and autism. *J. Inherit. Metab. Dis.* 29, 220–223.
- Puig, J.G., Torres, R.J., Mateos, F.A., Ramos, T.H., Arcas, J.M., Buño, A.S., O’Neill, P., 2001. The spectrum of hypoxanthine-guanine phosphoribosyltransferase (HPRT) deficiency. Clinical experience based on 22 patients from 18 Spanish families. *Medicine (Baltimore)*. 80, 102–12.
- Quan, R., 1992. Dietary nucleotides: potential for immune enhancement. In: Paubert-Braquet, M., Dupont, C., Poaoletti, R. (Eds.), *Foods, Nutrition and Immunity*. Karger, Dyn. Nutr. Res. Basel. Karger, New York, NY, pp. 13–21.
- Ramirez-Gomez, F., Greene, W., Rego, K., Hansen, J.D., Kataria, P., Bromage, E.S., 2017. Discovery and characterization of secretory IgD in rainbow trout: secretory IgD is produced through a novel splicing mechanism. *J. Immunol.* 7, 1341–1349.
- Rebl, A., Korytář, T., Köbis, J.M., Verleih, M., Krasnov, A., Jaros, J., Kühn, C., Köllner, B., Goldammer, T., 2014. Transcriptome profiling reveals insight into distinct immune responses to *Aeromonas salmonicida* in gill of two rainbow trout strains. *Mar. Biotechnol.* 16, 333–348.
- Rescher, U., Danielczyk, A., Markoff, A., Gerke, V., 2002. Functional activation of the formyl peptide receptor by a new endogenous ligand in human lung A549 cells. *J. Immunol.* 169, 1500–1504.
- Rescher, U., Gerke, V., 2004. Annexins – unique membrane binding proteins with diverse functions. *J. Cell Sci.* 117, 2631–2639.
- Ringø, E., Erik Olsen, R., Gonzalez Vecino, J.L., Wadsworth, S., Song, S.K., 2011. Use of immunostimulants and nucleotides in aquaculture: a review. *J. Mar. Sci. Res. Dev.* 2.
- Ripps, H., Shen, W., 2012. Review: taurine: a “very essential” amino acid. *Mol. Vis.* 18, 2673–86.
- Robertson, L.S., McCormick, S.D., 2012. Transcriptional profiling of the parr–smolt transformation in Atlantic salmon. *Comp. Biochem. Physiol. Part D Genomics Proteomics* 7, 351–60.
- Sacchi, R., Li, J., Villarreal, F., Gardell, A.M., Kültz, D., 2013. Salinity-induced regulation of the myo-inositol biosynthesis pathway in tilapia gill epithelium. *J. Exp. Biol.* 216, 4626–38.
- Saito, T., Nishino, T., 1989. Differences in redox and kinetic properties between NAD-dependent and O<sub>2</sub>-dependent types of rat liver xanthine dehydrogenase. *J. Biol. Chem.* 264, 10015–10022.
- Sakai, M., 1999. Current research status of fish immunostimulants. *Aquaculture* 172, 63–92.
- Sakai, M., Yoshida, T., Atusta, S., Kobayashi, M., 1995. Enhancement of resistance to vibriosis in rainbow trout, *Oncorhynchus mykiss* (Walbaum), by oral administration of *Clostridium butyricum* bacterin. *J. Fish Dis.* 18, 187–190.

- Saksida, S.M., Morrison, D., McKenzie, P., Milligan, B., Downey, E., Boyce, B., Eaves, A., 2013. Use of Atlantic salmon, *Salmo salar* L., farm treatment data and bioassays to assess for resistance of sea lice, *Lepeophtheirus salmonis*, to emamectin benzoate (SLICE<sup>®</sup>) in British Columbia, Canada. *J. Fish Dis.* 36, 515–520.
- Sangiao-Alvarellos, S., Arjona, F.J., Martín del Río, M.P., Míguez, J.M., Mancera, J.M., Soengas, J.L., 2005. Time course of osmoregulatory and metabolic changes during osmotic acclimation in *Sparus auratus*. *J. Exp. Biol.* 208, 4291–4304.
- Sangiao-Alvarellos, S., Laiz-Carrión, R., Guzmán, J.M., Martín del Río, M.P., Míguez, J.M., Mancera, J.M., Soengas, J.L., 2003. Acclimation of *S. aurata* to various salinities alters energy metabolism of osmoregulatory and nonosmoregulatory organs. *Am. J. Physiol. - Regul. Integr. Comp. Physiol.* 285, 897–907.
- Sauer, H., Wartenberg, M., Hescheler, J., 2001. Reactive oxygen species as intracellular messengers during cell growth and differentiation. *Cell. Physiol. Biochem.* 11, 173–86.
- Schulze, A., Battini, R., 2007. Pre-symptomatic treatment of creatine biosynthesis defects. In: Salomons, G.S., Wyss, M. (Eds.), *Creatine and Creatine Kinase in Health and Disease*. Springer Netherlands, Dordrecht, pp. 167–181.
- Scott, G.R., Brix, K. V., 2013. Evolution of salinity tolerance from transcriptome to physiological system. *Mol. Ecol.* 22, 3656–3658.
- Scottish Government, 2011. Scotland's National Marine Plan - Pre-consultation Draft.
- Seale, A.P., Watanabe, S., Grau, E.G., 2012. Osmoreception: perspectives on signal transduction and environmental modulation. *Gen. Comp. Endocrinol.* 176, 354–360.
- Seidelin, M., Madsen, S.S., Cutler, C.P., Cramb, G., 2001. Expression of gill vacuolar-type H<sup>+</sup>-ATPase B subunit, and Na<sup>+</sup>, K<sup>+</sup>-ATPase  $\alpha$ 1 and  $\beta$ 1 subunit messenger RNAs in smolting *Salmo salar*. *Zoolog. Sci.* 18, 315–324.
- Sharma, R., Perszyk, A.A., Marangi, D., Monteiro, C., Raja, S., 2003. Lethal neonatal carnitine palmitoyltransferase II deficiency: an unusual presentation of a rare disorder. *Am. J. Perinatol.* 20, 25–32.
- Shiau, S.-Y., Gabaudan, J., Lin, Y.-H., 2015. Dietary nucleotide supplementation enhances immune responses and survival to *Streptococcus iniae* in hybrid tilapia fed diet containing low fish meal. *Aquac. Reports* 2, 77–81.
- Shiau, S.-Y., Su, S.-L., 2005. Juvenile tilapia (*Oreochromis niloticus*×*Oreochromis aureus*) requires dietary myo-inositol for maximal growth. *Aquaculture* 243, 273–277.
- Silva, P., Solomon, R., Spokes, K., Epstein, F.H., 1977. Ouabain inhibition of gill Na-K-ATPase: Relationship to active chloride transport. *J. Exp. Zool.* 199, 419–426.
- Sinha, A.K., AbdElgawad, H., Zinta, G., Dasan, A.F., Rasoloniriana, R., Asard, H., Blust, R., De Boeck, G., 2015. Nutritional status as the key modulator of antioxidant responses induced by high environmental ammonia and salinity stress in European sea bass (*Dicentrarchus labrax*). *PLoS One* 10, e0135091.
- Smith, H.W., 1929. The Excretion of Ammonia and Urea by the Gills of Fish. *J. Biol. Chem.* 81, 727–742.
- Smith, M.D., Roheim, C.A., Crowder, L.B., Halpern, B.S., Turnipseed, M., Anderson, J.L.,

- Asche, F., Bourillón, L., Guttormsen, A.G., Khan, A., Liguori, L.A., McNevin, A., O'Connor, M.I., Squires, D., Tyedmers, P., Brownstein, C., Carden, K., Klinger, D.H., Sagarin, R., Selkoe, K.A., 2010. Economics. Sustainability and global seafood. *Science* (80- ). 327, 784–6.
- Soong, C.-L., Ogawa, J., Shimizu, S., 2001. Novel amidohydrolytic reactions in oxidative pyrimidine metabolism: analysis of the barbiturase reaction and discovery of a novel enzyme, ureidomalonase. *Biochem. Biophys. Res. Commun.* 286, 222–226.
- Souza, C.F., Verdi, C.M., Baldissera, M.D., Doleski, P.H., Vizzotto, B.S., Santos, R.C. V, Baldisserotto, B., 2017. Xanthine oxidase activity affects pro-oxidative and pro-inflammatory profiles in spleen of silver catfish experimentally infected with *Aeromonas caviae*. *Microb. Pathog.* 113, 25–28.
- Sozzani, S., Allavena, P., D'Amico, G., Luini, W., Bianchi, G., Kataura, M., Imai, T., Yoshie, O., Bonecchi, R., Mantovani, A., 1998. Cutting edge: differential regulation of chemokine receptors during dendritic cell maturation: a model for their trafficking properties. *J. Immunol.* 161, 1083–1086.
- SSPO, 2013. Sustainable Scottish Salmon - Scottish Salmon Farming Economic Report October 2013, Investing in sustainable jobs, communities and business.
- Staykov, Y., Spring, A.P., Denev, A.S., Sweetman, A.J., Denev, Á.S., Spring, P., Sweetman, J., 2007. Effect of a mannan oligosaccharide on the growth performance and immune status of rainbow trout (*Oncorhynchus mykiss*). *Aquac. Int.* 15, 153–161.
- Steenbergen, C., Hill, M.L., Jennings, R.B., 1985. Volume regulation and plasma membrane injury in aerobic, anaerobic, and ischemic myocardium in vitro. Effects of osmotic cell swelling on plasma membrane integrity. *Circ. Res.* 57, 864–875.
- Stefansson, S.O., Björnsson, B.T., Ebbesson, L.O., McCormick, S.D., 2008. Smoltification. In: Finn, R.N., Kapoor, B.G. (Eds.), *Fish Larval Physiology*. pp. 639–681.
- Stefansson, S.O., Nilsen, T.O., Ebbesson, L.O., Wargelius, A., Madsen, S.S., Th Björnsson, B., McCormick, S.D., 2007. Molecular mechanisms of continuous light inhibition of Atlantic salmon parr–smolt transformation. *Aquaculture* 273, 235–245.
- Street, T.O., Bolen, D.W., Rose, G.D., 2006. A molecular mechanism for osmolyte-induced protein stability. *Proc. Natl. Acad. Sci. U. S. A.* 103, 13997–4002.
- Subasinghe, R., 1997. Fish health and quarantine [WWW Document]. *Rev. State World Aquac.* FAO Fish. Dep. Rome. URL <http://www.fao.org/docrep/003/w7499e/w7499e23.htm>
- Sun, H.Q., Yamamoto, M., Mejillano, M., Yin, H.L., 1999. Gelsolin, a multifunctional actin regulatory protein. *J. Biol. Chem.* 274, 33179–33182.
- Sundh, H., Nilsen, T.O., Lindström, J., Hasselberg-Frank, L., Stefansson, S.O., McCormick, S.D., Sundell, K., 2014. Development of intestinal ion-transporting mechanisms during smoltification and seawater acclimation in Atlantic salmon *Salmo salar*. *J. Fish Biol.* 85, 1227–1252.
- Surette, M.E., Whelan, J., Broughton, K.S., Kinsella, J.E., 1992. Evidence for mechanisms of the hypotriglyceridemic effect of n – 3 polyunsaturated fatty acids. *Biochim. Biophys. Acta - Lipids Lipid Metab.* 1126, 199–205.

- Sveier, H., Nordas, H., Berge, G.E., Lied, E., 2001. Dietary inclusion of crystalline D- and L-methionine: effects on growth, feed and protein utilization, and digestibility in small and large Atlantic salmon (*Salmo salar* L.). *Aquac. Nutr.* 7, 169–181.
- Tacchi, L., Bickerdike, R., Douglas, A., Secombes, C.J., Martin, S. a. M., 2011. Transcriptomic responses to functional feeds in Atlantic salmon (*Salmo salar*). *Fish Shellfish Immunol.* 31, 704–715.
- Tacchi, L., Secombes, C.J., Bickerdike, R., Adler, M.A., Venegas, C., Takle, H., Martin, and S.A., 2012. Transcriptomic and physiological responses to fishmeal substitution with plant proteins in formulated feed in farmed Atlantic salmon (*Salmo salar*). *BMC Genomics* 13.
- Tacon, A.G.J., Metian, M., 2008. Global overview on the use of fish meal and fish oil in industrially compounded aquafeeds: Trends and future prospects. *Aquaculture* 285, 146–158.
- Tacon, A.G.J., Metian, M., Turchini, G.M., De Silva, S.S., 2010. Responsible aquaculture and trophic level implications to global fish supply. *Rev. Fish. Sci.* 18, 94–105.
- Tadiso, T.M., Sharma, A., Hordvik, I., 2011. Analysis of polymeric immunoglobulin receptor- and CD300-like molecules from Atlantic salmon. *Mol. Immunol.* 49, 462–473.
- Takagi, S., Takagi, Shusaku, Murata, H., Goto, T., Hayashi, M., Hatate, H., Endo, M., Yamashita, H., Ukawa, M., 2006. Hemolytic suppression roles of taurine in yellowtail *Seriola quinqueradiata* fed non-fishmeal diet based on soybean protein. *Fish. Sci.* 72, 546–555.
- Tateno, H., Yabe, R., Sato, T., Shibazaki, A., Shikanai, T., Gono, T., Narimatsu, H., Hirabayashi, J., 2012. Human ZG16p recognizes pathogenic fungi through non-self polyvalent mannose in the digestive system. *Glycobiology* 22, 210–220.
- Taylor, J.R., Grosell, M., 2006. Feeding and osmoregulation: dual function of the marine teleost intestine. *J. Exp. Biol.* 209, 2939–2951.
- Tejada, M., De las Heras, C., Kent, M., 2007. Changes in the quality indices during ice storage of farmed Senegalese sole (*Solea senegalensis*). *Eur. Food Res. Technol.* 225, 225–232.
- Terao, M., Romão, J.M., Leimkühler, S., Bolis, M., Fratelli, M., Coelho, C., Santos-Silva, T., Garattini, E., 2016. Structure and function of mammalian aldehyde oxidases. *Arch. Toxicol.* 90, 753–780.
- Torres, R.J., Prior, C., Puig, J.G., 2007. Efficacy and safety of allopurinol in patients with hypoxanthine-guanine phosphoribosyltransferase deficiency. *Metabolism* 56, 1179–1186.
- Torriglia, A., Martin, E., Jaadane, I., 2017. The hidden side of SERPINB1/Leukocyte Elastase Inhibitor. *Semin. Cell Dev. Biol.* 62, 178–186.
- Tse, W.K.F., 2014. The role of osmotic stress transcription factor 1 in fishes. *Front. Zool.* 11, 86.
- Tseng, Y.-C., Huang, C.-J., Chang, J.C.-H., Teng, W.-Y., Baba, O., Fann, M.-J., Hwang, P.-P., 2007. Glycogen phosphorylase in glycogen-rich cells is involved in the energy supply for ion regulation in fish gill epithelia. *Am J Physiol Regul Integr Comp Physiol*

293, 482–491.

- Tseng, Y.-C., Hwang, P.-P., 2008. Some insights into energy metabolism for osmoregulation in fish. *Comp. Biochem. Physiol. Part C* 148, 419–429.
- Uauy, R., 1994. Nonimmune system responses to dietary nucleotides. *J. Nutr.* 124, 157–159.
- Urquhart, N., Perry, T.L., Hansen, S., Kennedy, J., 1974. Passage of taurine into adult mammalian brain. *J. Neurochem.* 22, 871–2.
- Vijayan, M.M., Mommsen, T.P., Glémet, H.C., Moon, T.W., 1996. Metabolic effects of cortisol treatment in a marine teleost, the sea raven. *J. Exp. Biol.* 199, 1509–1514.
- Virág, L., Csaba, S., 2001. Purines inhibit poly(ADP-ribose) polymerase activation and modulate oxidant-induced cell death. *FASEB J.* 15, 99–107.
- Walker, G.C., Gunari, N.A., 2015. Compositions and methods for control of marine ectoparasites. WO 2015021534 A1.
- Wallimann, T., Wyss, M., Brdiczka, D., Nicolay, K., Eppenberger, H.M., 1992. Intracellular compartmentation, structure and function of creatine kinase isoenzymes in tissues with high and fluctuating energy demands: the “phosphocreatine circuit” for cellular energy homeostasis. *Biochem. J.* 281, 21–40.
- Walther, A., Riehemann, K., Gerke, V., 2000. A novel ligand of the formyl peptide receptor: annexin I regulates neutrophil extravasation by interacting with the FPR. *Mol. Cell* 5, 831–40.
- Wang, W., Sun, J., Liu, C., Xue, Z., 2017. Application of immunostimulants in aquaculture: current knowledge and future perspectives. *Aquac. Res.* 48, 1–23.
- Wehner, F., Olsen, H., Tinel, H., Kinne-Saffran, E., Kinne, R.K.H., 2003. Cell volume regulation: osmolytes, osmolyte transport, and signal transduction. *Rev. Physiol. Biochem. Pharmacol.* 148, 1–80.
- Wilkie, M.P., Wright, P.A., Iwama, G.K., Wood, C.M., 1993. The physiological responses of the Lahontan cutthroat trout (*Oncorhynchus Clarki Henshawi*), a resident of highly alkaline pyramid lake (pH 9.4), to challenge at pH 10. *J. Exp. Biol.* 175, 173–194.
- Willumsen, N., Skorve, J., Hexeberg, S., Rustan, A.C., Berge, R.K., 1993. The hypotriglyceridemic effect of eicosapentaenoic acid in rats is reflected in increased mitochondrial fatty acid oxidation followed by diminished lipogenesis. *Lipids* 28, 683–690.
- Willumsen, N., Vaagenes, H., Rustan, A.C., Grav, H., Lundquist, M., Skattebøl, L., Songstad, J., Berge, R.K., 1997. Enhanced hepatic fatty acid oxidation and upregulated carnitine palmitoyltransferase II gene expression by methyl 3-thiooctadeca-6,9,12,15-tetraenoate in rats. *J. Lipid Mediat. Cell Signal.* 17, 115–134.
- Wilson, M., Bengtén, E., Miller, N.W., Clem, L.W., Pasquier, L. Du, Warr, G.W., 1997. A novel chimeric Ig heavy chain from a teleost fish shares similarities to IgD. *Proc. Natl. Acad. Sci. USA* 94, 4593–4597.
- Wittmann, C., Chockley, P., Singh, S.K., Pase, L., Lieschke, G.J., Grabher, C., 2012. Hydrogen peroxide in inflammation: messenger, guide, and assassin. *Adv. Hematol.* 2012, 1–6.

- Wolff, S.D., Yancey, P.H., Stanton, T.S., Balaban, R.S., 1989. A simple HPLC method for quantitating major organic solutes of renal medulla. *Am. J. Physiol.* 256, 954–956.
- Woo, S.K., Lee, S. Do, Na, K.Y., Park, W.K., Kwon, H.M., 2002. TonEBP/NFAT5 stimulates transcription of HSP70 in response to hypertonicity. *Mol. Cell. Biol.* 22, 5753–60.
- Wood, C., Bergman, H., Laurent, P., Maina, J., Narahara, A., Walsh, P., 1994. Urea production, acid-base regulation and their interactions in the Lake Magadi tilapia, a unique teleost adapted to a highly alkaline environment. *J. Exp. Biol.* 189, 13–36.
- Wright, J.R., Bonen, A., Michael Conlon, J., Pohajdak, B., 2000. Glucose homeostasis in the teleost fish tilapia: insights from brockmann body xenotransplantation studies. *Am. Zool.* 40, 234–245.
- Wright, P.A., 1993. Nitrogen excretion and enzyme pathways for ureagenesis in freshwater tilapia (*Oreochromis niloticus*). *Physiol. Zool.* 66, 881–901.
- Wright, P.A., Land, M.D., 1998. Urea production and transport in teleost fishes. *Comp. Biochem. Physiol. Part A Mol. Integr. Physiol.* 119, 47–54.
- Wu, J.-Y., Prentice, H., 2010. Role of taurine in the central nervous system. *J. Biomed. Sci.* 17, 1–6.
- Wu, N., Liao, G.H., Li, D.F., Luo, Y.L., Zhong, G.M., 1991. The advantages of mosquito biocontrol by stocking edible fish in rice paddies. *Southeast Asian J. Trop. Med. Public Health* 22, 436–42.
- Xu, W.N., Liu, W. Bin, Lu, K. Le, Jiang, Y.Y., Li, G.F., 2012. Effect of trichlorfon on oxidative stress and hepatocyte apoptosis of *Carassius auratus gibelio* in vivo. *Fish Physiol. Biochem.* 38, 769–775.
- Yanagita, T., Han, S.-Y., Hu, Y., Nagao, K., Kitajima, H., Murakami, S., 2008. Taurine reduces the secretion of apolipoprotein B100 and lipids in HepG2 cells. *Lipids Health Dis.* 7, 38.
- Yancey, P., 2001. Water stress, osmolytes and proteins. *Am. Zool.* 41, 699–709.
- Yancey, P.H., 2005. Organic osmolytes as compatible, metabolic and counteracting cytoprotectants in high osmolarity and other stresses. *J. Exp. Biol.* 208, 2819–2830.
- Yancey, P.H., Clark, M.E., Hand, S.C., Bowlus, R.D., Somero, G.N., 1982. Living with water stress: evolution of osmolyte systems. *Science* (80- ). 217, 1214–1222.
- Yancey, P.H., Somero, G.N., 1979. Counteraction of urea destabilization of protein structure by methylamine osmoregulatory compounds of elasmobranch fishes. *Biochem. J.* 183, 317–323.
- Yegutkin, G.G., 2008. Nucleotide-and nucleoside-converting ectoenzymes: Important modulators of purinergic signalling cascade. *Biochim. Biophys. Acta* 1783, 673–694.
- Yin, H.L., Stull, J.T., 1999. Proteins that regulate dynamic actin remodeling in response to membrane signaling minireview series. *J. Biol. Chem.* 274, 32529–32530.
- Yudilevich, D.L., Boyd, C.A.R., 1987. Amino-acid transport in animal cells, 1st ed. Manchester University Press, Manchester.

- Zablocki, K., Millert, S.P.F., Garcia-Perez, A., Burg, A.M.B., 1991. Accumulation of glycerophosphocholine (GPC) by renal cells: Osmotic regulation of GPC:choline phosphodiesterase. *Proc. Natl. Acad. Sci. USA* 88, 7820–7824.
- Zhang, M., Bi, L.F., Fang, J.H., Su, X.L., Da, G.L., Kuwamori, T., Kagamimori, S., 2004a. Beneficial effects of taurine on serum lipids in overweight or obese non-diabetic subjects. *Amino Acids* 26, 267–71.
- Zhang, M., Izumi, I., Kagamimori, S., Sokejima, S., Yamagami, T., Liu, Z., Qi, B., 2004b. Role of taurine supplementation to prevent exercise-induced oxidative stress in healthy young men. *Amino Acids* 26, 203–207.
- Zhao, X., Gao, Y., Qi, M., 2014. Toxicity of phthalate esters exposure to carp (*Cyprinus carpio*) and antioxidant response by biomarker. *Ecotoxicology* 23, 626–632.
- Zydlewski, G.B., Zydlewski, J., 2012. Gill Na<sup>+</sup>,K<sup>+</sup>-ATPase of Atlantic salmon smolts in freshwater is not a predictor of long-term growth in seawater. *Aquaculture* 362–363, 121–126.
- Zydlewski, J., Wilkie, M.P., 2012. Freshwater to seawater transitions in migratory fishes. In: *Euryhaline Fishes, Fish Physiology*. Elsevier, pp. 253–326.

## Appendix 1 – Feeding trial growth data

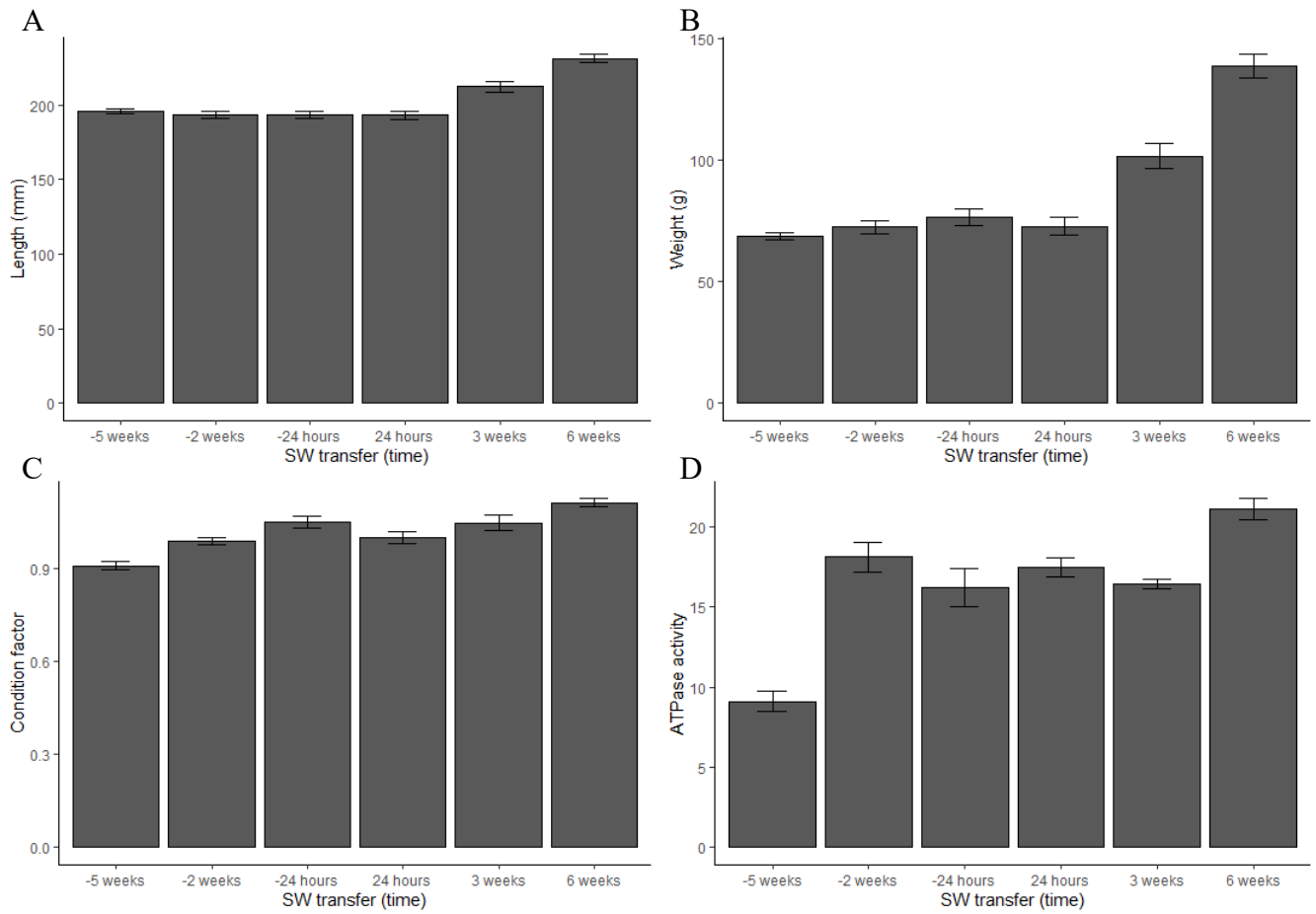


Figure A1.1. Mean length (A) weight (B) condition factor (C) and  $\text{Na}^+\text{K}^+$ -ATPase enzyme activity (D) throughout the feeding trial time course. Error bars represent standard error (n=19 or 20).

## Appendix 2 – Hypoxanthine and purine metabolism

### A2.1 Figures R code

```
#direct transfer trial
#data
nSWc <- NoSWChallengeR

#summary
library(dplyr)
my_summary <- nSWc %>%
  group_by(Days_To_SW_Transfer, Salinity) %>%
  summarise(n=n(),
            mean=mean(hypoxanthine_mmol),
            sd=sd(hypoxanthine_mmol),
            ) %>%
  mutate(se=sd/sqrt(n))

library(ggplot2)
#plot
MH.hyp.plot <- ggplot(my_summary, aes(x=Days_To_SW_Transfer, y=mean, fill = Salinity,
ymin=mean-se,ymax=mean+se))+
  geom_bar(stat = "identity", color = "black") +
  geom_errorbar(width=0.1, colour = "black")

MH.hyp.plot + scale_fill_grey() + theme_classic() +
  theme(panel.grid.major = element_blank(), panel.grid.minor = element_blank(),
        panel.background = element_blank(), axis.line = element_line(colour = "black"))+
  labs(x= "Days to SW transfer", y= "Hypoxanthine mmol/kg wet tissue")

#data
SWc <- SWChallengeR

#summary
my_summary2 <- SWc %>%
  group_by(Days_To_SW_Transfer, Salinity) %>%
  summarise(n=n(),
            mean=mean(hypoxanthine_mmol),
            sd=sd(hypoxanthine_mmol),
            ) %>%
  mutate(se=sd/sqrt(n))

#plot
MH.hyp.plot2 <- ggplot(my_summary2, aes(x=Days_To_SW_Transfer, y=mean, fill=Salinity,
ymin=mean-se, ymax=mean+se))+
  geom_bar(width = 0.9, color = "black", position=position_dodge(), stat = "identity")+
  geom_errorbar(position =position_dodge(0.9), width=0.1, colour = "black")

MH.hyp.plot2 + scale_fill_grey() + theme_classic() +
  theme(panel.grid.major = element_blank(), panel.grid.minor = element_blank(),
        panel.background = element_blank(), axis.line = element_line(colour = "black"))+
  labs(x= "Days to SW transfer", y= "Hypoxanthine mmol/kg wet tissue")

#feeding trial
```

```

#data
EWOS <- osmo_data_220219_w_diet_0

#summary
library(dplyr)
my_summary <- EWOS %>%
  group_by(Time_in_SW, Diet) %>%
  summarise(n=n(),
            mean=mean(Hypoxanthine),
            sd=sd(Hypoxanthine),
            ) %>%
  mutate(se=sd/sqrt(n))

library(ggplot2)

#plot
EWOS.hyp.plot <- ggplot(my_summary, aes(x=Time_in_SW, y=mean, fill = Diet, ymin=mean-
se,ymax=mean+se))+
  geom_bar(stat = "identity", color = "black", position = position_dodge()) +
  geom_errorbar(width=0.3, colour = "black", position = position_dodge(0.9))

EWOS.hyp.plot + scale_fill_grey() + theme_classic() +
  theme(panel.grid.major = element_blank(), panel.grid.minor = element_blank(),
        panel.background = element_blank(), axis.line = element_line(colour = "black"))+
  labs(x= "SW transfer (time)", y= "Hypoxanthine mmol/kg wet tissue")

#purine metabolism
#direct transfer trial
#data
MH_data <- MH_gene_expression

#AMPKa2a
library(dplyr)
AMPKa2a_summary <- MH_data %>%
  group_by(Time_in_SW) %>%
  summarise(n=n(),
            mean=mean(AMPKa2a),
            sd=sd(AMPKa2a),
            ) %>%
  mutate(se=sd/sqrt(n))

library(ggplot2)

#plot
MH.AMPKa2a.plot <- ggplot(AMPKa2a_summary, aes(x=Time_in_SW, y=mean, ymin=mean-
se,ymax=mean+se))+
  geom_bar(stat = "identity", color = "black", width = 0.5) +
  geom_errorbar(width=0.1, colour = "black")

MH.AMPKa2a.plot + scale_fill_grey() + theme_classic() +
  theme(panel.grid.major = element_blank(), panel.grid.minor = element_blank(),
        panel.background = element_blank(), axis.line = element_line(colour = "black"))+
  labs(x= "Time in SW", y= "Fold change in AMPKa2a expression")

#Hprt1
Hprt1_summary <- MH_data %>%
  group_by(Time_in_SW) %>%
  summarise(n=n(),
            mean=mean(Hprt1),
            sd=sd(Hprt1),

```

```

) %>%
mutate(se=sd/sqrt(n))

#plot
MH.Hprt1.plot <- ggplot(Hprt1_summary, aes(x=Time_in_SW, y=mean, ymin=mean-
se,ymax=mean+se))+
  geom_bar(stat = "identity", color = "black", width = 0.5) +
  geom_errorbar(width=0.1, colour = "black")

MH.Hprt1.plot + scale_fill_grey() + theme_classic() +
  theme(panel.grid.major = element_blank(), panel.grid.minor = element_blank(),
        panel.background = element_blank(), axis.line = element_line(colour = "black"))+
  labs(x= "Time in SW", y= "Fold change in Hprt1 expression")

#PNP5a
PNP5a_summary <- MH_data %>%
  group_by(Time_in_SW) %>%
  summarise(n=n(),
            mean=mean(PNP5a),
            sd=sd(PNP5a),
  ) %>%
  mutate(se=sd/sqrt(n))

#plot
MH.PNP5a.plot <- ggplot(PNP5a_summary, aes(x=Time_in_SW, y=mean, ymin=mean-
se,ymax=mean+se))+
  geom_bar(stat = "identity", color = "black", width = 0.5) +
  geom_errorbar(width=0.1, colour = "black")

MH.PNP5a.plot + scale_fill_grey() + theme_classic() +
  theme(panel.grid.major = element_blank(), panel.grid.minor = element_blank(),
        panel.background = element_blank(), axis.line = element_line(colour = "black"))+
  labs(x= "Time in SW", y= "Fold change in PNP5a expression")

#PNP5b
PNP5b_summary <- MH_data %>%
  group_by(Time_in_SW) %>%
  summarise(n=n(),
            mean=mean(PNP5b),
            sd=sd(PNP5b),
  ) %>%
  mutate(se=sd/sqrt(n))

#plot
MH.PNP5b.plot <- ggplot(PNP5b_summary, aes(x=Time_in_SW, y=mean, ymin=mean-
se,ymax=mean+se))+
  geom_bar(stat = "identity", color = "black", width = 0.5) +
  geom_errorbar(width=0.1, colour = "black")

MH.PNP5b.plot + scale_fill_grey() + theme_classic() +
  theme(panel.grid.major = element_blank(), panel.grid.minor = element_blank(),
        panel.background = element_blank(), axis.line = element_line(colour = "black"))+
  labs(x= "Time in SW", y= "Fold change in PNP5b expression")

#PNP6b
PNP6b_summary <- MH_data %>%
  group_by(Time_in_SW) %>%
  summarise(n=n(),
            mean=mean(PNP6b),

```

```

      sd=sd(PNP6b),
    ) %>%
    mutate(se=sd/sqrt(n))

#plot
MH.PNP6b.plot <- ggplot(PNP6b_summary, aes(x=Time_in_SW, y=mean, ymin=mean-
se,ymax=mean+se))+
  geom_bar(stat = "identity", color = "black", width = 0.5) +
  geom_errorbar(width=0.1, colour = "black")

MH.PNP6b.plot + scale_fill_grey() + theme_classic() +
  theme(panel.grid.major = element_blank(), panel.grid.minor = element_blank(),
    panel.background = element_blank(), axis.line = element_line(colour = "black"))+
  labs(x= "Time in SW", y= "Fold change in PNP6b expression")

#PNP6c
PNP6c_summary <- MH_data %>%
  group_by(Time_in_SW) %>%
  summarise(n=n(),
    mean=mean(PNP6c),
    sd=sd(PNP6c),
  ) %>%
  mutate(se=sd/sqrt(n))

#plot
MH.PNP6c.plot <- ggplot(PNP6c_summary, aes(x=Time_in_SW, y=mean, ymin=mean-
se,ymax=mean+se))+
  geom_bar(stat = "identity", color = "black", width = 0.5) +
  geom_errorbar(width=0.1, colour = "black")

MH.PNP6c.plot + scale_fill_grey() + theme_classic() +
  theme(panel.grid.major = element_blank(), panel.grid.minor = element_blank(),
    panel.background = element_blank(), axis.line = element_line(colour = "black"))+
  labs(x= "Time in SW", y= "Fold change in PNP6c expression")

#CNT3
CNT3_summary <- MH_data %>%
  group_by(Time_in_SW) %>%
  summarise(n=n(),
    mean=mean(CNT3),
    sd=sd(CNT3),
  ) %>%
  mutate(se=sd/sqrt(n))

#plot
MH.CNT3.plot <- ggplot(CNT3_summary, aes(x=Time_in_SW, y=mean, ymin=mean-
se,ymax=mean+se))+
  geom_bar(stat = "identity", color = "black", width = 0.5) +
  geom_errorbar(width=0.1, colour = "black")

MH.CNT3.plot + scale_fill_grey() + theme_classic() +
  theme(panel.grid.major = element_blank(), panel.grid.minor = element_blank(),
    panel.background = element_blank(), axis.line = element_line(colour = "black"))+
  labs(x= "Time in SW", y= "Fold change in CNT3 expression")
#feeding trial
#data
EWOSg <- EWOS_gene_ex_data_AHP_with_diet_0

library(dplyr)

```

```

AMPK_summary <- EWOSg %>%
  group_by(Time_in_SW, Diet) %>%
  summarise(n=n(),
            mean=mean(AMPKA2a),
            sd=sd(AMPKA2a),
            ) %>%
  mutate(se=sd/sqrt(n))

library(ggplot2)

#plot
EWOS.AMPK.plot <- ggplot(AMPK_summary, aes(x=Time_in_SW, y=mean, fill = Diet, ymin=mean-
se,ymax=mean+se))+
  geom_bar(stat = "identity", color = "black", position = position_dodge()) +
  geom_errorbar(width=0.3, colour = "black", position = position_dodge(0.9))

EWOS.AMPK.plot + scale_fill_grey() + theme_classic() +
  theme(panel.grid.major = element_blank(), panel.grid.minor = element_blank(),
        panel.background = element_blank(), axis.line = element_line(colour = "black"))+
  labs(x= "Time in SW", y= "Fold change in AMPKa2a expression")

Hprt_summary <- EWOSg %>%
  group_by(Time_in_SW, Diet) %>%
  summarise(n=n(),
            mean=mean(Hprt1),
            sd=sd(Hprt1),
            ) %>%
  mutate(se=sd/sqrt(n))

#plot
EWOS.Hprt.plot <- ggplot(Hprt_summary, aes(x=Time_in_SW, y=mean, fill = Diet, ymin=mean-
se,ymax=mean+se))+
  geom_bar(stat = "identity", color = "black", position = position_dodge()) +
  geom_errorbar(width=0.3, colour = "black", position = position_dodge(0.9))

EWOS.Hprt.plot + scale_fill_grey() + theme_classic() +
  theme(panel.grid.major = element_blank(), panel.grid.minor = element_blank(),
        panel.background = element_blank(), axis.line = element_line(colour = "black"))+
  labs(x= "Time in SW", y= "Fold change in Hprt1 expression")

PNP5a_summary <- EWOSg %>%
  group_by(Time_in_SW, Diet) %>%
  summarise(n=n(),
            mean=mean(`PNP5a1/2`),
            sd=sd(`PNP5a1/2`),
            ) %>%
  mutate(se=sd/sqrt(n))

#plot
EWOS.PNP5a.plot <- ggplot(PNP5a_summary, aes(x=Time_in_SW, y=mean, fill = Diet, ymin=mean-
se,ymax=mean+se))+
  geom_bar(stat = "identity", color = "black", position = position_dodge()) +
  geom_errorbar(width=0.3, colour = "black", position = position_dodge(0.9))

EWOS.PNP5a.plot + scale_fill_grey() + theme_classic() +
  theme(panel.grid.major = element_blank(), panel.grid.minor = element_blank(),
        panel.background = element_blank(), axis.line = element_line(colour = "black"))+
  labs(x= "Time in SW", y= "Fold change in PNP5a expression")

#nucleoside transporters

```

```

#data
nt <- EWOS_nucleoside_transporters

library(dplyr)
ENT1a_summary <- nt %>%
  group_by(Time_point, Diet) %>%
  summarise(n=n(),
            mean=mean(ENT1a),
            sd=sd(ENT1a),
            ) %>%
  mutate(se=sd/sqrt(n))

library(ggplot2)

#plot
EWOS.ENT1a.plot <- ggplot(ENT1a_summary, aes(x=Time_point, y=mean, fill = Diet, ymin=mean-
se,ymax=mean+se))+
  geom_bar(stat = "identity", color = "black", position = position_dodge()) +
  geom_errorbar(width=0.3, colour = "black", position = position_dodge(0.9))

EWOS.ENT1a.plot + scale_fill_grey() + theme_classic() +
  theme(panel.grid.major = element_blank(), panel.grid.minor = element_blank(),
        panel.background = element_blank(), axis.line = element_line(colour = "black"))+
  labs(x= "Time in SW", y= "Fold change in ENT1a expression")

ENT1b_summary <- nt %>%
  group_by(Time_point, Diet) %>%
  summarise(n=n(),
            mean=mean(ENT1b),
            sd=sd(ENT1b),
            ) %>%
  mutate(se=sd/sqrt(n))

#plot
EWOS.ENT1b.plot <- ggplot(ENT1b_summary, aes(x=Time_point, y=mean, fill = Diet, ymin=mean-
se,ymax=mean+se))+
  geom_bar(stat = "identity", color = "black", position = position_dodge()) +
  geom_errorbar(width=0.3, colour = "black", position = position_dodge(0.9))

EWOS.ENT1b.plot + scale_fill_grey() + theme_classic() +
  theme(panel.grid.major = element_blank(), panel.grid.minor = element_blank(),
        panel.background = element_blank(), axis.line = element_line(colour = "black"))+
  labs(x= "Time in SW", y= "Fold change in ENT1b expression")

ENT2_summary <- nt %>%
  group_by(Time_point, Diet) %>%
  summarise(n=n(),
            mean=mean(ENT2),
            sd=sd(ENT2),
            ) %>%
  mutate(se=sd/sqrt(n))

#plot
EWOS.ENT2.plot <- ggplot(ENT2_summary, aes(x=Time_point, y=mean, fill = Diet, ymin=mean-
se,ymax=mean+se))+
  geom_bar(stat = "identity", color = "black", position = position_dodge()) +
  geom_errorbar(width=0.3, colour = "black", position = position_dodge(0.9))

EWOS.ENT2.plot + scale_fill_grey() + theme_classic() +

```

```

theme(panel.grid.major = element_blank(), panel.grid.minor = element_blank(),
      panel.background = element_blank(), axis.line = element_line(colour = "black"))+
labs(x= "Time in SW", y= "Fold change in ENT2 expression")

ENT3_summary <- nt %>%
  group_by(Time_point, Diet) %>%
  summarise(n=n(),
            mean=mean(ENT3),
            sd=sd(ENT3),
  ) %>%
  mutate(se=sd/sqrt(n))

#plot
EWOS.ENT3.plot <- ggplot(ENT3_summary, aes(x=Time_point, y=mean, fill = Diet, ymin=mean-
se,ymax=mean+se))+
  geom_bar(stat = "identity", color = "black", position = position_dodge()) +
  geom_errorbar(width=0.3, colour = "black", position = position_dodge(0.9))

EWOS.ENT3.plot + scale_fill_grey() + theme_classic() +
  theme(panel.grid.major = element_blank(), panel.grid.minor = element_blank(),
        panel.background = element_blank(), axis.line = element_line(colour = "black"))+
  labs(x= "Time in SW", y= "Fold change in ENT3 expression")

ENT4_summary <- nt %>%
  group_by(Time_point, Diet) %>%
  summarise(n=n(),
            mean=mean(ENT4),
            sd=sd(ENT4),
  ) %>%
  mutate(se=sd/sqrt(n))

#plot
EWOS.ENT4.plot <- ggplot(ENT4_summary, aes(x=Time_point, y=mean, fill = Diet, ymin=mean-
se,ymax=mean+se))+
  geom_bar(stat = "identity", color = "black", position = position_dodge()) +
  geom_errorbar(width=0.3, colour = "black", position = position_dodge(0.9))

EWOS.ENT4.plot + scale_fill_grey() + theme_classic() +
  theme(panel.grid.major = element_blank(), panel.grid.minor = element_blank(),
        panel.background = element_blank(), axis.line = element_line(colour = "black"))+
  labs(x= "Time in SW", y= "Fold change in ENT4 expression")

CNT3_summary <- nt %>%
  group_by(Time_point, Diet) %>%
  summarise(n=n(),
            mean=mean(CNT3),
            sd=sd(CNT3),
  ) %>%
  mutate(se=sd/sqrt(n))

#plot
EWOS.CNT3.plot <- ggplot(CNT3_summary, aes(x=Time_point, y=mean, fill = Diet, ymin=mean-
se,ymax=mean+se))+
  geom_bar(stat = "identity", color = "black", position = position_dodge()) +
  geom_errorbar(width=0.3, colour = "black", position = position_dodge(0.9))

EWOS.CNT3.plot + scale_fill_grey() + theme_classic() +
  theme(panel.grid.major = element_blank(), panel.grid.minor = element_blank(),
        panel.background = element_blank(), axis.line = element_line(colour = "black"))+
  labs(x= "Time in SW", y= "Fold change in CNT3 expression")

```

```

#xanthine dehydrogenase
XDH <- XDH_qPCR_results

library(dplyr)
XDH_summary <- XDH %>%
  group_by(Time_in_SW, Diet) %>%
  summarise(n=n(),
            mean=mean(XDHex),
            sd=sd(XDHex),
            ) %>%
  mutate(se=sd/sqrt(n))

library(ggplot2)

#plot
XDH.plot <- ggplot(XDH_summary, aes(x=Diet, y=mean, fill = Time_in_SW, ymin=mean-
se,ymax=mean+se))+
  geom_bar(stat = "identity", color = "black", position = position_dodge(0.9)) +
  geom_errorbar(width=0.3, colour = "black", position = position_dodge(0.9))

XDH.plot + scale_fill_grey() + theme_classic() +
  theme(panel.grid.major = element_blank(), panel.grid.minor = element_blank(),
        panel.background = element_blank(), axis.line = element_line(colour = "black"))+
  labs(x= "Diet", y= "Fold change in XDH expression", fill = "Time in SW")

```

## *A2.2 Analysis R code*

```

#direct transfer trial
#Time course
#data
nSWc <- NoSWChallengeR

library(ggpubr)
library(car)
ggboxplot(nSWc, x = "timepoint", y = "hypoxanthine_mmol")
ggline(nSWc, x = "timepoint", y = "hypoxanthine_mmol", add = c("mean_se", "dotplot"))
nSWc.aov <- aov(hypoxanthine_mmol ~ timepoint, data = nSWc)
Anova(nSWc.aov, type = "II")
plot(nSWc.aov, 1)
leveneTest(hypoxanthine_mmol ~ timepoint, data = nSWc)
plot(nSWc.aov, 2)
nSWc.aov_residuals <- residuals(object = nSWc.aov)
shapiro.test(x = nSWc.aov_residuals)
nSWcpost <- TukeyHSD(x = nSWc.aov, 'timepoint', conf.level = 0.95)
nSWcpost

#SW challenge
SWc <- SWChallengeR
ggboxplot(SWc, x = "Days_To_SW_Transfer", y = "hypoxanthine_mmol", color = "Salinity")
ggline(SWc, x = "Days_To_SW_Transfer", y = "hypoxanthine_mmol", add = c("mean_se", "dotplot"),
color = "Salinity")
hypSW.aov <- aov(hypoxanthine_mmol ~ Days_To_SW_Transfer * Salinity, data = SWc)
Anova(hypSW.aov, type = "II")
plot(hypSW.aov, 1)
leveneTest(hypoxanthine_mmol ~ Days_To_SW_Transfer * Salinity, data = SWc)
plot(hypSW.aov, 2)

```

```

hypSW.aov_residuals <- residuals(object = hypSW.aov)
shapiro.test(x = hypSW.aov_residuals)
totSWP <- TukeyHSD(totSW.aov, conf.level = 0.95)
totSWP

#data
SWcO <- SWChallengeRoutlier
ggboxplot(SWcO, x = "Days_To_SW_Transfer", y = "hypoxanthine_mmol", color = "Salinity")
ggline(SWcO, x = "Days_To_SW_Transfer", y = "hypoxanthine_mmol", add = c("mean_se", "dotplot"),
color = "Salinity")
hypSW2.aov <- aov(hypoxanthine_mmol ~ Days_To_SW_Transfer * Salinity, data = SWcO)
Anova(hypSW2.aov, type = "II")
plot(hypSW2.aov, 1)
leveneTest(hypoxanthine_mmol ~ Days_To_SW_Transfer * Salinity, data = SWcO)
plot(hypSW2.aov, 2)
hypSW2.aov_residuals <- residuals(object = hypSW2.aov)
shapiro.test(x = hypSW2.aov_residuals)

#feeding trial

#distribution
E_osmo <- osmo_data_220219
E_osmo <- subset(osmo_data_220219, Diet == "1")
descdist(E_osmo$Hypoxanthine)
E_osmo <- subset(osmo_data_220219, Diet == "2")
descdist(E_osmo$Hypoxanthine)
E_osmo <- subset(osmo_data_220219, Diet == "3")
descdist(E_osmo$Hypoxanthine)
E_osmo <- subset(osmo_data_220219, Diet == "4")
descdist(E_osmo$Hypoxanthine)
E_osmo <- subset(osmo_data_220219, Diet == "5")
descdist(E_osmo$Hypoxanthine)
E_osmo <- subset(osmo_data_220219, Diet == "6")
descdist(E_osmo$Hypoxanthine)

Eo_data <- osmo_data_220219
library(car)
library(emmeans)
Ehyp_glm <- glm(Hypoxanthine ~ tp * Diet, family = Gamma(link = inverse), data = Eo_data)
summary(Ehyp_glm)
Anova(Ehyp_glm, type = "II", test = "F")
emmeans(Ehyp_glm, pairwise~tp)

#purine metabolism
#data
MH_data <- MH_gene_expression

library(ggpubr)
library(car)
library(emmeans)

#AMPKa2a
ggboxplot(MH_data, x = "Time_in_SW", y = "AMPKa2a")
ggline(MH_data, x = "Time_in_SW", y = "AMPKa2a", add = c("mean_se", "dotplot"))
lm.AMPK <- lm(AMPKa2a ~ Time_in_SW, data = MH_data)
summary(lm.AMPK)
MHA.aov <- Anova(lm.AMPK, type = "II")
MHA.aov
plot(MHA.aov, 1)

```

```

leveneTest(AMPKa2a ~ Time_in_SW, data = MH_data)
plot(MHA.aov,2)
MHA.aov_residuals <- residuals(MHA.aov)
shapiro.test(x = MHA.aov_residuals)

#Hprt1
ggboxplot(MH_data, x = "Time_in_SW", y = "Hprt1")
ggline(MH_data, x = "Time_in_SW", y = "Hprt1", add = c("mean_se", "dotplot"))
lm.Hprt <- lm(Hprt1 ~ Time_in_SW, data = MH_data)
summary(lm.Hprt)
MHH.avo <- Anova(lm.Hprt, type = "II")
MHH.avo
summary(MHH.avo)
plot(MHH.aov,1)
leveneTest(Hprt1 ~ Time_in_SW, data = MH_data)
plot(MHH.aov,2)
MHH.aov_residuals <- residuals(MHH.aov)
shapiro.test(x = MHH.aov_residuals)

#PNP5a
ggboxplot(MH_data, x = "Time_in_SW", y = "PNP5a")
ggline(MH_data, x = "Time_in_SW", y = "PNP5a", add = c("mean_se", "dotplot"))
lm.MHP5a <- lm(PNP5a ~ Time_in_SW, data = MH_data)
summary(lm.MHP5a)
plot(lm.MHP5a,1)
leveneTest(PNP5a ~ Time_in_SW, data = MH_data)
plot(MHP5a.aov,2)
MHP5a.aov_residuals <- residuals(MHP5a.aov)
shapiro.test(x = MHP5a.aov_residuals)
kruskal.test(PNP5a ~ Time_in_SW, data = MH_data)
library(FSA)
dunnTest(PNP5a ~ Time_in_SW, data = MH_data)

#PNP5b
ggboxplot(MH_data, x = "Time_in_SW", y = "PNP5b")
ggline(MH_data, x = "Time_in_SW", y = "PNP5b", add = c("mean_se", "dotplot"))
lm.MHP5b <- lm(PNP5b ~ Time_in_SW, data = MH_data)
summary(lm.MHP5b)
MHP5b.avo <- Anova(lm.MHP5b, type = "II")
MHP5b.avo
plot(lm.MHP5b,1)
leveneTest(PNP5b ~ Time_in_SW, data = MH_data)
plot(lm.MHP5b,2)
MHP5b.aov_residuals <- residuals(lm.MHP5b)
shapiro.test(x = MHP5b.aov_residuals)

#PNP6b
ggboxplot(MH_data, x = "Time_in_SW", y = "PNP6b")
ggline(MH_data, x = "Time_in_SW", y = "PNP6b", add = c("mean_se", "dotplot"))
lm.MHP6b <- lm(PNP6b ~ Time_in_SW, data = MH_data)
summary(lm.MHP6b)
MHP6b.avo <- Anova(lm.MHP6b, type = "II")
MHP6b.avo
plot(lm.MHP6b,1)
leveneTest(PNP6b ~ Time_in_SW, data = MH_data)
plot(lm.MHP6b,2)
MHP6b.aov_residuals <- residuals(lm.MHP6b.aov)
shapiro.test(x = MHP6b.aov_residuals)

#PNP6c

```

```

ggboxplot(MH_data, x = "Time_in_SW", y = "PNP6c")
ggline(MH_data, x = "Time_in_SW", y = "PNP6c", add = c("mean_se", "dotplot"))
lm.MHP6c <- lm(PNP6c ~ Time_in_SW, data = MH_data)
summary(lm.MHP6c)
MHP6c.avo <- Anova(lm.MHP6c, type = "II")
MHP6c.avo
plot(lm.MHP6c,1)
leveneTest(PNP6c ~ Time_in_SW, data = MH_data)
plot(lm.MHP6c,2)
MHP6c.aov_residuals <- residuals(lm.MHP6c)
shapiro.test(x = MHP6c.aov_residuals)
PNP6c.ph <- TukeyHSD(MHP6c.avo, conf.level = 0.95)

glm.MHP6c <- glm(PNP6c ~ Time_in_SW, data = MH_data)
glm.MHP6c
a6c <- Anova(glm.MHP6c, type = "II", test = "F")
a6c
emmeans(lm.MHP6c, pairwise~Time_in_SW)

#CNT3
ggboxplot(MH_data, x = "Time_in_SW", y = "CNT3")
ggline(MH_data, x = "Time_in_SW", y = "CNT3", add = c("mean_se", "dotplot"))
lm.CNT3 <- lm(CNT3 ~ Time_in_SW, data = MH_data)
summary(lm.CNT3)
MHC.aov <- Anova(lm.CNT3, type = "II")
MHC.aov
plot(lm.CNT3,1)
leveneTest(CNT3 ~ Time_in_SW, data = MH_data)
plot(lm.CNT3,2)
MHC.aov_residuals <- residuals(lm.CNT3)
shapiro.test(x = MHC.aov_residuals)

kruskal.test(CNT3 ~ Time_in_SW, data = MH_data)
library(FSA)
dunnTest(CNT3 ~ Time_in_SW, data = MH_data)

#feeding trial

#distribution
E_gene1 <- EWOS_gene_ex_data_AMPK_Hprt_PNP5a_corrected_270219
E_gene1 <- subset(EWOS_gene_ex_data_AMPK_Hprt_PNP5a_corrected_270219, Diet == "1")
descdist(E_gene1$AMPKA2ac)
E_gene1 <- subset(EWOS_gene_ex_data_AMPK_Hprt_PNP5a_corrected_270219, Diet == "2")
descdist(E_gene1$AMPKA2ac)
E_gene1 <- subset(EWOS_gene_ex_data_AMPK_Hprt_PNP5a_corrected_270219, Diet == "3")
descdist(E_gene1$AMPKA2ac)
E_gene1 <- subset(EWOS_gene_ex_data_AMPK_Hprt_PNP5a_corrected_270219, Diet == "4")
descdist(E_gene1$AMPKA2ac)
E_gene1 <- subset(EWOS_gene_ex_data_AMPK_Hprt_PNP5a_corrected_270219, Diet == "5")
descdist(E_gene1$AMPKA2ac)
E_gene1 <- subset(EWOS_gene_ex_data_AMPK_Hprt_PNP5a_corrected_270219, Diet == "6")
descdist(E_gene1$AMPKA2ac)

E_gene1 <- EWOS_gene_ex_data_AMPK_Hprt_PNP5a_corrected_270219
E_gene1 <- subset(EWOS_gene_ex_data_AMPK_Hprt_PNP5a_corrected_270219, Diet == "1")
descdist(E_gene1$Hprt1c)
E_gene1 <- subset(EWOS_gene_ex_data_AMPK_Hprt_PNP5a_corrected_270219, Diet == "2")
descdist(E_gene1$Hprt1c)
E_gene1 <- subset(EWOS_gene_ex_data_AMPK_Hprt_PNP5a_corrected_270219, Diet == "3")
descdist(E_gene1$Hprt1c)

```



```

E_gene2 <- subset(EWOS_gene_ex_data_AMPK_Hprt_PNP5a_corrected_270219, Diet == "6")
descdist(E_gene2$PNP6cc)

#data
AHP <- EWOS_gene_ex_data_AMPK_Hprt_PNP5a_corrected_270219

library(ggpubr)
library(car)
library(emmeans)

#AMPK
ggboxplot(AHP, x = "tp", y = "AMPKc", color = "diet", ylab = "AMPKa2a expression relative to
RPLP0", xlab = "Time point")
A_glm <- glm(AMPKc ~ tp * Diet, family = Gamma(link = inverse), data = AHP)
summary(A_glm)
Anova(A_glm, type = "II", test = "F")
emmeans(A_glm, pairwise~tp)
emmeans(A_glm, pairwise~tp|Diet)

#Hprt1
ggboxplot(AHP, x = "tp", y = "Hprt1", color = "Diet", ylab = "Hprt1 expression relative to RPLP0", xlab =
"Time point")
H_glm <- glm(Hprt1 ~ tp * Diet, family = Gamma(link = inverse), data = AHP)
summary(H_glm)
Anova(H_glm, type = "II", test = "F")
emmeans(H_glm, pairwise~tp)
emmeans(H_glm, pairwise~tp|Diet)

#PNP5a
ggboxplot(AHP, x = "tp", y = "PNP5a", color = "Diet", ylab = "PNP5a expression relative to RPLP0",
xlab = "Time point")
P5a_glm <- glm(PNP5a ~ tp * Diet, family = Gamma(link = inverse), data = AHP)
summary(P5a_glm)
Anova(P5a_glm, type = "II", test = "F")
emmeans(P5a_glm, pairwise~tp|Diet)
emmeans(P5a_glm, pairwise~tp)
emmeans(P5a_glm, pairwise~Diet)

#data
PNP <- EWOS_gene_ex_data_PNP5b_6b_6c_280219

#PNP5b
ggboxplot(PNP, x = "tp", y = "PNP5b", color = "Diet", ylab = "PNP5b expression relative to RPLP0",
xlab = "Time point")
P5b_glm <- glm(PNP5b ~ tp * Diet, family = Gamma(link = inverse), data = PNP)
summary(P5b_glm)
Anova(P5b_glm, type = "II", test = "F")
emmeans(P5b_glm, pairwise~tp|Diet)
emmeans(P5b_glm, pairwise~tp)

#PNP6b
ggboxplot(PNP, x = "tp", y = "PNP6b", color = "Diet", ylab = "PNP6b expression relative to RPLP0",
xlab = "Time point")
P6b_glm <- glm(PNP6b ~ tp * Diet, family = Gamma(link = inverse), data = PNP)
summary(P6b_glm)
Anova(P6b_glm, type = "II", test = "F")
emmeans(P6b_glm, pairwise~tp|Diet)
emmeans(P6b_glm, pairwise~tp)

#PNP6c

```

```

ggboxplot(PNP, x = "tp", y = "PNP6cc", color = "Diet", ylab = "PNP6b expression relative to RPLP0",
xlab = "Time point")
P6c_glm <- glm(PNP6cc ~ tp * Diet, family = Gamma(link = inverse), data = PNP)
summary(P6c_glm)
Anova(P6c_glm, type = "II", test = "F")
emmeans(P6c_glm, pairwise~tp|Diet)
emmeans(P6c_glm, pairwise~tp)

#nucleoside transporters
#data
nt <- EWOS_nucleoside_t_2

library(ggpubr)
library(car)
library(emmeans)

#ENT1a
ggboxplot(nt, x = "Time_point", y = "ENT1a", colour = "Diet")
ggline(nt, x = "Time_point", y = "ENT1a", add = c("mean_se", "dotplot"))
lm.ENT1a <- lm(ENT1a ~ Time_point, data = nt)
summary(lm.ENT1a)
MHE1a.aov <- Anova(lm.ENT1a, type = "II")
MHE1a.aov
plot(lm.ENT1a,1)
leveneTest(ENT1a ~ Time_point, data = nt)
plot(lm.ENT1a,2)
MHE1a.aov_residuals <- residuals(lm.ENT1a)
shapiro.test(x = MHE1a.aov_residuals)
kruskal.test(ENT1a ~ Time_point, data = nt)

E1a.glm <- glm(ENT1a ~ Time_point*Diet, family = Gamma(link = inverse), data = nt)
E1a.glm
a.E1a <- Anova(E1a.glm, type = "II", test = "F")
a.E1a
emmeans(E1a.glm, pairwise~Time_point*Diet)

#ENT1b
ggboxplot(nt, x = "Time_point", y = "ENT1b", colour = "Diet")
ggline(nt, x = "Time_point", y = "ENT1b", add = c("mean_se", "dotplot"))
lm.ENT1b <- lm(ENT1b ~ Time_point, data = nt)
summary(lm.ENT1b)
MHE1b.aov <- Anova(lm.ENT1b, type = "II")
MHE1b.aov
plot(lm.ENT1b,1)
leveneTest(ENT1b ~ Time_point, data = nt)
plot(lm.ENT1b,2)
MHE1b.aov_residuals <- residuals(lm.ENT1b)
shapiro.test(x = MHE1b.aov_residuals)
kruskal.test(ENT1b ~ Time_point, data = nt)

E1b.glm <- glm(ENT1b ~ Time_point*Diet, family = Gamma(link = inverse), data = nt)
E1b.glm
a.E1b <- Anova(E1b.glm, type = "II", test = "F")
a.E1b
emmeans(E1b.glm, pairwise~Time_point)

#ENT2
ggboxplot(nt, x = "Time_point", y = "ENT2", colour = "Diet")
ggline(nt, x = "Time_point", y = "ENT2", add = c("mean_se", "dotplot"))
lm.ENT2 <- lm(ENT2 ~ Time_point, data = nt)

```

```

summary(lm.ENT2)
MHE2.aov <- Anova(lm.ENT2, type = "II")
MHE2.aov
plot(lm.ENT2,1)
leveneTest(ENT2 ~ Time_point, data = nt)
plot(lm.ENT2,2)
MHE2.aov_residuals <- residuals(lm.ENT2)
shapiro.test(x = MHE2.aov_residuals)
kruskal.test(ENT2 ~ Time_point, data = nt)

E2.glm <- glm(ENT2 ~ Time_point*Diet, family = Gamma(link = inverse), data = nt)
E2.glm
a.E2 <- Anova(E2.glm, type = "II", test = "F")
a.E2
emmeans(E2.glm, pairwise~Time_point)

#ENT3
ggboxplot(nt, x = "Time_point", y = "ENT3", colour = "Diet")
ggline(nt, x = "Time_point", y = "ENT3", add = c("mean_se", "dotplot"))
lm.ENT3 <- lm(ENT3 ~ Time_point, data = nt)
summary(lm.ENT3)
MHE3.aov <- Anova(lm.ENT3, type = "II")
MHE3.aov
plot(lm.ENT3,1)
leveneTest(ENT3 ~ Time_point, data = nt)
plot(lm.ENT3,2)
MHE3.aov_residuals <- residuals(lm.ENT3)
shapiro.test(x = MHE3.aov_residuals)
kruskal.test(ENT3 ~ Time_point, data = nt)

E3.glm <- glm(ENT3c ~ Time_point*Diet, family = Gamma(link = inverse), data = nt)
E3.glm
a.E3 <- Anova(E3.glm, type = "II", test = "F")
a.E3
emmeans(E3.glm, pairwise~Time_point)

#ENT4
ggboxplot(nt, x = "Time_point", y = "ENT4", colour = "Diet")
ggline(nt, x = "Time_point", y = "ENT4", add = c("mean_se", "dotplot"))
lm.ENT4 <- lm(ENT4 ~ Time_point, data = nt)
summary(lm.ENT4)
MHE4.aov <- Anova(lm.ENT4, type = "II")
MHE4.aov
plot(lm.ENT4,1)
leveneTest(ENT4 ~ Time_point, data = nt)
plot(lm.ENT4,2)
MHE4.aov_residuals <- residuals(lm.ENT4)
shapiro.test(x = MHE4.aov_residuals)
kruskal.test(ENT4 ~ Time_point, data = nt)

E4.glm <- glm(ENT4c ~ Time_point*Diet, family = Gamma(link = inverse), data = nt)
E4.glm
a.E4 <- Anova(E4.glm, type = "II", test = "F")
a.E4
emmeans(E4.glm, pairwise~Time_point)

#CNT3
ggboxplot(nt, x = "Time_point", y = "CNT3", colour = "Diet")
ggline(nt, x = "Time_point", y = "CNT3", add = c("mean_se", "dotplot"))
lm.CNT3 <- lm(CNT3 ~ Time_point, data = nt)

```

```

summary(lm.CNT3)
MHC3.aov <- Anova(lm.CNT3, type = "II")
MHC3.aov
plot(lm.CNT3, 1)
leveneTest(CNT3 ~ Time_point, data = nt)
plot(lm.CNT3, 2)
CNT3.aov_residuals <- residuals(lm.CNT3)
shapiro.test(x = CNT3.aov_residuals)
kruskal.test(CNT3 ~ Time_point, data = nt)

c.glm <- glm(CNT3 ~ Time_point*Diet, family = Gamma(link = inverse), data = nt)
c.glm
C.aov <- Anova(c.glm, type = "II", test = "F")
C.aov
emmeans(c.glm, pairwise~Time_point*Diet)
emmeans(c.glm, pairwise~Time_point)

#Xanthine dehydrogenase
#data
XDH <- XDH_qPCR_results

ggboxplot(XDH, x = "tp", y = "XDHex", color = "Diet")
ggline(XDH, x = "tp", y = "XDHex", color = "Diet", add = c("mean_se", "dotplot"))
XDH.aov <- aov(XDHex ~ Time_in_SW, data = XDH)
Anova(XDH.aov, type = "II")
plot(XDH.aov, 1)
leveneTest(XDHex ~ Time_in_SW, data = XDH)
plot(XDH.aov, 2)
XDH.aov_residuals <- residuals(object = XDH.aov)
shapiro.test(x = XDH.aov_residuals)

ggboxplot(XDH, x = "Time_in_SW", y = "XDHex", color = "Diet", ylab = "XDH expression relative to
RPLP0", xlab = "Time in SW")
XDH_glm <- glm(XDHex ~ Time_in_SW * Diet, family = Gamma(link = inverse), data = XDH)
summary(XDH_glm)
Anova(XDH_glm, type = "II", test = "F")
emmeans(XDH_glm, pairwise~Time_in_SW|Diet)
emmeans(XDH_glm, pairwise~tp)

```

## Appendix 3 – Salmon xanthine dehydrogenase full sequence

CLUSTAL O (1.2.3) multiple sequence alignment for the 863bp fragment sequenced in this project from three clones and the SS2U007334 and SS2U045801 sequence fragments from SalmonDB.

```
SS2U007334      TCCTGACACCTGAGGAGGTTCTTTTATGTGTCCTGATCCCGTACACCAAGAAGGGTCAGT
SS2U045801      -----
XDH863c13T3revcomp -----
XDH863c13T7      -----
XDH863c11T3revcomp -----
XDH863c11T7      -----
XDH863c12T3      -----
XDH863c12T7revcomp -----
```

```
SS2U007334      ATTTTGCTGCCTATAAGCAGTCTCCTCGTCGTGAGGATGACATCAGCATTGTGACGTCAG
SS2U045801      -----
XDH863c13T3revcomp -----
XDH863c13T7      -----
XDH863c11T3revcomp -----
XDH863c11T7      -----
XDH863c12T3      -----
XDH863c12T7revcomp -----
```

```
SS2U007334      GGATGAGTGTGACATTCCGCCGAGGGGTCAACCGTCGTCGAAGCACCTGGCCCTTAGTTACG
SS2U045801      -----
XDH863c13T3revcomp -----GTC AACCGTCGTCGAAGCACCTGGCCCTTAGTTACG
XDH863c13T7      -----GTC AACCGTCGTCGAAGCACCTGGCCCTTAGTTACG
XDH863c11T3revcomp -----GTC AACCGTCGTCGAAGCACCTGGCCCTTAGTCACG
XDH863c11T7      -----GTC AACCGTCGTCGAAGCACCTGGCCCTTAGTCACG
XDH863c12T3      -----GTC AACCGTCGTCGAAGCACCTGGCCCTTAGTTACG
XDH863c12T7revcomp -----GTC AACCGTCGTCGAAGCACCTGGCCCTTAGTTACG
```

```
SS2U007334      GAGGGATGGCTGCTACTACCGTCATGGCCAAGAACACAGCCAGCAGACTTTTGGGAC----
SS2U045801      -----
XDH863c13T3revcomp GAGGGATGGCTGCTACTACCGTCATGGCCAAGAACACAGCCAGCAGACTTTTGGGACAAC
XDH863c13T7      GAGGGATGGCTGCTACTACCGTCATGGCCAAGAACACAGCCAGCAGACTTTTGGGACAAC
XDH863c11T3revcomp GAGGGATGGCTGCTACTACCGTCATGGCCAAGAACACAGCCAGCAGACTTTTGGGACAAC
XDH863c11T7      GAGGGATGGCTGCTACTACCGTCATGGCCAAGAACACAGCCAGCAGACTTTTGGGACAAC
XDH863c12T3      GAGGGATGGCTGCTACTACCGTCATGGCCAAGAACACAGCCAGCAGACTTTTGGGACAAC
XDH863c12T7revcomp GAGGGATGGCTGCTACTACCGTCATGGCCAAGAACACAGCCAGCAGACTTTTGGGACAAC
```

```
SS2U007334      -----
SS2U045801      -----
XDH863c13T3revcomp AATGGGGGGAAGAGCTTCTGCAGGATGCTTGTTCCCTCATTGGCTGAGGAGATGACCCTTC
XDH863c13T7      AATGGGGGGAAGAGCTTCTGCAGGATGCTTGTTCCCTCATTGGCTGAGGAGATGACCCTTC
XDH863c11T3revcomp AATGGGGGGAAGAGCTTCTGCAGGATGCTTGTTCCCTCATTGGCTGAGGAGATGACCCTTC
XDH863c11T7      AATGGGGGGAAGAGCTTCTGCAGGATGCTTGTTCCCTCATTGGCTGAGGAGATGACCCTTC
XDH863c12T3      AATGGGGGGAAGAGCTTCTGCAGGATGCTTGTTCCCTCATTGGCTGAGGAGATGACCCTTC
XDH863c12T7revcomp AATGGGGGGAAGAGCTTCTGCAGGATGCTTGTTCCCTCATTGGCTGAGGAGATGACCCTTC
```

```
SS2U007334      -----
SS2U045801      -----
XDH863c13T3revcomp ACCCCTCTGTGCCGGGTGGCATGGTGACCTACAGACGAACTCTGACCCTCAGCCTGTTTT
XDH863c13T7      ACCCCTCTGTGCCGGGTGGCATGGTGACCTACAGACGAACTCTGACCCTCAGCCTGTTTT
XDH863c11T3revcomp ACCCCTCTGTGCCGGGTGGCATGGTGACCTACAGACGAACTCTGACCCTCAGCCTGTTTT
XDH863c11T7      ACCCCTCTGTGCCGGGTGGCATGGTGACCTACAGACGAACTCTGACCCTCAGCCTGTTTT
XDH863c12T3      ACCCCTCTGTGCCGGGTGGCATGGTGACCTACAGACGAACTCTGACCCTCAGCCTGTTTT
XDH863c12T7revcomp ACCCCTCTGTGCCGGGTGGCATGGTGACCTACAGACGAACTCTGACCCTCAGCCTGTTTT
```

SS2U007334  
SS2U045801  
XDH863c13T3revcomp  
XDH863c13T7  
XDH863c11T3revcomp  
XDH863c11T7  
XDH863c12T3  
XDH863c12T7revcomp

-----  
-----  
ACAAGTTTACCTGACTGTACAACAGAACTGGCCAGTGAGGGTGCAGATATGGAGGGTG  
ACAAGTTTACCTGACTGTACAACAGAACTGGCCAGTGAGGGTGCAGATATGGAGGGTG  
ACAAGTTTACCTGACTGTACAACAGAACTGGCCAGTGAGGGTGCAGATATGGAGGGTG  
ACAAGTTTACCTGACTGTACAACAGAACTGGCCAGTGAGGGTGCAGATATGGAGGGTG  
ACAAGTTTACCTGACTGCACAACAGAACTGGCCAGTGAGGGTGCAGATATGGAGGGTG  
ACAAGTTTACCTGACTGCACAACAGAACTGGCCAGTGAGGGTGCAGATATGGAGGGTG

SS2U007334  
SS2U045801  
XDH863c13T3revcomp  
XDH863c13T7  
XDH863c11T3revcomp  
XDH863c11T7  
XDH863c12T3  
XDH863c12T7revcomp

-----  
-----  
TCAGGGCTGACTACATCAGTGCTACAGAGATCTACCACCAGACGTCCCCCTCCAGTGTCC  
TCAGGGCTGACTACATCAGTGCTACAGAGATCTACCACCAGACGTCCCCCTCCAGTGTCC  
TCAGGGCTGACTACATCAGTGCTACAGAGATCTACCACCAGACGTCCCCCTCCAGTGTCC  
TCAGGGCTGACTACATCAGTGCTACAGAGATCTACCACCAGACGTCCCCCTCCAGTGTCC  
TCAGGGCTGACTACATCAGTGCTACAGAGATCTACCACCAGACGTCCCCCTCCAGTGTCC  
TCAGGGCTGACTACATCAGTGCTACAGAGATCTACCACCAGACGTCCCCCTCCAGTGTCC

SS2U007334  
SS2U045801  
XDH863c13T3revcomp  
XDH863c13T7  
XDH863c11T3revcomp  
XDH863c11T7  
XDH863c12T3  
XDH863c12T7revcomp

-----  
-----  
-----GTTGGACGGTCAGAAGGAGGAGGACGTGGTGGGCCGTCCCATGA  
AGATTCTCCAGGCGGTTCCAGACGGTCAGAAGGAGGAGGACGTGGTGGGCCGTCCCATGA  
AGATTCTCCAGGCGGTTCCAGACGGTCAGAAGGAGGAGGACGTGGTGGGCCGTCCCATGA  
AGATTTTCCAGGCGGTTCCAGACGGTCAGAAGGAGGAGGACGTGGTGGGCCGTCCCATGA  
AGATTTTCCAGGCGGTTCCAGACGGTCAGAAGGAGGAGGACGTGGTGGGCCGTCCCATGA  
AGATTTTCCAGGCGGTTCCAGACGGTCAGAAGGAGGAGGACGTGGTGGGCCGTCCCATGA  
AGATTTTCCAGGCGGTTCCAGACGGTCAGAAGGAGGAGGACGTGGTGGGCCGTCCCATGA

SS2U007334  
SS2U045801  
XDH863c13T3revcomp  
XDH863c13T7  
XDH863c11T3revcomp  
XDH863c11T7  
XDH863c12T3  
XDH863c12T7revcomp

-----  
-----  
TGCACCTCTCAGCCATGAAGCAGGCGACGGGCGAGGCGGTTTACTGTGATGACATCCCTC  
TGCACCTCTCAGCCATGAAGCAGGCGACGGGCGAGGCGGTTTACTGTGATGACATCCCTC  
TGCACCTCTCAGCCATGAAGCAGGCGACGGGCGAGGCGGTTTACTGTGATGACATCCCTC  
TGCACCTCTCAGCCATGAAGCAGGCGACGGGCGAGGCGGTTTACTGTGATGACATCCCTC  
TGCACCTCTCAGCCATGAAGCAGGCGACGGGCGAGGCGGTTTACTGTGATGACATCCCTC  
TGCACCTCTCAGCCATGAAGCAGGCGACGGGCGAGGCGGTTTACTGTGATGACATCCCTC  
TGCACCTCTCAGCCATGAAGCAGGCGACGGGCGAGGCGGTTTACTGTGATGACATCCCTC

SS2U007334  
SS2U045801  
XDH863c13T3revcomp  
XDH863c13T7  
XDH863c11T3revcomp  
XDH863c11T7  
XDH863c12T3  
XDH863c12T7revcomp

-----  
-----  
TCTACGAGAATGAACTCTACCTCTGTCTTATAACCAGCACCAAGGCCACGCACGCATAC  
TCTACGAGAATGAACTCTACCTCTGTCTTATAACCAGCACCAAGGCCACGCACGCATAT  
TCTACGAGAATGAACTCTACCTCTGTCTTATAACCAGCACCAAGGCCACGCACGCATAT  
TCTACGAGAATGAACTCTACCTCTGTCTTATAACCAGCACCAAGGCCACGCACGCATAC  
TCTACGAGAATGAACTCTACCTCTGTCTTATAACCAGCACCAAGGCCACGCACGCATAC  
TCTACGAGAATGAACTCTACCTCTGTCTTATAACCAGCACCAAGGCCACGCACGCATAC  
TCTACGAGAATGAACTCTACCTCTGTCTTATAACCAGCACCAAGGCCACGCACGCATAC

SS2U007334  
SS2U045801  
XDH863c13T3revcomp  
XDH863c13T7  
XDH863c11T3revcomp  
XDH863c11T7  
XDH863c12T3  
XDH863c12T7revcomp

-----  
-----  
AGTCTATAGCTACATCGGAGGCAGAGAGTATGCCAGGTGTGGTGACGTGTGTGTTTGCCA  
AGTCTATAGATACATCGGAGGCAGAGAGTATGCCAGGTGTGGTGACGTGTGTGTTTGCCA  
AGTCTATAGATACATCGGAGGCAGAGAGTATGCCAGGTGTGGTGACGTGTGTGTTTGCCA  
AGTCTATAGATACATCGGAGGCAGAGAGTATGCCAGGTGTGGTGACGTGTGTGTTTGCCA  
AGTCTATAGATACATCGGAGGCAGAGAGTATGCCAGGTGTGGTGACGTGTGTGTTTGCCA  
AGTCTATAGATACATCGGAGGCAGAGAGTATGCCAGGTGTGGTGACGTGTGTGTTTGCCA  
AGTCTATAGATACATCGGAGGCAGAGAGTATGCCAGGTGTGGTGACGTGTGTGTTTGCCA

SS2U007334  
SS2U045801  
XDH863c13T3revcomp  
XDH863c13T7  
XDH863c11T3revcomp  
XDH863c11T7  
XDH863c12T3

-----  
-----  
AGGACATCCCTGGCAGCAACATGACAGGACCTATCATCTACGATGAGACTGTCTCTCGCTG  
AGGACATCCCTGGCAGCAACATGACAGGACCTATCATCTACGGTGAGACTGTCTCTCGCTG  
AGGACATCCCTGGCAGCAACATGACAGGACCTATCATCTACGGTGAGACTGTCTCTCGCTG  
AGGACATCCCTGGCAGCAACATGACAGGACCTATCATCTACGATGAGACTGTCTCTCGCTG  
AGGACATCCCTGGCAGCAACATGACAGGACCTATCATCTACGATGAGACTGTCTCTCGCTG  
AGGACATCCCTGGCAGCAACATGACAGGACCTATCATCTACGGTGAGACTGTCTCTCGCTG  
AGGACATCCCTGGCAGCAACATGACAGGACCTATCATCTACGATGAGACTGTCTCTCGCTG

XDH863c12T7revcomp	AGGACATCCCTGGCAGCAACATGACAGGACCTATCATCTACGATGAGACTGTCCTCGCTG
SS2U007334	-----
SS2U045801	TTGACACGGTGACCTGTGTGGGCCACATCATAGGAGCGGTAGTAGCAGACACTCAGGCTC
XDH863c13T3revcomp	TTGACACGGTGACCTGTGTGGGCCACATCATAGGAGCGGTAGTAGCAGACACTCAGGCTC
XDH863c13T7	TTGACACGGTGACCTGTGTGGGCCACATCATAGGAGCGGTAGTAGCAGACACTCAGGCTC
XDH863c11T3revcomp	TTGACACGGTGACCTGTGTGGGCCACATCATAGGAGCGGTAGTAGCAGACACTCAGGCTC
XDH863c11T7	TTGACACGGTGACCTGTGTGGGCCACATCATAGGAGCGGTAGTAGCAGACACTCAGGCTC
XDH863c12T3	TTGACACGGTGACCTGTGTGGGCCACATCATAGGAGCGGTAGTAGCAGACACTCAGGCTT
XDH863c12T7revcomp	TTGACACGGTGACCTGTGTGGGCCACATCATAGGAGCGGTAGTAGCAGACACTCAGGCTT
SS2U007334	-----
SS2U045801	ACGCTCAGAGAGCAGCCAAGGCTGTGAGGATCACCTACCAAGAACTACAGCCTGTAATCA
XDH863c13T3revcomp	ACGCTCAGAGAGCAGCCAAGGCTGTGAGGATCACCTACCAAGAACTACAGCCTGTAATCA
XDH863c13T7	ACGCTCAGAGAGCAGCCAAGGCTGTGAGGATCACCTACCAAGAACTACAGCCTGTAATCA
XDH863c11T3revcomp	ACGCTCAGAGAGCAGCCAAGGCTGTGAGGATCACCTACCAAGAACTACAGCCTGTAATCA
XDH863c11T7	ACGCTCAGAGAGCAGCCAAGGCTGTGAGGATCACCTACCAAGAACTACAGCCTGTAATCA
XDH863c12T3	ACGCTCAGAGAGCAGCCAAGGCTGTGAGGATCACCTACCAAGAACTACAGCCTGTAATCA
XDH863c12T7revcomp	ACGCTCAGAGAGCAGCCAAGGCTGTGAGGATCACCTACCAAGAACTACAGCCTGTAATCA
SS2U007334	-----
SS2U045801	TCACCATACAGGATGCCATTACACACCAGTCCTTCTTCCAGCCTGTTAGAACCATCCAGA
XDH863c13T3revcomp	TCACCATACAGGATGCCATTACACACCAGTCCTTCTTCCAGCCTGTTAGAACCATCCAGA
XDH863c13T7	TCACCATACAGGATGCCATTACACACCAGTCCTTCTTCCAGCCTGTTAGAACCATCCAGA
XDH863c11T3revcomp	TCACCATACAGGATGCCATTACACACCAGTCCTTCTTCCAGCCTGTTAGAACCATCCAGA
XDH863c11T7	TCACCATACAGGATGCCATTACACACCAGTCCTTCTTCCAGCCTGTTAGAACCATCCAGA
XDH863c12T3	TCACCATACAGGATGCCATTACACACCAGTCCTTCTTCCAGCCTGTTAGAACCATCCAGA
XDH863c12T7revcomp	TCACCATACAGGATGCCATTACACACCAGTCCTTCTTCCAGCCTGTTAGAACCATCCAGA
SS2U007334	-----
SS2U045801	GAGGAGACCTGGACCAAGGGTTACACACAGGCTGACCACATTCTGGAGGTGAGATGCATA
XDH863c13T3revcomp	GAGGAGACCTGGACCAAGGGTTACACACAGGCTGACCACATTCTGGAGG-----
XDH863c13T7	GAGGAGACCTGGACCAAGGGTTACACACAGGCTGACCACATTCTGGAGG-----
XDH863c11T3revcomp	GAGGAGACCTGGACCAAGGGTTACACACAGGCTGACCACATTCTGGAGG-----
XDH863c11T7	GAGGAGACCTGGACCAAGGGTTACACACAGGCTGACCACATTCTGGAGG-----
XDH863c12T3	GAGGAGACCTGGACCAAGGGTTACACACAGGCTGACCACATTCTGGAGG-----
XDH863c12T7revcomp	GAGGAGACCTGGACCAAGGGTTACACACAGGCTGACCACATTCTGGAGG-----
SS2U007334	-----
SS2U045801	TGGGAGGCCAGGAACACTTCTACCTGGAGACCAATGTTACTGTAGCTGTACCTAGAGGAG
XDH863c13T3revcomp	-----
XDH863c13T7	-----
XDH863c11T3revcomp	-----
XDH863c11T7	-----
XDH863c12T3	-----
XDH863c12T7revcomp	-----
SS2U007334	-----
SS2U045801	AGGATGGAGAGATGGAGCTGTTTGTCTCTACTCAGTCTGCTACCAAACCCAGTCTCTGG
XDH863c13T3revcomp	-----
XDH863c13T7	-----
XDH863c11T3revcomp	-----
XDH863c11T7	-----
XDH863c12T3	-----
XDH863c12T7revcomp	-----
SS2U007334	-----
SS2U045801	TAGCTAAGGCCTTGAGTGTCCCGCCAGTAGAGTGGTGATCAGAGTGAAGAGGATGGGAG
XDH863c13T3revcomp	-----
XDH863c13T7	-----
XDH863c11T3revcomp	-----

XDH863c11T7 -----  
XDH863c12T3 -----  
XDH863c12T7revcomp -----

SS2U007334 -----  
SS2U045801 GAGGATTCGGAGGGAAGGAGAGCAGGTCCACCACCCTGTCCACCCTGGTTCGCTGTGGCCG  
XDH863c13T3revcomp -----  
XDH863c13T7 -----  
XDH863c11T3revcomp -----  
XDH863c11T7 -----  
XDH863c12T3 -----  
XDH863c12T7revcomp -----

SS2U007334 -----  
SS2U045801 CTCAGAAGTTGAAGAGGCCAGTGAGATGTATGTTGGATAGAGATGAAGACATGCTGGTGA  
XDH863c13T3revcomp -----  
XDH863c13T7 -----  
XDH863c11T3revcomp -----  
XDH863c11T7 -----  
XDH863c12T3 -----  
XDH863c12T7revcomp -----

SS2U007334 -----  
SS2U045801 CGGGGGGGCGACACCCCTTCTATGGACGTTACAAGGTGGGCTTTATGAAGTCAGGTAAG  
XDH863c13T3revcomp -----  
XDH863c13T7 -----  
XDH863c11T3revcomp -----  
XDH863c11T7 -----  
XDH863c12T3 -----  
XDH863c12T7revcomp -----

SS2U007334 -----  
SS2U045801 TGGTGGCTCTAGAAGTGACCTACTACAACAACGCAGGAACTCCATAGACCTCTCTCTCT  
XDH863c13T3revcomp -----  
XDH863c13T7 -----  
XDH863c11T3revcomp -----  
XDH863c11T7 -----  
XDH863c12T3 -----  
XDH863c12T7revcomp -----

SS2U007334 -----  
SS2U045801 CAATCATGGAGCGTGCCTGTTCCACATGGAGAACTCTTACAGCATCGCTAACATTAGAG  
XDH863c13T3revcomp -----  
XDH863c13T7 -----  
XDH863c11T3revcomp -----  
XDH863c11T7 -----  
XDH863c12T3 -----  
XDH863c12T7revcomp -----

SS2U007334 -----  
SS2U045801 GGCGTGGCTACGTGTGTAAGACACACCTCCCGTCCAACACGGCCTTCCGAGGCTTTGGCG  
XDH863c13T3revcomp -----  
XDH863c13T7 -----  
XDH863c11T3revcomp -----  
XDH863c11T7 -----  
XDH863c12T3 -----  
XDH863c12T7revcomp -----

SS2U007334 -----  
SS2U045801 GGCCGAAGGAATGCTGATTGCTGAGAGTTGGATGAGTGACGTAGCTCTGAGCCTCGGGC  
XDH863c13T3revcomp -----  
XDH863c13T7 -----

XDH863c11T3revcomp -----  
XDH863c11T7 -----  
XDH863c12T3 -----  
XDH863c12T7revcomp -----

SS2U007334 -----  
SS2U045801 TGCCCTGCTGAACAGGTGCGTCGTCTGAACATGTACATCCAGGGAGAGACGACTCCCTACA  
XDH863c13T3revcomp -----  
XDH863c13T7 -----  
XDH863c11T3revcomp -----  
XDH863c11T7 -----  
XDH863c12T3 -----  
XDH863c12T7revcomp -----

SS2U007334 -----  
SS2U045801 GCCAGATCCTGGATCACATCACCCCTGGACCGCTGCTGGGACCAATGTCTGGAGATATCAT  
XDH863c13T3revcomp -----  
XDH863c13T7 -----  
XDH863c11T3revcomp -----  
XDH863c11T7 -----  
XDH863c12T3 -----  
XDH863c12T7revcomp -----

SS2U007334 -----  
SS2U045801 CCTTCAACCAACGCAGAGCTGGAGTAGAGACATACAACAGGGACCACCGTTGGACTAAGC  
XDH863c13T3revcomp -----  
XDH863c13T7 -----  
XDH863c11T3revcomp -----  
XDH863c11T7 -----  
XDH863c12T3 -----  
XDH863c12T7revcomp -----

SS2U007334 -----  
SS2U045801 GAGGGCTGTCTGTCTCCCCACCAAGTTCGGCATCAGCTTACCGCTCTCTTCTTAACC  
XDH863c13T3revcomp -----  
XDH863c13T7 -----  
XDH863c11T3revcomp -----  
XDH863c11T7 -----  
XDH863c12T3 -----  
XDH863c12T7revcomp -----

SS2U007334 -----  
SS2U045801 AGGCCGGTGC GTTGGCTCATATTTACACAGACGGCTCCGTGCTGTTGACTCACGGAGGGA  
XDH863c13T3revcomp -----  
XDH863c13T7 -----  
XDH863c11T3revcomp -----  
XDH863c11T7 -----  
XDH863c12T3 -----  
XDH863c12T7revcomp -----

SS2U007334 -----  
SS2U045801 CTGAGATGGGACAGGGTCTACACACCAAGATGGTACAGGTGGCCAGTAGGACCCTGGGTA  
XDH863c13T3revcomp -----  
XDH863c13T7 -----  
XDH863c11T3revcomp -----  
XDH863c11T7 -----  
XDH863c12T3 -----  
XDH863c12T7revcomp -----

SS2U007334 -----  
SS2U045801 TCCCCAGCAGTAAGATCCACATCACAGAGACCAGCACCAACACTGTTCCCAACACCAGCC

XDH863c13T3revcomp -----  
XDH863c13T7 -----  
XDH863c11T3revcomp -----  
XDH863c11T7 -----  
XDH863c12T3 -----  
XDH863c12T7revcomp -----

SS2U007334 -----  
SS2U045801 CTACTGCTGCCTCCGCTTCTCTGACCTCAATGGAGCCGCTGTGCATAATGCGTGTGAGA  
XDH863c13T3revcomp -----  
XDH863c13T7 -----  
XDH863c11T3revcomp -----  
XDH863c11T7 -----  
XDH863c12T3 -----  
XDH863c12T7revcomp -----

SS2U007334 -----  
SS2U045801 TCCTACTCCACCGTCTAGAACCCTACAAGACCAAGAATCCCAAAGGATGCTGGGAGGACT  
XDH863c13T3revcomp -----  
XDH863c13T7 -----  
XDH863c11T3revcomp -----  
XDH863c11T7 -----  
XDH863c12T3 -----  
XDH863c12T7revcomp -----

SS2U007334 -----  
SS2U045801 GGGTGAACACTGCCTACTTTGACCGGGTCAGTCTGTCTGCCAATGGATTCTACAAGACTC  
XDH863c13T3revcomp -----  
XDH863c13T7 -----  
XDH863c11T3revcomp -----  
XDH863c11T7 -----  
XDH863c12T3 -----  
XDH863c12T7revcomp -----

SS2U007334 -----  
SS2U045801 CAGACCTTGGTTATGACTTTGAGACCAACACAGGTCGTCCTTTCAACTACTTCAGTTATG  
XDH863c13T3revcomp -----  
XDH863c13T7 -----  
XDH863c11T3revcomp -----  
XDH863c11T7 -----  
XDH863c12T3 -----  
XDH863c12T7revcomp -----

SS2U007334 -----  
SS2U045801 GAGTGGCCTGCTCTGAGGTGGAGATAGACTGTCTGACCGGCAGCCACAAGAACATTGATA  
XDH863c13T3revcomp -----  
XDH863c13T7 -----  
XDH863c11T3revcomp -----  
XDH863c11T7 -----  
XDH863c12T3 -----  
XDH863c12T7revcomp -----

SS2U007334 -----  
SS2U045801 CGTCCATCGTCATTGATGTGGGAATAGTCTGAACCCAGCTCTGGACATAGGACAGGTAG  
XDH863c13T3revcomp -----  
XDH863c13T7 -----  
XDH863c11T3revcomp -----  
XDH863c11T7 -----  
XDH863c12T3 -----  
XDH863c12T7revcomp -----

SS2U007334  
SS2U045801  
XDH863c13T3revcomp  
XDH863c13T7  
XDH863c11T3revcomp  
XDH863c11T7  
XDH863c12T3  
XDH863c12T7revcomp

SS2U007334  
SS2U045801 GAGAGAATACATGCAGAGGAGAGAGAGAGAGAGAGAGAAGAGGGGAGAGACGGAG  
XDH863c13T3revcomp  
XDH863c13T7  
XDH863c11T3revcomp  
XDH863c11T7  
XDH863c12T3  
XDH863c12T7revcomp

SS2U007334  
SS2U045801 GGGGAAAAGAATAGGATAGCAAGCAGAGAGAGAGAAGGATAATCTGCTCCGAATTTATGC  
XDH863c13T3revcomp  
XDH863c13T7  
XDH863c11T3revcomp  
XDH863c11T7  
XDH863c12T3  
XDH863c12T7revcomp

SS2U007334  
SS2U045801 CATTAAATTCCTTTGTCTCAGTCTGAGGAAACGGCTGTTCTAATCAGTTTGAATGGAAT  
XDH863c13T3revcomp  
XDH863c13T7  
XDH863c11T3revcomp  
XDH863c11T7  
XDH863c12T3  
XDH863c12T7revcomp

SS2U007334  
SS2U045801 CAGAACCTAATCAGTTTGGAACTCTTACCCCAACGCACACATGGGTGGATCTCAGTGTA  
XDH863c13T3revcomp  
XDH863c13T7  
XDH863c11T3revcomp  
XDH863c11T7  
XDH863c12T3  
XDH863c12T7revcomp

SS2U007334  
SS2U045801 AAGGGGCTTCATCTCCTTGTCTCCTGTCTCTCATCCTTACTGAGCTGAGAACTCAGAACA  
XDH863c13T3revcomp  
XDH863c13T7  
XDH863c11T3revcomp  
XDH863c11T7  
XDH863c12T3  
XDH863c12T7revcomp

SS2U007334  
SS2U045801 ATATAGTGGATGTTGAGGGTCTGCTTTCACCTGTCCACTAGTTTTAGATCAGTGAAGAGG  
XDH863c13T3revcomp  
XDH863c13T7  
XDH863c11T3revcomp  
XDH863c11T7  
XDH863c12T3  
XDH863c12T7revcomp

SS2U007334  
SS2U045801 AAGAGACTATTAAGATGAAGCCCTGATCTGAAGCCTACCTGGCTATCAGCACTTTGACCT  
XDH863c13T3revcomp  
XDH863c13T7  
XDH863c11T3revcomp  
XDH863c11T7

XDH863c12T3 -----  
XDH863c12T7revcomp -----

SS2U007334 -----  
SS2U045801 AGGAAGCAATCCTAGTTCGGTCCGTCCCCCCCCCCCCCCCCCATAGCCACCATGGTGC  
XDH863c13T3revcomp -----  
XDH863c13T7 -----  
XDH863c11T3revcomp -----  
XDH863c11T7 -----  
XDH863c12T3 -----  
XDH863c12T7revcomp -----

SS2U007334 -----  
SS2U045801 ATTGTAAGTACAGGAGGCCACAGATTCTGATTGGAGGAAAGTTCGCTGAGGCCGC  
XDH863c13T3revcomp -----  
XDH863c13T7 -----  
XDH863c11T3revcomp -----  
XDH863c11T7 -----  
XDH863c12T3 -----  
XDH863c12T7revcomp -----

SS2U007334 -----  
SS2U045801 GGGAACTGACCAGACCAATCACACACCACATACAGTAACTGTTGAGGATCTTTTCAAGG  
XDH863c13T3revcomp -----  
XDH863c13T7 -----  
XDH863c11T3revcomp -----  
XDH863c11T7 -----  
XDH863c12T3 -----  
XDH863c12T7revcomp -----

SS2U007334 -----  
SS2U045801 GATGTCAATCATTTCAGACCTCACTGCATATCATATACAAATGACCTATGATCAATTCA  
XDH863c13T3revcomp -----  
XDH863c13T7 -----  
XDH863c11T3revcomp -----  
XDH863c11T7 -----  
XDH863c12T3 -----  
XDH863c12T7revcomp -----

SS2U007334 -----  
SS2U045801 ATATCTGTAATGATGCCTGTTATATACCTTTATCAAATAAGTCAACATCTTGTATTTGTG  
XDH863c13T3revcomp -----  
XDH863c13T7 -----  
XDH863c11T3revcomp -----  
XDH863c11T7 -----  
XDH863c12T3 -----  
XDH863c12T7revcomp -----

SS2U007334 -----  
SS2U045801 TGTAAAAGAGACAATATTTGTGTGTTAAATTTAATATAATTTCTAAATGTATATTTTAT  
XDH863c13T3revcomp -----  
XDH863c13T7 -----  
XDH863c11T3revcomp -----  
XDH863c11T7 -----  
XDH863c12T3 -----  
XDH863c12T7revcomp -----

SS2U007334 -----  
SS2U045801 ACATATTAATTTAATTTGACTTTTACTAGCAGAAATTGTGATTTTATTTAGTGGTTATGT  
XDH863c13T3revcomp -----  
XDH863c13T7 -----

XDH863c11T3revcomp -----  
XDH863c11T7 -----  
XDH863c12T3 -----  
XDH863c12T7revcomp -----

SS2U007334 -----  
SS2U045801 TGAGTGATAGAGATTTATTGAAATAATTTGTTTAATTTATTTTATGTGTAATCTCAGGTT  
XDH863c13T3revcomp -----  
XDH863c13T7 -----  
XDH863c11T3revcomp -----  
XDH863c11T7 -----  
XDH863c12T3 -----  
XDH863c12T7revcomp -----

SS2U007334 -----  
SS2U045801 TTAGTAAAACAGCACCATCTAGTGGCCGGTAGTGTGTCTGCAGTGCTACTGTTTTCAATT  
XDH863c13T3revcomp -----  
XDH863c13T7 -----  
XDH863c11T3revcomp -----  
XDH863c11T7 -----  
XDH863c12T3 -----  
XDH863c12T7revcomp -----

SS2U007334 -----  
SS2U045801 CAACTAGTTTTAATACTACTTGACTGACACAGAATAACTCAATTACTTCAACTACTTGATT  
XDH863c13T3revcomp -----  
XDH863c13T7 -----  
XDH863c11T3revcomp -----  
XDH863c11T7 -----  
XDH863c12T3 -----  
XDH863c12T7revcomp -----

SS2U007334 -----  
SS2U045801 AGACTGAGACAAATGAAAAGAGACTATCAAGCAATGGTGTAATTGAAGAATTTGCTTTAT  
XDH863c13T3revcomp -----  
XDH863c13T7 -----  
XDH863c11T3revcomp -----  
XDH863c11T7 -----  
XDH863c12T3 -----  
XDH863c12T7revcomp -----

SS2U007334 -----  
SS2U045801 TTTACATTTCAATAATGTACAGAGTTAGTCTGTTGAATAAACATACATTTCCAATCAAAA  
XDH863c13T3revcomp -----  
XDH863c13T7 -----  
XDH863c11T3revcomp -----  
XDH863c11T7 -----  
XDH863c12T3 -----  
XDH863c12T7revcomp -----

SS2U007334 -----  
SS2U045801 AAAAAAAAAAAAAAAAAAGA  
XDH863c13T3revcomp -----  
XDH863c13T7 -----  
XDH863c11T3revcomp -----  
XDH863c11T7 -----  
XDH863c12T3 -----  
XDH863c12T7revcomp -----

## Appendix 4 – Established osmolytes

### A4.1 Figures

```
#data
E.fig <- X260519_osmolyte_m_se_fig

library(ggplot2)

#total osmolyte
EWOS.tot.plot <- ggplot(E.fig, aes(x=Time_in_SW, y=total_osmolyte, fill = Diet, ymin=total_osmolyte-
total_osmolyte_SE,ymax=total_osmolyte+total_osmolyte_SE))+
  geom_bar(stat = "identity", color = "black", position = position_dodge(0.9)) +
  geom_errorbar(width=0.3, colour = "black", position = position_dodge(0.9))
EWOS.tot.plot + scale_fill_grey() + theme_classic() +
  theme(panel.grid.major = element_blank(), panel.grid.minor = element_blank(),
  panel.background = element_blank(), axis.line = element_line(colour = "black"))+
  labs(x= "SW transfer (time)", y= "Total osmolyte mmol/kg wet tissue")

#glucose
EWOS.glu.plot <- ggplot(E.fig, aes(x=Time_in_SW, y=Glucose, fill = Diet, ymin=Glucose-
Glucose_SE,ymax=Glucose+Glucose_SE))+
  geom_bar(stat = "identity", color = "black", position = position_dodge(0.9)) +
  geom_errorbar(width=0.3, colour = "black", position = position_dodge(0.9))
EWOS.glu.plot + scale_fill_grey() + theme_classic() +
  theme(panel.grid.major = element_blank(), panel.grid.minor = element_blank(),
  panel.background = element_blank(), axis.line = element_line(colour = "black"))+
  labs(x= "TSW transfer (time)", y= "Glucose mmol/kg wet tissue")

#Myoinositol
EWOS.myo.plot <- ggplot(E.fig, aes(x=Time_in_SW, y=Myoinositol, fill = Diet, ymin=Myoinositol-
Myoinositol_SE,ymax=Myoinositol+Myoinositol_SE))+
  geom_bar(stat = "identity", color = "black", position = position_dodge(0.9)) +
  geom_errorbar(width=0.3, colour = "black", position = position_dodge(0.9))
EWOS.myo.plot + scale_fill_grey() + theme_classic() +
  theme(panel.grid.major = element_blank(), panel.grid.minor = element_blank(),
  panel.background = element_blank(), axis.line = element_line(colour = "black"))+
  labs(x= "SW transfer (time)", y= "Myoinositol mmol/kg wet tissue")

#Taurine
EWOS.tau.plot <- ggplot(E.fig, aes(x=Time_in_SW, y=Taurine, fill = Diet, ymin=Taurine-
Taurine_SE,ymax=Taurine+Taurine_SE))+
  geom_bar(stat = "identity", color = "black", position = position_dodge(0.9)) +
  geom_errorbar(width=0.3, colour = "black", position = position_dodge(0.9))
EWOS.tau.plot + scale_fill_grey() + theme_classic() +
  theme(panel.grid.major = element_blank(), panel.grid.minor = element_blank(),
  panel.background = element_blank(), axis.line = element_line(colour = "black"))+
  labs(x= "SW transfer (time)", y= "Taurine mmol/kg wet tissue")

#GPC
EWOS.gpc.plot <- ggplot(E.fig, aes(x=Time_in_SW, y=GPC, fill = Diet, ymin=GPC-
GPC_SE,ymax=GPC+GPC_SE))+
  geom_bar(stat = "identity", color = "black", position = position_dodge(0.9)) +
```

```

geom_errorbar(width=0.3, colour = "black", position = position_dodge(0.9))
EWOS.gpc.plot + scale_fill_grey() + theme_classic() +
  theme(panel.grid.major = element_blank(), panel.grid.minor = element_blank(),
        panel.background = element_blank(), axis.line = element_line(colour = "black"))+
  labs(x= "SW transfer (time)", y= "GPC mmol/kg wet tissue")

```

#Urea

```

EWOS.ure.plot <- ggplot(E.fig, aes(x=Time_in_SW, y=Urea, fill = Diet, ymin=Urea-
Urea_SE,ymax=Urea+Urea_SE))+
  geom_bar(stat = "identity", color = "black", position = position_dodge(0.9)) +
  geom_errorbar(width=0.3, colour = "black", position = position_dodge(0.9))
EWOS.ure.plot + scale_fill_grey() + theme_classic() +
  theme(panel.grid.major = element_blank(), panel.grid.minor = element_blank(),
        panel.background = element_blank(), axis.line = element_line(colour = "black"))+
  labs(x= "SW transfer (time)", y= "Urea mmol/kg wet tissue")

```

#Alanine

```

EWOS.ala.plot <- ggplot(E.fig, aes(x=Time_in_SW, y=Alanine, fill = Diet, ymin=Alanine-
Alanine_SE,ymax=Alanine+Alanine_SE))+
  geom_bar(stat = "identity", color = "black", position = position_dodge(0.9)) +
  geom_errorbar(width=0.3, colour = "black", position = position_dodge(0.9))
EWOS.ala.plot + scale_fill_grey() + theme_classic() +
  theme(panel.grid.major = element_blank(), panel.grid.minor = element_blank(),
        panel.background = element_blank(), axis.line = element_line(colour = "black"))+
  labs(x= "SW transfer (time)", y= "Alanine mmol/kg wet tissue")

```

#Betaine

```

EWOS.bet.plot <- ggplot(E.fig, aes(x=Time_in_SW, y=Betaine, fill = Diet, ymin=Betaine-
Betaine_SE,ymax=Betaine+Betaine_SE))+
  geom_bar(stat = "identity", color = "black", position = position_dodge(0.9)) +
  geom_errorbar(width=0.3, colour = "black", position = position_dodge(0.9))
EWOS.bet.plot + scale_fill_grey() + theme_classic() +
  theme(panel.grid.major = element_blank(), panel.grid.minor = element_blank(),
        panel.background = element_blank(), axis.line = element_line(colour = "black"))+
  labs(x= "SW transfer (time)", y= "Betaine mmol/kg wet tissue")

```

#Creatine

```

EWOS.cre.plot <- ggplot(E.fig, aes(x=Time_in_SW, y=Creatine, fill = Diet, ymin=Creatine-
Creatine_SE,ymax=Creatine+Creatine_SE))+
  geom_bar(stat = "identity", color = "black", position = position_dodge(0.9)) +
  geom_errorbar(width=0.3, colour = "black", position = position_dodge(0.9))
EWOS.cre.plot + scale_fill_grey() + theme_classic() +
  theme(panel.grid.major = element_blank(), panel.grid.minor = element_blank(),
        panel.background = element_blank(), axis.line = element_line(colour = "black"))+
  labs(x= "SW transfer (time)", y= "Creatine mmol/kg wet tissue")

```

## *A4.2 Analysis*

```
library(fitdistrplus)
```

```
#total osmolyte
```

```

E_osmo <- osmo_data_220219
E_osmo <- subset(osmo_data_220219, Diet == "1")
descdist(E_osmo$total_osmolyte)
E_osmo <- subset(osmo_data_220219, Diet == "2")
descdist(E_osmo$total_osmolyte)
E_osmo <- subset(osmo_data_220219, Diet == "3")

```

```
descdist(E_osmo$total_osmolyte)
E_osmo <- subset(osmo_data_220219, Diet == "4")
descdist(E_osmo$total_osmolyte)
E_osmo <- subset(osmo_data_220219, Diet == "5")
descdist(E_osmo$total_osmolyte)
E_osmo <- subset(osmo_data_220219, Diet == "6")
descdist(E_osmo$total_osmolyte)
```

```
#myoinositol
E_osmo <- osmo_data_220219
E_osmo <- subset(osmo_data_220219, Diet == "1")
descdist(E_osmo$Myoinositol)
E_osmo <- subset(osmo_data_220219, Diet == "2")
descdist(E_osmo$Myoinositol)
E_osmo <- subset(osmo_data_220219, Diet == "3")
descdist(E_osmo$Myoinositol)
E_osmo <- subset(osmo_data_220219, Diet == "4")
descdist(E_osmo$Myoinositol)
E_osmo <- subset(osmo_data_220219, Diet == "5")
descdist(E_osmo$Myoinositol)
E_osmo <- subset(osmo_data_220219, Diet == "6")
descdist(E_osmo$Myoinositol)
```

```
#taurine
E_osmo <- osmo_data_220219
E_osmo <- subset(osmo_data_220219, Diet == "1")
descdist(E_osmo$Taurine)
E_osmo <- subset(osmo_data_220219, Diet == "2")
descdist(E_osmo$Taurine)
E_osmo <- subset(osmo_data_220219, Diet == "3")
descdist(E_osmo$Taurine)
E_osmo <- subset(osmo_data_220219, Diet == "4")
descdist(E_osmo$Taurine)
E_osmo <- subset(osmo_data_220219, Diet == "5")
descdist(E_osmo$Taurine)
E_osmo <- subset(osmo_data_220219, Diet == "6")
descdist(E_osmo$Taurine)
```

```
#GPC
E_osmo <- osmo_data_220219
E_osmo <- subset(osmo_data_220219, Diet == "1")
descdist(E_osmo$GPC)
E_osmo <- subset(osmo_data_220219, Diet == "2")
descdist(E_osmo$GPC)
E_osmo <- subset(osmo_data_220219, Diet == "3")
descdist(E_osmo$GPC)
E_osmo <- subset(osmo_data_220219, Diet == "4")
descdist(E_osmo$GPC)
E_osmo <- subset(osmo_data_220219, Diet == "5")
descdist(E_osmo$GPC)
E_osmo <- subset(osmo_data_220219, Diet == "6")
descdist(E_osmo$GPC)
```

```
#alanine
E_osmo <- osmo_data_220219
E_osmo <- subset(osmo_data_220219, Diet == "1")
descdist(E_osmo$Alanine)
E_osmo <- subset(osmo_data_220219, Diet == "2")
descdist(E_osmo$Alanine)
E_osmo <- subset(osmo_data_220219, Diet == "3")
```

```
descdist(E_osmo$Alanine)
E_osmo <- subset(osmo_data_220219, Diet == "4")
descdist(E_osmo$Alanine)
E_osmo <- subset(osmo_data_220219, Diet == "5")
descdist(E_osmo$Alanine)
E_osmo <- subset(osmo_data_220219, Diet == "6")
descdist(E_osmo$Alanine)
```

#betaine

```
E_osmo <- osmo_data_220219
E_osmo <- subset(osmo_data_220219, Diet == "1")
descdist(E_osmo$Betaine)
E_osmo <- subset(osmo_data_220219, Diet == "2")
descdist(E_osmo$Betaine)
E_osmo <- subset(osmo_data_220219, Diet == "3")
descdist(E_osmo$Betaine)
E_osmo <- subset(osmo_data_220219, Diet == "4")
descdist(E_osmo$Betaine)
E_osmo <- subset(osmo_data_220219, Diet == "5")
descdist(E_osmo$Betaine)
E_osmo <- subset(osmo_data_220219, Diet == "6")
descdist(E_osmo$Betaine)
```

#creatine

```
E_osmo <- osmo_data_220219
E_osmo <- subset(osmo_data_220219, Diet == "1")
descdist(E_osmo$Creatine)
E_osmo <- subset(osmo_data_220219, Diet == "2")
descdist(E_osmo$Creatine)
E_osmo <- subset(osmo_data_220219, Diet == "3")
descdist(E_osmo$Creatine)
E_osmo <- subset(osmo_data_220219, Diet == "4")
descdist(E_osmo$Creatine)
E_osmo <- subset(osmo_data_220219, Diet == "5")
descdist(E_osmo$Creatine)
E_osmo <- subset(osmo_data_220219, Diet == "6")
descdist(E_osmo$Creatine)
```

#glucose

```
MH_data <- Glucose_arb_an
MH_data <- subset(Glucose_arb_an, Diet == "1")
descdist(MH_data$Glucose_arb)
MH_data <- subset(Glucose_arb_an, Diet == "2")
descdist(MH_data$Glucose_arb)
MH_data <- subset(Glucose_arb_an, Diet == "3")
descdist(MH_data$Glucose_arb)
MH_data <- subset(Glucose_arb_an, Diet == "4")
descdist(MH_data$Glucose_arb)
MH_data <- subset(Glucose_arb_an, Diet == "5")
descdist(MH_data$Glucose_arb)
MH_data <- subset(Glucose_arb_an, Diet == "6")
descdist(MH_data$Glucose_arb)
```

#urea

```
MH_data <- urea_arb_an
MH_data <- subset(urea_arb_an, Diet == "1")
descdist(MH_data$Urea_arb)
MH_data <- subset(urea_arb_an, Diet == "2")
descdist(MH_data$Urea_arb)
```

```

MH_data <- subset(urea_arb_an, Diet == "3")
descdist(MH_data$Urea_arb)
MH_data <- subset(urea_arb_an, Diet == "4")
descdist(MH_data$Urea_arb)
MH_data <- subset(urea_arb_an, Diet == "5")
descdist(MH_data$Urea_arb)
MH_data <- subset(urea_arb_an, Diet == "6")
descdist(MH_data$Urea_arb)
#data
Eo_data <- osmo_data_220219

library(car)
library(emmeans)

#total osmolyte
Etot_glm <- glm(total_osmolyte ~ tp * Diet, family = Gamma(link = inverse), data = Eo_data)
summary(Etot_glm)
Anova(Etot_glm, type = "II", test = "F")
emmeans(Etot_glm, pairwise~tp)

#Glucose
Eglu_glm <- glm(Glucose ~ tp * Diet, family = Gamma(link = inverse), data = Eo_data)
summary(Eglu_glm)
Anova(Eglu_glm, type = "II")
Anova(Eglu_glm, type = "II", test = "F")
emmeans(Eglu_glm, pairwise~tp)

#Myoinositol
Emyo_glm <- glm(Myoinositol ~ tp * Diet, family = Gamma(link = inverse), data = Eo_data)
summary(Emyo_glm)
Anova(Emyo_glm, type = "II", test = "F")
emmeans(Emyo_glm, pairwise~tp|Diet)

#Taurine
Etau_glm <- glm(Taurine ~ tp * Diet, family = Gamma(link = inverse), data = Eo_data)
summary(Etau_glm)
Anova(Etau_glm, type = "II", test = "F")
emmeans(Etau_glm, pairwise~tp)

#GPC
Egpc_glm <- glm(GPC ~ tp * Diet, family = Gamma(link = inverse), data = Eo_data)
summary(Egpc_glm)
Anova(Egpc_glm, type = "II", test = "F")
emmeans(Egpc_glm, pairwise~tp|Diet)

#Urea
Eure_glm <- glm(Urea ~ tp * Diet, family = Gamma(link = inverse), data = Eo_data)
summary(Eure_glm)
Anova(Eure_glm, type = "II", test = "F")
emmeans(Eure_glm, pairwise~tp|Diet)

#Alanine
Eala_glm <- glm(Alanine ~ tp * Diet, family = Gamma(link = inverse), data = Eo_data)
summary(Eala_glm)
Anova(Eala_glm, type = "II", test = "F")
emmeans(Eala_glm, pairwise~tp|Diet)

#Betaine
Ebet_glm <- glm(Betaine ~ tp * Diet, family = Gamma(link = inverse), data = Eo_data)
summary(Ebet_glm)

```

```

Anova(Ebet_glm, type = "II", test = "F")
emmeans(Ebet_glm, pairwise~tp|Diet)

#Creatine
Ecre_glm <- glm(Creatine ~ tp * Diet, family = Gamma(link = inverse), data = Eo_data)
summary(Ecre_glm)
Anova(Ecre_glm, type = "II", test = "F")
emmeans(Ecre_glm, pairwise~tp)
#creatine kinase
CKA_data <- creatine_kinase_expression

library(dplyr)
CKA_summary <- CKA_data %>%
  group_by(Diet, Salinity) %>%
  summarise(n=n(),
            mean=mean(CKA),
            sd=sd(CKA),
            ) %>%
  mutate(se=sd/sqrt(n))

library(ggplot2)

#plot
CKA.plot <- ggplot(CKA_summary, aes(x=Diet, y=mean, fill = Salinity, ymin=mean-
se,ymax=mean+se))+
  geom_bar(stat = "identity", color = "black", position = position_dodge()) +
  geom_errorbar(width=0.1, colour = "black", position = position_dodge(0.9))

CKA.plot + scale_fill_grey() + theme_classic() +
  theme(panel.grid.major = element_blank(), panel.grid.minor = element_blank(),
        panel.background = element_blank(), axis.line = element_line(colour = "black"))+
  labs(x= "Diet", y= "Fold change in CKA expression")

#ANOVA
library(ggpubr)
library(car)
ggboxplot(CKA_data, x = "Diet", y = "CKA", fill = "Salinity")
ggline(CKA_data, x = "Diet", y = "CKA", color = "Salinity", add = c("mean_se", "dotplot"))
CKA.aov1 <- aov(CKA ~ Diet*Salinity, data = CKA_data)
summary(CKA.aov1)
#test for equal variance
plot(CKA.aov1, 1)
leveneTest(CKA ~ Diet*Salinity, data = CKA_data)
#test for normal distribution
plot(CKA.aov1, 2)
CKA.aov1_residuals <- residuals(object = CKA.aov1)
shapiro.test(x = CKA.aov1_residuals)

#generalised linear model
CKA.glm <- glm(CKA ~ Diet*Salinity, family = Gamma(link = log), data = CKA_data)
CKA.glm
CKA.g.a <- Anova(CKA.glm, test = "F")
CKA.g.a
library(emmeans)
emmeans(CKA.glm, pairwise~Diet*Salinity)

```

## Appendix 5 – Biomarkers of smoltification

### A5.1 Figures R code

```
#data
NKA_fig <- NKA_alpha_MH_original
library(dplyr)
Expression_summary <- NKA_fig %>%
  group_by(Life_stage, Gene) %>%
  summarise(n=n(),
            mean=mean(Expression),
            sd=sd(Expression),
            ) %>%
  mutate(se=sd/sqrt(n))

#plot NKA
Expression.plot <- ggplot(Expression_summary, aes(x=Life_stage, y=mean, color = Gene, fill = Gene,
ymin=mean-se,ymax=mean+se))+
  geom_bar(stat = "identity", position = position_dodge(), color = "black") +
  geom_errorbar(width=0.5, colour = "black", position = position_dodge(0.9))
Expression.plot + scale_fill_grey() + theme_classic() +
  theme(panel.grid.major = element_blank(), panel.grid.minor = element_blank(),
        panel.background = element_blank(), axis.line = element_line(colour = "black"))+
  labs(x= "Life stage", y= "Fold change in NKA  $\alpha$ 1a and  $\alpha$ 1b expression")

#data
NKA_data2 <- NKA_MH_new_tc_fig
library(dplyr)
Expression_summary <- NKA_data2 %>%
  group_by(Days_to_SW_transfer, Gene) %>%
  summarise(n=n(),
            mean=mean(Expression),
            sd=sd(Expression),
            ) %>%
  mutate(se=sd/sqrt(n))

library(ggplot2)
#plot NKA
Expression.plot <- ggplot(Expression_summary, aes(x=Days_to_SW_transfer, y=mean, color = Gene,
fill = Gene, ymin=mean-se,ymax=mean+se))+
  geom_bar(stat = "identity", position = position_dodge(), color = "black") +
  geom_errorbar(width=0.2, colour = "black", position = position_dodge(0.9))
Expression.plot + scale_fill_grey() + theme_classic() +
  theme(panel.grid.major = element_blank(), panel.grid.minor = element_blank(),
        panel.background = element_blank(), axis.line = element_line(colour = "black"))+
  labs(x= "Days to SW transfer", y= "Fold change in NKA  $\alpha$ 1a and  $\alpha$ 1b expression")

#data
NKA_last <- NKA_MH_latest_time_course
library(dplyr)
Expression_summary <- NKA_last %>%
  group_by(SW_transfer, Gene) %>%
  summarise(n=n(),
            mean=mean(Expression),
            sd=sd(Expression),
```

```

) %>%
mutate(se=sd/sqrt(n))

library(ggplot2)
#plot NKA
Expression.plot <- ggplot(Expression_summary, aes(x=SW_transfer, y=mean, color = Gene, fill =
Gene, ymin=mean-se,ymax=mean+se))+
  geom_bar(stat = "identity", position = position_dodge(), color = "black") +
  geom_errorbar(width=0.2, colour = "black", position = position_dodge(0.9))

Expression.plot + scale_fill_grey() + theme_classic() +
  theme(panel.grid.major = element_blank(), panel.grid.minor = element_blank(),
  panel.background = element_blank(), axis.line = element_line(colour = "black"))+
  labs(x= "SW transfer (days)", y= "Fold change in NKA α1a and α1b expression")

#data
NKAa1a_wfig <- NKAa1a_western_for_fig

library(dplyr)
library(ggplot2)

NKAaw_summary <- NKAa1a_wfig %>%
  group_by(Days_to_SW_transfer, Size) %>%
  summarise(n=n(),
            mean=mean(NKA_a1a),
            sd=sd(NKA_a1a)
  ) %>%
  mutate(se=sd/sqrt(n))

NKAaw_summary$stacked_mean<-NA
# Add the height of bars below in order to plot error bars at top of each bar
NKAaw_summary$stacked_mean[1]<- NKAaw_summary$mean[3] + NKAaw_summary$mean[1] +
NKAaw_summary$mean[2]
NKAaw_summary$stacked_mean[2]<- NKAaw_summary$mean[3] + NKAaw_summary$mean[1]
NKAaw_summary$stacked_mean[3]<- NKAaw_summary$mean[3]
NKAaw_summary$stacked_mean[4]<- NKAaw_summary$mean[6] + NKAaw_summary$mean[4] +
NKAaw_summary$mean[5]
NKAaw_summary$stacked_mean[5]<- NKAaw_summary$mean[6] + NKAaw_summary$mean[4]
NKAaw_summary$stacked_mean[6]<- NKAaw_summary$mean[6]
NKAaw_summary$stacked_mean[7]<- NKAaw_summary$mean[9] + NKAaw_summary$mean[7] +
NKAaw_summary$mean[8]
NKAaw_summary$stacked_mean[8]<- NKAaw_summary$mean[9] + NKAaw_summary$mean[7]
NKAaw_summary$stacked_mean[9]<- NKAaw_summary$mean[9]
NKAaw_summary$stacked_mean[10]<- NKAaw_summary$mean[12] + NKAaw_summary$mean[10]
+ NKAaw_summary$mean[11]
NKAaw_summary$stacked_mean[11]<- NKAaw_summary$mean[12] + NKAaw_summary$mean[10]
NKAaw_summary$stacked_mean[12]<- NKAaw_summary$mean[12]
NKAaw_summary$stacked_mean[13]<- NKAaw_summary$mean[15] + NKAaw_summary$mean[13]
+ NKAaw_summary$mean[14]
NKAaw_summary$stacked_mean[14]<- NKAaw_summary$mean[15] + NKAaw_summary$mean[13]
NKAaw_summary$stacked_mean[15]<- NKAaw_summary$mean[15]
NKAaw_summary$stacked_mean[16]<- NKAaw_summary$mean[18] + NKAaw_summary$mean[16]
+ NKAaw_summary$mean[17]
NKAaw_summary$stacked_mean[17]<- NKAaw_summary$mean[18] + NKAaw_summary$mean[16]
NKAaw_summary$stacked_mean[18]<- NKAaw_summary$mean[18]
NKAaw_summary$stacked_mean[19]<- NKAaw_summary$mean[21] + NKAaw_summary$mean[19]
+ NKAaw_summary$mean[20]
NKAaw_summary$stacked_mean[20]<- NKAaw_summary$mean[21] + NKAaw_summary$mean[19]
NKAaw_summary$stacked_mean[21]<- NKAaw_summary$mean[21]

```

```

NKAaw_summary$stacked_mean[22]<- NKAaw_summary$mean[24] + NKAaw_summary$mean[22]
+ NKAaw_summary$mean[23]
NKAaw_summary$stacked_mean[23]<- NKAaw_summary$mean[24] + NKAaw_summary$mean[22]
NKAaw_summary$stacked_mean[24]<- NKAaw_summary$mean[24]
NKAaw_summary$Size <- factor(NKAaw_summary$Size, levels = c("180kDa", "110kDa", "95kDa"))

```

```

#plot NKAa1a western
NKA_a1aw.plot <- ggplot(NKAaw_summary, aes(x=Days_to_SW_transfer, fill = Size, y=mean,
ymin=stacked_mean-se,ymax=stacked_mean+se))+
  geom_bar(stat = "identity", width = 0.9, color = "black") +
  geom_errorbar(width=0.1, colour = "black")
NKA_a1aw.plot + scale_fill_grey() + theme_classic() +
  theme(panel.grid.major = element_blank(), panel.grid.minor = element_blank(),
  panel.background = element_blank(), axis.line = element_line(colour = "black"))+
  labs(x= "SW transfer (days)", y= "Relative expression of NKA α1a proteins")

```

```

#data
NKAa1b <- NKAa1b_western_data

```

```

NKAbw_summary <- NKAa1b %>%
  group_by(SW_transfer, Salinity) %>%
  summarise(n=n(),
            mean=mean(NKA_a1b),
            sd=sd(NKA_a1b)
  ) %>%
  mutate(se=sd/sqrt(n))

```

```

#plot NKAa1b western
NKA_a1bw.plot <- ggplot(NKAbw_summary, aes(x=SW_transfer, fill = Salinity, y=mean, ymin=mean-
se,ymax=mean+se))+
  geom_bar(stat = "identity", position = position_dodge(), color = "black") +
  geom_errorbar(width=0.1, colour = "black", position = position_dodge(0.9))
NKA_a1bw.plot + scale_fill_grey() + theme_classic() +
  theme(panel.grid.major = element_blank(), panel.grid.minor = element_blank(),
  panel.background = element_blank(), axis.line = element_line(colour = "black"))+
  labs(x= "SW transfer (days)", y= "Relative expression of NKA α1b protein")

```

```

#data
B_data <- Biomarker_gene_expression_sorted_data

```

```

NKCC_summary <- B_data %>%
  group_by(SW_transfer) %>%
  summarise(n=n(),
            mean=mean(NKCC),
            sd=sd(NKCC),
  ) %>%
  mutate(se=sd/sqrt(n))

```

```

#plot NKCC
NKCC.plot <- ggplot(NKCC_summary, aes(x=SW_transfer, y=mean, ymin=mean-
se,ymax=mean+se))+
  geom_bar(stat = "identity", color = "black", position = position_dodge()) +
  geom_errorbar(width=0.1, colour = "black", position = position_dodge())
NKCC.plot + scale_fill_grey() + theme_classic() +
  theme(panel.grid.major = element_blank(), panel.grid.minor = element_blank(),
  panel.background = element_blank(), axis.line = element_line(colour = "black"))+
  labs(x= "SW transfer (days)", y= "Fold change in NKCC1 expression")

```

```

CFTR_summary <- B_data %>%
  group_by(SW_transfer) %>%

```

```

summarise(n=n(),
          mean=mean(CFTR),
          sd=sd(CFTR),
) %>%
mutate(se=sd/sqrt(n))

#plot CFTR
CFTR.plot <- ggplot(CFTR_summary, aes(x=SW_transfer, y=mean, ymin=mean-
se,ymax=mean+se))+
  geom_bar(stat = "identity", color = "black", position = position_dodge()) +
  geom_errorbar(width=0.1, colour = "black", position = position_dodge())
CFTR.plot + scale_fill_grey() + theme_classic() +
  theme(panel.grid.major = element_blank(), panel.grid.minor = element_blank(),
        panel.background = element_blank(), axis.line = element_line(colour = "black"))+
  labs(x= "SW transfer (days)", y= "Fold change in CFTR expression")

NKAb2ab_summary <- B_data %>%
  group_by(SW_transfer) %>%
  summarise(n=n(),
            mean=mean(NKAb2ab),
            sd=sd(NKAb2ab),
) %>%
mutate(se=sd/sqrt(n))

#plot NKAb2ab
NKAb2ab.plot <- ggplot(NKAb2ab_summary, aes(x=SW_transfer, y=mean, ymin=mean-
se,ymax=mean+se))+
  geom_bar(stat = "identity", color = "black", position = position_dodge()) +
  geom_errorbar(width=0.1, colour = "black", position = position_dodge())
NKAb2ab.plot + scale_fill_grey() + theme_classic() +
  theme(panel.grid.major = element_blank(), panel.grid.minor = element_blank(),
        panel.background = element_blank(), axis.line = element_line(colour = "black"))+
  labs(x= "SW transfer (days)", y= "Fold change in NKA  $\beta$ 2ab expression")

NKAb2c_summary <- B_data %>%
  group_by(SW_transfer) %>%
  summarise(n=n(),
            mean=mean(NKAb2c),
            sd=sd(NKAb2c),
) %>%
mutate(se=sd/sqrt(n))

#plot NKAb2c
NKAb2c.plot <- ggplot(NKAb2c_summary, aes(x=SW_transfer, y=mean, ymin=mean-
se,ymax=mean+se))+
  geom_bar(stat = "identity", color = "black", position = position_dodge()) +
  geom_errorbar(width=0.1, colour = "black", position = position_dodge())

NKAb2c.plot + scale_fill_grey() + theme_classic() +
  theme(panel.grid.major = element_blank(), panel.grid.minor = element_blank(),
        panel.background = element_blank(), axis.line = element_line(colour = "black"))+
  labs(x= "SW transfer (days)", y= "Fold change in NKA  $\beta$ 2c expression")

NKAb3b_summary <- B_data %>%
  group_by(SW_transfer) %>%
  summarise(n=n(),
            mean=mean(NKAb3b),
            sd=sd(NKAb3b),
) %>%
mutate(se=sd/sqrt(n))

```

```

#plot NKAb3b
NKAb3b.plot <- ggplot(NKAb3b_summary, aes(x=SW_transfer, y=mean, ymin=mean-
se,ymax=mean+se))+
  geom_bar(stat = "identity", color = "black", position = position_dodge()) +
  geom_errorbar(width=0.1, colour = "black", position = position_dodge())

NKAb3b.plot + scale_fill_grey() + theme_classic() +
  theme(panel.grid.major = element_blank(), panel.grid.minor = element_blank(),
    panel.background = element_blank(), axis.line = element_line(colour = "black"))+
  labs(x= "SW transfer (days)", y= "Fold change in NKA  $\beta$ 3b expression")

NKAb3c_summary <- B_data %>%
  group_by(SW_transfer) %>%
  summarise(n=n(),
    mean=mean(NKAb3c),
    sd=sd(NKAb3c),
  ) %>%
  mutate(se=sd/sqrt(n))

#plot NKAb3c
NKAb3c.plot <- ggplot(NKAb3c_summary, aes(x=SW_transfer, y=mean, ymin=mean-
se,ymax=mean+se))+
  geom_bar(stat = "identity", color = "black", position = position_dodge()) +
  geom_errorbar(width=0.1, colour = "black", position = position_dodge())
NKAb3c.plot + scale_fill_grey() + theme_classic() +
  theme(panel.grid.major = element_blank(), panel.grid.minor = element_blank(),
    panel.background = element_blank(), axis.line = element_line(colour = "black"))+
  labs(x= "SW transfer (days)", y= "Fold change in NKA  $\beta$ 3c expression")

NKAb4_summary <- B_data %>%
  group_by(SW_transfer) %>%
  summarise(n=n(),
    mean=mean(NKAb4),
    sd=sd(NKAb4),
  ) %>%
  mutate(se=sd/sqrt(n))

#plot NKAb4
NKAb4.plot <- ggplot(NKAb4_summary, aes(x=SW_transfer, y=mean, ymin=mean-
se,ymax=mean+se))+
  geom_bar(stat = "identity", color = "black", position = position_dodge()) +
  geom_errorbar(width=0.1, colour = "black", position = position_dodge())
NKAb4.plot + scale_fill_grey() + theme_classic() +
  theme(panel.grid.major = element_blank(), panel.grid.minor = element_blank(),
    panel.background = element_blank(), axis.line = element_line(colour = "black"))+
  labs(x= "SW transfer (days)", y= "Fold change in NKA  $\beta$ 4 expression")

CaATPase_summary <- B_data %>%
  group_by(SW_transfer) %>%
  summarise(n=n(),
    mean=mean(CaATPase),
    sd=sd(CaATPase),
  ) %>%
  mutate(se=sd/sqrt(n))

#plot CaATPase
CaATPase.plot <- ggplot(CaATPase_summary, aes(x=SW_transfer, y=mean, ymin=mean-
se,ymax=mean+se))+
  geom_bar(stat = "identity", color = "black", position = position_dodge()) +

```

```

geom_errorbar(width=0.1, colour = "black", position = position_dodge())
CaATPase.plot + scale_fill_grey() + theme_classic() +
  theme(panel.grid.major = element_blank(), panel.grid.minor = element_blank(),
        panel.background = element_blank(), axis.line = element_line(colour = "black"))+
  labs(x= "SW transfer (days)", y= "Fold change in Ca ATPase expression")

```

```

Copine_summary <- B_data %>%
  group_by(SW_transfer) %>%
  summarise(n=n(),
            mean=mean(Copine),
            sd=sd(Copine),
  ) %>%
  mutate(se=sd/sqrt(n))

```

```

#plot Copine
Copine.plot <- ggplot(Copine_summary, aes(x=SW_transfer, y=mean, ymin=mean-
se,ymax=mean+se))+
  geom_bar(stat = "identity", color = "black", position = position_dodge()) +
  geom_errorbar(width=0.1, colour = "black", position = position_dodge())
Copine.plot + scale_fill_grey() + theme_classic() +
  theme(panel.grid.major = element_blank(), panel.grid.minor = element_blank(),
        panel.background = element_blank(), axis.line = element_line(colour = "black"))+
  labs(x= "SW transfer (days)", y= "Fold change in Copine expression")

```

```

ApoA1_summary <- B_data %>%
  group_by(SW_transfer) %>%
  summarise(n=n(),
            mean=mean(ApoA1),
            sd=sd(ApoA1),
  ) %>%
  mutate(se=sd/sqrt(n))

```

```

#plot ApoA1
ApoA1.plot <- ggplot(ApoA1_summary, aes(x=SW_transfer, y=mean, ymin=mean-
se,ymax=mean+se))+
  geom_bar(stat = "identity", color = "black", position = position_dodge()) +
  geom_errorbar(width=0.1, colour = "black", position = position_dodge())
ApoA1.plot + scale_fill_grey() + theme_classic() +
  theme(panel.grid.major = element_blank(), panel.grid.minor = element_blank(),
        panel.background = element_blank(), axis.line = element_line(colour = "black"))+
  labs(x= "SW transfer (days)", y= "Fold change in Apo A1 expression")

```

```

ApoA1b_summary <- B_data %>%
  group_by(SW_transfer) %>%
  summarise(n=n(),
            mean=mean(ApoA1b),
            sd=sd(ApoA1b),
  ) %>%
  mutate(se=sd/sqrt(n))

```

```

#plot ApoA1b
ApoA1b.plot <- ggplot(ApoA1b_summary, aes(x=SW_transfer, y=mean, ymin=mean-
se,ymax=mean+se))+
  geom_bar(stat = "identity", color = "black", position = position_dodge()) +
  geom_errorbar(width=0.1, colour = "black", position = position_dodge())
ApoA1b.plot + scale_fill_grey() + theme_classic() +
  theme(panel.grid.major = element_blank(), panel.grid.minor = element_blank(),
        panel.background = element_blank(), axis.line = element_line(colour = "black"))+
  labs(x= "SW transfer (days)", y= "Fold change in Apo A1b expression")

```

```

ApoA4_summary <- B_data %>%
  group_by(SW_transfer) %>%
  summarise(n=n(),
            mean=mean(ApoA4),
            sd=sd(ApoA4),
  ) %>%
  mutate(se=sd/sqrt(n))

#plot NKAb4
ApoA4.plot <- ggplot(ApoA4_summary, aes(x=SW_transfer, y=mean, ymin=mean-
se,ymax=mean+se))+
  geom_bar(stat = "identity", color = "black", position = position_dodge()) +
  geom_errorbar(width=0.1, colour = "black", position = position_dodge())
ApoA4.plot + scale_fill_grey() + theme_classic() +
  theme(panel.grid.major = element_blank(), panel.grid.minor = element_blank(),
        panel.background = element_blank(), axis.line = element_line(colour = "black"))+
  labs(x= "SW transfer (days)", y= "Fold change in Apo A4 expression")

ApoB100_summary <- B_data %>%
  group_by(SW_transfer) %>%
  summarise(n=n(),
            mean=mean(ApoB100),
            sd=sd(ApoB100),
  ) %>%
  mutate(se=sd/sqrt(n))

#plot ApoB100
ApoB100.plot <- ggplot(ApoB100_summary, aes(x=SW_transfer, y=mean, ymin=mean-
se,ymax=mean+se))+
  geom_bar(stat = "identity", color = "black", position = position_dodge()) +
  geom_errorbar(width=0.1, colour = "black", position = position_dodge())
ApoB100.plot + scale_fill_grey() + theme_classic() +
  theme(panel.grid.major = element_blank(), panel.grid.minor = element_blank(),
        panel.background = element_blank(), axis.line = element_line(colour = "black"))+
  labs(x= "SW transfer (days)", y= "Fold change in Apo B100 expression")

LDLR_summary <- B_data %>%
  group_by(SW_transfer) %>%
  summarise(n=n(),
            mean=mean(LDLR),
            sd=sd(LDLR),
  ) %>%
  mutate(se=sd/sqrt(n))

#plot LDLR
LDLR.plot <- ggplot(LDLR_summary, aes(x=SW_transfer, y=mean, ymin=mean-
se,ymax=mean+se))+
  geom_bar(stat = "identity", color = "black", position = position_dodge()) +
  geom_errorbar(width=0.1, colour = "black", position = position_dodge())

LDLR.plot + scale_fill_grey() + theme_classic() +
  theme(panel.grid.major = element_blank(), panel.grid.minor = element_blank(),
        panel.background = element_blank(), axis.line = element_line(colour = "black"))+
  labs(x= "SW transfer (days)", y= "Fold change in LDLR expression")

AnnA1_summary <- B_data %>%
  group_by(SW_transfer) %>%
  summarise(n=n(),
            mean=mean(AnnA1),
            sd=sd(AnnA1),

```

```

) %>%
mutate(se=sd/sqrt(n))

#plot AnnA1
AnnA1.plot <- ggplot(AnnA1_summary, aes(x=SW_transfer, y=mean, ymin=mean-
se,ymax=mean+se))+
  geom_bar(stat = "identity", color = "black", position = position_dodge()) +
  geom_errorbar(width=0.1, colour = "black", position = position_dodge())
AnnA1.plot + scale_fill_grey() + theme_classic() +
  theme(panel.grid.major = element_blank(), panel.grid.minor = element_blank(),
  panel.background = element_blank(), axis.line = element_line(colour = "black"))+
  labs(x= "SW transfer (days)", y= "Fold change in Annexin A1 expression")

AnnA2_summary <- B_data %>%
group_by(SW_transfer) %>%
summarise(n=n(),
  mean=mean(AnnA2),
  sd=sd(AnnA2),
) %>%
mutate(se=sd/sqrt(n))

#plot AnnA2
AnnA2.plot <- ggplot(AnnA2_summary, aes(x=SW_transfer, y=mean, ymin=mean-
se,ymax=mean+se))+
  geom_bar(stat = "identity", color = "black", position = position_dodge()) +
  geom_errorbar(width=0.1, colour = "black", position = position_dodge())
AnnA2.plot + scale_fill_grey() + theme_classic() +
  theme(panel.grid.major = element_blank(), panel.grid.minor = element_blank(),
  panel.background = element_blank(), axis.line = element_line(colour = "black"))+
  labs(x= "SW transfer (days)", y= "Fold change in Annexin A2 expression")

AnnA3_summary <- B_data %>%
group_by(SW_transfer) %>%
summarise(n=n(),
  mean=mean(AnnA3),
  sd=sd(AnnA3),
) %>%
mutate(se=sd/sqrt(n))

#plot AnnA3
AnnA3.plot <- ggplot(AnnA3_summary, aes(x=SW_transfer, y=mean, ymin=mean-
se,ymax=mean+se))+
  geom_bar(stat = "identity", color = "black", position = position_dodge()) +
  geom_errorbar(width=0.1, colour = "black", position = position_dodge())

AnnA3.plot + scale_fill_grey() + theme_classic() +
  theme(panel.grid.major = element_blank(), panel.grid.minor = element_blank(),
  panel.background = element_blank(), axis.line = element_line(colour = "black"))+
  labs(x= "SW transfer (days)", y= "Fold change in Annexin A3 expression")

AnnA6b_summary <- B_data %>%
group_by(SW_transfer) %>%
summarise(n=n(),
  mean=mean(AnnA6b),
  sd=sd(AnnA6b),
) %>%
mutate(se=sd/sqrt(n))

#plot AnnA6b

```

```

AnnA6b.plot <- ggplot(AnnA6b_summary, aes(x=SW_transfer, y=mean, ymin=mean-se,ymax=mean+se))+
  geom_bar(stat = "identity", color = "black", position = position_dodge()) +
  geom_errorbar(width=0.1, colour = "black", position = position_dodge())
AnnA6b.plot + scale_fill_grey() + theme_classic() +
  theme(panel.grid.major = element_blank(), panel.grid.minor = element_blank(),
    panel.background = element_blank(), axis.line = element_line(colour = "black"))+
  labs(x= "SW transfer (days)", y= "Fold change in Annexin A6b expression")

lgK_summary <- B_data %>%
  group_by(SW_transfer) %>%
  summarise(n=n(),
    mean=mean(lgK),
    sd=sd(lgK),
  ) %>%
  mutate(se=sd/sqrt(n))

#plot AnnA2
lgK.plot <- ggplot(lgK_summary, aes(x=SW_transfer, y=mean, ymin=mean-se,ymax=mean+se))+
  geom_bar(stat = "identity", color = "black", position = position_dodge()) +
  geom_errorbar(width=0.1, colour = "black", position = position_dodge())
lgK.plot + scale_fill_grey() + theme_classic() +
  theme(panel.grid.major = element_blank(), panel.grid.minor = element_blank(),
    panel.background = element_blank(), axis.line = element_line(colour = "black"))+
  labs(x= "SW transfer (days)", y= "Fold change in lgK expression")

lgD_summary <- B_data %>%
  group_by(SW_transfer) %>%
  summarise(n=n(),
    mean=mean(lgD),
    sd=sd(lgD),
  ) %>%
  mutate(se=sd/sqrt(n))

#plot lgD
lgD.plot <- ggplot(lgD_summary, aes(x=SW_transfer, y=mean, ymin=mean-se,ymax=mean+se))+
  geom_bar(stat = "identity", color = "black", position = position_dodge()) +
  geom_errorbar(width=0.1, colour = "black", position = position_dodge())
lgD.plot + scale_fill_grey() + theme_classic() +
  theme(panel.grid.major = element_blank(), panel.grid.minor = element_blank(),
    panel.background = element_blank(), axis.line = element_line(colour = "black"))+
  labs(x= "SW transfer (days)", y= "Fold change in lgD expression")

plgRLT1_summary <- B_data %>%
  group_by(SW_transfer) %>%
  summarise(n=n(),
    mean=mean(plgRLT1),
    sd=sd(plgRLT1),
  ) %>%
  mutate(se=sd/sqrt(n))

#plot plgRLT1
plgRLT1.plot <- ggplot(plgRLT1_summary, aes(x=SW_transfer, y=mean, ymin=mean-se,ymax=mean+se))+
  geom_bar(stat = "identity", color = "black", position = position_dodge()) +
  geom_errorbar(width=0.1, colour = "black", position = position_dodge())
plgRLT1.plot + scale_fill_grey() + theme_classic() +
  theme(panel.grid.major = element_blank(), panel.grid.minor = element_blank(),

```

```

    panel.background = element_blank(), axis.line = element_line(colour = "black"))+
labs(x= "SW transfer (days)", y= "Fold change in pIgRL1 expression")

pIgRLT1a_summary <- B_data %>%
  group_by(SW_transfer) %>%
  summarise(n=n(),
            mean=mean(pIgRLT1a),
            sd=sd(pIgRLT1a),
            ) %>%
  mutate(se=sd/sqrt(n))

#plot pIgRLT1a
pIgRLT1a.plot <- ggplot(pIgRLT1a_summary, aes(x=SW_transfer, y=mean, ymin=mean-
se,ymax=mean+se))+
  geom_bar(stat = "identity", color = "black", position = position_dodge()) +
  geom_errorbar(width=0.1, colour = "black", position = position_dodge())
pIgRLT1a.plot + scale_fill_grey() + theme_classic() +
  theme(panel.grid.major = element_blank(), panel.grid.minor = element_blank(),
        panel.background = element_blank(), axis.line = element_line(colour = "black"))+
  labs(x= "SW transfer (days)", y= "Fold change in pIgRL1a expression")

UP584_summary <- B_data %>%
  group_by(SW_transfer) %>%
  summarise(n=n(),
            mean=mean(UP584),
            sd=sd(UP584),
            ) %>%
  mutate(se=sd/sqrt(n))

#plot UP584
UP584.plot <- ggplot(UP584_summary, aes(x=SW_transfer, y=mean, ymin=mean-
se,ymax=mean+se))+
  geom_bar(stat = "identity", color = "black", position = position_dodge()) +
  geom_errorbar(width=0.1, colour = "black", position = position_dodge())
UP584.plot + scale_fill_grey() + theme_classic() +
  theme(panel.grid.major = element_blank(), panel.grid.minor = element_blank(),
        panel.background = element_blank(), axis.line = element_line(colour = "black"))+
  labs(x= "SW transfer (days)", y= "Fold change in UP584 expression")

Elast_in_summary <- B_data %>%
  group_by(SW_transfer) %>%
  summarise(n=n(),
            mean=mean(Elast_in),
            sd=sd(Elast_in),
            ) %>%
  mutate(se=sd/sqrt(n))

#plot Elast_in
Elast_in.plot <- ggplot(Elast_in_summary, aes(x=SW_transfer, y=mean, ymin=mean-
se,ymax=mean+se))+
  geom_bar(stat = "identity", color = "black", position = position_dodge()) +
  geom_errorbar(width=0.1, colour = "black", position = position_dodge())
Elast_in.plot + scale_fill_grey() + theme_classic() +
  theme(panel.grid.major = element_blank(), panel.grid.minor = element_blank(),
        panel.background = element_blank(), axis.line = element_line(colour = "black"))+
  labs(x= "SW transfer (days)", y= "Fold change in LEI expression")

Gelsolin_summary <- B_data %>%
  group_by(SW_transfer) %>%
  summarise(n=n(),

```

```

        mean=mean(Gelsolin),
        sd=sd(Gelsolin),
    ) %>%
    mutate(se=sd/sqrt(n))

#plot Gelsolin
Gelsolin.plot <- ggplot(Gelsolin_summary, aes(x=SW_transfer, y=mean, ymin=mean-
se,ymax=mean+se))+
  geom_bar(stat = "identity", color = "black", position = position_dodge()) +
  geom_errorbar(width=0.1, colour = "black", position = position_dodge())
Gelsolin.plot + scale_fill_grey() + theme_classic() +
  theme(panel.grid.major = element_blank(), panel.grid.minor = element_blank(),
        panel.background = element_blank(), axis.line = element_line(colour = "black"))+
  labs(x= "SW transfer (days)", y= "Fold change in Gelsolin expression")

ZP16_summary <- B_data %>%
  group_by(SW_transfer) %>%
  summarise(n=n(),
            mean=mean(ZP16),
            sd=sd(ZP16),
  ) %>%
  mutate(se=sd/sqrt(n))

#plot ZP16
ZP16.plot <- ggplot(ZP16_summary, aes(x=SW_transfer, y=mean, ymin=mean-se,ymax=mean+se))+
  geom_bar(stat = "identity", color = "black", position = position_dodge()) +
  geom_errorbar(width=0.1, colour = "black", position = position_dodge())
ZP16.plot + scale_fill_grey() + theme_classic() +
  theme(panel.grid.major = element_blank(), panel.grid.minor = element_blank(),
        panel.background = element_blank(), axis.line = element_line(colour = "black"))+
  labs(x= "SW transfer (days)", y= "Fold change in ZG16 expression")

CPT2_summary <- B_data %>%
  group_by(SW_transfer) %>%
  summarise(n=n(),
            mean=mean(CPT2),
            sd=sd(CPT2),
  ) %>%
  mutate(se=sd/sqrt(n))

#plot CPT2
CPT2.plot <- ggplot(CPT2_summary, aes(x=SW_transfer, y=mean, ymin=mean-
se,ymax=mean+se))+
  geom_bar(stat = "identity", color = "black", position = position_dodge()) +
  geom_errorbar(width=0.1, colour = "black", position = position_dodge())
CPT2.plot + scale_fill_grey() + theme_classic() +
  theme(panel.grid.major = element_blank(), panel.grid.minor = element_blank(),
        panel.background = element_blank(), axis.line = element_line(colour = "black"))+
  labs(x= "SW transfer (days)", y= "Fold change in CPT2 expression")

```

## *A5.2 Analysis R code*

```

#data
NKA_data <- NKA_a1a_a1b_MH_early_time_course

#NKAa1a

```

```

ggboxplot(NKA_data, x = "Life_stage", y = "NKA_a1a")
ggline(NKA_data, x = "Life_stage", y = "NKA_a1a", add = c("mean_se", "dotplot"))
NKA_a1a.aov <- aov(NKA_a1a ~ Life_stage, data = NKA_data)
summary(NKA_a1a.aov)
plot(NKA_a1a.aov, 1)
leveneTest(NKA_a1a ~ Life_stage, data = NKA_data)
plot(NKA_a1a.aov, 2)
NKA_a1a.aov_residuals <- residuals(object = NKA_a1a.aov)
shapiro.test(x = NKA_a1a.aov_residuals)

#NKAa1b
ggboxplot(NKA_data, x = "Life_stage", y = "NKA_a1b")
ggline(NKA_data, x = "Life_stage", y = "NKA_a1b", add = c("mean_se", "dotplot"))
NKA_a1b.aov <- aov(NKA_a1b ~ Life_stage, data = NKA_data)
summary(NKA_a1b.aov)
plot(NKA_a1b.aov, 1)
leveneTest(NKA_a1b ~ Life_stage, data = NKA_data)
plot(NKA_a1b.aov, 2)
NKA_a1b.aov_residuals <- residuals(object = NKA_a1b.aov)
shapiro.test(x = NKA_a1b.aov_residuals)
kruskal.test(NKA_a1b ~ Life_stage, data = NKA_data)
dunnTest(NKA_a1b ~ Life_stage, data = NKA_data)

#data
NKA_Ldata <- NKA_latest_for_analysis

library(ggpubr)
library(car)
library(FSA)

#NKAa1a
ggboxplot(NKA_Ldata, x = "SW_transfer", y = "NKAa1a")
ggline(NKA_Ldata, x = "SW_transfer", y = "NKAa1a", add = c("mean_se", "dotplot"))
NKAa1a.aov <- aov(NKAa1a ~ SW_transfer, data = NKA_Ldata)
summary(NKAa1a.aov)
plot(NKAa1a.aov, 1)
leveneTest(NKAa1a ~ SW_transfer, data = NKA_Ldata)
plot(NKAa1a.aov, 2)
NKAa1a.aov_residuals <- residuals(object = NKAa1a.aov)
shapiro.test(x = NKAa1a.aov_residuals)
kruskal.test(NKAa1a ~ SW_transfer, data = NKA_Ldata)
dunnTest(NKAa1a ~ SW_transfer, data = NKA_Ldata)

#NKAa1b
ggboxplot(NKA_Ldata, x = "SW_transfer", y = "NKAa1b")
ggline(NKA_Ldata, x = "SW_transfer", y = "NKAa1b", add = c("mean_se", "dotplot"))
NKAa1b.aov <- aov(NKAa1b ~ SW_transfer, data = NKA_Ldata)
summary(NKAa1b.aov)
plot(NKAa1b.aov, 1)
leveneTest(NKAa1b ~ SW_transfer, data = NKA_Ldata)
plot(NKAa1b.aov, 2)
NKAa1b.aov_residuals <- residuals(object = NKAa1b.aov)
shapiro.test(x = NKAa1b.aov_residuals)
kruskal.test(NKAa1b ~ SW_transfer, data = NKA_Ldata)
dunnTest(NKAa1b ~ SW_transfer, data = NKA_Ldata)

#data
NKAa1a_west <- NKAa1a_western_results

```

```

library(ggpubr)
library(car)

#180kDa
ggboxplot(NKAa1a_west, x = "Days_to_SW_transfer", y = "A")
ggline(NKAa1a_west, x = "Days_to_SW_transfer", y = "A", add = c("mean_se", "dotplot"))
A.aov <- aov(A ~ Days_to_SW_transfer, data = NKAa1a_west)
summary(A.aov)
plot(A.aov, 1)
leveneTest(A ~ Days_to_SW_transfer, data = NKAa1a_west)
plot(A.aov, 2)
A.aov_residuals <- residuals(object = A.aov)
shapiro.test(x = A.aov_residuals)
kruskal.test(A ~ Days_to_SW_transfer, data = NKAa1a_west)

#110kDa
ggboxplot(NKAa1a_west, x = "Days_to_SW_transfer", y = "B")
ggline(NKAa1a_west, x = "Days_to_SW_transfer", y = "B", add = c("mean_se", "dotplot"))
B.aov <- aov(B ~ Days_to_SW_transfer, data = NKAa1a_west)
summary(B.aov)
plot(B.aov, 1)
leveneTest(B ~ Days_to_SW_transfer, data = NKAa1a_west)
plot(B.aov, 2)
B.aov_residuals <- residuals(object = B.aov)
shapiro.test(x = B.aov_residuals)

#95kDa
ggboxplot(NKAa1a_west, x = "Days_to_SW_transfer", y = "C")
ggline(NKAa1a_west, x = "Days_to_SW_transfer", y = "C", add = c("mean_se", "dotplot"))
C.aov <- aov(C ~ Days_to_SW_transfer, data = NKAa1a_west)
summary(C.aov)
plot(C.aov, 1)
leveneTest(C ~ Days_to_SW_transfer, data = NKAa1a_west)
plot(C.aov, 2)
C.aov_residuals <- residuals(object = C.aov)
shapiro.test(x = C.aov_residuals)
kruskal.test(C ~ Days_to_SW_transfer, data = NKAa1a_west)

#SUM
ggboxplot(NKAa1a_west, x = "Days_to_SW_transfer", y = "SUM")
ggline(NKAa1a_west, x = "Days_to_SW_transfer", y = "SUM", add = c("mean_se", "dotplot"))
SUM.aov <- aov(SUM ~ Days_to_SW_transfer, data = NKAa1a_west)
summary(SUM.aov)
plot(SUM.aov, 1)
leveneTest(SUM ~ Days_to_SW_transfer, data = NKAa1a_west)
plot(SUM.aov, 2)
SUM.aov_residuals <- residuals(object = SUM.aov)
shapiro.test(x = SUM.aov_residuals)

library(FSA)
dunnTest(A ~ Days_to_SW_transfer, data = NKAa1a_west)
dunnTest(C ~ Days_to_SW_transfer, data = NKAa1a_west)
TukeyHSD(B.aov)
TukeyHSD(SUM.aov)

#data
NKAa1b <- NKAa1b_western_data

#NKAa1b
ggboxplot(NKAa1b, x = "Days_to_SW_transfer", y = "NKA_a1b")

```

```

ggline(NKAa1b, x = "Days_to_SW_transfer", y = "NKA_a1b", add = c("mean_se", "dotplot"))
NKA_a1b.aov <- aov(NKA_a1b ~ Days_to_SW_transfer, data = NKAa1b)
summary(NKA_a1b.aov)
plot(NKA_a1b.aov, 1)
leveneTest(NKA_a1b ~ Days_to_SW_transfer, data = NKAa1b)
plot(NKA_a1b.aov, 2)
NKA_a1b.aov_residuals <- residuals(object = NKA_a1b.aov)
shapiro.test(x = NKA_a1b.aov_residuals)
kruskal.test(NKA_a1b ~ Days_to_SW_transfer, data = NKAa1b)
dunnTest(NKA_a1b ~ Days_to_SW_transfer, data = NKAa1b)

#data
B_data <- Biomarker_gene_expression_sorted_data

library(ggpubr)
library(car)

#NKA a1a
ggboxplot(B_data, x = "days_to_SW_transfer", y = "NKA_a1a")
ggline(B_data, x = "days_to_SW_transfer", y = "NKA_a1a", add = c("mean_se", "dotplot"))
NKAa1a.aov <- aov(NKA_a1a ~ days_to_SW_transfer, data = B_data)
summary(NKAa1a.aov)
plot(NKAa1a.aov, 1)
leveneTest(NKA_a1a ~ days_to_SW_transfer, data = B_data)
plot(NKAa1a.aov, 2)
NKAa1a.aov_residuals <- residuals(object = NKAa1a.aov)
shapiro.test(x = NKAa1a.aov_residuals)

#NKA a1b
ggboxplot(B_data, x = "days_to_SW_transfer", y = "NKA_a1b")
ggline(B_data, x = "days_to_SW_transfer", y = "NKA_a1b", add = c("mean_se", "dotplot"))
NKA_a1b.aov <- aov(NKA_a1b ~ days_to_SW_transfer, data = B_data)
summary(NKA_a1b.aov)
plot(NKA_a1b.aov, 1)
leveneTest(NKA_a1b ~ days_to_SW_transfer, data = B_data)
plot(NKA_a1b.aov, 2)
NKA_a1b.aov_residuals <- residuals(object = NKA_a1b.aov)
shapiro.test(x = NKA_a1b.aov_residuals)

#AnnA2
ggboxplot(B_data, x = "days_to_SW_transfer", y = "AnnA2")
ggline(B_data, x = "days_to_SW_transfer", y = "AnnA2", add = c("mean_se", "dotplot"))
AnnA2.aov <- aov(AnnA2 ~ days_to_SW_transfer, data = B_data)
summary(AnnA2.aov)
plot(AnnA2.aov, 1)
leveneTest(AnnA2 ~ days_to_SW_transfer, data = B_data)
plot(AnnA2.aov, 2)
AnnA2.aov_residuals <- residuals(object = AnnA2.aov)
shapiro.test(x = AnnA2.aov_residuals)

#AnnA6b
ggboxplot(B_data, x = "days_to_SW_transfer", y = "AnnA6b")
ggline(B_data, x = "days_to_SW_transfer", y = "AnnA6b", add = c("mean_se", "dotplot"))
AnnA6b.aov <- aov(AnnA6b ~ days_to_SW_transfer, data = B_data)
summary(AnnA6b.aov)
plot(AnnA6b.aov, 1)
leveneTest(AnnA6b ~ days_to_SW_transfer, data = B_data)
plot(AnnA6b.aov, 2)
AnnA6b.aov_residuals <- residuals(object = AnnA6b.aov)
shapiro.test(x = AnnA6b.aov_residuals)

```

```

#ApoA1b
ggboxplot(B_data, x = "days_to_SW_transfer", y = "ApoA1b")
ggline(B_data, x = "days_to_SW_transfer", y = "ApoA1b", add = c("mean_se", "dotplot"))
ApoA1b.aov <- aov(ApoA1b ~ days_to_SW_transfer, data = B_data)
summary(ApoA1b.aov)
plot(ApoA1b.aov, 1)
leveneTest(ApoA1b ~ days_to_SW_transfer, data = B_data)
plot(ApoA1b.aov, 2)
ApoA1b.aov_residuals <- residuals(object = ApoA1b.aov)
shapiro.test(x = ApoA1b.aov_residuals)

#ApoA4
ggboxplot(B_data, x = "days_to_SW_transfer", y = "ApoA4")
ggline(B_data, x = "days_to_SW_transfer", y = "ApoA4", add = c("mean_se", "dotplot"))
ApoA4.aov <- aov(ApoA4 ~ days_to_SW_transfer, data = B_data)
summary(ApoA4.aov)
plot(ApoA4.aov, 1)
leveneTest(ApoA4 ~ days_to_SW_transfer, data = B_data)
plot(ApoA4.aov, 2)
ApoA4.aov_residuals <- residuals(object = ApoA4.aov)
shapiro.test(x = ApoA4.aov_residuals)

#NKAb2ab
ggboxplot(B_data, x = "days_to_SW_transfer", y = "NKAb2ab")
ggline(B_data, x = "days_to_SW_transfer", y = "NKAb2ab", add = c("mean_se", "dotplot"))
NKAb2ab.aov <- aov(NKAb2ab ~ days_to_SW_transfer, data = B_data)
summary(NKAb2ab.aov)
plot(NKAb2ab.aov, 1)
leveneTest(NKAb2ab ~ days_to_SW_transfer, data = B_data)
plot(NKAb2ab.aov, 2)
NKAb2ab.aov_residuals <- residuals(object = NKAb2ab.aov)
shapiro.test(x = NKAb2ab.aov_residuals)

#NKAb2c
ggboxplot(B_data, x = "days_to_SW_transfer", y = "NKAb2c")
ggline(B_data, x = "days_to_SW_transfer", y = "NKAb2c", add = c("mean_se", "dotplot"))
NKAb2c.aov <- aov(NKAb2c ~ days_to_SW_transfer, data = B_data)
summary(NKAb2c.aov)
plot(NKAb2c.aov, 1)
leveneTest(NKAb2c ~ days_to_SW_transfer, data = B_data)
plot(NKAb2c.aov, 2)
NKAb2c.aov_residuals <- residuals(object = NKAb2c.aov)
shapiro.test(x = NKAb2c.aov_residuals)

#NKAb3b
ggboxplot(B_data, x = "days_to_SW_transfer", y = "NKAb3b")
ggline(B_data, x = "days_to_SW_transfer", y = "NKAb3b", add = c("mean_se", "dotplot"))
NKAb3b.aov <- aov(NKAb3b ~ days_to_SW_transfer, data = B_data)
summary(NKAb3b.aov)
plot(NKAb3b.aov, 1)
leveneTest(NKAb3b ~ days_to_SW_transfer, data = B_data)
plot(NKAb3b.aov, 2)
NKAb3b.aov_residuals <- residuals(object = NKAb3b.aov)
shapiro.test(x = NKAb3b.aov_residuals)

#NKAb3c
ggboxplot(B_data, x = "days_to_SW_transfer", y = "NKAb3c")
ggline(B_data, x = "days_to_SW_transfer", y = "NKAb3c", add = c("mean_se", "dotplot"))
NKAb3c.aov <- aov(NKAb3c ~ days_to_SW_transfer, data = B_data)

```

```

summary(NKAb3c.aov)
plot(NKAb3c.aov, 1)
leveneTest(NKAb3c ~ days_to_SW_transfer, data = B_data)
plot(NKAb3c.aov, 2)
NKAb3c.aov_residuals <- residuals(object = NKAb3c.aov)
shapiro.test(x = NKAb3c.aov_residuals)

#NKAb4
ggboxplot(B_data, x = "days_to_SW_transfer", y = "NKAb4")
ggline(B_data, x = "days_to_SW_transfer", y = "NKAb4", add = c("mean_se", "dotplot"))
NKAb4.aov <- aov(NKAb4 ~ days_to_SW_transfer, data = B_data)
summary(NKAb4.aov)
plot(NKAb4.aov, 1)
leveneTest(NKAb4 ~ days_to_SW_transfer, data = B_data)
plot(NKAb4.aov, 2)
NKAb4.aov_residuals <- residuals(object = NKAb4.aov)
shapiro.test(x = NKAb4.aov_residuals)

#UP584
ggboxplot(B_data, x = "days_to_SW_transfer", y = "UP584")
ggline(B_data, x = "days_to_SW_transfer", y = "UP584", add = c("mean_se", "dotplot"))
UP584.aov <- aov(UP584 ~ days_to_SW_transfer, data = B_data)
summary(UP584.aov)
plot(UP584.aov, 1)
leveneTest(UP584 ~ days_to_SW_transfer, data = B_data)
plot(UP584.aov, 2)
UP584.aov_residuals <- residuals(object = UP584.aov)
shapiro.test(x = UP584.aov_residuals)

#CaATPase
ggboxplot(B_data, x = "days_to_SW_transfer", y = "CaATPase")
ggline(B_data, x = "days_to_SW_transfer", y = "CaATPase", add = c("mean_se", "dotplot"))
CaATPase.aov <- aov(CaATPase ~ days_to_SW_transfer, data = B_data)
summary(CaATPase.aov)
plot(CaATPase.aov, 1)
leveneTest(CaATPase ~ days_to_SW_transfer, data = B_data)
plot(CaATPase.aov, 2)
CaATPase.aov_residuals <- residuals(object = CaATPase.aov)
shapiro.test(x = CaATPase.aov_residuals)

#Copine
ggboxplot(B_data, x = "days_to_SW_transfer", y = "Copine")
ggline(B_data, x = "days_to_SW_transfer", y = "Copine", add = c("mean_se", "dotplot"))
Copine.aov <- aov(Copine ~ days_to_SW_transfer, data = B_data)
summary(Copine.aov)
plot(Copine.aov, 1)
leveneTest(Copine ~ days_to_SW_transfer, data = B_data)
plot(Copine.aov, 2)
Copine.aov_residuals <- residuals(object = Copine.aov)
shapiro.test(x = Copine.aov_residuals)

#Elast_in
ggboxplot(B_data, x = "days_to_SW_transfer", y = "Elast_in")
ggline(B_data, x = "days_to_SW_transfer", y = "Elast_in", add = c("mean_se", "dotplot"))
Elast_in.aov <- aov(Elast_in ~ days_to_SW_transfer, data = B_data)
summary(Elast_in.aov)
plot(Elast_in.aov, 1)
leveneTest(Elast_in ~ days_to_SW_transfer, data = B_data)
plot(Elast_in.aov, 2)
Elast_in.aov_residuals <- residuals(object = Elast_in.aov)

```

```

shapiro.test(x = Elast_in.aov_residuals)

#AnnA3
ggboxplot(B_data, x = "days_to_SW_transfer", y = "AnnA3")
ggline(B_data, x = "days_to_SW_transfer", y = "AnnA3", add = c("mean_se", "dotplot"))
AnnA3.aov <- aov(AnnA3 ~ days_to_SW_transfer, data = B_data)
summary(AnnA3.aov)
plot(AnnA3.aov, 1)
leveneTest(AnnA3 ~ days_to_SW_transfer, data = B_data)
plot(AnnA3.aov, 2)
AnnA3.aov_residuals <- residuals(object = AnnA3.aov)
shapiro.test(x = AnnA3.aov_residuals)

#Gelsolin
ggboxplot(B_data, x = "days_to_SW_transfer", y = "Gelsolin")
ggline(B_data, x = "days_to_SW_transfer", y = "Gelsolin", add = c("mean_se", "dotplot"))
Gelsolin.aov <- aov(Gelsolin ~ days_to_SW_transfer, data = B_data)
summary(Gelsolin.aov)
plot(Gelsolin.aov, 1)
leveneTest(Gelsolin ~ days_to_SW_transfer, data = B_data)
plot(Gelsolin.aov, 2)
Gelsolin.aov_residuals <- residuals(object = Gelsolin.aov)
shapiro.test(x = Gelsolin.aov_residuals)

#IgK
ggboxplot(B_data, x = "days_to_SW_transfer", y = "IgK")
ggline(B_data, x = "days_to_SW_transfer", y = "IgK", add = c("mean_se", "dotplot"))
IgK.aov <- aov(IgK ~ days_to_SW_transfer, data = B_data)
summary(IgK.aov)
plot(IgK.aov, 1)
leveneTest(IgK ~ days_to_SW_transfer, data = B_data)
plot(IgK.aov, 2)
IgK.aov_residuals <- residuals(object = IgK.aov)
shapiro.test(x = IgK.aov_residuals)

#IgD
ggboxplot(B_data, x = "days_to_SW_transfer", y = "IgD")
ggline(B_data, x = "days_to_SW_transfer", y = "IgD", add = c("mean_se", "dotplot"))
IgD.aov <- aov(IgD ~ days_to_SW_transfer, data = B_data)
summary(IgD.aov)
plot(IgD.aov, 1)
leveneTest(IgD ~ days_to_SW_transfer, data = B_data)
plot(IgD.aov, 2)
IgD.aov_residuals <- residuals(object = IgD.aov)
shapiro.test(x = IgD.aov_residuals)

#LDLR
ggboxplot(B_data, x = "days_to_SW_transfer", y = "LDLR")
ggline(B_data, x = "days_to_SW_transfer", y = "LDLR", add = c("mean_se", "dotplot"))
LDLR.aov <- aov(LDLR ~ days_to_SW_transfer, data = B_data)
summary(LDLR.aov)
plot(LDLR.aov, 1)
leveneTest(LDLR ~ days_to_SW_transfer, data = B_data)
plot(LDLR.aov, 2)
LDLR.aov_residuals <- residuals(object = LDLR.aov)
shapiro.test(x = LDLR.aov_residuals)

#ApoA1
ggboxplot(B_data, x = "days_to_SW_transfer", y = "ApoA1")
ggline(B_data, x = "days_to_SW_transfer", y = "ApoA1", add = c("mean_se", "dotplot"))

```

```

ApoA1.aov <- aov(ApoA1 ~ days_to_SW_transfer, data = B_data)
summary(ApoA1.aov)
plot(ApoA1.aov, 1)
leveneTest(ApoA1 ~ days_to_SW_transfer, data = B_data)
plot(ApoA1.aov, 2)
ApoA1.aov_residuals <- residuals(object = ApoA1.aov)
shapiro.test(x = ApoA1.aov_residuals)

#NKCC
ggboxplot(B_data, x = "days_to_SW_transfer", y = "NKCC")
ggline(B_data, x = "days_to_SW_transfer", y = "NKCC", add = c("mean_se", "dotplot"))
NKCC.aov <- aov(NKCC ~ days_to_SW_transfer, data = B_data)
summary(NKCC.aov)
plot(NKCC.aov, 1)
leveneTest(NKCC ~ days_to_SW_transfer, data = B_data)
plot(NKCC.aov, 2)
NKCC.aov_residuals <- residuals(object = NKCC.aov)
shapiro.test(x = NKCC.aov_residuals)

#CFTR
ggboxplot(B_data, x = "days_to_SW_transfer", y = "CFTR")
ggline(B_data, x = "days_to_SW_transfer", y = "CFTR", add = c("mean_se", "dotplot"))
CFTR.aov <- aov(CFTR ~ days_to_SW_transfer, data = B_data)
summary(CFTR.aov)
plot(CFTR.aov, 1)
leveneTest(CFTR ~ days_to_SW_transfer, data = B_data)
plot(CFTR.aov, 2)
CFTR.aov_residuals <- residuals(object = CFTR.aov)
shapiro.test(x = CFTR.aov_residuals)

#plgRLT1
ggboxplot(B_data, x = "days_to_SW_transfer", y = "plgRLT1")
ggline(B_data, x = "days_to_SW_transfer", y = "plgRLT1", add = c("mean_se", "dotplot"))
plgRLT1.aov <- aov(plgRLT1 ~ days_to_SW_transfer, data = B_data)
summary(plgRLT1.aov)
plot(plgRLT1.aov, 1)
leveneTest(plgRLT1 ~ days_to_SW_transfer, data = B_data)
plot(plgRLT1.aov, 2)
plgRLT1.aov_residuals <- residuals(object = plgRLT1.aov)
shapiro.test(x = plgRLT1.aov_residuals)

#ApoB100
ggboxplot(B_data, x = "days_to_SW_transfer", y = "ApoB100")
ggline(B_data, x = "days_to_SW_transfer", y = "ApoB100", add = c("mean_se", "dotplot"))
ApoB100.aov <- aov(ApoB100 ~ days_to_SW_transfer, data = B_data)
summary(ApoB100.aov)
plot(ApoB100.aov, 1)
leveneTest(ApoB100 ~ days_to_SW_transfer, data = B_data)
plot(ApoB100.aov, 2)
ApoB100.aov_residuals <- residuals(object = ApoB100.aov)
shapiro.test(x = ApoB100.aov_residuals)

#plgRLT1a
ggboxplot(B_data, x = "days_to_SW_transfer", y = "plgRLT1a")
ggline(B_data, x = "days_to_SW_transfer", y = "plgRLT1a", add = c("mean_se", "dotplot"))
plgRLT1a.aov <- aov(plgRLT1a ~ days_to_SW_transfer, data = B_data)
summary(plgRLT1a.aov)
plot(plgRLT1a.aov, 1)
leveneTest(plgRLT1a ~ days_to_SW_transfer, data = B_data)
plot(plgRLT1a.aov, 2)

```

```

plgRLT1a.aov_residuals <- residuals(object = plgRLT1a.aov)
shapiro.test(x = plgRLT1a.aov_residuals)

#ZP16
ggboxplot(B_data, x = "days_to_SW_transfer", y = "ZP16")
ggline(B_data, x = "days_to_SW_transfer", y = "ZP16", add = c("mean_se", "dotplot"))
ZP16.aov <- aov(ZP16 ~ days_to_SW_transfer, data = B_data)
summary(ZP16.aov)
plot(ZP16.aov, 1)
leveneTest(ZP16 ~ days_to_SW_transfer, data = B_data)
plot(ZP16.aov, 2)
ZP16.aov_residuals <- residuals(object = ZP16.aov)
shapiro.test(x = ZP16.aov_residuals)

#AnnA1
ggboxplot(B_data, x = "days_to_SW_transfer", y = "AnnA1")
ggline(B_data, x = "days_to_SW_transfer", y = "AnnA1", add = c("mean_se", "dotplot"))
AnnA1.aov <- aov(AnnA1 ~ days_to_SW_transfer, data = B_data)
summary(AnnA1.aov)
plot(AnnA1.aov, 1)
leveneTest(AnnA1 ~ days_to_SW_transfer, data = B_data)
plot(AnnA1.aov, 2)
AnnA1.aov_residuals <- residuals(object = AnnA1.aov)
shapiro.test(x = AnnA1.aov_residuals)

#CPT2
ggboxplot(B_data, x = "days_to_SW_transfer", y = "CPT2")
ggline(B_data, x = "days_to_SW_transfer", y = "CPT2", add = c("mean_se", "dotplot"))
CPT2.aov <- aov(CPT2 ~ days_to_SW_transfer, data = B_data)
summary(CPT2.aov)
plot(CPT2.aov, 1)
leveneTest(CPT2 ~ days_to_SW_transfer, data = B_data)
plot(CPT2.aov, 2)
CPT2.aov_residuals <- residuals(object = CPT2.aov)
shapiro.test(x = CPT2.aov_residuals)

#TukeysHSD test
#NKAA1a
TukeyHSD(NKAA1a.aov)
#NKAA1b
TukeyHSD(NKA_a1b.aov)
#ApoA4
TukeyHSD(ApoA4.aov)
#NKAb3c
TukeyHSD(NKAb3c.aov)
#Elast_in
TukeyHSD(Elast_in.aov)
#IgK
TukeyHSD(IgK.aov)
#CFTR
TukeyHSD(CFTR.aov)
#ZP16
TukeyHSD(ZP16.aov)

B_SWc <- Biomarkers_SW_challenge

library(ggpubr)
library(car)

```

```

#TTP1
ggboxplot(B_SWc, x = "category", y = "TTP1")
ggline(B_SWc, x = "category", y = "TTP1", add = c("mean_se", "dotplot"))
TTP1.aov <- aov(TTP1 ~ category, data = B_SWc)
summary(TTP1.aov)
plot(TTP1.aov, 1)
leveneTest(TTP1 ~ category, data = B_SWc)
plot(TTP1.aov, 2)
TTP1.aov_residuals <- residuals(object = TTP1.aov)
shapiro.test(x = TTP1.aov_residuals)

#TTP2
ggboxplot(B_SWc, x = "category", y = "TTP2")
ggline(B_SWc, x = "category", y = "TTP2", add = c("mean_se", "dotplot"))
TTP2.aov <- aov(TTP2 ~ category, data = B_SWc)
summary(TTP2.aov)
plot(TTP2.aov, 1)
leveneTest(TTP2 ~ category, data = B_SWc)
plot(TTP2.aov, 2)
TTP2.aov_residuals <- residuals(object = TTP2.aov)
shapiro.test(x = TTP2.aov_residuals)

#AHRT1
ggboxplot(B_SWc, x = "category", y = "AHRT1")
ggline(B_SWc, x = "category", y = "AHRT1", add = c("mean_se", "dotplot"))
AHRT1.aov <- aov(AHRT1 ~ category, data = B_SWc)
summary(AHRT1.aov)
plot(AHRT1.aov, 1)
leveneTest(AHRT1 ~ category, data = B_SWc)
plot(AHRT1.aov, 2)
AHRT1.aov_residuals <- residuals(object = AHRT1.aov)
shapiro.test(x = AHRT1.aov_residuals)

#plgR
ggboxplot(B_SWc, x = "category", y = "plgR")
ggline(B_SWc, x = "category", y = "plgR", add = c("mean_se", "dotplot"))
plgR.aov <- aov(plgR ~ category, data = B_SWc)
summary(plgR.aov)
plot(plgR.aov, 1)
leveneTest(plgR ~ category, data = B_SWc)
plot(plgR.aov, 2)
plgR.aov_residuals <- residuals(object = plgR.aov)
shapiro.test(x = plgR.aov_residuals)

#plgRL1
ggboxplot(B_SWc, x = "category", y = "plgRL1")
ggline(B_SWc, x = "category", y = "plgRL1", add = c("mean_se", "dotplot"))
plgRL1.aov <- aov(plgRL1 ~ category, data = B_SWc)
summary(plgRL1.aov)
plot(plgRL1.aov, 1)
leveneTest(plgRL1 ~ category, data = B_SWc)
plot(plgRL1.aov, 2)
plgRL1.aov_residuals <- residuals(object = plgRL1.aov)
shapiro.test(x = plgRL1.aov_residuals)

#plgRL2
ggboxplot(B_SWc, x = "category", y = "plgRL2")
ggline(B_SWc, x = "category", y = "plgRL2", add = c("mean_se", "dotplot"))
plgRL2.aov <- aov(plgRL2 ~ category, data = B_SWc)
summary(plgRL2.aov)

```

```

plot(plgRL2.aov, 1)
leveneTest(plgRL2 ~ category, data = B_SWc)
plot(plgRL2.aov, 2)
plgRL2.aov_residuals <- residuals(object = plgRL2.aov)
shapiro.test(x = plgRL2.aov_residuals)

#CLM8
ggboxplot(B_SWc, x = "category", y = "CLM8")
ggline(B_SWc, x = "category", y = "CLM8", add = c("mean_se", "dotplot"))
CLM8.aov <- aov(CLM8 ~ category, data = B_SWc)
summary(CLM8.aov)
plot(CLM8.aov, 1)
leveneTest(CLM8 ~ category, data = B_SWc)
plot(CLM8.aov, 2)
CLM8.aov_residuals <- residuals(object = CLM8.aov)
shapiro.test(x = CLM8.aov_residuals)

#XBP1
ggboxplot(B_SWc, x = "category", y = "XBP1")
ggline(B_SWc, x = "category", y = "XBP1", add = c("mean_se", "dotplot"))
XBP1.aov <- aov(XBP1 ~ category, data = B_SWc)
summary(XBP1.aov)
plot(XBP1.aov, 1)
leveneTest(XBP1 ~ category, data = B_SWc)
plot(XBP1.aov, 2)
XBP1.aov_residuals <- residuals(object = XBP1.aov)
shapiro.test(x = XBP1.aov_residuals)

#NKCC
ggboxplot(B_SWc, x = "category", y = "NKCC")
ggline(B_SWc, x = "category", y = "NKCC", add = c("mean_se", "dotplot"))
NKCC.aov <- aov(NKCC ~ category, data = B_SWc)
summary(NKCC.aov)
plot(NKCC.aov, 1)
leveneTest(NKCC ~ category, data = B_SWc)
plot(NKCC.aov, 2)
NKCC.aov_residuals <- residuals(object = NKCC.aov)
shapiro.test(x = NKCC.aov_residuals)

#CFTR
ggboxplot(B_SWc, x = "category", y = "CFTR")
ggline(B_SWc, x = "category", y = "CFTR", add = c("mean_se", "dotplot"))
CFTR.aov <- aov(CFTR ~ category, data = B_SWc)
summary(CFTR.aov)
plot(CFTR.aov, 1)
leveneTest(CFTR ~ category, data = B_SWc)
plot(CFTR.aov, 2)
CFTR.aov_residuals <- residuals(object = CFTR.aov)
shapiro.test(x = CFTR.aov_residuals)

#ZG16
ggboxplot(B_SWc, x = "category", y = "ZG16")
ggline(B_SWc, x = "category", y = "ZG16", add = c("mean_se", "dotplot"))
ZG16.aov <- aov(ZG16 ~ category, data = B_SWc)
summary(ZG16.aov)
plot(ZG16.aov, 1)
leveneTest(ZG16 ~ category, data = B_SWc)
plot(ZG16.aov, 2)
ZG16.aov_residuals <- residuals(object = ZG16.aov)
shapiro.test(x = ZG16.aov_residuals)

```

TukeyHSD(plgRL1.aov)  
TukeyHSD(plgRL2.aov)  
TukeyHSD(NKCC.aov)

## Appendix 6 – SWATH methodology

### *A6.1 Protein assay*

Protein was extracted from tissue as for Western blot (Material and Methods section 2.3.1).

Bicinchoninic acid (BCA) Assay: Samples were diluted 1:40 with water and 10 µl samples were added to 96 well plates along with a series of BSA standards (62.5 – 1000 µg/ml). BCA working reagent (200 µl: prepared by addition of 50 parts Solution A and 1 part Solution B; BCA assay kit, Pierce, Thermo Fisher Scientific) was added to each well and samples incubated at 37°C for 20 minutes. Plates were cooled at room temperature for 5 minutes and absorbance measured at 560 nm on a Dynex plate reader. This assay was used for protein samples for SWATH analysis as it was recommended by the Mass Spectrometry and Proteomics Facility at the University of St Andrews.

### *A6.2 Sequential Windowed Acquisition of All Theoretical Fragment Ion Mass Spectra (SWATH-MS) proteomics*

In order to quantify changes in proteins expressed in the gill during smoltification and following subsequent seawater transfer, a proteomic study was carried out using SWATH, a liquid chromatography coupled-mass spectrometry method. HPLC-MS/MS analysis involves digestion of proteins by trypsin. The resultant peptides are then separated by reverse phase liquid chromatography (LC) on a C18 column coupled directly to a mass spectrometer. Peptides eluting from the LC are transferred into the mass spectrometer where the mass to charge (m/z) ratio of peptides is determined. These peptides are then fragmented in the collision cell and fragments are detected. The fragmentation pattern forms a fingerprint specific to the parent molecule, which can be used for identification. The method used was

the SWATH-MS technique developed by Gillet *et al.* (2012). This targeted proteomic method, which systematically interrogates samples, enabling rapid detection and quantification of proteins of interest in multiple samples, requires the generation of a library of spectra associated with the study population.

The SWATH-MS technique consists of two modes of analysis. The first is data dependent acquisition mode (DDA), used to create a library of spectra for the sample, in which for each MS scan the program selects a defined number of peptides for fragmentation dependent on their abundance. The second mode is data independent acquisition (DIA) in which selection is not based on abundance, but instead a full MS scan is conducted between the  $m/z$  400-1250. The machine then scans across overlapping  $m/z$  windows of a defined width ( $m/z$  25), and oligopeptides which fall within the window are fragmented. Information in the fragment ion library is used to mine the complete fragment ion maps produced in the DIA mode. This method allows the identification and quantification of peptides of interest with comparable consistency and accuracy to that of the gold standard proteomic method, selected reaction monitoring.

### *A6.3 Creation of peptide database*

A database of peptides was created based on the proteins and transcripts in the NCBI Salmon 8030 database, corrected to remove a number of known duplicated sequences and to re-annotate incorrectly labelled submissions. This was achieved by aligning sequences of related genes using Clustal, and identifying and re-grouping known paralogues of genes and repeated sequences that had been submitted with different annotations. Equivalent forms of proteins were then given specific annotations to allow the identification of individual paralogues in the SWATH runs.

#### *A6.4 Generation of spectral library*

Lysates of gill samples, taken from 24 Atlantic salmon at different developmental stages, ranging from FW parr through to 2 year old SW adults, were prepared as detailed in Section 3.1. Particulate extracts were solubilised by treatment with homogenizing buffer (Section 3.1) containing 4% sodium deoxycholate (DOC) for 2 h at 4°C before centrifugation at 15500 rpm (28388 G, Beckman J2 centrifuge; JA18.1 rotor) for 90 min at 4°C to remove insoluble material. The protein content of the solubilised particulate extract was determined by Bradford protein assay as detailed in Section 3.2.

The lysates were then further processed by the Mass Spectrometry and Proteomics Facility at the University of St Andrews.

#### *A6.5 Denaturing, and digestion of protein samples*

Proteins samples were denatured, disulphide bonds broken, and cysteines alkylated, before the proteins were fragmented by treatment with trypsin. The details of this procedure are given below. The volume of sample required to give 47 µg of protein was taken, and 50 mM ammonium bicarbonate was added to make the volume up to 10 µl. Samples were treated with 15 µl of 10 M urea to denature proteins, giving a final urea concentration of 6 M and a volume of 25 µl for digestion. Samples were then incubated with 1.25 µl of 100 mM tris 2-carboxyethyl phosphine hydrochloride (TCEP) in 50 mM ammonium bicarbonate at room temperature for 45 minutes, then for a further 30 minutes in the dark after the addition of 1.05 µl of 250 mM iodoacetamide (IAA) in 50 mM ammonium bicarbonate. To reduce all disulphide bonds, 1.09 µl of 0.5 M dithiothreitol (DTT) in 50 mM ammonium bicarbonate was added and samples incubated at room temperature for 10 minutes before addition of 71.61 µl of 50 mM ammonium bicarbonate to dilute the urea concentration to 1.5 M. Trypsin

was added to a ~1:50 ratio between enzyme:substrate (w/w) (4  $\mu$ l, stock 0.2  $\mu$ g/ $\mu$ l in 0.1% formic acid) and incubated for 16 h at 30°C. Samples were acidified with 0.52  $\mu$ l of 100% trifluoroacetic acid (TFA), followed by the addition of 5.23  $\mu$ l 100% acetonitrile (MeCN). Samples were then desalted on micro-prep columns. Micro Spin C18 columns (Harvard Apparatus) were activated by washing sequentially with 2 x with 200  $\mu$ l of 100% MeCN, 3 x with 200  $\mu$ l of 50% MeCN and finally 3 x with 200  $\mu$ l of 5% MeCN/0.5%TFA centrifuging at 0.5 x g for 30 seconds. Samples were re-loaded twice, spinning for 1 minute at 0.5 x g and finally 1 minute at 1.5 x g before drying samples in a Savant SpeedVac concentrator (Thermo Fisher Scientific). Dried peptides were dissolved to give a final concentration of 1  $\mu$ g/ $\mu$ l in loading buffer (2% MeCN/0.5% TFA).

A sample representative of all life stages, for the spectral library, was prepared by combining 10  $\mu$ g of peptides from each individually digested gill sample. This mixture was analysed on a Sciex Triple TOF 5600+ system mass spectrometer (Sciex, Framingham, MA, USA) coupled to an Eksigent nanoLC AS-2/2Dplus system in data dependent mode to achieve in depth identification of the proteins. Prior to mass spectrometric analysis reference iRT peptides (Biognosys, Schlieren, Switzerland) were added according to manufacturer's specifications to correct for retention times. Samples were loaded in 2% MeCN/ 0.05% trifluoroacetic acid (TFA) buffer and bound to an Aclaim pepmap 100  $\mu$ m x 2 cm trap (Thermo Fisher Scientific). After 10 min washing to waste, the trap was turned in-line with the analytical column (Aclaim pepmap RSLC 75  $\mu$ m x 15 cm). The analytical solvent system consisted of buffer A (2% MeCN with 0.1% formic acid in water) and buffer B (2% water with 0.1% formic acid in MeCN) at a flow rate of 300 nl/min with the following gradient: linear 1-20% of buffer B over 90 min, linear 20-40% of buffer B over 30 min, linear 40-99% of buffer B over 10 min, isocratic 99% buffer B over 5 min, linear 99 -1% of buffer B over 2.5 min and isocratic 1% buffer B over 12.5 min. The mass spectrometer was operated in

DDA top 20 positive ion mode, with 250 and 150 ms acquisition time for the MS1 (m/z 400-1200) and MS2 (m/z 230-1800) scans respectively, and 15s dynamic exclusion. Rolling collision energy with a collision energy spread of 5 eV was used for fragmentation. A search result was generated from raw.wiff files using Protein Pilot v5.0.1 (Sciex) with the following search parameters: urea denaturation as special factors, trypsin as the cleavage enzyme (/K-\P and /R-\P) and carbamidomethylation as a fixed modification of the cysteines. Within the Triple TOF 5600+ instrument setting option, MS tolerance was pre-set to 0.05 Da and MS/MS tolerance to 0.1 Da. The search was carried out in “rapid ID” mode with a detected protein threshold of 1% plus false discovery rate analysis against the *Salmo salar* database (dbID 8030, see modification as described above). Note that the iRT peptides were included in this database.

#### *A6.6 SWATH-MS data acquisition*

For SWATH-MS data acquisition, the same mass spectrometer and LC-MS/MS setup was used, essentially as described above, but operated in SWATH (DIA) mode. The method uses 50 windows of variable Da effective isolation width with a 1 Da overlap using ABSciex Variable Window Calculator tool. Each window has a dwell time of 150 ms to cover the mass range of 400-1250 m/z in TOF-MS mode and MS/MS data was acquired over a range of 230-1800 m/z with high sensitivity setting and a dwell time of 70ms, resulting in a cycle time of 3.6 s. the collision energy for each window was set using a collision energy of a 2+ ion centred in the middle of the window with a spread of 5 eV.

For SWATH analyses soluble/supernatant and solubilised particulate samples were prepared from gill samples for 18 salmon at different stages of the parr/smolt transformation. Gill tissue from parr, freshwater smolts immediately before transfer to SW and smolts sampled 72 hours post SW transfer were prepared as detailed in Section 2. Study samples were derived

from 6 fish per group. Membrane fractions from protein extraction were combined to give three experimental samples per group, each containing material from two fish. The volume of protein lysate required to give 1  $\mu\text{g}$  of protein (as determined by Bradford protein assay) was made up to 8  $\mu\text{l}$  with 2% MeCN/0.1% formic acid for injection onto the column as described above.

The data were analysed using the programs Protein Pilot, Protein Peak View, and Marker View. The HPLC/MS/MS and data analysis was carried out by Dr Silvia Synowsky of the Mass spectrometry and proteomic facility in the Biomedical Sciences Research Complex Core Facility at the University of St Andrews.